



# **Glycosynthases — tuning glycosidase activity towards glycoside diversification and synthesis**

Inaugural-Dissertation

zur Erlangung des Doktorgrades  
der Mathematisch-Naturwissenschaftlichen Fakultät  
der Heinrich-Heine-Universität Düsseldorf

vorgelegt von

**Marc Richard Hayes**  
aus Lindlar

Düsseldorf, Juli 2019

aus dem Institut für Bioorganische Chemie  
der Heinrich-Heine-Universität Düsseldorf

Gedruckt mit der Genehmigung der  
Mathematisch-Naturwissenschaftlichen Fakultät der  
Heinrich-Heine-Universität Düsseldorf

Berichtersteller:

1. Prof. Dr. Jörg Pietruszka

2. Prof. Dr. Vlada Urlacher

Tag der mündlichen Prüfung: 24.09.2019



# PUBLICATIONS

Parts of this thesis have been published in scientific journals or presented at scientific conferences.

## Published in Journals

M. R. Hayes, K. A. Bochinsky, L. S. Seibt, L. Elling, J. Pietruszka, *J. Biotechnol.* **2017**, *257*, 162–170; ‘Development of a colourimetric assay for glycosynthases’.

M. R. Hayes, J. Pietruszka, *Molecules* **2017**, *22(9)*, 1434; ‘Synthesis of glycosides by glycosynthases’.

A. Fulton, M. R. Hayes, U. Schwaneberg, J. Pietruszka, K.-E. Jaeger, *Methods Mol. Biol.* **2018**, *1685*, 209–231; ‘High-Throughput Screening Assays for Lypolytic Enzymes’.

## Conference participation

### Poster

Final Aachen-Osaka Symposium, International Research Training Group ‘Selectivity in Chemo- and Biocatalysis’, 26<sup>th</sup>–27<sup>th</sup> November 2018, Super C, Ford Saal, RWTH Aachen University, Germany; M. R. Hayes, »Glycosynthases — Creating a versatile, biocatalytic toolbox towards glycoside synthesis«

Enzyme Engineering XXIV, 24<sup>th</sup>–28<sup>th</sup> September 2017, Pierre Baudis Congress Center, Toulouse, France; M. R. Hayes, L. Elling, K. Fujiyama, T. Ohashi, J. Pietruszka, »Glycodiversification: Glycosynthases towards variation of flavonoid glycosides«

19<sup>th</sup> European Carbohydrate Symposium, EUROCARB 2017, 2<sup>nd</sup>–6<sup>th</sup> July 2017, Centre de Convencions International de Barcelona, Barcelona, Spain; M. R. Hayes, L. Elling, J. Pietruszka, »Glycosynthases: Identification, Characterisation, and Application«

Joint Symposium Aachen-Osaka, International Research Training Group ‘Selectivity in Chemo- and Biocatalysis’, 20<sup>th</sup>–21<sup>st</sup> September 2017, RWTH Aachen University, Germany; M. R. Hayes, L. Elling, K. Fujiyama, T. Ohashi, J. Pietruszka, »Glycosynthases: Biocatalysis Towards the Glycodiversification of Flavonoids«

8<sup>th</sup> International Congress on Biocatalysis, Biocat 2016, 28<sup>th</sup> August–1<sup>st</sup> September 2016, Hamburg University of Technology, Hamburg, Germany; M. R. Hayes, L. Elling, J. Pietruszka, »Glycosynthases as Versatile Biocatalysts in Organic Synthesis«

## **Presentation**

Biotechnology and Chemistry for Green Growth, JSPS Japanese-German Graduate Externship Program, 9<sup>th</sup>–10<sup>th</sup> March 2016, Osaka University, Japan; M. R. Hayes, »Glycosynthases in Organic Synthesis«

Joint Symposium Aachen-Osaka, International Research Training Group 'Selectivity in Chemo- and Biocatalysis', 6<sup>th</sup>–7<sup>th</sup> September 2016, RWTH Aachen University, Germany; M. R. Hayes, »Glycosynthases: A New Approach to Screening and Characterisation«

Biotechnology and Chemistry for Green Growth, JSPS Japanese-German Graduate Externship Program, 6<sup>th</sup>–7<sup>th</sup> March 2017, Yumebutai, Awaji, Hyogo, Japan; M. R. Hayes, »Development and Characterisation of Glycosynthases for Organic Synthesis«

Biotechnology and Chemistry for Green Growth, JSPS Japanese-German Graduate Externship Program, 13<sup>th</sup>–14<sup>th</sup> March 2018, Yumebutai, Awaji, Hyogo, Japan; M. R. Hayes, »Glycosynthases: Towards the biocatalytic synthesis of glycosides«

Annual Conference 2018 of the Association for General and Applied Microbiology, VAAM 2018, 15<sup>th</sup>–18<sup>th</sup> April 2018, Wolfsburg, Germany; M. R. Hayes, J. Pietruszka, »Glycosynthases: Biocatalytic synthesis of glycosides«

9<sup>th</sup> International Congress on Biocatalysis, Biocat 2018, 26<sup>th</sup>–30<sup>th</sup> August 2018, Hamburg, Germany; M. R. Hayes, J. Pietruszka, »Glycosynthases: A biocatalytic approach to the synthesis of glycosides«

## **Theses**

The current thesis contains results of the following bachelor theses and master thesis:

M. Sc. Marc Richard Hayes (Heinrich Heine University Düsseldorf, Master thesis), 2014: »Glycosidases in Organic Synthesis«

M. Sc. Lisa Sabrina Seibt (Heinrich Heine University Düsseldorf, Bachelor thesis), 2015: »Charakterisierung von psychrophilen  $\beta$ -Glycosidasen und -synthasen«

B. Sc. Bianca-Georgiana Axinte (Heinrich Heine University Düsseldorf, Bachelor thesis), 2018:  
» $\alpha$ -L-Rhamnosidase from *Bacillus* sp. GL1: First Attempts on Systematically Altering  
Hydrolytic Activity«

The respective theses were conducted under the author's supervision and is indicated throughout the thesis.

# TABLE OF CONTENTS

1	Abbreviations.....	1
2	Abstract .....	1
3	Kurzzusammenfassung .....	3
4	Introduction.....	5
4.1	Importance of glycosides.....	5
4.2	Thesis objective.....	7
5	State of knowledge .....	9
5.1	Glycosynthases — from hydrolysis to synthesis .....	9
5.2	Biocatalysis towards $\beta$ -linked glycosides .....	12
5.2.1	Synthesis of $\beta$ -glycosides .....	12
5.2.2	Glycosidase candidates — a versatile toolbox for $\beta$ -glycoside synthesis .....	21
5.3	Biocatalysis towards $\alpha$ -linked glycosides .....	27
5.3.1	Synthesis with $\alpha$ -glycosynthases .....	27
5.3.2	Biocatalysis towards rhamnosides .....	31
5.4	Transferring glycans by <i>endo</i> - $\beta$ - <i>N</i> -acetylglucosaminidases.....	34
5.4.1	Glycosynthases derived from <i>endo</i> - $\beta$ - <i>N</i> -acetylglucosaminidases.....	34
5.4.2	Endo-CC — an ENGase with high potential .....	36
6	Results.....	38
6.1	From hot to cold — searching for optimal glycosynthase conditions by varying temperature optima .....	38
6.1.1	Glucosidase gene isolation .....	38
6.1.2	Characterisation of the wild type glycosidases .....	43
6.1.3	Structural analysis and mutagenesis of the $\beta$ -glucosidases .....	49
6.1.4	Detecting glycosynthase activity .....	57
6.1.5	Development of a high-throughput assay for glycosynthase characterisation .	66
6.1.6	Glycosynthase kinetics and acceptor screening .....	71
6.2	A substrate based approach for glycosynthase development.....	77
6.2.1	Choice and isolation of $\beta$ -glucosidase Cbg1 .....	77
6.2.2	Characterisation of Cbg1 .....	80
6.2.3	Mutagenesis and screening for synthetic activity .....	83

6.2.4	Expanding the mutant library of Cbg1 for synthetic application .....	88
6.2.5	Cbg1 for transglycosylation .....	97
6.3	Creating a rhamnosynthase .....	101
6.3.1	Synthesis of rhamnosyl substrates.....	101
6.3.2	Characterisation of the <i>wt</i> $\alpha$ -L-rhamnosidase .....	104
6.3.3	Mutagenesis of $\alpha$ -L-rhamnosidase RhaB .....	109
6.3.4	Screening for azide release.....	111
6.3.5	Attempts to find a $\alpha$ -L-rhamnosynthase.....	114
6.4	From monosaccharides to <i>en bloc</i> glycan transfer .....	125
6.4.1	<i>En bloc</i> glycosylation.....	125
6.4.2	Glycosylating RNase B-GlcNAc.....	126
6.4.3	Transferring glycans to low molecular weight acceptors .....	127
6.4.4	Heterologous expression of Endo-CC N180H.....	130
7	Summary and Outlook .....	133
8	Experimental Section.....	144
8.1	General.....	144
8.1.1	Devices.....	144
8.1.2	Consumables .....	145
8.1.3	Chemicals and enzymes .....	146
8.1.4	Oligonucleotides and plasmids.....	146
8.1.5	Bacterial strains.....	151
8.1.6	Software .....	151
8.2	Molecular biological methods .....	152
8.2.1	Isolation of genomic DNA from <i>R. radiobacter</i> .....	152
8.2.2	Plasmid isolation .....	152
8.2.3	DNA concentration determination .....	153
8.2.4	Agarose gel electrophoresis.....	153
8.2.5	DNA gel elution .....	154
8.2.6	DNA ligation and restriction.....	154
8.2.7	DNA amplification by PCR .....	155
8.2.8	Mutagenesis by inverse-PCR.....	156

8.2.9	Gibson Assembly cloning.....	157
8.2.10	DNA sequencing .....	158
8.3	Microbiological methods.....	158
8.3.1	Chemically competent cells.....	158
8.3.2	Transformation of chemically competent <i>E. coli</i> strains .....	159
8.3.3	Cultivation of <i>E. coli</i> strains .....	160
8.3.4	Heterologous expression of enzymes .....	160
8.3.5	Esculin-agar plate assay .....	161
8.4	Protein biochemical methods .....	162
8.4.1	Cell lysis .....	162
8.4.2	Protein isolation.....	162
8.4.3	Buffer exchange, desalting, and concentrating protein samples.....	163
8.4.4	Protein concentration determination .....	164
8.4.5	Lyophilisation .....	164
8.4.6	SDS-PAGE.....	165
8.5	Biocatalytic assays .....	166
8.5.1	Hydrolytic activity .....	166
8.5.2	Coniferin hydrolysis.....	167
8.5.3	Glycosynthase activity assay .....	167
8.5.4	Chemical recovery experiments.....	168
8.5.5	Glycosylation modification of RNase B .....	169
8.5.6	Naringinase deactivation and activity assay .....	169
8.6	Chemical synthesis .....	171
8.6.1	Chromatography .....	171
8.6.2	LC-MS analysis .....	171
8.6.3	Mass spectrometry.....	172
8.6.4	NMR-Spectroscopy .....	172
8.6.5	IR-Spectroscopy.....	173
8.6.6	Measurement of rotatory power ( $[\alpha]_D^{20}$ ).....	173
8.6.7	Melting points.....	173
8.6.8	Peracetylation of monosaccharides .....	173

8.6.9	Fluorination of peracetylated glycosides .....	174
8.6.10	O-Glycosylation .....	176
8.6.11	One-pot peracetylation and bromination of $\alpha$ -L-rhamnose ( <b>11e</b> ).....	178
8.6.12	Synthesis of 2,3,4-tri-O-acetyl $\beta$ -L-rhamnopyranosyl azide ( <b>22v</b> ) .....	179
8.6.13	Deprotection of acetylated compounds .....	180
8.6.14	Synthesis of triisopropyl-(4-nitrophenoxy)-silane (TIPSpNP, <b>23</b> ) .....	183
8.6.15	Enzymatic synthesis of prunin ( <b>1b</b> ) from naringin ( <b>1c</b> ).....	184
8.6.16	Biocatalytic synthesis of $\beta$ -D-glucosides.....	185
8.6.17	Glycosylation of glycoside molecules by Endo-CC N180H .....	189
9	Appendix.....	192
9.1	Gene and protein sequences .....	192
9.1.1	Standard expression vectors.....	192
9.1.2	<i>abg</i> — $\beta$ -Glucosidase of <i>R. radiobacter</i> .....	193
9.1.3	<i>bglU</i> — $\beta$ -Glucosidase of <i>M. antarcticus</i> .....	195
9.1.4	<i>bglC</i> — $\beta$ -Glycosidase of <i>P. furiosus</i> .....	196
9.1.5	<i>cbg1</i> — $\beta$ -Glucosidase of <i>R. radiobacter</i> .....	198
9.1.6	<i>rhaB</i> — $\alpha$ -L-Rhamnosidase of <i>Bacillus</i> sp. GL1 .....	200
9.1.7	<i>endo-CC N180H</i> — <i>Endo-N</i> -acetylglucosaminidase variant of <i>C. cinerea</i> .....	202
9.2	Codon harmonisation of <i>bglU</i> .....	204
9.3	Content of own contribution to the published publications during the work of this thesis .....	206
10	References .....	207
11	List of Synthesised Molecules .....	219
12	Acknowledgements.....	222
13	Declaration.....	225

# 1 ABBREVIATIONS

Amino acids		
Amino acid	3-Letter code	1-Letter code
Alanine	Ala	A
Arginine	Arg	R
Asparagine	Asn	N
Aspartic acid	Asp	D
Cysteine	Cys	C
Glutamine	Gln	Q
Glutamic acid	Glu	E
Glycine	Gly	G
Histidine	His	H
Isoleucine	Ile	I
Leucine	Leu	L
Lysine	Lys	K
Methionine	Met	M
Phenylalanine	Phe	F
Proline	Pro	P
Serine	Ser	S
Threonine	Thr	T
Tryptophan	Trp	W
Tyrosine	Tyr	Y
Valine	Val	V

## Organisms

<i>Alicyclobacillus acidocaldarius</i> , <i>A. acidocaldarius</i>	<i>Kluyveromyces fragilis</i> , <i>K. fragilis</i>
<i>Alternaria</i> sp. L1, <i>Alternaria</i> sp. L1,	<i>Micrococcus antarcticus</i> , <i>M. antarcticus</i>
<i>Alteromonas haloplanctis</i> , <i>A. haloplanctis</i>	<i>Mucor hiemalis</i> , <i>M. hiemalis</i>
<i>Arabidopsis thaliana</i> , <i>A. thaliana</i>	<i>Mycobacterium tuberculosis</i> , <i>M. tuberculosis</i>
<i>Arthrobacter protophormiae</i> , <i>A. protophormiae</i>	<i>Paecilomyces thermophile</i> , <i>P. thermophile</i>
<i>Bacillus circulans</i> , <i>B. circulans</i>	<i>Paenibacillus pabuli</i> , <i>P. pabuli</i>
<i>Bacillus halodurans</i> , <i>B. halodurans</i>	<i>Paenibacillus polymyxa</i> , <i>P. polymyxa</i>
<i>Bacillus licheniformis</i> , <i>B. licheniformis</i>	<i>Penicillium decumbens</i> , <i>P. decumbens</i>
<i>Bacteroides thetaiotaomicron</i> , <i>B thetaiotaomicron</i>	<i>Picea abies</i> , <i>P. abies</i>
<i>Bifidobacterium bifidum</i> , <i>B. bifidum</i>	<i>Pseudotsuga menziesii</i> , <i>P. menziesii</i>

---

### Organisms

---

<i>Calotomus japonicus</i> , <i>C. japonicus</i>	<i>Pyrococcus furiosus</i> , <i>P. furiosus</i>
<i>Candida rugosa</i> , <i>C. rugosa</i>	<i>Pyrococcus horikoshii</i> , <i>P. horikoshii</i>
<i>Cellulomonas fimi</i> , <i>C. fimi</i>	<i>Rhodococcus equi</i> , <i>R. equi</i>
<i>Cellvibrio gilvus</i> , <i>C. gilvus</i>	<i>Rhizobium radiobacter</i> , <i>R. radiobacter</i> (formerly <i>Agrobacterium tumefaciens</i> or <i>Agrobacterium radiobacter</i> )
<i>Cicer arietum</i> , <i>C. arietum</i>	<i>Solanum lycopersicum</i> , <i>S. lycopersicum</i>
<i>Clostridium stercorarium</i> , <i>C. stercorarium</i>	<i>Streptococcus pneumonia</i> , <i>S. pneumonia</i>
<i>Coprinopsis cinerea</i> , <i>C. cinerea</i>	<i>Sulfolobus solfataricus</i> , <i>S. solfataricus</i>
<i>Cryptococcus albidus</i> , <i>C. albidus</i>	<i>Thermococcus kodakaraensis</i> , <i>T. kodakaraensis</i>
<i>Eudendrium antarcticum</i> B7, <i>E. antarcticum</i> B7	<i>Thermotoga maritima</i> , <i>T. maritima</i>
<i>Escherichia coli</i> , <i>E. coli</i>	<i>Thermotoga neapolitana</i> , <i>T. neapolitana</i>
<i>Geobacillus stearothermophilus</i> , <i>G. stearothermophilus</i>	<i>Thermoplasma acidophilum</i> , <i>T. acidophilum</i>
<i>Helicobacter pylori</i> , <i>H. pylori</i>	<i>Thermosphaera aggregans</i> , <i>T. aggregans</i>
<i>Homo sapiens</i> , <i>H. sapiens</i>	<i>Thermus nonproteolyticus</i> , <i>T. nonproteolyticus</i>
<i>Humicola insolens</i> , <i>H. insolens</i>	<i>Thermus thermophiles</i> , <i>T. therophiles</i>
<i>Kluyveromyces marxianus</i> , <i>K. marxianus</i> (formerly <i>K. fragilis</i> )	<i>Volvariella volvacea</i> , <i>V. volvacea</i>

---

### Glycosides

---

Ara	L-Arabinose	IPTG	Isoproyl $\beta$ -D-thiogalactopyranoside
Gal	D-Galactose	LacNAc	N-Acetyl D-lactosamine
Glc	D-Glucose	Le <sup>a/x</sup>	Lewis antigen <sup>a/x</sup>
GlcNAc	N-Acetyl D-glucosamine	Le <sup>b/y</sup>	Lewis antigen <sup>b/y</sup>
Fuc	L-Fucose	LNB I	Lacto-N-biose I
Lac	Lactose	LNFP II	Lacto-N-fucopentaose II
Mal	Maltose	LNT	Lacto-N-tetraose
Man	D-Mannose	pNP Ara	p-Nitrophenyl $\alpha$ -L-arabinopyranoside
Rha	L-Rhamnose	pNP Gal	p-Nitrophenyl $\beta$ -D-galactopyranoside
Xyl	D-Xylose	pNP Glc	p-Nitrophenyl $\beta$ -D-glucopyranoside

---

Glycosides			
$\alpha$ -GalF	$\alpha$ -D-Galactopyranosyl fluoride	<i>p</i> NP <sub>GlcNAc</sub>	<i>p</i> -Nitrophenyl <i>N</i> -acetyl $\beta$ -D-glucosaminide
$\alpha$ -GlcF	$\alpha$ -D-Glucopyranosyl fluoride	<i>p</i> NP- $\beta$ -D-Fuc	<i>p</i> -Nitrophenyl $\beta$ -D-fucopyranoside
$\alpha$ -FucF	$\alpha$ -L-Fucopyranosyl fluoride	<i>p</i> NP- $\alpha$ -L-Fuc	<i>p</i> -Nitrophenyl $\alpha$ -L-fucopyranoside
$\alpha$ -LacF	$\alpha$ -D-Lactosyl fluoride	<i>p</i> NPLac	<i>p</i> -Nitrophenyl $\beta$ -D-lactoside
$\alpha$ -ManF	$\alpha$ -D-Mannopyranosyl fluoride	<i>p</i> NPMan	<i>p</i> -Nitrophenyl $\beta$ -D-mannopyranoside
$\alpha$ -Man <sub>2</sub> F	$\alpha$ -D-Mannobiosyl fluoride	<i>p</i> NPRha	<i>p</i> -Nitrophenyl $\alpha$ -L-rhamnopyranoside
$\alpha$ -XylF	$\alpha$ -D-Xylopyranosyl fluoride	<i>p</i> NPXyl	<i>p</i> -Nitrophenyl $\beta$ -D-xylopyranoside
$\beta$ -GalN <sub>3</sub>	$\beta$ -D-Galactopyranosyl azide	<i>p</i> NPXyl <sub>2</sub>	<i>p</i> -Nitrophenyl $\beta$ -D-xylobioside
$\beta$ -FucN <sub>3</sub>	$\beta$ -L-Fucopyranosyl azide		Xyloglucans
$\beta$ -FucF	$\beta$ -L-Fucopyranosyl fluoride	XLFG; XLLG/XLLG $\alpha$ F; XXXG/XXXG $\alpha$ F	(G = Glc; X = Xyl- $\alpha$ 1,6-Glc; L = Gal- $\beta$ 1,2-Xyl- $\alpha$ 1,6-Glc; F = Fuc- $\alpha$ 1,2-Gal- $\beta$ 1,2-Xyl- $\alpha$ 1,6-Glc; $\alpha$ F = fluoride in $\alpha$ -configuration)
$\beta$ -RhaN <sub>3</sub>	$\beta$ -L-Rhamnopyranosyl azide		
BTXyl <sub>2</sub>	Benzylthio- $\beta$ -xylobioside	Xyl <sub>2</sub> F/X <sub>2</sub> F	$\alpha$ -D-Xylobiosyl fluoride
2-Cl- <i>p</i> NPRha	2-Chloro- <i>p</i> -nitrophenyl $\alpha$ -L-rhamnopyranoside	Xyl <sub>3</sub> F	$\alpha$ -D-Xylotriosyl fluoride
HMO	Human milk oligosaccharides	UDP-GlcNAc	Uridine diphosphate <i>N</i> -acetylglucosamine

Enzymes			
Abg	$\beta$ -Glucosidase of <i>R. radiobacter</i>	Gan42B	$\beta$ -Galactosidase of <i>G. stearothermophilus</i>
A4- $\beta$ -gal	$\beta$ -Galactosidase of <i>T. thermophilus</i>	GlmA <sub>TK/Ph</sub>	$\beta$ -Glucosaminidases of <i>T. kodakarensis</i> or <i>P. hirokoshii</i>
Aa $\beta$ Gal-D361G	$\beta$ -Galactosynthase of <i>A. acidocaldarius</i>	HiCel7B	Cellobiase of <i>H. insolens</i>
Abg-2F6	Mutant variant of Abg	Hs- $\beta$ -gal	$\beta$ -Galactosidase of <i>H. sapiens</i>
Abg-NNT	Mutant variant of Abg	KmBglI	$\beta$ -Glucosidase of <i>K. marxianus</i>

Enzymes			
AglA	$\alpha$ -Glucosidase of <i>T. acidophilum</i>	LacZ	$\beta$ -Galactosidase of <i>E. coli</i>
AHA	$\alpha$ -Amylase of <i>A. haloplanctis</i>	LamA	<i>Endo</i> -1,3- $\beta$ -glucanase of <i>P. furiosus</i>
AtFUT1	Fucosyltransferase of <i>A. thaliana</i>	MalA	$\alpha$ -Glucosidase of <i>S. solfataricus</i>
BbAfcA	$\alpha$ -Fucosidase of <i>B. bifidum</i>	Man26a	$\beta$ -Mannosidase of <i>C. japonicus</i>
BgaC	$\beta$ -Galactosidase of <i>B. circulans</i>	Man2a	$\beta$ -Mannosidase of <i>C. fimi</i>
BglC	$\beta$ -Glucosaminidase of <i>P. furiosus</i>	Pfu	Polymerase of <i>P. furiosus</i>
BglU	$\beta$ -Glucosidase of <i>M. antarcticus</i>	PpXG5	<i>Endo</i> -xyloglucanase of <i>P. pabuli</i>
BglU1-E386G	$\beta$ -Glucosidase mutant of rice	REX	Reducing-end xylose-releasing <i>exo</i> -xylanase
BglY	$\beta$ -Glucosidase of <i>Paenibacillus</i> sp.	RhaB	$\alpha$ -L-Rhamnosidase of <i>Bacillus</i> sp. GL1
BgtA	Glycosyltransferase	RhaL1	$\alpha$ -L-Rhamnosidase of <i>Alternaria</i> sp. L1
Bhx	<i>Exo</i> - $\beta$ -xylosidase of <i>B. halodurans</i>	RNase B	Ribonuclease B of bovine pancreas
Cbg1	Coniferin specific $\beta$ -glucosidase of <i>R. radiobacter</i>	Ss	Fucosidase of <i>S. solfataricus</i>
Cel5A	Cellobiase of <i>C. fimi</i>	Taq	Polymerase of <i>T. aquaticus</i>
Cex	Xylanase of <i>C. fimi</i>	Tm	Fucosidase of <i>T. maritima</i>
CFXcd-E235G	Xylanase of <i>C. fimi</i>	TmGalA	$\beta$ -Galactosidase of <i>T. maritima</i>
CstI	Sialyltransferase	TnBgl1A/TnBgl3B	$\beta$ -Glucosidases of <i>T. neapolitana</i>
EGALC-E341S	<i>Endo</i> -galactosyl ceramidase of <i>R. equi</i>	TnG-E338A	$\beta$ -Glycosidase of <i>T. nonproteolyticus</i>
EGCase	<i>Endo</i> -glycoceraminidase	WbgL	Glycotransferase
Endo-CC	<i>Endo</i> - <i>N</i> -acetyl glucosaminidases of <i>C. cinerea</i>	XylB	Xylanase of <i>T. maritima</i>

Enzymes			
Endo-H	Endoglycosidase H	XynA	Xylanase of <i>B. halodurans</i>
Endo-M	<i>Endo-N</i> -acetyl glucosaminidases of <i>M. hiemalis</i>	XynB	Xylanase of <i>C. stercoarium</i>
ENGase	<i>Endo-N</i> -acetyl glucosaminidase	XynB2	<i>Exo</i> -glycosidase of <i>G. stearothermophilum</i>
ExoI	Barley $\beta$ -D-glucan <i>exo</i> -glucohydrolase	$\beta$ -GalT-1	Human galactosyltransferase

General			
APS	Ammonium persulfate	LOQ	Limit of quantification
BLAST	Basic local alignment search tool	AU	Auxillary units
bp	Base pairs	NMR	Nuclear magnetic resonance
CaZY	Carbohydrate active enzymes	NTA	Nitrilotriacetic acid
CDMBI	2-Chloro-1,3-dimethyl-1 <i>H</i> -benzimidazol-3-ium chloride	PCR	Polymerase chain reaction
Da	Dalton (g/mol)	PDB	Protein data base
DMC	2-Chloro-1,3-dimethylimidazolium chloride	PE	Petrol ether
DMF	<i>N,N</i> -Dimethylformamide	<i>p</i> NP	<i>p</i> -Nitrophenol
DMPU	<i>N,N'</i> -Dimethylpropyleneurea	rpm	Rounds per minute
DP	Degree of polymerisation	RP-TLC	Reversed phase thin layer chromatography
DSMZ	Deutsche Stammsammlung von Mikroorganismen und Zellkulturen	SDS-PAGE	Sodium dodecylsulfate polyacrylamide gel electrophoresis
E.C.	Enzyme class	SGP	Sialylglycopeptide
EA	Ethyl acetate	<i>T</i>	Temperature
EDTA	Ethylenediaminetetraacetic acid	<i>t</i>	Time
equiv	Equivalents	TB	Terrific broth
GH	Glycohydrolase	TEMED	<i>N,N,N',N'</i> -Tetramethyl ethylenediamine
HEPES	4-(2-Hydroxyethyl)-1-piperazineethanesulfonic acid	TIM	Triosephosphateisomerase

---

**General**

---

His <sub>6</sub>	Tag comprising of six histidines	TIPSpNP	Triisopropyl-(4-nitrophenoxy)-silane
HIV	Human immunodeficiency virus	TLC	Thin layer chromatography
HIV-1 gp41	Glycopeptide of HIV-1	TRIS	Tri(hydroxymethyl)aminomethane
HMPA	Hexamethylphosphoramide	U	Unit (μmol substrate/min)
HPLC	High-performance liquid chromatography	UM	Umbelliferone
HTS	High-throughput screening	UV	Ultra violet
IgG	Immunoglobulin G	$\tilde{\nu}$	Wave number
IMAC	Ion metal affinity chromatography	wt	Wild type
IR	Infra red	X-gal/X-glc	5-bromo-4-chloro-3-indoyl $\beta$ -D-galacto-/glucopyranoside
ISE	Ion selective electrode	$^xJ$	Coupling constant (NMR)
KEGG	Kyoto encyclopedia of genes and genomes	$\delta$	Chemical shift
KP <sub>i</sub>	Potassium phosphate	$\epsilon$	Extinction coefficient
LB	Lysogeny broth	$\lambda$	Wavelength
LOD	Limit of detection		

---

## 2 ABSTRACT

With the aim of producing and applying new glycosynthases towards the synthesis of glycosides, the results obtained during the work of this thesis highlighted various aspects not only of the glycosynthase-catalysed reaction but also of the process of transforming a glycosidase into a glycosynthase.

The influence of temperature on glycosynthetic reactions was examined in detail by applying mutated glycosidases with hyperthermophilic, mesophilic, and psychrophilic properties. An elevated temperature proved as unsuitable for glycosynthetic reaction utilising glycosyl fluoride donors. The application of a hyperthermophilic enzyme was attempted with mutants of the putative  $\beta$ -galactosidase BglC, which was provided by the group of Prof. Elling (RWTH Aachen). A general unsuitability of high temperatures for glycosynthetic reactions was determined as thermal degradation of the glycosyl fluoride donor dominated the reaction. The unsuitability of elevated temperatures turned the focus towards low and moderate temperatures for the glycosynthetic reaction in order to minimise glycosyl fluoride hydrolysis. The mesophilic  $\beta$ -glucosidase mutant Abg-E358S acted, not only as an example of a mesophilic glycosynthase, but also as a positive control as this variant was literature known to possess glycosynthetic activity. The psychrophilic glucosidase BglU of *M. antarcticus* was characterised and the catalytic residue mutated with the aim of producing a cold-adapted  $\beta$ -glycosynthase. Mutation of the nucleophilic residue and  $\beta$ -glucosidase activity screening via esculin-agar resulted in the discovery of the glycosynthetic active variant BglU-E377A. Similar to the *wt*, the glycosynthase BglU-E377A exhibited a lower synthetic activity than the mesophilic Abg-E354S and despite the lower activity, a repeated glycosylation of the product similar to the reaction catalysed by Abg-E358S was observed.

Following the method of *Andrés et al.*, a modification of the glycosynthase activity assay, exploiting the capability of fluoride to cleave silyl ether bonds, was developed shortening the assay time and increasing the maximal detection limit greatly.<sup>[1]</sup> The modifications enabled the measurement of glycosynthase activity and the determination of the conversion during synthetic reactions within the short time of 10 min. The application of the assay was demonstrated by the determination of the conversion of the glycosyl fluoride donor, kinetic measurements, substrate scope, and optimal acceptor:donor ratio of the glycosynthases Abg-E358S and BglU-E377A. Both the development and application of the assay was successfully published.<sup>[2]</sup>

Due to the limitation of the substrate spectrum of the examined glycosynthases, glycosylating only glycosidic acceptor molecules, a substrate-based approach of glycosynthase candidate identification was carried out. The coniferin-specific  $\beta$ -glucosidase Cbg1 of *R. radiobacter* was

identified as a glycosynthase candidate, which could potentially glycosylate phenolic compounds. Structural analysis identified the catalytic residues and nine mutant variants were created by mutagenesis and tested for hydrolytic and glycosynthase activity utilising glycosyl fluoride or the chemical recovery method. With respect to hydrolysis, the mutants Cbg1-D222S and -H144A exhibited much higher hydrolytic activity than the *wt* form. A chemical recovery was only observed for the mutant variants of the D559 position. Additionally, transglycosylation experiments were attempted applying phenolic compounds.

The conversion of the  $\alpha$ -L-rhamnosidase RhaB of *Bacillus* sp. GL1 into a rhamnosynthase was attempted, by applying the strategy of an *in situ* production and transfer of the  $\beta$ -glycosyl azide donor. The reference substances and substrates were synthesised successfully for the application in activity and chemical recovery experiments. The *wt* RhaB of *Bacillus* sp. GL1 was expressed and characterised. New mutant variants of RhaB, RhaB-E567C/N, -E579Q, and -E841A were created by mutagenesis. The mutant variants were tested for hydrolytic activity, activity mediated by chemical recovery, and glycosynthetic activity. A colourimetric detection assay for azide ions by acidic ferric solution was adapted for a microplate format and applied for the identification of glycosynthetic activity of RhaB mutant variants.

In cooperation with the group of Prof. Fujiyama (Osaka University) the synthetic potential of the glycosynthase variant of Endo-CC N180H of *C. cinerea* for the diversification of flavonoids was evaluated. The transfer of a sialo biantennary glycan catalysed by commercially obtained Endo-CC N180H was successfully demonstrated for different substrates. The acceptor scope was further tested towards the flavonoids, revealing the limitation of the acceptor scope lying in the glycoside (glucoside vs. galactoside) rather than the aglycone of the acceptor. Active Endo-CC N180H was also expressed in *E. coli* BL21(DE3) and isolated for glycan transfer reactions.

### 3 KURZZUSAMMENFASSUNG

Die vorliegende Dissertation beschäftigt sich mit der Generierung und dem Einsatz neuer Glykosynthasen in der biokatalytischen Synthese von Glykosiden. Durch die erlangten Ergebnisse konnten verschiedene Aspekte der Glykosynthasen-katalysierten Reaktion und des Prozesses der Umwandlung einer Glykosidase zur Glykosynthase aufgeklärt werden.

Der Einfluss der Temperatur auf synthetische Reaktionen mit Glykosynthasen wurde durch den Einsatz von mutierten hyperthermophilen, mesophilen und psychophilen Glykosidasen untersucht. Die Anwendung eines hyperthermophilen Enzyms wurde erprobt mit Mutanten der putativen  $\beta$ -Galaktosidase BglC aus *P. furiosus*, dessen *wild typ* (*wt*) Enzym von der AG Elling (RWTH Aachen) zur Verfügung gestellt wurde. Erhöhte Temperaturen erwiesen sich jedoch generell als ungeeignet für synthetische Reaktionen mit Glykosylfluoriden als Donor. Somit rückte der Fokus auf niedrige und moderate Temperaturen für die glykosynthetische Reaktion, um die Glykosylfluoridhydrolyse zu minimieren. Die mesophile  $\beta$ -Glucosidase Mutante Abg-E358S ist nicht nur ein Beispiel für eine mesophile Glykosynthase, sondern diente auch als positive Kontrolle, da diese Variante in der Literatur als Glykosynthase bekannt war. Die psychophile  $\beta$ -Glucosidase BglU aus *M. antarcticus* wurde charakterisiert und mutiert mit dem Ziel, eine kälteangepasste  $\beta$ -Glykosynthase zu produzieren. Die Mutation des katalytisch aktiven Zentrums und ein  $\beta$ -Glucosidase-Aktivitätsscreening auf Esculin-Agar führten zur Entdeckung der glykosynthetisch aktiven Variante BglU-E377A. Ähnlich wie der *wt* zeigte die Glykosynthase BglU-E377A eine geringere synthetische Aktivität als die mesophile Abg-E354S. Trotz der geringeren Aktivität wurde eine wiederholte Glykosylierung des Produkts ähnlich der durch Abg-E358S katalysierten Reaktion beobachtet.

Nach dem Verfahren von *Andrés et al.* wurde eine Modifikation des Glykosynthase-Aktivitätsassays unter Ausnutzung der Spaltung von Silyletherbindungen durch Fluorid-Ionen entwickelt, die die Assayzeit verkürzt und die maximale Nachweisgrenze stark erhöht.<sup>[1]</sup> Die Modifikation ermöglichte die Messung der Glykosynthaseaktivität und die Bestimmung der Umsatzes bei synthetischen Reaktionen innerhalb von 10 Minuten. Die Anwendung des Assays wurde durch die Bestimmung des Umsatzes des Glykosylfluorid-Donors, kinetischer Messungen, Bestimmung des Substratspektrums und des optimalen Akzeptor : Donor-Verhältnisses der Glykosynthasen Abg-E358S und BglU-E377A demonstriert. Sowohl die Entwicklung als auch die Anwendung des Assays wurden erfolgreich veröffentlicht.<sup>[2]</sup>

Aufgrund der Einschränkung des Substratspektrums der untersuchten Glykosynthasen, die nur glykosidische Akzeptormoleküle glykosylieren können, wurde ein substratbasierter Ansatz zur Identifizierung von Glykosynthase-Kandidaten durchgeführt. Die Coniferin-spezifische

$\beta$ -Glucosidase Cbg1 von *R. radiobacter* wurde als Kandidat identifiziert, der potenziell phenolische Verbindungen glykosylieren könnte. Eine Strukturanalyse lieferte die katalytischen Aminosäuren und neun verschiedene Mutanten wurden erzeugt und auf hydrolytische und Glykosynthaseaktivität unter Verwendung von Glykosylfluorid oder der ‚chemical recovery‘ methode untersucht. In Bezug auf die Hydrolyse zeigten die Mutanten Cbg1-D222S und -H144A eine viel höhere hydrolytische Aktivität als das *wt*-Enzym. Eine Rückgewinnung der enzymatischen Aktivität wurde nur für die mutierten Varianten der D559-Position beobachtet. Zusätzlich wurden Transglykosylierungsexperimente mit phenolischen Verbindungen durchgeführt.

Die Umwandlung der  $\alpha$ -L-Rhamnosidase RhaB aus *Bacillus* sp. GL1 zu eine Rhamnosynthase wurde untersucht, indem die Strategie einer *in situ* Produktion und Übertragung des  $\beta$ -Glykosylazid-Donors angewendet wurde. Die Referenzsubstanzen und Substrate wurden erfolgreich für den Einsatz in Aktivitäts- und ‚chemical recovery‘-Versuchen synthetisiert. Der *wt*-Glykosidase von RhaB wurde heterolog exprimiert und charakterisiert. Neue mutierte Varianten von RhaB, RhaB E567C/N, E579Q und E841A wurden erzeugt und auf hydrolytische Aktivität, auf rückgewonnene Aktivität durch ‚chemical recovery‘ und auf glykosynthetische Aktivität getestet. Ein Nachweisassay für Azid-Ionen wurde für ein Mikrotiterplattenformat angepasst und zur Identifizierung der glykosynthetischen Aktivität von RhaB-Varianten eingesetzt.

In Zusammenarbeit mit der Arbeitsgruppe von Prof. Fujiyama (Osaka University) wurde das synthetische Potenzial der Glykosynthasevariante von Endo-CC N180H aus *C. cinerea* zur Glykodiversifizierung von Flavonoiden untersucht. Die Übertragung eines Glykans (des komplexen Types) katalysiert durch das kommerziell erhältliche Endo-CC N180H, wurde erfolgreich für verschiedene Substrate nachgewiesen. Das Akzeptorspektrum wurde weiterhin auf Flavonoide getestet, welche die Einschränkung des Akzeptorspektrums zeigt, der im Glykosid (Glucosid vs. Galaktosid) und nicht im Aglykon des Akzeptors liegt. Aktives Endo-CC N180H wurde auch in *E. coli* BL21(DE3) heterolog exprimiert und für die Glykanübertragung getestet.

## 4 INTRODUCTION

### 4.1 Importance of glycosides

The most abundant biological molecules on earth are carbohydrates. Their simplest form, created during the photosynthesis of plants by the use of sunlight and CO<sub>2</sub>, which are then converted to complex carbohydrates, glycoconjugates or glycans, take part in the biology of all living organisms. They cover the surface of all cellular organisms (either forming the glycocalyx or a cell wall) and are added to the structure of numerous macromolecules produced by these cells. Glycosides are essential for the given biological and physicochemical properties of the specific compound, and exert major influence on the functionality and stability of peptides, cell recognition, health and immunity and many other processes throughout biology. Many advances in glycoscience have brought more and more to light the crucial role of glycosides and glycoconjugates in biological processes and have defined their importance for applications of the pharmaceutical-, medicinal-, food-, energy-, and material industry. Due to their natural occurrence and production in plants for example, carbohydrates are proving to be viable and sustainable alternative to fossil resources.<sup>[3, 4]</sup>

The role of glycosylation is also increasing immensely in the pharmaceutical industry. Since the introduction of the first biologically based pharmaceutical Insulin, approved by the US Food and Drug Administration in 1982, many biopharmaceuticals in form of cytokines, hormones, enzymes, monoclonal antibodies, and fusion proteins have been introduced to the market.<sup>[5]</sup> This has changed the pharmaceutical industry drastically with now eight of the top ten selling pharmaceuticals in 2017 being of biological origin (Figure 1, **A**).<sup>[6]</sup>

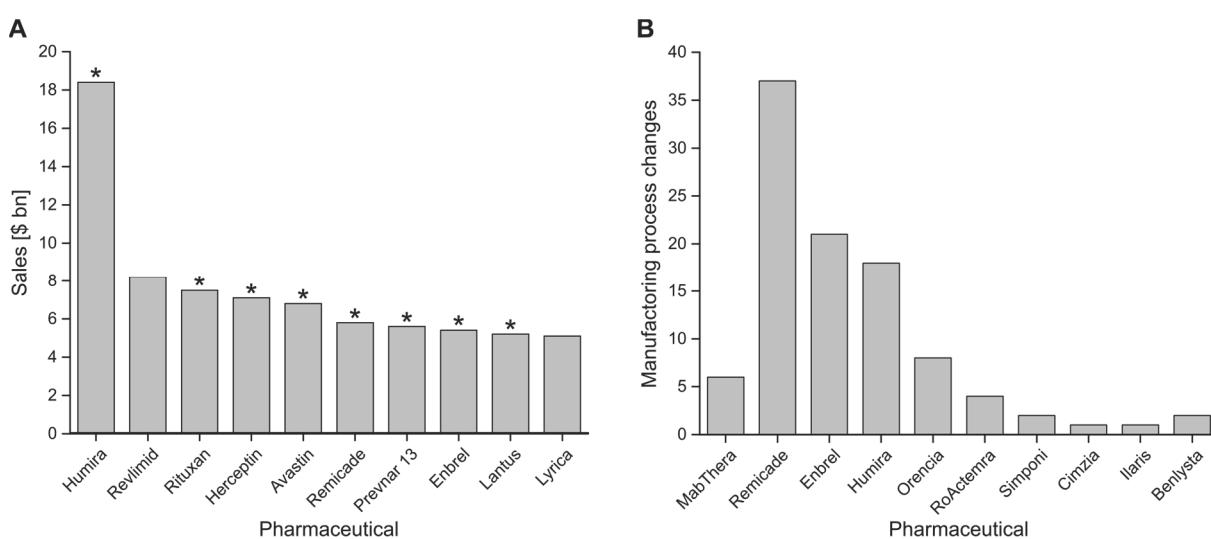


**Figure 1 (A)** Overview of the top ten selling pharmaceuticals of 2017.<sup>[6]</sup> The pharmaceuticals based on biological complex molecules are highlighted by an asterisks. **(B)** Number of production changes after approval of pharmaceuticals, which can have an effect on the posttranslational modifications such as glycosylation.<sup>[7]</sup>

However, these large complex molecules are subject to diverse posttranslational modifications, which are influenced by subtle changes such as culture conditions, production cell type, and purification strategies (Figure 1, **B**). The in-depth understanding of these modifications, as for example functionally relevant glycans, are essential for the maintenance of quality and safety of biopharmaceuticals. The recent introduction of biosimilars, follow-on versions of biopharmaceuticals designed to match protein drugs for which production patents have expired, has increased the importance of state of the art analytics for the detection and control of critical quality attributes.<sup>[5, 7]</sup>

Glycosides play a further major role in the food industry modulating biological activities and the bioavailability of nutritional compounds. Flavonoids and their respective glycosides are the most abundant type of polyphenols in food and have been attributed considerable biological effects concerning diseases such as cancer, diabetes, HIV, inflammation, and obesity. Glycosylation of the flavonoid structures, most commonly O-glycosylation in the 3- or 7-position, can influence the absorption, distribution and metabolism. A generalisation of the glycosylation effects on flavonoids is difficult as glycosylation position, flavonoid structure, and the type of glycosyl residue influence the increase or decrease in activities. Activities such as anti-obesity, anti-HIV, tyrosinase inhibition, and anti-allergic can be greatly increased by glycosylation, whereas the antioxidant, anti-cancer, anti-coagulant and anti-fungal activity have been reported to decrease.<sup>[6]</sup> The diversification of the glycosylation of such compounds could lead to the discovery of further beneficial activities.

Due to the large impact of glycosylation, the demand for simple methods for the synthesis of defined glycosides is therefore constantly rising. In the area of organic synthesis, especially the synthesis of natural compounds, enzymatic conversions are becoming more and more popular. Many properties of enzymes such as, regio-, stereo- and chemo-selectivity make enzymes ideal candidates for organic synthetic conversions. The ability of enzymes to catalyse reactions under mild conditions also shows their potential as 'green' catalysts. Due to the huge variety of enzymes throughout nature, many different reaction types can be catalysed with the use of enzymes, e.g. redox reactions, carbon-carbon bond formations, hydrolytic reactions or isomerisations, making enzymes versatile tools to develop synthetic methods. The use of enzymes such as glycosyltransferases and glycosidases capable of transferring and hydrolysing glycosidic structures has gained much interest by organic chemists. The high regio-selectivity and often complete anomeric control of the enzymatic conversions cancel out the need of tedious protection and activation procedures which often lead to low yields. Recent developments in genetic engineering have also made the use of glycosynthases possible, raising the yields and synthetic potential of these enzymes greatly.

## 4.2 Thesis objective

As described above, the importance of synthesising glycosidic structures due to their crucial roles in biological processes is evident. The simple production of complex glycans or glycosylated compounds will help to develop new pharmaceuticals, modulate nutritional food values and new analytical methods. The main objective of the presented thesis is the development of new glycosynthases in the aim of creating a versatile biocatalytic toolbox for glycosylation and glycodiversification in organic synthesis. The focus lies hereby on the production of the glycosynthases by mutagenesis and the evaluation of their suitability for the application in synthetic reactions.

The objective is approached in four separate projects, each focussing on a different aspect of the glycosylation reaction carried out by glycosynthases. However, in each case, gained insights and the developed glycosynthases are applied to a set of flavonoid substrates **1** as a model reaction (Figure 2). The flavonone naringenin (**1a**) and its respective glycosides, prunin (**1b**, naringenin-7-O- $\beta$ -D-glucoside), and naringin (**1c**) are well known throughout literature and therefore ideal model substrates, with the focus lying on the production of the 7-O-glucoside prunin (**1b**) and its subsequent glycodiversification possibly modulating its properties such as bioavailability, biological activity and taste.

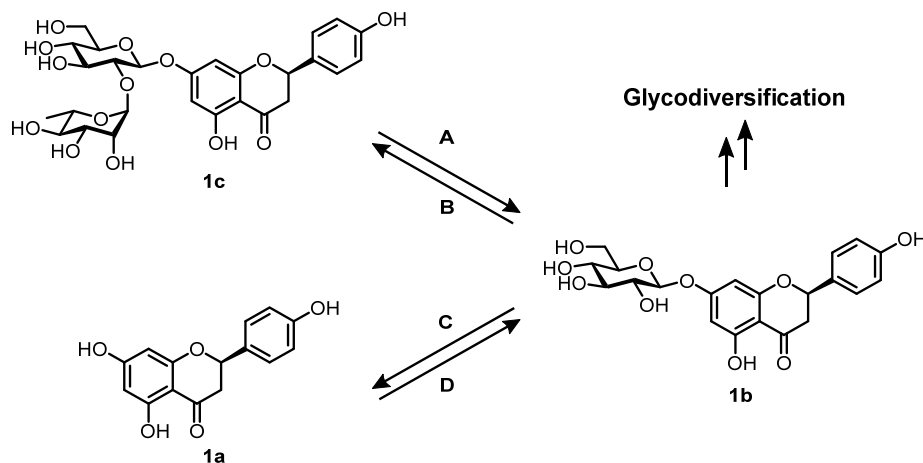


**Figure 2** Flavonoid substrates naringenin (**1a**), prunin (**1b**) and naringin (**1c**) applied in model reaction set for the evaluation of glycosynthase applicability. The examined glycosidases and potential glycosynthases are to be tested in de-glycosylation (A & C) and glycosylation (B & D) reactions. Furthermore, the glycodiversification of prunin (**1b**) is examined.

Firstly, with the aim of producing  $\beta$ -linked glucosides, two extremophile  $\beta$ -glycosidases, the psychrophilic BglU of *Micrococcus antarcticus*, and hyperthermophilic BglC of *Pyrococcus furiosus* are to be characterised biochemically and subsequently transformed by site-directed mutagenesis to potential glycosynthases. The suitability of extremophile glycosidases for the production of potential glycosynthases and their use in synthetic reactions is to be evaluated by comparison of the potential new glycosynthases with the characteristics

of a literature known  $\beta$ -glycosynthase variant of Abg of *Rhizobium radiobacter*. The development of a high throughput assay is also to be targeted, in order to simplify the biochemical characterisation of newly created potential glycosynthases. Secondly, a focus is to be set on the acceptor substrate specificity of glycosynthases by choosing a glycosidase with a known natural substrate. With the aim of glycosylating non-glycosidic phenolic acceptor substrates, the coniferin specific  $\beta$ -glucosidase Cbg1 of *R. radiobacter* is to be examined for glycosynthetic potential by mutagenesis.

Though many advances have been made towards the production of  $\alpha$ -glycosynthases, the establishment of  $\alpha$ -L-rhamnosynthases has not yet been described. The third project focusses on the transferral of methods developed for  $\alpha$ -galacto- and  $\alpha$ -fucosynthases towards the transformation of the  $\alpha$ -L-rhamnosidase RhaB of *Bacillus sp.* GL1 into a  $\alpha$ -L-rhamnosynthase. Beside the site-directed mutagenesis of the rhamnosidase, a suitable assay for the evaluation and analysis of potential synthetic reactions is to be developed.

In a cooperation with the group of Prof. Fujiyama of the Osaka University, the fourth project switches the focus from the transferal of monosaccharide moieties to large glycan moieties. The potential of transferring a sialyl biantennary glycan onto flavonoid and aryl glycosides is examined with the *endo-N*-acetyl-glucosaminidase mutant variant EndoCC-N180H of *Coprinopsis cinerea*.

## 5 STATE OF KNOWLEDGE

### 5.1 *Glycosynthases — from hydrolysis to synthesis*

Glycosidic structures are ubiquitous throughout nature, covering the surface of all cellular organisms and even many of the macromolecules inside of these. Therefore, glycosides fulfil various functions in biological systems acting on the one hand as recognition motifs, as for example, in blood group antigens, but also providing function, structure, and stability for cells and enzymes. The importance of glycosidic structures for the pharmaceutical industry is clearly demonstrated by the many bacterial and viral infections mediated by glycoside recognition.<sup>[9]</sup> Furthermore, specific oligosaccharides, such as human milk oligosaccharides (HMOs), have been reported to have probiotic and antimicrobial effects making them highly desired targets for the food and nutrition industry.<sup>[10]</sup> Originating from renewable resources, polysaccharides also play an important role in discovering new sustainable materials. The demand for simple synthetic methods for the synthesis of defined glycosides is rising constantly with the increasingly growing knowledge of the major role glycosides and glycoconjugates play in biological processes. The high biological functionality and complex structure of glycosides is a direct result of their numerous functional moieties, diverse stereochemistry, and abundant linkage possibilities. Synthesis of glycoside structures would greatly improve the possibility in producing new materials and pharmaceuticals, and allow targeted research on functional and structural properties of these compounds. The chemical synthesis of glycosidic structures is well developed, but remains a strenuous task. Addressing for example, solely single functional groups, many protection and selective deprotection steps are required in order to avoid side product formation.<sup>[11-14]</sup> A complete anomeric control of the newly formed glycosidic bond is also prerequisite to bypass lengthy separation methods.

Throughout nature, the enzyme group of glycosyltransferases (E.C. 2.4.1.n) accomplish the biosynthesis of glycosidic structures. These enzymes transfer activated sugar-nucleotide donor molecules with high selectivity onto various acceptor molecules. Even though their use in biocatalysis has been extensively researched, a large scale use is still limited by the high cost of the nucleotide-phosphate donor molecules and the difficulty in expression and handling of these mostly membrane bound enzymes.<sup>[15]</sup> Alternative carbohydrate active enzymes are glycohydrolases (E.C. 3.2.1.n), also referred to as glycosidases, of which a high variety are readily available due to their occurrence in most primary and secondary metabolic pathways of all organisms.<sup>[16]</sup> These enzymes are structurally diverse and have been categorised by the carbohydrate active enzyme database (CAZy) into over 150 glycosyl hydrolase families (GH) based on amino acid sequence similarities. Similarities in protein folding have also enabled the classification of 18 different glycohydrolase clans (GH A–R). The natural function of this

group of enzymes is the degradation of glycosidic structures and are defined into two groups depending on their catalytic mechanism (Figure 3, **A & B**).<sup>[17]</sup>

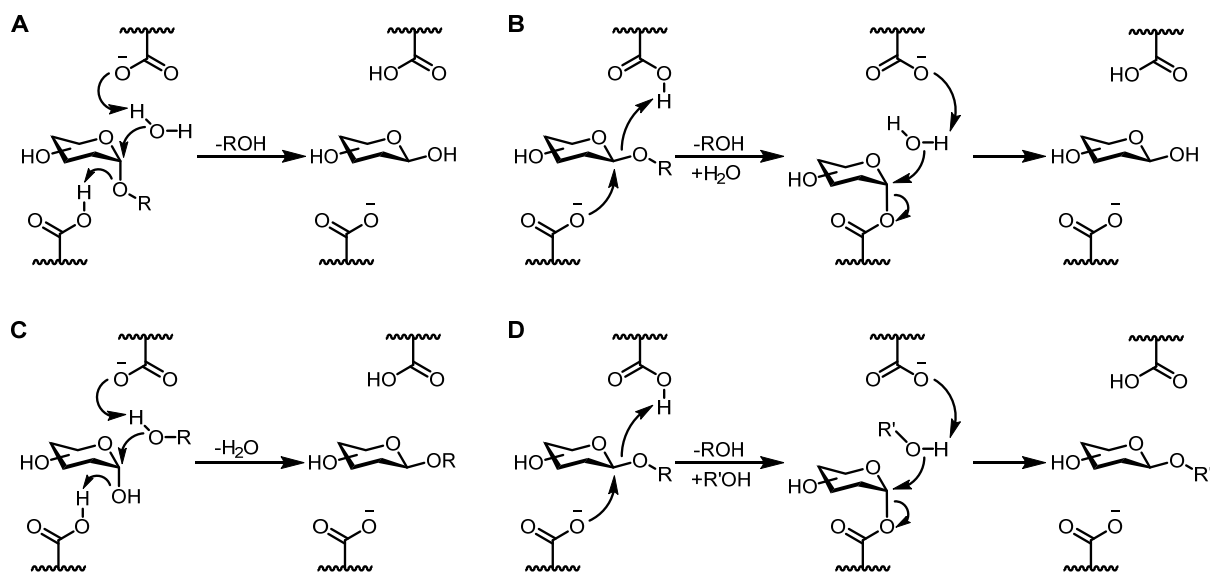


**Figure 3** Hydrolytic (**A & B**) and synthetic (**C & D**) mechanisms of glycosyl hydrolases. (**A**) Inverting hydrolases: A single displacement mechanism, supported by acid/base residues, inverts the anomeric configuration of the product compared to the substrate. (**B**) Retaining hydrolases: The double displacement mechanism allows the anomeric configuration of the substrate to be retained in the product *via* a glycosyl-enzyme-intermediate. (**C**) Reverse hydrolysis: The presence of high acceptor concentrations shifts the equilibrium of the reaction to the formation of a glycosidic bond. (**D**) Transglycosylation: The enzyme-glycosyl-intermediate is intercepted by and transferred to an acceptor molecule in place of a hydrolysis of the intermediate.

A double displacement mechanism catalysed by a nucleophilic and acid/base residue in the enzymes active site is carried out by retaining glycosidases, resulting in a retention of the anomeric configuration of the substrate in the yielded product (Figure 3, **B**). Inverting glycosidases in comparison follow a single displacement mechanism with two catalytic acid/base residues supporting the nucleophilic substitution at the anomeric centre of the substrate, inverting the anomeric configuration of the resulting product compared to the substrate (Figure 3, **A**). Due to the vast variety of glycosidases, a consensus nomenclature for the description of the carbohydrate binding subsites was developed.<sup>[18]</sup> The nomenclature adopts a -n to +n form whereby -n represents the non-reducing end and +n the reducing end binding subsites. The cleavage catalysed by the glycosidase takes place between the -1 and +1 subsites (Figure 4). The consensus nomenclature is necessary in order to compare glycosidases consistently throughout literature.

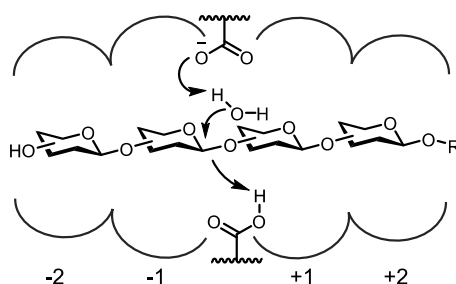


**Figure 4** Depiction of the consensus nomenclature for the carbohydrate binding subsites of the active site of glycosidases. The  $-n$  subsites represent binding sites of the non-reducing end, while  $+n$  subsites bind to the reducing end of the cleaved oligosaccharide.<sup>[18]</sup>

Glycosidases can be utilized in two different ways for synthetic reactions by reverse hydrolysis or transglycosylation methods (Figure 3, **C & D**).<sup>[19, 20]</sup> Nevertheless, the ability of the glycosidase in hydrolysing the produced product most often leads to strongly diminished yields. *Mackenzie et al.* and *Malet et al.* (working on *exo*- and *endo*-glycosidases, respectively) reported the production of genetically engineered glycosidases, namely glycosynthases, which were lacking a nucleophilic residue and therefore void of hydrolytic activity, to overcome the disadvantage of product hydrolysis.<sup>[21, 22]</sup> The intact structure of the enzyme allowed the formation of glycosidic bonds in the presence of activated glycosyl donors such as glycosyl fluorides, which mimic the glycosyl-enzyme-intermediate (Figure 5, **A**). Following the introduction of this 'classical' glycosynthase method mostly restricted to retaining glycosidases, alternative methods such as *in situ* generation of donor molecules have been described, greatly expanding the repertoire of glycosynthases.<sup>[23]</sup> The *in situ* donor synthesis is enabled by a recovery of the 'hydrolytic' activity of glycosidase mutants by the presence of an external nucleophile (Figure 5, **B**). The external nucleophile can then act as a new leaving group, allowing the transferral of the glycosyl residue onto an acceptor molecule. This method has been termed 'chemical rescue' throughout literature.

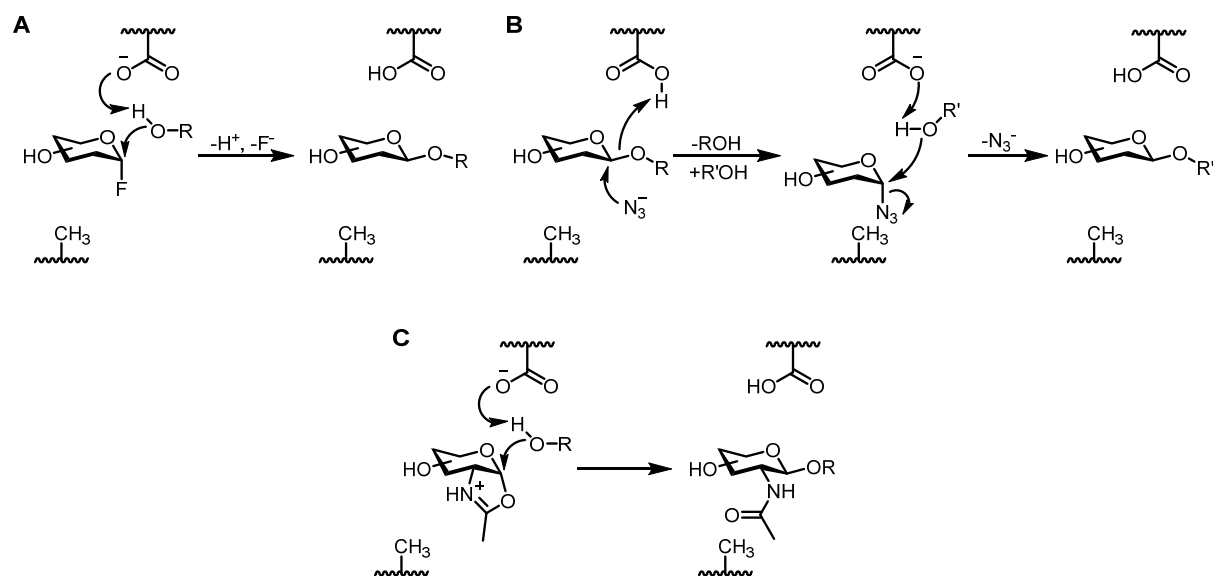


**Figure 5** Mechanisms for mutant glycosidases without hydrolytic activity acting as glycosynthases. **(A)** A ‘classic’ approach in which a chemically synthesised activated glycosyl donor with an opposite anomeric configuration to the natural substrate is utilised. **(B)** The activated glycosyl donor is produced *in situ* by addition of an external nucleophile (chemical recovery) and subsequently transferred onto an acceptor. **(C)** Activated glycosyl donors in the shape of glycosyl oxazoline compounds derived from *N*-acetyl-D-glucosamine can be transferred to acceptors by glycosynthases based on *endo*- $\beta$ -*N*-acetylglucosaminidases.

Glycosidases of various origins have been transformed into glycosynthases allowing the production of  $\alpha$ - and  $\beta$ -glycosyl linkages with glucosyl-, galactosyl-, fucosyl-, arabinosyl-, mannosyl- or even lactosyl-residues.<sup>[24]</sup> Recently, the method has been applied to *endo*- $\beta$ -*N*-acetylglucosaminidases, such as the enzyme Endo-M of the fungal plant pathogen *Mucor hiemalis*, which play important roles in protein post-translational glycosylation. Elucidation of the mechanistic properties of these enzymes led to the development of synthase mutants, which transfer oxazoline glycoside structures onto different acceptors enabling the complete (*en bloc*) transfer of large (nonasaccharide) glycans (Figure 5, **C**).<sup>[25]</sup> This has resulted in a powerful tool for modifying peptides with high pharmaceutical interest with defined glycan structures.

## 5.2 Biocatalysis towards $\beta$ -linked glycosides

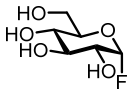
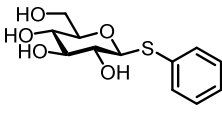
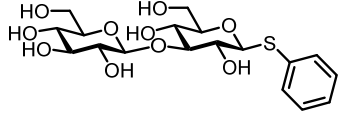
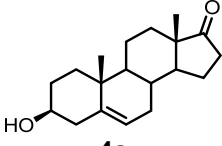
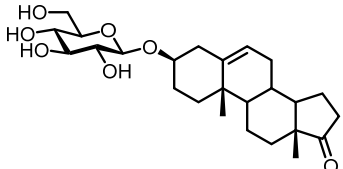
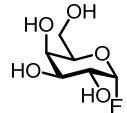
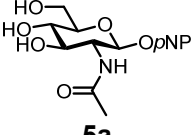
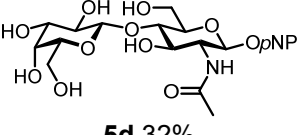
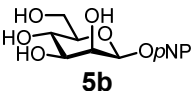
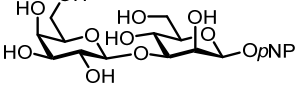
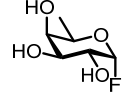
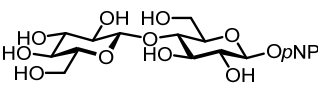
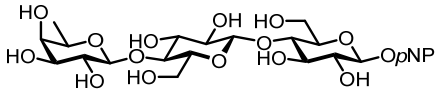
### 5.2.1 Synthesis of $\beta$ -glycosides

#### Biocatalytic synthesis with $\beta$ -glycosynthases

After the introduction of the genetically engineered glycosynthases by *Mackenzie et al.* in 1998, glucosynthases, transferring glucosyl moieties, derived from glucosidases (*exo*- or *endo*-) originating from a variety of organisms have been the most commonly produced type of these enzymes.<sup>[21]</sup> This type of variant is often generally referred to as ‘glycosynthase’ throughout literature, due to the often-observed promiscuity concerning the donor glycoside.

The Abg E358A glucosynthase derived from *R. radiobacter* (formerly *Agrobacterium tumefaciens*), for example, catalysed not only the transfer of glucosyl but also galactosyl residues to *para*-nitrophenyl (pNP) glycosides. *Shim et al.* and *Kim et al.* reported further modulation of this enzyme broadening the scope of donor substrates even more.<sup>[26, 27]</sup> The use of the glucosynthase variant Abg 2F6 was thereby extended to a xylosyl donor and Abg NNT to C3-modified (methylated) gluco- and galactosyl donors (producing  $\beta$ -1,4 linkages), giving a much broader range of synthesisable glycosides. *Wei et al.* also impressively demonstrated the promiscuity of glucosynthases to accept different glycosyl fluoride donors with the  $\beta$ -glycosidase mutant TnG-E338A of *Thermus nonproteolyticus*.<sup>[28]</sup> The glucosynthase showed high promiscuity towards the donor substrate, transferring  $\alpha$ -D-glucosyl-,  $\alpha$ -D-galactosyl-, and  $\alpha$ -D-fucosyl fluoride donors (**2a**,  $\alpha$ -GlcF; **2b**,  $\alpha$ -GalF; **2c**,  $\alpha$ -D-FucF) to different acceptors **3a**, **4a**, **5a–5c** in yields for **3b**, **4b**, **5d–5f** varying between 15–100% depending on the donor and acceptor combination (Table 1). Interestingly the enzyme also catalysed donor transferal towards dehydroepiandrosterone (**4a**), an unusually large and lipophilic acceptor, with  $\alpha$ -GlcF **2a** as the donor glycoside (49% yield).

**Table 1** Synthetic glycosylation examples catalysed by TnG-E338A.<sup>[28]</sup> The reactions were carried out with  $\alpha$ -GlcF (**2a**),  $\alpha$ -GalF (**2b**), or  $\alpha$ -D-FucF (**2c**) as the donor substrates. Donor and acceptor molecules were employed in equal amounts unless otherwise described. Yields were determined after isolation.

Donor	Acceptor	Product Yield [%]
 <b>2a</b>	 <b>3a</b>	 <b>3b</b> 80%
	 <b>4a</b>	 <b>4b</b> 49%
 <b>2b</b>	 <b>5a</b>	 <b>5d</b> 32%
	 <b>5b</b>	 <b>5e</b> 14% <sup>a</sup>
 <b>2c</b>	 <b>5c</b>	 <b>5f</b> 91%

<sup>a</sup> Donor was applied in 2 equiv.

An even more extensive donor scope was exhibited by the glucosynthase BGluc1-E386G originating from the  $\beta$ -glucosidase of rice examined by *Pengthaisong et al.*<sup>[29]</sup> The glucosynthase was shown to transfer the glycosyl residues of  $\alpha$ -D-glucosyl (**2a**),  $\alpha$ -D-galactosyl (**2b**),  $\alpha$ -D-fucosyl (**2c**),  $\alpha$ -D-arabinosyl,  $\alpha$ -D-xylosyl (**2d**), and  $\alpha$ -D-mannosyl (**2e**) fluoride donor to *p*-nitrophenyl  $\beta$ -D-cellobioside (**5c**) producing yields of 57%, 42%, 59%, 99%, 3%, and 79%, respectively.

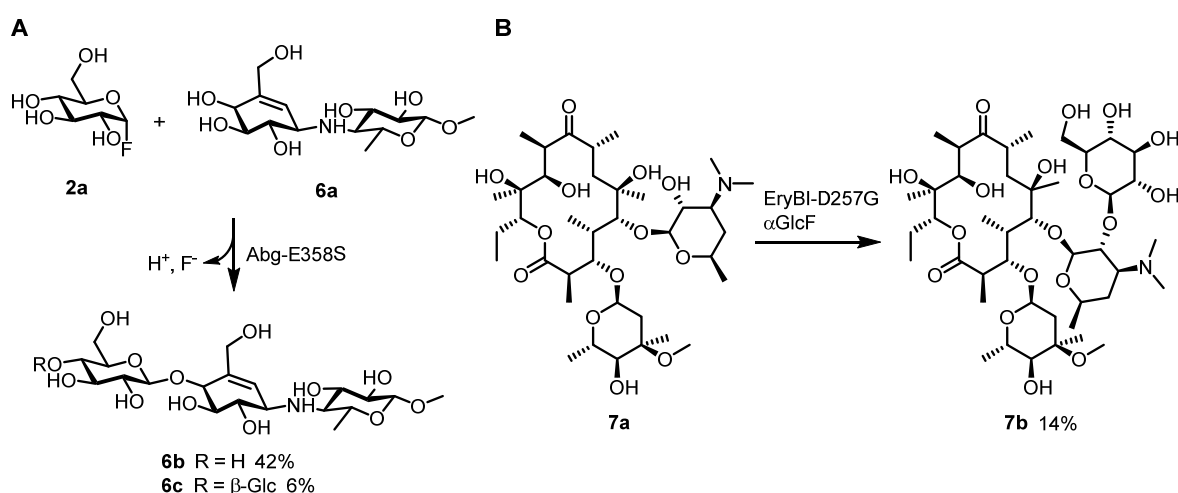


**Figure 6** Glucosylation of natural and unnatural glycosides by glucosynthases. **(A)** Synthesis of glucosylated methyl  $\beta$ -acarviosin (**6**) by *Fairweather et al.*<sup>[30]</sup> The mono- and diglycosylated products **6b** and **6c** were isolated in yields of 42% and 6%; **(B)** Enzymatic glucosylation of erythromycin A (**7a**) by the glucosynthase EryBI-D257G. The enzyme showed high tolerance towards the bulky dimethylated amino group in the C3-position.<sup>[31]</sup>

The use of Abg-E358S as a glucosynthase in syntheses of natural or unnatural glycosides was also demonstrated efficiently by *Fairweather et al.* in the synthesis of glucosylated versions of methyl  $\beta$ -acarviosin (**6a**), an inhibitor of cellulases (Figure 6, **A**).<sup>[30]</sup> The inhibitor was glucosylated, with a  $\beta$ -1,4 connection, to the pseudo-tri- **6b** and pseudo-tetrasaccharide **6c** in yields of 42% and 6%, respectively. Further putative cellulose inhibitors, derivatives of tetrahydrooxazine and isofagomine, were produced by *MacDonald et al.* producing a mixture of cello-oligosaccharide inhibitor variants with different lengths.<sup>[32]</sup> The reported glucosylation of erythromycin A (**7a**) by *Jakeman et al.* displayed the possibility of transferal of a glucosyl residue, in a  $\beta$ -1,2 fashion, to a more complex type of acceptor in a yield of 14% (Figure 6, **B**).<sup>[31]</sup>

Additionally to the 'classical' glucosynthase approach catalysing the transfer of glycosyl fluoride donors, *Pozzo et al.* improved glucosylation yields by utilizing the chemical rescue method for *in situ* donor production with the  $\beta$ -glucosynthase (TnBgl1A-E349G) derived from *Thermotoga neapolitana*.<sup>[33]</sup> The group reached a 3.7  $\times$  higher yield during the synthesis of quercetin-3,4'-di- $O$ - $\beta$ -D-glucopyranoside, with *ortho*-nitrophenyl glucopyranoside and formate for *in situ* donor production, compared to the synthesis using  $\alpha$ -GlcF **2a** (10% yield). This



### Biocatalytic synthesis with $\beta$ -galactosynthases

By combining the glycosynthase Abg 2F6, in a reaction sequence with the glycosyltransferases WbgL and BgtA, towards the synthesis of the type 2 blood group A oligosaccharide **8a**, *Kwan et al.* demonstrated the importance of the glycosynthase method in the production of glycoside structures for biological or pharmaceutical research.<sup>[39]</sup> The enzyme effectively transferred  $\alpha$ -D-galactosyl fluoride (**2b**,  $\alpha$ -GalF) onto 4-methylumbelliferyl  $\beta$ -N-acetylglucosaminide (**8b**, UM- $\beta$ -GlcNAc) in yields of 84% (Figure 8).

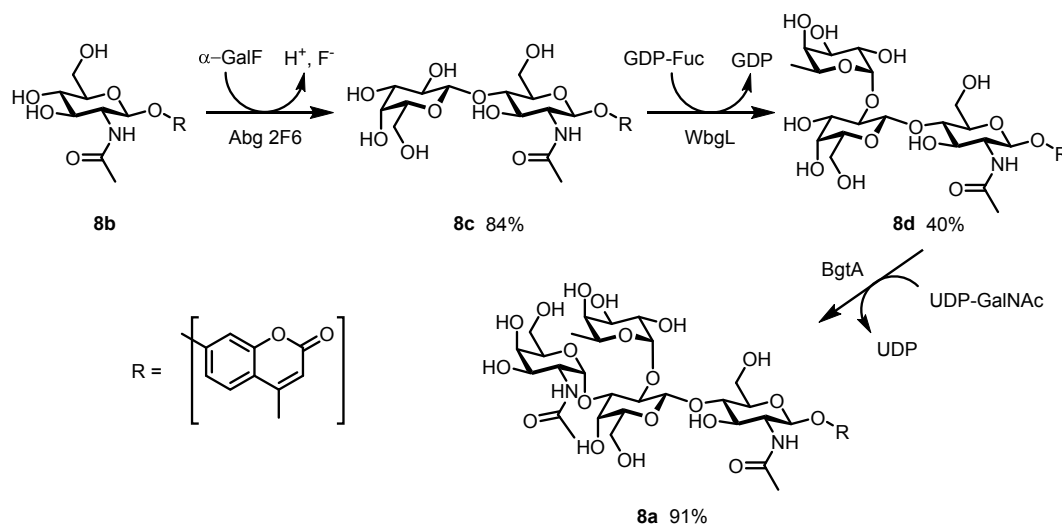


**Figure 8** Synthetic route towards the methyl-umbelliferone derivative of the type 2 blood group A oligosaccharide **8a** by *Kwan et al.*<sup>[39]</sup> The synthesis combined the engineered glycosynthase Abg 2F6 (containing the mutations A19T, E358G, Q248R, M407V) with two glycosyltransferases WbgL and BgtA. WbgL and BgtA could also be applied in a one-pot reaction giving a higher yield of 62% compared to 37% for the sequential reaction.

Exploiting the chemical rescue method usually carried out in the case of  $\alpha$ -glycosynthases (described in detail in section 5.3), *Strazulli et al.* catalysed the formation of various  $\beta$ -galactosyl glycosides by the  $\beta$ -galactosynthase Aa $\beta$ Gal-D361G (*Alicyclobacillus acidocaldarius*) and the simple donor pNPGal **5g** as starting material.<sup>[40]</sup> Though a high transglycosylation was achieved, the enzyme displayed high promiscuity by producing different regioisomers and polyglycosylated products.

*Goddard-Borger et al.* demonstrated the use of a glycosynthase in the synthesis of the natural product psychosine, a 1- $\beta$ -D-galactopyranosyl sphingosine found in the central nervous system.<sup>[41]</sup> The neural signalling dysfunction often observed in individuals with Krabbe disease can be led back to an accumulation of this compound. The  $\beta$ -glycosynthase EGALC-E341S (*endo*-galactosyl ceramidase of *Rhodococcus equi*) was successfully applied in the one-step synthesis of psychosine from  $\alpha$ -GalF **2b** and sphingosine (**9a**) in a yield of 21%, mainly due to the low solubility of sphingosine (**9a**) and precipitation of the enzyme. Further glycosphingolipids were synthesised by the efficient combination of glycosyltransferases and

*endo*-glycoceramamidase (EGCase) derived synthases. *Rich et al.* described the synthesis of the glycolipid *lyso*-G<sub>M3</sub> (**9b**) by combining  $\alpha$ -LacF **2f** with sphingosine (**9a**) catalysed by EGCase II-D351S, followed by a sialylation with the Cst-I  $\alpha$ -2,3-sialyltransferase reaching an overall yield of 51% (**9b**, Figure 9).<sup>[42]</sup> *Yang et al.* varied the same synthesis to a FRET-probe of *lyso*-G<sub>M3</sub> (**9b**) to allow visualisation of the enzymatic processing of the glycolipid.<sup>[43]</sup> A further combination of glycosyltransferases and glycosynthases was performed in sequential and also one-pot reactions by *Henze et al.*<sup>[44]</sup> The report demonstrated the synthesis of *N*-acetylactosamine type 1 (-3-Gal- $\beta$ 1,3-GlcNAc-1-) and type 2 (-3-Gal- $\beta$ 1,4-GlcNAc-1-) oligomers by combining the glycosynthase His<sub>6</sub>BgaC-D233G (*Bacillus circulans*) either in a one-pot or sequential reaction with the glycosyltransferases  $\beta$ 3GlcNAcT (*Helicobacter pylori*) and the  $\beta$ GalT-1 (human origin).<sup>[45]</sup> By sequential use of this combination of enzymes it was even possible to create neo-*N*-acetylactosamine (LacNAc) oligomers with alternating type 1 and type 2 units.

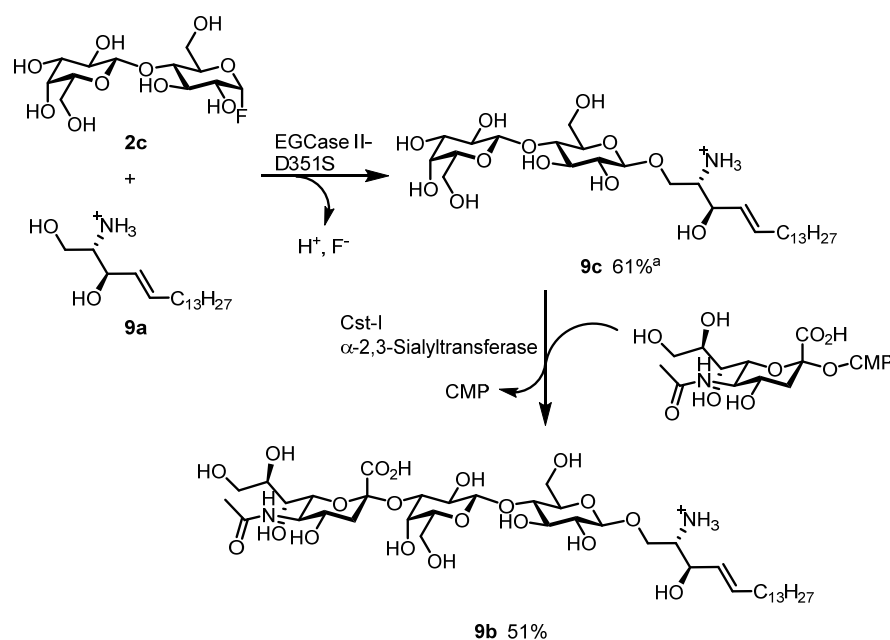


**Figure 9** Synthesis of the glycolipid *lyso*-G<sub>M3</sub> (**9b**) performed by *Rich et al.*<sup>[42]</sup> The synthesis of the lactosyl sphingosine acceptor **9c** for the Cst-I  $\alpha$ -2,3-sialyltransferase was catalysed by the EGCCase II glycosynthase variant in an overall yield of 61%. <sup>a</sup> Yield encompassing the chemical synthesis of  $\alpha$ -LacF **2c** and the glycosynthase reaction.

### Biocatalytic synthesis of $\beta$ -xylosides

The pharmaceutical industry has gained much interest in xylooligosaccharides, due to their anti-freezing activity, non-digestibility, non-cariogenic and beneficial properties for the intestinal flora.<sup>[46]</sup> One of the first attempts towards the synthesis of xylosides was carried out by *Kim et al.* using the  $\beta$ -glycosynthase Abg 2F6 (A19T, E358G, Q248R, M407V) derived from a  $\beta$ -glucosidase from *A. tumefaciens* (now *R. radiobacter*).<sup>[27]</sup> The glycosynthase variant

exhibited a broad donor substrate range and an increased specificity toward  $\alpha$ -D-xylosyl fluoride (**2d**,  $\alpha$ -XylF; 34 $\times$  higher) compared to the original mutant Abg-E358G. This was later utilised in 2005 by the same group in the synthesis of xylooligosaccharides with *p*NPGlc **5h** ( $\beta$ -1,4), *p*-nitrophenyl xylopyranoside (**5i**, *p*NPXyl;  $\beta$ -1,3/1,4) and *p*-nitrophenyl xylobioside (**5j**, *p*NPXyl<sub>2</sub>;  $\beta$ -1,4) as acceptors in yields of 35–98%. Xylosylated 1-deoxyxylojirimycin (**10a**), a xylose derived nitrogen-containing inhibitor was also synthesised by this mutant in a yield of 28% (acetylated product; Figure 10).<sup>[47]</sup>

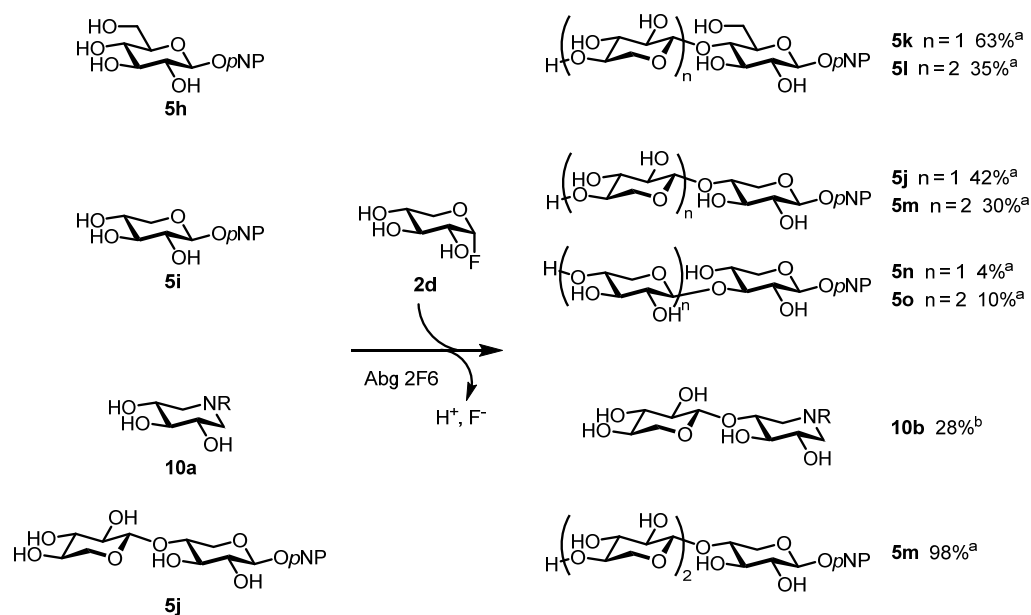


**Figure 10** Synthetic route towards various xylosides **5j–5o** and **10b** by the  $\beta$ -glycosynthase Abg 2F6 derived from the  $\beta$ -glucosidase Abg of *R. radiobacter*.<sup>[47]</sup> The enzyme exhibited variable selectivity depending on the acceptor molecule, producing predominantly  $\beta$ -1,4 linkages. <sup>a</sup> Yields based on HPLC analysis of the reaction mixture; <sup>b</sup> Yield of isolated, acetylated product.

After these first biocatalytic syntheses, various groups accomplished syntheses of xylooligomers with glycosynthases derived from actual xylanases. The reducing-end xylose-releasing *exo*-xylanase (REX), with a mutation of the acid/base catalytic residue (E236C), was utilised by *Honda et al.* in the synthesis of xylotrimers from xylobiosyl fluoride (**2g**, X<sub>2</sub>F) and xylose (**11a**).<sup>[48]</sup> This was also the first example of a glycosynthase derived from an inverting glycosidase. *Kim et al.* also produced xylooligosaccharides with the CFXcd-E235G mutant of the retaining xylanase of *Cellulomonas fimi*.<sup>[49]</sup> The enzyme catalysed the oligomerisation of X<sub>2</sub>F **2g** and *p*NPXyl<sub>2</sub> **5j** or benzylthio- $\beta$ -xylobioside (**3c**, BTXyl<sub>2</sub>) resulting in a mixture of different oligomers ranging from xylo-tetrasaccharides to -dodecasaccharides with a total yield of transfer products of 61 and 66%, respectively. *Sugimura et al.* expanded the repertoire of xylanase derived glycosynthases by four examples of the GH 10 family (XylB *Thermotoga maritima*; XynA *Bacillus halodurans*; XynB *Clostridium stercorarium*; Cex *C. fimi*) enabling the synthesis of xylooligomers from X<sub>2</sub>F **2g** in yields from 29–69% (7.8–18.4 mg).<sup>[50]</sup> Product precipitation enabled easy isolation and these were of high interest as unsubstituted

xylan, a homopolymer of  $\beta$ -1,4-xylopyranose units, does not exist in nature. The production of even larger xylooligomers was achieved by *Ben-David et al.*<sup>[51]</sup> The XynB2-E335G recombinant enzyme of the retaining *exo*-glycosidase (GH 52) of *Geobacillus stearothermophilus* catalysed the synthesis of xylosides with  $\alpha$ -XylF **2d** and *p*NPGlc **5h**, *p*NPXyl **5i**, and *p*-nitrophenyl mannopyranoside (**5b**, *p*NPMan) with a  $\beta$ -1,4 linkage in yields of 49%, 42%, and 10% (disaccharide yields), respectively. By exploiting the self-condensation of  $\alpha$ -XylF **2d** by the XynB2-E335G to Xyl<sub>2</sub>F **2g**, a combinatorial synthesis with a glycosynthase variant of the xylanase XT6 (E265G; also of *G. stearothermophilus*) resulted in xylooligomers comprising of 6–100 monomers (Figure 11).<sup>[51, 52]</sup>

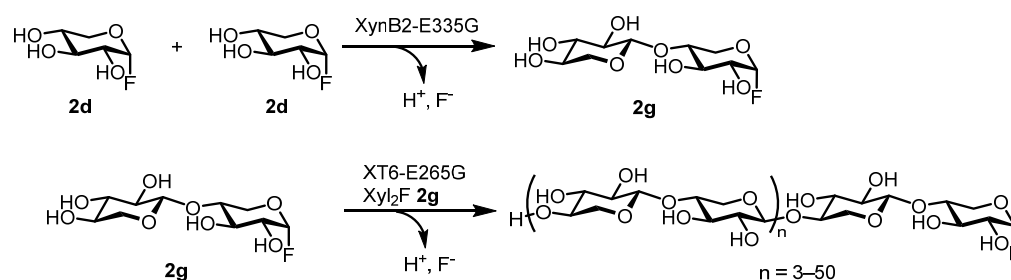


**Figure 11** Synthesis of xylooligomers comprising of 6–100 monomers, exploiting the self-condensation of  $\alpha$ -XylF **2d** and Xyl<sub>2</sub>F **2g** catalysed by the combination of XynB2-E335G and XT6-E265G.<sup>[51, 52]</sup>

The activity of the XynB2-E335G glycosynthase in production of Xyl<sub>2</sub>F **2g** and Xyl<sub>3</sub>F **2h** was improved by the development of a general screening assay utilizing the pH indicator Methyl Red, resulting in variants with much higher  $k_{\text{cat}}$  values than the original synthase.<sup>[53]</sup> However, no yields of the reactions catalysed by the improved variants were reported. More recently, *Goddard-Borger et al.* demonstrated the efficient synthesis of various xylanase inhibitors by the *exo*- $\beta$ -xylosidase mutant Bhx-E334G (*B. halodurans*).<sup>[54]</sup> The enzyme accepted various sugar derivatives such as thioglycosides, iminosugar derived carbamates, and a 2-deoxy-2-fluoroxylsides giving yields of 67–86% of glycosylated products (acetylated products). A further important type of xyloside are xyloglucans ( $\alpha$ -1,4 glucan backbone containing  $\alpha$ -1,6-D-xylose branches) which are the major hemicellulose components of the primary cell wall of plant cells and are also an abundant type of storage polysaccharide in seeds.<sup>[55]</sup> They often find use in the paper, textile, food, and pharmaceutical industry as for example cellulose cross-linkers or rheology modifiers (fluid mechanics). With the xyloglucan glycosynthase PpXG5-E323G (*Paenibacillus pabuli*), the synthesis of xyloglucans, as custom polysaccharides, was recently carried out by *Spaduit et al.*<sup>[56]</sup> The group synthesised XXXG- **12a** and XLLG-structure **12b** type xyloglucans with molecular masses of up to 30,000 (n = 29) and 60,000 (n = 44) by self-condensation of the XXXG $\alpha$ F **2i** and XLLG $\alpha$ F **2j** donor blocks respectively (Figure 12, Nomenclature: G = Glc; X = Xyl- $\alpha$ 1,6-Glc; L = Gal- $\beta$ 1,2-Xyl- $\alpha$ 1,6-Glc; F = Fuc- $\alpha$ 1,2-Gal- $\beta$ 1,2-Xyl- $\alpha$ 1,6-Glc;  $\alpha$ F = fluoride in  $\alpha$ -configuration). These were subsequently modified to fucosylated XLFG-type glucans **12c**

with a ratio of 3 : 1 XLFG : XLLG catalysed by the fucosyltransferase AtFUT1 (originating from *Arabidopsis thaliana*).

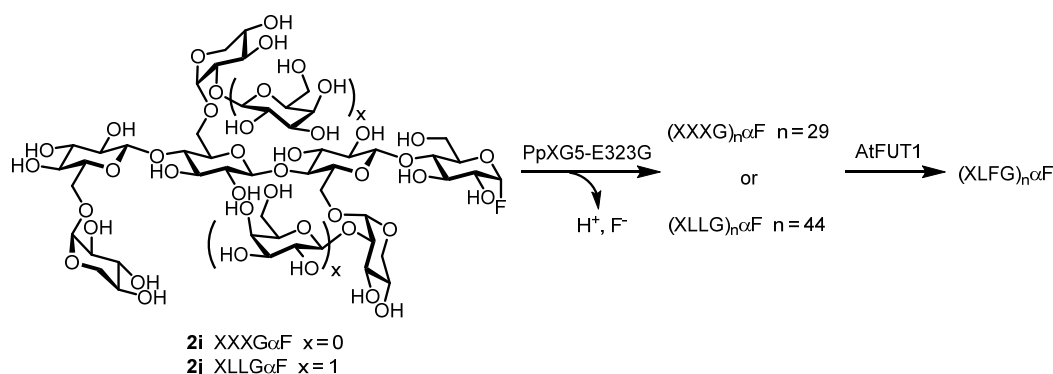


**Figure 12** Combinatorial glycosynthase / glycosyltransferase approach for the synthesis of defined, homogenous xyloglucans.<sup>[56]</sup> Polysaccharide synthesis using compound **2i** or **2j** was catalysed by PpXG5-E323G resulting in polymers with a maximal molecular weight of 30,000 ( $n=29$ ) and 60,000 ( $n=44$ ), respectively. Subsequent fucosylation by the fucosyltransferase AtFUT1 reached a fucosylation of 75% of the oligosaccharide repeats. Nomenclature: G = Glc; X = Xyl- $\alpha$ 1,6-Glc; L = Gal- $\beta$ 1,2-Xyl- $\alpha$ 1,6-Glc; F = Fuc- $\alpha$ 1,2-Gal- $\beta$ 1,2-Xyl- $\alpha$ 1,6-Glc;  $\alpha$ F = fluoride in  $\alpha$ -configuration.

### Biocatalytic synthesis of $\beta$ -mannosides

Apart from the xyloglucans, mannans are also highly abundant polysaccharides in plant cell walls and mannosyl moieties are common components of biological structures such as *N*-linked glycans, viral and microbial antigens.<sup>[57, 58]</sup> The enzymatic synthesis of  $\beta$ -mannosyl linkages has raised much interest, as the chemical synthesis is complex and demanding due to no beneficial effects promoting the synthesis of the  $\beta$ -anomeric configuration. Utilisation of  $\beta$ -mannosynthases is therefore a simple and practical solution for the synthesis of this type of linkage. Nevertheless, not much research has been carried out toward the creation of mannosynthases. *Nashiru et al.* produced a  $\beta$ -mannosynthase by the 'classical' glycosynthase method with a retaining  $\beta$ -mannosidase mutant of Man2a (E519S, GH 2) of *C. fimi*.<sup>[57]</sup> Man2a-E519S catalysed the formation of  $\beta$ -1,4 (major linkage) and  $\beta$ -1,3 mannosides with  $\alpha$ -D-mannosyl fluoride (**2e**,  $\alpha$ -ManF) and various acceptors (*p*NPMan **5b**, -Xyl **5i**, -Glc **5h**, -cellobioside **5c**, -gentiobioside, and 2,4-dinitrophenyl-2-deoxy-2-fluoro- $\beta$ -mannoside) in yields from 70–99% comprising di-, tri-, and tetrasaccharides. The yield was mostly restricted due to the instability of  $\alpha$ -ManF **2e**, which can easily undergo hydrolysis by epoxide-formation. The enzyme also displayed high activity in chemical rescue experiments using 2,4-dinitrophenyl- $\beta$ -D-mannopyranoside (**5p**) and external nucleophiles such as azide, formate or acetate, but also in the presence of fluoride ions allowing an *in situ* production of the  $\alpha$ -ManF donor **2e** (Figure 13).

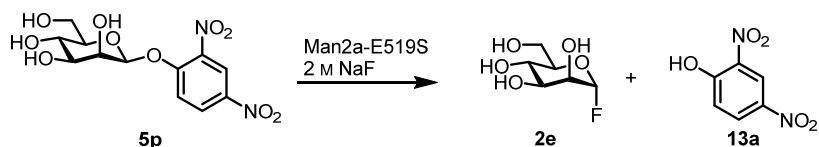


**Figure 13** *In situ* synthesis of the glycosynthase donor substrate  $\alpha$ -ManF (**2e**) by applying the chemical rescue method with Man2a-E519S in the presence of sodium fluoride as an external nucleophile.<sup>[57]</sup>

Larger manno oligosaccharides were synthesised by *Jahn et al.* using the glycosynthase derived from the  $\beta$ -mannosidase Man26A of *Calotomus japonicus*.<sup>[59]</sup> The glycosynthase produced manno oligosaccharides using the  $\alpha$ -Man<sub>2</sub>F donor **2e** and *p*NPGlc **5h** as the acceptor in a total yield of 59%. The tri- (36%), penta- (18%), and heptasaccharides (5%) contained exclusively  $\beta$ -1,4 linkages. In comparison, the acceptor *p*NPMan **5b** resulted in a trisaccharide in 35% yield.

### 5.2.2 Glycosidase candidates — a versatile toolbox for $\beta$ -glycoside synthesis

Even though much research and progress has been carried out and achieved on the development of glycosynthases for the synthesis of glycosides, there is still no general method, which can be applied for the definite production of a potential glycosynthase. In order to reach the goal of developing a versatile biocatalytic toolbox for the synthesis of glycosides, new glycosynthases exhibiting a broad substrate scope and a tolerance towards a wide range of reaction conditions need to be discovered. The following glucosidases were chosen to help step closer to this goal.

#### Learning from the first glycosynthase

An important point to developing new methods is to test the developed methods with a control, which is already literature known and well characterised. In order to evaluate methods developed for glycosynthase identification and characterisation in this thesis, one of the first developed glycosynthases, a mutant of the  $\beta$ -glucosidase Abg of *R. radiobacter* (also known as *Agrobacterium faecalis*, *Agrobacterium sp.*, *A. tumefaciens*, *A. radiobacter*) was chosen for use as a positive control.<sup>[21]</sup> The catalytic nucleophilic residue of the  $\beta$ -glucosidase Abg was identified by trapping the glycosyl-enzyme-intermediate using 2',4'-dinitrophenyl 2-deoxy-2-fluoro- $\beta$ -D-glucopyranoside and identifying the thereby marked residue by *Edman* degradation.<sup>[60]</sup> After the identification, many mutagenesis studies were carried out characterising the influence of the variation of the nucleophilic residue and the surrounding amino acids.<sup>[61, 62]</sup> Further mutagenic studies led to the identification of the catalytic acid/base residue of Abg, determining the catalytic residues to be E358 and E170 (nucleophile and acid/base respectively).<sup>[63]</sup> The wild type (*wt*) enzyme was first used in synthesis by *Prade et al.* in transglycosylation reactions. The group demonstrated the glycosylation of acceptors, such

as phenyl-1-thio- or benzyl-1-thio-glycopyranosides using (e.g.) *p*-nitrophenyl  $\beta$ -D-galactopyranoside (**5g**) as the glycosyl donor.<sup>[64]</sup> Shortly thereafter the mutant variant Abg-E358A was described as a glycosynthase by *Mackenzie et al.*, transferring the donors  $\alpha$ -GlcF (**2a**) and  $\alpha$ -GalF (**2b**) onto aryl glycosides. The glycosynthase activity was then optimised, by introducing a serine or glycine instead of the alanine residue at the E358 position, creating much more active glycosynthases.<sup>[65, 66]</sup> The combination of glycosynthase activity and the hydrolysis of the respective glycosynthetic product by the cellobiase Cel5A (*C. fimi*), releasing a detectable chromo- or fluorophore, allowed the screening for further optimised variants of Abg by directed evolution.<sup>[27, 65]</sup> This process led to the highly active and versatile glycosynthases Abg-2F6 and Abg-NNT described in section 5.2.1.<sup>[26, 47]</sup>

### Temperature variation towards the optimal glycoside synthesis

For many industrial applications, the tolerance of enzymes towards extreme conditions such as elevated or low temperatures has become of high relevance in order to make many biocatalytic processes even viable. Thereby, the interest towards enzymes of extremophiles has gained much interest in recent years. With respect to these developments two glycosidases originating from different extremophiles were examined in this thesis.

Putative hyperthermophilic ' $\beta$ -galactosidase' BglC<sup>1</sup> of *P. furiosus*:

The marine microorganism *P. furiosus*, belonging to the domain of the archaea, has hyperthermophilic properties, growing optimally under conditions near 100 °C in its natural habitat.<sup>[67]</sup> The genome of *P. furiosus* (2.05 Mbp) has been sequenced and extensively examined by *Borges et al.*<sup>[67]</sup> Genome comparisons with other representatives of the *Pyrococcus* phylum such as *Pyrococcus horikoshii* have also been carried out.<sup>[68]</sup> Enzymes isolated from this organism mostly show high thermal stability as for example the Pfu-polymerase, a thermostable DNA-polymerase with proof-reading activity. The glycosidase BglC [WP\_011011477.1 / PF\_RS01865 (gene), AAL80487 (protein)] chosen for this thesis of the *P. furiosus* DSM3638 strain (isolated and provided by *Elling and Merker*)<sup>2</sup> also exhibits hyperthermophilic properties (activity optimum around 85 °C) and was annotated as a putative ' $\beta$ -galactosidase'.<sup>[69]</sup> The enzyme is classified as part of the GH A clan containing a typical ( $\beta/\alpha$ )<sub>8</sub>-fold (TIM-barrel), belonging to the glycohydrolase family GH 35.<sup>[70, 71]</sup> In initial experiments of *Elling and Merker*, the enzyme has shown to exhibit weak  $\beta$ -glucosidase and  $\beta$ -xylosidase rather than  $\beta$ -galactosidase activity. The application of this specific enzyme in transglycosylation reactions or mutation to a glycosynthase has not been reported in literature.

---

<sup>1</sup> Referred to as 'GalPF' in the publication *Hayes et al.*<sup>[2]</sup>

<sup>2</sup> RWTH Aachen University, Laboratory for Biomaterials, Institute for Biotechnology and Helmholtz Institute for Biomedical Engineering

Nevertheless, the use of other glycosidases originating from *P. furiosus* as hydrolases or synthases in organic synthesis has often been reported. *Gelo-Pujic et al.* described transglycosylation reactions in dry media under microwave irradiation with a  $\beta$ -glucosidase of *P. furiosus* and successfully transferred glucose onto propane-1,3-diol.<sup>[72]</sup> The group of *Lieshout et al.* carried out hydrolytic and glycosynthetic reactions utilising the *endo*-1,3- $\beta$ -glucanase (laminarinase, LamA).<sup>[73]</sup> A mutant variant of LamA with reduced hydrolytic activity was able to catalyse synthetic reactions using glycosyl fluorides. They also describe the drawback of the use of hyperthermophilic enzymes, as the thermo-stability of the glycosyl fluoride substrates is not high. *Perugino et al.* and *Trincone et al.* further investigated the application of *P. furiosus* glycosidases.<sup>[74, 75]</sup> They developed three hyperthermophilic glycosynthases of *Sulfolobus solfataricus*, *Thermosphaera aggregans* and *P. furiosus* (CelB,  $\beta$ -glucosidase) and described the activating effects of buffer below pH neutrality on the activity of the synthases using the chemical rescue method.

#### Psychrophilic $\beta$ -glucosidase of *Micrococcus antarcticus*:

In contrast to the hyperthermophilic enzymes, psychrophilic enzymes exhibit high catalytic activity at lower temperatures and originate most often from organisms living in permanently cold areas such as the Antarctic. These types of enzymes have high potential for industrial purposes as for example in the food industry avoiding the deterioration of nutritional value and flavour of heat-sensitive products.<sup>[76]</sup> They could also prove useful in the second generation bio-ethanol production allowing simultaneous biomass hydrolysis/saccharification (usually carried out at higher temperatures) and fermentation (yeast prefer cool temperatures) without the need of multiple heat/cooling stages.<sup>[77]</sup> Despite these promising applications, only little research has been carried out towards this type of enzyme in comparison to mesophilic and thermophilic enzymes. The research on psychrophilic glycosidases is mostly limited to a few such as  $\beta$ -glucosidases (BglIU, *M. antarcticus*; PtBglu, *Paecilomyces thermophile*), xylanases (*Criptomycoccus albidus*), and  $\alpha$ -amylases (AHA, *Alteromonas haloplanctis*).<sup>[78-81]</sup> Recently the group of *Zanphorlin et al.* elucidated the crystal structure of the psychrophilic  $\beta$ -glucosidase EaBglA1 (GH 1) of *Eudendrium antarcticum* B7, examining in detail the structural properties leading to cold tolerance.<sup>[82]</sup> The use of these enzymes in synthetic reactions of glycosidic bonds instead of hydrolysis has not been reported. The modification of a psychrophilic  $\beta$ -glucosidase to a glycosynthase and its application in synthesis was attempted in this thesis for the  $\beta$ -glucosidase BglIU [FJ483828 (gene), ACM66669 (protein)] of *M. antarcticus*. The glucosidase was discovered by an activity screening of the genomic library of *M. antarcticus* by *Fan et al.* and was the first example of a cold adapted  $\beta$ -glucosidase of the GH 1 family.<sup>[81]</sup> The protein structure was elucidated and consisted of the characteristic  $(\beta / \alpha)_8$ -fold, typical for GH 1 glycosidases. The amino acid sequence displayed the conserved sequence motifs [ENP]

and [ENG] allowing determination of the acid/base and nucleophilic residue to be E170 and E377 respectively. The enzyme was characterised and found to hydrolyse  $\beta$ -1,2;  $\beta$ -1,3;  $\beta$ -1,4; and  $\beta$ -1,6-diglycosides and aryl glycosides optimally at 25 °C and pH 6.5. Further structural analysis by *Miao et al.* revealed two key structural elements conveying the cold adaptedness exhibited by BglU (Figure 14).<sup>[83]</sup> First, a unique long loop structure (35 amino acids long compared to around 7 usually observed in GH 1 glucosidases) involved in the substrate binding ensures higher activity at lower temperatures. Mutagenesis experiments revealed the correlation of a shorter loop with lower activities at lower temperatures. The second key element found was a histidine residue H299, which contributes to the stabilisation of an ordered water molecule chain within the active site pocket. This residue is mostly responsible for the thermo-lability of BglU. The exchange of the histidine with a tyrosine residue, found in meso- and thermophilic glycosidases at this position, greatly increased catalytic activity, the optimal temperature, and the thermostability of the enzyme.

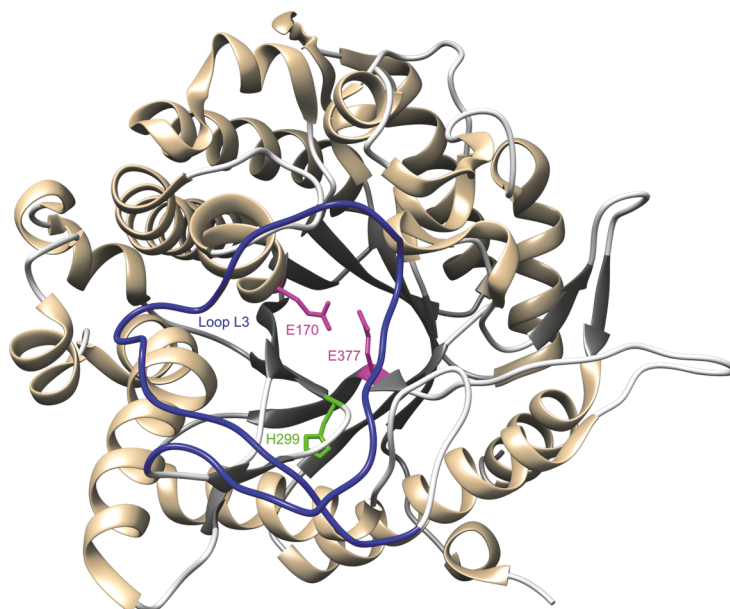


**Figure 14** Depiction of the key structural elements conveying the cold adaptedness properties of the  $\beta$ -glucosidase BglU of *M. antarcticus* (PDB 3W53).<sup>[83]</sup> The non-conserved long loop L3 (blue) and H299 residue (green) give BglU the characteristic cold adapted activity. Also depicted are the catalytic acid/base and nucleophile residues E170 and E377.

### Substrate based prediction of glycosynthase specificity

Many glycosynthases were created by mutation of characterised glycosidases of which preferentially the crystal structure has already been elucidated. However, most commonly the exact natural substrates of these glycosidases are unknown and therefore rendering the acceptor specificity of the resulting potential glycosynthase equally unknown. The

$\beta$ -glucosidase Cbg1 of *R. radiobacter* (formerly *A. tumefaciens*) on the other hand is a glycosidase with a known natural substrate.

Coniferin specific  $\beta$ -glucosidase of *R. radiobacter*:

The  $\beta$ -glucoside coniferin (**14a**) produced by conifers such as *Pseudotsuga menziesii* has been described as a major *vir* region inducer (virulence region encoding enzymes responsible for mediating conjugative transfer of T-DNA), which induces the successful infection of the host plant cells by *R. radiobacter*.<sup>[84]</sup> The active inducer, coniferyl alcohol (**14b**), is the aglycone of coniferin (**14a**), which is released by the  $\beta$ -glucosidases Cbg1 of *R. radiobacter*. *Castle et al.* discovered the enzyme by screening the genomic library of *R. radiobacter* for  $\beta$ -glucosidase activity.<sup>[85]</sup> Two enzymes were identified, but only one exhibiting activity towards the  $\beta$ -glucoside coniferin (**14a**). The gene *cbg1* was identified and showed similarities to  $\beta$ -glucosidase genes of the glycohydrolase family GH 3, which allowed the identification of the catalytic nucleophilic residue D222 as part of the [-SDW-] consensus sequence found in GH 3 glycosidases. Later, as no structural data was available for GH 3 glycosidases, the construction of chimeric enzymes of Cbg1 and the  $\beta$ -glucosidase of *Cellvibrio gilvus*, led to insights to the domain functions of Cbg1.<sup>[86, 87]</sup> *Watt et al.* carried out the biochemical characterisation of Cbg1, demonstrating hydrolytic activity towards aryl glucosides, xylosides,  $\alpha$ -L-arabinosides,  $\beta$ -D-fucosides, and galactosides.<sup>[88]</sup> The enzyme exhibited a 20,000-fold preference to coniferin (**14a**) than towards the cellobiose disaccharide. The group also describes a high transglycosylation activity of the enzyme in the presence of hydrophobic alcohols, the highest activity observed for the transglycosylation of 1-butanol (**15a**). The first assignment of the catalytic acid/base residue was proposed as E616 by *Goyal et al.* comparing the sequence of Cbg1 with the  $\beta$ -glucosidase BglB of *T. maritima* during the creation of further chimeric  $\beta$ -glucosidases.<sup>[89]</sup> Truncation studies, deleting parts of the non-homologous regions of Cbg1 compared to the barley  $\beta$ -D-glucan *exo*-glucohydrolase ExoI, revealed the structural function of this region in maintaining the affinity of Cbg1 toward hydrophobic compounds.<sup>[90]</sup> Further insights on the transglycosylation activity of Cbg1 were gained by *Kitaoka et al.* describing a self-transferring product inhibition when a high concentration of *p*NPGlc **5h** was present.<sup>[91]</sup> The inhibition was observed by a non-linear time profile of the initial enzyme reaction. The transfer of the glucosyl residue of *p*NPGlc **5h** to already released *p*-nitrophenol (**13b**) was determined to be the cause of the non-linearity of the reactions time profile (Figure 15).

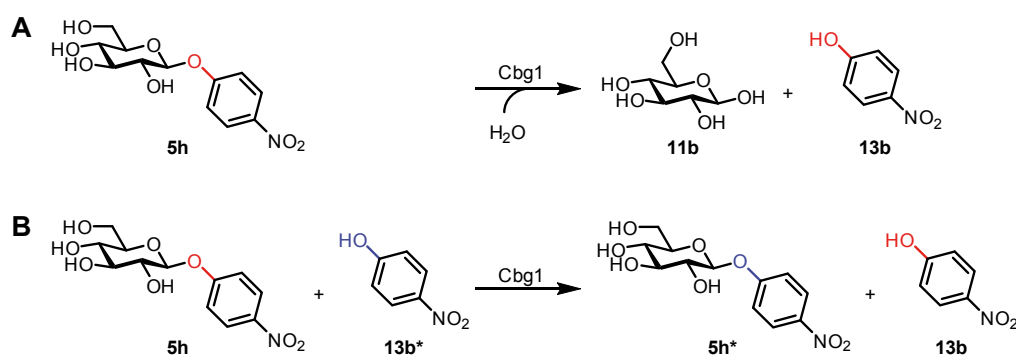


**Figure 15** Proposed self-transferring inhibition of Cbg1 of *R. radiobacter* described by Kitaoka *et al.* when incubating Cbg1 with high concentrations of pNPGlc 5h.<sup>[91]</sup> **A:** Regular hydrolysis of pNPGlc 5h by Cbg1. **B:** Transglycosylation of before released pNP 13b (marked with \*) occurring at high concentrations of pNPGlc 5h.

Even though the structure of Cbg1 has not been elucidated, an idea of the structure can be obtained by the structure of KmBglI, a GH 3  $\beta$ -glucosidase of *Kluyveromyces marxianus* (formerly known as *Kluyveromyces fragilis*), which shows 40% identity and 64% similarity to Cbg1.<sup>[92]</sup> The structure of KmBglI shows the combination of a  $(\beta/\alpha)_8$ -barrel and a  $(\alpha/\beta)_6$ -sandwich fold, which is characteristic to GH 3 glycosidases. The  $(\alpha/\beta)_6$ -sandwich is separated into two units by the insertion of a PA14 domain, consisting of a two layered  $\beta$ -sheet, which is also present in Cbg1. The PA14 domain was determined to play a critical role in the substrate specificity of the +1 subsite, hindering the binding of long oligosaccharides.

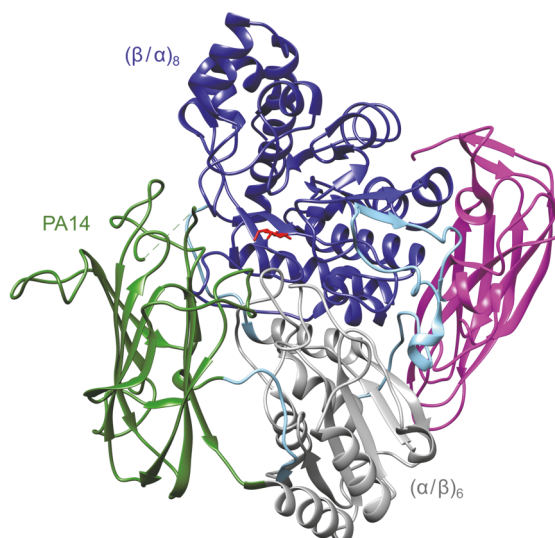


**Figure 16** Structural overview of the GH 3  $\beta$ -glucosidase KmBglI of *K. marxianus* (PDB: 3AC0).<sup>[92]</sup> KmBglI shows 40% identity and 64% similarity to Cbg1 and can therefore be used as a model for the structure of Cbg1. The domain structure is depicted by colouration:  $(\beta/\alpha)_8$ -fold (TIM-barrel), blue;  $(\alpha/\beta)_6$ -sandwich, gray; PA14, green; C-terminal domain, magenta; glucose, red.

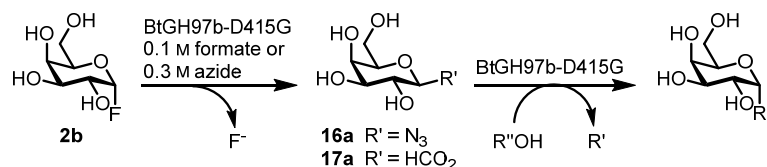
## 5.3 Biocatalysis towards $\alpha$ -linked glycosides

### 5.3.1 Synthesis with $\alpha$ -glycosynthases

Even though much research and many advances have occurred in the synthesis of  $\beta$ -glycosidic linkages, the synthesis of  $\alpha$ -glycosidic linkages utilizing  $\alpha$ -glycosynthases is still limited and poses a challenge. The 'classical' glycosynthase method utilising a glycosyl fluoride donor is majorly hindered by the necessity of  $\beta$ -glycosyl fluorides, which are much more unstable and difficult to synthesise compared to their  $\alpha$ -configured counterparts.<sup>[93]</sup> Therefore, alternative methods are required in order to create this kind of linkage biocatalytically with glycosynthases.

### Biocatalysis towards $\alpha$ -galactosides

With the aim of producing  $\alpha$ -galactosides, *Cobucci-Ponzano et al.* reported the efficient conversion of  $\beta$ -D-galactopyranosyl azide (**16a**,  $\beta$ -GalN<sub>3</sub>) to  $\alpha$ -galactooligosaccharides by the glycosynthase TmGalA-D327G derived from *T. maritima*.<sup>[94]</sup> The enzyme synthesised galactooligosaccharides in high yields and the method was recently expanded by *Okuyama et al.* with the glycosynthase BtGH97b-D415G to the *in situ* formation of a  $\beta$ -D-galactosyl formate donor (**17a**), which exhibited a higher transglycosylation rate compared to the azide donor **16a** (Figure 17).<sup>[95]</sup> The method enabled the galactosylation of carbohydrates such as glucose ( $\alpha$ -D-Gal-1,1- $\beta$ -D-Glc, non-reducing sugar), xylose ( $\alpha$ -1,4), maltose ( $\alpha$ -D-Gal-1,1- $\beta$ -D-Man), cellobiose ( $\alpha$ -D-Gal-1,1- $\beta$ -D-Cel;  $\alpha$ -1,6), lactose ( $\alpha$ -D-Gal-1,1- $\beta$ -D-Lac), and *p*NP derivatives of glucose (*p*NPGlc **5h**), and mannose (*p*NPMan **5b**; exclusively  $\alpha$ -1,6) in yields ranging from 75% to 95%. *Bayón et al.* examined the effect of ionic liquids as cosolvents on the synthesis of  $\alpha$ -galactosyl residues with  $\beta$ -GalN<sub>3</sub> **16a** and reported increased conversion and yield for the glycosynthase TmGalA D327G producing  $\alpha$ -1,6 bonds with *p*NPGlc **5h** and *p*NPMan **5b**.<sup>[96]</sup>

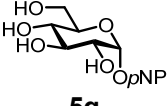
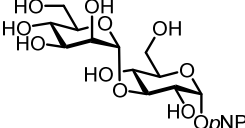
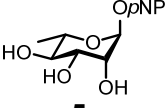
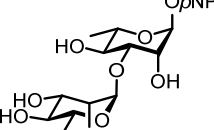
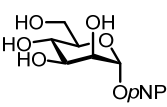
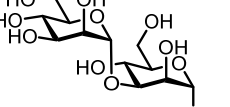
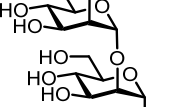
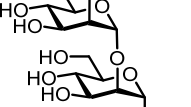
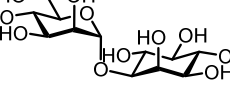
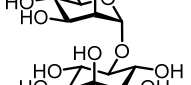


**Figure 17** *In situ* synthesis of the galactosyl donors  $\beta$ -GalN<sub>3</sub> **16a** and  $\beta$ -Gal-formate **17a** by incubation with  $\alpha$ -GalF **2b** with the galactosynthase BtGH97b-D415G and the external nucleophiles sodium azide or formate.<sup>[95]</sup> The *in situ* produced donor can then be directly transferred to a suitable acceptor (R''OH).

### Biocatalytic $\alpha$ -mannosylation

For the synthesis of  $\alpha$ -mannosyl linkages *Yamamoto et al.* described the possibility of mono- $\alpha$ -mannosylating acceptors with a glycosynthase derived from a broad glycosidase scaffold.<sup>[58]</sup> The  $\alpha$ -mannosynthase was produced by mutation of an  $\alpha$ -glucosidase of *S. solfataricus* with hydrolysis of glucosides preferred over mannosides. The synthase variant MalA-D320G catalysed the formation of oligosaccharides if  $\beta$ -D-glucopyranosyl fluoride (**2k**,  $\beta$ -GlcF) was used, but only mono-glycosylation was observed in the case of the  $\beta$ -D-mannopyranosyl fluoride donor ( $\beta$ -ManF). The enzyme was tested on various *p*NP-glycosides **5** resulting in yields up to 77% ( $\alpha$ -1,4 being the major type of linkage,  $\alpha$ -1,3 and  $\alpha$ -1,2 were also observed) and the preparation of naturally occurring  $\alpha$ -mannosyl motifs, such as Man- $\alpha$ (1,4)-Glc (**5t**), Man- $\alpha$ (1,3)-L-Rha (**5u**), and Man- $\alpha$ (1,2)-Man (**5w**, Table 2). The production of mannosylated *myo*-inositol (**18a**), a component of the cell wall glycolipids of *Mycobacterium tuberculosis* was also demonstrated with this method. The mono-mannosylated inositols were isolated in a yield of 41% (mixture of Man- $\alpha$ (1,5)- and Man- $\alpha$ (1,1)-*myo*-inositol **18b** and **18c** in a 3 : 1 ratio).

**Table 2** Examples of  $\alpha$ -mannosylated synthetic products **5t–5w**, **18b/c** catalysed by MalA-D320G. All reactions were carried out with  $\beta$ -ManF as the donor. Different regioselectivities were observed depending on the acceptor structure and anomeric configuration. Yields were determined after purification or isolation.

Acceptor	Product	Yield (Selectivity)
 <b>5q</b>	 <b>5t</b>	26% <sup>a</sup> (>95%, $\alpha$ -1,3)
 <b>5r</b>	 <b>5u</b>	44% <sup>a</sup> (92%, $\alpha$ -1,3)
 <b>5s</b>	 <b>5v</b>	55% (60 : 40 $\alpha$ -1,3 / $\alpha$ -1,2)
 <b>5w</b>	 <b>5w</b>	
 <b>18a</b>	 <b>18b</b>	41% <sup>a</sup> (3 : 2 $\alpha$ -1,5 / $\alpha$ -1,1)
	 <b>18c</b>	

<sup>a</sup> Isolated as peracetate.

## Biocatalysis towards $\alpha$ -fucosides

A further important group of glycosyl compounds relevant in many biological processes are fucosyl residues. Throughout nature, this deoxy-aldohexose occurs in comparison to most other natural carbohydrates as an L-configured glycoside and is linked predominantly in  $\alpha$ -configuration at the anomeric centre. Many biological processes involve fucosylated compounds such as, cell-to-cell communication, cell development, recognition structures for pathogens, and antigenic structures.

The first production of fucosylated structures using a glycosynthase method was reported by *Wada et al.* with a mutated  $\alpha$ -fucosidase of *Bifidobacterium bifidum* BbAfcA-D766G.<sup>[97]</sup> The recombinant enzyme was successfully applied in the synthesis of a Fuc- $\alpha$ (1,2)-Gal linkage in 2'-fucosyllactose by combining  $\beta$ -fucopyranosyl fluoride (**21**,  $\beta$ -FucF) with lactose. However, the low stability of  $\beta$ -FucF **21** led to yields of 6%. The low yields caused by the instability of the  $\beta$ -fluoride donor were overcome by *Cobucci-Ponzano et al.* by the implementation of the more stable  $\beta$ -azide fucosylpyranoside (**16b**,  $\beta$ -FucN<sub>3</sub>) donor for two new  $\alpha$ -fucosynthases (Figure 18).<sup>[98]</sup>

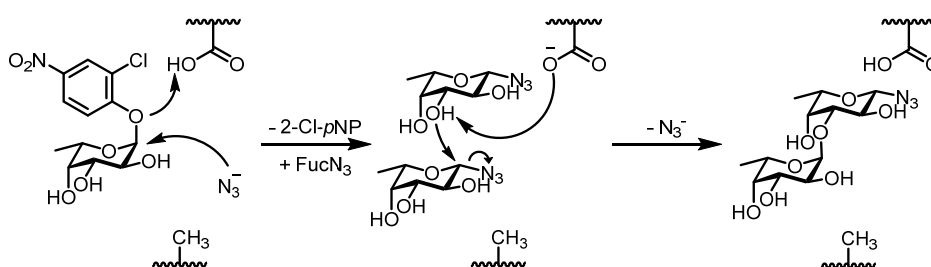


**Figure 18** *In situ* production of a glycosyl donor and subsequent transference to an acceptor demonstrated by *Cobucci-Ponzano et al.* The  $\alpha$ -fucosynthases Ss-D242S and Tm-D224G were derived from the fucosidases of *S. solfataricus* and *T. maritima*.<sup>[98]</sup>

The  $\alpha$ -fucosynthase Ss-D242S displayed a broad acceptor range (shown for various aryl-glycosides) though also catalysing the self-condensation of  $\beta$ -FucN<sub>3</sub> **16b** in all cases. In comparison, the second fucosynthase Tm-D224G exhibited a more restricted acceptor range, but the self-condensation reaction was not observed. The reactions were also carried out with Ss-D242S in a preparative scale with total transufucosylation efficiencies ranging from 29–86% [for the acceptors *p*NPXyl **5i**, *p*NPGal **5g**, and *p*-nitrophenyl *N*-acetylglucosaminide (**5a**, *p*NPGlcNAc)] resulting mostly in  $\alpha$ -1,4 and 1,3 linkages and additionally  $\alpha$ -1,6 linkages in the case of the galactoside acceptor **5g**. The Tm-D224G variant could even reach a transufucosylation efficiency of 91% providing a mixture of Fuc- $\alpha$ (1,3)- and Fuc- $\alpha$ (1,4)- $\beta$ -Xyl*p*NP in a near 1 : 1 ratio. The application of  $\alpha$ -L-fucosynthases was recently transferred to biological structures such as epitopes of the Lewis and ABO antigens. These glycosides can be found on, e.g., red blood cells, contributing to the phenotype of the blood group system. *Sakurama et al.* reported the synthesis of the Lewis antigens Le<sup>a</sup> and Le<sup>x</sup>

[Gal- $\beta$ 1,3/4-(Fuc- $\alpha$ 1,4/3)-GlcNAc: Le<sup>a/x</sup> **19a/19b**] catalysed by the 1,3-1,4- $\alpha$ -L-fucosyltransferase BbAfcB-D703S.<sup>[99]</sup> The antigen structures were produced by the reaction of  $\beta$ -FucF **21** and lacto-*N*-biose I [**19c**, LNB, Gal- $\beta$ (1,3)-GlcNAc] and *N*-acetyllactosamine [**19d**, LacNAc, Gal- $\beta$ (1,4)-GlcNAc] resulting in yields of 47% and 55% for Le<sup>a</sup> **19a** and Le<sup>x</sup> **19b**, respectively (Figure 19). An increase in the yield using the more stable donor  $\beta$ -FucN<sub>3</sub> **16b** as described by *Cobucci-Ponzano et al.* could not be achieved as no transfucosylation products could be observed using this donor. The enzyme also interestingly only acted on di- or trisaccharide acceptors, unable to fucosylate monosaccharides such as, glucose, galactose, *N*-acetylglucosamine, and *N*-galactosamine. The specific synthesis of lacto-*N*-fucopentaose II [LNFP II: Gal- $\beta$ 1,3-(Fuc- $\alpha$ 1,4)-GlcNAc- $\beta$ 1,3-Gal- $\beta$ 1,4-Glc] was also achieved in a yield of 41% with lacto-*N*-tetraose (LNT: Gal- $\beta$ 1,3-GlcNAc- $\beta$ 1,3-Gal- $\beta$ 1,4-Glc) as the acceptor.

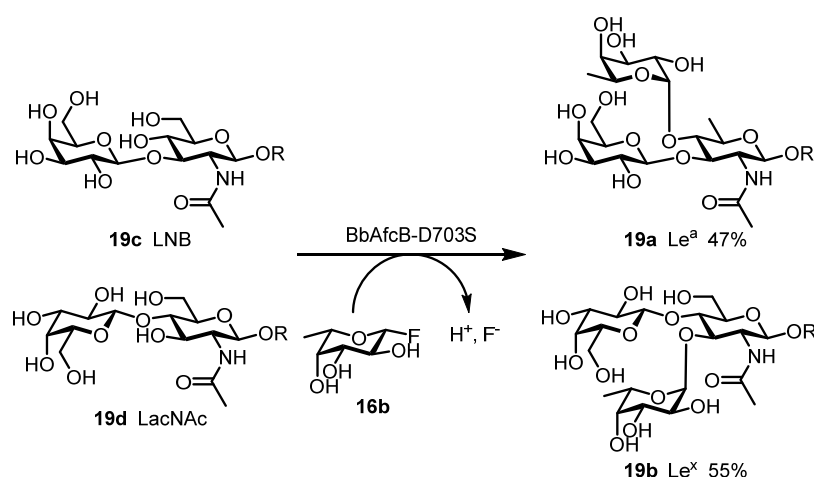


**Figure 19** Synthesis of the Lewis antigens Le<sup>a</sup> **19a** and Le<sup>x</sup> **19b** by  $\alpha$ -fucosylation of LNB **19c** of LacNAc **19d**, respectively, catalysed by the  $\alpha$ -1,3-1,4-L-fucosyltransferase BbAfcB-D703S.<sup>[99]</sup>

The repertoire of synthesised antigen epitope structures was broadened by the work of *Sugiyama et al.* introducing the 1,2- $\alpha$ -L-fucosyltransferase BbAfcA-N423H.<sup>[100]</sup> In addition to  $\alpha$ -fucosylating various types of mono- and disaccharides, producing for example H type-1 or H type-2 chains from LNB **19c** or LacNAc **19d** respectively, the antigens Le<sup>b</sup> and Le<sup>y</sup> [Fuc- $\alpha$ 1,2-Gal- $\beta$ 1,3/4-(Fuc- $\alpha$ 1,4/3)-GlcNAc: Le<sup>b/y</sup>] were produced in yields of 43% and 62% from the Le<sup>a</sup> **19a** and Le<sup>x</sup> **19b** trisaccharides. In comparison to the BbAfcB-D703S synthase, BbAfcA-N423H produced LNFP I (Fuc- $\alpha$ 1,2-Gal- $\beta$ 1,3-GlcNAc- $\beta$ 1,3-Gal- $\beta$ 1,4-Glc) rather than LNFP II with an efficiency of 75%. Later, the transfer of fucosyl residues to the non-reducing end of *O*-linked glycans was demonstrated by the successful reintroduction of H-antigen structures to pretreated glycopeptide porcine gastric mucin. The reaction was even further expanded by the group introducing H-antigens to the non-reducing ends of *N*- and *O*-glycans in fetuin glycoproteins, GM1 ganglioside (**9d**), and a xyloglucan nonasaccharide.<sup>[101]</sup> It was determined that BbAfcA-N423H could fucosylate asialo-bi-, asialo-tri-, and

monosialo-triantennary *N*-glycans of the asialo fetuin glycopeptide with transfer efficiencies of 9%, 26%, and 20% respectively. BbAfcA-N423H was also capable of fucosylating the sialo form of the fetuin peptide containing di-sialo-bi-, di-sialo-tri-, tri-sialo-tri-, and tetra-sialo-triantennary glycans, yet with lower transfer efficiencies. Fucosylation of the xyloglucan nonasaccharide XLLG **12b** (Structure in Figure 12) occurred with an efficiency of 57% giving a mixture of mono- ( $\alpha$ -1,2-Gal), di- ( $\alpha$ -1,2-Gal), and trifucosylated ( $\alpha$ -1,3-Glc) XLLG glycosides. The enzyme also fucosylated glycolipids, transferring the  $\alpha$ -1,2-fucosyl residue to the glycoside of the GM1 ganglioside (**9d**, Figure 20).

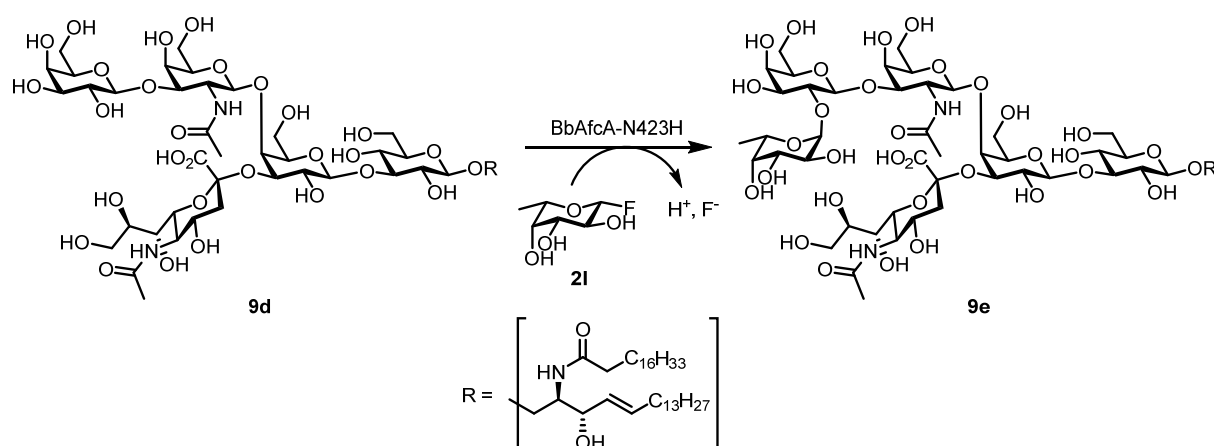


**Figure 20** Selective  $\alpha$ -fucosylation of the glycoside GM1 ganglioside (**9e**) described by Sugiyama *et al.*<sup>[101]</sup> BbAfcA N423H showed a wide acceptor range exhibiting fucosylation activity towards *N*- and *O*-glycans and the nonasaccharide xyloglucan XLLG (**12b**).

### 5.3.2 Biocatalysis towards rhamnosides

Similar to fucose,  $\alpha$ -L-rhamnose, a 6-deoxy-hexopyranoside occurs predominantly in the L-configuration.  $\alpha$ -L-Rhamnosides are widely distributed in plants and bacteria and occur often for example in plant glycosides, cell walls, bacterial rhamnolipids and other polysaccharides.<sup>[102]</sup> Many biological active compounds of pharmaceutical interest contain rhamnose as a glycoside. The de-rhamnosylation and even rhamnosylation can vary the active properties and bioavailability of certain compounds greatly. The bioavailability of flavonoid glycosides such as prunin (**1b**) or isoquercetin (**1h**) differ greatly from naringin (**1c**) or hesperidin, respectively, strengthening the effects of the molecules by far.<sup>[8, 103, 104]</sup> On the other hand, myricetin, a natural flavonol in plants and fruits with anti-oxidant and anti-mutagenic activities, can be rhamnosylated to myricetin-3-*O*-rhamnoside, modifying its physicochemical and biological properties to a neural nitric oxide synthase or protein kinase C inhibitor.<sup>[105]</sup>

The use of  $\alpha$ -L-rhamnosidases for biocatalytic synthesis of natural products containing rhamnosyl residues is limited throughout literature. The most common use of rhamnosidases occurs in the food industry, for example in debittering and clarification of fruit juices [hydrolysis

of naringin (**1c**), hesperidin, and pectin] and aroma optimisation of wine (liberation of monoterpenols).<sup>[102, 106]</sup> Chemoenzymatic synthetic reactions with rhamnosidases have been limited to the use of reverse hydrolysis. *De Winter et al.* produced various rhamnosides, rhamnosylating acceptors such as 2-phenylethanol, anisyl alcohol, catechol, and resorcinol, though with lengthy reaction times up to 48 h, high co-solvent amounts and low yields.<sup>[107]</sup> The  $\alpha$ -rhamnosidase RhaL1 of *Alternaria sp.* L1 was also applied in reverse hydrolysis reactions by *Lu et al.*, glycosylating mannitol, fructopyranose, and esculin in yields of 36%, 12%, and 18% respectively.<sup>[108]</sup> The relative yield of the reverse hydrolysis reaction with mannitol was improved up to 43% by site directed mutagenesis studies on RhaL1.<sup>[109]</sup> The use and development of  $\alpha$ -L-rhamnosynthases via mutation has not been reported up to date. An application of the chemical rescue method, applied for the closely related  $\alpha$ -fucosynthases, has not yet been transferred or tested for  $\alpha$ -L-rhamnosidases and is examined in this thesis.

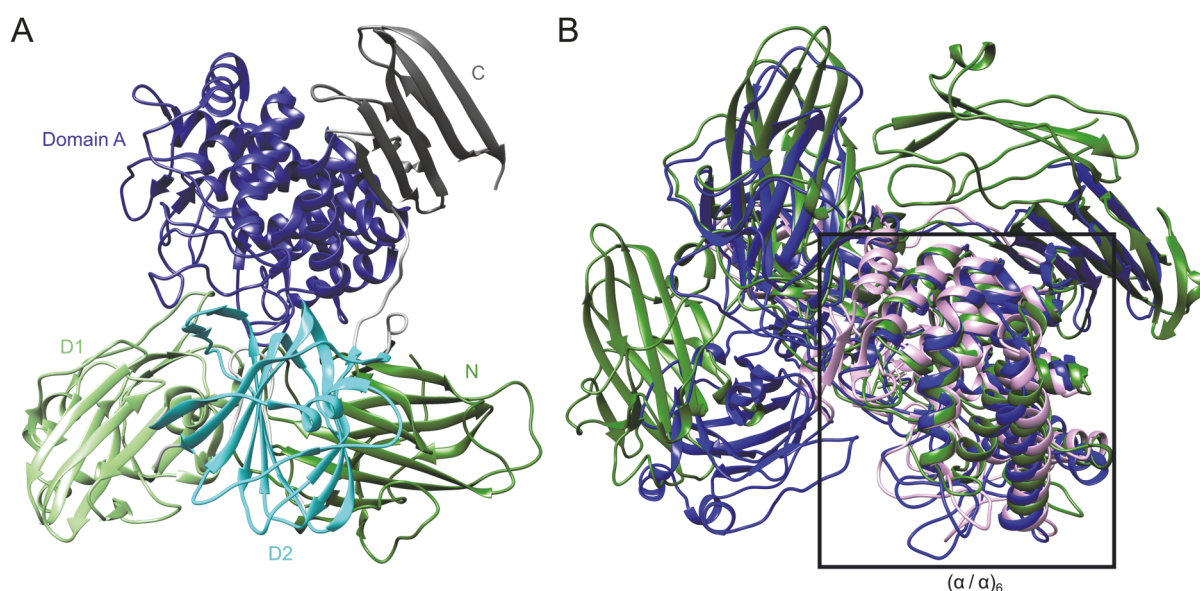


**Figure 21** Domain structure of RhaB of *Bacillus sp.* GL1 (**A**) and structural comparison of GH 78 rhamnosidases (**B**). The five domains, N, D1, D2, A, and C of RhaB (2OKX) are marked in (**A**) by colour. Domain A contains the proposed catalytic residues. In the structural comparison (RhaB, blue, 2OKX; KoRha, lilac, 4XHC; SaRha78A, green, 3W5N) the conserved  $(\alpha/\alpha)_6$  fold characteristic for GH 78 glycosidases is highlighted.<sup>[110-112]</sup>

For the studies of this thesis, the  $\alpha$ -L-rhamnosidase RhaB (sometimes also referred to as BaRhaB) of *Bacillus sp.* GL1 was chosen. Activity of an  $\alpha$ -L-rhamnosidase produced by *Bacillus sp.* GL1 induced by the presence of gellan during cultivation was first described by *Hashimoto et al.*<sup>[113]</sup> The activity was attributed to a protein with a molecular weight of about 100 kDa and an optimal activity at pH 7 and 50 °C. Upon later analysis of the genome, the group identified two  $\alpha$ -L-rhamnosidase genes *rhaA* and *rhaB*.<sup>[114]</sup> The before observed activity was identified as the enzyme product of *rhaB*, as the production of RhaA was not induced by the presence of gellan. Nevertheless, both were shown to accept degraded gellan as substrates for de-rhamnosylation. The identified rhamnosidase RhaB of the glycohydrolase

---

family GH 78 was recombinantly expressed in *E. coli* BL21(DE3)pLysS and further characterised. The enzyme was proposed to act as an inverting glycosidase and exhibited a high affinity towards rhamnose with a  $K_M$  value of 0.28 mM, though also being inhibited by the monosaccharide with a  $K_i$  of 1.8 mM. The enzyme interestingly showed activity towards the flavonoid glycoside naringin (**1c**) producing the naringenin-7-*O*- $\beta$ -D-glucoside (**1b**) by de-rhamnosylation, indicating to a potential industrial application of the enzyme. *Cui et al.* later elucidated the crystal structure of RhaB with and without the presence of rhamnose, which was the first structure to be elucidated of an enzyme of the GH 78 family (Figure 21).<sup>[112, 115]</sup> The group confirmed the size and structural family of the enzyme and showed RhaB to be a homodimer. The monomer itself consists of the five domains N, D1, D2, A and C (in order from the N- to C-terminus). The four Domains N, C, D1 and D2 are small and abundant in  $\beta$ -strands showing  $\beta$ -sandwich motives. The largest and catalytic domain A consists of 15  $\alpha$ -helices and four  $\beta$ -strands folded as a  $(\alpha/\alpha)_6$ -barrel. Based on the structural analysis and mutagenesis experiments the residues D567, E572, W576, D579, and E841 were ascribed a catalytic or substrate recognition function.

## 5.4 Transferring glycans by *endo*- $\beta$ -*N*-acetylglucosaminidases

### 5.4.1 Glycosynthases derived from *endo*- $\beta$ -*N*-acetylglucosaminidases

Different to the *exo*- and *endo*-glycosidases described above, the hydrolytic mechanism of *endo*- $\beta$ -*N*-acetylglucosaminidases (ENGase) follows a substrate-assisted pathway in which the anomeric centre of *N*-acetylglucosamine located in the chitobiose moiety undergoes a nucleophilic attack by the *N*-linked acetyl group creating an oxazoline structure (Figure 23). This kind of activated compound can be employed by mutant forms of the *endo*- $\beta$ -*N*-acetylglucosaminidases, which are deficient in the promotion of the oxazoline formation, as glycan donors in glycosynthetic reactions. Umekawa *et al.* reported the first glycosynthase like form of an *endo*- $\beta$ -*N*-acetylglucosaminidase as the N175A mutant variant of Endo-M (originating from *M. hiemalis*).<sup>[25, 116, 117]</sup>

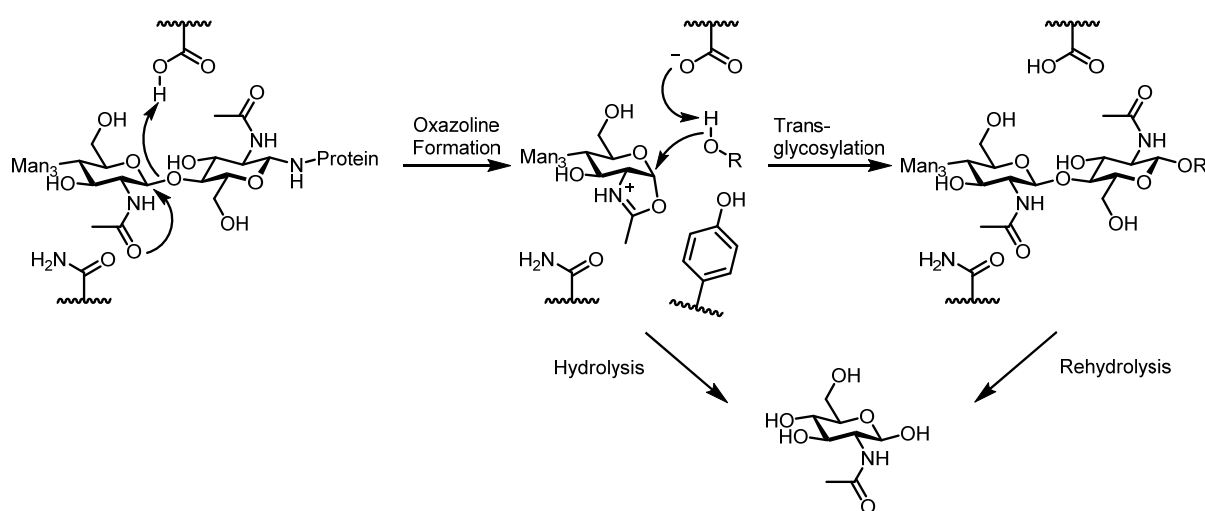


**Figure 22** Hydrolytic and synthetic mechanisms of *endo*- $\beta$ -*N*-acetylglucosaminidases. The enzyme promotes a cleavage by oxazoline formation within the substrate, which can then be hydrolysed by H<sub>2</sub>O or transferred to an acceptor in a transglycosylation. The Asn/Gln residue, conserved throughout GH 85 ENGases, assists in the appropriate orientation of the 2-acetamido group for the oxazoline formation. The hydrolysis of the oxazoline is promoted by the coordination of a water molecule by the conserved tyrosine residue. The transglycosylation product may also be hydrolysed by the same mechanism if the hydrolytic activity of the enzyme is high.

The enzyme was able to utilize the oxazoline donor Man<sub>9</sub>GlcNAc-oxazoline in the synthesis of the HIV-1 gp41 derived glycopeptide Man<sub>9</sub>GlcNAc<sub>2</sub>C<sub>34</sub>, producing the glycopeptide in a yield of 72%. A large improvement for the glycosynthase method using *endo*- $\beta$ -*N*-acetylglucosaminidases was the simplified donor synthesis by Noguchi *et al.*<sup>[118, 119]</sup> The synthesis of the oxazoline structure catalysed by 2-chloro-1,3-dimethylimidazolium chloride (DMC) and later 2-chloro-1,3-dimethyl-1*H*-benzimidazol-3-ium chloride (CDMBI) allowed the production in aqueous solution and without the need of protection groups, therefore ideal for subsequent conversion by enzymatic glycosylation. In 2010, Umekawa *et al.* described a new variant Endo-M N175Q, which exhibited a much higher synthase activity and

transglycosidase activity.<sup>[120]</sup> This enabled the use of natural glycan donors such as the sialoglycopeptide (**20**, SGP), though leading to a lower yield compared to the use of oxazoline donors. The variant enabled the synthesis of a high-mannose (84%) and complex-type glycoform (76%) of the sperm antigen CD52 (**21a/b**) using the GlcNAc-CD52 peptide (**21c**) as the acceptor (Figure 23).

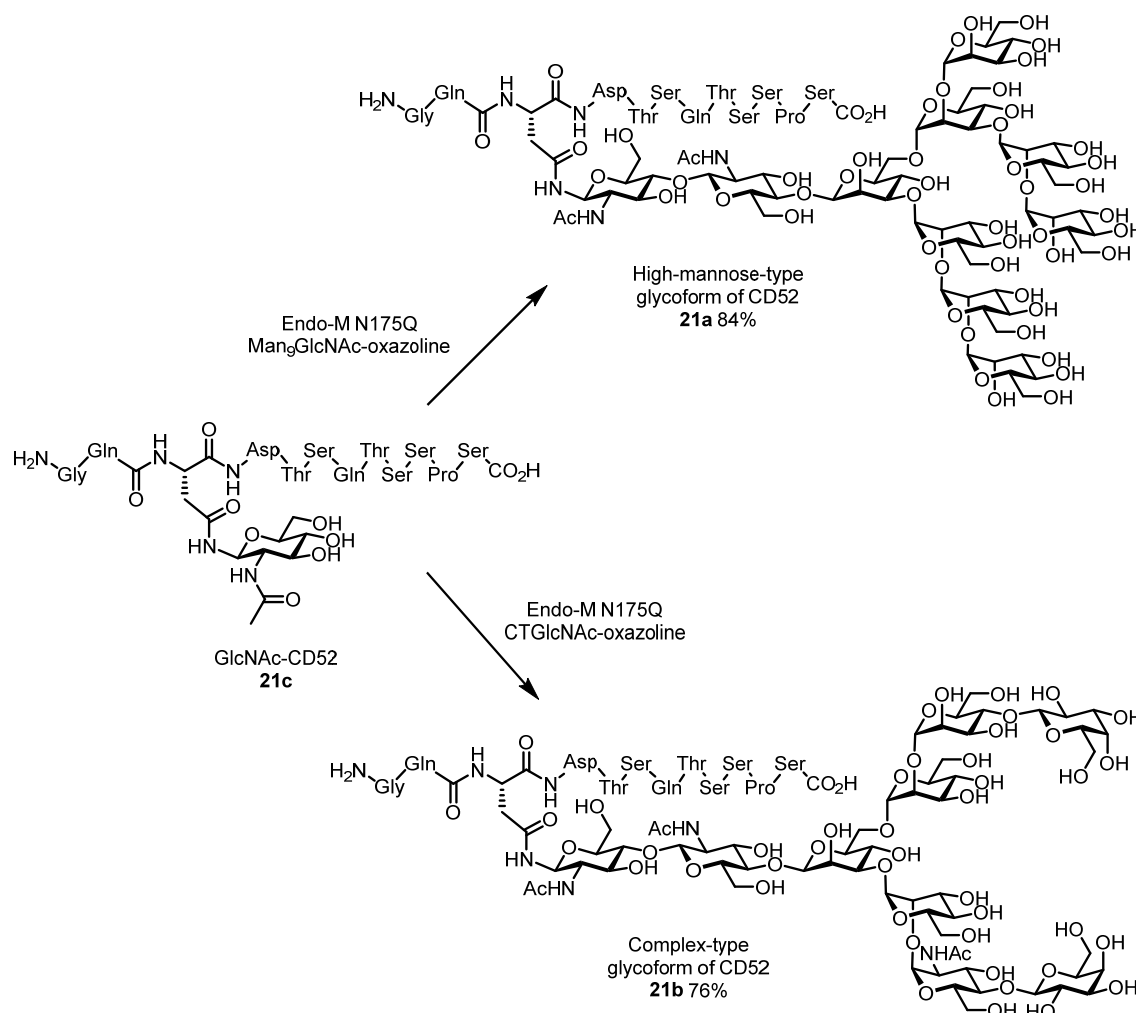


**Figure 23** Synthesis of two glycoforms of the sperm antigen CD52 (**2a/b**) by the *endo*- $\beta$ -*N*-acetylglucosaminidase derived glycosynthase Endo-M N175Q.<sup>[116]</sup> The high-mannose and complex-type glycoforms were produced under utilisation of oxazoline donors and the GlcNAc-CD52 peptide (**21c**).

The group also described the successful synthesis of sialo-complex-type glycoforms of the bioactive peptides PAMP12 and 'Substance P' in high yields (95% and 98%, respectively). The glycosylation reaction was also shown for the protein RNase B bearing a single GlcNAc moiety therefore allowing glycan modification of proteins/enzymes by this method.<sup>[121]</sup> *Amin et al.* also described the production of monoglycoforms of RNase B by the glycosynthase Endo-A N171A (*Arthrobacter protophormiae*) in yields up to 80% with chemically synthesized oxazoline glycans.<sup>[122]</sup> The Endo-M and Endo-A glycosynthase variants were additionally employed in the synthesis of four glycoforms of the glycopeptide pramlintide with yields varying from

59–96% by *Tomabechi et al.*, in an attempt to vary the low circulatory half-life and poor solubility of the pharmaceutical compound.<sup>[123]</sup> The produced glycoforms were tested *in vitro* and *in vivo* and exhibited varying properties in dependency of the type of transferred glycan and its position in the glycopeptide. The glycoform library was subsequently expanded with the same enzymes by *Kowalczyk et al.* to 18 *N*-glycosylated pramlintide analogues bearing either a GlcNAc, pentasaccharide or undecasaccharide residue at different positions of the peptide.<sup>[124]</sup> In comparison to the Endo-A and Endo-M glycosynthases, *Fan et al.* developed a glycosynthase variant of Endo-D originating from *Streptococcus pneumoniae*, which could glycosylate fucosylated GlcNAc residues.<sup>[125]</sup> This unique property allowed the remodelling of the glycans of the IgG Fc-domain. However, the strict substrate specificity for Man<sub>3</sub>GlcNAc oxazoline and not complex-type *N*-glycan oxazolines limits the use of the enzyme greatly. A more variable glycosylation of  $\alpha$ -1,6-fucosylated GlcNAc-polypeptides was demonstrated by *Giddens et al.* with the Endo-F3 mutants D165A/Q.<sup>[126]</sup> The mutant was capable of synthesising asialo-biantennary and complex triantennary core-fucosylated glycoforms of rituximab (intact antibody) in yields over 95%. Further applications, indicating the high potential of the method for the synthesis of pharmaceutical relevant compounds were the chemoenzymatic production of vaccine candidates, the site-selective glycosylation of HIV-1 polypeptide antigen bearing two different glycans (yields up to 95%), the glycan remodelling of human erythropoietin (EPO), and the synthesis of mannose-6-phosphate-containing glycoproteins.<sup>[127-130]</sup> *Tang et al.* impressively demonstrated a one-pot *N*-glycan remodelling of IgG proteins by combining the wild type (*wt*) Endo-M glycosidase with the synthase variant Endo-S D322S.<sup>[131]</sup> This synthesis comprised the donor production by Endo-M catalysed SGP (**20**) hydrolysis, subsequent conversion to the oxazoline with DMC and donor transfer to the protein by Endo-S D322S with near complete conversion within 30 min.

### 5.4.2 Endo-CC — an ENGase with high potential

The transfer of different types of high-mannose and complex type glycans to various acceptor molecules by Endo-M variants leading to homogenously glycosylated compounds has been examined extensively (as described in the section 5.4.1). The use of this enzyme on a larger scale is limited by the high cost of commercially available samples and the low recombinant expression of Endo-M and its variants in *E. coli* strains. *Eshima et al.* described the isolation of a new ENGase Endo-CC from *C. cinerea*, which could act as an alternative to Endo-M for glycan transfer.<sup>[132]</sup> The enzyme was identified by the *in silico* analysis of amino acid sequences of ENGases from different organisms. The ENGase, also from the GH 85 family, shows 46% similarity to Endo-M and hydrolyses high-mannose and biantennary complex-type oligosaccharides, but not asialo-bi-, tri-, and tetraantennary oligosaccharides. The enzyme exhibited high activity at a neutral pH of 7.5 in comparison to the acidic pH in the range of 4–6,

---

which most other *endo*- $\beta$ -*N*-acetylglucosaminidases require for activity. It also exhibited a higher thermal stability, retaining its activity even after an incubation of 10 min at 50 °C. A mutation of the position N180 (equivalent to N175 in Endo-M) produced a mutant with high transglycosylation activities using SGP (**20**) as a glycan donor. *Higuchi et al.* later demonstrated and optimised the use of Endo-CC N180H with a sialo-complex-type oxazoline donor.<sup>[133]</sup> The pH optimum of Endo-CC acted as a great advantage for yield improvement due to the increased stability of the oxazoline donors at this pH. Most recently, *Manabe et al.* examined the acceptor range of Endo-CC N180H.<sup>[134]</sup>

## 6 RESULTS

### 6.1 From hot to cold — searching for optimal glycosynthase conditions by varying temperature optima

The production of  $\beta$ -glucosides has been the most commonly examined reaction catalysed by glycosynthases. Even though many  $\beta$ -glucosynthases have been created with a variety of different properties, methods for the analysis and characterisation are still limited and much research is needed with respect to finding the optimal reaction conditions for these enzymes. In this first chapter, the factor of temperature on the enzymatic glycosylation reaction by glycosynthases was to be examined by the application of glycosidases with varying temperature optima. Mutant variants of two glycosidases, BglC (hyperthermophilic, *P. furiosus*) and BglU (psychrophilic, *M. antarcticus*), originating from extremophile organisms were compared to the mesophilic glycosynthase Abg-E358S (*R. radiobacter*) in order to assess the optimal temperature range for the synthesis of glycosides with glycosynthases. Additionally, an activity assay in a microplate format was to be developed for the characterisation of the potential glycosynthases.

#### 6.1.1 Glucosidase gene isolation

The  $\beta$ -glucosidase Abg of *R. radiobacter* (formerly *A. tumefaciens* / *A. radiobacter*) is a well-characterised glycosyl hydrolase, of which the gene sequence and catalytic active residues have been described. The mutant variant of Abg, Abg E358S, was demonstrated to exhibit glycosynthase activity by *Mackenzie et al.*, catalysing the synthesis of 1,4-glycosidic bonds.<sup>[21]</sup> Therefore, Abg was chosen to create a reference example of a glycosynthase with mesophilic properties. The glucosidase gene *abg* consists of 1401 bp coding for 466 amino acids. In order to create mutant variants of the gene, coding for the glycosynthase variants of Abg, the gene needed to be amplified from the genomic DNA and cloned into an appropriate expression vector. A commercial strain of *R. radiobacter* was obtained from the DSMZ<sup>3</sup> and cultivated to give access to the genomic DNA. Amplification of the gene, from a cell suspension of *R. radiobacter* (colony re-suspended and lysed by heat denaturation) by the polymerase chain reaction (PCR), was first attempted with the *RedTaq® ready mix™*. The primer oligonucleotides were designed for a direct subsequent integration into the pET-21a(+) expression vector via the *Gibson assembly* method.<sup>[135]</sup> The primers therefore contained not only the beginning and end of the *abg* gene (fw- and rev-primer respectively) but also a sequence complementary to the position of insertion in the target vector. The PCR reaction was carried out on a broad scale varying the annealing temperature from 45–55 °C. These first

<sup>3</sup> Leibniz Institute DSMZ-German Collection of Microorganisms and Cell Cultures

reactions did not result in an amplification product of the desired gene. Therefore, the genomic DNA of *R. radiobacter* culture was isolated by a phenol/chloroform extraction. The isolated genomic DNA acted as a template for further PCR reactions towards the amplification of the *abg* gene. Keeping the conditions identical and using the genomic DNA as a template, the PCR still occurred without amplification of the gene. Variation of various parameters, such as the polymerase (*Phire Hot-Start II*, *Phusion High-Fidelity*, Pfu), annealing temperature, buffer system (HF-, GC-buffer), and the addition of DMSO did not yield an amplification product. The *touchdown*-PCR method was applied in case an unspecific binding of the primers to the template was occurring. This method added a set of ten PCR cycles with decreasing annealing temperature (55–45 °C), allowing only specific primer binding at higher temperatures, before running the standard PCR conditions. Nevertheless, the combination of *touchdown*-PCR and different annealing temperatures did not lead to an amplification of the desired gene. To enhance the specificity of the employed primers, the vector overlapping sequence of the primers was removed. As these changes also did not yield the desired result, a further variation of the PCR method to a *nested*-PCR was attempted. Additional primers binding -144 bp upstream and +200 bp downstream of *abg* in the genomic context were designed and applied in a single PCR reaction together with the standard primers binding at the beginning and end of *abg*. The *nested*-PCR generated two distinct amplicons of the expected size of ~1.5 kbp and ~1.4 kbp (Figure 24, **A**).

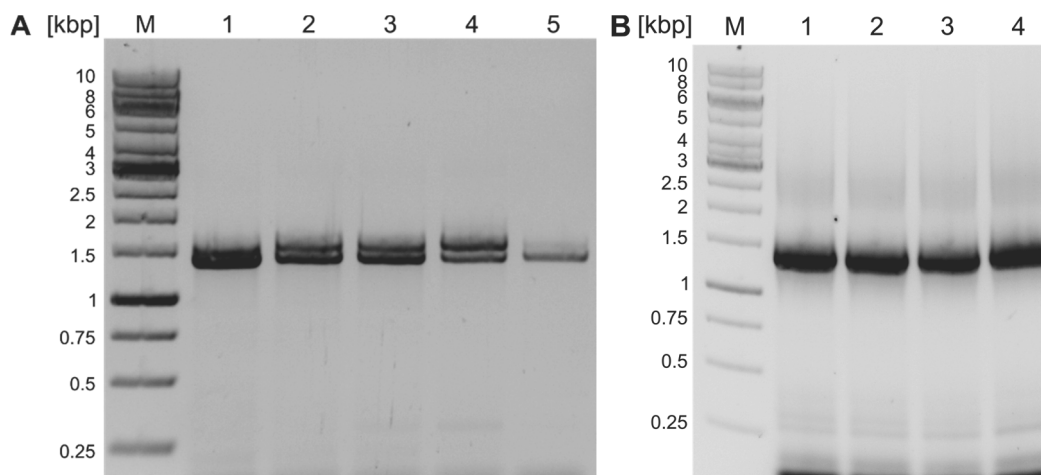


**Figure 24** Amplification of the *abg* gene from genomic DNA of *R. radiobacter* by *nested*-PCR (**A**) and subsequent amplification of the *Gibson assembly* insert (**B**). (**A**) The *nested*-PCR occurred with four primers (#2–4), the *Phire Hot Start II* polymerase, and varying annealing temperatures (1: 48 °C; 2: 51 °C; 3: 55 °C; 4: 59 °C; 5: 63 °C). (**B**) Using the amplicon of the *nested*-PCR as a template, the vector overlapping sequences were added to the gene by primers #1 & 2 (1: 59 °C; 2: 61 °C; 3: 66 °C; 4: 69 °C).

The amplicon mixture of the *nested*-PCR was subsequently utilised in a further PCR reaction as a template in order to add the vector overlapping sequences required for the *Gibson assembly* (Figure 24, **B**). The reaction resulted in an amplicon of the expected size of 1.4 kbp. For the insertion of *abg* into the pET-21a(+) vector (linearized prior with NdeI/XhoI)

via the *Gibson assembly*, different insert to vector ratios were tested leading to strongly differing colony numbers of transformed *E. coli* DH5 $\alpha$  colonies after selection on LB-agar plates containing ampicillin. Twelve of the resulting transformants were checked via colony PCR for the presence of the desired *abg* gene, which was found to be present in a single colony. The high amount of colonies containing only vector without the desired insert indicates strongly to a religation of the vector and therefore to an incomplete restriction of the vector. In addition, the higher concentration of vector and insert shows to be advantageous for the *Gibson assembly* itself. *Sanger*-sequencing verified the correct insertion of *abg* into the vector.

The comparison of hydrolytic and glycosynthetic activity of the *wt* and mutant variants of the mesophilic  $\beta$ -glucosidase Abg was to be carried out with a hyperthermophilic and psychrophilic glycosidase and their possible glycosynthase variants. The comparison is important as many of the substrates and products required or produced by glycosynthases can differ strongly in their thermostability. As an example for a hyperthermophilic glycosidase, the gene of the putative  $\beta$ -glucosidase BglC of *P. furiosus* was provided by the group of *Prof. Elling* of the RWTH Aachen<sup>4</sup>. The *bglC* gene was inserted by *Merker*<sup>4</sup> into the pET-Duet-1 vector between the restriction sites of NcoI and Sall fusing to the vector's sequence of the N-terminal His<sub>6</sub>-tag. The function of the enzyme has been annotated by sequence analysis as a putative  $\beta$ -galactosidase.<sup>[67, 68]</sup> However, initial results of *Merker*<sup>4</sup> indicated to a lack of galactosidase activity and to weak gluco- and xylosidase activity, therefore rendering this enzyme viable as a comparison to Abg even without annotation as a  $\beta$ -glucosidase.

In contrast to thermophilic glycosidases, only scarce amounts of studies on psychrophilic  $\beta$ -glucosidases and their biochemical characterisation can be found throughout the literature.<sup>[136]</sup> A few examples of cold tolerant  $\beta$ -glucosidases of the GH 3 family, such as BglA49 of *Serratia sp.* TN79 (ADK91094) and BglY of *Paenibacillus sp.* C7 (AAX35883), have been characterised biochemically, but the protein structure has not been elucidated making a rational design towards a glycosynthase more difficult.<sup>[137, 138]</sup> For the purposes of this study, the psychrophilic  $\beta$ -glucosidase BglU of *M. antarcticus*, discovered and characterised by *Fan et al.*, was chosen. Additionally to the elucidated crystal structure, the amino acid sequence showed a high similarity to Abg of *R. radiobacter*. A functional screening of a genomic library of *M. antarcticus* in *E. coli* by *Fan et al.* led to the identification of the *bglU* gene. Analysis of the amino acid sequence revealed the typical conserved amino acid sequences [NEP] and [ENG] often found in glycohydrolases in the GH 1 family (Figure 25).

---

<sup>4</sup> RWTH Aachen University, Laboratory for Biomaterials, Institute for Biotechnology and Helmholtz Institute for Biomedical Engineering

The catalytically active residues could therefore be determined to be E170 and E377, acting as the acid/base catalyst and nucleophile residue respectively.

Abg	MTDPQTLAARFPGDFLFGVATASFQIEGATKVDGRKPSIWDAFCNMPGHVFGRHNGDVAC	60
BglU	MMNHLSQKFAWPKEFLWGSATAAAQIEGAGHSYGKEDSVWDAFARKEGAIAGGENLEVAV	60
	* : : : * : ** : * ** : * ** : * : : * : ** : * : * . * : **	
Abg	DHYNRWEDDLDIKEMGVEAYRFSIAWPRIIPDGFPGINEKGLDFYDRLVDGCKARGIKT	120
BglU	DHYHRYREDVQLMRELGLDSYRFSTSWARVVPGR-TVNPEGLDFYSRLVDELLENGILP	119
	** : * : . : * : : * : : * : : * : : * : : * : : * : : * : : * : : * : : *	
Abg	YATLYHWDLPPLTLMGDGGWASRSTAHAFQRYAKTVMARLGDRDLDAVATFNEPWC	180
BglU	WLTLYHWDLPQALEERGGWNTRETSYKFLYAEVHEKLGDRVKHWTTFNEPLCSSLIGY	179
	: * * * * * * * : * * * * : * : * : * . * * : * : * * * : * * * : * : * * * * * : * : : :	
Abg	LYGIHAPGERNMEAALAAMHHINLAHGFVGEASRHVAPKVPVGLVNLNAHSVIPASN-SDA	239
BglU	AAGEHAPGRQEPQAALAAVHHQHHLAHLATARLRELGA-EHIGITLNLNAVPNNPGDPV	238
	* * * * * : : : * * * * * : * * : * * * * : . . . : * : . * * . . . * . . .	
Abg	DMKAAERAFQFHNGAFFDPVFKGEYPAEMMEALGS--RMPVVEAEDLSIISQKLDWWGLN	297
BglU	DLEAARRVDALWNRMYLDPVLRGYPEDLLEDVQQLGLAEVIEAGDLEIISQPIDFLGVN	298
	* : : * * . * . : * : : * * * : : * * * : : * : . * : * * * * . * * * * : * : * : *	
Abg	YYTPMRVADDATEGAEFPATKPAPA-----VSDVKTDIGWEVYA	336
BglU	HYHDDNV-----SGHPLPAGQPQPVVPTDSPKSSPFVVGSEYVTFPARDLPRTAMGWEVNP	353
	: * . * . * . * * : * * * . : * : * * * *	
Abg	PALHSLVETLYERY-ELPDCYITENGACYNMGV-ENGEVDDQPRLDYYAEHLGIVADLVK	394
BglU	EGLRVLLNRLNQDYANLPSLYITENGASVYTDVTEAGTVEDPEREYIILNHLDAVVRAIA	413
	. * : * : * : * : * * . * * * * * . * . * * * * * * : * : * * . * . :	
Abg	DGYPMRGYFAWSLMDNFEWAEGYRMRFGLVHVDYETQVRTLKNSGKWYSALASGFPKGNH	454
BglU	DGVDVRGYFVWSLLDNFEWAAGYAKRFGIIHVDYQTQVRTIKNSGKAYAGLIAANRTMA-	472
	** : * * * . * * * : * * * * * * * * * * : * * * : * * * * * * * * * * * * * : * : . . .	
Abg	GVVKG 459	
BglU	----- 472	

**Figure 25** Alignment of the amino acid sequences of BglU of *M. antarcticus* and Abg of *A. radiobacter* using *Clustal Omega*.<sup>[139]</sup> The conserved catalytic domains found in GH 1 glycohydrolases are highlighted by the coloured boxes (red - domain of acid/base residue; green - domain of nucleophilic residue; \* conserved; : high similarity; . low similarity).

Due to the difficulty in cultivation of psychrophilic strains such as *M. antarcticus*, the *bglU* gene was synthesised commercially and inserted between the NdeI and XhoI restriction sites of pET-21a(+) thereby adding a C-terminal His<sub>6</sub>-tag to the enzyme for later purification via ion metal affinity chromatography (IMAC). As the production of the enzyme was to be conducted heterologous in *E. coli* BL21(DE3), the codons of the *bglU* sequence were optimised for the codon usage of *E. coli* before synthesis of the gene. For this purpose, the method of codon harmonisation was chosen exchanging codons not just to the most frequently used by the host *E. coli*, but more with codons matching the usage within the original organism *M. antarcticus* (Figure 26). The resulting sequence showed 74% identity to the original DNA sequence and a 100% identity for the amino acid sequence. Upon further analysis, the harmonised sequence displayed two new restriction enzyme sites for XhoI (CTCGAG) and BamHI (GGATCC), both relatively commonly used enzymes. In order to avoid later complications, these restriction sites

were removed by inserting silent mutations at the positions 396 (CTC<sub>2</sub>GAG→CTA<sub>2</sub>GAG) and 778 (GGA<sub>1</sub>TCC→GGA<sub>2</sub>CCC) in the nucleotide sequence.

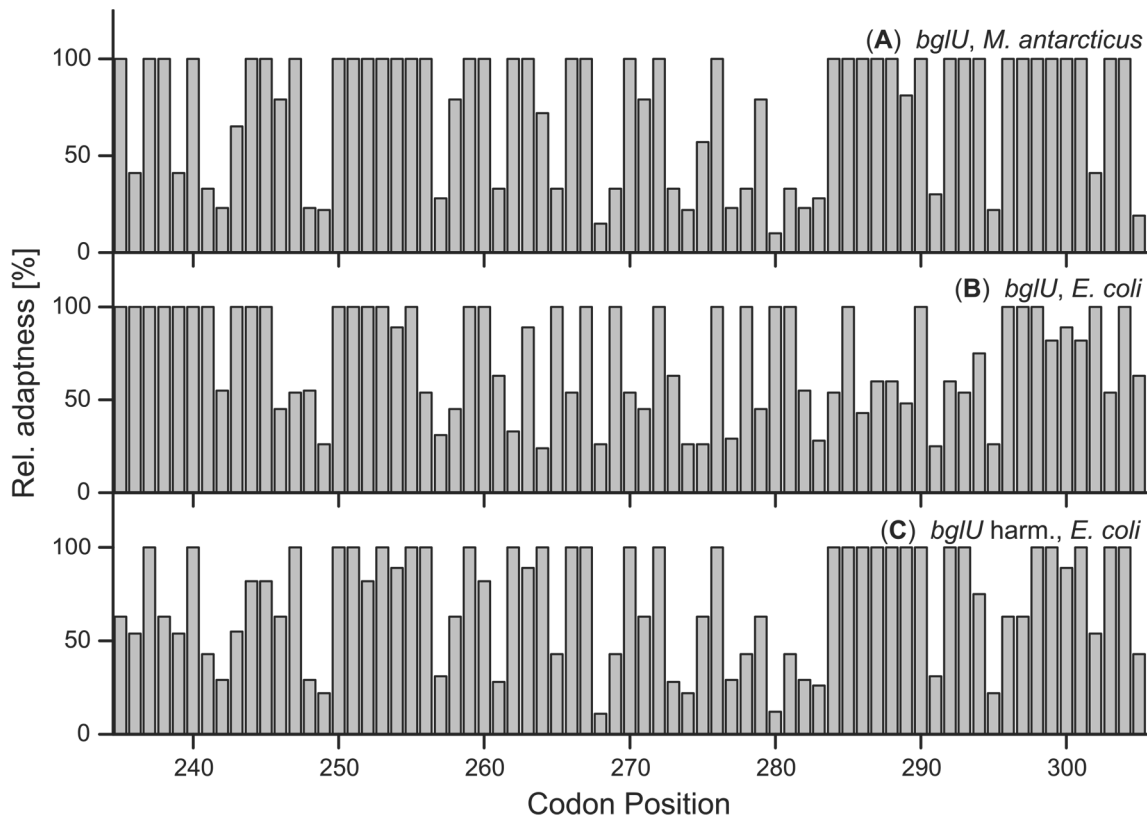


**Figure 26** Excerpt of the codon harmonisation of the gene *bglU* for the heterologous production in *E. coli* BL21(DE3). **(A)** Codon usage of *bglU* in *M. antarcticus*. **(B)** Codon usage of the *bglU* gene in *E. coli* without adaptation of the sequence towards the expression host. **(C)** Codon usage of the harmonised *bglU* sequence for the expression host *E. coli*, which was optimised to match the usage of the original organism. As no data could be found for the codon usage of *M. antarcticus*, the codon usage data of *Micrococcus sp. 28* was chosen as a reference (Appendix 9.2, Figure 118). Data was processed by the online tool *Graphical Codon Usage Analyser* (gcua) of Fuhrmann *et al.*<sup>[140]</sup>

### 6.1.2 Characterisation of the wild type glycosidases

Before mutation of the three  $\beta$ -glucosidases to potential glycosynthases, the wild type (*wt*) enzymes were expressed, isolated, and characterised. Throughout literature, the *wt*  $\beta$ -glucosidases have been characterised with temperature and buffer conditions giving the optimal activity for the natural hydrolysis reaction. Nevertheless, the glycosynthases derived from these characterised enzymes were applied with completely different conditions allowing for an easier analysis and product isolation, though not making the parameters determined for the *wt* glucosidases comparable to the glycosynthase variants. Therefore, the  $\beta$ -glucosidases were characterised using the conditions of the planned glycosynthetic reactions. All glycosidases were incorporated into the expression vector fusing a His<sub>6</sub>-tag to either the C- (Abg and BglU) or N-terminus (BglC) of the enzyme for simple purification of the proteins via IMAC. The expression of the enzymes was carried out in *E. coli* BL21(DE3) under standard expression conditions (25 °C, 24 h, 120 rpm) after induction with isopropyl  $\beta$ -D-1-thiogalactopyranoside (IPTG). The glycosidases Abg and BglU were isolated by IMAC purification, leading to enzyme solutions of high purity.

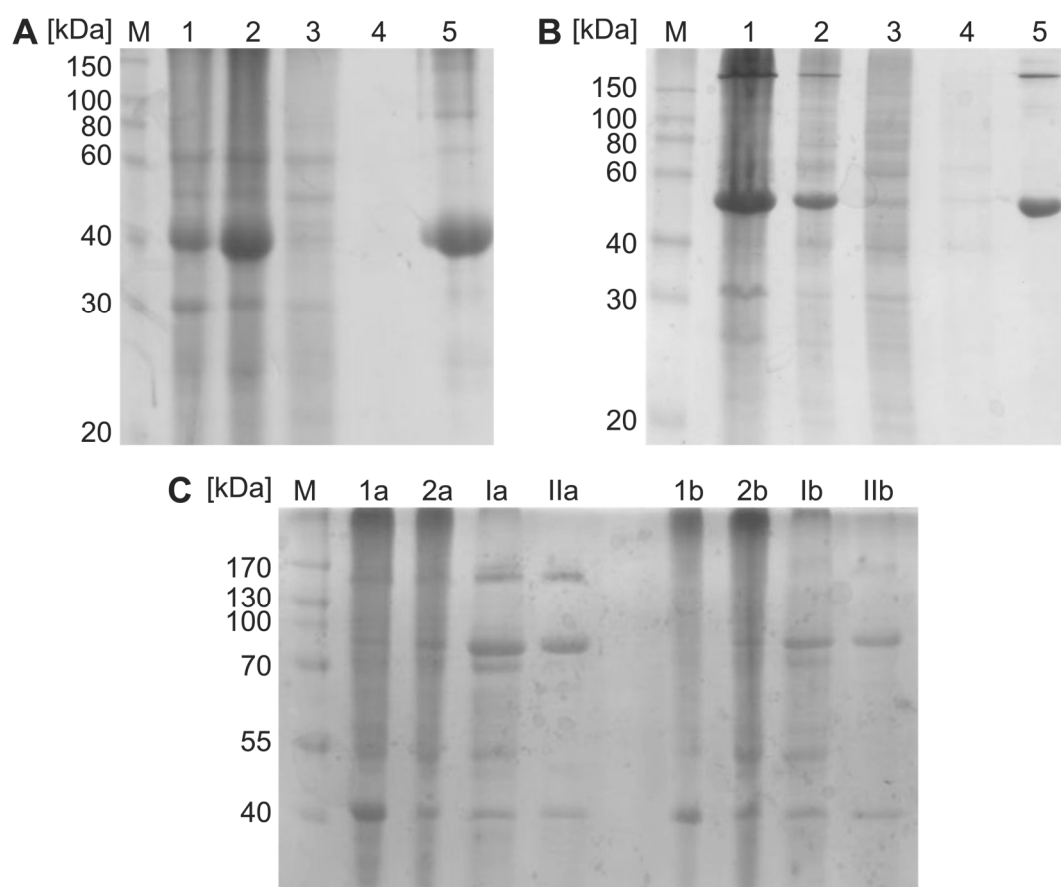


**Figure 27** SDS-PAGE analysis of the IMAC purification of the *wt*  $\beta$ -glucosidases Abg of *R. radiobacter* (A) and BglU of *M. antarcticus* (B) expressed in *E. coli* BL21(DE3). Different steps of the purification are depicted: 1 cell lysate; 2 cell-free lysate; 3 flow-through; 4 wash fraction; 5 elution. Roti-Mark 10–150 was applied as a standard (M) for size determination. The expression of BglC of *P. furiosus* (C) is shown for expression in *E. coli* BL21(DE3) (a) and *E. coli* Rosetta™ 2 (b). The enzyme was purified by heat-denaturation (1a/b: 30 min, 75 °C; 1b/a: 30 min, 85 °C).

SDS-PAGE analysis indicated to proteins with a molecular weight of 40 and 56 kDa for Abg and BglU respectively, roughly corresponding to the molecular weights found in literature (Figure 27, **A & B**). The lower molecular weight of Abg observed in the SDS-PAGE may have been caused by inhomogeneity of the polyacrylamide gel, but also by the high concentration of the loaded protein sample. After a buffer-exchange *via* ultrafiltration, enzyme solutions with protein concentrations of  $3.3 \pm 2.3 \cdot 10^{-1}$  mg/mL of Abg and  $1.4 \pm 3.7 \cdot 10^{-1}$  mg/mL of BglU could be obtained.

Due to the hyperthermophilic properties of putative  $\beta$ -galactosidase BglC, a simplified purification utilising heat-denaturation could be implemented. After expression, the cells were disrupted *via* sonification and subsequent to removal of the cell debris, the solution was heated to 75 °C (30 min) and then further to 85 °C (30 min). The heat-denaturation process removed a large amount of the undesired proteins from the solution, leaving the desired protein of ~85 kDa in a near constant amount, which could be easily observed by SDS-PAGE analysis (Figure 27, **Ca**). As the gene sequence of *bglC* was not harmonised to the codon usage of *E. coli*, the expression was repeated in *E. coli* Rosetta™ 2 in order to compensate for the rare codons of the *bglC* sequence. Analysis of the purification steps show, when expressed in Rosetta™ 2, a slightly better purification can be achieved after the heat-denaturation steps (Figure 27; **Cb**). The heat-denaturated solutions are, compared to the expression using *E. coli* BL21(DE3), near free of the protein band at 135 kDa. Nevertheless, even with near identical specific activities the expression of BglC in *E. coli* Rosetta™ 2 led to a lower protein concentration of 1.2 mg/mL than when expressed in *E. coli* BL21(DE3) (2.2 mg/mL).

To evaluate the purification of the  $\beta$ -glycosidases, the protein concentration and specific activity of each purification step fraction was analysed (Table 3). In each case, the protein concentration decreased largely due to the removal of impurities (cellular proteins, cell debris) from the enzyme solution. The increase of the specific activity for each enzyme also pointed to a successful purification of the desired  $\beta$ -glycosidase. The highest increase of specific activity could be observed for BglC increasing 8.4× from  $1.2 \cdot 10^{-3} \pm 3.0 \cdot 10^{-4}$  U/mg in the cell lysate to  $10.3 \cdot 10^{-3} \pm 1.65 \cdot 10^{-3}$  U/mg in the final enzyme solution (after heat-denaturation II, activity towards *pNPXyl 5i*). Yet, the highest specific activity could be observed for the mesophilic  $\beta$ -glucosidase Abg, exhibiting an activity of  $20.3 \pm 1.73$  U/mg towards *pNPGlc 5h*.

**Table 3** Parameters determined for the evaluation of the protein purification of the  $\beta$ -glycosidases Abg, BglU and BglC. The specific activity was determined for the hydrolysis of *p*NPGlc **5h** and *p*NPXyl **5i** for Abg and BglU, and BglC respectively.

$\beta$ -Glycosidase	Fraction	Protein conc. [mg/mL]	Spec. activity [U/mg]	Purification factor
Abg <sup>a</sup>	Cell-free lysate	12 $\pm$ 2.2	5.9 $\pm$ 1.2	1 $\times$
	Flow-through	4.7 $\pm$ 1.8 $\cdot$ 10 <sup>-1</sup>	0.1 $\pm$ 1 $\cdot$ 10 <sup>-2</sup>	—
	Wash	1.2 $\pm$ 11 $\cdot$ 10 <sup>-2</sup>	2.7 $\cdot$ 10 <sup>-1</sup> $\pm$ 3.0 $\cdot$ 10 <sup>-2</sup>	—
	Elution	3.3 $\pm$ 2.3 $\cdot$ 10 <sup>-1</sup>	2.0 $\cdot$ 10 <sup>1</sup> $\pm$ 1.7	3.4 $\times$
	2 <sup>nd</sup> Wash	8.4 $\cdot$ 10 <sup>-1</sup> $\pm$ 3.0 $\cdot$ 10 <sup>-2</sup>	2.5 $\pm$ 2.4 $\cdot$ 10 <sup>-1</sup>	—
BglU <sup>b</sup>	Cell-free lysate	116 $\pm$ 6.75	0.34 $\pm$ 0.07	1
	Flow-through	40 $\pm$ 1.0	0.0 $\pm$ 2 $\cdot$ 10 <sup>-4</sup>	—
	Wash	1.31 $\pm$ 0.09	0.01 $\pm$ 1.8 $\cdot$ 10 <sup>-3</sup>	—
	Elution	2.9 $\pm$ 1.8 $\cdot$ 10 <sup>-1</sup>	1.4 $\pm$ 3.7 $\cdot$ 10 <sup>-1</sup>	4.1 $\times$
BglC <sup>c</sup>	Cell lysate	21 $\pm$ 3.0	1.2 $\cdot$ 10 <sup>-3</sup> $\pm$ 3.0 $\cdot$ 10 <sup>-4</sup>	1 $\times$
	Cell-free	15 $\pm$ 7.0 $\cdot$ 10 <sup>-1</sup>	1.7 $\cdot$ 10 <sup>-4</sup> $\pm$ 2.0 $\cdot$ 10 <sup>-5</sup>	—
	Heat-Denat. I <sup>d</sup>	3.7 $\pm$ 3.0 $\cdot$ 10 <sup>-1</sup>	2.4 $\cdot$ 10 <sup>-3</sup> $\pm$ 2.4 $\cdot$ 10 <sup>-4</sup>	2.0 $\times$
	Heat-Denat. II <sup>e</sup>	1.7 $\pm$ 2.0 $\cdot$ 10 <sup>-1</sup>	10 $\cdot$ 10 <sup>-3</sup> $\pm$ 1.7 $\cdot$ 10 <sup>-3</sup>	8.4 $\times$

<sup>a</sup> 25 °C, NH<sub>4</sub>HCO<sub>3</sub>-buffer 150 mM, pH 7.9, **5h** 18 mM; <sup>b</sup> 25 °C, KP<sub>i</sub>-buffer 50 mM, pH 7, **5h** 36 mM; <sup>c</sup> 85 °C, citrate-phosphate-buffer (35 mM and 128 mM), pH 6, **5i** 4 mM; <sup>d</sup> 30 min, 75 °C; <sup>e</sup> 30 min, 85 °C

While the mesophilic and psychrophilic  $\beta$ -glucosidases, Abg and BglU, respectively, have already been characterised in literature by *Withers et al.* and *Fan et al.*, the hyperthermophilic BglC on the other hand has not yet been biochemically characterised.<sup>[62, 81, 125]</sup> When looking into literature, the function of the *bg/C* gene was derived from sequential analysis and annotated as a putative  $\beta$ -galactosidase.<sup>[141]</sup> Contrary to this annotation, the isolated enzyme did not exhibit any hydrolytic activity towards *p*-nitrophenyl  $\beta$ -D-galactopyranoside (**5g**, *p*NPGal), but rather to *p*NPGlc **5h** and *p*NPXyl **5i** with activities of  $2.2 \cdot 10^{-2} \pm 3.1 \cdot 10^{-3}$  U/mL and  $1.8 \cdot 10^{-2} \pm 2.3 \cdot 10^{-3}$  U/mL, respectively (incubation at 85 °C, Figure 28).

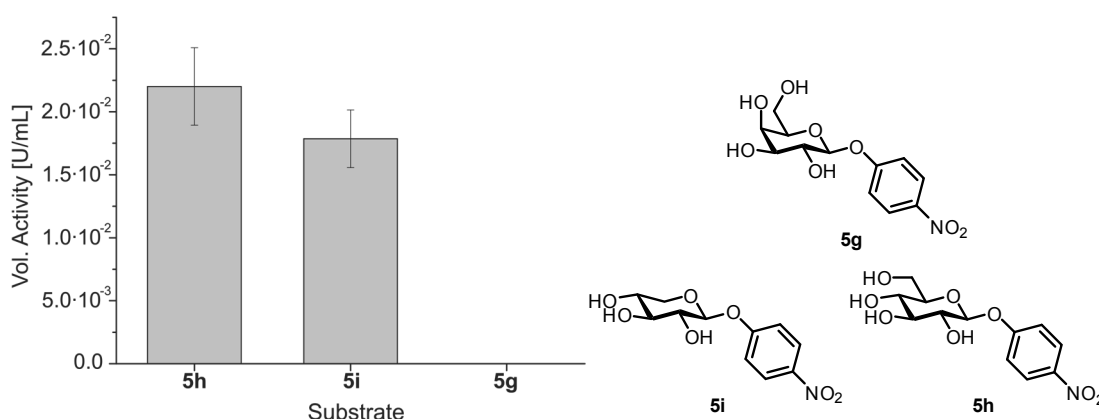


**Figure 28** Volumetric activity of BglC towards *p*-nitrophenyl  $\beta$ -glycopyranosides **5g–i**. The reaction mixture was incubated in citrate-phosphate-buffer (pH 6) at 85 °C with 4 mM substrate for 5 min.

The exhibited activity of BglC clearly illustrates a mistake in the annotation of the enzyme, as no galactosidase activity could be observed despite the similarity of homologues in this glycohydrolase family (GH 35). As the enzyme exhibited the highest activity towards *p*NPGlc **5h**, an annotation as a  $\beta$ -glucosidase would be more appropriate. Nevertheless, the low activity exhibited towards *p*NPGlc **5h** and *p*NPXyl **5i** by BglC can indicate to a natural substrate different to the tested glycosides **5g–i**. Furthermore, the storage and temperature stability of BglC was examined to further characterise the enzyme. Storage of the enzyme solution was examined at 4 °C or -20 °C either containing 50% glycerol (v/v) or being flash frozen or lyophilised. The  $\beta$ -glucosidase showed a high stability towards freezing, with only a decrease of initial activity by 21% after flash freezing in liquid nitrogen and after subsequent lyophilisation. High stability was also observed in solution at 4 °C and -20 °C containing 50% glycerol (v/v) retaining near 100% activity after 15 days of storage. It must be noted, that the storage of enzyme solutions by addition of 50% glycerol, even though effective, was excluded in further experiments of this thesis. The cryo-protectant can also act as an acceptor molecule for potential glycosynthases and is difficult to remove from the reaction products after a glycosynthetic reaction. A short-term stability was determined for BglC at a reaction temperature of 85 °C, which was described by *Elling* and co-workers as the optimal temperature for BglC. The enzyme retained 90% hydrolytic activity after 1 h incubation at 85 °C. Further incubation up to 3 h caused a decrease of the hydrolytic activity down to 54%, indicating a poor suitability of the enzyme for long reaction times.

To compare the three isolated  $\beta$ -glucosidases, the temperature dependency was determined with respect to the hydrolytic activity towards glucoside **5h** (Figure 29). The lowest activity (max.  $3.2 \cdot 10^{-2} \pm 1.0 \cdot 10^{-3}$  U/mg) and highest temperature dependency (83% activity decrease from 85 °C to 65 °C) was observed for the hyperthermophile BglC. Temperatures above 85 °C were omitted from these studies, on the one hand due to evaporation of buffer causing measurement difficulties, on the other hand as higher temperatures are not suited well for future glycosynthase experiments with thermolabile substrates [e.g. the donor substrate  $\alpha$ -D-glucopyranosyl fluoride (**2a**)]. The psychrophilic BglU exhibited maximal activity at 35 °C with  $7.5 \pm 0.2$  U/mg. The highest temperature dependent activity was observed for the mesophilic  $\beta$ -glucosidase Abg showing an activity of  $64 \pm 6.1$  U/mg at 45 °C. With respect to glycosynthetic reactions, reaction conditions at around 25 °C would be desired as this would be the most energy efficient and keep the autohydrolysis of the glycosyl fluoride donors low. Only the mesophilic Abg and psychrophilic BglU exhibited activity ( $19 \pm 3.0 \cdot 10^{-1}$  and  $3.7 \pm 0.1$  U/mg at 25 °C, respectively) at this desired reaction condition.

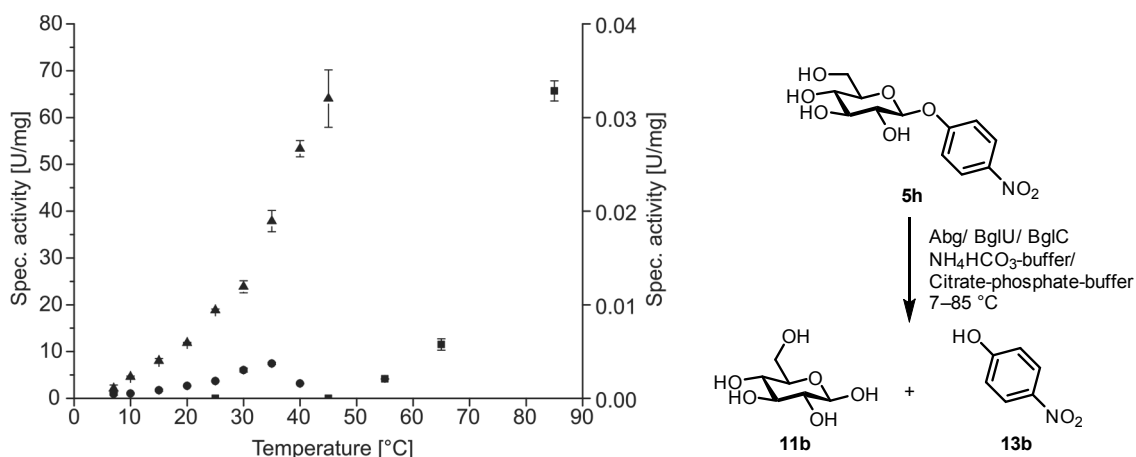


**Figure 29** Temperature dependency of the hydrolytic activity of  $\beta$ -glucosidases Abg, BglU ( $\blacktriangle$  and  $\bullet$  respectively, left y-axis) and BglC ( $\blacksquare$ , right y-axis). The activity of each enzyme was determined for *p*NPGlc **5h** (20 mM for Abg and BglU,  $\text{NH}_4\text{HCO}_3$ -buffer 150 mM, pH 7.9; 40 mM for BglC, citrate-phosphate-buffer, pH 6.5). Activity was determined in triplicate by measurement of released *p*-nitrophenol (**13b**).

For a more effective comparison of the three isolated  $\beta$ -glucosidases, kinetic parameters such as  $v_{\max}$ ,  $k_{\text{cat}}$ ,  $K_M$ ,  $K_i$  and the resulting catalytic efficiency  $k_{\text{cat}}/K_M$  of each enzyme were determined (Figure 30, Table 4). The highest parameters were observed for the mesophilic enzyme Abg with a  $v_{\max}$  of  $23 \pm 2.1 \cdot 10^{-1}$  U/mg and a catalytic efficiency of  $18.2 \pm 1.01$   $\text{s}^{-1} \cdot \text{mM}^{-1}$ . These results align well with the initial activity measurements at fixed substrate concentrations. Nevertheless, the kinetic analysis indicated to a high substrate-excess inhibition by the glucoside **5h**, showing a  $K_i$  value of  $1.9 \cdot 10^2 \pm 0.0$  M, which was determined by fitting the kinetic data by using substrate-excess-inhibition formula derived by Murray (Equation 1).<sup>[142]</sup>

$$\text{Equation 1} \quad v = \frac{v_{\max}}{\left(1 + \left(\frac{K_M}{S}\right) + \left(\frac{S}{K_i}\right)\right)}$$

## 6 Results

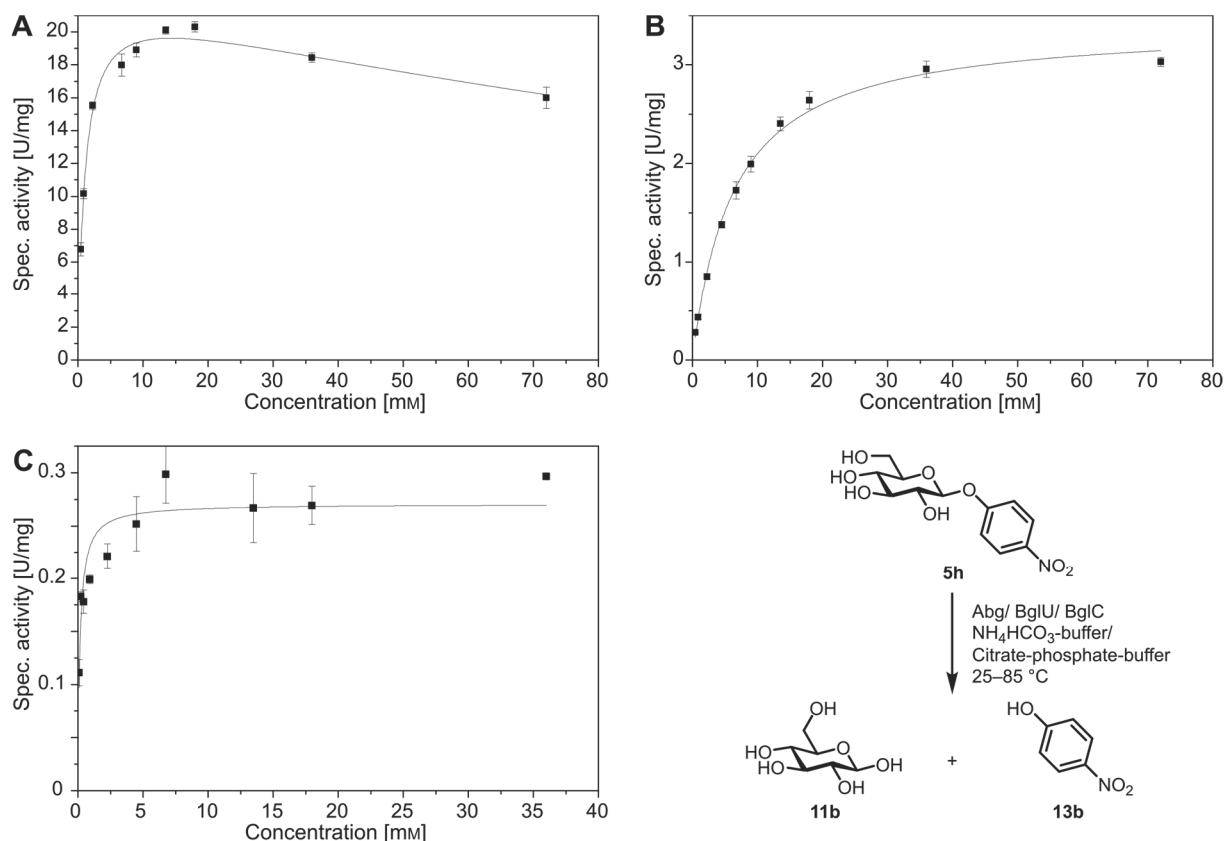


**Figure 30** Characterisation of the kinetic parameters of Abg (**A**), BglU (**B**), and BglC (**C**) for the hydrolysis of *p*NPGlc **5h**. Parameters were determined for Abg and BglU in  $\text{NH}_4\text{HCO}_3$ -buffer (150 mM, pH 7.9) at 25 °C, and for BglC in citrate-phosphate-buffer (35 mM, 128 mM respectively, pH 6) at 85 °C.

**Table 4** Summary of the kinetic parameters determined for the wild type  $\beta$ -glycosidases Abg, BglU, and BglC. Parameters were determined towards *p*NPGlc **5h** for Abg and BglU in  $\text{NH}_4\text{HCO}_3$ -buffer (150 mM, pH 7.9), and for BglC in citrate-phosphate-buffer (35 mM, 128 mM respectively, pH 6). For  $v_{\text{max}}$ ,  $K_{\text{M}}$ , and  $K_{\text{i}}$  the errors are uncertainties from least-square fitting of triplicate data. The errors for  $k_{\text{cat}}$  and  $k_{\text{cat}}/K_{\text{M}}$  were determined by error-propagation from their parental parameters.

	$v_{\text{max}}$ [U/mg]	$k_{\text{cat}}$ [ $\text{s}^{-1}$ ]	$K_{\text{M}}$ [mM]	$K_{\text{i}}$ [M]	$k_{\text{cat}}/K_{\text{M}}$ [ $\text{s}^{-1}\cdot\text{mM}^{-1}$ ]
Abg	$23 \pm 2.1 \cdot 10^{-1}$	$20 \pm 1.8 \cdot 10^{-1}$	$1.1 \pm 5.0 \cdot 10^{-2}$	$1.9 \cdot 10^2 \pm 0.0$	$18 \pm 1.01$
BglU	$3.4 \pm 5.0 \cdot 10^{-2}$	$3.1 \pm 5.0 \cdot 10^{-2}$	$6.3 \pm 2.8 \cdot 10^{-1}$	—	$4.8 \cdot 10^{-1} \pm 3.0 \cdot 10^{-2}$
BglC	$2.7 \cdot 10^{-1} \pm 1.0 \cdot 10^{-2}$	$4.1 \cdot 10^{-1} \pm 2.3 \cdot 10^{-2}$	$1.6 \cdot 10^{-1} \pm 2.0 \cdot 10^{-2}$	—	$2.5 \pm 4.0 \cdot 10^{-1}$

The psychrophilic BglU exhibited a maximal activity at  $3.2 \pm 5.0 \cdot 10^{-2}$  U/mg, which is 6.6 $\times$  lower than the maximal activity of Abg. In combination with a lower affinity to *p*NPGlc **5h** ( $K_{\text{M}} = 6.3 \pm 2.8 \cdot 10^{-1}$  M), the catalytic efficiency of BglU was very low at  $4.8 \cdot 10^{-1} \pm 3.0 \cdot 10^{-2}$   $\text{s}^{-1}\cdot\text{mM}^{-1}$ . The inhibition of the hydrolytic activity by *p*NPGlc **5h** could also be observed for BglU, though the theoretical value of  $K_{\text{i}}$  being far above the solubility range of compound **5h**, hindering the reliable determination of the inhibition constant. The lowest turnover number of  $4.1 \cdot 10^{-1} \pm 2.3 \cdot 10^{-2}$   $\text{s}^{-1}$  (even at 85 °C) was exhibited by BglC, partially compensated by the high affinity of *p*NPGlc **5h** ( $K_{\text{M}} = 1.6 \cdot 10^{-1} \pm 2.0 \cdot 10^{-2}$  mM) resulting in a catalytic efficiency of  $2.5 \pm 4.0 \cdot 10^{-1}$   $\text{s}^{-1}\cdot\text{mM}^{-1}$ .

### 6.1.3 Structural analysis and mutagenesis of the $\beta$ -glucosidases

In order to transform a glycosidase to a glycosynthase the natural hydrolytic activity of the glycosidase needs to be eliminated. The intact overall structure of the mutated glycosidase is able to facilitate the regio-specific transfer of a glycosyl donor onto an acceptor molecule. This was first demonstrated by *Mackenzie et al.* and *Planas et al.* for the  $\beta$ -glucosidases Abg of *R. radiobacter* (then known as *Agrobacterium sp.*) and HiCel7B of *Humicola insolens* and has since been transferred to various glycosidases.<sup>[21, 22]</sup> For retaining glycosidases, the nucleophilic catalytic residue is most commonly exchanged for a non-nucleophilic residue, in order to knock-out the hydrolytic activity and enable glycosynthetic activity. This approach was applied successfully to Abg by replacing the nucleophilic glutamate residue at position E358 with a non-nucleophilic alanine or less nucleophilic serine. A transfer of this method was taken into account for the psychrophilic BglU (GH 1) and hyperthermophilic BglC (GH 35), as these are both part of glycohydrolase families with retaining mechanisms.

As afore mentioned, the mesophilic  $\beta$ -glucosidase Abg of *R. radiobacter* was one of the first glycosidases to be transformed into a glycosynthase by *Mackenzie et al.*<sup>[21]</sup> The catalytic residues were determined and replaced by mutation with non-nucleophilic residues. The Abg variant E358A was found to transfer  $\alpha$ -D-glucopyranosyl fluoride (**2a**,  $\alpha$ -GlcF) and  $\alpha$ -D-galactopyranosyl fluoride (**2b**,  $\alpha$ -GalF) onto various aryl glycoside acceptors. Further variants were tested and characterised for the transferal of  $\alpha$ -GalF **2b** onto glycoside acceptors. Following this example, the corresponding codon for E358 in *abg* was mutated by *QuikChange*<sup>TM</sup>-PCR resulting in the *abg* variants coding for Abg-E358A and Abg-E358S (Table 5). The mutations of the *abg* gene were verified by *Sanger*-sequencing.

**Table 5** Mutation of the nucleophilic amino acid residues E358 of Abg of *R. radiobacter*. The mutations were acquired by *QuikChange*<sup>TM</sup>-PCR by mutation of the wild type gene in a pET-21a(+) vector. Obtained plasmids were sequenced for confirmation of the resulting mutation.

Original AA	Introduced mutation	Codon variation	Verification
E358	A	GAA $\rightarrow$ GCG	+
	S	GAA $\rightarrow$ AGC	+

As the crystal structure of the putative  $\beta$ -galactosidase BglC was and still is not elucidated, the identification of the catalytically active residues was required by comparison of the BglC amino acid sequence with other homologous  $\beta$ -galactosidase structures. The amino acid sequence of BglC shows parts of the conserved domain structure GanA which is most commonly attributed to  $\beta$ -galactosidases.<sup>[143]</sup> An amino acid sequence similarity based classification of BglC of the carbohydrate-active enzyme database (CAZy) pointed to the GH-A clan [glycohydrolases containing a ( $\beta$  /  $\alpha$ )<sub>8</sub>-fold] and the glycohydrolase family GH 35.<sup>[70, 71]</sup> A first

comparison of the amino acid sequence of BglC was carried out with the sequences and the elucidated protein structures of four GH 35  $\beta$ -galactosidases of *Solanum lycopersicum*<sup>[144]</sup>, *Homo sapiens*<sup>[145]</sup>, *Bacteroides thetaiotaomicron*<sup>[146]</sup>, and *S. pneumoniae*<sup>[147]</sup>. Even though these enzymes show a low sequence identity to BglC (e.g. 16.0% for Hs- $\beta$ -gal of *H. sapiens*), the comparison led to three conserved residues, which were candidates for mutation towards a glycosynthase variant of BglC (Figure 31, **E**). The residues corresponded to the amino acid positions E97, E173, and E300 in the sequence of BglC. Noteworthy at this point is the close proximity of the positions E188 and E268 (E173 and E300 in BglC) to the anomeric centre of the galactose molecule, which points to the high likelihood of these being the catalytic acid/base and nucleophilic residue. These two residues also share the conserved positions with respect to the nucleophilic and acid/base residues of GH 35 glycosidases (Figure 31, **F**). A recent publication by *Mine et al.* has introduced the structures of two  $\beta$ -glucosaminidases, GlmA<sub>TK</sub> and GlmA<sub>PH</sub> originating from *Thermococcus kodakaraensis* und *P. horikoshii*.<sup>[148]</sup> Comparing these glycosidases, also belonging to the GH 35 family, with the sequence of BglC, a high sequence identity 81.3% and 61.9% (GlmA<sub>PH</sub> and GlmA<sub>TK</sub> respectively) could be found. Due to the high sequence identity of BglC with these  $\beta$ -glucosaminidases, the identical comparison of structures and sequences, carried out for GlmA<sub>TK</sub> and GlmA<sub>PH</sub> by *Mine et al.*, was applied to the amino acid sequence of BglC (Figure 31).

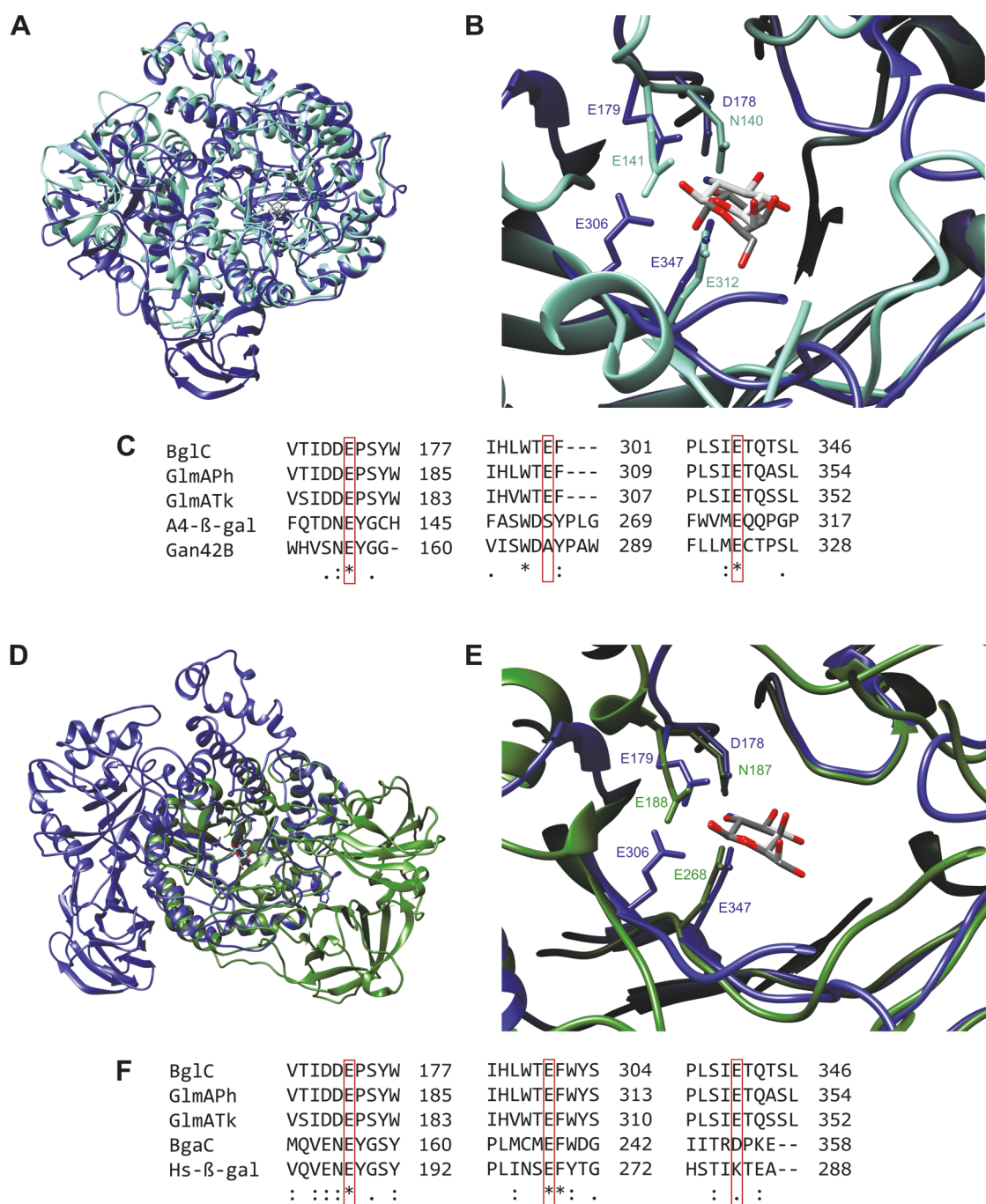


**Figure 31** Structural analysis and sequence alignment of BglC with GH 35 and GH 42 glycosidases for the determination of the acid/base and nucleophile residue. The structure of GlmA<sub>TK</sub> acts representative for BglC due to the high sequence identity. **A:** Overview of the structure alignment GlmA<sub>TK</sub> (*T. kodakaraensis*, 5GSM, blue) with GH 42 A4-β-gal (*Thermus thermophilus*, 1KWK, cyan). **B:** Close up of the superimposed active sites of GlmA<sub>TK</sub> and A4-β-gal. The potential catalytic and conserved residues are depicted and marked respectively. **C:** Excerpt of the amino acid alignment of BglC with GlmA<sub>TK/Ph</sub>, A4-β-gal, and Gan42B (*G. stearothermophilus*, 4OIF) showing potential conserved catalytic residues (red box, \* conserved; : high similarity; . low similarity; via *Clustal Omega*).<sup>[139]</sup> **D:** Overview of the alignment of GlmA<sub>TK</sub> (blue) with GH 35 Hs-β-gal (*H. sapiens*, 3THC, green). **E:** Close up of the superimposed active sites of GlmA<sub>TK</sub> and Hs-β-gal. The potential catalytic and conserved residues are depicted and marked respectively. **F:** Excerpt of the amino acid alignment of BglC with GlmA<sub>TK/Ph</sub>, Hs-β-gal, and BgaC (*S. pneumoniae*, 4E8C) showing potential conserved catalytic residues (red box, \* conserved; : high similarity; . low similarity; via *Clustal Omega*).<sup>[139]</sup>

As was discovered for GlmA<sub>TK</sub> and GlmA<sub>Ph</sub>, the sequence alignment showed conserved sequences for the acid/base and nucleophile residues of the TIM-barrel domain [(β/α)<sub>8</sub>-fold]

of the GH 42 glycosidases A4- $\beta$ -gal and Gan42B (Figure 31, **C**). This alignment would designate the residues E173 and E342 of BglC as the acid/base and nucleophile residue respectively. Nevertheless, the alignment of the BglC sequence with the GH 35 galactosidases Hs- $\beta$ -gal and BgaC, as mentioned above, also showed conserved sequences for the acid/base and nucleophile residues of GH 35 galactosidases, designating these roles to the residues E173 and E300 (Figure 31, **F**). An equivalent of the position E342 could not be found and is therefore not conserved in the GH 35 galactosidases as was also stated by *Mine et al.* when comparing the  $\beta$ -glucosaminidases to these sequences. The structural analysis of GlnA<sub>TK</sub> compared to the structure of GH 35 galactosidases, revealed the position of the E347 residue (corresponding to E342 in BglC and the conserved nucleophile position in GH 42 galactosidases) to take up the same position as the nucleophilic residue in the GH 35 galactosidases. The E306 residue (corresponding to E300 in BglC and the conserved nucleophile position in GH 35 galactosidases) is located in a different position, taking part in the catalysis by electrostatic interaction with the substrate (thereby lowering the activation energy of the chemical transformation). Due to the high similarity of BglC to the  $\beta$ -glucosaminidases, it can be assumed that the positions E173 and E342 are most likely to be the acid/base and nucleophile residues respectively, and position E300 will facilitate the catalysis in a similar way to the E306 residue in GlnA<sub>TK</sub>. The resemblance of BglC to GlnA<sub>Ph</sub> and GlnA<sub>TK</sub> also explains the observed hydrolytic activities of BglC described during the characterisation of the *wt* enzyme (section 6.1.2). Both  $\beta$ -glucosaminidases exhibit no galactosidase activity and GlnA<sub>TK</sub> was reported to exhibit very weak  $\beta$ -glucosidase activity, similar to the observation made for BglC in this thesis.<sup>[149]</sup> A second indication, supporting the assumption of BglC being a  $\beta$ -glucosaminidase, can be found in a further analysis of the amino acid sequence. The aspartate residue D172 which precedes the acid/base residue E173 in BglC, usually an asparagine (N) residue in GH 35 glycosidases, is also present in GlnA<sub>TK</sub> and GlnA<sub>Ph</sub>. The negative charge of this residue stabilises the binding and recognition of a  $\beta$ -D-glucosamine glycoside, which holds a positively charged amino group at the C<sub>2</sub>-position when located in the active site pocket of the  $\beta$ -glucosaminidase.

As the characterisation and mutagenesis of BglC, presented in this thesis, was carried out before the publication of the  $\beta$ -glucosaminidase structures elucidated by *Mine et al.*, the presented mutagenesis of BglC focuses on of the three positions E97, E173, and E300 determined by the amino acid sequence comparison with the GH 35 galactosidases. Due to the N-terminal fusion of a His<sub>6</sub>-tag to BglC by the insertion of *bgIC* in the pET-Duet-1 vector, the positions E97, E173, and E300 of the natural protein correspond to the residues E113, E189, and E316 in the recombinant protein. The *bgIC* gene was mutated by application of the *QuikChange*<sup>™</sup>-PCR method with primers containing the degenerate codon KSC [(T/G)-(G/C)-C], coding for the four amino acids serine, alanine, glycine, and cysteine.

Identical to the procedure for *abg* mutagenesis, the isolated plasmids resulting from the mutagenesis procedure were checked by sequencing for mutation of *bgI/C*. In total three variants of each examined position could be generated (Table 6).

**Table 6** Variation of the proposed catalytically active amino acid residues E113, E189 and E316 of BglC of *P. furiosus*. The mutations were acquired by *QuikChange*<sup>TM</sup>-PCR by mutation of the wild type gene in a pET-Duet-1 vector. Obtained plasmids were sequenced for confirmation of the resulting mutation.

Original AA	Introduced mutation	Codon variation	Verification
E113	A	GAG → GCC	+
	C	GAG → TGC	—
	G	GAG → GGC	+
	S	GAG → TCC	+
E189	A	GAA → GCC	—
	C	GAA → TGC	+
	G	GAA → GGC	+
	S	GAA → TCC	+
E316	A	GAA → GCC	+
	C	GAA → TGC	—
	G	GAA → GGC	+
	S	GAA → TCC	+

To create a glycosynthase variant of BglU, the catalytic residues of BglU, E170 and E377, identified by sequence alignment, needed to be mutated to non-nucleophilic residues. Examination of the crystal structure of BglU also indicated to the involvement of these residues in the hydrolysis of glycosidic bonds, as the distances of these glutamic acid residues to each other are between 3–4 Å, which is typical for retaining glycosyl hydrolases (Figure 32).<sup>[150]</sup> The variants mutated at position E377 were most likely to act as potential glycosynthases as this position was proposed to be the catalytic nucleophilic residue of BglU by *Fan et al.*<sup>[81]</sup>

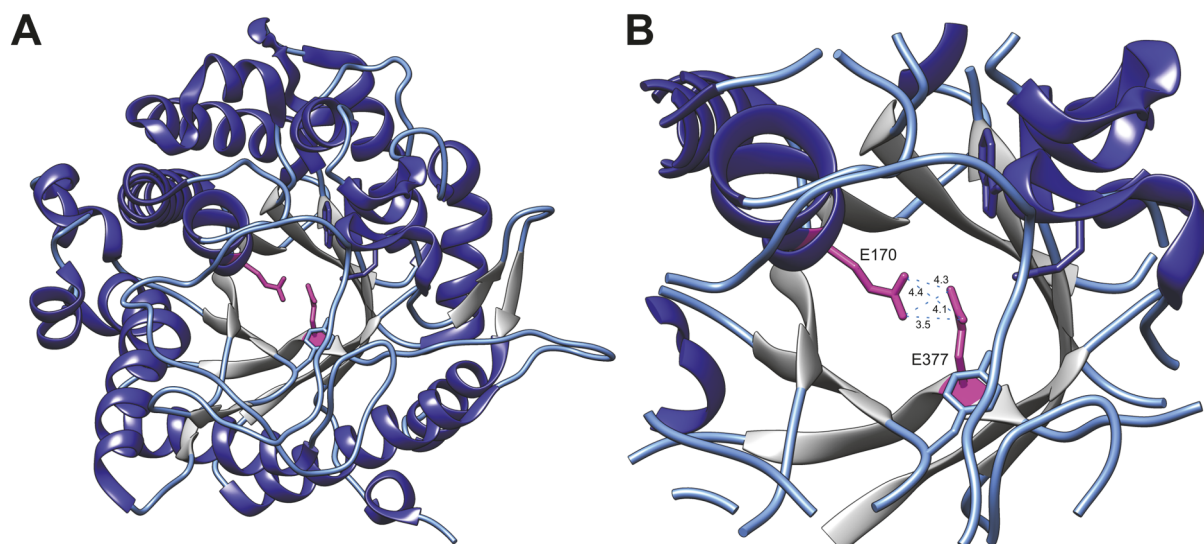


**Figure 32** Analysis of the crystal structure of BglU of *M. antarcticus* (PDB 3W53). The  $(\beta/\alpha)_8$ -barrel structure (TIM-barrel; helices, blue; strands, gray) can be observed in the overview (A) with the catalytically active residues (magenta) located inside the active site pocket. The residues E170 and E377 are at average around 4.1 Å apart, a typical distance for retaining hydrolases (B). The distances are depicted and given in Å.

As was chosen for the mutagenesis of *bglC*, the introduction of various single mutations into the *bglU* gene was to occur via the *QuikChange*<sup>™</sup>-PCR method. Primers containing the same degenerate codon KSC [(T/G)-(G/C)-C] as for the mutagenesis of *bglC*, were designed and applied in the PCR reactions. Products of the *QuikChange*<sup>™</sup>-PCR were used to transform *E. coli* BL21(DE3), which were cultivated on ampicillin containing agar plates for selection. As the proportion of *wt* genes, even after DpnI digestion of the template vector, was often still high after the *QuikChange*<sup>™</sup>-PCR reaction (observed during the mutagenesis of *abg* and *bglC*), a screening was applied to easily recognise  $\beta$ -glucosidase variants deficient of hydrolytic activity. The screening method was based on the hydrolysis of 6,7-dihydroxycoumarin 6- $\beta$ -D-glucopyranoside (**21a**), also known as esculin, which when hydrolysed forms a complex with iron(III) ions causing a black colouration (Figure 33).

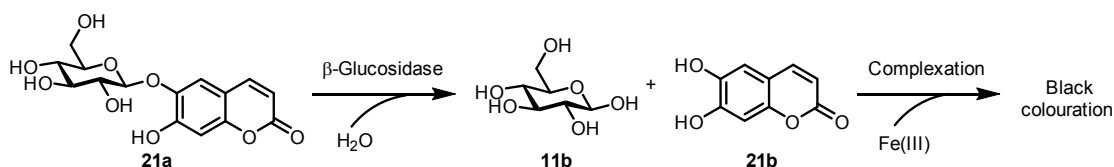


**Figure 33** Hydrolysis of esculin (**21a**) by a  $\beta$ -glucosidase releasing glucose (**11b**) and 6,7-dihydroxycoumarin (**21b**). Coumarin **21b** causes a black colouration when in complex with Fe(III) ions.

This activity test was developed by *Harrison et al.* to detect the presence of *E. coli* in water samples.<sup>[151]</sup> Common as an assay for the detection of  $\beta$ -glucosidase activity, the assay has not yet been applied as a mutagenesis screening for glycosynthase variants. Transformed *E. coli* BL21(DE3) colonies containing a mutant form of a  $\beta$ -glucosidase deficient of hydrolytic activity would therefore not cause any colouring of the agar and be easily identifiable. The

assay has high similarity to the blue-white-screening detecting the insertion of a target gene into the desired vector by inactivating the  $\beta$ -galactosidase LacZ and consequently hindering the hydrolysis of X-gal (5-bromo-4-chloro-3-indolyl- $\beta$ -D-galactopyranoside) and a blue colouration.<sup>[152]</sup> The choice towards a screening based on esculin agar plates instead of X-glc (5-bromo-4-chloro-3-indolyl- $\beta$ -D-glucopyranoside) was based on the high cost of X-glc (100 mg, 848 €<sup>5</sup>) in comparison to esculin (**21a**, monohydrate 100 g, 464 €<sup>5</sup>). Before screening for mutant variants of BglU, a control was carried out by incubating *E. coli* BL21(DE3), transformed prior with a pET-21a(+) vector (not containing an insert), on esculin agar in order to rule out the expression of an endogenous  $\beta$ -glucosidase by the *E. coli* strain. The colonies did not cause a dark colouration, therefore rendering the strain as suitable for the screening assay. First attempts of cultivating *E. coli* BL21(DE3), transformed with the *QuikChange*<sup>™</sup>-PCR product, on esculin agar plates already containing IPTG at a concentration of 50  $\mu$ M failed as no bacterial growth could be found on the agar plates after 24 h incubation at 37 °C. Therefore, the transformed bacteria were first incubated on esculin agar plates without the presence of IPTG and the expression later induced (after colony formation) by adding 0.7  $\mu$ L of 50  $\mu$ M IPTG onto the agar plate. After a further incubation of up to 16 h, colonies containing functional  $\beta$ -glucosidases showed a dark brown colouration in contrast to non-functional glucosidases, which left the colonies uncoloured (Figure 34). The presence of IPTG in the agar when cultivating freshly transformed bacteria seems to exert stress on the bacteria hindering a normal growth and therefore the formation of visible colonies. By use of the esculin screening, bacteria containing mutated *bglU* genes were easily identified and a total of five *bglU* variants of the possible eight planned variants (4 each at E170 and E377) were isolated and confirmed by DNA sequencing (Table 7).

---

<sup>5</sup> *Sigma-Aldrich* 21<sup>st</sup> Feb 2019

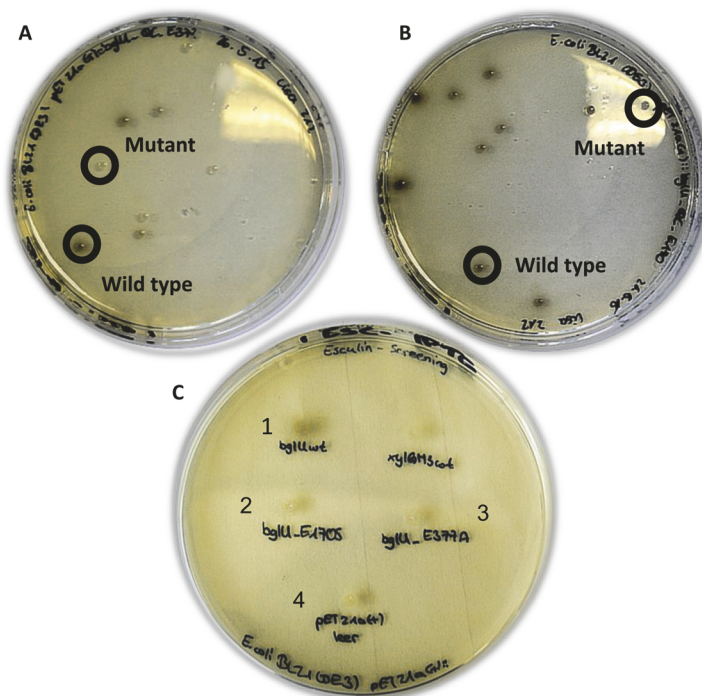


**Figure 34** Mutagenesis screening of BglU by cultivation on esculin agar. After transformation and incubation of *E. coli* BL21(DE3) with plasmids derived from the *QuikChange*<sup>TM</sup>-PCR mutagenesis of *bglU*, IPTG was added to the agar to induce  $\beta$ -glucosidase expression and dark colouring of active variants. **(A)** Mutagenesis screening of position E377 of BglU. **(B)** Mutagenesis screening of position E170 of BglU. **(C)** Control plate testing defined *E. coli* BL21(DE3) strains with BglU variants; 1: *wt* BglU; 2: BglU-E170S; 3: BglU-E377A; 4: *E. coli* BL21(DE3) containing pET-21a(+) without *bglU* gene.

**Table 7** Variation of the catalytically active amino acid residues E170 and E377 of BglU of *M. antarcticus*. The mutations were acquired by *QuikChange*<sup>TM</sup>-PCR by mutation of the *wt* gene in a pET-21a(+) vector. Obtained plasmids were sequenced for confirmation of the resulting mutation.

Original AA	Introduced mutation	Codon variation	Verification
E170	A	GAG → GCC	—
	C	GAG → TGC	+
	G	GAG → GGC	+
	S	GAG → TCC	+
E377	A	GAA → GCC	+
	C	GAA → TGC	—
	G	GAA → GGC	+
	S	GAA → TCC	—

After mutagenesis of the three  $\beta$ -glucosidases Abg, BglC, and BglU the potential glycosynthase variants were expressed under the identical conditions as the expression of the *wt* enzymes. The heterologous expression occurred for the mutant forms of Abg and BglU in *E. coli* BL21(DE3). In contrast to the experiments for *wt* BglC, the expression of the BglC variants E113S, E189S and E316S in *E. coli* BL21(DE3) did not lead to the target enzyme and

therefore was carried out in *E. coli* Rosetta™ 2. All mutant glycosidases were isolated by IMAC and checked for purity by SDS-PAGE analysis (Figure 35).

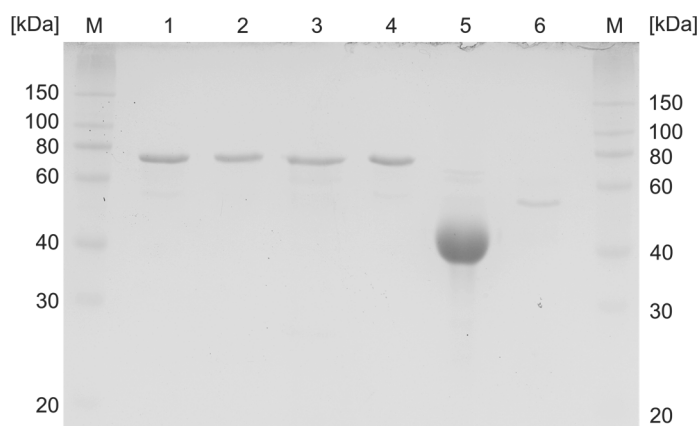


**Figure 35** SDS-PAGE analysis of the expression and purification of the mutated  $\beta$ -glycosidases. All proteins were isolated by IMAC. The glycosidases *wt* BglC (1), Abg-E358S (5), and BglU-E377A (6) were expressed in *E. coli* BL21(DE3), the variants BglC-E113S (2), -E189S (3), and -E316S in *E. coli* Rosetta™ 2. Roti-Mark 10–150 was applied as a standard (M) for size determination.

#### 6.1.4 Detecting glycosynthase activity

##### Synthesis of glycoside substrates

Required in a larger amount for activity assays and synthetic experiments, the substrates *p*-nitrophenyl  $\beta$ -D-glucopyranoside (**5h**, *p*NPGlc),  $\alpha$ -D-glucopyranosyl fluoride (**2a**,  $\alpha$ -GlcF), and  $\alpha$ -D-xylopyranosyl fluoride (**2d**,  $\alpha$ -XylF) were synthesised chemically (Figure 36). The *p*NPGlc **5h** substrate, used later in all activity measurements, was prepared beginning from 1,2,3,4,6-penta-*O*-acetyl  $\alpha$ -D-glucopyranoside (**22a**) according to the *O*-glycosylation method of *Lee et al.* and subsequent deprotection of glycoside **22b**.<sup>[153]</sup> The glycoside **22b** was obtained in a yield of only 46% most probably due to hydrolysis during the alkaline extraction of *p*-nitrophenol (**13b**) with saturated carbonate solution and incomplete crystallisation during the work-up procedure. The deprotection using sodium methoxide in methanol led to a quantitative yield of product **5h**. For glycosynthetic reactions the glycosyl fluorides **2a** and **2d** were prepared according to the procedure of *Steinmann et al.* from acetylated glucose (**22a**) and xylose (**22c**).<sup>[154]</sup> The acetylated fluoride derivatives **22d** and **22e** were both obtained as anomeric mixtures. The  $\alpha$ -anomer was isolated in both cases via flash column chromatography in yields of 45% and 56% for compound **22d** and **22e** respectively. Deprotection of the acetylated glycosyl fluorides **22d** and **22e** using ammonia in methanol occurred in a quantitative yield.<sup>[58]</sup>

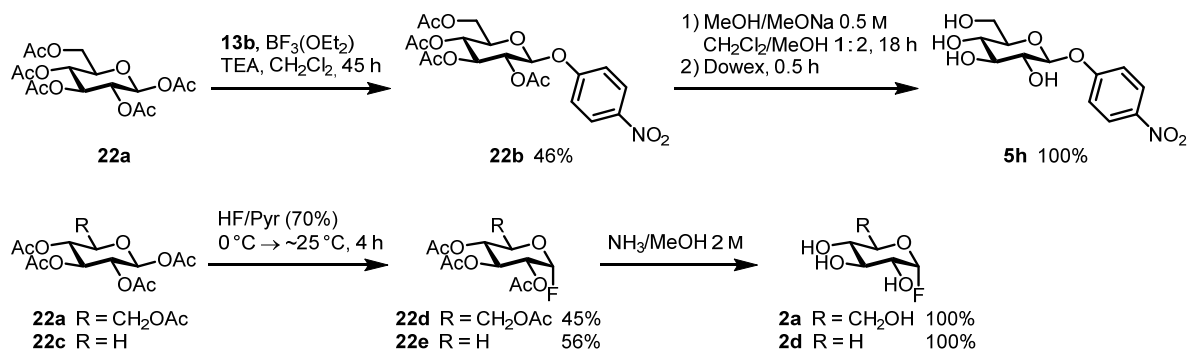


**Figure 36** Chemical synthesis of the glycosyl donor/acceptor molecules  $\alpha$ -D-glucopyranosyl-,  $\alpha$ -D-xylopyranosyl fluoride (**2a** & **2d**), and *p*-nitrophenyl  $\beta$ -D-glucopyranoside (**5h**).

### Testing for synthetic activity

To determine whether the produced  $\beta$ -glucosidase variants displayed glycosynthase activity, a model reaction of the glucosylation of *p*NPGlc **5h** (acceptor) with the glucosyl donor  $\alpha$ -GlcF **2a** was examined for each variant (Figure 37). The mutant  $\beta$ -glucosidases were tested beforehand for residual hydrolytic activity towards *p*NPGlc **5h** before application in the model reaction.

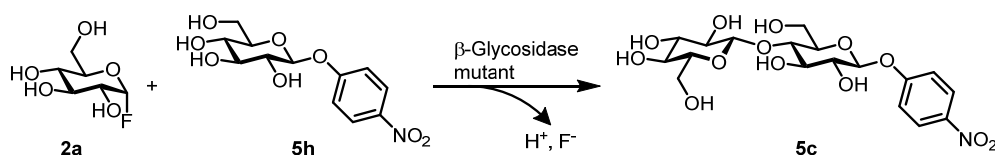


**Figure 37** Model glycosylation reaction applied for the detection of synthetic activity of mutant  $\beta$ -glucosidase variants of BglC, Abg and BglU.  $\alpha$ -GlcF **2a** and *p*NPGlc **5h** were incubated with the respective  $\beta$ -glucosidase mutant at 25 °C (Abg & BglU) or 85 °C (BglC) and the respective buffer employed in the characterisation of the *wt* enzyme.

### Potential glycosynthase variants of BglC

The first set of  $\beta$ -glucosidase mutants tested for glycosynthetic activity were the mutants of the hyperthermophilic glycosidase BglC, BglC-E113S, -E189S, and -E316S. Hydrolytic activity towards *p*NPGlc **5h** exhibited by the mutants could not be detected, strongly indicating to the catalytic importance of all of the chosen residues. In addition, the enzymes showed no activity during chemical recovery experiments using glucoside **5h** and sodium formate (2 M) as an external nucleophile. This initial result was a first indication for the unsuitability of the BglC mutants as glycosynthases. Further tests for glycosynthase activity were carried out using the synthesised  $\alpha$ -GlcF **2a** (20 mM) and *p*NPGlc **5h** (40 mM) as the donor and acceptor respectively (Figure 37). The excess of acceptor was chosen to repress the transfer of the glycosyl donor to itself (homocoupling) or water (hydrolysis). A control reaction was also

conducted using identical conditions without enzyme. The reactions were followed by reverse phase thin-layer chromatography (RP-TLC) revealing a hydrolysis of substrate **2a** in all tested reactions. The degradation was also visible in the reference reaction ruling out enzymatic hydrolysis by the BglC mutants and indicating to a thermal hydrolysis due to the high temperature of 85 °C. Thermal hydrolysis can be expected at high temperatures such as 85 °C, as glycosyl fluorides show high instability even at lower temperatures.<sup>[93]</sup> Therefore, to use the glycosyl fluoride **2a** as a donor substrate in a synthase reaction using BglC, the reaction conditions would need to be changed to lower temperatures. However, as shown during the characterisation of BglC (section 6.1.2, Figure 29), the enzyme showed no activity at temperatures below 55 °C. High temperatures are therefore prerequisite for the activity of the *wt* enzyme BglC, which was to be expected due to the hyperthermophilic nature of this particular enzyme. An increase in synthetic activity of different mutated glycosidases, using buffers with more acidic conditions (around pH 4) than for the respective *wt* hydrolysis reactions was reported by *Perugino et al.*<sup>[74]</sup> Therefore, the pH tolerance of *wt* BglC was tested by measuring the activity at pH 6, 5, 4 and 3. The *wt* enzyme exhibited no activity at pH values of 4 and lower. The activity of BglC at pH 5 was only 14.3% of the activity measured under the same conditions at pH 6 ( $1.2 \cdot 10^{-2}$  U/mg, pH 5 compared to  $8.4 \cdot 10^{-2}$  U/mg, pH 6). A further explanation for the lack of synthetic activity can be considered with respect to the positions of the incorporated mutations. As described during the comparison of the amino acid sequence of BglC with the  $\beta$ -glucosaminidases GlmA<sub>Ph</sub> and GlmA<sub>Tk</sub>, the glutamate residue E358 (E342 without the C-terminal fused His<sub>6</sub>-tag) is most likely the catalytic nucleophilic residue and not one of the three residues examined in this experiment. Despite of this insight, the suitability of BglC as a glycosynthase was hindered by the strict temperature dependency of the enzyme and was not further considered as a potential glycosynthase.

### **$\beta$ -Glucosynthase Abg-E358S**

To verify the non-suitability of BglC and thermophilic glycosidases as glycosynthases in general, due to the instability of the glycosyl fluoride donors at elevated temperatures but not the applied analytical method, the literature known glycosynthase Abg-E358S was applied as a reference for the model glycosylation reaction. As expected from literature, the mutant did not show hydrolytic activity towards *p*NPGlc **5h** and was then tested in the same model reaction as carried out for BglC (Figure 37). Incubation of the Abg-E358S (0.8 mg/mL, NH<sub>4</sub>HCO<sub>3</sub>-buffer 150 mM, pH 7.9) with  $\alpha$ -GlcF **2a** (40 mM) and *p*NPGlc **5h** (20 mM) resulted in a mixture of new products, which could be observed by RP-TLC. The products were derivatised by peracetylation, with acetic anhydride in pyridine, and isolated by preparative TLC. As was

described by *Mackenzie et al.*, the glycosynthase catalysed the transfer of the glucosyl moiety onto *p*NPGlc **5h** with a  $\beta$ -1,4 linkage.<sup>[21]</sup> Nevertheless, due to repeated transfer of  $\alpha$ -GlcF **2a** by Abg-E358S a mixture of *p*-nitrophenyl  $\beta$ -D-cellobioside (**5c**), *p*-nitrophenyl  $\beta$ -D-cellobioside (**5x**), and *p*-nitrophenyl  $\beta$ -D-cellobioside (**5y**) was produced of which the trisaccharide **5x** was the major product.

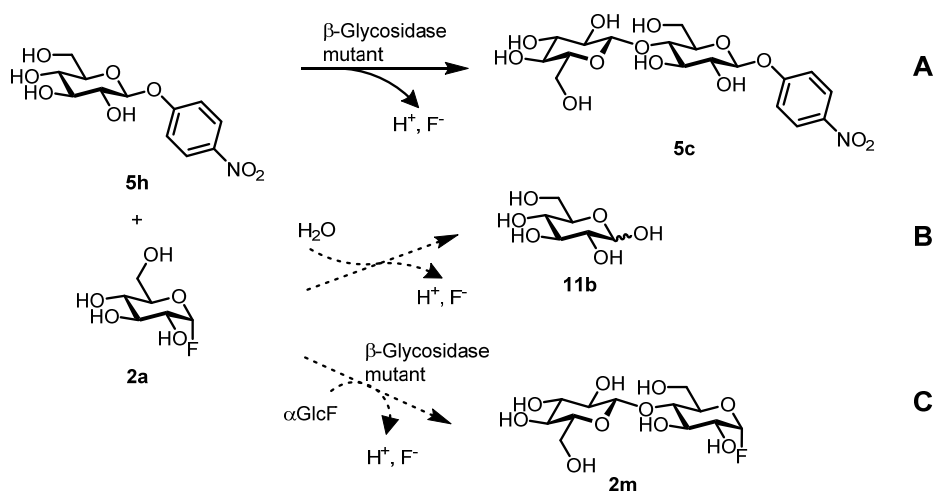


**Figure 38** Possible reaction pathways of the glycosylation of the acceptor *p*NPGlc **5h** with Abg-E358S and  $\alpha$ -GlcF **2a** as the glycosyl donor. **(A)** Transfer of the glucosyl moiety onto the acceptor molecule **5h**. **(B)** Autohydrolysis of the glycosyl fluoride donor **2a**. **(C)** Self-coupling of the glycosyl donor **2a** catalysed by the glycosynthase.

The purification and yield determination of synthesised glycosylation products produced by Abg-E358S proved difficult as a substantial amount of side products were produced in addition to the glucose (**11b**) side product caused by autohydrolysis (Figure 38). Upon closer analysis of the side product signals in the  $^1H$ -NMR spectra of the isolated mixed fractions, more than one signal with a coupling constant of 52.8 Hz, which is characteristic for a proton of an anomeric centre coupling to a fluorine atom in  $\alpha$ -configuration, could be observed. This observation indicated to Abg-E358S catalysing the transfer of the glucosyl residue of the donor not only onto the acceptor but also onto the donor molecule itself. To verify a self-coupling of the donor  $\alpha$ -GlcF **2a** by Abg-E358S, a test was carried out incubating the enzyme with the donor **2a** in the absence of an acceptor molecule. After incubation of the reaction (24 h, 25 °C), the products were peracetylated and separated by flash chromatography.  $^1H$ -NMR analysis confirmed the homocoupling of the donor  $\alpha$ -GlcF **2a** by the identification of not only  $\alpha$ -D-cellobiosyl fluoride (**2m**) and  $\alpha$ -D-cellobiosyl fluoride (**2n**), but also the respective di- and trisaccharide caused by hydrolysis of the glycosyl fluorides (Figure 39). The major product of the homocoupling reaction,  $\alpha$ -D-cellobiosyl fluoride (**2m**), was only produced in a 6.8% yield, which displays the low affinity of the +1 subsite of Abg towards glycosides without an aryl aglycone. Therefore, in the presence of a suitable acceptor Abg-E358S will first glycosylate the acceptor, but with decreasing amounts of acceptor molecules the glycosynthase will also

catalyse the homocoupling reaction. The use of an excess of acceptor molecules should cause a suppression of the self-coupling reaction.

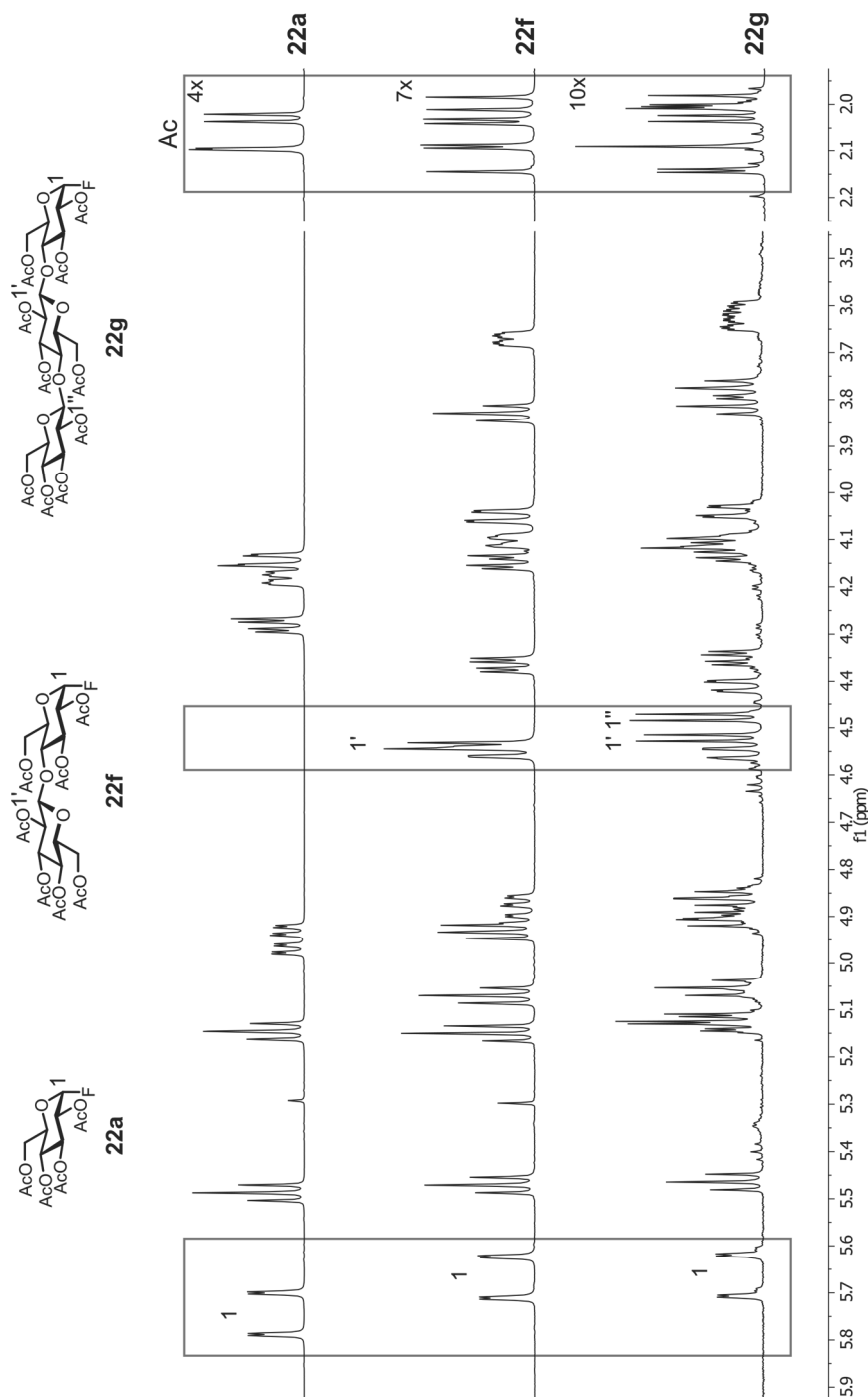


**Figure 39**  $^1\text{H-NMR}$  analysis of homocoupling products produced by Abg-E358S with  $\alpha\text{-GlcF}$  (**2a**, 80 mM) in the absence of an acceptor molecule. The reaction was incubated 24 h at 25 °C and the reaction products subsequently peracetylated for isolation by flash chromatography. Boxes highlight the shift of the anomeric centre (1), the additional anomeric centres (1', 1''), and the increase in acetate (Ac) signals. The  $^1\text{H-NMR}$  spectra were recorded in  $\text{CDCl}_3$ .

The synthase activity of Abg-E358S was further applied for the glycodiversification of the flavanone glycoside prunin (**1b**, naringenin-7- $\text{O-}\beta\text{-D-glucoside}$ ). This glycoside of the flavanone naringenin (**1a**) has a higher solubility mediated by the glucosyl residue and thereby

a higher bioavailability than naringenin (**1a**), but lacks the bitter taste exhibited by naringin (**1c**, naringenin-7-O- $\beta$ -neohesperidoside). A diversification of the glycosylation of naringenin (**1a**) could improve the bioavailability and bioactive properties of the flavanone. Due to the high cost of prunin (**1b**, 206 €/mg<sup>6</sup>) in comparison to naringin (**1c**, 2.25 €/g<sup>6</sup>), the flavanone glucoside **1b** was produced by a de-rhamnosylation procedure described by *Vila-Real et al.*<sup>[103]</sup> The de-rhamnosylation was catalysed by a naringinase of *Penicillium decumbens*, an enzyme complex exhibiting  $\alpha$ -L-rhamnosidase and  $\beta$ -D-glucosidase activity. To avoid a de-glucosylation, the  $\beta$ -D-glucosidase activity was deactivated prior to the reaction with naringin (**1c**) by incubating the enzyme in 20 mM citrate buffer at pH 3.9 and 82 °C for 16 min. The procedure, determined by *Vila-Real et al.* by the use of response surface methodology, eliminated the  $\beta$ -D-glucosidase activity, while keeping 40% residual  $\alpha$ -L-rhamnosidase activity.<sup>[103]</sup> The pretreated naringinase was then added to a solution of naringin (**1c**, 10 mM) at 60 °C and afforded the desired glucoside **1b** in a yield of 84% (Figure 40).

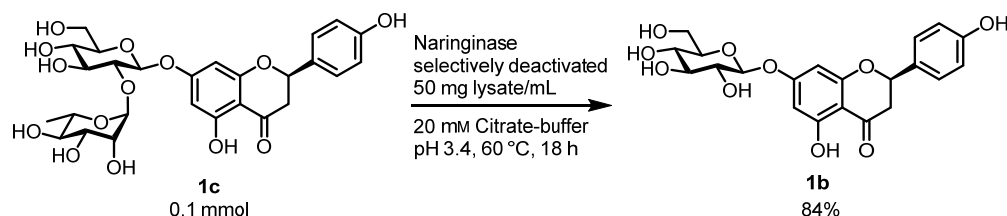


**Figure 40** De-rhamnosylation of naringin (**1c**) for the synthesis of prunin (**1b**) catalysed by selectively deactivated naringinase of *P. decumbens*. The  $\beta$ -glucosidase activity was deactivated by incubation in 20 mM citrate-buffer, pH 3.9, at 82 °C for 16 min.

The resulting glycoside **1b** (40 mM) was applied as an acceptor in a glycosylation reaction with Abg-E358S (3 mg purified, lyophilised) and the donor  $\alpha$ -GlcF **2a** (80 mM). DMSO (10% v/v) was added to the reaction as a co-solvent to improve the solubility of prunin (**1b**). After an incubation of 24 h the product mixture was derivatised by acetylation, identically to the glycosylation of *p*NPGlc **5h**, and the products isolated by flash chromatography. Analysis of the isolated fractions by <sup>1</sup>H-NMR revealed many similar products of which the spectra only slightly varied from each other. The acceptor prunin (**1b**) was reisolated from the reaction and the major reaction product was identified as a glucosylated derivative of prunin (**1b**), naringenin-7-O- $\beta$ -D-cellobioside (**1g**). The derivatisation using peracetylation caused difficulties for the purification with flash chromatography. The acetyl group of the A-ring of the flavonoid scaffold seemed to be labile and partially cleaved during the chromatography, leading to mixtures of the peracetylated and partly non-acetylated products **22h–k** (Figure 41).

<sup>6</sup> *Sigma-Aldrich* 22<sup>nd</sup> March 2019

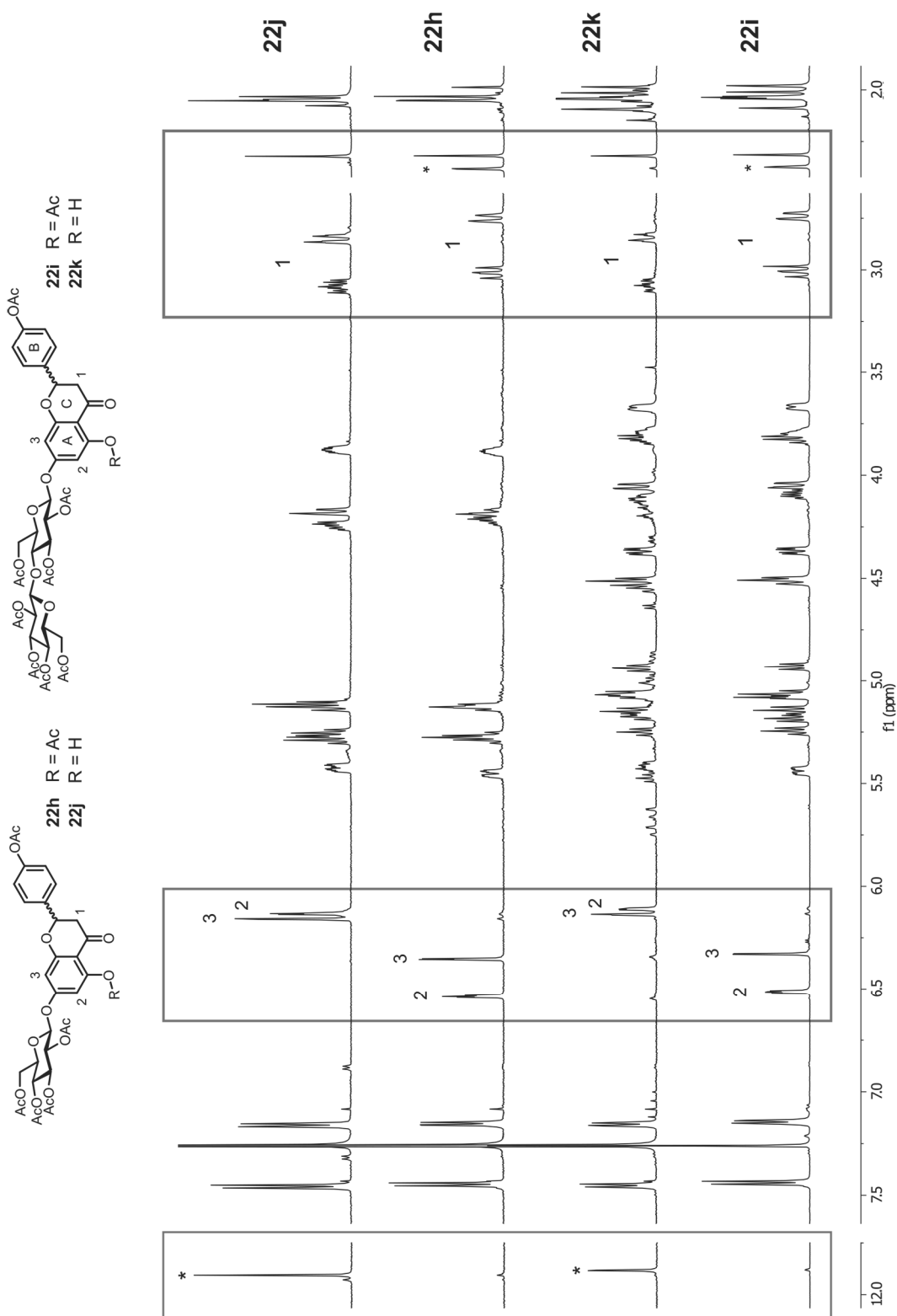


**Figure 41**  $^1\text{H-NMR}$  analysis of isolated compounds of the glycosylation of prunin (**1b**) with Abg-E358S and  $\alpha\text{-GlcF 2a}$ . Compounds of the reaction mixture were acetylated and separated by flash chromatography. The acceptor **1b** and product **1i** were isolated in two forms, completely acetylated **22h/i** and mono-deacetylated **22j/k** (signals indicating to a mono-deacetylation are marked by boxes; \* shows signal of the acyl group or proton of R).  $^1\text{H-NMR}$  spectra were measured in  $\text{CDCl}_3$ .

Considering all versions of the respective product (peracetylated and mono-deacetylated), the glucosylated prunin derivative **1i** was isolated in a yield of 15%. The product was further

confirmed by high-resolution mass spectroscopy. Furthermore, traces of a diglycosylated product and homocoupling of the glycosyl fluoride donor **2a** was observed in the <sup>1</sup>H-NMR spectra. The reaction parameters seem to have not been optimal for the enzyme as 55% of the glycosyl donor **2a** was reisolated from the reaction. Possible oligomerisation products were also observed in trace amounts but were not further examined due to a high amount of impurities.

The application of an alternative glycosyl fluoride,  $\alpha$ -XylF **2d**, as a glycosyl donor was also examined for the glycosylation of *p*NPGlc **5h**. Identically to the afore mentioned reactions, the donor **2d** was applied in an excess (80 mM) with respect to the acceptor **5h** (40 mM) and incubated for 24 h at 25 °C with Abg-E358S. Subsequent derivatisation (peracetylation) and flash chromatography led mostly to the reisolation of the donor **2d** and *p*NPGlc **5h** in their acetylated form. A mixture of 1,2,3,4-tetra-*O*-acetyl  $\alpha/\beta$ -D-xylopyranoside (**22c**), representing 30% of the employed donor **2d**, was also isolated indicating to a high rate of autohydrolysis of the donor. The glycosylation product, *p*-nitrophenyl-(4-*O*- $\beta$ -D-xylopyranosyl)- $\beta$ -D-glucopyranoside (**5k**), was identified only in trace amounts. The low synthase activity of Abg-E358S towards the transfer of xylosyl residues was expected, as this has been described in literature for the Abg-E358G mutant.<sup>[27]</sup> Even though further mutations have been described, which enhance the xylosynthase activity of Abg mutants, the optimisation of this reaction was not further examined in this thesis.

The results obtained for Abg-E358S in the examined glycosylation reactions, verified the applicability of the chosen analytical methods for the identification of glycosynthase activity and product analysis. Therefore, the unsuitability of BglC as a glycosynthase was due to the enzymes hyperthermophilic properties and not the possible problematic product detection by the applied analytical methods.

### **BglU variants as potential psychrophilic glycosynthases**

The preceding results defined the BglC mutant variants as unsuitable for the application as a glycosynthase, as the strict temperature dependency of the activity only caused thermal degradation of the glycosyl fluoride donor. The psychrophilic  $\beta$ -glucosidase mutants of BglU with a potential optimal activity at low temperatures should therefore be more suitable for this type of reaction. The successful detection of synthetic activity by a mutant of BglU, would also present the first cold-adapted glycosynthase in literature.

Site-directed mutagenesis of *bglU* utilising the *QuikChange*<sup>TM</sup>-PCR method, resulted in the production of the variants E170S, E170G, and E170C for the catalytic acid/base residue, and E377A and E377G for the catalytic nucleophile residue of BglU (section 6.1.3). All variants

were heterologously expressed, isolated, and tested for hydrolytic activity towards *p*NPGlc **5h**. As expected for the mutation of the acid/base residue E170, all variants exhibited weak or no hydrolytic activity compared to the *wt* form of BglU. The highest specific activity was observed for BglU-E170C at  $2.1 \cdot 10^{-2} \pm 4.5 \cdot 10^{-2}$  U/mg, followed by BglU-E170S with  $2.0 \cdot 10^{-3} \pm 4.9 \cdot 10^{-3}$  U/mg, representing 1.3% and 0.1% residual activity compared to *wt* BglU measured at  $1.6 \pm 3.4 \cdot 10^{-1}$  U/mg. No hydrolytic activity was detected for BglU-E170G. The mutation of the nucleophilic residue of BglU, E377, to alanine or serine, displayed similar results for the measurement of the hydrolytic activity towards *p*NPGlc **5h**. A low specific activity of  $2.98 \cdot 10^{-2} \pm 2.40 \cdot 10^{-2}$  U/mg was detected for BglU-E377G, whereas no hydrolytic activity could be detected for BglU-E377A.

The variants of BglU were then applied in the model glycosylation reaction with  $\alpha$ -GlcF **2a** and *p*NPGlc **5h** as was carried out for BglC and Abg. Due to the low activity of *wt* BglU in comparison to Abg, the reaction for each BglU variant was carried out with high substrate concentrations of the donor  $\alpha$ -GlcF **2a** at 80 mM and the acceptor *p*NPGlc **5h** at 40 mM. Following the reactions by RP-TLC, the variants BglU-E170G, -E170S, and -E170C showed only a slight production of glucose, but no other product formation and therefore no synthetic activity. The production of glucose (**11b**) was attributed to the autohydrolysis of  $\alpha$ -GlcF **2a**, which occurred over time due to the instability of the glycosyl fluoride in aqueous solution. This result was expected as glycosynthases derived from retaining glycosidases are obtained by mutation of the catalytic nucleophilic residue and not the catalytic acid/base residue. In contrast, for the reaction incubated with BglU-E377A, three new product spots were observed by RP-TLC. For further analysis, the solvent of the reaction batch was removed under reduced pressure and all compounds peracetylated with acetic anhydride in pyridine according to the method of *Steinmann et al.* (Figure 42).<sup>[154]</sup> Separation of the reaction products via flash column chromatography and subsequent analysis by <sup>1</sup>H-NMR determined the products as the acetylated forms of 4-nitrophenyl cellobioside (**5c**), -cellotrioside (**5x**), and -cellotetraside (**5y**). The production of these products confirms the transformation of  $\beta$ -glucosidase BglU into a glycosynthase. The enzyme BglU-E377A catalysed the transfer of glucosyl residues onto the acceptor with complete anomeric control in a  $\beta$ -1,4 linkage.

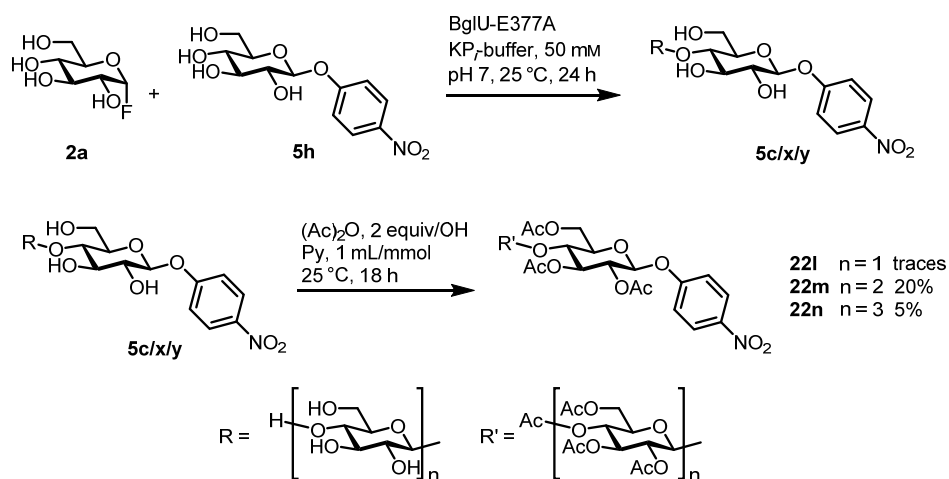


**Figure 42** Glycosylation of *p*NPGlc **5h** catalysed by BglU-E377A with  $\alpha$ -GlcF **2a** as the glycosyl donor. The reaction was incubated at 25 °C in  $\text{KP}_7$ -buffer (50 mM, pH 7) for 24 h. After solvent removal, all reaction products were acetylated for product isolation by flash chromatography.

The glycosynthase also catalysed the subsequent glucosylation of the first reaction product, leading to an oligomerisation as was observed for Abg-E358S. For the case of BglU-E377A the *p*-nitrophenyl cellotrioside (**5x**) was the main product of the reaction after a 24 h incubation with a yield of 20%. Only trace amounts of the *p*-nitrophenyl cellobioside (**5c**) were isolated allowing the measurement of the  $^1\text{H-NMR}$  spectrum but not of the respective  $^{13}\text{C-NMR}$  spectrum. The low amount of *p*-nitrophenyl cellobioside (**5c**) strongly indicates to a high affinity of BglU-E377A towards the disaccharide product facilitating a further glycosylation to the trisaccharide **5x**. The affinity of BglU-E377 towards the trisaccharide **5x** on the other hand seems to be lower as the reaction yielded only 5% of the *p*-nitrophenyl cellotetraside (**5y**). Nevertheless, the low conversion of the trisaccharide **5x** might also have been caused by a depletion of the donor **2a** concentration leading to a decrease of the reaction rate.

### 6.1.5 Development of a high-throughput assay for glycosynthase characterisation<sup>7</sup>

The analysis of biocatalytic reactions by glycosynthases are most commonly carried out by lengthy high-pressure liquid chromatography (HPLC) measurements, requiring a sufficient separation of the reaction products, or by the measurement of the fluoride release by an ion-selective electrode (ISE). The measurement of glycosynthase activity *via* an ISE was exemplary demonstrated for the glucosylation of *p*NPGlc **5h** by Abg-E358S with  $\alpha$ -GlcF **2a** as the donor. The conversion of the donor molecule **2a** releases fluoride ions, which can be detected by the ISE in a decrease of the electric potential of the solution. By plotting the

<sup>7</sup> The development of the glycosynthase activity assay and glycosynthase characterisation were published in Hayes *et al.*<sup>[2]</sup>

negative decadic logarithm of various fluoride concentrations against the measured electric potential, a calibration for quantification of the fluoride ions released by the glycosynthase can be created. By following the release of fluoride over time, a specific activity of  $7.4 \cdot 10^{-1} \pm 6.0 \cdot 10^{-2}$  U/mg could be determined for Abg-E358S for this reaction (Figure 43). However, the measurement of the reaction using the ISE is laborious, as firstly, the measured values must be precisely timed and noted manually during the reaction, and secondly, conduction of parallel measurements was not possible. Additionally, due to the size of the ISE, a downscaling of the reaction volume was only possible down to 500  $\mu$ L. A characterisation or screening of glycosynthases by ISE measurements is therefore highly time consuming and requires high substrate amounts due to the larger reaction volume.

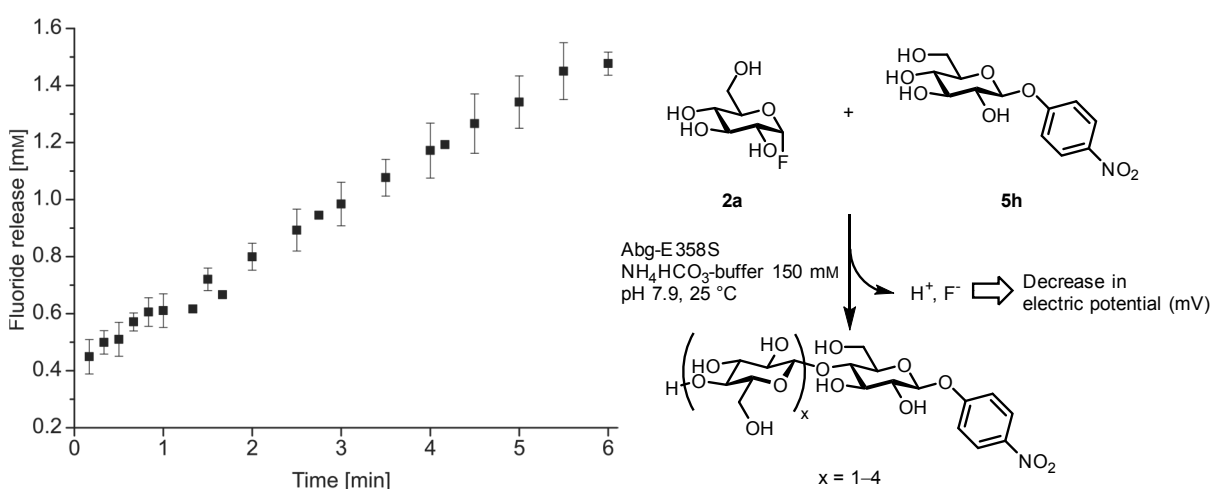


**Figure 43** Glycosynthase activity measurement via an ion selective electrode (ISE). The conversion of  $\alpha$ -GlcF **2a** catalysed by Abg-E358S was detected by the decrease of electric potential measured by the ISE.

As an alternative to the ISE measurements and a possible high-throughput screening method (HTS), a colourimetric assay was developed allowing quantification of released fluoride in a microplate format. The assay is a modification of a method developed by *Andrés et al.*<sup>[1]</sup> In mutagenesis libraries of glycosidases the group identified glycosynthetic activity by the cleavage of *tert*-butyldimethylsilyl-protected 4-methylumbelliferone. The compound was added to a reaction solution of a cell-free lysate containing a glycosyl fluoride donor and the resulting fluorescence was measured after 40 min. The demonstrated assay showed a low detection maximum of 500  $\mu$ M fluoride, limiting the use of the assay for biocatalytic conversion measurements, identification and characterisation of potential highly-active glycosynthase variants. To overcome these limitations, a modified assay using triisopropyl-(4-nitrophenoxy)-silane (**23**, TIPS $\rho$ NP) was developed. Similar to the method of *Andrés et al.*<sup>[1]</sup> the release of fluoride by conversion of  $\alpha$ -GlcF **2a** will cause a cleavage of the triisopropylsilyl group of TIPS $\rho$ NP **23** (Figure 44).

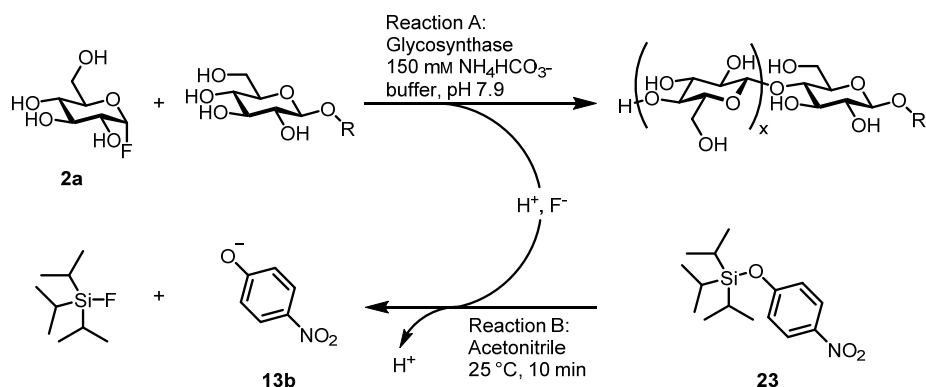


**Figure 44** Example reaction mechanism of the developed glycosynthase activity assay. The enzymatic glycosylation is catalysed in reaction A by the  $\alpha/\beta$ -glucosynthase releasing hydrogen fluoride as a side product. A sample of the enzymatic reaction is then transferred into acetonitrile containing 1 mM TIPSpNP **23** initiating the cleavage of the silyl ether as reaction B. A quantification of the enzymatically released fluoride can then occur by photometric measurements of the released pNP **13b** at 410 nm.

The chemical synthesis of the TIPSpNP **23** in a preparative scale resulted in yields of 97% (1.4 g, 4.8 mmol, Figure 45). The possibility of a continuous assay using the synthesised fluoride chemosensor TIPSpNP **23** was ruled out by the low solubility of the sensor **23**, therefore requiring the assay to be carried out in a discontinuous fashion. Even the use of co-solvents such as DMSO, acetonitrile, or acetone in concentrations of 10–20% could not greatly enhance the solubility of TIPSpNP **23** in aqueous solution. The use of DMSO as a co-solvent was also problematic, due to partial cleavage of TIPSpNP **23** by the presence of DMSO in the solution.

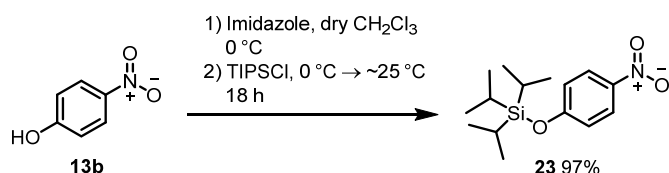


**Figure 45** Synthesis of triisopropyl-(4-nitrophenoxy)-silane (**23**) used for the fluoride detection during glycosynthase activity assays.

The low solubility of fluorogenic molecules protected by a triisopropylsilyl ether was also described by *Sokkalingam and Lee*.<sup>[155]</sup> They also observed a strong decrease in the reaction rate of the silyl ether cleavage with increasing amount of aqueous solvent. The low solubility and therefore low concentration, resulting in a low cleavage reaction rate of TIPS ethers could cause a false representation of the enzymatic reaction rate in a continuous assay. As an alternative, the addition of fluoride containing samples for the cleavage of TIPSpNP **23** and quantification of fluoride was examined in acetonitrile as the bulk solvent. By testing different amounts of buffer, containing pNP **13b** in acetonitrile, a buffer content of 10% was chosen. This amount would keep to a low aqueous content (with respect to the cleavage reaction rate), but ensure a sufficient absorption signal at 410 nm (Figure 46).

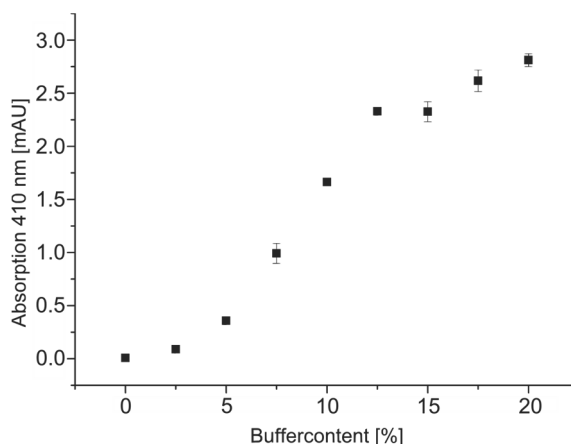


**Figure 46** Influence of the buffer content in acetonitrile on the absorption on *p*-nitrophenol (**13b**) at 410 nm and 25 °C. The chromophore **13b** concentration was held constant at 0.5 mM and the amount of  $\text{NH}_4\text{HCO}_3$ -buffer (150 mM, pH 7.9) in acetonitrile varied from 0–20%.

The cleavage of TIPS $\rho$ NP **23** (1 mM) was measured in a time-dependent manner in acetonitrile containing 10% buffer and varying concentrations of sodium fluoride (15  $\mu\text{M}$ –2 mM). A reliable completion of the cleavage after 10 min was observable independent of the fluoride concentration (Figure 47, **A**). This reaction rate is in accordance to the rate observed by *Sokkalingam and Lee*.<sup>[155]</sup> After a 10 min incubation, a linear dependency of the absorption towards the fluoride concentration could be recognised when using an  $\text{NH}_4\text{HCO}_3$ -buffer (pH 7.9), which is most commonly used in synthetic reactions with glycosynthases (Figure 47, **B**).

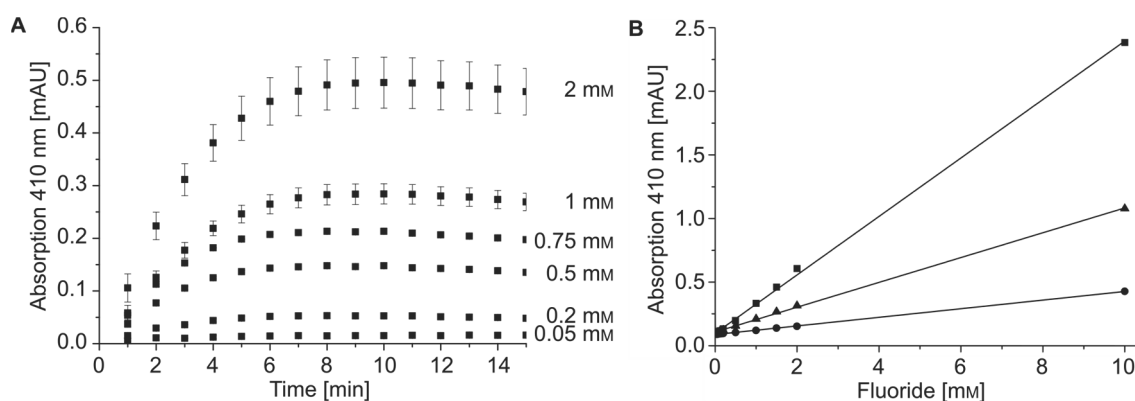


**Figure 47 (A)** Time course of the cleavage reaction of TIPS $\rho$ NP **23** (1 mM) by the addition of varying concentrations of NaF (0.05–2 mM) in acetonitrile with 10%  $\text{NH}_4\text{HCO}_3$ -buffer (150 mM, pH 7.9) at 25 °C. **(B)** Calibration of the fluoride quantification assay with TIPS $\rho$ NP **23** (1 mM) in acetonitrile using  $\text{NH}_4\text{HCO}_3^-$  (■, 150 mM, pH 7.9),  $\text{KP}_i^-$  (▲, 50 mM, pH 6.5), and citrate-phosphate-buffer (●, 35 mM, 128 mM, pH 6) after the addition of NaF (0.05–2 mM) and 10 min incubation. For the measurements with  $\text{KP}_i^-$  and citrate-phosphate-buffer an additional basification step was added ahead of the cleavage reaction.

The addition of sodium bicarbonate solution (0.2 M) to the sample in a 1:1 ratio was added before the cleavage of TIPS $\rho$ NP **23** by the released fluoride. This basification further broadened the applicability of the quantification to enzymatic reactions carried out in buffers with a pH lower than 7 (Figure 47, **B**). Calibrations carried out after this additional basification step led to reliable regression lines using a citrate-phosphate buffer (35 mM, 128 mM, pH 6)

## 6 Results

and  $KP_i$ -buffer (150 mM, pH 6.5). The measurement of the absorption of  $pNP$  **13b**, in comparison to the fluorescence of 4-methylumbelliferone, raised the maximal detection limit to ranges of 2–4 mM fluoride and above, which lowered the limitation of the assay. The limit of detection (LOD) and limit of quantification (LOQ) of the assay was determined by linear regression to be 25  $\mu\text{M}$  and 82  $\mu\text{M}$  respectively (calibration with fluoride concentrations in the range of 50–150  $\mu\text{M}$ ).<sup>[156]</sup> The determined LOQ was verified by repeated measurements of samples with a sodium fluoride concentration of 85  $\mu\text{M}$  with a precision of 10%. The high maximal limit and low LOQ of the assay allows simple determination of substrate conversions at low and high substrate concentrations, which is vital for kinetic characterisation of glycosynthases.

The literature known  $\beta$ -glucosynthase Abg-E358S was first examined to determine the applicability of the developed assay for measurement of enzymatic activity. The kinetic parameters of this  $\beta$ -glucosynthase were determined by *Mackenzie et al.* using  $\alpha$ -GlcF **2b** instead of  $\alpha$ -GlcF **2a** in order to avoid self-condensation of the donor molecules.<sup>[21]</sup> As a model reaction for glycosylation with Abg-E358S, the glycosylation of the acceptor  $pNPGlc$  **5h** (40 mM) with  $\alpha$ -GlcF **2a** (20 mM) was chosen. An excess of the acceptor **5h** was employed to reduce the rate of self-condensation of the donor molecules, which has been observed when using  $\alpha$ -GlcF **2a**. The determination of the conversion of  $\alpha$ -GlcF **2a** by Abg-E358S *via* the concentration of released fluoride (25 °C, 5 min reaction time) with the TIPSpNP-assay resulted in a specific activity of  $0.83 \pm 0.05$  U/mg. Importantly, the rate of autohydrolysis of  $\alpha$ -GlcF **2a** and  $pNPGlc$  **5h** was measured by control reactions and subtracted from the enzymatic reaction if any occurred.

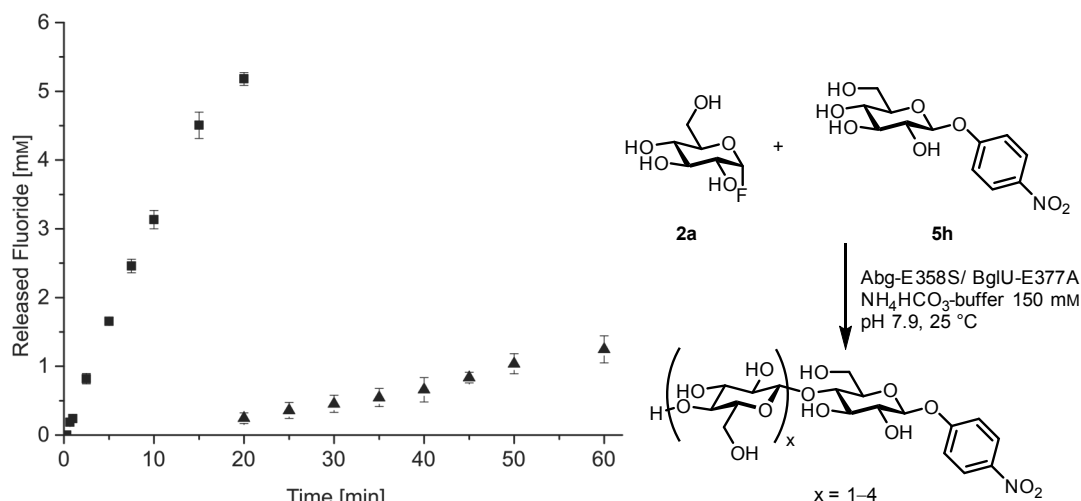


**Figure 48** Time course of the glycosylation reaction catalysed by Abg-E358S ( $\blacksquare$ , 0.7 g/mL) and BglU-E377A ( $\bullet$ , 0.2 g/mL) in the presence of the glycosyl fluoride donor **2a** (20 mM; 40 mM for BglU-E377A) and the glycosyl acceptor **5h** (40 mM) in  $\text{NH}_4\text{HCO}_3$ -buffer (150 mM, pH 7.9) at 25 °C.

An expected linear conversion of  $\alpha$ -GlcF **2a**, releasing the leaving group fluoride accordingly, could be observed during the first 15 min of the enzymatic reaction, indicating to a rapid

conversion of the  $\alpha$ -GlcF **2a** by Abg-E358S (Figure 48). Furthermore, the activity and time course of the glucosylation using the newly developed glucosynthase BglU-E377A was examined. The enzyme exhibited a much lower activity than Abg-E358S and the time of the enzymatic reaction needed to be lengthened to determine a reliable activity. A specific activity of  $1.8 \cdot 10^{-2} \pm 2.0 \cdot 10^{-3}$  U/mg was determined for the enzyme (1 : 1 donor **2a** : acceptor **5h**), which was around 46 $\times$  lower than the specific activity of Abg-E358S even after doubling the donor concentration. However, the 3.5 $\times$  lower enzyme concentration of BglU-E377A employed in the reaction must be considered. The potential synthase mutants BglC-E113S, -E189S, and -E316S, which were already ruled out for use as glycosynthases, were also tested for synthetic activity using the fluoride quantification assay. The identical reaction as tested for Abg-E358S and BglU-E377A was carried out at optimal temperature of 85 °C of the *wt* enzyme. As before, no synthetic activity was observed for each mutant. Only thermal hydrolysis of  $\alpha$ -GlcF **2a** could be detected. The thermal instability of glycosyl fluoride derived donors has also been described by *Williams and Withers*.<sup>[93]</sup> Therefore, to avoid a thermal hydrolysis, the reaction was assayed for each mutant at lowered temperatures of 25–65 °C. Instead of enzymatic activity, only an increase in autohydrolysis for each reaction (observable by the control reaction) with increasing temperature was detected. These results verify the non-suitability of the variants of BglC for glycosynthetic reactions. They also illustrate the limitation of hyperthermophilic glycosidases with narrow temperature optima as candidates for glycosynthases when using glycosyl fluoride derived donors.

### 6.1.6 Glycosynthase kinetics and acceptor screening

The first experiments demonstrated the applicability of the fluoride quantification assay for detection of the synthetic activity of glycosynthases. Further applicability was to be shown by characterisation of the glycosynthases Abg-E358S and BglU-E377A. The kinetic parameters of these enzymes were determined for the same reaction as in section 6.1.5 in  $\text{NH}_4\text{HCO}_3$ -buffer (150 mM, pH 7.9). This buffer is most commonly used for synthetic reactions but not for the characterisation of the enzymatic properties used for the synthesis. A two-dimensional approach, varying both the acceptor and donor molecule concentration (0–80 mM) for the measurement of the *Michaelis-Menten* kinetics was taken. Therefore, the activity of the glucosynthases was measured with 37 different ratios of donor and acceptor concentrations (Figure 49).

## 6 Results

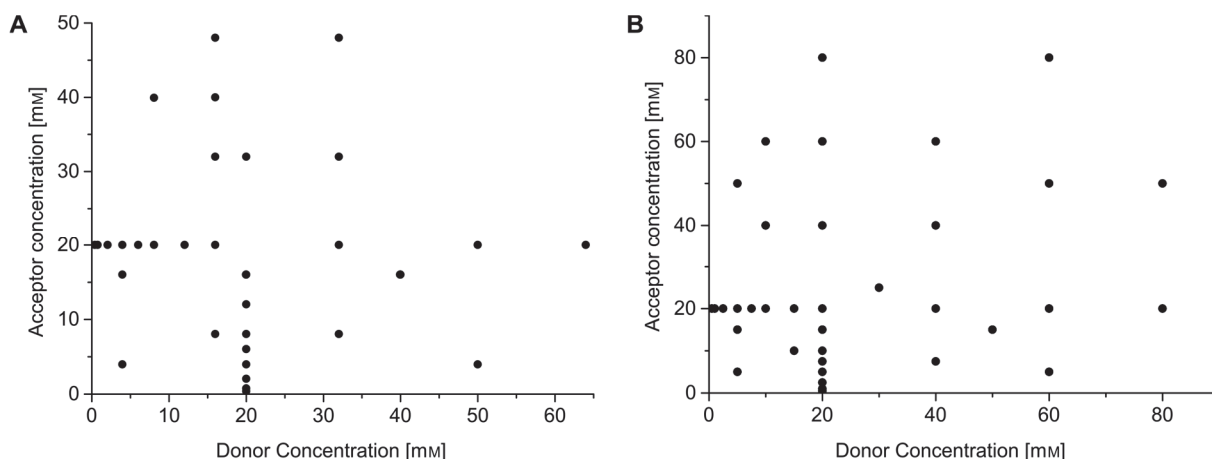


**Figure 49** Donor ( $\alpha$ -GlcF **2a**) and acceptor ( $p$ NPGlc **5h**) concentration ratios chosen for the determination of kinetic parameters for Abg-E358S (**A**) and BglU-E377A (**B**).

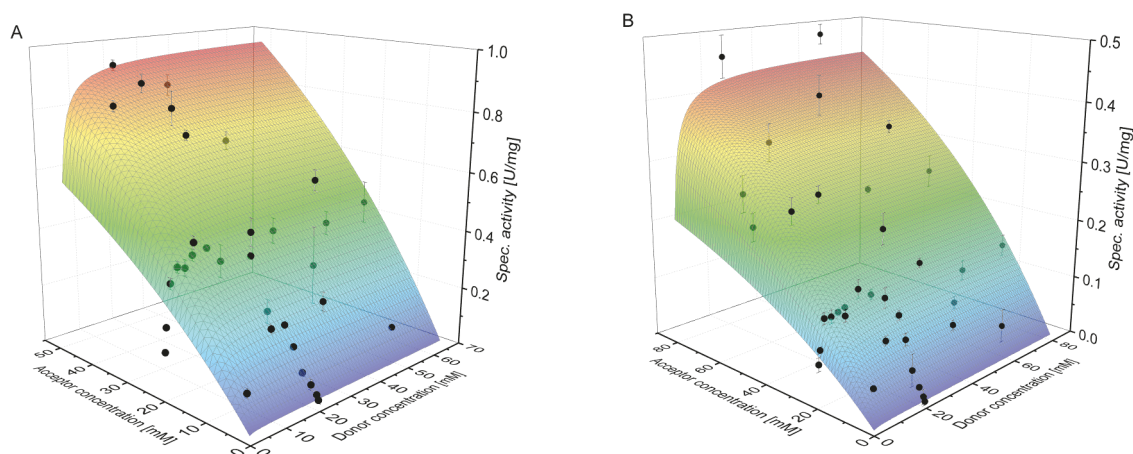


**Figure 50** Characterisation of the glycosynthases Abg-E358S (**A**) and BglU-E377A (**B**) by 2D-Michaelis-Menten kinetics determined in  $\text{NH}_4\text{HCO}_3$ -buffer (150 mM, pH 7.9). The specific activity (U/mg) of the enzyme variants was determined for 37 different acceptor **5h**: donor **2a** ratios. Subsequent fitting of the data was carried out using the data set of each triplicate measurement.

$$\text{Equation 2} \quad v = \frac{(v_{\max} \times x \times y)}{(K_{Ma} \times K_{Mb} + K_{Mb} \times x + K_{Ma} \times y + x \times y)} \quad [157]$$

Each reaction was measured in triplicate and the complete set of data was fitted to a *Michaelis-Menten*-equation for a two substrate reaction (Figure 50, Equation 2).<sup>[157]</sup> The maximal activity ( $v_{\max}$ ) of the enzymes was determined as  $2.9 \pm 2.1 \cdot 10^{-1}$  U/mg and  $1.1 \pm 1.2 \cdot 10^{-1}$  U/mg for Abg-E358S and BglU-E377A, respectively (Table 8). The low activity of the  $\beta$ -glucosynthase BglU-E377A was also observed in the activity measurements described in section 6.1.5. However, in this case the maximal activity of Abg-E358S is only 2.6 $\times$  higher than for BglU-E377A, indicating to non-optimal conditions for BglU-E377A during the activity measurement in section 6.1.5. A high affinity towards the donor  $\alpha$ -GlcF **2a** with low  $K_{M, \alpha\text{-GlcF}}$  values of  $6.7 \cdot 10^{-1} \pm 1.5 \cdot 10^{-1}$  mM and  $1.1 \pm 2.8 \cdot 10^{-1}$  mM (Abg-E358S and BglU-E377A, respectively) was exhibited by both enzymes. The affinity of the enzymes towards the acceptor **5h** was much lower, observable by the high  $K_{M, p\text{NPGlc}}$  values of  $94 \pm 19$  mM and

$11 \cdot 10^1 \pm 18$  mM. The large standard deviations of the determined  $K_M$  values towards the acceptor **5h** (16–20% deviation) are due to the low solubility of the acceptor molecule. This issue can be easily recognised in the curve of the plotted fit of the kinetic measurements (Figure 50). The concentration of *p*NPGlc **5h** is far from the theoretical  $v_{max}$  value, leading to the high uncertainty of the  $K_{M, pNPGlc}$  value.

**Table 8** Kinetic parameters  $v_{max}$  and  $K_M$  (for the donor and acceptor respectively) for the glycosynthase Abg-E358S and BglU-E377A. The reaction velocities of 37 acceptor **5h**:donor **2a** ratios were determined and fitted with *Michaelis-Menten* kinetics considering two substrates.

	$v_{max}$ [U/mg]	$k_{cat}$ [s <sup>-1</sup> ]	$K_M, \alpha\text{-GlcF}$ [mM]	$K_M, pNPGlc$ [mM]
Abg-E358S	$2.9 \pm 2.1 \cdot 10^{-1}$	$2.5 \pm 1.8 \cdot 10^{-1}$	$6.7 \cdot 10^{-1} \pm 1.5 \cdot 10^{-1}$	$94 \pm 19$
BglU-E377A	$1.1 \pm 1.2 \cdot 10^{-1}$	$9.6 \cdot 10^{-1} \pm 1.1 \cdot 10^{-1}$	$1.1 \pm 2.8 \cdot 10^{-1}$	$11 \cdot 10^1 \pm 18$

The difference in affinity towards the donor and acceptor molecules give indications towards the natural substrate range of both examined enzymes. The -1 sub-site of both  $\beta$ -glucosidases are optimally designed for the recognition of the non-reducing terminus of a glucoside substrate. In comparison, the +1 and possibly +2 sub-site of the  $\beta$ -glucosidases are not suitably arranged for the recognition of glucose or an aryl substituent containing a nitro group in the *para*-position of the benzyl ring.

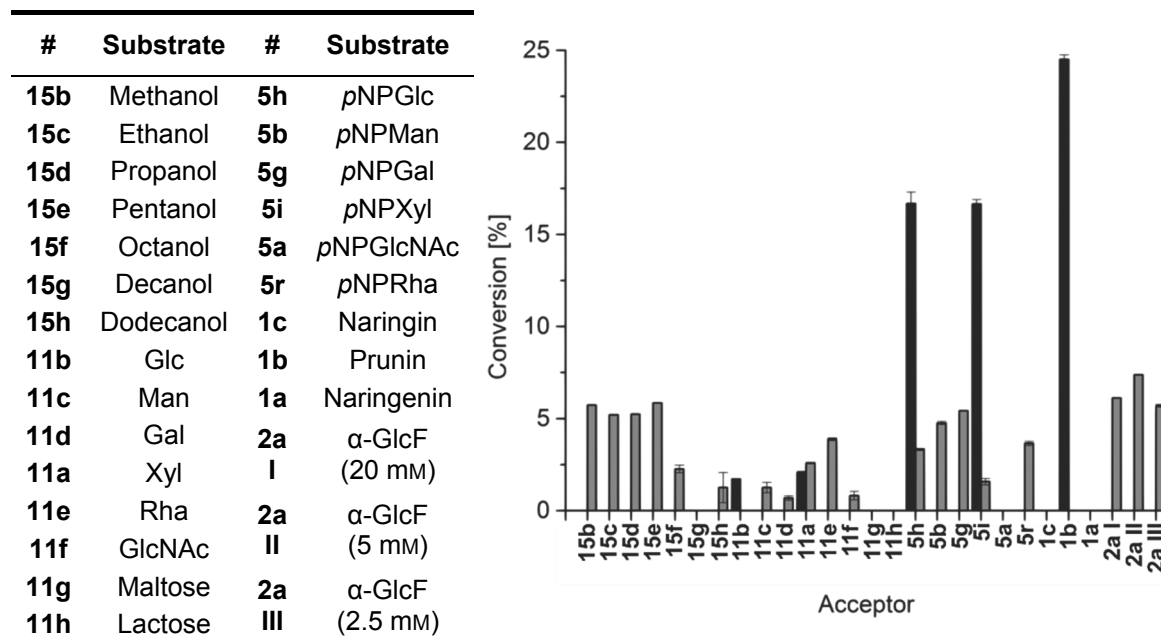


**Figure 51** Acceptor scope screening for the glycosynthases Abg-E358S (0.12  $\mu$ M; black) and BglU-E377A (0.20  $\mu$ M; grey). The reactions were carried out in  $\text{NH}_4\text{HCO}_3$ -buffer (150 mM, pH 7.9) with  $\alpha$ -GlcF **2a** as donor and the respective acceptor in a 1 : 2 ratio. Homocoupling was tested in **2aI–III** with absence of an acceptor molecule. Conversion was determined by the quantification of fluoride release after 1 h. The reactions were carried out in triplicate and control reactions were carried out without addition of enzyme.

To characterise further the  $\beta$ -glucosynthases and scope of the assay applicability, the substrate scope towards the acceptor molecule structure was screened. A batch of 24 different acceptor molecules were incubated in a 1 : 2 donor : acceptor ratio with  $\alpha$ -GlcF **2a** as the donor and the respective glycosynthase for up to 1 h at 25 °C. Different acceptor molecule types, such as alcohols **15b–g** varying in alkyl chain length, various glycosides **11a–h**, **5a/b**, **5g–l**, **5r**, and three derivatives of the naringenin flavonoid **1a–c** were chosen for the screening in order to determine factors, which promote the glycosylation activity (Figure 51). The screening showed an obvious preference of Abg-E358S for glucosyl and xylosyl moieties with respect to the acceptor. The enzyme featured a moderate activity towards the monosaccharidic acceptor molecules **11a** and **11b**. Addition of the aromatic *p*-nitrophenyl aglycone to these moieties (**5i** and **5h**) increased the activity largely. This increase could indicate to a favourable interaction of the aromatic aglycone with the enzymes +2 sub-site. An increased activity of the Abg-E358S was also observed towards prunin **1b**, a glucoside of the naringenin flavonoid **1a** (Figure 52).

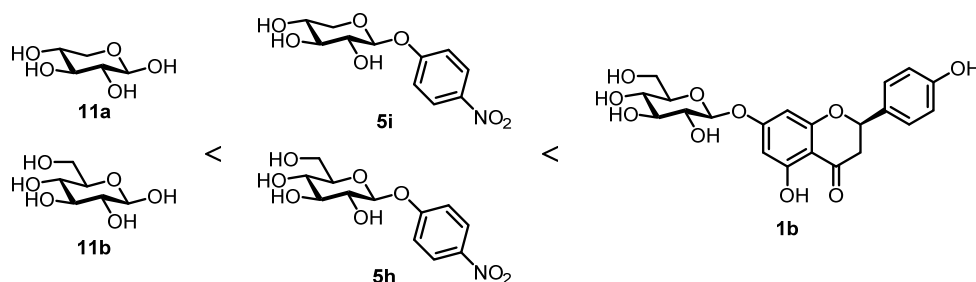


**Figure 52** Substrate preference with respect to the acceptor molecule of the  $\beta$ -glucosynthase Abg-E358S. The screening of 24 acceptor molecules displayed a preference of Abg-E358S for glucosides and xylosides, preferably with an aryl aglycone.

In contrast, the screening of the acceptor scope of BglU-E377A did not lead to a clarification of the psychrophilic enzymes acceptor preference. For various acceptors, a conversion of the donor **2a** could be detected by the assay. However, control reactions containing donor **2a** in absence of an acceptor molecule also showed a conversion in a similar percentage, indicating to a high self-coupling reaction of the donor molecules (Figure 51). Therefore, identification of the coupling products would be requisite in order to determine if solely a self-coupling of the donor molecules is catalysed by the enzyme or not. The results clearly illustrate the importance of the self-coupling control reactions in addition to the autohydrolysis controls for the characterisation of newly developed glycosynthases, as these types of side reactions can lead to false depictions of the glycosynthases properties.

Furthermore, the effect of the donor : acceptor ratio on the glucosylation reaction of *p*NPGlc **5h** catalysed by Abg-E358S was examined. The release of fluoride, representing the conversion of the glycosyl donor **2a**, was determined for the reaction with different donor **2a** : acceptor **5h** ratios ranging from 5 : 1 up to 1 : 5 (Figure 53). An excess of the donor molecule  $\alpha$ -GlcF **2a** did not influence the glycosylation reaction as similar amounts of fluoride were released for the

ratios ranging from 5 : 1 up to 1 : 1 (donor : acceptor). The application of an excess of the acceptor **5h** on the other hand had a strong influence on the conversion by the enzyme. A donor : acceptor ratio of 1 : 2 caused a near doubling of the conversion of  $\alpha$ -GlcF **2a** and a 1 : 4 ratio caused the maximal increase. Applying a further excess of the acceptor (1 : 5) caused a decrease of the conversion compared a ratio at 1 : 4. The different effects of the donor : acceptor ratios on the conversion of the glycosyl fluoride donor are most likely competitive effects concerning the binding of the glycosidases active site sub-sites. A high donor concentration will cause an increased binding of the  $\alpha$ -GlcF **2a** in the +1 sub-site, thereby competing with the acceptor **5h** and promoting the homocoupling reaction. A too high excess of the acceptor *p*NPGlc **5h** on the other hand will block the -1 sub-site and therefore decrease the conversion of the donor **2a**. The positive effects of a slight excess of acceptor **5h** can also be explained by the lower affinity of Abg-E358S towards *p*NPGlc **5h** ( $K_{M, pNPGlc} = 93.82 \pm 19.02$  mM) observed during the determination of the kinetic parameters.

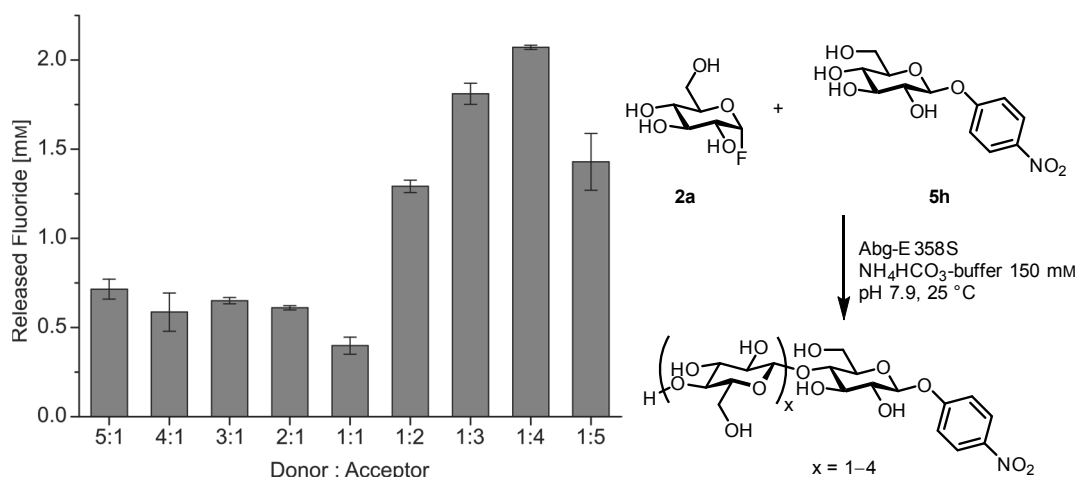


**Figure 53** Effect of the donor : acceptor ratio on the glycosylation reaction of Abg-E358S. The donor **2a** and acceptor **5h** concentrations were varied in 10 mM steps (from 50 mM : 10 mM to 10 mM : 50 mM) the reactions were carried out in NH<sub>4</sub>HCO<sub>3</sub>-buffer (150 mM, pH 7.9), incubated for 10 min at 25 °C. The released fluoride was determined by cleavage of TIPS*p*NP **23** and absorption measurement.

The obtained results show the applicability of the fluoride quantification assay for a reliable determination of a glycosynthases' kinetic parameters. Throughout literature, the kinetic parameters are usually determined by lengthy HPLC analyses or fluoride quantification *via* the ion-selective electrode. Therefore, the presented assay is the first method of determining a glycosynthases' kinetic parameters in a fast and efficient microplate format.

Chapter synopsis:

- The *wt* genes *abg*, *bglU*, and *bglC* were isolated/synthesised and incorporated into expression vectors. These glycosidase genes were mutated *via QuikChange*<sup>™</sup> PCR producing two variants of *abg*, five variants of *bglU*, and nine variants of *bglC*.
- The *wt* enzymes Abg, BglU and BglC were expressed and characterised with respect to temperature dependency and their kinetic parameters. BglC was further characterised towards substrate specificity, temperature and storage stability, and pH optimum.
- Structural analysis of BglC determined the function of the annotated 'β-galactosidase' as a potential β-glucosaminidase.
- The mutant variants of the hyperthermophilic, mesophilic and psychrophilic glycosidases were tested for glycosynthetic activity, which was found for the glycosidase variants Abg-E358S and E358A, and BglU-E377A.
- A fluoride quantification assay was developed in a microplate format based on the cleavage of triisopropyl-(4-nitrophenoxy)-silane (**23**, TIPSpNP) by released fluoride ions. The assay allowed for fast and reliable measurement of glycosynthase conversions.
- The kinetic parameters and substrate scope of the glycosynthases Abg-E358S and BglU-E377A were determined by use of the developed glycosynthase activity assay.

## 6.2 A substrate based approach for glycosynthase development

### 6.2.1 Choice and isolation of the $\beta$ -glucosidase Cbg1

The mutation of mostly *exo*-glycosidases to glycosynthases has resulted in many glycosynthases, which transfer glycosyl residues specifically to glycosidic acceptors. Examples of glycosynthases glycosylating non-glycosidic structures are still only few, such as TnG-E388A, HiCel7B-E197S, and EGCCase II-D351S, glycosylating the acceptors dehydroepiandrosterone (**4a**), flavonoids **1d/e**, and sphingosine (**9a**) respectively.<sup>[28, 36, 42]</sup> The latter two enzymes belong to the group of *endo*-glycosidases transferring only oligo- or disaccharide donors such as cellobiosyl or lactosyl fluoride, requiring further modification reactions in order to receive a product with a single glycosyl residue. The only *exo*-glycosidase-derived synthase is thereby TnG-E388A, which, as described in section 5.2.1 (Table 1), exhibits a wide acceptor range including a steroidal type.

Most *exo*-glycosidases isolated from a diverse array of organisms, take part in the primary carbohydrate metabolism. Their function is most commonly the release of monosaccharides from large polysaccharides in order to process these further in pathways such as the glycolysis. Therefore, their +1 sub-sites have most likely evolved to optimally bind glycosidic moieties. To find *exo*-glycosidases, which do not act on polysaccharides, possibly possessing sub-sites with a high affinity to non-glycosidic compounds, the focus must be shifted to enzymes of the secondary metabolism. With help of the KEGG pathway database different secondary metabolisms were examined for the presence of glycosides with non-glycosidic aglycones.<sup>[158]</sup> Additionally to the specification of a non-glycosidic aglycone, it was important to find compounds of which the attributed hydrolysing enzyme (cleaving the glycoside from the non-glycosidic aglycone) has also been described in literature. A search through the KEGG pathway database revealed interesting compounds such as coniferin (**14a**), syringin (**24**), and 4-hydroxycinnamyl alcohol 4- $\beta$ -D-glucoside (**25**) as part of the phenylpropanoid biosynthetic pathway (Figure 54). All three compounds belong to the group of monolignols and contain a  $\beta$ -glucoside directly linked to a phenolic hydroxyl group.

## 6 Results

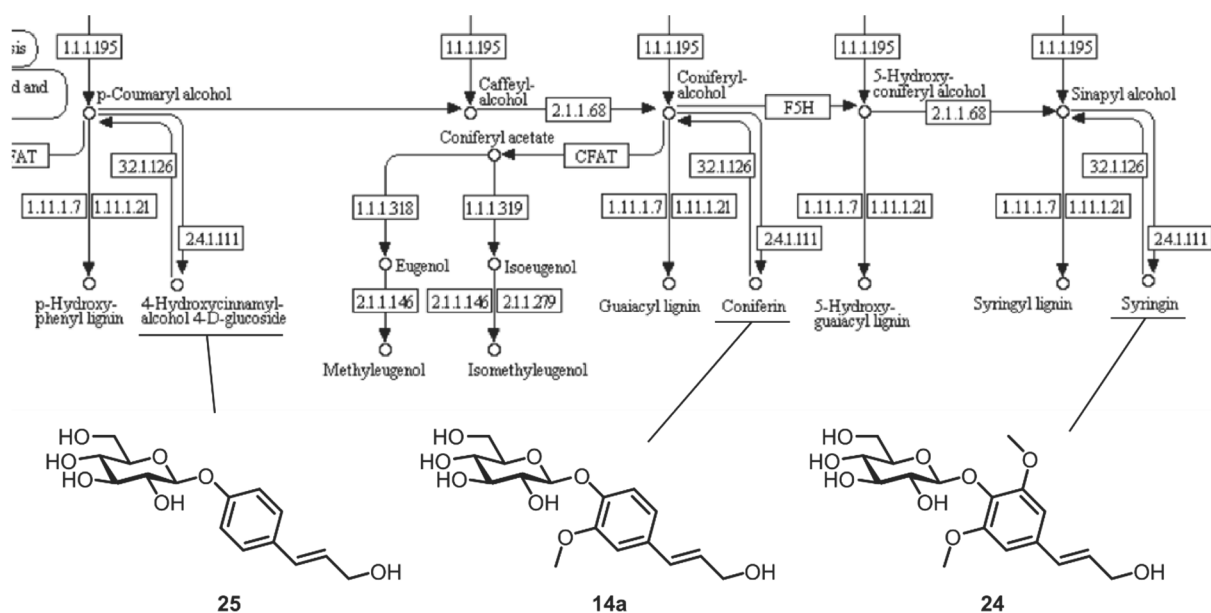


**Figure 54** Excerpt from the phenylpropanoid biosynthetic pathway (KEGG pathway) for the identification of glycosides with non-glycosidic aglycones.<sup>[158]</sup> The boxed numbers represent the E.C. number of a respective enzyme. Three glycosides, syringin (**24**), coniferin (**14a**), and 4-hydroxycinnamyl alcohol 4-D-glucoside (**25**) were identified, which are all hydrolysed by the same enzyme, coniferin-hydrolysing  $\beta$ -glucosidase (E.C.3.2.1.126).

Recognisable in the phenylpropanoid biosynthesis, all three glycosides **14a**, **24**, and **25** can be cleaved by the coniferin-hydrolysing  $\beta$ -glucosidase (E.C.3.2.1.126). This type of enzyme has been described by *Marcinowsdki et al.* as a cell wall bound  $\beta$ -glucosidase in *Picea abies* (Norway spruce), and by *Hösel et al.* as an enzyme possibly involved in lignification from *Cicer arietinum* (chickpea).<sup>[159, 160]</sup> *Castle et al.* also identified a bacterial coniferin-specific  $\beta$ -glucosidase Cbg1 produced by the plant pathogen *R. radiobacter* (formerly *A. tumefaciens*), which was induced by the presence of coniferin (**14a**) and is proposed to play a crucial role in the virulence of *R. radiobacter* towards conifers.<sup>[85]</sup> The enzyme was further characterised by *Watt et al.* and described to have a high transglycosylation activity in the presence of hydrophobic alcohols.<sup>[88]</sup> This  $\beta$ -glucosidase therefore has a high potential to act as a glycosynthase, which can create glycosidic bonds directly bound to a phenolic aglycone instead of a glycosidic acceptor.

Identically to the  $\beta$ -glucosidase gene *abg*, described in section 6.1.1, the *cbg1* gene was to be isolated from the genomic DNA of *R. radiobacter*. The isolated *cbg1* gene was subsequently to be inserted into a pET-21a(+) vector between the XhoI and NdeI restriction sites fusing a C-terminal His<sub>6</sub>-tag to the protein for IMAC purification. Due to the difficulties in the isolation of *abg* from the genomic DNA, two approaches for the isolation and amplification of *cbg1* were carried out simultaneously. Firstly, simple primers (#17 & 18) binding at the beginning and end of the gene were designed to amplify the gene from the genomic DNA in a standard PCR reaction. Secondly, a pair of primers with overlaps (complementary to the vector insertion site, #19 & 20) were designed for a direct use of the amplicon in a *Gibson assembly*.<sup>[135]</sup>

Nonetheless, despite variation of the annealing temperature (50–70 °C), no amplification product could be observed for both PCR reactions. Therefore, a third set of primers (#21 & 22) was developed binding -107 bp upstream and +110 bp downstream of *cbg1* for the use in a *nested*-PCR as was carried out for the isolation of *abg*. The combination of the four primers (#17–18, 21–22) led to an array of amplification products of different sizes (Figure 55, **A**). A variation of the employed primers (#18 & 21, #17 & 22; Figure 55, **B & C**) did not lead to a reduction of undesired side products. The amplicon of ~2 kbp, possibly an amplification of *cbg1* (2,457 bp), was only produced in a low amount. Isolation of this amplicon and use as a template in a further PCR reaction led to further mixture of amplification products.

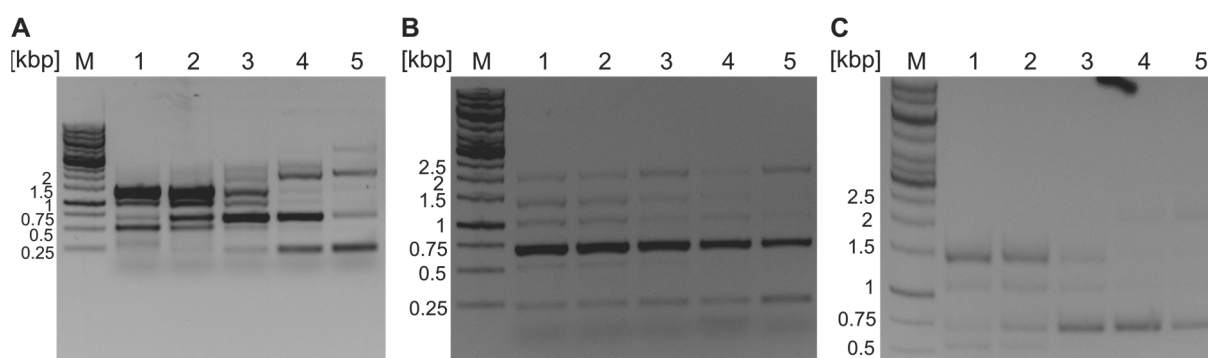


**Figure 55** Analysis of the *nested*-PCR reaction mixtures for the amplification of *cbg1*. Variation of the annealing temperature (1: 51 °C; 2: 54 °C; 3: 58 °C; 4: 63 °C; 5: 68 °C) and combination of primers (**A** #17–18, 21–22; **B** #18 & 21; **C** #17 & 22) did not reduce the amount of undesired side products. All depicted PCR reactions were carried out with the *Phire Hot-Start II* DNA-polymerase

For the insertion of a gene into an expression vector, the direct use of these PCR reaction mixtures is highly disadvantageous as many products can be inserted and lead to false vectors. In an attempt to reduce undesired side products, five different DNA-polymerases, the *Phire Hot-Start II*, *Phusion High-Fidelity*, KAPA-HiFi, *Herculase II Fusion*, and Taq DNA-polymerase were tested (Figure 56). Of the five tested polymerases, the *Herculase II Fusion* polymerase produced the highest amount of amplicon at ~2.5 kbp while producing the least side products (with an annealing temperature set at 63 °C). Variation of the PCR method to a *touchdown*- or sequential *nested*-PCR (use of the PCR-mixture with primers #21 & 22 as a template for a PCR reaction with primers #17 & 18) did not improve the amount of desired and undesired products.

## 6 Results

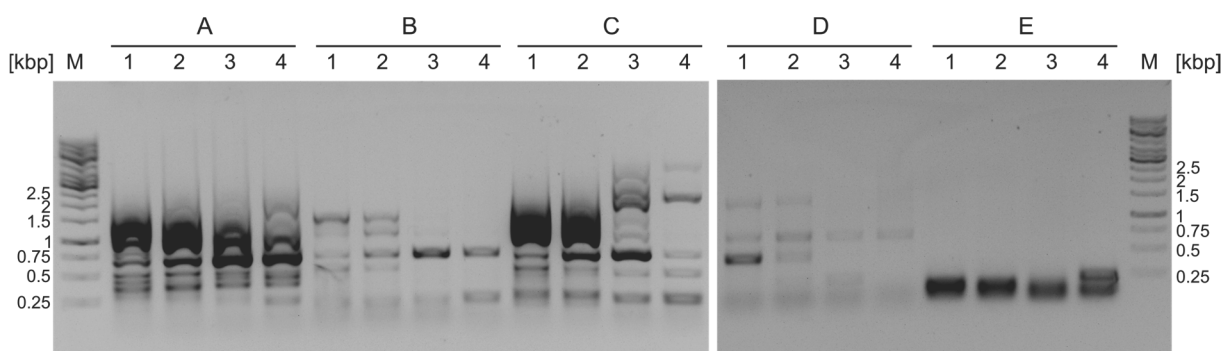


**Figure 56** Variation of the DNA-polymerase for the amplification of *cbg1* from the genomic DNA of *R. radiobacter*. Each polymerase, *Phire Hot-Start II* (A), *Phusion High-Fidelity* (B), *Herculase II Fusion* (C), Taq (D), and Kappa-HiFi (E) was tested with a variation of annealing temperatures (1: 52 °C; 2: 55 °C; 3: 58 °C; 4: 63 °C).

In a final attempt, the use of the TOPO-TA cloning method was attempted. This method utilises the topoisomerase I, which acts both as a restriction enzyme and as a ligase. The topoisomerase is covalently bound to the TOPO-cloning vector and ligates PCR products with a 3'-adenine overhang directly into the cloning vector. Such an overhang is automatically added by the Taq polymerase, therefore allowing direct use of PCR products produced by the Taq polymerase for TOPO-TA cloning. Nevertheless, the *cbg1* gene was not amplified by the Taq polymerase for TOPO-TA cloning. Nevertheless, the *cbg1* gene was not amplified by the Taq polymerase using the genomic DNA as a template, but also when applying the PCR product obtained by the *Herculase II fusion* polymerase as the template. The isolation and insertion of *cbg1* was therefore also not possible considering this cloning method. Due to these difficulties in amplification and isolation of *cbg1* from the genomic DNA of *R. radiobacter*, the gene was then synthesised commercially into a pET-21a(+) vector at the desired position and chemically competent *E. coli* BL21(DE3) cells were transformed for expression and characterisation of the *wt* enzyme.

### 6.2.2 Characterisation of Cbg1

The characterisation of the *wt* form of Cbg1 was carried out by *Watt et al.* applying a temperature of 30 °C. This was determined by the group as the optimal temperature for Cbg1 for the hydrolysis of *pNPGlc 5h*. In regard to employing mutant variants of Cbg1 as glycosynthases, at temperatures preferably lower than 30 °C, the *wt* glycosidase Cbg1 was expressed and characterised with respect to the kinetic parameters and substrate scope of the enzyme at 25 °C. After transformation of chemically competent *E. coli* BL21(DE3) with the pET-21a(+) expression vector containing *cbg1*, the expression of Cbg1 was induced by the addition of IPTG. A 24 h incubation at 25 °C resulted in an overexpression of the enzyme visible by SDS-PAGE analysis (Figure 57). The purification by IMAC yielded an enzyme solution with high purity and a protein concentration of  $1.3 \pm 1.0 \cdot 10^{-1}$  mg/mL (after desalting and concentrating). The molecular weight of the isolated enzyme was determined, by

comparison with the standard in the SDS-PAGE, as 86 kDa, which corresponds well to the theoretical value of 89 kDa and the values observed in literature.<sup>[85, 88]</sup>

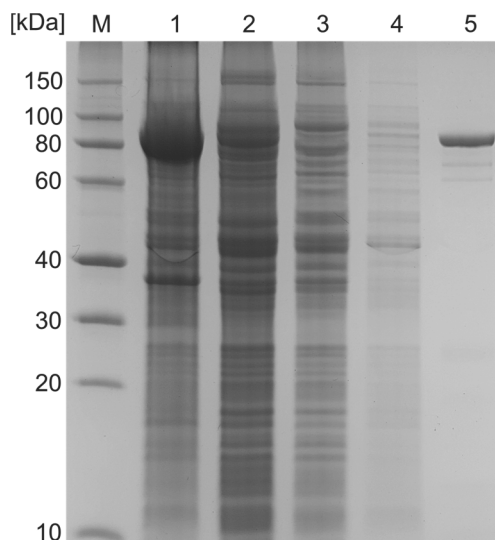


**Figure 57** SDS-PAGE analysis of the IMAC purification of the *wt*  $\beta$ -glucosidase Cbg1 of *R. radiobacter* expressed in *E. coli* BL21(DE3). Different steps of the purification are depicted: 1 cell lysate; 2 cell-free lysate; 3 flow-through; 4 wash fraction; 5 elution. Roti-Mark 10–150 was applied as a standard (M) for size determination.

Furthermore, the kinetic parameters exhibited by Cbg1 for the hydrolysis of *p*NPGlc **5h** at 25 °C and a pH of 7.5 (K<sub>P</sub>-buffer, 50 mM) were determined (Figure 58). The enzyme showed a maximal activity of  $23.7 \pm 1.41$  U/mg and a high affinity to *p*NPGlc **5h**, recognisable by the low  $K_M$  value of  $36 \pm 4.7 \cdot 10^{-3}$  mM. Due to a decrease of the specific activity caused by high concentrations of *p*NPGlc **5h**, the collected data was fitted according to *Murray* (section 6.1.2, Equation 1), as was carried out for Abg (section 6.1.2; Figure 30, **A**).<sup>[142]</sup> The decrease in activity indicated to a substrate-excess inhibition and the  $K_i$  was determined to be  $2.0 \pm 5.2 \cdot 10^{-1}$  mM. The activity decrease may be caused by a competitive inhibition of glucose (**11b**), which is released by the hydrolysis of *p*NPGlc **5h**. *Watt et al.* also observed an inhibition by glucose (**11b**) and determined the inhibition constant of glucose (**11b**) towards Cbg1 to be 2.9 mM.

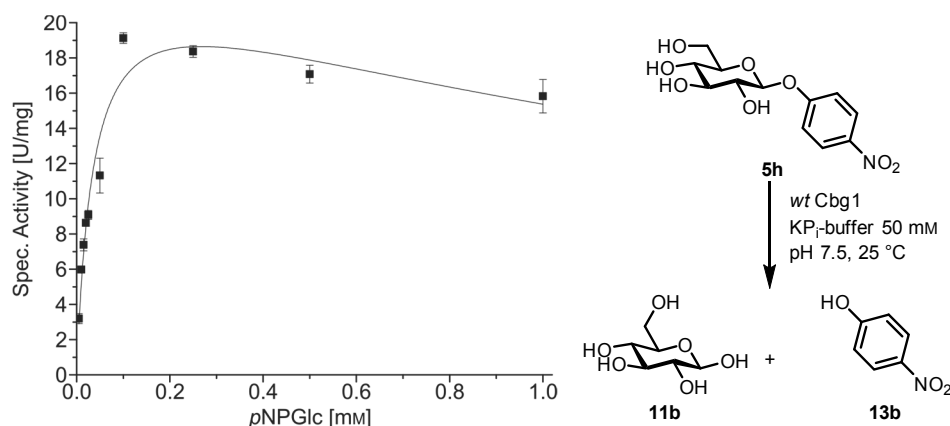


**Figure 58** Determination of the kinetic parameters of the  $\beta$ -glucosidase Cbg1 of *R. radiobacter*. Parameters were determined for the hydrolysis of pNPGlc **5h** in KP<sub>i</sub>-buffer 50 mM, pH 7.5 at 25 °C. Collected data was fitted according to Murray (Equation 1).<sup>[142]</sup>

The substrate scope of Cbg1 was examined for eleven different *p*-nitrophenyl glycosides, to determine important recognition motifs of the -1 sub-site, which would in turn determine the scope of glycosyl donor types for a glycosynthase derived from Cbg1 (Figure 59).

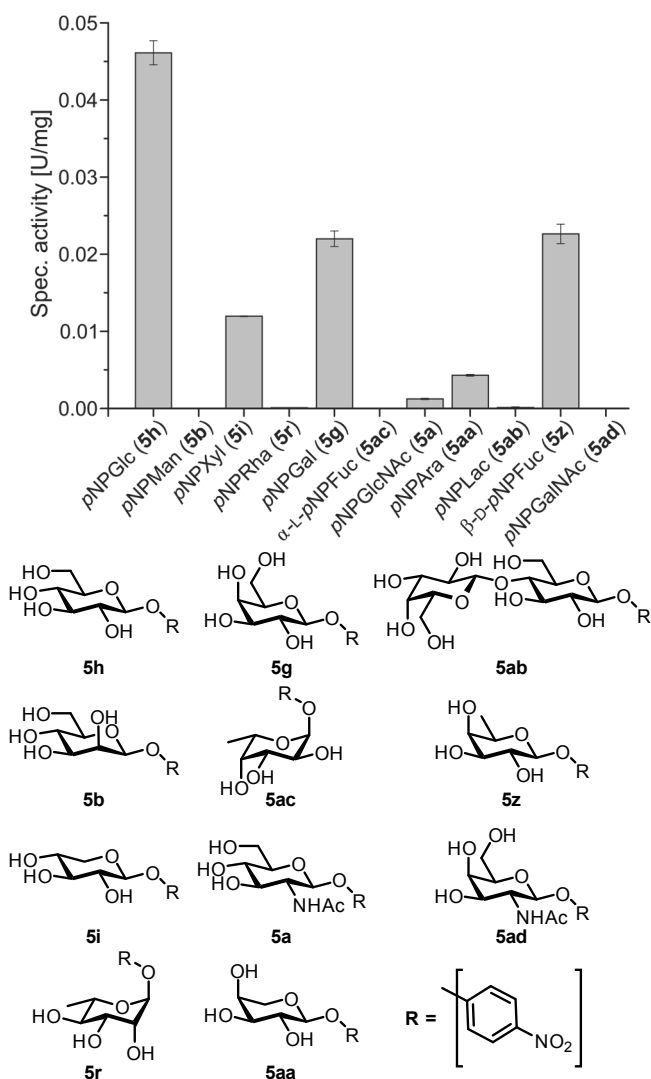


**Figure 59** Determination of the substrate scope for Cbg1 with respect to the glycoside, which binds to the -1 sub-site of the active site. Each reaction was incubated at 25 °C in 50 mM KP<sub>i</sub>-buffer, pH 7.5.

As expected, the highest hydrolytic activity of Cbg1 was exhibited towards *p*NPGlc **5h** with a specific activity of  $4.6 \cdot 10^{-2} \pm 1.6 \cdot 10^{-3}$  U/mg. The hydrolytic activity towards *p*NPXyl **5i** on the other hand was 3.9× lower ( $1.2 \cdot 10^{-2} \pm 5.1 \cdot 10^{-5}$  U/mg) than towards *p*NPGlc **5h**, clearly displaying the importance of the hydroxyl group of the C<sub>6</sub>-position for the binding of the glycosyl substrate. The glycosidase also showed hydrolytic activity towards *p*NPGal **5g** with an activity of  $2.2 \cdot 10^{-2} \pm 1.0 \cdot 10^{-3}$  U/mg. The axial configuration in the C<sub>4</sub>-position of the pyranoside significantly decreased the hydrolytic activity compared to *p*NPGlc **5h** with an equatorial hydroxyl group in the same position. The near equal activity towards β-D-*p*NPFuc **5z**, which possesses the identical configuration as β-D-*p*NPGal **5g** but no hydroxyl group at C<sub>6</sub>, indicated a major participation of the methylene moiety at C<sub>6</sub>. This was also evident by the even lower activity of  $4.3 \cdot 10^{-3} \pm 1.2 \cdot 10^{-4}$  U/mg towards *p*-nitrophenyl α-L-arabinopyranoside **5aa** (*p*NPAra), in which the C<sub>6</sub>-methylene group is absent. An even higher impact on the substrate recognition was exhibited by modification of the C<sub>2</sub>-configuration. Cbg1 displayed no activity towards *p*NPMan **5b**, and only weak activity towards *p*NPGlcNAc **5a**. The enzyme also did not accept disaccharidic substrates, showing no activity towards *p*-nitrophenyl lactoside (**5ab**).

### 6.2.3 Mutagenesis and screening for synthetic activity

In order to create a glycosynthase derived from the β-glucosidase Cbg1, mutagenesis studies were carried out to exchange the catalytic nucleophilic residue, eliminating the hydrolytic activity of the hydrolase. The nucleophilic residue D222 was identified by *Castle et al.* by amino acid sequence alignment with other GH 3 glycosidases.<sup>[85]</sup> The consensus sequence [-SDW-] containing the nucleophilic residue typical for this glycohydrolase family was also present in Cbg1. To identify the catalytic acid/base residue, proposed by *Goyal et al.* to be residue E616, a structural analysis of Cbg1 using the crystal structure of *KmBglI* (*K. marxianus*) as a model was carried out. This model structure was chosen as the amino acid sequence shows 40% identity and 64% similarity to Cbg1.<sup>[89, 92]</sup> The sequence of Cbg1 and *KmBglI* was additionally aligned with the amino acid sequence of *VvBglIII* (*Volvariella volvacea*), which also shares a high identity of 38.2% with Cbg1, to identify the conserved areas of the proteins structure. The alignment clearly demonstrated a high level of conserved residues in the (β/α)<sub>8</sub>- and (α/β)<sub>6</sub>-domains, in particular in the region of the active site (Figure 60). The PA14-domain inserted into the (α/β)<sub>6</sub>-domain, present in all three aligned glycosidases, showed a lower level of conservation. This difference most likely explains the different specificity of the enzymes towards the aglycone of the glycoside substrate as a direct result of a different structure of the +1 sub-site created by the PA14 domain.



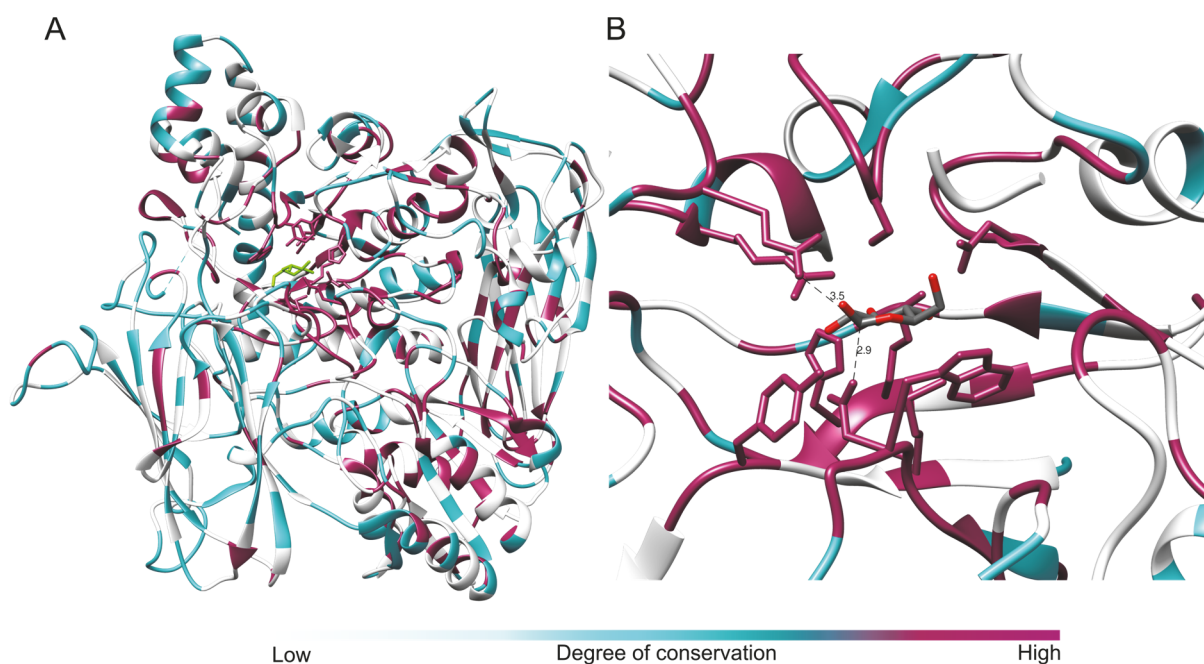


**Figure 61** Structural analysis of the overall structure (A) and active site (B) of the  $\beta$ -glucosidase *KmBglI* (PDB 3AC0) as a model for the structure of *Cbg1*. The degree of conservation was determined by alignment of the amino acid sequences of *Cbg1* with *KmBglI* and *VvBglIII* and is depicted by the colour gradient. Distances of the catalytic residues, corresponding to D222 (2.9 Å) and E559 (3.5 Å) in *Cbg1*, to the anomeric centre of the glucose molecule are depicted (B).

The catalytic nucleophile is conserved in all three glycosidases, in contrast to the proposed acid/base residue E616, which is only found in *KmBglI* but not *VvBglIII*. The position of the residue far from the active site also negates the possibility of this residue acting as the acid/base catalyst during hydrolysis. In comparison, the position of the acid/base residue determined for *KmBglI* by *Yoshida et al.* is also conserved in all three  $\beta$ -glycosidases, therefore the residue E559 in *Cbg1* was established as the acid/base catalyst.

After identification of the catalytic residues as D222 and E559, the nucleophilic residue D222 was to be exchanged with the less nucleophilic residues cysteine and serine and the non-nucleophilic amino acid alanine. Glycine was excluded from the mutagenesis as the exchange with glycine can often lead to structural problems due to a high increase in flexibility of the protein back-bone caused by this residue. Initially, mutation of the D222 residue was to be carried out by the *QuikChange*<sup>TM</sup>-PCR method. Primers containing the respective point mutations were designed and applied in the PCR reaction. Similar to the attempts to isolate *cbg1* from the genomic DNA from *R. radiobacter*, the PCR did not yield the desired product but many side products. The variation of the annealing temperature also did not lead to the desired mutated gene. As an alternative option the *round the horn*-PCR mutagenesis method was chosen. First PCR reactions with the respective designed primers led to the desired amplicon, but with the presence of many side products. Changing the procedure to a two-step protocol, consisting of only a denaturation step (98 °C) and a combined annealing and extension step (72 °C), resulted in the production of an around 8 kbp amplicon with little side

products. The mutagenesis procedure allowed the isolation and identification of the three vectors containing the D222A, D222S, and D222C variants of *cbg1* (Table 9).

**Table 9** Variation of the catalytic nucleophilic amino acid residues D222 of Cbg1 of *R. radiobacter*. The mutations were acquired by *round the horn*-PCR by mutation of the *wt* gene in pET-21a(+). Obtained plasmids were sequenced for confirmation of the resulting mutation.

Original AA	Introduced mutation	Codon variation	Verification
D222	A	GAC → GCC	+
	C	GAC → TCC	+
	S	GAC → TCG	+

The mutant variants of Cbg1 were examined for hydrolytic activity towards the enzymes natural substrate coniferin (**14a**). The hydrolysis was determined by the quantification of coniferyl alcohol (**14b**), which can be detected by a reaction with the *Fast Blue RR Salt* reagent (Figure 62). The assay was described by *Castle et al.* during the identification of Cbg1.<sup>[85]</sup> The exchange of the nucleophilic residue D222 with the non-nucleophilic residue alanine, decreased as expected the hydrolytic activity greatly by 97% compared to *wt* Cbg1. The Cbg1-D222C variant showed a weak activity, 3× higher than Cbg1-D222A. On the contrary, the Cbg1-D222S mutant unexpectedly retained the hydrolytic activity towards coniferin (**14b**) with a slightly higher activity of  $1.01 \cdot 10^{-1}$  U/mg than the *wt* activity of  $9.44 \cdot 10^{-2}$  U/mg. Even though unexpected, the retained hydrolytic activity could be caused by a nucleophilic attack on the substrate by the introduced serine residue despite the most likely different position of the nucleophile compared to the glutamate residue of the *wt* enzyme.

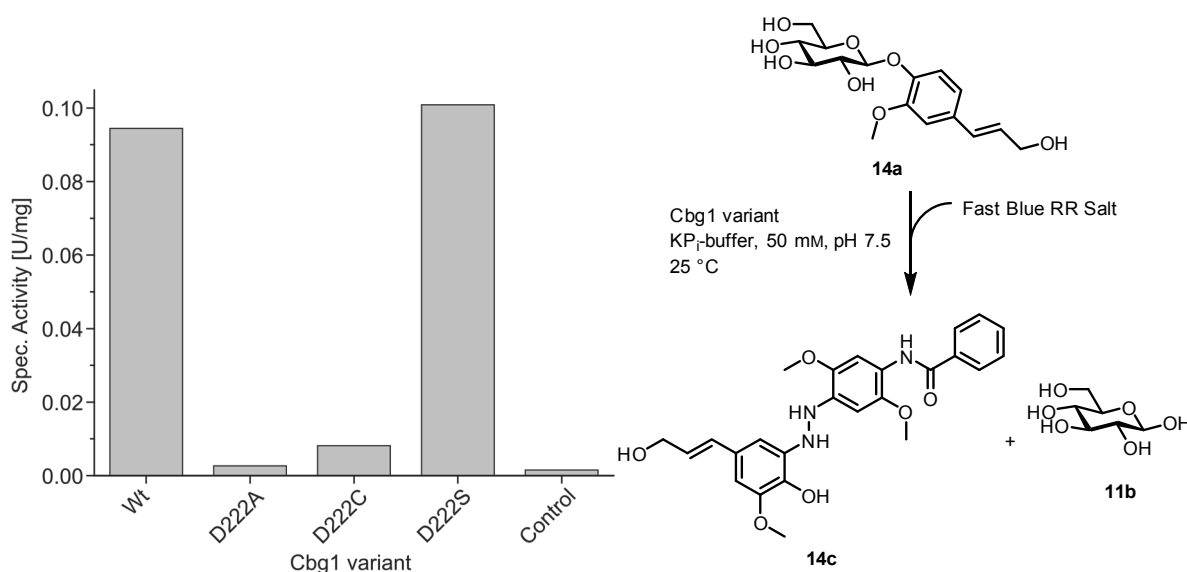


**Figure 62** Colourimetric assay detecting the hydrolysis of coniferin (**14a**, 0.41 mM) to coniferyl alcohol (**14b**) catalysed by variants of Cbg1. The hydrolysis was carried out for 50 min at 25 °C, and stopped by the addition of 0.1 M sodium carbonate solution. The quantity of released coniferyl alcohol (**14b**) is determined by the addition of the *Fast Blue RR salt* (5 mg/mL) and absorption measurement at 490 nm.

The three mutants were then tested for glycosynthase activity for the glucosylation of coniferyl alcohol (**14b**) with  $\alpha$ -GlcF **2a** as the glycosyl donor (Figure 63). Applying the fluoride quantification assay, a conversion of  $\alpha$ -GlcF **2a** in 1 : 1 ratio with the acceptor **14b** was detected for all three mutants, indicating to a possible synthetic reaction. Different to the glycosynthase Abg-E358S, an excess of the acceptor in a 1 : 4 ratio lowered the release of fluoride and therefore the conversion of  $\alpha$ -GlcF **2a**. The highest activity was detected during incubation of the donor **2a** in the absence of the acceptor **14b**, thereby ruling out a transfer of the glucosyl moiety onto coniferyl alcohol (**14b**). Incubation of *wt* Cbg1 with  $\alpha$ -GlcF **2a** also led to a release of fluoride, which implied to a hydrolysis of the donor **2a** despite having the opposite configuration to the natural substrate.

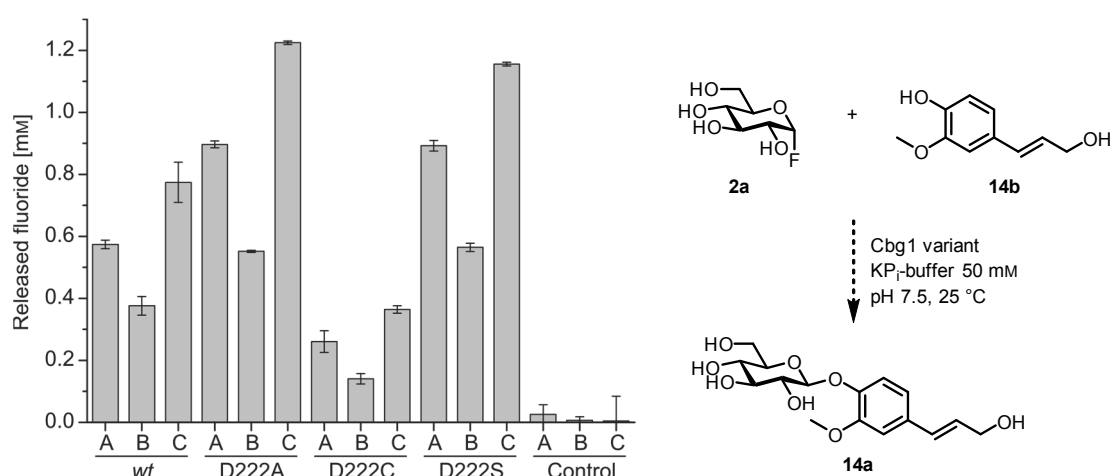


**Figure 63** Cbg1 variants applied in the glycosylation of coniferyl alcohol (**14b**) with  $\alpha$ -GlcF **2a** as the glycosyl donor (donor : acceptor ratio A: 1 : 1; B: 1 : 4; C: only donor). Activity was detected as the release of fluoride quantified by the cleavage of TIPS<sub>p</sub>NP **23**. The reaction was incubated with 16  $\mu$ g/mL of the Cbg1 variant for 1 h at 25 °C in KP<sub>i</sub>-buffer (50 mM, pH 7.5).

An alternative method to the use of a glycosyl fluoride donor in a glycosynthase catalysed reaction is the use of the chemical recovery method. The glycosyl donor is thereby created *in situ* by the reaction with an external nucleophile and subsequently transferred to the acceptor. For the Cbg1 mutants the possibility of recovering the “hydrolytic” activity by employing an external nucleophile was examined for the cleavage of *p*NPGlc **5h** (Figure 64). The specific activity of the *wt* form of Cbg1 towards *p*NPGlc **5h** was barely effected by the presence of sodium azide at concentrations of 0.5 M or 1 M. The presence of sodium formate at these concentrations on the other hand lowered the activity of the *wt* enzyme to  $9.37 \cdot 10^{-2} \pm 1.20 \cdot 10^{-3}$  U/mg and  $7.31 \cdot 10^{-2} \pm 2.92 \cdot 10^{-3}$  U/mg respectively. The presence of any external nucleophile did not recover any activity for Cbg1-D222A and only low activities of around  $3.94 \cdot 10^{-3} \pm 7.35 \cdot 10^{-5}$  U/mg could be recovered for Cbg-D222C. Opposite to these results, Cbg1-D222S exhibited a high specific activity of  $4.8 \cdot 10^{-1} \pm 1.1 \cdot 10^{-2}$  U/mg towards *p*NPGlc **5h** even without the presence of an external nucleophile. The addition of sodium azide activated the activity of Cbg1-D222S even further up to  $5.95 \cdot 10^{-1} \pm 4.27 \cdot 10^{-3}$  U/mg (1 M NaN<sub>3</sub>).

## 6 Results

Despite the 3.6× higher specific activity of Cbg1-D222S compared to *wt* Cbg1, the addition of sodium formate deactivated the mutant enzyme with increasing concentration in a similar rate as for *wt* Cbg1. The high hydrolytic activity of Cbg1-D222S rendered the application of this mutant unsuitable as a glycosynthase.

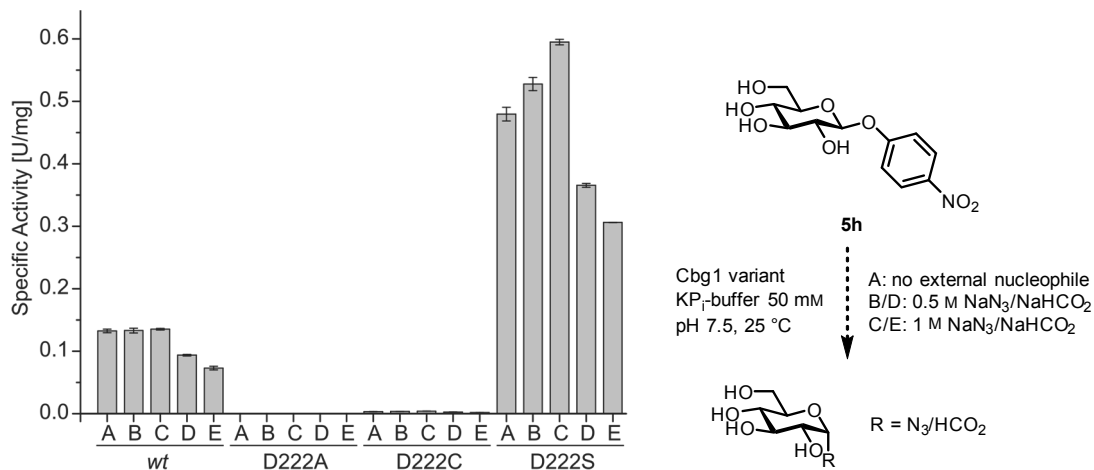


**Figure 64** Chemical recovery of the cleavage activity of Cbg1 mutants Cbg1-D222A, Cbg1-D222S, and Cbg1-D222C in the presence of sodium azide (B: 0.5 M; C: 1 M) and sodium formate (D: 0.5 M, E: 1 M) as external nucleophiles. Activity was measured by the release of *p*-nitrophenol (**13b**) and absorption measurement at 410 nm. The hydrolytic activity without the presence of an external nucleophile was also measured as a control reaction (A).

### 6.2.4 Expanding the mutant library of Cbg1 for synthetic application

The initial studies testing the synthetic potential of the Cbg1 mutant variants led to very mixed results. A complete deactivation of the hydrolytic activity was only observed for Cbg1-D222A. Both Cbg1-D222C and D222S retained hydrolytic activity, whereby the D222S mutant even surpassed the hydrolytic activity of the *wt* enzyme with respect to *p*NPGlc **5h**. All mutants showed a hydrolysis of the  $\alpha$ -GlcF **2a** donor, indicating to possible alternate hydrolysis mechanisms occurring in the active site, facilitated by the mutation of the catalytic nucleophilic residue. A further analysis of the potential active site, again using the structure of *KmBglI* as a model, was carried out in order to identify potentially interfering residues. As the structure is only a model for the active site of Cbg1, only the conserved amino acid residues were considered (Figure 65). Viewing the distances of the two catalytic residues towards the anomeric centre of the co-crystallised glucose molecule, it was apparent that the D222 residue with a 2.9 Å distance should act as the nucleophilic residue rather than D559 with a distance of 3.5 Å. Nevertheless, the potential acid/base residue D559 was considered for mutation to prove the importance of the residue for the hydrolytic mechanism. In addition to the two aspartates D222 and D559, a hydroxyl group of the tyrosine residue Y190, with a distance of 3.3 Å, is in close proximity to the anomeric centre of the glucose molecule (Figure 65, **A**). This residue, most likely mediating substrate recognition, could act as a nucleophile and thereby

cause hydrolytic activity in the Cbg1 mutants. Depending on the mutation at position D222, the position of the tyrosine residue might shift further towards the anomeric centre, thereby facilitating a nucleophilic attack.

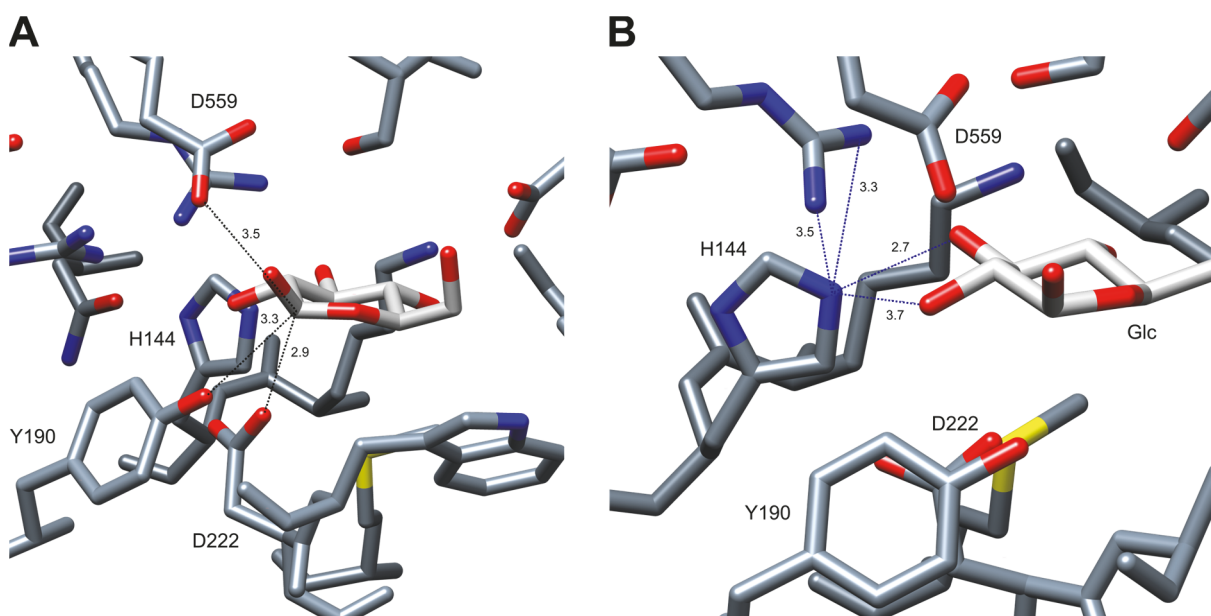


**Figure 65** Analysis of the conserved active site amino acid residues of Cbg1 (structure of *KmBglI* as model, PDB 3AC0). Potential nucleophilic atoms like oxygen (red), nitrogen (blue) and sulphur (yellow) are marked by colour. All distances are given in Å. **(A)** In addition to the catalytic nucleophile D222 and acid/base residue D559 the nucleophilic residue Y190 is located close to the anomeric centre of the glucose molecule. **(B)** The residue H144 coordinates to the C<sub>2</sub>- and C<sub>3</sub>-hydroxyl group of the glucose molecule and is possibly essential for catalysis.

Replacement of the tyrosine residue Y190 with a phenylalanine residue would retain any effects of the aromatic ring on the enzymes structure, but remove the potential nucleophile. Furthermore, the role of the histidine residue (H144) located centrally in the active site pocket closely to the glucose molecule was also examined (Figure 65, **B**). Enzymes originating from the glycohydrolase family GH 3 have not only been characterised as glycosidases, but also as glycoside phosphorylases. This type of enzyme utilises phosphate as an acceptor for cleavage of the glycosyl-enzyme-intermediate. Additionally to a catalytic aspartate (nucleophile), a catalytic diad consisting of a histidine and aspartate are employed to reduce coulombic repulsion between the acid/base and the phosphate acceptor. The catalytic diad is commonly found in the conserved sequence [KH(F/I)PG(H/L)GXXXXD(S/T)H]. Even though the sequence is not conserved in Cbg1, the H144 residue is located in the active site and is part of a [KHF] sequence and was therefore considered for mutation. The possibility of Cbg1 acting as a phosphorylase, instead of a hydrolase was examined by comparing the hydrolysis in the presence and absence of phosphate (Figure 66). The hydrolysis rate of *p*NPGlc **5h** by Cbg1, was identical in both reactions, one in phosphate buffer (50 mM, pH 7.5) the other in HEPES buffer (50 mM, pH 7.5). This result confirmed Cbg1 as a hydrolase as the enzyme was unaffected by the presence of phosphate during the hydrolytic reaction.

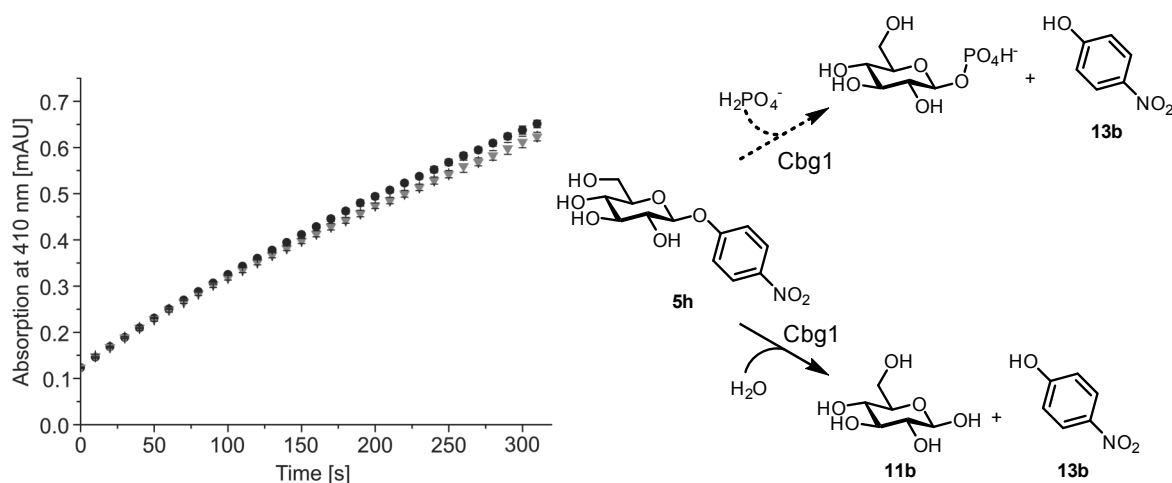


**Figure 66** Hydrolysis of *p*NPGlc **5h** (20 mM) by *wt* Cbg1 in the presence (●) and absence (▼) of phosphate. *Wt* Cbg1 was isolated and purified in 50 mM HEPES-buffer, pH 7.5 (▼) and in 50 mM KPi-buffer, pH 7.5 (●) to determine whether Cbg1 acts as a glycohydrolase or phosphorylase. Both reactions were carried out with an identical protein concentration of 15  $\mu\text{g}/\text{mL}$  at 25 °C. Hydrolysis was detected by *p*-nitrophenol (**13b**) release at 410 nm.

The mutagenesis of the positions D559, Y190, and H144 was carried out with the *round the horn*-PCR method similar to the D222 mutants described before. The mutant library of Cbg1 was thereby expanded by six further variants of Cbg1 including a double mutant Cbg1-Y190F D222A (Table 10).

**Table 10** Variation of the catalytically important amino acid residues E559, H144, and Y190 of Cbg1 of *R. radiobacter*. The mutations were acquired by *round the horn*-PCR by mutation of the wild type gene in pET-21a(+). Obtained plasmids were sequenced for confirmation of the resulting mutation.

Original AA	Introduced mutation	Codon variation	Verification
E559	A	GAA → GCA	+
	C	GAA → TGC	+
	S	GAA → TCA	+
H144	A	CAC → GCC	+
Y190	F	TAC → TTC	+
Y190 D222	Y190F	TAC → TCC	+
	D222A	GAC → GCC	

All of the mutant variants of Cbg1 were expressed heterologously in *E. coli* BL21(DE3) and isolated via IMAC. All isolated protein solutions were diluted to an identical concentration of 95.5  $\mu\text{g}/\text{mL}$  for the application in various activity assays.

The hydrolytic activity of all Cbg1 variants was determined for the hydrolysis of *p*NPGlc **5h** (Figure 67). The *wt* Cbg1 exhibited an activity  $2.5 \cdot 10^{-1} \pm 1.0 \cdot 10^{-2}$  U/mg towards the glucoside **5h**. Replacement of the tyrosine Y190 with a phenylalanine residue decreased the activity by 4.3×. The decline in activity clearly demonstrates the importance of the hydroxyl group of Y190 during catalysis. As the variant retained hydrolytic activity, the involvement as

a nucleophilic residue for the hydrolysis mechanism of *wt* Cbg1 could be ruled out. The mutation of the histidine in position 144 resulted in a high increase of hydrolytic activity. The mutant Cbg1-H144A reached a specific activity of  $5.06 \pm 0.09$  U/mg, 20× higher than the *wt* Cbg1 and 2.7× higher than the Cbg1-D222S mutant. Due to the proximity of H144 to the C<sub>2</sub>- and C<sub>3</sub>-hydroxyl groups of the glucose moiety, a decrease of the hydrolytic activity was expected by a lower binding of the substrate to the -1 sub-site. Nevertheless, the results demonstrate a highly favourable effect for the hydrolysis of *p*NPGlc **5h**. The replacement of the histidine moiety may allow a shift of the proposed acid/base catalyst D559 towards the substrate, thereby allowing a higher hydrolysis rate.

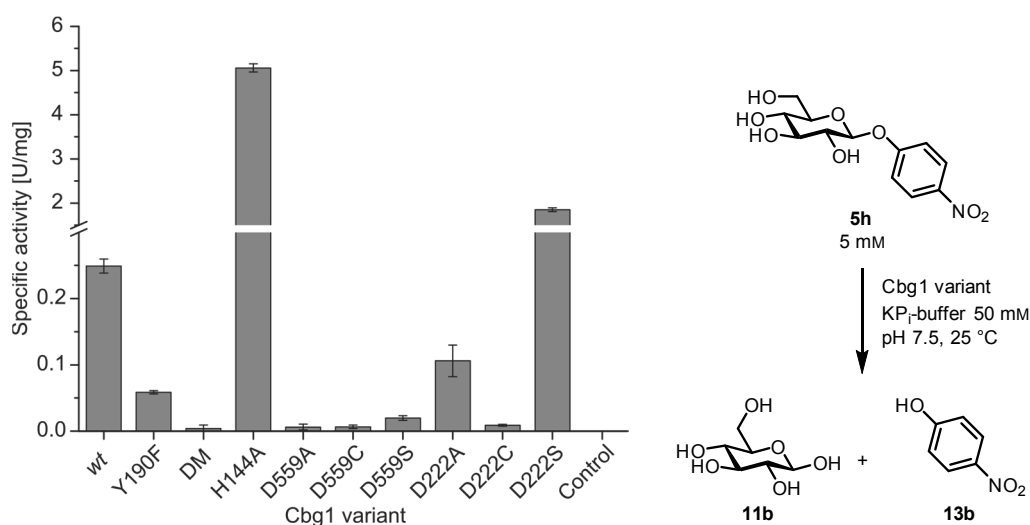


**Figure 67** Hydrolytic activity of all Cbg1 variants towards the substrate *p*NPGlc **5h**. The respective variant (19.1  $\mu$ g/mL) was incubated with the substrate **5h** (5 mM) in 50 mM KP<sub>i</sub>-buffer, pH 7.5 at 25 °C for 10 min. Hydrolysis was detected by *p*-nitrophenol (**13b**) release and absorption measurement at 410 nm. DM : double mutant Cbg1-Y190F D222A

Mutation of the D559 residue to alanine, cysteine, or serine reduced the hydrolytic activity greatly down to specific activities of around  $1 \cdot 10^{-2} \pm 0$  U/mg. For the mutations of D222 on the other hand, Cbg1-D222A and Cbg1-D222S retained hydrolytic activity with specific activities of  $1.1 \cdot 10^{-1} \pm 2.0 \cdot 10^{-2}$  U/mg and  $1.9 \pm 4.1 \cdot 10^{-2}$  U/mg respectively. The addition of the Y190F mutation in Cbg1-D222A eliminated the hydrolytic activity, implying a participation of the Y190 residue in the retained hydrolysis of Cbg1-D222A.

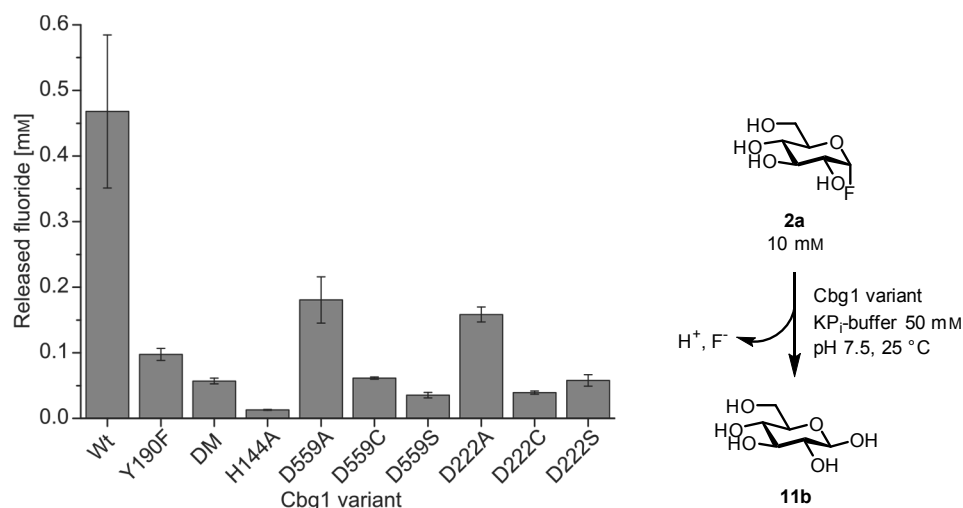


**Figure 68** Conversion of  $\alpha$ -GlcF **2a** by Cbg1 variants. The enzyme variant (19.1  $\mu$ g/mL) was incubated with  $\alpha$ -GlcF **2a** (10 mM) in 50 mM  $\text{KP}_i$ -buffer, pH 7.5, at 25 °C for 140 min. The conversion was detected by fluoride release and subsequent quantification by cleavage of TIPS $\rho$ NP **23**.

Furthermore, the variants were incubated with  $\alpha$ -GlcF **2a** to determine whether the variants hydrolyse the glycosyl fluoride **2a**, as was observed for the *wt* and D222 mutants (Figure 68). The highest release of fluoride by conversion of  $\alpha$ -GlcF **2a** was observed for *wt* Cbg1. The hydrolysis rate of the substrate **2a** by Cbg1 is low only releasing  $0.47 \pm 0.15$  mM fluoride of possible 10 mM (starting concentration of  $\alpha$ -GlcF **2a** after an incubation time of 140 min). Further hydrolysis of  $\alpha$ -GlcF **2a** was observed for Cbg1-D559A and -D222A by the release of  $0.18 \pm 0.06$  mM and  $0.15 \pm 0.02$  mM fluoride respectively. This release could indicate to a hydrolysis or self-coupling of the substrate **2a**. Nevertheless, the hydrolysis or self-coupling reaction was neglected for the mutants of Cbg1, due to the low reaction rate representing only a 1% conversion of the glycosyl fluoride **2a** after a 2 h incubation. Therefore, the Cbg1 variants were tested in a glycosynthase reaction with the donor  $\alpha$ -GlcF **2a** (2.5 mM) and coniferyl alcohol (**14b**, 5 mM) acting as the acceptor substrate. The protein concentration of the mutants Cbg1-H144 and -D222S were diluted tenfold, in order to lower the hydrolysis of potential reaction products due to the high hydrolytic activity exhibited by these variants. However, the glycosynthase reaction displayed for each mutant the same pattern observed for the reaction with  $\alpha$ -GlcF **2a** in the absence of the acceptor **14b**. A possible transferal of the glucosyl residue of  $\alpha$ -GlcF **2a** onto the acceptor molecule **14b** by a Cbg1 variant was therefore dismissed.

As described for the Cbg1-D222 variants in section 6.2.3, the chemical recovery of glycosidase activity by an external nucleophile, is a feasible alternative to classic glycosynthase reactions utilising glycosyl fluoride donors. All of the produced Cbg1 mutants were tested for activity recovery by the addition of sodium azide in an equal concentration to the substrate *p*NPGlc **5h** (5 mM, Figure 69). As observed before, the activity of *wt* Cbg1 and the D222 variants were not significantly effected by the presence of the external nucleophile. The single mutant Cbg1-Y190F and double mutant Cbg1-Y190F D222A were also not effected. On the contrary,

the presence of the external nucleophile increased the activity of Cbg1-H144A from  $5.1 \pm 9.0 \cdot 10^{-2}$  U/mg to  $6.0 \pm 5.9 \cdot 10^{-1}$  U/mg (1.2× increase). An even higher recovery in activity was observed for all the Cbg1-D559 variants. The two variants, Cbg1-D559C and -D559S showed an 8.3× and 3.8× increase in activity compared to hydrolysis without sodium azide present. Cbg1-D559A exhibited the highest recovery, rising from  $6.5 \cdot 10^{-3} \pm 4.4 \cdot 10^{-3}$  U/mg up to  $2.4 \cdot 10^{-1} \pm 5.0 \cdot 10^{-3}$  U/mg, a 38× increase. The Cbg1-D559A mutant therefore regained over 100% of the wt activity ( $2.3 \cdot 10^{-1} \pm 5.0 \cdot 10^{-3}$  U/mg) in the presence of the external nucleophile.

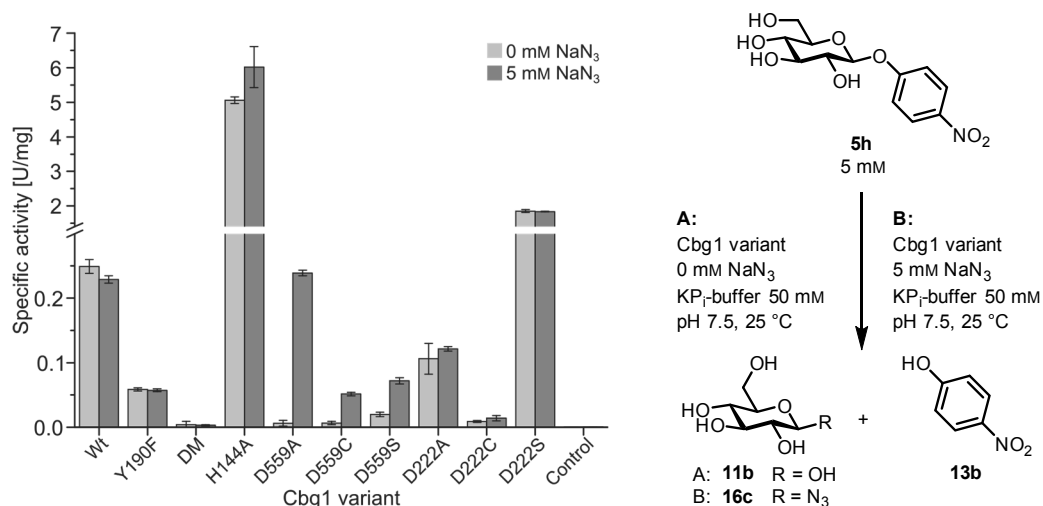


**Figure 69** Detection of the recovered ‘hydrolytic’ activity of Cbg1 variants towards *p*NPGlc **5h** (5 mM) in the presence of sodium azide (5 mM) as an external nucleophile. All variants were applied in a concentration of 19.1  $\mu$ g/mL in 50 mM KP<sub>i</sub>-buffer, pH 7.5, and incubated for 10 min at 25 °C. Enzymatic activity was detected by the release of *p*-nitrophenol (**13b**) and subsequent absorption measurements at 410 nm.

The reactivation of the Cbg1 variant mutated in the position of the proposed catalytic acid/base residue can indicate to two different reactivation mechanisms. The first type of mechanism is also observed for thioglycoligases, mutant glycosidases, which catalyse the production of thioglycosides.<sup>[161]</sup> The glycoside substrate is attacked by the nucleophilic residue of the mutant glycosidase, resulting in a glycosyl-enzyme-intermediate, which is not hydrolysed due to the absence of the mutated acid/base residue. An external nucleophile/acceptor such as a thiol can cleave the glycosyl-enzyme-intermediate, thereby producing a  $\beta$ -thioglycoside. The second, more unlikely mechanism, would not produce a glycosyl-enzyme-intermediate, but allow a direct attack of the external nucleophile (in this case azide) on the substrate.

To further investigate the option of glycosynthetic reactions *via* a chemical recovery, the Cbg1-D559 mutants was tested for synthesis in the presence of *p*NPGlc **5h**, sodium azide and the potential acceptor molecules coniferyl alcohol (**14b**) and hydroquinone (**26a**). These acceptor molecules were chosen, as their respective glucosides, coniferin (**14a**) and arbutin (**26b**), are known substrates cleaved by the *wt* Cbg1. The variants were tested for activity after an incubation at 25 °C for 30 min with equal amounts of *p*NPGlc **5h**, sodium azide,

## 6 Results

and acceptor **14b** or **26a** (5 mM, Figure 70). All three variants displayed different behaviour depending on the substrates present during the reaction. As observed before, the activity of Cbg1-D559A was most effected by the addition of sodium azide, followed by the Cbg1-D559C variant. The addition of coniferyl alcohol (**14b**) as an acceptor for the glycosylation reaction inhibited the activity recovery by the external nucleophile for Cbg1-D559A and -D559C. The activity recovery for Cbg1-D559S on the other hand was not affected. In the presence of the acceptor hydroquinone (**26a**), the recovered activity of both Cbg1-D559A and -D559S increased by  $1.6 \cdot 10^{-2}$  U/mg and  $1.4 \cdot 10^{-2}$  U/mg ( $\Delta$ U/mg). The increase in recovered activity could indicate to a transfer of the glucosyl residue of *p*NPGlc **5h** onto the acceptor **26a**.

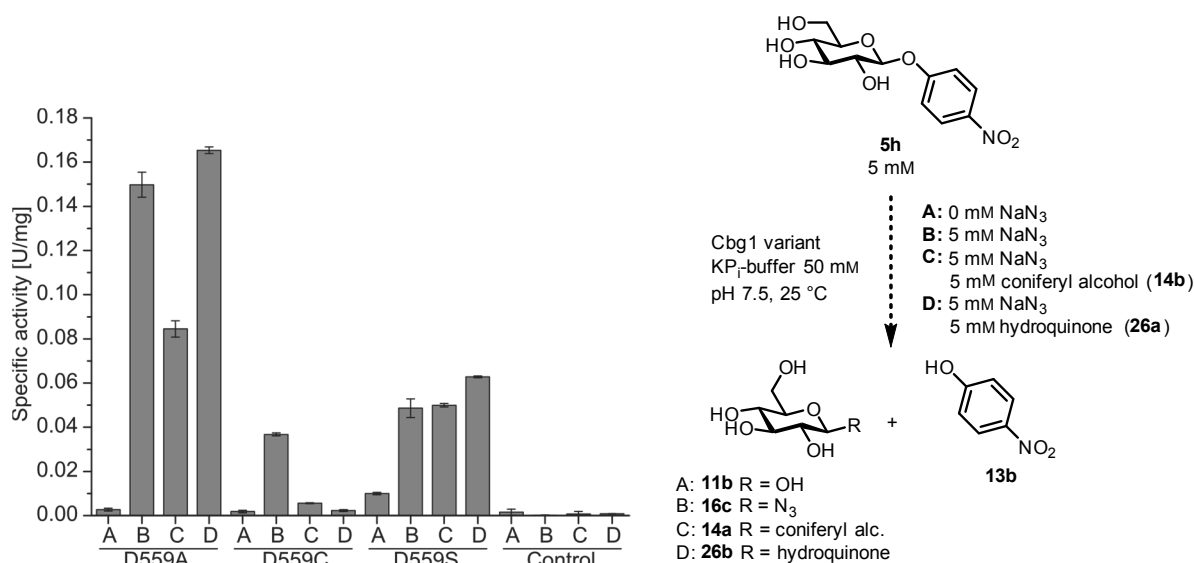


**Figure 70** Analysis of glycosynthetic reactions utilising the chemical recovery method and Cbg1-D222 variants. Each variant (19.1  $\mu$ g/mL) was incubated with *p*NPGlc **5h** (5 mM) and: A 0 mM NaN<sub>3</sub>; B 5 mM NaN<sub>3</sub>; C 5 mM NaN<sub>3</sub>, 5 mM **14b**; D 5 mM NaN<sub>3</sub>, 5 mM **26a**; in 50 mM KP<sub>i</sub>-buffer, pH 7.5 at 25 °C. Activity was determined by the release of *p*-nitrophenol (**13b**) and absorption measurement at 410 nm.

To determine firstly, by what mechanism the azide is incorporated into the glycosyl substrate **5h**, and secondly, whether a transfer of the glucosyl residue of the potential glycosyl azide occurred onto one of the acceptor molecules or not, <sup>1</sup>H-NMR analysis of the reaction mixtures was carried out. The product mixture produced by Cbg1-D559A in the presence of sodium azide (5 mM) with and without the acceptors **14b** or **26a** (5 mM) was peracetylated after removal of the buffer solution under reduced pressure. The analysis of the reaction products *via* <sup>1</sup>H-NMR clearly displayed the production of a single new compound in all three examined reactions (Figure 72). In addition

to the signals of the starting material *p*NPGlc **5h**, coniferyl alcohol (**14b**), and hydroquinone (**26a**) in their peracetylated form, a time dependant increase of signals belonging to a new compound could be detected. Comparing the newly formed signals with literature values for 2,3,4,6-tetra-*O*-acetyl  $\alpha/\beta$ -D-glucopyranosyl azide **22o- $\alpha/\beta$**  allowed the identification of the new compound as  $\beta$ -configured 2,3,4,6-tetra-*O*-acetyl- $\beta$ -D-glucopyranosyl

azide (**22o-β**). The production of the  $\beta$ -configured glycoside confirmed the mechanism to follow the thioglycoligase mechanism by producing a glycosyl-enzyme-intermediate, which is cleaved by the external nucleophile azide ion (Figure 71). Nevertheless, the production of a  $\beta$ -configured glycosyl donor inhibited the transfer of the glycosyl donor onto the acceptor, as the donor would require a leaving group in  $\alpha$ -configuration. The transfer of a glycosyl residue onto hydroquinone (**26a**) or coniferyl alcohol (**14b**) could not be observed by  $^1\text{H-NMR}$ . The inhibitory effect of coniferyl alcohol (**14b**) on the activity recovery of Cbg1-D559A observed before was also evident in the  $^1\text{H-NMR}$  analysis, as this reaction showed the weakest production of signals belonging to 2,3,4,6-tetra-*O*-acetyl- $\beta$ -D-glucopyranosyl azide (**22o**).

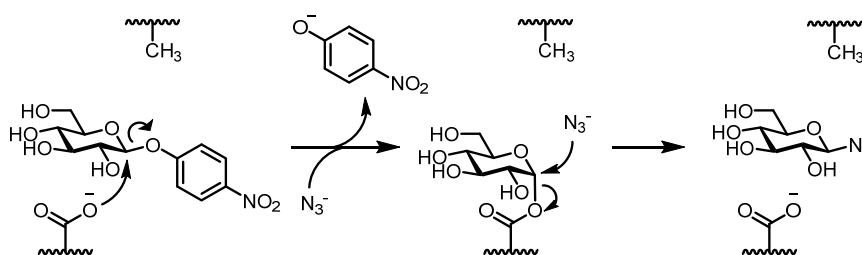


**Figure 71** Proposed reaction mechanism of the chemical recovery reaction catalysed by Cbg1-D559A in the presence of the external nucleophile sodium azide and *p*NPGlc **5h** as the substrate. A nucleophilic attack occurs by the catalytic residue D222 creating a glucosyl-enzyme-intermediate, which can only be cleaved by the external nucleophile as the acid/base residue is missing.

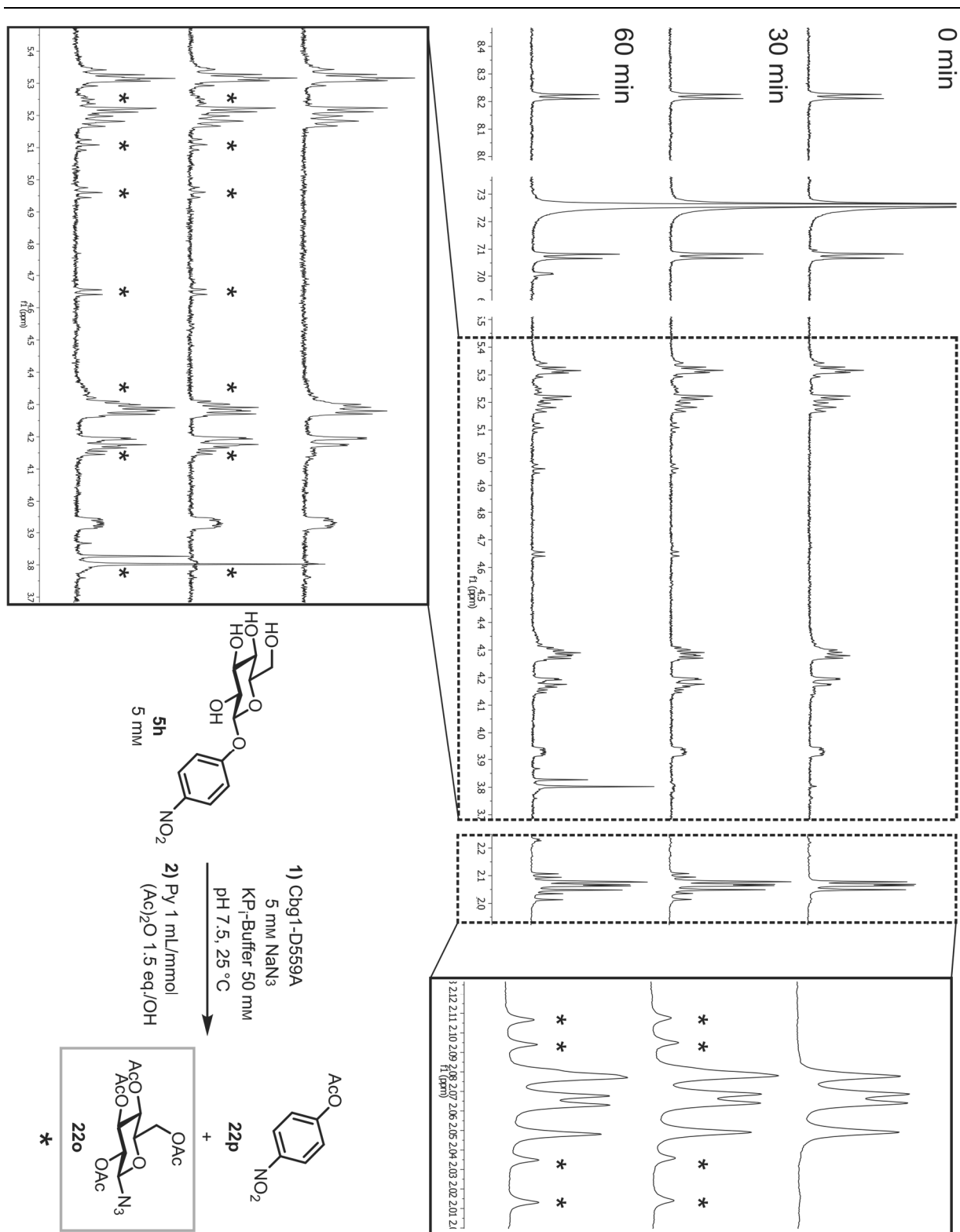


**Figure 72**  $^1\text{H-NMR}$  analysis of the chemical recovery reaction catalysed by Cbg1-D559A in the presence of sodium azide (5 mM) after 0 min, 30 min and 60 min. The reaction was incubated at 25 °C in 50 mM KP-buffer, pH 7.5 and stopped by removal of the solvent under reduced pressure. The dry reaction was peracetylated and analysed by  $^1\text{H-NMR}$  in  $\text{CDCl}_3$ . The signals of the newly produced glycosyl azide **22o** are marked with \*. Unmarked signals belong to the peracetylated form of *p*NPGlc **5h**, representing not converted starting material.

### 6.2.5 Cbg1 for transglycosylation

Even though no suitable conditions were yet determined for the use of Cbg1 as a glycosynthase, the glycosidase could still be a potential biocatalyst for glycoside synthesis by transglycosylation. *Watt et al.* described the activation of *wt* Cbg1 in the presence of aliphatic alcohols and determined the activation as a transglycosylation of the glucosyl moiety of *p*NPGlc **5h** onto the alcohol by  $^1\text{H-NMR}$  analysis.<sup>[88]</sup> The highest activation was observed for *n*-butanol (**15a**), whereby the larger aliphatic alcohols most likely show solubility issues leading to the lower transglycosylation. *Kitaoka et al.* also observed the transglycosylation of *p*-nitrophenol (**13b**) causing a self-transferring product inhibition during the hydrolysis of *p*NPGlc **5h**.<sup>[91]</sup> The activation of *wt* Cbg1 towards *p*NPGlc **5h** by the presence of *n*-butanol (**15a**) was examined for three different concentration ratios, 1 : 1, 1 : 2, and 1 : 10 (Figure 73) by measurement of the time profile of the *p*-nitrophenol (**13b**) release. A high activation of the *wt* Cbg1 activity was observed in all cases. Equimolar concentrations of the acceptor *n*-butanol (**15a**) doubled the activity of the enzyme. Excess of the acceptor raised the activity of *wt* Cbg1 even further up to 2.8× of the activity observed without any acceptor.

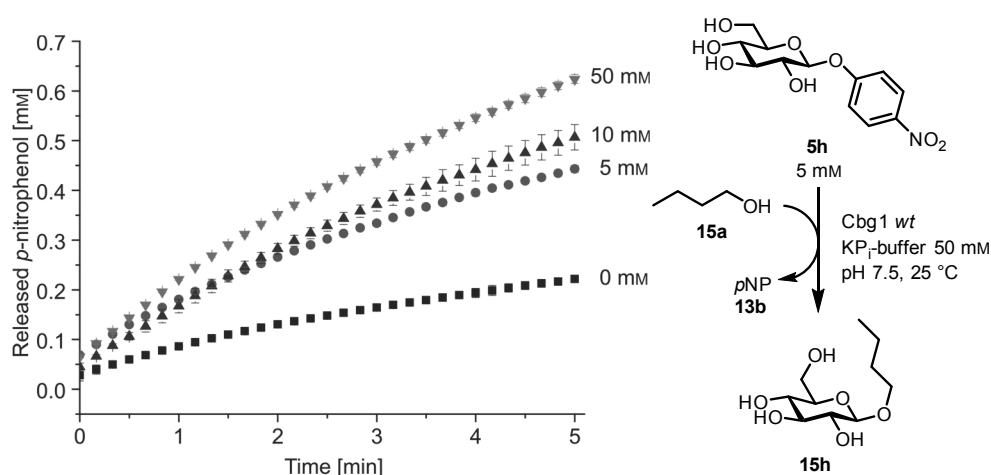


**Figure 73** Activation of *wt* Cbg1 (26.8  $\mu\text{g}/\text{mL}$ ) towards *p*NPGlc **5h** (5 mM) by the presence of *n*-butanol (**15a**) in various concentrations (0 mM, 5 mM, 10 mM, 50 mM). The reaction was incubated at 25 °C in 50 mM  $\text{KPi}$ -buffer, pH 7.5 and the release of *p*-nitrophenol (**13b**) was followed by absorption measurement at 410 nm.

## 6 Results

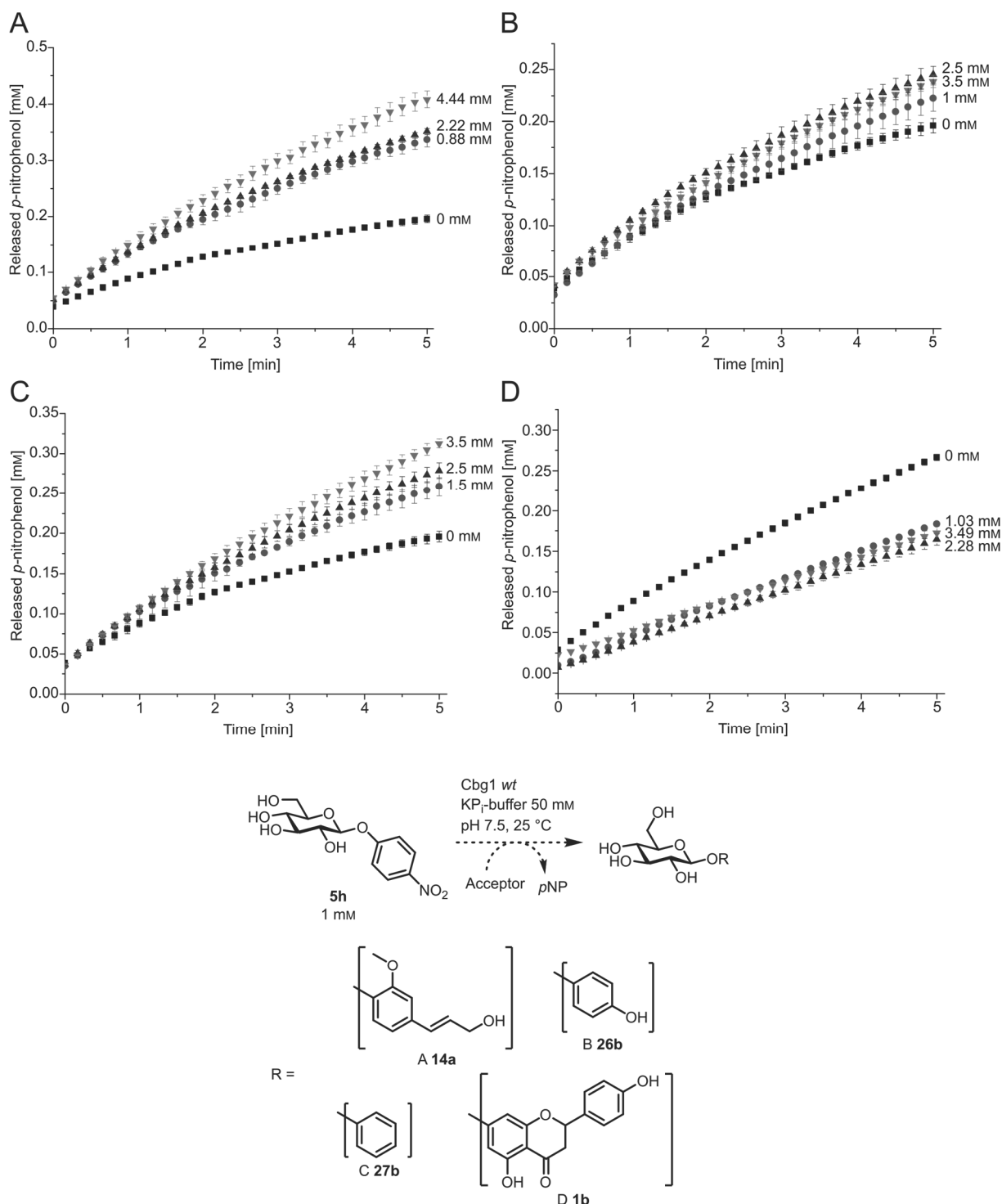


**Figure 74** Activation of *wt* Cbg1 (26.8 µg/mL) towards *p*NPGlc **5h** (5 mM) by the presence of the phenolic alcohols, coniferyl alcohol (**14b**, **A**), hydroquinone (**26a**, **B**), phenol (**27a**, **C**), and naringenin (**1a**, **D**) in various concentrations. The reaction was incubated at 25 °C in 50 mM KP<sub>i</sub>-buffer, pH 7.5 and the release of *p*-nitrophenol (**13b**) was followed by absorption measurement at 410 nm. In the case of naringenin (**1a**) 10% (v/v) DMSO was added as a co-solvent.

To further determine the potential of the transglycosylation reaction for synthesis, the activation reaction of *wt* Cbg1 by an additional acceptor was expanded to the phenolic alcohols, coniferyl alcohol (**14b**), hydroquinone (**26a**), phenol (**27**), and naringenin (**1a**, Figure 74, **A–D**). The acceptor molecules coniferyl alcohol (**14b**) and hydroquinone (**26a**) were chosen, as their

respective glucosides coniferin (**14a**) and arbutin are known substrates hydrolysed by Cbg1. With the exception of naringenin (**1a**) the presence of phenolic alcohols increased the activity of *wt* Cbg1. The highest activation was observed for coniferyl alcohol (**14b**), increasing the rate of *p*-nitrophenol (**13b**) release from  $3.9 \cdot 10^{-2} \pm 1.3 \cdot 10^{-3}$  mM/min up to  $8.2 \cdot 10^{-2} \pm 2.9 \cdot 10^{-3}$  mM/min when in an excess of 4.4× compared to the *p*NPGlc **5h** concentration. Both hydroquinone (**26a**) and phenol (**27**) increased the activity of Cbg1, but with a lower effect compared to coniferyl alcohol (**14b**). The increase of *p*-nitrophenol (**13b**) release strongly indicated to an activation by transglycosylation. The presence of naringenin (**1a**) on the other hand, inhibited the activity of Cbg1 irrespective of the concentration of the acceptor. Due to the low solubility, transglycosylation reactions with naringenin (**1a**) were carried out with 10% (*v/v*) DMSO as a co-solvent. A control reaction with *wt* Cbg1 and *p*NPGlc **5h** in the presence of 10% (*v/v*) DMSO but without naringenin (**1a**) displayed no inhibition of the hydrolytic activity. A possibility of successful glycosylation of naringenin (**1a**) by transglycosylation catalysed by Cbg1 was therefore ruled out. <sup>1</sup>H-NMR analysis was carried out for the transglycosylation reactions with coniferyl alcohol (**14b**), hydroquinone (**26a**), phenol (**27**), and *n*-butanol (**15a**). The compounds of the reaction mixture were peracetylated before analysis. A transglycosylation product could only be observed in the case of the reaction containing *n*-butanol (**15a**), resulting in the production of 1-butyl β-D-glucopyranoside (**15i**). However, the high concentration of the respective acceptor molecules and *p*NPGlc **5h**, compared to the produced product, hindered the identification of product signals in the <sup>1</sup>H-NMR spectra. The production of aryl glycosides by transglycosylation may also be hindered by the higher affinity and activity of Cbg1 towards aryl glycosides compared to glycosides with aliphatic aglycones.

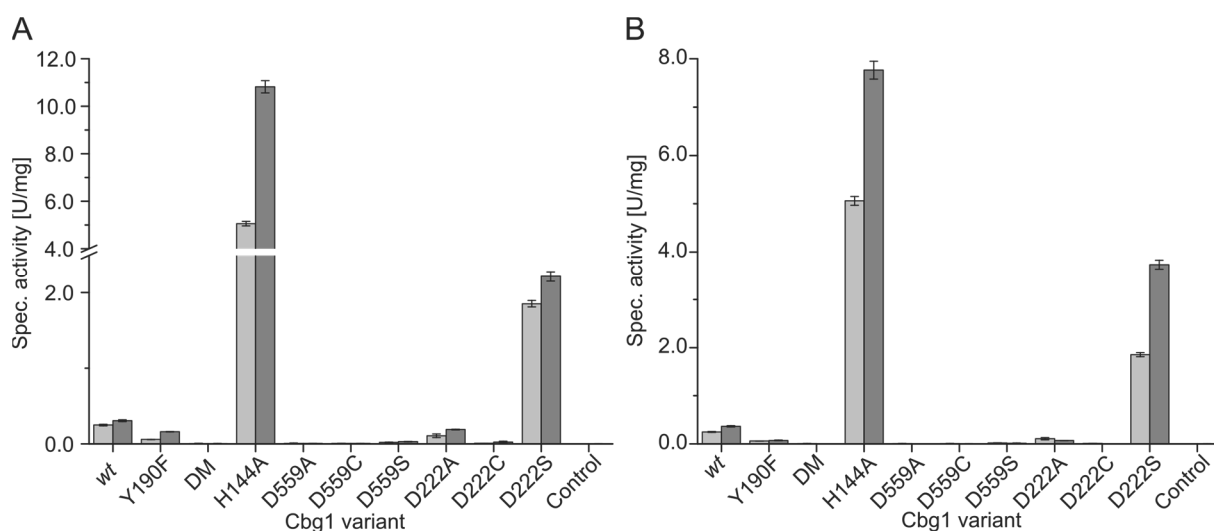


**Figure 75** Activation of mutant Cbg1 variants (19.1 μg/mL) towards *p*NPGlc **5h** (5 mM) by the presence of hydroquinone (**26a**, 5 mM, **A**) or coniferyl alcohol (**14b**, 5 mM, **B**). The spec. activity in the presence of the acceptor **26a** or **14b** (dark gray) is compared to the activity without addition (light gray). The reaction was incubated at 25 °C in 50 mM KPi-buffer, pH 7.5 and the release of *p*-nitrophenol (**13b**) was followed by absorption measurement at 410 nm.

The effect on the enzymatic activity, exhibited by the phenolic acceptors coniferyl alcohol (**14b**) and hydroquinone (**26a**), was also examined for the mutant variants of Cbg1 (Figure 75). As was observed for the *wt* enzyme, the addition of the phenolic alcohols generally led to an increase in activity towards *p*NPGlc **5h**. The Cbg1-H144A mutant displayed the highest increase in activity. Addition of hydroquinone increased the activity from  $5.1 \pm 9.0 \cdot 10^{-2}$  U/mg to  $11 \pm 2.6 \cdot 10^{-1}$  U/mg (2.1 $\times$ ). Coniferyl alcohol (**14b**) in comparison only increased the activity of Cbg1-H144A up to  $7.8 \pm 1.8 \cdot 10^{-1}$  U/mg corresponding to a 1.5 $\times$  increase. On the contrary, the addition of coniferyl alcohol (**14b**) increased the activity of the Cbg1-D222S mutant to  $3.7 \pm 9.1 \cdot 10^{-2}$  U/mg and hydroquinone (**26a**) only up to  $2.2 \pm 7.2 \cdot 10^{-2}$  U/mg. These activities could indicate to potential transglycosylation activity similar to the *wt* enzyme. Yet, the increased hydrolytic activity of the Cbg1-H144A and -D222S may hinder the isolation of transglycosylation products in high yields. Initial analysis of the transglycosylation reaction by RP-TLC could not lead to the identification of new produced products.

#### Chapter synopsis:

- The coniferin-specific  $\beta$ -glucosidase Cbg1 of *R. radiobacter* was identified as a glycosynthase candidate, which could potentially glycosylate phenolic compounds.
- Cbg1 was successfully heterologously expressed in *E. coli* BL21(DE3) and isolated by IMAC. The *wt* enzyme was characterised with respect to its kinetic properties and substrate scope.
- Structural analysis identified the catalytic residues D222 and D559 as the nucleophilic and acid/base respectively. The mutants Cbg1-D222A, -D222S, and D222C were created by *round the horn*-PCR mutagenesis and tested for glycosynthetic activity.
- The mutant library of Cbg1 was expanded by Cbg1-D559A, -D559S, -D559C, -Y190F, -Y190F D222A, and -H144A variants. Each mutant was examined for hydrolytic activity and glycosynthase activity utilising glycosyl fluorides or the chemical recovery method.
- $\beta$ -D-Glucopyranosyl azide (**16c**) was identified as the product of the chemical recovery reaction catalysed by Cbg1-D559A with *p*NPGlc **5h** and sodium azide.
- Transglycosylation reactions were tested for phenolic alcohols, which showed an activating effect on *wt* Cbg1 and various mutant variants. Successful transglycosylation was only proven for the aliphatic alcohol *n*-butanol (**15a**).

### 6.3 Creating a rhamnosynthase

A glycosynthetic approach, using a mutated form of a rhamnosidase as a rhamnosynthase for the incorporation of rhamnosyl moieties onto various acceptors, has not yet been demonstrated throughout literature. One of the largest limitations towards the creation of a rhamnosynthase is the low amount of structural and mechanistic data available for this type of carbohydrate active enzyme. Therefore, the  $\alpha$ -L-rhamnosidase RhaB of *Bacillus sp.* GL1 was selected for this project, as the enzyme (as described in section 5.3.2) is well characterised and the crystal structure was elucidated by *Cui et al.*<sup>[112, 115]</sup> However, even though the enzyme displayed structural similarities with other inverting carbohydrate enzymes, the sequence similarity was low and suggested to a new, undescribed hydrolysis mechanism.

#### 6.3.1 Synthesis of rhamnosyl substrates

As described before in section 6.1.4, in order to analyse and characterise enzymatic catalysis, reference compounds and substrates are required. For the analysis of the activity of  $\alpha$ -L-rhamnosidase RhaB of *Bacillus sp.* GL1 and potential rhamnosynthase variants of this rhamnosidase, the reference compounds and donor molecules **5r/ae** and **16d** were required and synthesised chemically (Figure 76 & Figure 77).

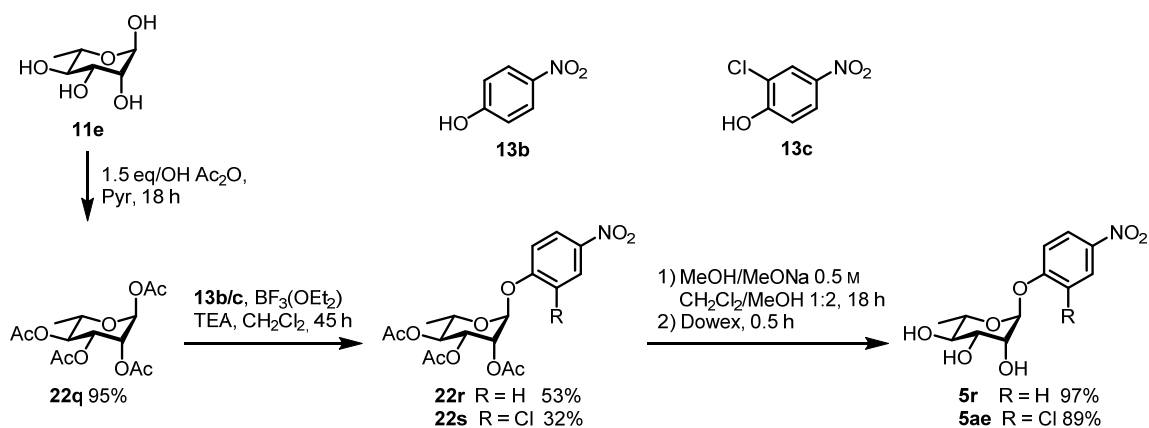


**Figure 76** Synthesis of the  $\alpha$ -L-rhamnopyranoside derivatives **5r** and **5ae** following the O-glycosylation method of *Steinmann et al.*<sup>[154]</sup>

With respect to the rhamnosidase hydrolytic activity assay, and as potential rhamnosyl donors used in the chemical recovery method, the *p*-nitrophenyl rhamnosyl derivatives **5r** and **5ae** were synthesised chemically (Figure 76). The monosaccharide  $\alpha$ -L-rhamnose (**11e**) was peracetylated to 1,2,3,4-tetra-O-acetyl- $\alpha$ -L-rhamnose (**22q**) with acetic anhydride in pyridine according to the literature known procedure of *Steinmann et al.* in yields of around 95%.<sup>[162]</sup> The O-glycosylation, resulting in the rhamnosyl derivatives **22r** and **22s** in a yield of 53 and 32% respectively, was prepared according to the method described by *Lee et al.*<sup>[153]</sup> The yield

of the rhamnoside **22s** in comparison to rhamnoside **22r** is most likely limited by the lower nucleophilicity of the phenol **13c** caused by the electron withdrawing chlorine substituent in the *ortho*-position. The general yields of the reaction are also much lower than the yields reported by *Lee et al.*, though their procedure was only performed on gluco- and not rhamnopyranosides, making the direct comparison of these yields difficult.<sup>[153]</sup> The reaction procedure led specifically to the formation of the 1,2-*trans* configured  $\alpha$ -L-rhamnopyranoside **22r** due to the participating neighbouring 2-O-acetyl group. A modified work-up procedure utilising a crystallisation step circumvented the requirement of a lengthy chromatography work-up. The crude product was therefore recrystallized in hot ethanol and simply purified by filtration. The compounds **5r** and **5ae** were produced by a deprotection reaction using the Zemplén conditions described by *Steinmann et al.*<sup>[162]</sup> The glycosides **5r** and **5ae** were obtained in yields of 97% and 89% respectively. The lower nucleophilicity and therefore increased leaving group potential of the phenol **13c** compared to *p*-nitrophenol (**13b**), is underlined by the higher instability and lower obtained yield of the glycosides **22s** and **5ae** compared to the glycosides **22r** and **5r**.

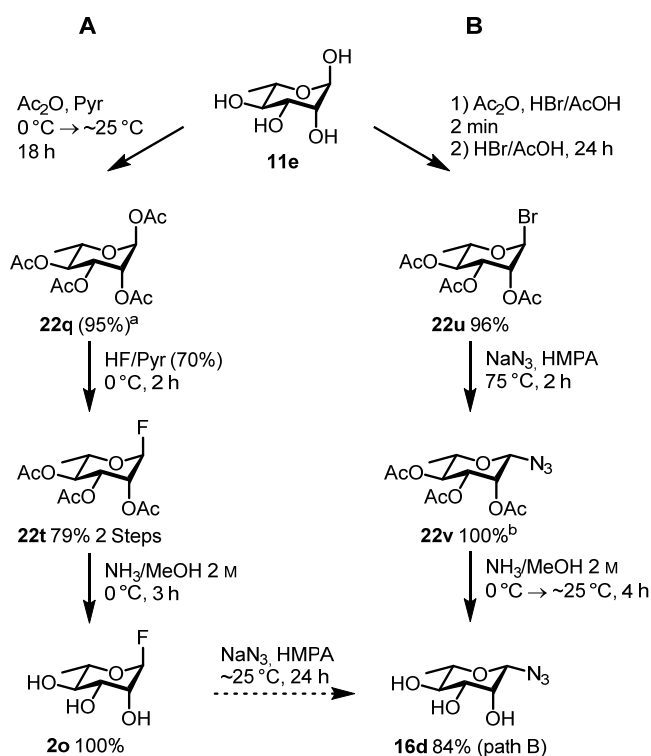


**Figure 77** Synthetic routes (**A** & **B**) towards the rhamnosyl donor **16d**. The  $\beta$ -L-rhamnopyranosyl azide (**16d**) was synthesised exclusively by the synthetic route **B**, as purification difficulties arose during the last step of route **A**. (<sup>a</sup> Yield of the single reaction, <sup>b</sup> Uncertain yield as residual HMPA was present)

Two different synthetic routes were attempted for the synthesis of the reference and potential rhamnosyl donor  $\beta$ -L-rhamnopyranosyl azide (**16d**,  $\beta$ -RhaN<sub>3</sub>, Figure 77). *Györgydeák et al.* described the conversion of a pyranosyl halide with NaN<sub>3</sub> in HMPA which was carried out in the first synthetic route (Figure 77, **A**).<sup>[162]</sup> Their review described the synthesis of

1,2-*cis*-glycosyl azides as generally difficult and discussed the reaction as an S<sub>N</sub>2 substitution of the halide by the azide anion in HMPA or DMSO. The first route (Figure 77, **A**), began with a peracetylation of rhamnose (**11e**) and subsequent fluorination following the procedure described by *Steinmann et al.*, which resulted in a yield of 79% of the 2,3,4-tri-*O*-acetyl- $\alpha$ -L-rhamnopyranosyl fluoride (**22t**) after both steps.<sup>[154]</sup> After a deprotection of compound **22t** with quantitative yields (*Yamamoto et al.*), the glycoside **2o** was treated with sodium azide in HMPA for the substitution of the halide.<sup>[58]</sup> It was not possible to follow the reaction *via* TLC, as many degradation spots were visible after staining, making a distinction of the putative product **16d** and remaining starting material **2o** not possible. The analysis of the crude reaction *via* <sup>1</sup>H-NMR showed the production of the rhamnosyl azide **16d** (anomeric proton signal was detectable). However, the work-up of rhamnoside **16d** proved difficult due to the high boiling point of the HMPA solvent and high solubility of HMPA and the non-acetylated  $\beta$ -RhaN<sub>3</sub> **16d** in water rendering a removal of HMPA *via* extraction not possible. To avoid an unwanted neighbouring group effects of the 2-*O*-acetyl group ( $\alpha$ -directing effect) and to improve the solubility of rhamnoside **16d** in organic solvents a selective deprotection of compound **22t** at the 2-position was attempted chemically and enzymatically (Table 11).

**Table 11** Chemical and enzymatic conditions for the selective deprotection of the 2-*O*-acetyl group of 2,3,4-tri-*O*-acetyl- $\alpha$ -L-rhamnopyranosyl fluoride (**22t**). The chemical deprotection occurred at ~25 °C whereas the enzymatic reaction was incubated at 37 °C.

Entry	Conditions
A	0.2 mmol <b>22t</b> , 10 mL/mmol CH <sub>2</sub> Cl <sub>2</sub> :MeOH (1 : 2) 0.5 M NaOMe/MeOH
B	0.2 mmol <b>22t</b> , 10 mL/mmol CH <sub>2</sub> Cl <sub>2</sub> :MeOH (1 : 2) 5 mM NaOMe/MeOH
C	0.1 M <b>22t</b> , 1 M NH <sub>3</sub> /MeOH
D	0.07 mmol <b>22t</b> , 50 mg Lipase of <i>Candida rugosa</i> (~70 U/mg), 1 mL toluene, 100 $\mu$ L 50 mM KP <sub>i</sub> -buffer pH 7
E	0.07 mmol <b>22t</b> , 1 mL 50 mM KP <sub>i</sub> -buffer pH 7 20 mg Lipase of <i>C. rugosa</i> (~70 U/mL), 50 mg $\beta$ -cyclodextrin

The chemical deprotection methods exhibited no selectivity during the deacetylation, removing all hydroxyl groups too fast in order to isolate a single intermediate. The enzymatic deprotection showed no effect and was abandoned as most literature states the most common position of acetyl cleavage to be the 4-position and not the 2-position.<sup>[163-165]</sup> A second synthetic route was carried out in order to avoid a prolonged synthesis route *via* acetylation and subsequent deacetylation and the difficult retrieval of the  $\beta$ -RhaN<sub>3</sub> **16d** from the reaction. The route followed a different procedure also proposed by *Györgydeák et al.*<sup>[166]</sup> The route encompasses an one-pot acetylation and bromination of  $\alpha$ -L-rhamnose (**11e**) and substitution of the acetylated halide **22u** with sodium azide. The one-pot acetylation and bromination procedure

of *Kartha et al.* was carried out to receive the acetylated bromide **22u** directly from rhamnose (**11e**), which was obtained in a yield of 96%.<sup>[167]</sup> Residual traces of hydrobromic acid were removed by repeated dissolution of the product in toluene and co-evaporation under reduced pressure. <sup>1</sup>H-NMR analysis indicated to an instability of the glycosyl halide **22u** as small amounts of degradation products of the bromide **22u** were present. Therefore, the compound was always stored below -20 °C and continuously kept on ice when in use. The substitution of the bromide using sodium azide in HMPA yielded the product **22v** in a virtually quantitative yield. The high solubility of the acetylated product **22v** in organic solvents (CH<sub>2</sub>Cl<sub>2</sub>) simplified the purification by extracting HMPA using water. A complete removal of the residual HMPA was not achieved, making the determination of the exact yield difficult. Using ammonia in methanol (2 M) for the deprotection of glycoside **22v** resulted in a yield of 84% of rhamnoside **16d**.<sup>[58]</sup> Similar to rhamnoside **22u**, β-RhaN<sub>3</sub> **16d** also displayed slight instability indicated by the <sup>1</sup>H-NMR-spectrum. A residual amount of HMPA was also still detectable in the <sup>1</sup>H-NMR-spectrum after the deprotection of the acetylated rhamnoside **22v**. In order to avoid the use of the highly toxic solvent HMPA, the synthesis of the rhamnosyl azide **16d** was attempted using the less toxic DMPU as a substitute solvent. The substitution of the solvent led to an unfavourable anomeric ratio of 1 : 2 (α : β) of the resulting product **22v** which was observable via <sup>1</sup>H-NMR. This unfavourable ratio clearly indicates to a strong participation of HMPA in the substitution reaction directing the azide into the equatorial position (β-configuration). The reaction in DMPU also showed side products and difficulty in separation of solvent from the desired product **22v**.

β-RhaN<sub>3</sub> **16d** was used on the one hand as a reference compound for the enzymatic synthesis of β-L-rhamnopyranosyl azide (**16d**) but also as a donor substrate for the potential rhamnosynthase variants.

### 6.3.2 Characterisation of the *wt* α-L-rhamnosidase

Before attempting the mutagenesis of RhaB to a glycosynthase, the *wt* form of the rhamnosidase was characterised. The *wt* gene *rhaB*, encoding the rhamnosidase RhaB containing a C-terminal His<sub>6</sub>-tag, was synthesised commercially into a pUC57 vector (*GenScript USA Inc.*, Piscataway, NJ, USA). The expression of the enzyme was carried out, identical to the expression of Cbg1 (section 6.2.2), heterologously in *E. coli* BL21(DE3) and isolated by IMAC. SDS-PAGE analysis of the purification steps displayed a successful isolation of *wt* RhaB in the elution fraction (Figure 78). The determined molecular weight (size comparison in the SDS-PAGE) of 101.2 kDa corresponds to the theoretical value of 107.6 kDa. The enzyme was isolated in concentrations of 0.75 ± 0.23 mg/mL after desalting and concentrating *via* ultrafiltration.

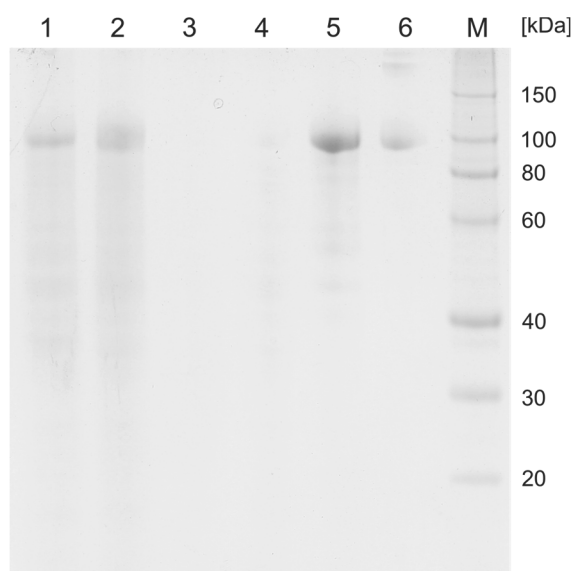


**Figure 78** SDS-PAGE analysis of the IMAC purification of the *wt*  $\alpha$ -L-rhamnosidases RhaB of *Bacillus* sp. GL1 expressed in *E. coli* BL21(DE3). Different steps of the purification are depicted: 1 cell lysate; 2 cell-free lysate; 3 flow-through; 4 wash fraction; 5 elution; 6 column wash. Roti-Mark 10–150 was applied as a standard (M) for size determination.

The kinetic parameters exhibited by RhaB for the hydrolysis of *p*NPRha **5r** were determined at 25 °C and a pH of 7.5 (K<sub>P</sub>-buffer, 50 mM; Figure 79). The rhamnosidase showed a high maximal activity of  $168 \pm 16.6$  U/mg and a high affinity to *p*NPRha **5r**, recognisable by the low  $K_M$  value of  $1.18 \pm 0.18$  mM. Due to the low solubility of *p*NPRha **5r**, concentrations higher than 1 mM were not tested for the determination of the kinetic parameters. Considering the fit of the kinetic data, it is evident that the maximal activity of RhaB was not reached under the chosen conditions, causing the relative high uncertainty of the determined  $v_{max}$  value (~10%).

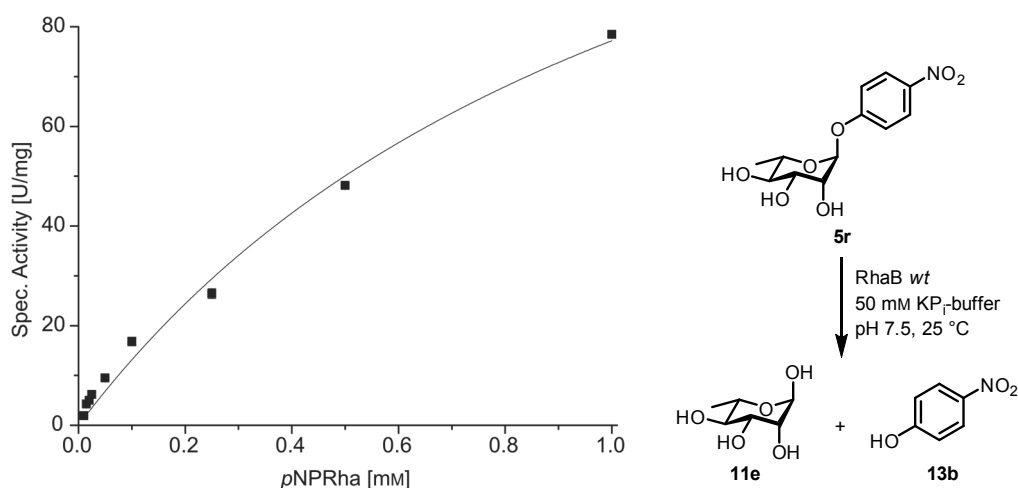


**Figure 79** Determination of the kinetic parameters of the  $\alpha$ -L-rhamnosidase RhaB of *Bacillus* sp. GL1. Parameters were determined for the hydrolysis of *p*NPRha **5r** in 50 mM K<sub>P</sub>-buffer, pH 7.5 at 25 °C. Hydrolysis was detected by absorption at 410 nm after 5 min incubation.

The  $k_{cat}$  value was calculated as  $302 \pm 30$  s<sup>-1</sup> resulting in a catalytic efficiency of  $255 \pm 64.2$  s<sup>-1</sup>·mM<sup>-1</sup>. Further characterisation of RhaB was carried out towards the storage stability, substrate scope and tolerance of co-solvents and external nucleophiles.

The low solubility of *p*NPRha **5r** and some glycosides, such as naringin (**1c**), caused the necessity of a co-solvent in order to make the substrate available for the enzyme in aqueous solution. Therefore, the influence of increasing the DMSO concentration on the activity of the rhamnosidase was examined (Figure 80, **A**). Lower concentrations up to 10% (*v/v*) did not affect the hydrolytic activity. The activity was improved at concentrations between 15–20%, most likely caused by an increased solubility of the substrate *p*NPRha **5r** in the presence of the co-solvent. High concentrations of 40% did not influence the activity of RhaB significantly, rendering DMSO as an ideal co-solvent. As residual HMPA was found in the product of the synthesis of  $\beta$ -L-rhamnopyranosyl azide (**16d**), the effect of HMPA on RhaB was also determined. In contrast to the tolerance of RhaB to DMSO, the presence of HMPA had a strong deactivating effect on the rhamnosidase (Figure 80, **B**). The activity of RhaB continually decreased with increasing HMPA concentrations resulting in residual activity of 34% at a HMPA concentration of 40% (*v/v*).

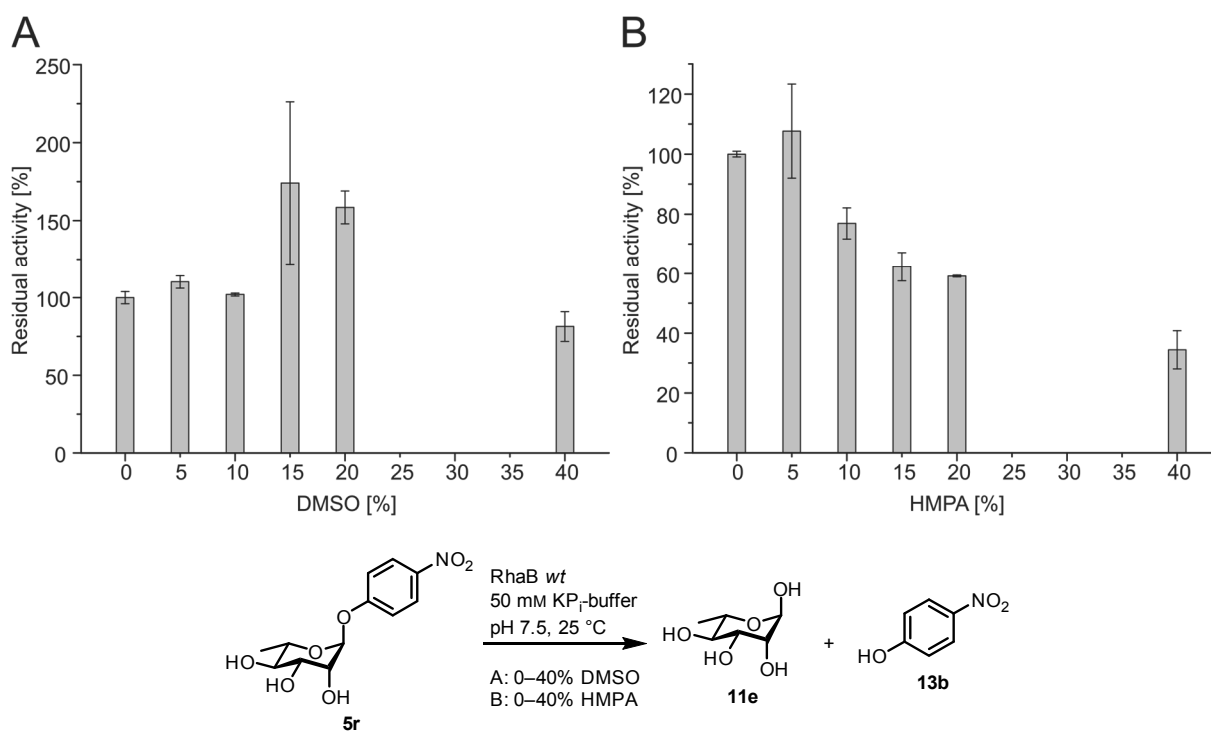


**Figure 80** DMSO- (**A**) and HMPA-tolerance (**B**) of RhaB of *Bacillus* sp. GL1 during hydrolysis of *p*NPRha **5r**. The hydrolysis of *p*NPRha **5r** was measured in the presence of 5, 10, 15, 20 and 40% DMSO/HMPA (*v/v*) in 50 mM  $\text{KP}_i$ -buffer, pH 7.5, at 28 °C for 5 min by absorption measurement at 410 nm.

In addition to the tolerance of co-solvents, the effect of different concentrations of glucose (**11b**) and sodium azide on the activity of RhaB was examined as these were employed as a possible acceptor or external nucleophile respectively (Figure 81, **B**). The activity of RhaB towards 2-Cl-*p*NPRha **5ae** was not affected significantly by low glucose (**11b**) concentrations. A slight activation of RhaB could be observed for low concentrations of 20 mM glucose (**11b**) increasing from  $15 \pm 4.5$  U/mg to  $17 \pm 3.0$  U/mg (17% increase). A high

concentration of 1 M on the other hand, exhibited a deactivating effect on the specific activity, lowering the activity down to  $10.4 \pm 1.03$  U/mg. Nevertheless, this represents only a decrease of 29% activity, therefore indicating to a high tolerance of RhaB towards glucose (**11b**). In comparison, the effect of the potential external nucleophile sodium azide on the activity of RhaB towards 2-Cl-*p*NPRha **5ae** was much higher (Figure 81, **A**). Similar to glucose (**11b**), low concentrations of sodium azide activated the enzyme increasing the activity from  $10 \pm 8.4 \cdot 10^{-1}$  U/mg to  $21 \pm 4.7 \cdot 10^{-1}$  U/mg. Concentrations of 40 mM and higher exhibited a strong deactivating effect, lowering the activity down to  $6.3 \pm 6.4 \cdot 10^{-1}$  U/mg corresponding to only 62% residual activity (compared to 0 mM sodium azide).

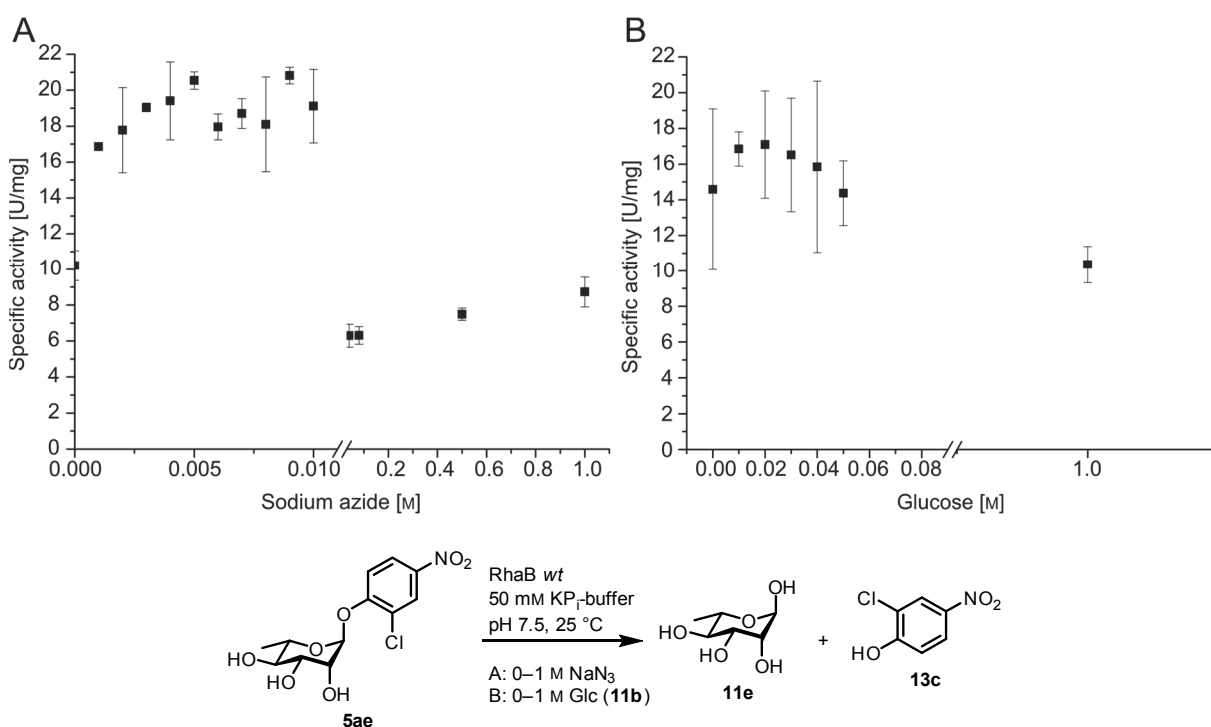


**Figure 81** Influence of sodium azide (**A**) and glucose (**B**) on the hydrolytic activity of RhaB of *Bacillus* sp. GL1 during hydrolysis of 2-Cl-*p*NPRha **5ae**. The hydrolysis of 2-Cl-*p*NPRha **5ae** was measured in the presence of different concentrations of sodium azide or glucose (**11b**) in 50 mM KP<sub>i</sub>-buffer, pH 7.5, at 28 °C for 3.3 min by absorption measurement at 410 nm.

To determine the versatility of a potential glycosynthase derived from RhaB with respect to possible donor substrates, the hydrolytic activity of RhaB towards ten different *p*-nitrophenyl glycosides were tested and compared to the activity towards 2-Cl-*p*NPRha **5ae**. The rhamnosidase exhibited only weak activity to different glycosides such as, *p*NPGlcNAc **5a** and *p*NPXyl **5i**, with relative activities around 0.04% when compared to the activity towards 2-Cl-*p*NPRha **5ae**. To all other glycosides, *p*NPGlc **5h**, *p*NPMan **5b**, *p*NPGal **5g**, *p*NPGalNAc **5ad**,  $\alpha$ -L-*p*NPFuc **5ac**,  $\beta$ -D-*p*NPFuc **5z**, and  $\alpha$ -L-*p*NPPara **5aa** relative activities below 0.03% were observed. The disaccharidic glycoside *p*NPLac **5ab** was also not hydrolysed by the enzyme. The substrate scope of RhaB is therefore very specific for  $\alpha$ -L-rhamnosyl moieties.

The application of the  $\alpha$ -L-rhamnosidase RhaB for the production of flavanone glucoside prunin (**1b**), which was also synthesised with the selectively deactivated naringinase (section 6.1.4), was tested using various conditions (Table 12). The reaction was followed by TLC at certain intervals in order to detect conversion of naringin (**1c**) to the desired product prunin (**1b**). For all conditions, no conversion of naringin (**1c**) could be observed. Precipitation of the substrate **1c** was often observed after less than 1 h incubation at 27 °C even after preliminary solubilisation of flavonoid **1c** at higher temperatures. Therefore, the reaction might have not occurred due to the precipitation of the flavonoid **1c**, becoming unavailable for RhaB in solution. A further possibility could be, that naringin (**1c**) is not naturally accepted by RhaB, as the natural substrate of this specific enzyme is gellan, which contains a  $\alpha$ -1,3 linkage between the rhamnosyl and glucosyl moieties and not a  $\alpha$ -1,2 linkage (Figure 82). These results contradict the findings described by *Hashimoto et al.*<sup>[114]</sup> The group reported the hydrolysis of naringin (**1c**) to prunin (**1b**) by RhaB detected via TLC analysis while incubating 10  $\mu$ g RhaB with 25  $\mu$ g of glycoside **1c**. A suitability of the model system for the development of reaction methods using  $\alpha$ -L-rhamnosidase RhaB as a rhamnosynthase could therefore not be verified.

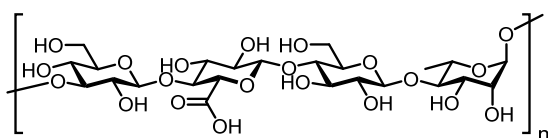


**Figure 82** Chemical structure of the linear repeating tetrasaccharide unit of gellan, the natural substrate of  $\alpha$ -L-rhamnosidase RhaB of *Bacillus* sp. GL1. ([,3- $\beta$ -D-Glc-1,4- $\beta$ -D-GlcA-1,4- $\beta$ -D-Glc-1,4- $\alpha$ -L-Rha-1,],<sub>n</sub>, GlcA = glucuronic acid)

**Table 12** Conditions tested for the hydrolysis of naringin (**1c**) to prunin (**1b**) by  $\alpha$ -L-rhamnosidase RhaB of *Bacillus* sp. GL1. All reactions were carried out in 50 mM KPi-buffer, pH 7 and reaction components/products analysed via TLC.

Entry	Conditions
A <sup>1</sup>	0.01 mg/mL RhaB lyophilised, 10 mM naringin <b>1c</b> , 2 h 30 °C, 18 h 40 °C
B <sup>1</sup>	0.05 mg/mL RhaB lyophilised, 10 mM naringin <b>1c</b> solubilised in DMSO (5% final-concentration v/v), 24 h 30 °C
C/D/E/F/G <sup>2</sup>	0.1 mg/mL RhaB lyophilised, 17 mM naringin <b>1c</b> , DMSO 5/10/20/30% v/v, 42 h 30 °C
H/I <sup>2</sup>	0.1 mg/mL RhaB lyophilised, 17 mM naringin <b>1c</b> , DMF 10/20% v/v, 42 h 30 °C
J <sup>2</sup>	0.1 g/mL RhaB lyophilised, 17 mM naringin <b>1c</b> , acetone 10% v/v, 42 h 30 °C
K <sup>2</sup>	0.1 mg/mL RhaB lyophilised, 17 mM naringin <b>1c</b> , ethanol 5% v/v, 42 h 30 °C

<sup>1</sup> Reaction volume 10 mL

<sup>2</sup> Reaction volume 1 mL

### 6.3.3 Mutagenesis of $\alpha$ -L-rhamnosidase RhaB

In order to create a rhamnosynthase, the hydrolytic activity needed to be eliminated by replacing the catalytically active residues with non-nucleophilic residues. The initial work towards this goal was carried out during the doctoral thesis of *Kamila Morka*.<sup>8</sup> Based on the description of the catalytically relevant amino acid residues by *Cui et al.* (Figure 83), mutations replacing each of the three conserved residues D567, E572 and E841 by a serine or glycine were introduced.<sup>[112]</sup> The mutations were incorporated by the *QuikChange*<sup>TM</sup>-PCR method and verified by *Sanger* DNA sequencing.

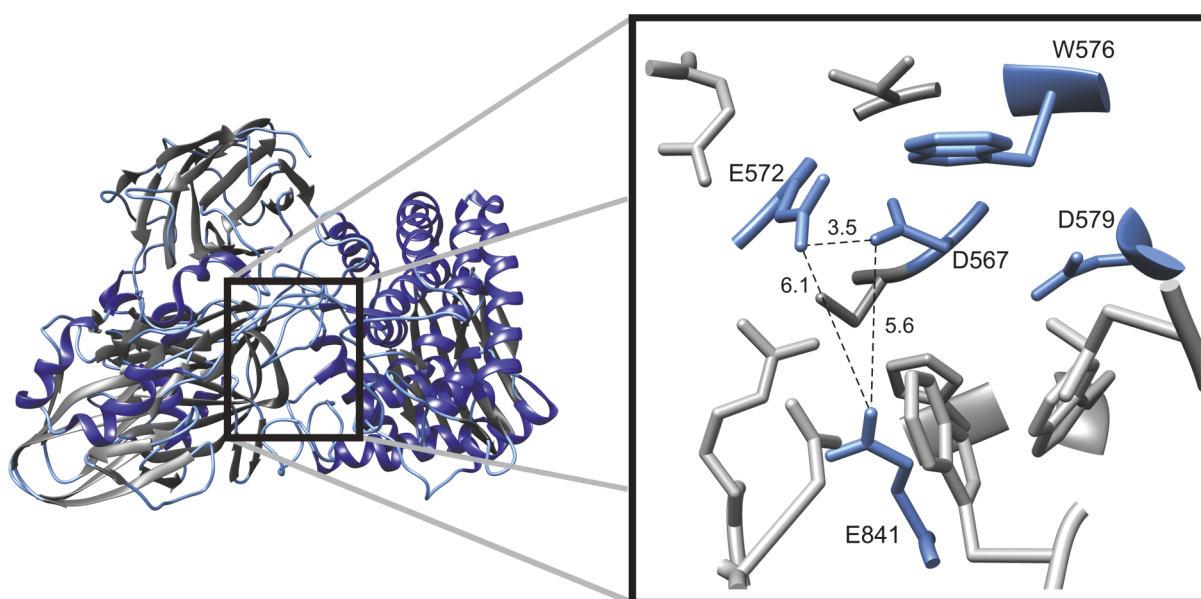


**Figure 83** Overview of RhaB of *Bacillus* sp. GL1 and a close up of the proposed active site cleft. Residues described by *Cui et al.* participating in the catalytic hydrolysis of RhaB are marked in the close up.<sup>[112]</sup> As RhaB is an inverting glycosidase, a definite determination of the catalytic acid/base pair is not possible, as the distances between these can vary. Distances in the close up are given in Å.

The wild type and mutated variants *rhaB-D567G/S*, *-E572G/S*, *-E841G/S* were then transferred into the expression vector pET-28a(+). Upon further consideration, it was decided to expand the variant library by not only varying the mutations further to alanine, cysteine, asparagine, and glutamine but adding mutations of the fourth highly conserved residue D579 as well.<sup>9</sup> The addition of alanine and cysteine mutations was considered, as they are common residues, which are usually tested for the production of glycosynthases throughout literature. The exchange with asparagine or glutamine would retain the structural properties of the replaced amino acids, but without the possibility of acting as an acid/base residue. Due to the high number of unique primers required for the creation of the additional twelve variants and the low yield of mutated genes created due to the linear amplification in the *QuikChange*<sup>TM</sup>-PCR method, the mutagenesis method was changed to *round the horn*-PCR.

<sup>8</sup> K. Morka, 'Yeasts as Production Hosts for Biocatalysts', Dissertation, Heinrich Heine University Düsseldorf, 2015

<sup>9</sup> B.-G. Axinte, ' $\alpha$ -L-Rhamnosidase from *Bacillus* sp. GL1: First Attempts on Systematically Altering Hydrolytic Activity', Bachelor thesis, Heinrich Heine University Düsseldorf, 2018

As this method does not utilise complementary primers, the change entailed the use of single reverse primers for each position in combination with a unique forward primer containing the new mutation, reducing the required amount of primers from 24 to 15.

Despite the successful use of the *round the horn*-PCR for the mutagenesis of *cbg1*, the mutagenesis of *rhaB* proved difficult when applying this method. For each mutation, PCR protocols with varying annealing temperatures were tested and desired fragments of around 8 kbp [size of pET-28a(+) with *rhaB* insert] were observed. Nevertheless, side products of smaller size were also produced indicating to non-selective binding of the primers within the *rhaB* gene. PCR products in batches containing a side product were separated by agarose gel electrophoresis and gel elution prior to ligation. Isolated plasmids were tested for the *rhaB* gene in a test PCR with primers binding the T7 promoter and terminator region of the vector. In many cases, the test PCR showed amplicons of varying size, most probably caused by an incorrect binding of one of the mutagenesis primers within *rhaB*. Isolated plasmids harbouring incomplete gene fragments were discarded. Sequencing was also carried out for a definite determination of the obtained mutant variant of *rhaB* (Table 13).

**Table 13** Variation of the proposed catalytically active amino acid residues D567, E572, D579, and E841 of RhaB of *Bacillus* sp. GL1. The mutations were acquired by *round the horn*-PCR by mutation of the *wt* gene in a pET-28a(+). Obtained plasmids were sequenced for confirmation of the resulting mutation.

Original AA	Introduced mutation	Codon variation	Verification
D567	A	GAC → GCC	—
	C	GAC → TGC	+ <sup>a</sup>
	N	GAC → AAC	+ <sup>a</sup>
	Q	GAC → CAG	—
	G	GAC → GGC	+ <sup>b</sup>
	S	GAC → AGC	+ <sup>b</sup>
D579	A	GAC → GCC	—
	C	GAC → TGC	—
	N	GAC → AAC	—
	Q	GAC → CAG	+ <sup>a</sup>
	G	GAC → GGC	—
	S	GAC → TCC	—
E841	A	GAG → GCC	+ <sup>a</sup>
	C	GAG → TGC	—
	N	GAG → AAC	—
	Q	GAG → CAG	—
	G	GAG → GGC	+ <sup>b</sup>
	S	GAG → AGC	+ <sup>b</sup>
E572	G	GAA → GGC	+ <sup>b</sup>
	S	GAA → AGC	+ <sup>b</sup>

<sup>a</sup> Mutations created by Bianca-Giorgiana Axinte during her bachelor thesis work.

<sup>b</sup> Plasmids obtained from the doctoral thesis of Kamila Morka

The expression of mutant variants of RhaB was carried out in *E. coli* BL21(DE3) following the standard expression procedure, incubating for 24 h at 25 °C after induction with 0.1 M IPTG. The expression was successful in all cases and the desired variants were isolated by the IMAC procedure (Figure 84). Expression of the RhaB variants by *E. coli* BL21(DE3) occurred at different levels resulting in highly varying protein concentrations ranging from  $1.1 \pm 7.2 \cdot 10^{-1}$  mg/mL for RhaB-E841S down to  $5.1 \cdot 10^{-2} \pm 2.0 \cdot 10^{-3}$  mg/mL for RhaB-D567C. The difference in expression might indicate to a disruption of the protein folding by the introduced mutation or a less suitable codon for expression in *E. coli*. All mutant variants were expressed in a lower level than the *wt* rhamnosidase.

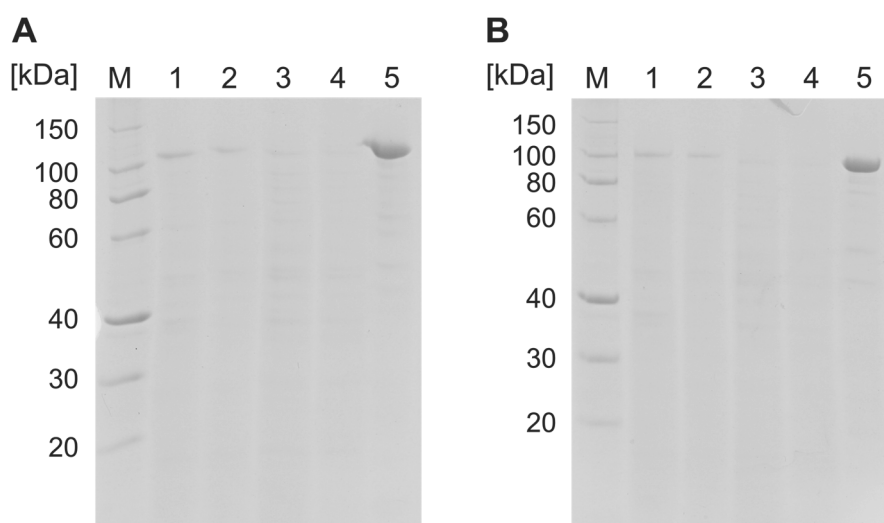


**Figure 84** Exemplary SDS-PAGE analysis of the expression and purification of the mutated  $\alpha$ -L-rhamnosidases. The variants RhaB-E841G (**A**) and RhaB-E841S (**B**) were isolated by IMAC. The glycosidases were expressed in *E. coli* BL21(DE3). Different steps of the purification are depicted: 1 cell lysate; 2 cell-free lysate; 3 flow-through; 4 wash fraction; 5 elution. Roti-Mark 10–150 was applied as a standard (M) for size determination.

#### 6.3.4 Screening for azide release

As discussed earlier in this thesis (section 6.1.4), the measurement of the activity of glycosynthases is a laborious task, as most glycosidic compounds are not easily detected by simple methods such as absorption or mass spectrometry without further derivatisation steps. In the case of the ‘classic’ glycosynthases, which utilise a glycosyl fluoride donor in the synthetic reaction, the release and quantification of the fluoride ion could be easily detected by a colourimetric assay containing triisopropyl-(4-nitrophenoxy)-silane (**23**). The release of the fluoride allowed the detection of the conversion of the glycosyl fluoride donor and therefore determine the rate of the enzymatic reaction. Due to the instability of  $\beta$ -glycosyl fluorides in general and the preliminary results observed in the work of *Kamila Morka* (high instability of  $\beta$ -L-rhamnopyranosyl fluoride in aqueous buffer), the classical donor could not be utilised for the identification and subsequent characterisation of potential rhamnosynthases. Therefore,

the developed assay for fluoride detection and quantification could also not serve as an adequate method for rhamnosynthase activity.

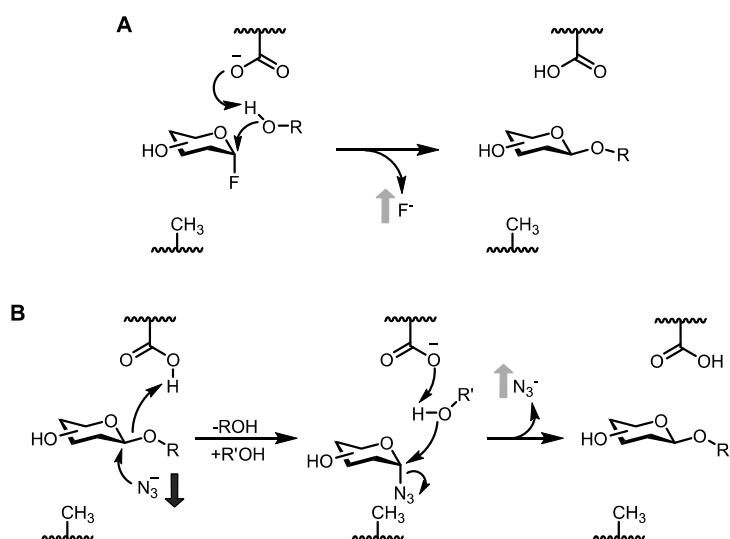


**Figure 85** Comparison of glycosynthetic reaction schemes *via* a ‘classical’ glycosynthase (**A**) utilising a glycosyl fluoride donor and a glycosynthase following the ‘chemical recovery’ method (**B**) creating *in situ* the glycosyl donor with assistance of an external nucleophile (e.g. azide-, acetate-, formate- or fluoride-ion). The arrows indicate an increase (gray) or decrease (black) of a detectable leaving group/nucleophile.

When comparing the proposed synthetic reaction scheme of a glycosynthase following a chemical recovery method, producing a glycosyl donor *in situ* in the presence of an external nucleophile, and the reaction scheme of a ‘classical’ glycosynthase (Figure 85), it is evident that also for the rhamnosynthase a successful glycosylation will be indicated by the release of the donor leaving group. Even more, a detection method quantifying the donors leaving group, which acts as the external nucleophile in the *in situ* production of the glycosyl donor would also allow the detection of the glycosyl donor’s production. A suitable assay would allow the characterisation and optimisation of both the *in situ* donor production and the glycosyl transfer onto an acceptor. In respect to the proposed rhamnosynthase reaction, a detection assay for azide ions would be required. For this purpose, the suitability of a spectrophotometric rapid determination method developed by *Seto et al.*, originally for the determination of cyanide and azide in beverages, was examined.<sup>[168]</sup> The method follows the formation of an azide ferric complex in acidic solution by photometry. After addition of  $\text{NaN}_3$ , the yellow acidic ferric solution (50 mM  $\text{FeCl}_3$  in 10 mM HCl) develops a red colour with an absorption maximum at 450 nm. The assay was carried out by the group in a microplate format, rendering the assay suitable for high-throughput screening. The detection limit of the assay for  $\text{NaN}_3$  was determined by the group to be 0.25 mM (S/N=3).

Before application of the assay towards the identification and characterisation of possible rhamnosynthase candidates, the handling and applicability was evaluated. The absorption spectrum of the acidic ferric solution after addition of  $\text{NaN}_3$  (in concentrations of 1–10 mM)

showed a maximum at 456 nm (Figure 86, **B**). The increase of absorption followed a linear fashion allowing a simple linear fit ( $R^2 = 0.999$ ) which can be utilised for quantification of the azide concentration.

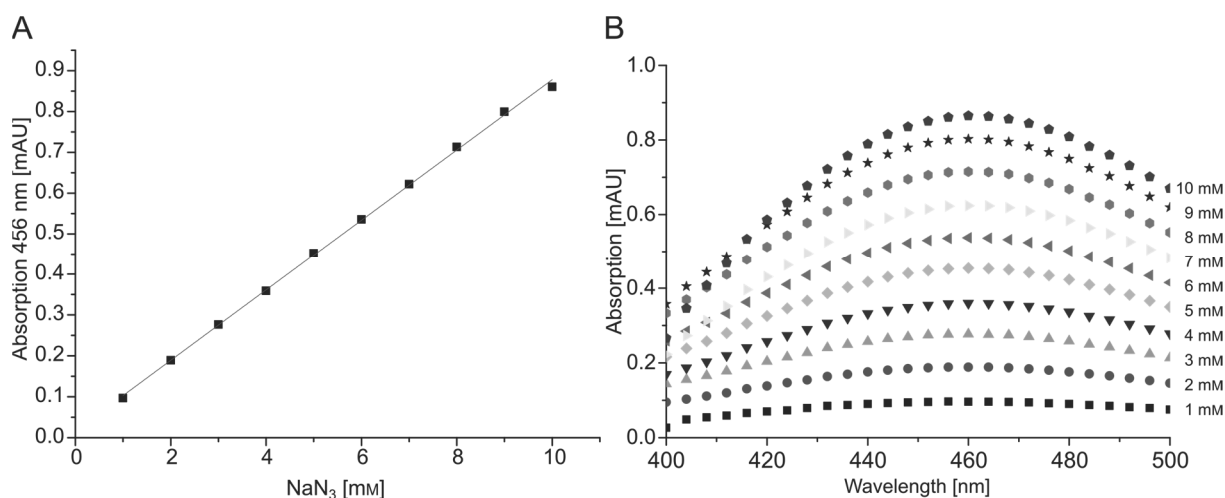


**Figure 86** Evaluation of the absorption changes of the acidic ferric solution (40 mM FeCl<sub>3</sub> in 10 mM HCl) in the presence of NaN<sub>3</sub> in different concentrations (1–10 mM). The absorption spectra (**B**) show a maximum at 456 nm and the increase of absorption with increasing azide amounts follows a linear fashion (**A**). Linear regression led to a calibration straight with a  $R^2 = 0.999$ .

The variation of the FeCl<sub>3</sub> concentration (10–50 mM) also exhibited a strong effect on the absorption up to a concentration of 30 mM. Above 30 mM FeCl<sub>3</sub> the absorption only increased slightly and a concentration of 40 mM was chosen as the standard condition for the assay. In order to determine the amount of released azide ions due to the conversion of the glycosyl donor, the possible formation of an azide ferric complex by the glycosyl donor **16d** itself needed to be ruled out. Therefore, the effects of  $\beta$ -L-rhamnopyranosyl azide (**16d**) at different concentrations and in the presence of free azide ions was tested (Figure 87). The absorption spectra measured in the presence of the glycoside **16d** at concentrations ranging from 1–5 mM showed only a slight increase of 0.01 ( $\Delta$ Abs) at 456 nm. The rhamnoside **16d** also showed no influence in the formation of the azide ferric complex when NaN<sub>3</sub> was added simultaneously to the rhamnoside **16d**. The absorption at 456 nm still followed a linear increase dependent of the NaN<sub>3</sub> concentration even in the presence of  $\beta$ -L-rhamnopyranosyl azide (**16d**). These results confirmed the applicability of the azide quantification assay as a useful tool for the identification and characterisation of potential rhamnosynthases.

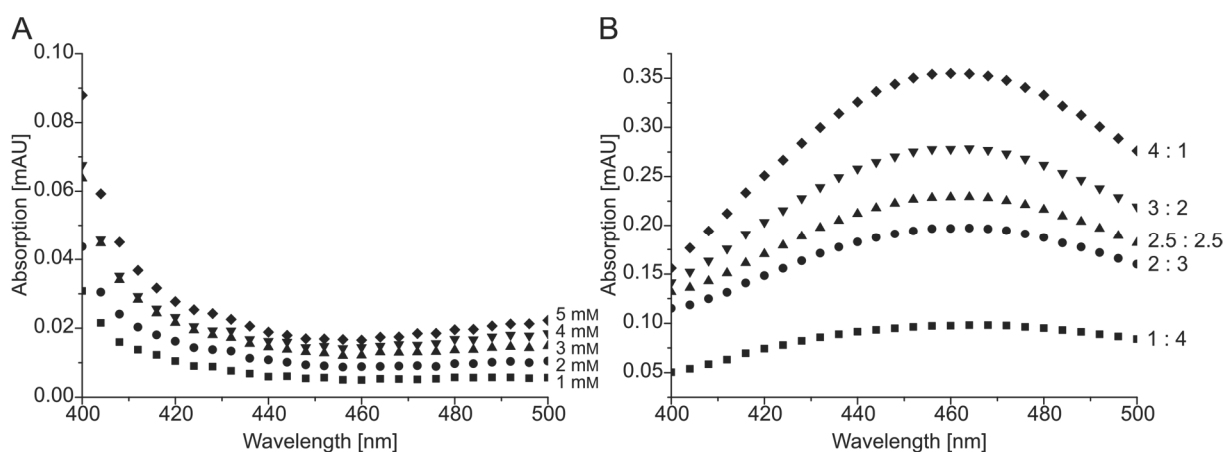


**Figure 87** Analysis of the effect of  $\beta$ -L-rhamnopyranosyl azide (**16d**) on the absorption of the acidic ferric assay solution (40 mM  $\text{FeCl}_3$  in 10 mM HCl). (A) The absorption spectra showed no significant increase when varying the concentration of compound **16d** (1–5 mM). (B) Different ratios of  $\text{NaN}_3$  and  $\beta$ -L-rhamnopyranosyl azide (**16d**) showed an absorption solely dependent of the free azide ion concentration (1 : 4 = 1 mM  $\text{NaN}_3$  : 4 mM  $\beta$ -Rha $\text{N}_3$  **16d**).

### 6.3.5 Attempts to find a $\alpha$ -L-rhamnosynthase

In contrast to the glycosynthases derived from  $\beta$ -glycosidases, which utilise  $\alpha$ -configured glycosyl fluoride donors, a glycosynthase derived from a  $\alpha$ -glycosidase requires a donor glycoside with  $\beta$ -configuration. The instability of  $\beta$ -glycosyl fluorides in aqueous solution renders these unsuitable for synthetic reactions. As described in section 5.3.1,  $\alpha$ -glycosynthases have been developed by utilising the *in situ* production of  $\beta$ -glycosyl azides, which exhibit a higher stability than their fluoride counterparts and are directly transferred to an adequate acceptor molecule. The *in situ* synthesis of the  $\beta$ -azide donor by chemical recovery was to be examined for the potential rhamnosynthase variants of RhaB (Figure 88).

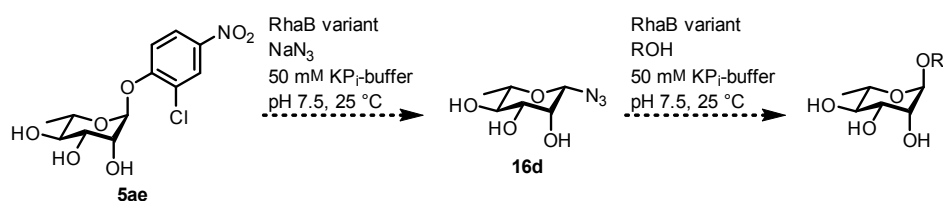


**Figure 88** Proposed mechanism for a  $\alpha$ -L-rhamnosynthase by applying the chemical recovery method. The  $\beta$ -rhamnopyranosyl azide (**16d**) is synthesised *in situ* by addition of the external nucleophile sodium azide and subsequently transferred to an acceptor molecule.

Before examining the potential of the produced RhaB variants in the chemical recovery experiments, with sodium azide acting as an external nucleophile, the mutant variants were tested for hydrolytic activity. Lyophilisate samples of the isolated rhamnosidase variants RhaB-D567G, -D567S, -E841G, and -E841S, provided by *Kamila Morka*, exhibited towards  $p\text{NPRha } \mathbf{5r}$  no residual activity above 0.5% compared to the *wt* RhaB and were therefore further considered for glycosynthetic reactions (Figure 89, A). The variant RhaB-D572G on the

other hand showed a residual activity of 10.9%, possibly displaying the importance of this residue for substrate recognition as the activity was not fully eliminated. The serine mutant at this position exhibited nearly no residual activity, which strengthens the possibility of a substrate recognition function, as unfavourable substrate-enzyme interactions may be caused by the incorporated serine residue. Addition of the external nucleophile at concentrations of 40 mM and 80 mM resulted in no significant recovery of activity for any of the RhaB variants (Figure 89, **A**). The presence of sodium azide decreased the residual activity of RhaB-E572G from 10.9% to 8.2% and 7.7% at concentrations of 40 mM and 80 mM azide respectively. The deactivation of the rhamnosidase variant is in keeping with the results observed for the *wt* rhamnosidase.

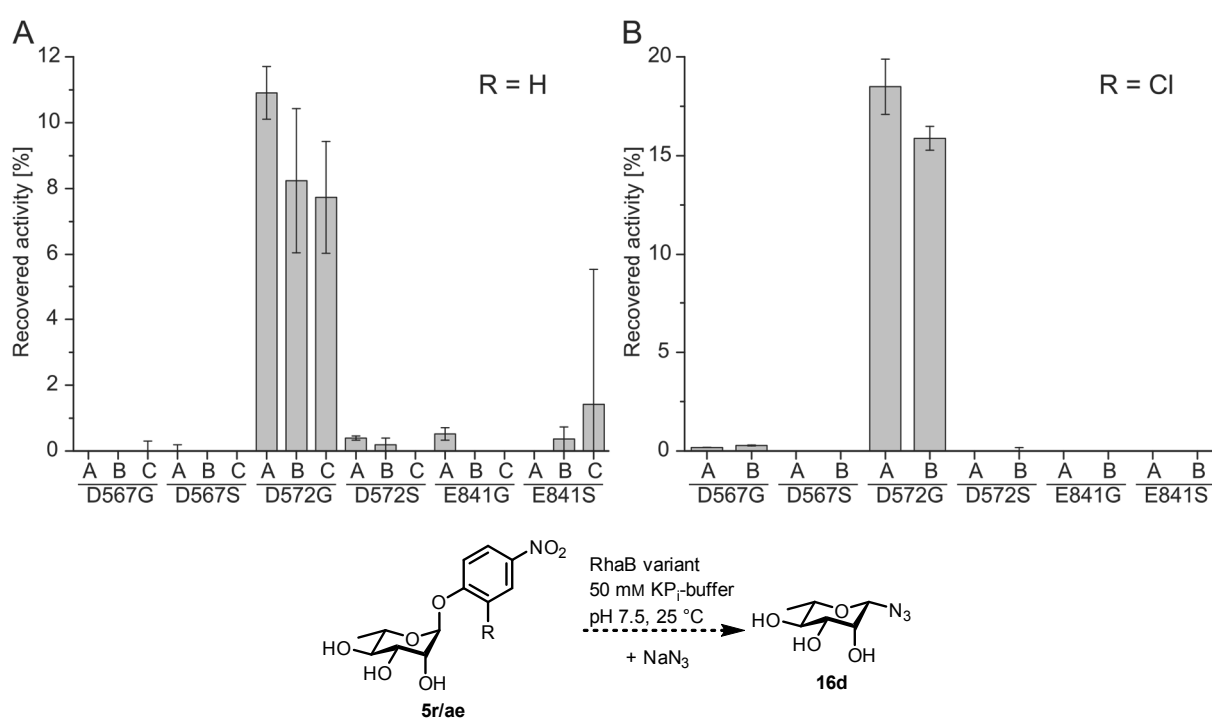


**Figure 89** Chemical recovery with various RhaB mutants (2 mg/ml lyophilisate). The residual activity of each mutant compared to the activity of the *wt* enzyme (taken as 100% activity) with identical conditions is depicted. **(A)** Incubation with *p*NPRha **5r** (10 mM) and sodium azide (A = 0 mM, B = 40 mM, C = 80 mM); **(B)** Incubation with 2-Cl-*p*NPRha (**5ae**, 5 mM) and sodium azide (A = 0 mM; B = 5 mM).

The reactions were repeated with the 2-chloro-4-nitrophenyl derivative of *p*NPRha **5ae**, as *Cobbuci-Ponzano et al.* described the respective fucoside to be more efficient than *p*NPFuc **5ac** in chemical recovery experiments while developing the  $\alpha$ -fucosynthase.<sup>[98]</sup> The substrate was employed in a much lower concentration (5 mM) due to the lower solubility of the compound and also the stronger absorption of 2-chloro-4-nitrophenolate (**13c**) compared to *p*-nitrophenolate (**13b**). Nevertheless, the mutant variants displayed the same behaviour towards the rhamnoside **5ae** as to *p*NPRha **5r**. The residual activity of RhaB-E572G was higher for 2-Cl-*p*NPRha **5ae** (18%), but was also deactivated by the presence of

## 6 Results

sodium azide (16%, 5 mM). Due to the residual hydrolytic activity of RhaB-E572G, the mutant variants of this position were excluded from further examination of glycosynthetic activity.

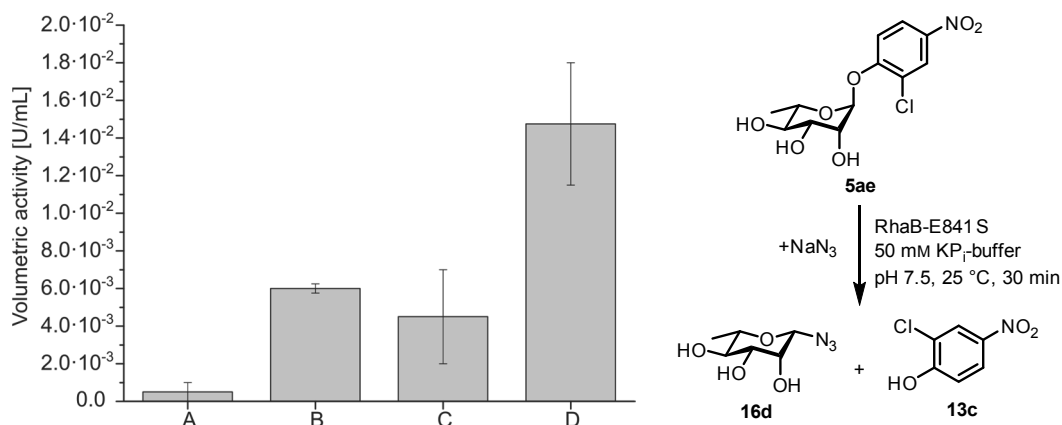


**Figure 90** Chemical recovery with the mutant variant RhaB-E841S, 2-Cl-*p*NPRha **5ae** (5 mM) and sodium azide (5 mM or 10 mM) incubated for 30 min at 25 °C in 50 mM KP<sub>i</sub>-buffer, pH 7. In the reactions A–C contained 2 mg/mL lyophilisate and reaction D 5 mg/mL lyophilisate. Sodium azide concentrations: A 0 mM, B 5 mM, C 10 mM, D 5 mM.

Upon further testing, a slight recovery of activity was observed for the RhaB-E841S variant. The recovery could be observed in the chemical recovery reaction with *p*NPRha **5r** (Figure 89; **A**), but not for 2-Cl-*p*NPRha **5ae** (Figure 89, **B**). Due to the high error, the results were considered with uncertainty. Nevertheless, the reaction with substrate **5ae** was repeated with RhaB-E841S and followed for a longer duration of 30 min (Figure 90). The mutant exhibited virtually no volumetric activity ( $4.0 \cdot 10^{-4}$  U/mL) when incubated in the absence of the external nucleophile azide. When incubated with equimolar concentrations of sodium azide (5 mM), the enzyme regained activity up to  $6.2 \cdot 10^{-3}$  U/mL, reconfirming the possibility of a chemical recovery of the activity observed with *p*NPRha **5r**. An increase of azide to 10 mM showed as expected a deactivating effect, decreasing the volumetric activity of the solution to  $4.5 \cdot 10^{-3}$  U/mL. The increase of lyophilisate from 2 mg/mL to 5 mg/mL (and therefore increasing the amount of enzyme) increased the volumetric activity  $2.4 \times$  ( $1.5 \cdot 10^{-2}$  U/mL). This increase in activity corresponds linearly to the increase of the protein concentration. These results strongly pointed to RhaB-E841S being a possible candidate for a  $\alpha$ -L-rhamnosynthase. The substrate was only cleaved in the presence of the external nucleophile and therefore cannot have been caused by natural hydrolysis. The reaction was carried out on a larger scale, but the detection of the presence of  $\beta$ -L-rhamnopyranosyl azide (**16d**), as a reaction product of the enzymatic conversion, was not possible *via* RP-TLC. Analysis of the crude reaction mixture, after removal of the aqueous solvent by reduced pressure, and comparison with the chemically synthesised  $\beta$ -RhaN<sub>3</sub> **16d** *via* <sup>1</sup>H-NMR displayed indications of the production of rhamnoside **16d** (Figure 91). A weak signal, with a chemical shift of 4.8 ppm (in D<sub>2</sub>O), could be observed next to the large solvent peak of HDO. The signal indicated to the possible presence of the anomeric proton of  $\beta$ -RhaN<sub>3</sub> **16d**. Closer examination of the <sup>1</sup>H-NMR spectrum and additional

---

comparison with the chemical shift values of  $\alpha$ - and  $\beta$ -L-rhamnose (**11e- $\alpha/\beta$** ) determined the produced product to be  $\beta$ -L-rhamnose (**11e- $\beta$** ). Despite the different functional group of the anomeric centre in  $\beta$ -L-rhamnose (**11e**, OH) and  $\beta$ -L-rhamnopyranosyl azide (**16d**, N<sub>3</sub>), the chemical shift of the anomeric proton of both compounds are near identical. Nevertheless, a differentiation between the two compounds **11e** and **16d** can be more easily made by comparison of the proton signals of the C<sub>2</sub>- and C<sub>3</sub>-positions of the rhamnosides. The <sup>1</sup>H-NMR spectrum shows apart from remaining starting material, a mixture of  $\alpha$ - and  $\beta$ -L-rhamnose (**11e**) and released 2-chloro-*p*-nitrophenol (**13c**). The presence of the hydrolysis product of 2-Cl-*p*NPRha **5ae** was unexpected as RhaB-E841S showed no hydrolytic activity without the presence of the external nucleophile. Nonetheless, due to low concentration and therefore low intensity of the proton signals the <sup>1</sup>H-NMR spectrum, a production of the  $\beta$ -rhamnopyranosyl azide (**16d**) cannot be excluded.

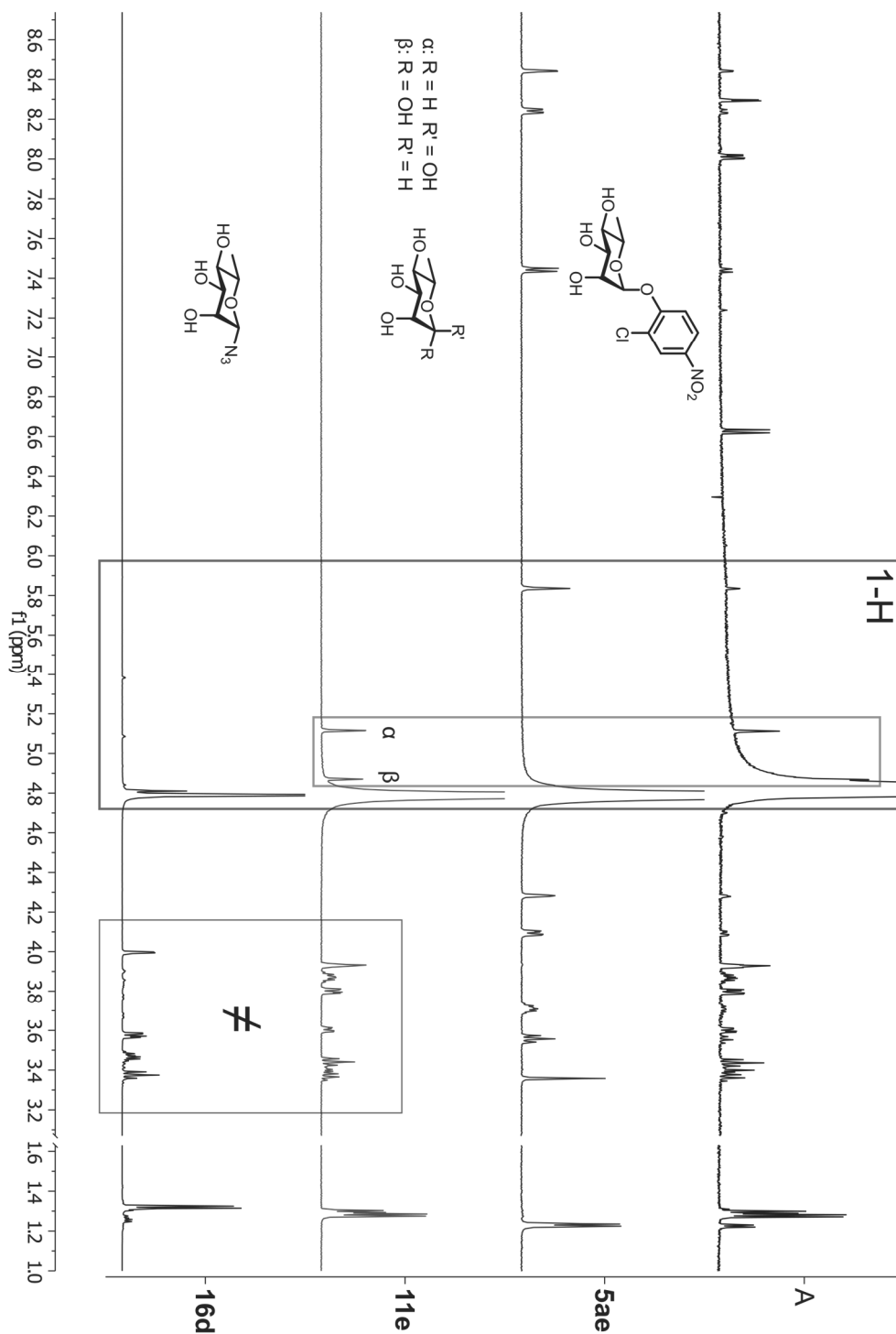


**Figure 91** <sup>1</sup>H-NMR analysis of the conversion of 2-Cl-pNPRha **5ae** (5 mM) by RhaB-E842S (5 mg/mL lyophilisate) in the presence of sodium azide (10 mM) incubated 18 h at 25 °C. The resulting spectrum of the reaction mixture (**A**; after solvent removal under reduced pressure) was compared to the references 2-Cl-pNPRha **5ae**, α/β-L-rhamnose (**11e**), and β-RhaN<sub>3</sub> **16d**. Each <sup>1</sup>H-NMR-spectrum was recorded in D<sub>2</sub>O.

During the Bachelor thesis of *B.-G. Axinte*, the variants of RhaB mutated at the positions E841 and E567 were freshly expressed in *E. coli* BL21(DE3) and isolated by IMAC. However, the RhaB-D567G mutant was excluded from further experiments, as resequencing of the inserted gene *rhaB-D567G* revealed a section of six mutated amino acids (N547–I552; NATWEI changed to ISHVAF) additionally to the desired D567G mutation. The results obtained

beforehand with the lyophilisate of this RhaB variant can therefore not be taken into account, as an exchange of six consecutive amino acids will most likely lead to the deficiency in hydrolytic activity, which was observed in the previous experiments.

Contrary to the chemical recovery experiments using the lyophilisated samples, the freshly expressed RhaB variants displayed a much higher recovery in the presence of the external nucleophile (Figure 92). With exception of RhaB-E841S, all examined variants RhaB-E841G, -D567S, and -D567C exhibited a residual hydrolytic activity even without the presence of the external nucleophile. The absence of this residual activity in the lyophilisated samples may be due to denaturation of the rhamnosidase during the freeze-drying process. In the presence of sodium azide at a concentration of 16 mM, RhaB-E841G, -D567S, and -D567C all showed 100% recovery of the cleavage activity. As the activity of the *wt* enzyme was deactivated by high concentrations of sodium azide, the recovered activity will not have been caused or influenced by the residual activity observed in the absence of sodium azide. Higher concentrations of azide such as 0.1 M and 0.2 M exhibited a deactivating effect on the RhaB-D567S variant. RhaB-D567C was also deactivated by the high concentration, though the large deviations in recovered activity might indicate to disturbances during the measurement. Different to the other variants, RhaB-E841G was not deactivated by the high concentrations of azide. The high percentage of recovered activity in the presence of the external nucleophile points to an incorporation of the azide into the substrate **5ae**. The RhaB-D567G variant showed the most promising properties for use as a rhamnosynthase, as this mutant recovered activity without any deactivation during all of the tested conditions. The missing recovery of the variant RhaB-E841S contradicts the results found for the lyophilisate sample. This apparent absence in recovered activity might be due to the short measurement time of 5 min as, with the lyophilisated sample, long reaction times of 30 min and longer were necessary to detect a cleavage of the substrate *p*NPRha **5r** with RhaB-E841S.

## 6 Results

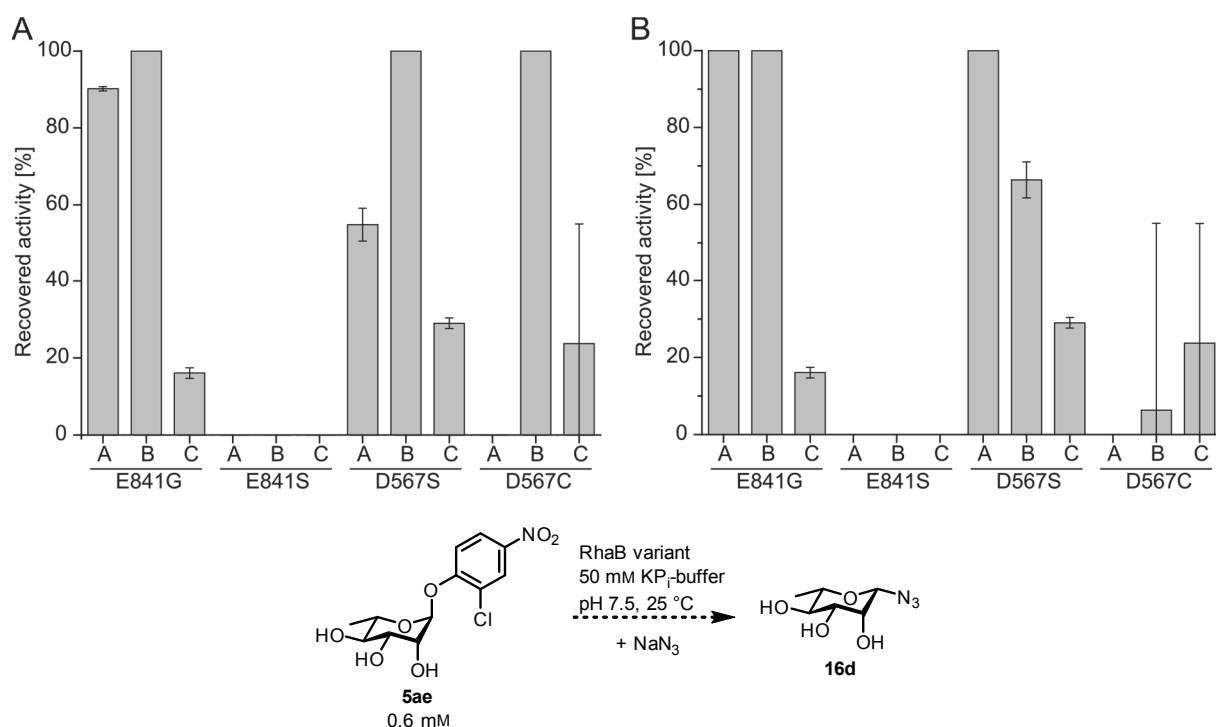


**Figure 92** Recovered activity of the RhaB mutant variants towards 2-Cl-*p*-NPRha **5ae** (0.6 mM) in the presence of sodium azide. The concentration of sodium azide was varied (**A**: A 8 mM; B 16 mM; C 0 mM / **B**: A 0.1 M; B 0.2 M; C 0 M) and the reaction followed for 5 min at 25 °C in 50 mM KP<sub>i</sub>-buffer, pH 7.5. Activity was compared to the *wt* activity, which was set as 100%. Enzyme concentrations: E842G 94.8 µg/mL; E841S 73.2 µg/mL; D567S 2.0 µg/mL; D567C 0.1 µg/mL.

To determine whether the recovered activity of the RhaB variants led to the formation of the β-L-rhamnopyranosyl azide (**16d**) donor, the chemical recovery reactions were repeated but instead of the release of 2-chloro-*p*-nitrophenolate (**13c**) the depletion of the sodium azide concentration was examined (Figure 93). The azide concentration of the reaction mixture could be determined by applying the assay described in section 6.3.4 using acidic ferric solution. The measurement of a reference sample containing no enzyme did not lead to the expected azide concentrations of 8 mM and 16 mM (starting concentrations of the external nucleophile) but concentrations of  $5.9 \pm 0.4$  mM and  $12.3 \pm 2.0$  mM respectively and also showed a concentration of  $2.3 \pm 0.5$  mM when no sodium azide was present. The assay therefore seems to contain a slight uncertainty and the results should only be considered for indications of the donor **16d** formation. When considering these measurements, the most promising variants of RhaB for the conversion of azide are RhaB-E841G and -D567S. In the presence of a starting concentration of 16 mM sodium azide RhaB-E841G and -D567S catalysed a reduction of the azide concentration of 6.6 mM and 4.9 mM respectively ( $\Delta N_3$  concentration after 1 h). The reduction catalysed by these variants is larger than the difference of the reference sample ( $\Delta N_3 = 3.7$  mM) and therefore could possibly indicate to a conversion by the enzymes and the production of the rhamnosyl donor **16d**. The large standard deviation of the measurements also point towards the necessity of further optimisation of the azide quantification assay.

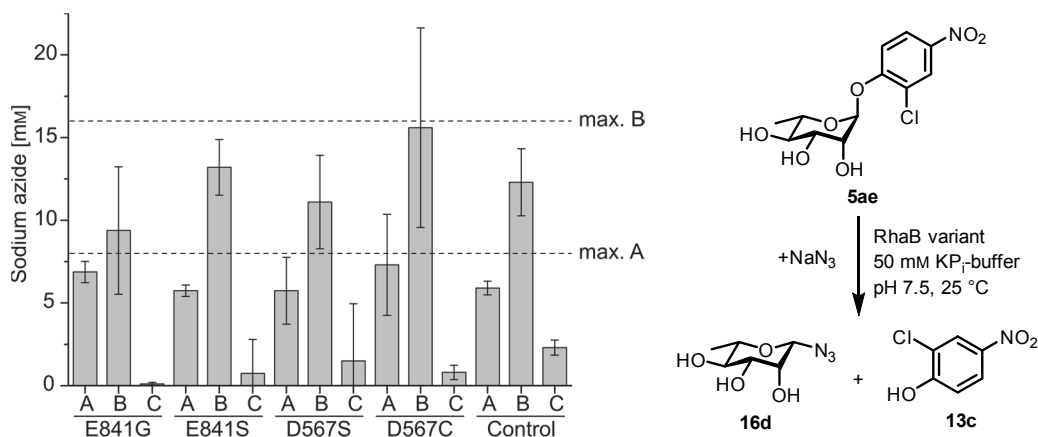


**Figure 93** Quantification of the sodium azide concentration decreased by the potential conversion of 2-Cl-*p*NPRha **5ae** to donor **16d** by mutant variants of RhaB. The concentration of sodium azide was varied (A 8 mM; B 16 mM; C 0 mM) and the concentration measured after 1 h at 25 °C in 50 mM KPi-buffer, pH 7.5. Quantification was carried out measuring the absorption of the reaction in acidic ferric solution (40 mM FeCl<sub>3</sub> in 10 mM HCl) at 456 nm. A control reaction was performed by adding buffer without enzyme to the reaction mixture. Enzyme concentrations: E842G 94.8 µg/mL; E841S 73.2 µg/mL; D567S 2.0 µg/mL; D567C 0.1 µg/mL.

Furthermore, it was attempted to observe the production of the donor  $\beta$ -RhaN<sub>3</sub> **16d** by the RhaB variants using infrared (IR) spectroscopy and <sup>1</sup>H-NMR analysis. The characteristic absorption band at 2113 cm<sup>-1</sup> in the IR spectrum of  $\beta$ -L-rhamnopyranosyl azide (**16d**) represents the vibration of the azide functionality when bound to the rhamnosyl moiety. Measurement of sodium azide displayed an absorption band around 2042 cm<sup>-1</sup>, which therefore allowed a differentiation between the bound and free form of the azide molecule. All IR spectra of the enzymatic reactions, containing 0.2 M sodium azide and 0.6 mM 2-Cl-*p*NPRha **5ae** and one of the RhaB variants RhaB-E841G, -E841S, or -D567S, displayed an absorption band around 2041 cm<sup>-1</sup> belonging to the unbound azide ion (Figure 94). The absence of an absorption band at 2113 cm<sup>-1</sup> therefore indicated to no production of the rhamnosyl donor **16d**. Analysis of the chemical recovery reaction via <sup>1</sup>H-NMR also could not lead to the identification of  $\beta$ -RhaN<sub>3</sub> **16d**. For the cases of RhaB-E841G and -D567S, hydrolysis of the substrate **5ae** to rhamnose (**11e**) was observed. For RhaB-D567S the hydrolysis was even observed for the reaction without the presence of sodium azide, suggesting a hydrolysis of substrate **5ae** without the external nucleophile participating. RhaB-E841G on the other hand, displayed hydrolysis of substrate **5ae** only in presence of the nucleophile, with an increase of sodium azide causing a proportional increase of the hydrolysis product **11e**. These results for the RhaB variant RhaB-E841G correspond to the results observed by <sup>1</sup>H-NMR analysis for the chemical recovery of RhaB-E841S lyophilisate sample.

## 6 Results

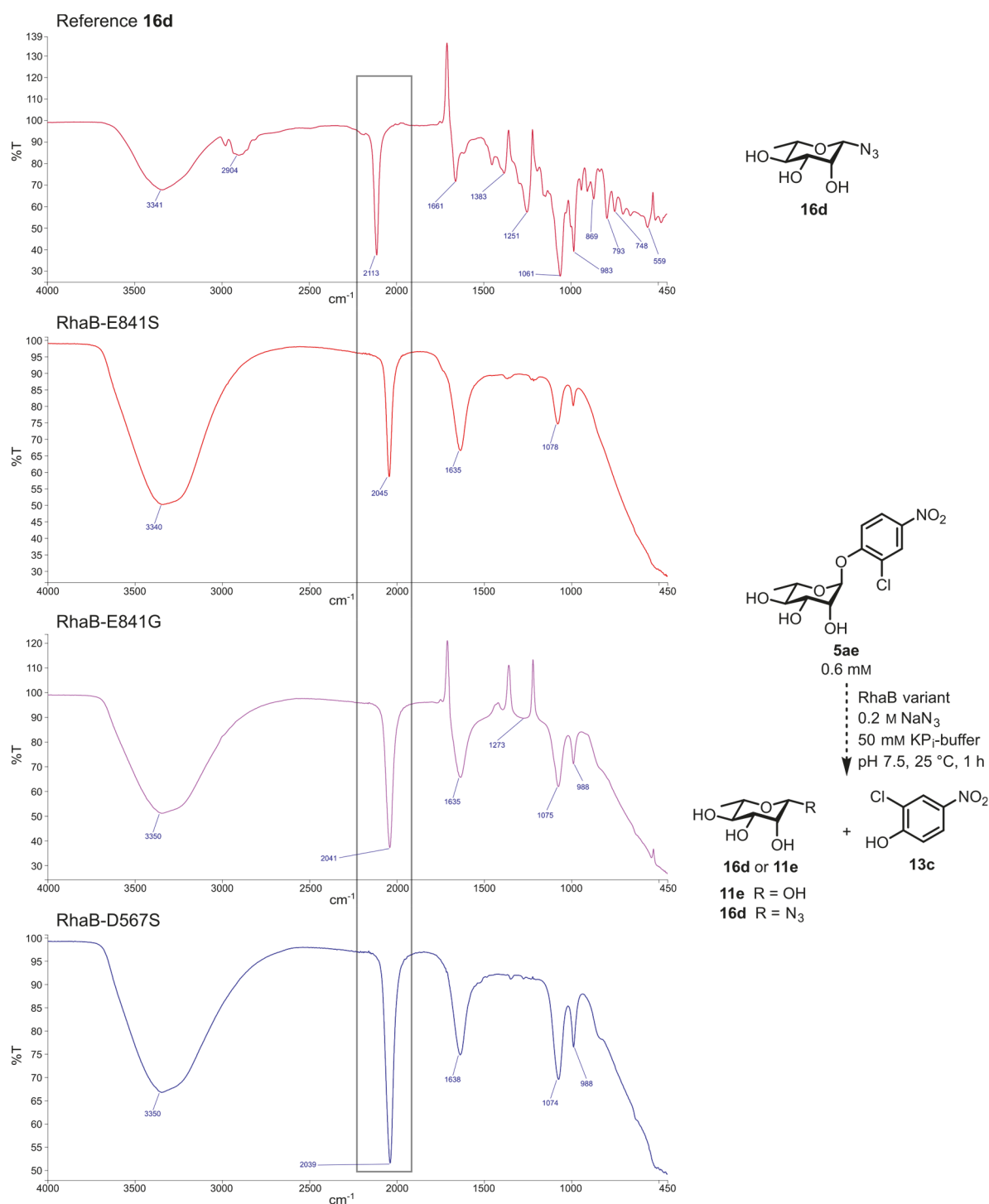


**Figure 94** IR analysis of the chemical recovery experiments with RhaB variants RhaB-E841S, -E841G, and D567S in the presence of 2-Cl-*p*NPRha **5ae** (0.6 mM) and sodium azide (0.2 M). The reaction was incubated for 1 h in 50 mM KP<sub>i</sub>-buffer, pH 7.5 at 25 °C. The vibrational bands applied for differentiation between free (~2041 cm<sup>-1</sup>) and bound azide (2113 cm<sup>-1</sup>) are marked by the box.

The glycosynthetic reaction, utilising difficult synthesisable donor molecules, would be facilitated by the *in situ* production of the glycosyl donor catalysed by the glycosynthase itself, yet the incapability of the *in situ* production of the glycosyl donor does not exclude the mutant glycosidase as a potential glycosynthase. Therefore, the mutant variants of RhaB were also tested for glycosynthetic activity by applying the chemically synthesised rhamnosyl donor

---

$\beta$ -L-rhamnopyranosyl azide (**16d**) in the presence of the monosaccharide glucose (**11b**) as an acceptor. Glucose (**11b**) was chosen as the acceptor as the disaccharidic substrate 3-O-( $\alpha$ -L-rhamnopyranosyl)- $\beta$ -D-glucopyranose was proposed by *Cui et al.* as the natural substrate of RhaB.<sup>[112]</sup> Analysis of the potential rhamnosylation reaction was carried out by <sup>1</sup>H-NMR. After incubation of the reaction containing a RhaB mutant (E841G/S, D567S/C),  $\beta$ -RhaN<sub>3</sub> **16d** as the donor, and the acceptor glucose (**11b**) in concentrations of 0.2 M and 0.1 M, the solvent was removed by reduced pressure and dissolved in D<sub>2</sub>O for <sup>1</sup>H-NMR analysis. Control reactions without the addition of the acceptor molecule **11b** displayed the inactivity of the RhaB mutants towards the potential donor **16d**. Nevertheless, the addition of glucose **11b** did not lead to the production of the expected disaccharide. The identification of newly formed signals and the analysis of the left over starting material **11b** in the <sup>1</sup>H-NMR spectrum was hindered greatly by the high intensity of the acceptor proton signals caused by the high concentration of the acceptor (chosen to benefit the equilibrium towards product formation).

Chapter synopsis:

- The substrates *p*-nitrophenyl rhamnopyranoside (**5r**) and 2-chloro-4-nitrophenyl rhamnopyranoside (**5ae**) were synthesised successfully as substrates for RhaB, applied in the activity and chemical recovery experiments.
- $\beta$ -L-Rhamnopyranosyl azide (**16d**) was successfully synthesised by conversion of the pyranosyl halide **22u** with  $\text{NaN}_3$  in HMPA. The compound **16d** was employed as a reference molecule and potential donor substrate for rhamnosynthase candidates.
- The *wt* RhaB of *Bacillus* sp. GL1 was characterised for kinetic parameters, substrate scope and tolerance towards co-solvents (DMSO and HMPA) and the additives  $\text{NaN}_3$  and glucose (**11b**).
- Additionally to the mutant variants of RhaB created by *Kamila Morka*, RhaB-D567G/S, -E572G/S, -E841G/S, four further variants RhaB-E567C, -E567N, -E579Q, and -E841A were created by *round the horn*-PCR.
- The colourimetric detection assay for azide ions by acidic ferric solution was adapted for a microplate format.
- Mutant variants of RhaB were tested for hydrolytic activity, examined for regained activity by chemical recovery and glycosynthetic activity with glucose as an acceptor molecule.

## 6.4 From monosaccharides to en bloc glycan transfer

In comparison to the glycosynthases, Abg-E358S and BglU-E377A, which transfer monosaccharide moieties to an acceptor molecule, glycosynthases derived from *endo*- $\beta$ -*N*-acetylglucosaminidases (ENGase) of the glycohydrolase family GH 85, are able to transfer large glycan molecules *en bloc* onto various acceptor molecules. These acceptor molecules can range from small low-molecular-weight molecules (e. g. monosaccharides, 1,3-diols) to large protein structures. Glycosyl oxazolines or *N*-glycans containing a  $\beta$ -1,4-linked *N,N'*-diacetylchitobiose core can act as donor molecules for glycosynthases of this family. *Eshima et al.* described the mutant variant of the *endo*- $\beta$ -*N*-acetylglucosaminidase of *C. cinerea* Endo CC-N180H to have high transglycosylation and glycosynthase-like activity.<sup>[132]</sup> The enzymes activity pH-optimum of 7.5 is advantageous for synthetic reactions, as the stability of the oxazoline donor compounds is greatly increased at an alkaline pH. The high heterologous expression in *E. coli* strains would also allow easy scalability of the desired reactions. The transfer of the sialo biantennary complex type glycan by Endo CC-N180H, derived from the sialylglycopeptide (**20**, SGP) as the glycan donor, was demonstrated by *Manabe et al.* for various acceptor molecules.<sup>[134]</sup> The acceptor repertoire of Endo CC-N180H was to be expanded to flavonoid and sugar nucleotide compounds and was attempted during the work of this thesis for the flavonoid glycosides naringenin-7-*O*- $\beta$ -D-glucopyranoside (**1b**, prunin), quercetin-3-*O*- $\beta$ -D-glucopyranoside (**1h**, isoquercetin), quercetin-3-*O*- $\beta$ -D-galactopyranoside (**1j**, hyperoside), quercetin-3-*O*- $\alpha$ -L-arabinofuranoside (**1k**, avicularin) and uridine diphosphate *N*-acetylglucosamine (**28**, UDP-GlcNAc).

### 6.4.1 En bloc glycosylation

Glycosynthases derived from *endo*- $\beta$ -*N*-acetylglucosaminidases mostly utilise oxazoline donors for the glycosylation reaction. If residual hydrolytic activity is present, the mutant glycosidase can also apply natural occurring glycans containing a *N,N'*-diacetylchitobiose core as glycan donors. The ENGase variant Endo-CC N180H is able to utilise the natural glycopeptide, sialylglycopeptide (**20**, SGP), as a donor for the transferral of a sialo biantennary glycan (complex type) onto a 1,3-diol acceptor (Figure 95). SGP **20** can be isolated from egg yolk powder and is commercially available in a purified form.<sup>[169, 170]</sup> For the presented experiments commercial SGP **20** was obtained and was applied in glycosylation reactions with a commercial version of Endo-CC N180H and a version heterologously expressed in *E. coli* BL21(DE3).

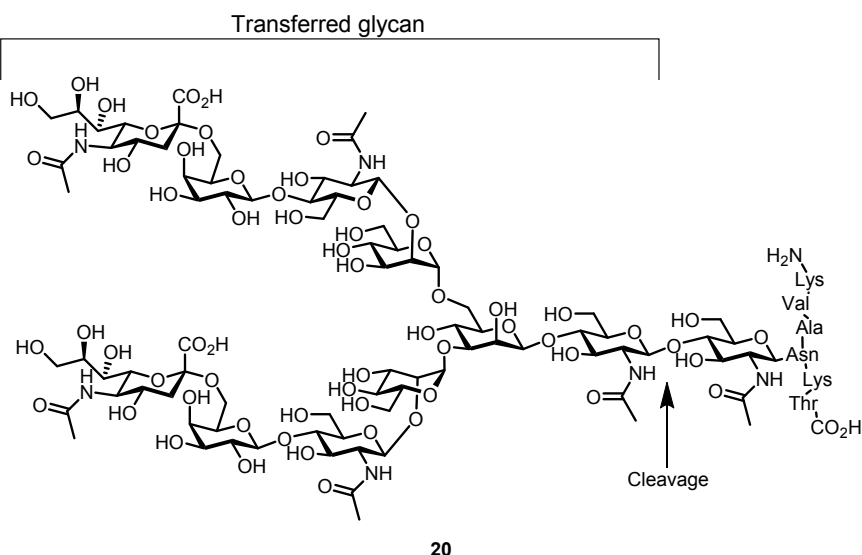


**Figure 95** Structure of the sialylglycopeptide SGP **20**, which acts as a glycan donor in glycosylation reactions with Endo-CC N180H. The *N,N'*-diacetylchitobiose core of the glycan is cleaved and then transferred onto a suitable acceptor.

#### 6.4.2 Glycosylating RNase B-GlcNAc

Native RNase B, which possesses a single glycan structure of the high mannose type, was enabled to act as an acceptor for transglycosylation, by cleavage of the *N,N'*-diacetylchitobiose core of the glycan with commercially available Endo-H. The cleavage of the glycan proceeded with complete conversion, decreasing the proteins molecular weight from 15 kDa to 14 kDa, which was observable by Tricine-SDS-PAGE analysis. A Tricine-SDS-PAGE was chosen for the analysis of the transglycosylation, as this type of SDS-PAGE technique is more suited for proteins below 30 kDa.<sup>[171]</sup> By comparison with a dilution series of albumin, with protein amounts ranging from 1–10  $\mu\text{g}$ , the amount of produced RNase B-GlcNAc was estimated to be 0.002 mg/ $\mu\text{L}$ . The obtained peptide (2  $\mu\text{g}$ ) was subsequently incubated as an acceptor with the commercial ENGase glycosynthase variant Endo-CC N180H (0.75 mU) and SGP **20** (150  $\mu\text{g}$ ) as the glycan donor. Further Tricine-SDS-PAGE analysis displayed an increase in the molecular weight confirming the transfer of the biantennary complex type glycan to the RNase B-GlcNAc. These results were in accordance to the observations in literature.<sup>[132]</sup> A dilution of the Endo-CC N180H concentration caused an improved glycosylation, possibly due to residual hydrolytic activity of the mutant ENGase.

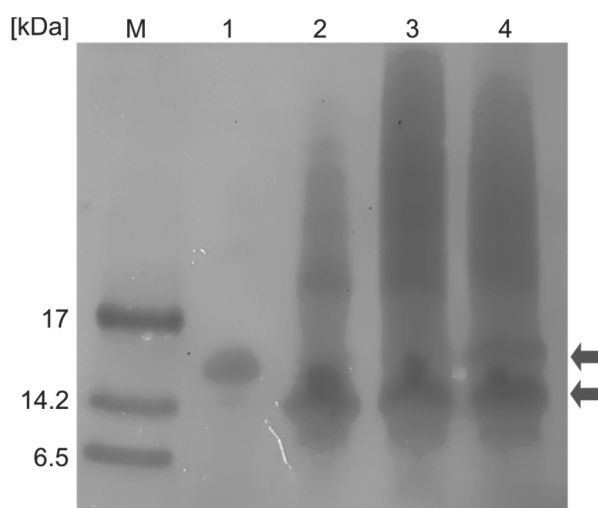


**Figure 96** Tricine-SDS-PAGE analysis of the glycosylation of RNase B-GlcNAc with the mutant ENGase Endo-CC N180H and SGP **20**. Native RNase B (1) was de-glycosylated to RNase B-GlcNAc (2) by incubation with Endo-H (theor. 29 kDa; impurities above 17 kDa). The glycosylation reaction with Endo-CC N180H in 25 mM KPi-buffer, pH 7.5 (3: 75  $\mu$ U; 4: 7.5  $\mu$ U) caused an increase in molecular weight of RNase B-GlcNAc back to approx. 15 kDa.

### 6.4.3 Transferring glycans to low molecular weight acceptors

To test the versatility of the transglycosylation method using Endo-CC N180H different acceptors were chosen for the reaction. The acceptor range of Endo-CC was described to be similar to Endo-M N175Q, therefore rendering *p*NPGlcNAc **5a** as a possible acceptor, which was the first acceptor tested in the Endo-CC N180H glycosylation reaction. After a 2 h incubation of *p*NPGlcNAc **5a** (1 mM) with commercial Endo-CC N180H (75  $\mu$ U) and the glycan donor SGP **20** (7.5 mM) at 30 °C, a new peak was detectable *via* HPLC. The conversion was determined by the peak area to be 21%. For further proof of glycosylation activity catalysed by the glycosynthase, a time conversion was measured after 0 h, 1 h, 2 h and 4 h (Figure 97). The newly formed peak was not visible after 0 h incubation and increased over the time of the incubation. Hydrolysis of the isolated product **5af** with *wt* Endo-M (ENGase of *M. hiemalis*; commercially obtained) led to the production of the starting material *p*NPGlcNAc **5a**, giving a further indication to the successful transfer of the sialyl biantennary glycan onto *p*NPGlcNAc **5a**. The mass of the peak could not be determined in definite, as the analyte concentration of the isolated product was too low. Nevertheless, as the glycan transfer catalysed by Endo-CC N180H onto *p*NPGlcNAc **5a** has been described in literature, the assumption of a successful transfer can be made.

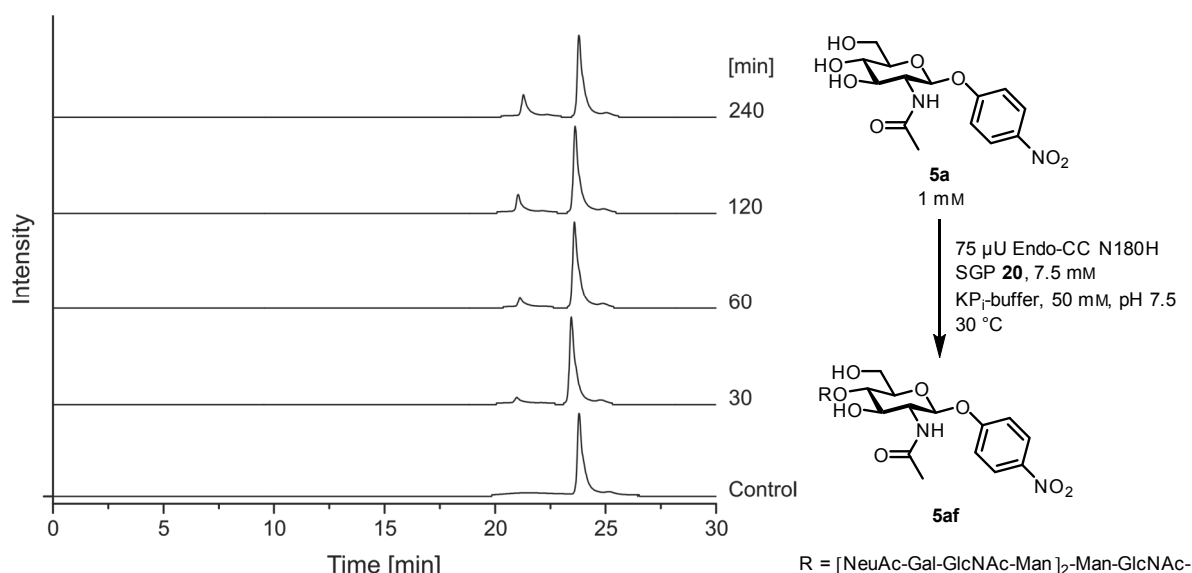


**Figure 97** Time profile of the glycan transfer catalysed by commercial Endo-CC N180H of *C. cinerea*. The enzyme (75  $\mu$ U) was incubated with *p*NPGlcNAc **5a** (1 mM) and the donor **20** (7.5 mM) for 30–240 min at 30 °C (KP<sub>i</sub>-buffer, 50 mM, pH 7.5). Product formation and substrate conversion was analysed by HPLC.

Additionally to the transfer of the sialo biantennary glycan of SGP **20** onto *p*NPGlcNAc **5a**, *Manabe et al.* also described the transfer onto acceptors such as *p*NPGlc **5h** and *p*NPMan **5b**.<sup>[134]</sup> Therefore, the transfer should also be possible for the flavonone glucoside prunin (**1b**). Incubation of the commercial Endo-CC N180H with SGP **20** and naringenin-7-*O*- $\beta$ -D-glucoside (**1b**), under identical conditions as the glycosylation of *p*NPGlcNAc **5a**, also led to a newly formed product observable by HPLC analysis. The conversion over 2 h was with 31% similar to the conversion of the *p*NPGlcNAc **5a**, which is most likely due to the identical configuration of the hydroxyl groups of the two glycosyl moieties. The acetyl group in the 2-position of *p*NPGlcNAc **5a** therefore seems to play a secondary role in the acceptor recognition of Endo-CC N180H. As expected, an incubation over 18 h increased the conversion of the acceptor **1b** to 54% (Figure 98). The peak of the possible glycosylated product was isolated via HPLC and the molecular weight was determined to be 2436 g/mol confirming the presence of the expected product **1i**. The hydrolysis of the isolated glycoside **1i** by incubation with the ENGase *wt* Endo-M also led in this case to the starting material **1b**.

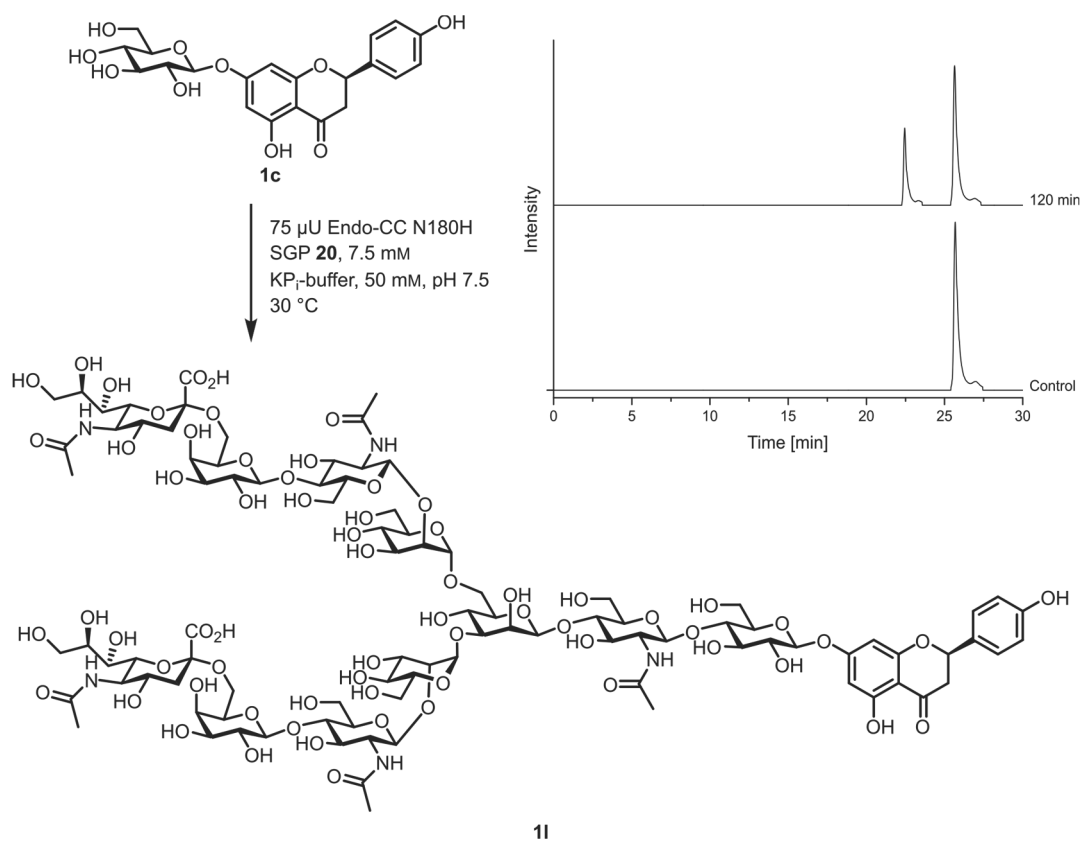


**Figure 98** Conversion of prunin (**1b**) during the glycan transfer catalysed by commercial Endo-CC N180H of *C. cinerea*. The enzyme (75  $\mu$ U) was incubated with prunin (**1b**, 1 mM) and the donor **20** (7.5 mM) for 2–18 h at 30 °C (KP<sub>i</sub>-buffer, 50 mM, pH 7.5). Product formation and substrate conversion was analysed by HPLC.

The flavonoid derivatives isoquercetin (**1h**), avicularin (**1k**) and hyperoside (**1j**) were also applied as acceptor substrates for the glycan transfer catalysed by Endo-CC N180H (Figure 99).

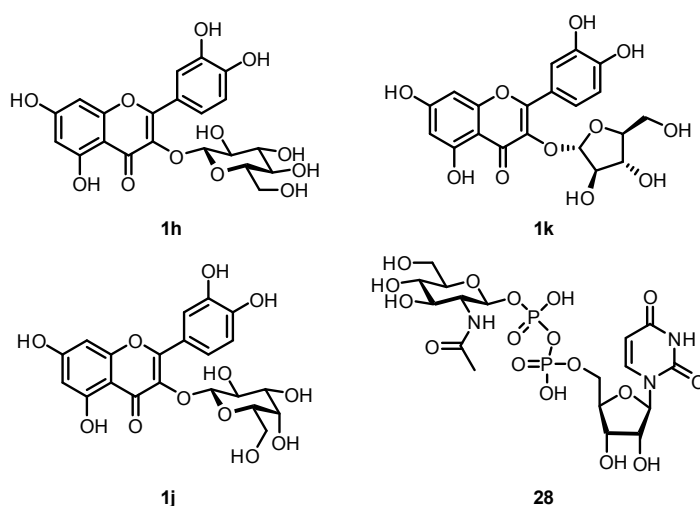


**Figure 99** Acceptor molecules tested for glycosylation catalysed by Endo-CC N180H with SGP **20** as the glycan donor. A glycosylation product was observed for isoquercetin (**1h**), but not avicularin (**1k**), hyperoside (**1j**) or UDP-GlcNAc **28**.

Only in the case of isoquercetin (**1h**) could the formation of a new product be observed by HPLC analysis. As the flavonol structure is identical in isoquercetin (**1h**) and hyperoside (**1j**) the difference in acceptance could only result from the glycoside configuration. The hydroxyl group of the C-4 atom in the glycosidic ring being in an equatorial position (compared to axial in, for example, the galactose residue of hyperoside) is prerequisite for Endo-CC N180H. Similar results were reported by *Manabe et al.* for the acceptor *p*NPGal **5g**.<sup>[134]</sup> The nucleotide sugar UDP-GlcNAc **28** was also tested as a possible acceptor substrate for Endo-CC N180H. A new product formation could not be observed by HPLC. Nevertheless, this might be due to an inadequate HPLC separation. Due to the previous results glycosylating *p*NPGlcNAc **5a** and as *N*-acetylglucosamine derivatives are usually readily accepted by ENGases, UDP-GlcNAc **28** should be a possible candidate for glycan transfer. Though the negative charges of the phosphate residues of UDP-GlcNAc **28** might cause unfavourable interactions in the active site of Endo-CC N180H and therefore render the compound not suitable as an acceptor.

#### 6.4.4 Heterologous expression of Endo-CC N180H

In order to characterise a certain enzyme fully, it is important to have access to a large amount of the respective enzyme as not to be restricted in the scope of feasible experiments. The production of Endo-CC N180H of *C. cinerea* was carried out in literature by the heterologous expression in *E. coli* BL21 CodonPlus (DE3).<sup>[132]</sup> The heterologous expression of Endo-CC N180H was tested in *E. coli* BL21(DE3) and the gene *endo-CC N180H* was therefore synthesised commercially and inserted between the NdeI and XhoI restriction sites of pET-21a(+) adding a C-terminal His<sub>6</sub>-tag to the enzyme for later purification via IMAC. After transformation of the *E. coli* strain, the expression was induced by the addition of IPTG and incubated 24 h at 25 °C (120 rpm). IMAC purification of Endo-CC N180H led to an enzyme solution with a protein concentration of  $4.2 \cdot 10^{-1} \pm 4.1 \cdot 10^{-2}$  mg/mL and SDS-analysis indicated to a protein with a calculated size of 89 kDa and a solution of high purity (Figure 100). Isolation of Endo-CC N180H from 1 g *E. coli* BL21(DE3) (cell mass; not dry) resulted in 2.1 mg isolated protein. *Eshima et al.* described the isolation of 0.1 mg *wt* Endo-CC from 250 mL *E. coli* culture after a 12 h incubation at 30 °C. These values are difficult to compare, as the cell mass or OD<sub>600</sub> values of the cell cultures from which the ENGase was isolated, were not determined by *Eshima et al.* at the point of harvest. Due to uncertain factors, such as cell growth, a direct comparison of the amount of isolated protein is therefore not possible.

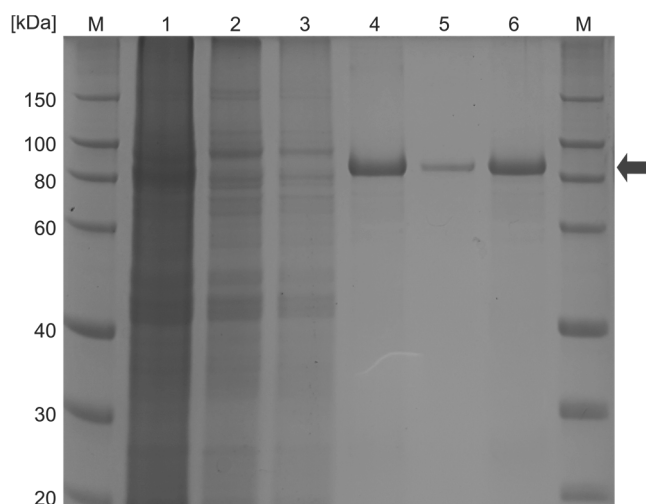


**Figure 100** Tricine-SDS-PAGE analysis of the IMAC-purification of Endo CC-N180H from *E. coli* BL21(DE3). Samples of six stages of the purification were analysed: 1 cell-free extract; 2 flow through; 3 wash-fraction; 4 elution; 5 column wash; 6 final enzyme solution (desalted, concentrated). M: RotiMark 10–150

The heterologous expressed Endo-CC N180H was examined for transglycosylation activity using commercially obtained SGP **20** and the acceptor molecules *p*NPGlc **5h**, *p*NPGlcNAc **5a**, and prunin (**1b**). The glycan donor **20** (7.5 mM) was applied in a 7.5× excess with respect to the acceptor compound **5h**, **5a** and **1b** (1 mM) and incubated at 30 °C for 18 h (Figure 101). A yellow colouration of the reaction solution containing the acceptors **5h** and **5a** after the deactivation of Endo-CC N180H (100 °C, 3 min), indicated to a release of *p*-nitrophenol (**13b**) by hydrolysis of the *p*-nitrophenyl glycosides. The temperature of the deactivation process was therefore lowered to 80 °C to avoid product degradation. Transglycosylation activity was detected via liquid chromatography coupled mass spectroscopy (LC/MS) measurements for the acceptors **5h** and **5a** by detection of the expected product mass peaks 1152.4 ( $M + 2H / 2$ ) and 1172 ( $M + 2H / 2$ ) respectively. A product for the glycosylation of prunin (**1b**) could not be detected *via* the LC/MS method. Nevertheless, this result is most probably attributed to the analytical method, as the possibility of glycosylation of prunin (**1b**) was confirmed applying the commercially available Endo-CC N180H. The obtained results therefore confirm the possibility of heterologous expression of active Endo-CC N180H in *E. coli* BL21(DE3).

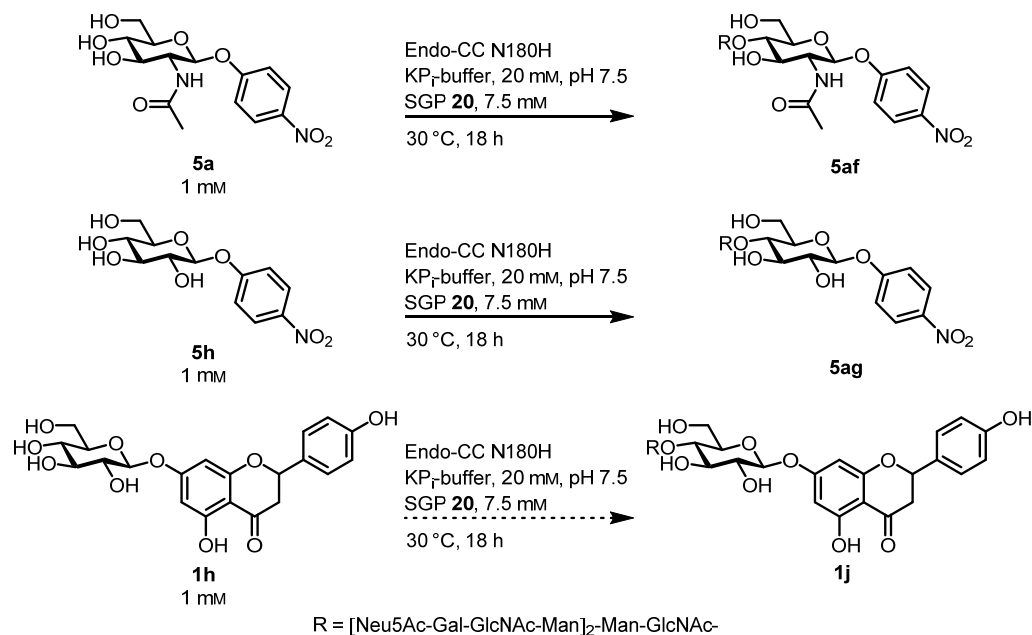


**Figure 101** Glycan transfer reactions catalysed by, in *E. coli* BL21(DE3) heterologous expressed, Endo-CC N180H of *C. cinerea*. The enzyme (0.21 mg/mL) was incubated with the respective acceptor **5a**, **5h** and **1b** (1 mM) and donor **20** (7.5 mM) for 18 h at 30 °C (KP<sub>i</sub>-buffer, 20 mM, pH 7.5). Product formation was analysed by LC/MS measurement.

#### Chapter synopsis:

- The transfer of the sialo biantennary glycan of SGP **20** catalysed by commercially obtained Endo-CC N180H was successfully demonstrated for RNase B-GlcNAc, pNPGlcNAc **5a** and naringenin-7-O-β-D-glucoside (**1b**).
- The acceptor scope of Endo-CC N180H was tested towards isoquercetin (**1h**), hyperoside (**1j**), and avicularin (**1k**).
- Active Endo-CC N180H was expressed in *E. coli* BL21(DE3) and tested for the glycan transfer onto pNPGlc **5h**, pNPGlcNAc **5a**, and naringenin-7-O-β-D-glucoside (**1b**) with SGP **20** as the glycan donor.

## 7 SUMMARY AND OUTLOOK

The biocatalytic synthesis of glycosides by application of glycosynthases has many advantages over chemical synthesis, but also numerous challenges, which still need to be addressed in order to turn this synthetic approach into a universal method. The results obtained during the work of this thesis highlighted various aspects not only of the glycosynthase-catalysed reaction but also of the process of transforming a glycosidase into a glycosynthase.

### Application of extremophilic glycosidases as glycosynthase candidates

The influence of temperature on glycosynthetic reactions by applying mutated glycosidases with hyperthermophilic, mesophilic, and psychrophilic properties was examined in detail. The mesophilic  $\beta$ -glucosidase mutant Abg-E358S acted, not only as an example of a mesophilic glycosynthase, but also as a positive control as this variant was literature known to possess glycosynthetic activity. The synthetic activity was demonstrated by the glycosylation of *p*NPGlc **5h** and the naringenin-7-O- $\beta$ -D-glucoside (**1b**, Figure 102). As has been described in literature, the enzyme did not only catalyse a single glycosylation, but in both cases led to oligomeric products.<sup>[21]</sup> Beside the repeated glycosylation of the produced product, the self-coupling of the donor  $\alpha$ -GlcF **2a**, producing  $\alpha$ -D-cellobiosyl and  $\alpha$ -D-cellotriosyl fluoride (**2m** and **2n**) as undesired side products, was observed.

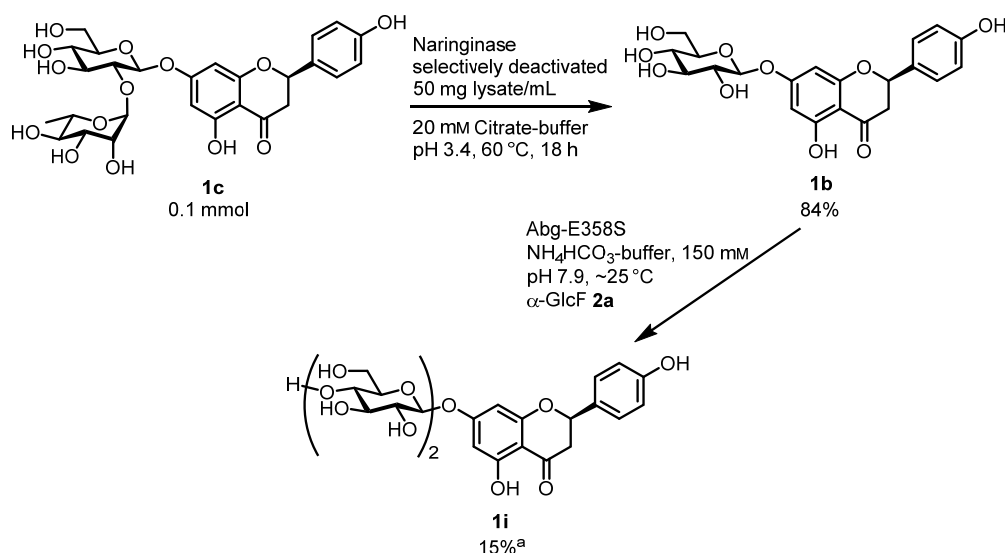


**Figure 102** Glycodiversification of the flavonoid naringin (**1c**). The rhamnoside was cleaved by the deactivated form of the naringinase of *P. decumbens*. Subsequently, the glucoside **1b** was glycosylated by the  $\beta$ -glucosynthase Abg-E358S. <sup>a</sup> Yield of the acetylated derivative of **1i**.

An elevated temperature proved unsuitable for glycosynthetic reactions utilising glycosyl fluoride donors. In literature, thermophilic enzymes have been applied as glycosynthases, but mostly by employing the *in situ* production of the glycosyl donor by chemical recovery.<sup>[23, 74, 172]</sup>

The application of a hyperthermophilic enzyme was attempted in this thesis with mutants of the putative  $\beta$ -galactosidase BglC, which was provided by the group of Prof. *Elling* (RWTH Aachen). Analysis of the glycosidases amino acid sequence with glycosidases of the respective glycohydrolase family (GH 35) led to the determination of potential catalytic residues, which were mutated by *QuikChange*<sup>TM</sup>-PCR. No glycosynthetic activity could be detected for the generated variants of BglC and a general unsuitability of high temperatures for glycosynthetic reactions was determined as thermal degradation of the glycosyl fluoride donor dominated the reaction. A further analysis of the sequence of BglC with the  $\beta$ -glucosaminidases GImA<sub>Tk</sub> and GImA<sub>Ph</sub> revealed a high similarity of BglC to this type of enzyme and a most likely miss-identification of the catalytic residue, which might explain the absence of glycosynthetic activity by the tested BglC variants. Nevertheless, the high thermal degradation of the glycosyl donor at high reaction temperatures would still lead to diminished yields and BglC was therefore not further considered as a glycosynthase candidate.

The unsuitability of elevated temperatures turned the focus towards low and moderate temperatures for the glycosynthetic reaction in order to minimalise glycosyl fluoride hydrolysis. The psychrophilic glucosidase BglU of *M. antarcticus* was therefore characterised and the catalytic residue mutated with the aim of producing a cold-adapted  $\beta$ -glycosynthase. The *wt* enzyme exhibited generally a much lower hydrolytic activity than the mesophilic glucosidase Abg. Mutation of the nucleophilic residue by *QuikChange*<sup>TM</sup>-PCR and  $\beta$ -glucosidase activity screening via esculin-agar resulted in the identification of the glycosynthetic active variant BglU-E377A, which transferred the glucosyl donor onto glycosidic acceptors producing a  $\beta$ -1,4 linkage. Similar to the *wt*, the glycosynthase BglU-E377A exhibited a lower synthetic activity than the mesophilic Abg-E354S and despite the lower activity, a repeated glycosylation of the product similar to the reaction catalysed by Abg-E358S was observed.

The  $\beta$ -glycosynthase BglU-E377A is to the best of our knowledge the first glycosynthase derived from a cold-adapted glucosidase. Nevertheless, the low activity of the generated glycosynthase limited the application of the enzyme for synthetic purposes. Characterisation of the substrate scope of BglU-E377A proved difficult most likely due to the low reaction rate of the glycosynthase. In order to make this glucosynthase synthetically useful, an increase of the catalytic activity of the enzyme would be required. Observations described by *Miao et al.* (mentioned in section 5.2.2), examining the effect of certain amino acid residues and the long L3-loop structure on the cold-adapted activity of BglU, could contribute greatly to this goal.<sup>[83, 173]</sup> While deletion of the flexible L3-loop caused a loss of the low-temperature activity for BglU, the exchange of H299 with tyrosine, found most commonly in this position in meso- and thermophilic glucosidases, increased the catalytic activity, thermostability and

optimal temperature (Figure 103). The combination of the E377A mutation, giving the desired glycosynthase activity, with the H299Y mutation might increase the activity of the glycosynthase as observed for the *wt* glycosidase. *Miao et al.* postulated the activation being caused by the interaction of the tyrosine hydroxyl group (H299Y) with the backbone of H331. This interaction on the one hand, stabilises the conformation of the catalytic pocket and on the other, cuts off an essential water chain usually ranging from the surface of BglU into the catalytic pocket by interaction with the H299 residue. The BglU-H299Y mutant exhibited a 3.4× higher hydrolytic activity (*wt*:  $k_{\text{cat}} = 6.7 \cdot 10^3 \text{ s}^{-1}$ ; H299Y:  $k_{\text{cat}} = 22.6 \cdot 10^3 \text{ s}^{-1}$ ) and a higher affinity to the substrate *p*NPGlc **5h** (*wt*:  $K_{\text{M}} = 5.9 \text{ M}$ ; H299Y:  $K_{\text{M}} = 3.9 \text{ M}$ ) at 25 °C. This stabilising effect could also be beneficial for the glycosynthases activity.

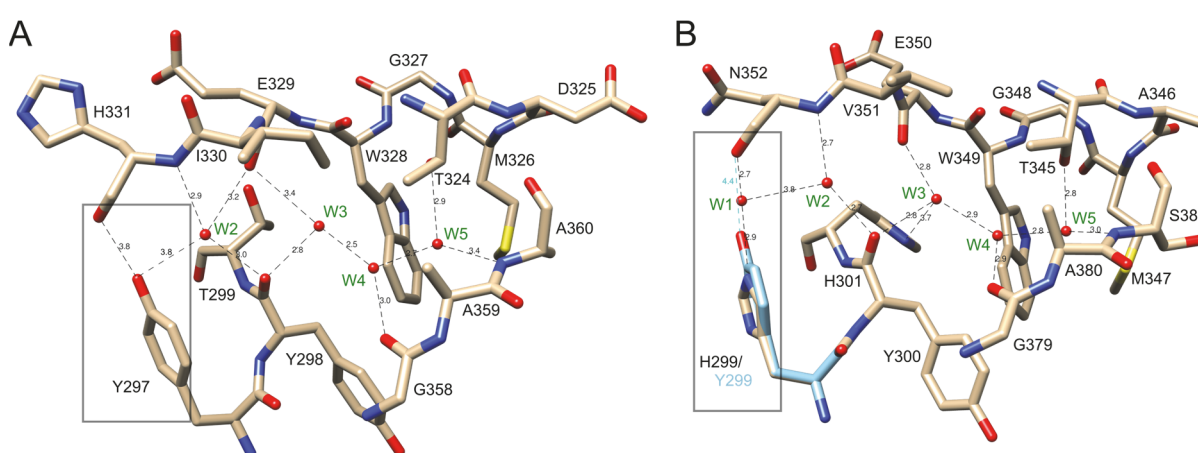


**Figure 103** Structural comparison of the function of Y297 in the mesophilic glucosidase BglB (*Paenibacillus polymyxa*) and the corresponding residue H299 in the cold-adapted glucosidase BglU (*M. antarcticus*). **(A)** The hydroxyl group of Y297 in BglB interacts with the backbone of H331, exhibiting a stabilising effect on the catalytic pocket and cutting off the water chain (W2–W5) from the surface of the enzyme. **(B)** The H299 residue of BglU interacts with a water molecule belonging to a hydrogen bond network reaching from the surface into the catalytic pocket. Introduction of H299Y in BglU could also lead to a displacement of W1 and result in a stabilising effect, increasing activity and thermostability (depicted in blue, **B**).

While an increase in glycosynthetic activity is desirable for an efficient synthesis of glycosides, the increased activity will also cause a disadvantage in the form of glycoside product mixtures due to repeated glycosylation. This is in general a drawback in particular for glycosynthases as the produced glycoside can act as a new acceptor for the enzyme. In literature, repeated glycosylation catalysed by glycosynthases is avoided by applying  $\alpha$ -D-galactopyranosyl fluoride (**2b**), which after transferral is not recognised as an acceptor by the enzyme.<sup>[21]</sup> This solution is effective if the type of glycosylation in the product is not essential, but ineffective if a glycosylation is the desired. A solution possibly enabling mono-glycosylation could be the application of glycosynthases in a flow-reactor set up. The immobilisation of the glycosynthase to a stationary phase in a reactor column would allow the removal of the product from the enzyme after catalysing the first glycosylation reaction in a simple flow system (Figure 104). The degree of glycosylation might even be adjustable by employing different flow rates through

the reactor column and variation of the donor:acceptor ratios in the mobile phase. Most recently, *Haneda et al.* demonstrated the application of the glycosynthase Endo-M N175Q immobilised on *N*-hydroxysuccinimide-activated sepharose resin in a microbioreactor for the production of neo-glycoconjugates.<sup>[174]</sup> The transferral of the oxazoline derivative of the sialo complex-type glycoside onto *N*-Fmoc-*N*-acetylglucosaminyl-L-aprarginine was successfully demonstrated with this method. This is, up to date, the only example in literature of an immobilised glycosynthase for synthetic uses. However, immobilisation and flow reactors have been successfully applied for transglycosylation reactions producing lactulose and  $\beta$ -glucosylglycerol using the thermophilic  $\beta$ -glycosidase CelB of *P. furiosus*, demonstrating the high potential of continuous flow reactors for reaction time sensitive reactions.<sup>[175, 176]</sup>

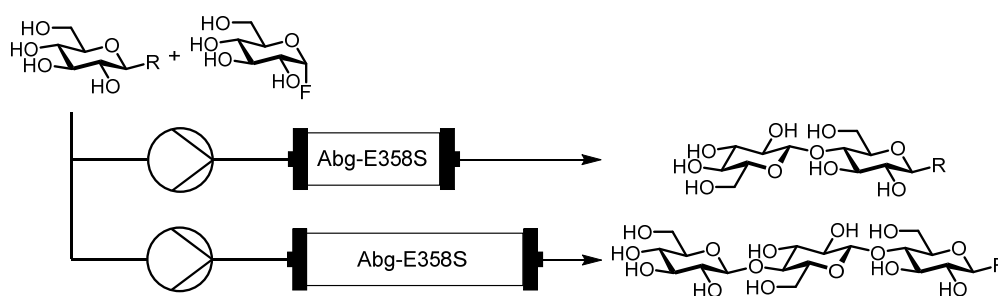


**Figure 104** Immobilisation of glucosynthases and application in continuous flow-reactors could improve the control of repeated glycosylation of the produced product by ensuring removal of the product from the enzyme reactor. Length of the reactor column or the flow rate could be variable parameters to influence the enzymatic glycosylation.

Despite the unsuitability of the hyperthermophilic  $\beta$ -glycosidase BglC as a  $\beta$ -glucosynthase, due to the high temperature dependency and low activity towards glucoside substrates, a characterisation and verification of the natural function of BglC would be of great interest. The high sequential similarity of BglC to GlmA<sub>TK/Ph</sub> indicates strongly in the direction of a  $\beta$ -glucosaminidase, which could easily be confirmed by testing the activity of BglC towards *p*-nitrophenyl  $\beta$ -D-glucosaminide or other glucosaminide derivatives. The high temperature dependency of the hydrolytic activity of BglC might then be cancelled out, should the activity towards glucosaminide compounds be much higher than the activity towards glucosides (as observed for GlmA<sub>TK</sub> and GlmA<sub>Ph</sub>). A decrease of the temperature dependency would reintroduce the possibility of applying BglC as a glycosynthase, serving as a new biocatalytic synthesis route towards glycosaminoglycans. The diverse structures of glycosaminoglycans, encompassing polymers such as hyaluronan, dermatan sulfate, and heparan sulfate are of high pharmaceutical interest due to their diverse biological activities, especially concerning carcinogenesis.<sup>[177, 178]</sup> The enzymatic synthesis of glycosaminoglycans has mostly been carried out by transglycosylation, applying  $\beta$ -*N*-acetylhexosaminidases or hyaluronidases with *p*-nitrophenyl glucosaminide or oxazoline derivatives as glycosyl donors.<sup>[179-183]</sup> A synthetic approach towards glycosaminoglycans by a glycosynthase has yet only been described by

Müllegger *et al.*<sup>[184]</sup> by transferring  $\alpha$ -D-glucuronyl fluoride onto various glycoside acceptors catalysed by a mutant variant of the thermostable  $\beta$ -glucuronidase (TMGUA-E476A) of *T. maritima*. A glycosynthase derived from BglC transferring the glucosamine moiety towards the synthesis of a glycosaminoglycan would complement the synthesis approach of Müllegger *et al.* well.

### Colourimetric glycosynthase activity assay

Following the method of Andrés *et al.*, a modification of the glycosynthase activity assay, exploiting the capability of fluoride to cleave silyl ether bonds, was developed shortening the assay time and increasing the maximal detection limit greatly (Figure 105).<sup>[1]</sup> The use of TIPSpNP **23** in acetonitrile for the quantification of fluoride ions, released by conversion of the glycosyl fluoride donor, enabled the measurement of glycosynthase activity and the determination of the conversion during synthetic reactions within the short time of 10 min. Despite the use of a less sensitive absorption assay instead of a fluorescence probe, the quantitation limit (LOQ) is only slightly higher, thereby still allowing reliable detection of low fluoride concentrations. The increased detection maximum, which is vital for determination of kinetic parameters, for which high substrate concentrations are required, broadened the applicability of the method towards biochemical characterisation of glycosynthases.

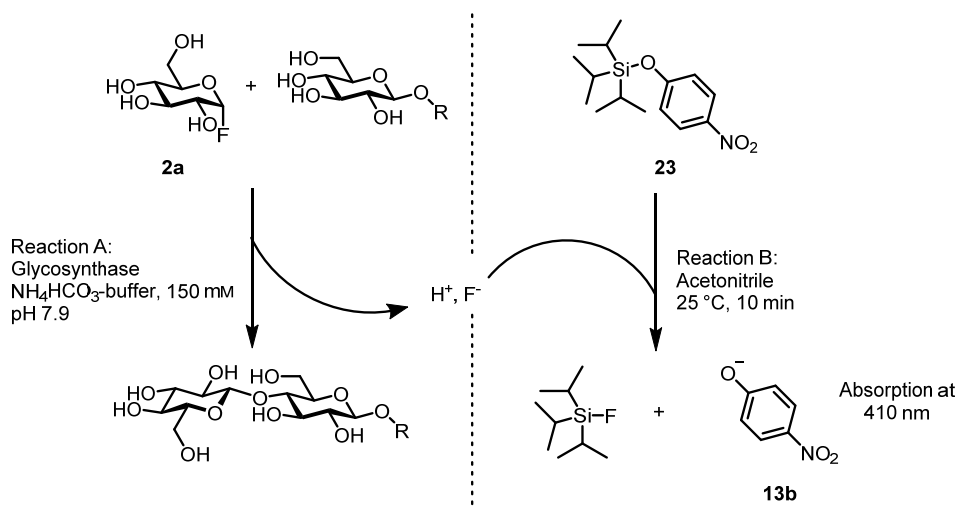


**Figure 105** Reaction mechanism of the developed glycosynthase activity assay. The enzymatic glycosylation is catalysed in reaction A by the  $\alpha/\beta$ -glycosynthase releasing hydrogen fluoride as a side product. A sample of the reaction is then transferred into acetonitrile containing 1 mM TIPSpNP **23** initiating the cleavage of the silyl ether as reaction B. A quantification of the enzymatically released fluoride can then occur by photometric measurements of the released pNP **13b** at 410 nm.

The developed assay allowed the characterisation of glycosynthases in a fast and efficient microtiter plate format, omitting the need of lengthy ion-selective electrode analyses. The application of the assay was demonstrated by the determination of the conversion of the glycosyl fluoride donor, kinetic measurements, substrate scope, and optimal acceptor : donor

ratio of the glycosynthases Abg-E358S and BglU-E377A. Both the development and application of the assay was successfully published.<sup>[2]</sup> The utilisation of the assay could also be broadened from the characterisation of glycosynthase properties to the identification or improvement of glycosynthases in mutagenesis libraries. The high-throughput microplate format also has high potential in automated screening processes. Therefore, the quantification of the fluoride concentration being separate from the enzymatic reaction would bring the advantage of allowing subsequent analysis of the reaction by HPLC or multiplex capillary electrophoresis after identifying positive hits in a mutant library.

### Glycosylation of phenolic compounds by Cbg1

Due to the limitation of the substrate spectrum of the examined glycosynthases, glycosylating only glycosidic acceptor molecules, a substrate-based approach of glycosynthase candidate identification was carried out. By analysis of the secondary metabolic pathways of *R. radiobacter* the coniferin-specific  $\beta$ -glucosidase Cbg1 was identified as a glycosynthase candidate, which could potentially glycosylate phenolic compounds. Cbg1 was successfully heterologously expressed, and characterised with respect to its kinetic properties and substrate scope. Structural analysis identified the catalytic residues D222 and D559 as the nucleophilic and acid/base residue respectively. The mutants Cbg1-D222A, -D222S, and D222C were created by *round the horn*-PCR mutagenesis and tested for glycosynthetic activity. As none of these variants showed glycosynthetic activity, but low hydrolysis of the glycosyl fluoride donor, a further structural examination was conducted. The mutant library of Cbg1 was therefore expanded by Cbg1-D559A/S/C, -Y190F, -Y190F D222A, and -H144A variants. Each mutant was examined for hydrolytic activity and glycosynthase activity utilising a glycosyl fluoride donor or the chemical recovery method. In regard to the hydrolysis, the mutants Cbg1-D222S and -H144A exhibited much higher hydrolytic activity (3.6 $\times$  and 20 $\times$ , respectively) than the *wt* form. A chemical recovery of *p*NPGlc **5h** cleavage was only observed for the mutant variants of the D559 position.  $\beta$ -D-Glucopyranosyl azide (**16c**) was identified as the product of the chemical recovery reaction catalysed by Cbg1-D559A with *p*NPGlc (**5h**) and sodium azide. The production of this compound verified the position D559 as the acid/base catalyst in Cbg1. As the glycosynthetic activity was not yet observed, transglycosylations following the experiments of *Watt et al.* were attempted applying phenolic compounds. Successful transglycosylation was only observed for the aliphatic alcohol *n*-butanol (**15a**), even though the phenolic alcohols showed an activating effect on *wt* Cbg1 and various mutant variants similar to the transglycosylation onto *n*-butanol (**15a**).

Despite not having identified a mutant variant of Cbg1 with glycosynthase activity, there is much potential for application of Cbg1 in glycoside synthesis. The various mutant variants of

Cbg1 showed very different effects on the enzymes activity and could prove synthetically useful. The mutation of the acid/base catalyst D559 enabled the single step synthesis of  $\beta$ -D-glucopyranosyl azide (**16c**) by chemical recovery using sodium azide from a commercially available starting material *p*NPGlc **5h** (Figure 106). This synthesis avoids the longer chemical procedure encompassing acetylation, bromination, and substitution of the halide by an azide ion or the use of hypervalent silicate intermediates and occurs with complete anomeric control.<sup>[162, 185]</sup> This glycosyl azide can be applied as a building block for the synthesis of  $\beta$ -glucopyranosyl triazols in a Cu<sup>I</sup>-catalysed azide alkyne 1,3-dipolar cycloaddition ('click chemistry').<sup>[186, 187]</sup> These structures have been shown to possess interesting glucosidase inhibitory properties. Starting from the glycosyl azide, the synthesis of amide-linked *N*-glycosides by Staudinger-aza-Wittig chemistry or the respective glycosylamines by reduction of the azide are possible. Furthermore, considering the substrate scope of wt Cbg1, an array of glycosyl azides may possibly be synthesised by the mutant variant Cbg1-D559A.

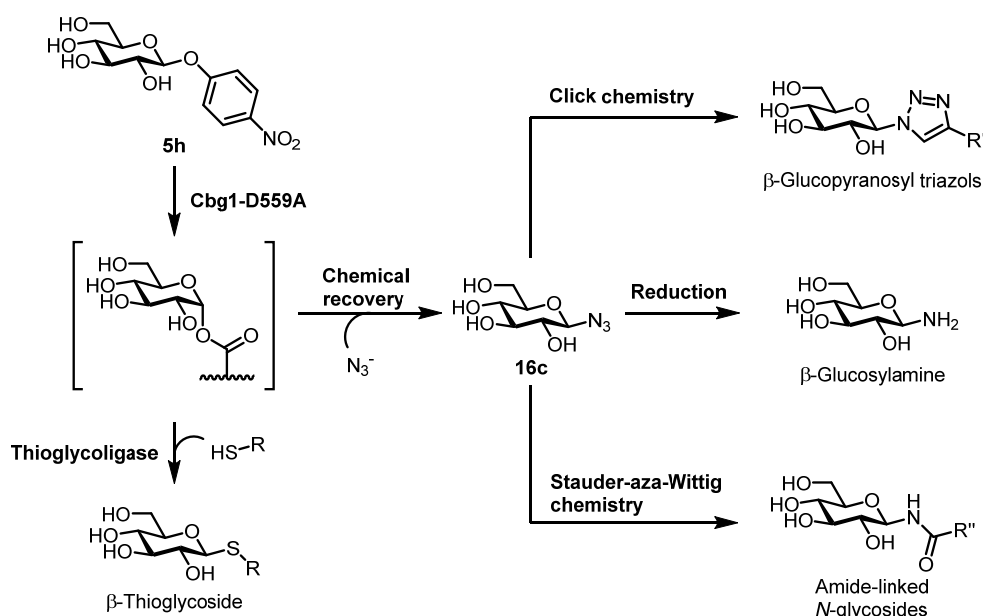


**Figure 106** Possible synthetic applications of the generated variant Cbg1-D559A. The glycosyl-enzyme-intermediate, formed during the cleavage of *p*NPGlc **5h**, can be cleaved by an external nucleophile such as a thiol (acting as a thioglycoligase) resulting in a  $\beta$ -thioglycoside or by an azide ion producing  $\beta$ -glucopyranosyl azide (**16c**).<sup>[161]</sup> This product can be utilised as a building block for the synthesis of  $\beta$ -glycopyranosyl triazols (click chemistry),  $\beta$ -glycosylamines (reduction), or amide-linked *N*-glycosides (Stauder-aza-Wittig chemistry).<sup>[162, 186, 187]</sup>

By utilising the same reaction mechanism, Cbg1-D559A could also be applied as a thioglycoligase for the synthesis of  $\beta$ -thioglycosides by adding thiols as acceptors instead of sodium azide.<sup>[161, 188]</sup> When utilising a deoxythio sugar acceptor, the regioselectivity of the produced glycosidic linkage can be influenced by the position of the thiol group in the acceptor. The increased activity by mutation of the position H144A could also be exploited for synthetic purposes in different ways. In the case of the single mutation, the strong activation in the presence of an alcohol acceptor, which is higher than the activation of the *wt* enzyme, indicates

to an increased potential of synthesis by transglycosylation. Nevertheless, due to the increased activity of the variant, reaction control will be critical in order to avoid low yields by hydrolysis of the produced glycoside. Of great interest would be the combination of the H144A mutation with a further mutation such as D559A. The activation of the enzymes activity by the mutation H144A might also occur for Cbg1-D559A, possibly resulting in a double mutated variant Cbg1-H144A D559A with increased synthetic potential towards glycosyl azides or thioglycoligase activity.

### Transforming RhaB into a glycosynthase

The transformation of a  $\alpha$ -L-rhamnosidase into a glycosynthase has not yet been described in literature and therefore, the conversion of the  $\alpha$ -L-rhamnosidase RhaB of *Bacillus* sp. GL1 was attempted, by applying the strategy of an *in situ* production and transfer of the  $\beta$ -glycosyl azide donor as demonstrated by *Cobucci-Ponzano et al.* for  $\alpha$ -fucosynthases.<sup>[98]</sup> The substrates, *p*-nitrophenyl rhamnopyranoside (**5r**) and 2-chloro-4-nitrophenyl rhamnopyranoside (**5ae**), required for enzyme characterisation and glycosynthase development were synthesised successfully and applied in activity and chemical recovery experiments.  $\beta$ -L-Rhamnopyranosyl azide (**16d**) was successfully synthesised by conversion of the pyranosyl halide **22u** with  $\text{NaN}_3$  in HMPA. The compound **16d** was employed as a reference molecule and potential donor substrate for rhamnosynthase candidates. The *wt* RhaB of *Bacillus* sp. GL1 was expressed and characterised for kinetic parameters and substrate scope, which revealed a high specificity towards rhamnosides and none of the other examined glycosides. The enzyme exhibited a high tolerance towards DMSO as a co-solvent but additives such as HMPA,  $\text{NaN}_3$ , and glucose (**11b**) inhibited the rhamnosidase when present in high concentrations. In addition to the six mutant variants of RhaB created by *Kamila Morka*, RhaB-D567G/S, -E572G/S, -E841G/S, four further mutant variants RhaB-E567C/N, -E579Q, and -E841A were produced by *round the horn*-PCR. The mutant variants of RhaB were tested for hydrolytic activity, examined for regained activity by chemical recovery, and glycosynthetic activity, applying glucose (**11b**) as an acceptor molecule. Mutant variants of the position D572 were excluded as potential glycosynthases due to the retained hydrolytic activity. Mutants of the positions E841 and D567, on the other hand, recovered activity in the presence of an external nucleophile, but the formation of  $\beta$ -L-rhamnopyranosyl azide (**16d**) was not detected by  $^1\text{H-NMR}$  or IR analysis. A colourimetric detection assay for azide ions by acidic ferric solution was adapted for a microplate format and applied for the identification of glycosynthetic activity of RhaB mutant variants. The assay allowed the distinction between free and bound azide molecules, yet the relative high deviations during azide quantification for enzymatic conversions indicates to the requirement of further optimisation.

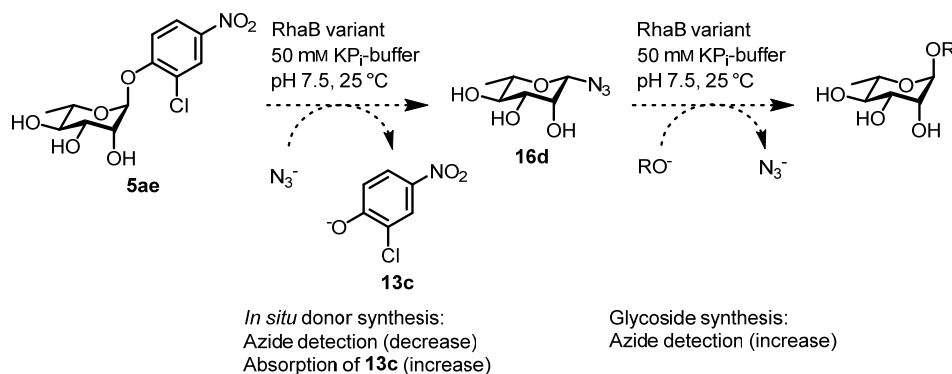


**Figure 107** Reaction scheme and detection methods for the characterisation of an  $\alpha$ -L-rhamnosynthase by applying the chemical recovery method. The  $\beta$ -rhamnopyranosyl azide (**16d**) is synthesised *in situ* by addition of the external nucleophile sodium azide and subsequently transferred to an acceptor molecule. The *in situ* donor synthesis can be detected either by the decrease of the azide concentration or by the increase of absorption at 410 nm (release of **13c**). Rhamnosylation can then be detected by the release of azide.

Although the protein structure of RhaB has been elucidated, the absence of a clearly defined reaction mechanism is the main challenge for transforming this particular glycosidase into its glycosynthase counterpart. The instability issues of the  $\beta$ -glycosyl fluoride donor can be overcome by the application of the respective glycosyl azides, yet a general approach for mutation of the inverting glycosidase can still not be described. Acquisition of further mutant variants of the residues potentially involved in the enzymatic catalysis and their characterisation would give more insight into the glycoside hydrolysis and contribute to glycosynthase production. Further analysis of the rhamnoside cleavage by RhaB-E841 and -D567 mutants observed in the chemical recovery experiments with sodium azide is also required. The cleavage occurring only in the presence of azide ions, yet absence of a cleavage product containing the external nucleophile indicates to an undescribed catalytic mechanism. Elucidation of this hydrolytic mechanism could be key to optimising the rhamnosidase towards glycosynthetic activity. Nevertheless, should further examination of RhaB variants not lead to glycosynthase activity, the rhamnosidase could alternatively be considered for rhamnoside synthesis by transglycosylation or reverse hydrolysis. *De Winter et al.* and *Ge et al.* both successfully demonstrated the use of fungal rhamnosidases towards the synthesis of phenolic rhamnosides and rhamnosyl mannitol by the reverse hydrolysis approach, which could also be attempted using the *wt* RhaB.<sup>[107, 189]</sup>

### Glycan transfer by Endo-CC N180H

The transfer of larger glycans catalysed by glycosynthases was enabled by the introduction of mutant *endo*- $\beta$ -*N*-acetylglucosaminidases (ENGases) exhibiting glycosynthase like activity. In cooperation with the group of Prof. *Fujiyama* the synthetic potential of the glycosynthase variant of Endo-CC N180H of *C. cinerea* for the diversification of flavonoids was evaluated. The transfer of the sialo biantennary glycan of SGP **20** catalysed by commercially obtained

Endo-CC N180H was successfully demonstrated for RNase B-GlcNAc, *p*NPGlcNAc **5a** and naringenin-7-*O*- $\beta$ -D-glucoside (**1b**), which demonstrates the large scope of possible glycosides acting as an acceptor for Endo-CC N180H. The acceptor scope was further tested towards the flavonoids isoquercetin (**1h**), hyperoside (**1j**), and avicularin (**1k**), revealing the limitation of the acceptor scope lying in the glycoside (glucoside vs. galactoside) rather than the aglycone of the acceptor. Similar observations were made by *Manabe et al.*, also transferring the glycan of SGP **20** to the anti-CCR4 antibody.<sup>[134]</sup> Active Endo-CC N180H was also expressed in *E. coli* BL21(DE3) and tested for the glycan transfer onto *p*NPGlc **5h**, *p*NPGlcNAc **5a**, and naringenin-7-*O*- $\beta$ -D-glucoside (**1b**) with SGP **20** as the glycan donor.

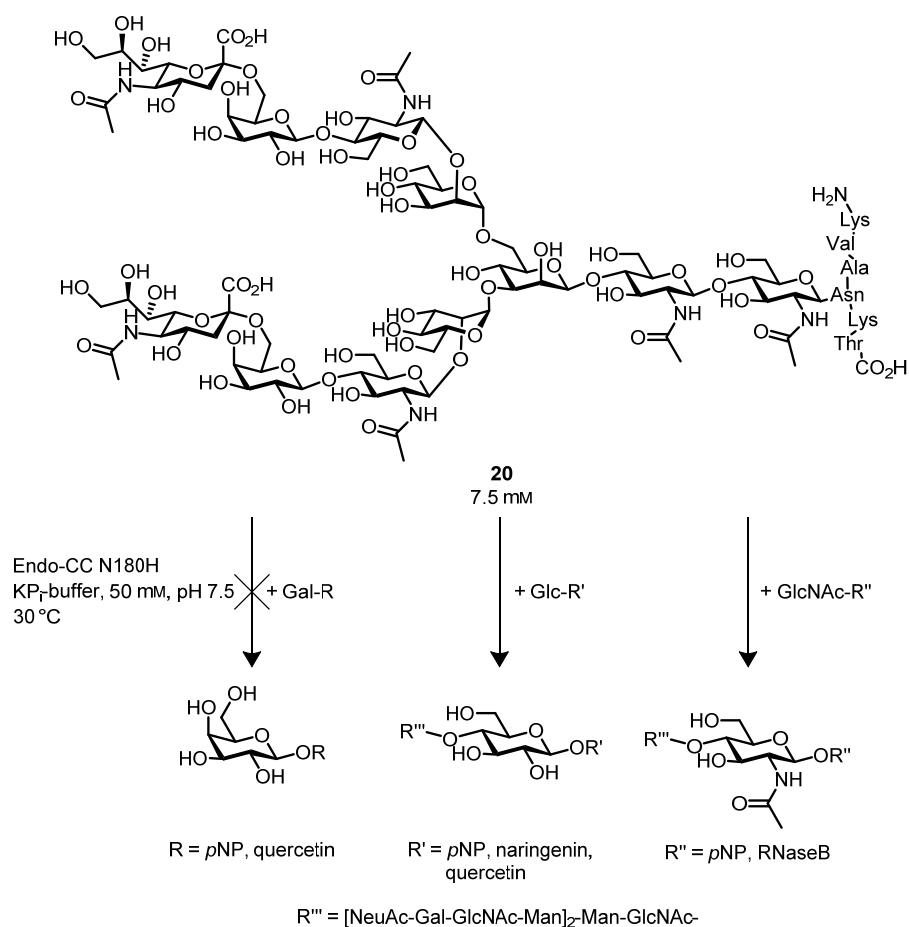


**Figure 108** Overview of the examined glycosylation reactions catalysed by Endo-CC N180H. The sialo biantennary glycan was transferred from SGP (**20**) onto different glucosides and *N*-acetyl glucosaminides. Galactosides were not accepted by the enzyme as acceptor molecules.

The results obtained during this thesis demonstrate the high potential of Endo-CC N180H in the synthesis of new glycosides with large glycan structures. The transfer of the glycan of SGP **20** onto the flavonoids naringenin-7-*O*- $\beta$ -D-glucoside (**1b**) and isoquercetin (**1h**) reveals a new possibility of glycodiversification of flavonoid glycosides. Depending on the scope of the glycan donor structure of Endo-CC N180H, which has not yet been fully described, the biological activity and pharmacokinetics of flavonoids could be tailored by adding the required glycan to the flavonoid by glycosynthase catalysis. The high cost of commercially available

---

SGP **20**, limits the possibility of up-scaling of the reaction. Nevertheless, this limitation can be circumvented by extraction of the glycan from cost efficient sources such as egg yolk powder.<sup>[170, 190, 191]</sup> Endo-CC N180H could also be similarly applied for the production of neo-glycoconjugates as was demonstrated by *Haneda et al.* immobilising the glycosynthase Endo-M-N175Q in a microbioreactor.<sup>[174]</sup> The capability of Endo-CC N180H in transferral of glycans to large protein structures will be highly advantageous for the production of homogeneously glycosylated biopharmaceuticals and biosimilars. The use of this glycosynthase in the modification of the post-translational glycosylation will help to understand the functional role of relevant glycans and facilitate the maintenance of biopharmaceutical and biosimilar quality and safety.

## 8 EXPERIMENTAL SECTION

### 8.1 General

#### 8.1.1 Devices

Devices used for biochemical, molecular, and microbiological methods are listed in Table 14. An overview of the devices used for the chemical analysis of synthetic reaction products can be found in section 8.6.

**Table 14** Overview of the utilised devices.

Device	Description	Producer
Electrophoresis	300 V Power source <i>Mini-Protean® Tetra System</i> <i>Agarose gel chambers</i>	<i>VWR International GmbH</i> , Darmstadt, Germany <i>Bio-Rad Laboratories GmbH</i> , Munich, Germany <i>peqLab Biotechnology</i>
Gel documentation	<i>INTAS GeliX Imager</i>	<i>INTAS Science Imaging Instruments GmbH</i> , Göttingen, Germany
Photometer	<i>NanoDrop 2000c</i> <i>UV-1800</i> (cuvettes), tempered	<i>Thermo Fisher Scientific</i> , Waltham, MA, USA <i>Shimadzu</i> , Duisburg, Germany
Photometer/Fluorometer for microplates	<i>Infinite® M1000Pro</i>	<i>TECAN Trading AG</i> , Männedorf, Switzerland
pH-Meter	pH-Meter 766 combined with electrode <i>IJ44C</i>	<i>Calimetic Knick Nordantec GmbH</i> , Bremerhafen, Germany
Pipettes	<i>Eppendorf Research</i> , 0.1–2.5 µL <i>Eppendorf Research</i> , 1–10 µL <i>Eppendorf Research</i> , 10–100 µL <i>Eppendorf Research</i> , 100–1000 µL <i>Gilson Pipetman</i> , 0.5–5mL	<i>Eppendorf AG</i> , Hamburg, Germany  <i>Gilson</i> , Middleton, WI, USA
Peristaltic pump	Peristaltic pump P-1	<i>Pharmacia Fine Chemicals</i> , now <i>Pharmacia &amp; Upjohn</i> , Uppsala, Sweden
Rotatory evaporator	<i>Rotavapor R-205</i> combined with <i>B-490 Waterbath</i>	<i>Büchi Labortechnik GmbH</i> , Essen, Germany
Thermocycler	<i>Biometra TProfessional Basic Gradient</i> <i>VWR Doppio</i>	<i>Analytik Jena AG</i> , Jena, Germany <i>VWR International GmbH</i> , Darmstadt, Germany
Ultrasonic bath	<i>Sonorex RK 100H</i>	<i>Bandelin electronic GmbH</i> , Berlin, Germany
UV-light	254/366 nm UV-light	<i>Camag</i> , Muttenz, Switzerland
Scales	ME253S LA1200S	<i>Satorius AG</i> , Göttingen, Germany
Cell lysis equipment	Sonoplus	<i>Bandelin electronic GmbH</i> , Berlin, Germany

Centrifuges	<i>Eppendorf Centrifuge 5424R</i> , cooled with fixed angle rotor (reaction vessels 1.5 mL, 2 mL)	<i>Eppendorf AG</i> , Hamburg, Germany
	<i>Eppendorf Centrifuge 5810R</i> , cooled with fixed angle rotor (reaction vessels 15 mL, 50 mL)	<i>Eppendorf AG</i> , Hamburg, Germany
	<i>Eppendorf Concentrator 5301</i> , vacuum centrifuge	<i>Eppendorf AG</i> , Hamburg, Germany
	<i>Sorvall RC6+</i> , cooled centrifuge	<i>Thermo Fisher Scientific</i> , Waltham, MA, USA
	<i>Sorvall F10S-4x1000</i> , fixed angle rotor	<i>Thermo Fisher Scientific</i> , Waltham, MA, USA
	<i>Sorvall F9S</i> , fixed angle rotor	<i>Thermo Fisher Scientific</i> , Waltham, MA, USA
Incubator	<i>New Brunswick™ Innova® 42</i>	<i>Eppendorf AG</i> , Hamburg, Germany
Shaker	<i>BioCote Stuart rotator SB2</i>	<i>BioCote Ltd</i> , Wolverhampton, UK
	<i>Eppendorf Thermomixer compact</i> , shaking heatblock for reaction vessels of 1.5–2 mL	<i>Eppendorf AG</i> , Hamburg, Germany
	<i>HLC MKR23</i> , shaking heatblock for reaction vessels of 1.5–50 mL	<i>HLC BioTech</i> , Bovenden, Germany
Magnetic stirrer	<i>Heidolph MR 3001 K</i> , heatable magnetic stirrer combined with the <i>EKT HeiCon</i> thermometer	<i>Heidolph Instruments GmbH &amp; Co.KG</i> , Schwabach, Germany
Heat gun (50–650 °C)	<i>Steinel HG3002LCD Type 3458</i>	<i>Steinel Vertrieb GmbH</i> , Herzebrock-Clarholz
Heat cabinet (120 °C, for glas ware)	<i>Jouan Innovens 234 EU1</i>	<i>Thermo Fisher Scientific</i> , Waltham, MA, USA
Lyophilisator	<i>Zirbus VaCo2 Lyophilisator</i>	<i>Zirbus Technology GmbH</i> , Bad Grund, Germany

### 8.1.2 Consumables

Consumables such as pipette tips of various sizes (0.1–1,000  $\mu\text{L}$ ), reaction vessels (1.5 mL, 2 mL, 15 mL, 50 mL), and petri dishes were acquired from *neoLab Migge GmbH* (Heidelberg, Germany). Sterile syringe filters (0.20  $\mu\text{m}$ , cellulose acetate) were purchased from *VWR International GmbH* (Darmstadt, Germany). Single use syringes of the *Injekt®* series (polypropylene/polyethylene) were purchased from *B. Braun Melsungen AG* (Melsungen, Germany). For absorption measurements microplates, 96 well (PS, F-bottom, clear) of *Greiner Bio-one GmbH* (Frickenhausen, Germany) and single use cuvettes (LLG-cuvettes, PS, semi-micro, 1.6 mL) of *Lab Logistics Group GmbH* (Meckenheim, Germany) were utilised.

### 8.1.3 Chemicals and enzymes

The chemicals used in chemical syntheses and for the production of buffers, cultivation media, and various solutions were obtained from the companies *Sigma-Aldrich*, *Alfa Aesar*, *TCl*, *Apollo Scientific*, *AppliChem*, *Carl Roth*, *Fluka*, and *CarboSynth*. Organic solvents were purchased commercially and distilled before use in order to remove stabilising agents. Dry solvents such as dichloromethane, tetrahydrofurane, diethyl ether and toluene were taken from the solvent drying system MB-SPS-800 (*M. Braun Inertgas-Systeme GmbH*, Garching, Germany).

The *Phusion High-Fidelity* DNA polymerase (2 U/ $\mu$ L), *Phire Hot-Start II* DNA polymerase, T4 DNA ligase, dNTP mix (10 mM), and all restriction endonucleases were obtained from *Thermo Fisher Scientific* (Waltham, MA, USA). The *Vent<sup>®</sup>* DNA polymerase, *Q5<sup>®</sup> High-Fidelity* DNA polymerase, *Taq* DNA ligase (40,000 U/mL), T5-Exonuclease (10,000 U/mL) were obtained from *New England BioLabs GmbH* (Frankfurt a. Main, Germany). The *Herculase II Fusion* DNA polymerase and KAPA-HiFi DNA polymerase (1 U/ $\mu$ L), were purchased from *Agilent* (Santa Clara, CA, USA) and *KAPA Biosystems* (Roche, Basel, Switzerland) respectively.

### 8.1.4 Oligonucleotides and plasmids

Oligonucleotides were obtained as lyophilisate from *Sigma-Aldrich* (Steinheim, Germany) and dissolved in H<sub>2</sub>O creating a 100 mM solution. Synthetic genes were ordered from *GenScript USA Inc.* (Piscataway, NJ, USA), synthesised directly into the pET-21a(+)-vector flanked by NdeI and XhoI restriction sites. The plasmids utilised, synthesised and produced during this thesis with their respective target genes are listed in Table 16.

**Table 15** Oligonucleotide overview displaying each sequence in 5'→3' orientation and the desired application method. The description fw (forward) and rv (reverse) of each oligonucleotide describe the orientation of the oligonucleotide binding either the sense or antisense strand respectively. Mismatching nucleotides for mutagenesis are depicted in bold. The target gene overlapping sequences of oligonucleotides designed for Gibson Assembly (GA) are underlined. (GA – Gibson assembly<sup>®</sup>; N – Nested-PCR; QC – QuikChange<sup>™</sup>; RTH – Round the horn-PCR; A – Analysis/Sequencing)

#	Description	Sequence (5'→3')	Method
1	abg1_GA_rv	<u>AGTGGTGGTGGTGGTGGTGGTCTCGAGCCCC</u> TTCACCACAC	GA
2	abg1_GA_fw	<u>ATTTTGTTTAACTTTAAGAAGGAGATATACA</u> <u>CATATGACCGATCCCCAAACG</u>	GA
3	abg1_fw_2	ATGACCGATCCCCAAACGCTTGCA	N
4	abg1_rv_2	CACCCCTTCACCACCCATGGTTCCC	N
5	abg1_+200_rv	ATGACGGGTGCAAGCAGGCACC	N
6	abg1_-144_fw	ATTAGTGCATGCAAAGCGCTTTGGA	N
7	QC_abg1_E358S_fw	TACATTACC <b>AGCA</b> ACGGCGCCTG	QC

8	QC_abg1_E358S_rv	CAGGCGCCGTT <b>GCT</b> GGTAATGTA	QC
9	QC_abg1_E358A_fw	TACATTACC <b>GCG</b> AACGGCGCCTG	QC
10	QC_abg1_E358A_rv	CAGGCGCCGTT <b>GCG</b> GGTAATGTA	QC
11	QC_abg1_E358_KCA_fw	TACATCACCK <b>CAA</b> ATGGCGCCTG	QC
12	QC_abg1_E358_KCA_rv	CAGGCGCCATTT <b>G</b> MGGTGTATGTA	QC
13	QC_bgIU_E377_KSC_fw	GTACATTACCK <b>SCA</b> ACGGTGCTAG	QC
14	QC_bgIU_E170_KSC_fw	CCTTCAACK <b>SCC</b> CGCTGTGTT	QC
15	QC_bgIU_E377_KSC_rv	CTAGCACCGTT <b>GSM</b> GGTAATGTAC	QC
16	QC_bgIU_E170_KSC_rv	AACACAGCGG <b>GSM</b> GTTGAAGG	QC
17	cbg1_fw	ATGATCGACGATATTCTCGATAAGAT	N
18	cbg1_rv	CTACGGCTCCATCACATGATCG	N
19	cbg1_GA_fw	<u>ATTTTGTTTAACTTTAAGAAGGAGATATA</u> <u>CATATGATCGACGATATTCTCG</u>	GA
20	cbg1_GA_rv	<u>TGGTGGTGGTGGTGGTGGTGGTGGTGGT</u> <u>CATCACATGA</u>	GA
21	cbg1_fw_-107	GCTGGCAATCGTGCCGGT	N
22	cbg1_rv_+110	CAGGTATGTACATTAAGAGAGCGA	N
23	cbg1_rv_ver2	CTACGGCTCCATCACATGATC	N
24	QC_cbg1_D222A_fw	TCATGTCC <b>GCC</b> TGGTTCGG	QC
25	QC_cbg1_D222S_fw	TCATGTCC <b>AGC</b> TGGTTCGG	QC
26	QC_cbg1_D222C_fw	TCATGTCC <b>TGCT</b> GTTTCGG	QC
27	QC_cbg1_D222A_rv	CCGAACC <b>AGGC</b> GGACATGA	QC
28	QC_cbg1_D222S_rv	CCGAACC <b>AGCT</b> GGACATGA	QC
29	QC_cbg1_D222C_rv	CCGAACC <b>AGCAG</b> GGACATGA	QC
30	RTH_cbg1_rv_phos	GGACATGACCACGCCGTCAAGCCCCATT C	RTH
31	RTH_cbg1_fw_D222A_phos	<b>GCCT</b> GGTTCGGCTCGCACTCGACGGCTGA A	RTH
32	RTH_cbg1_fw_D222C_phos	<b>TCCT</b> GGTTCGGCTCGCACTCGACGGCTGA A	RTH
33	RTH_cbg1_fw_D222S_phos	<b>TGCT</b> GGTTCGGCTCGCACTCGACGGCTGA A	RTH
34	RTH_cbg1_rev2_phos	GGAGGACATGACGG	RTH
35	RTH_cbg1_fw_Y190F_phos	<b>TTC</b> AACAAGCTCAACGG	RTH
36	RTH_cbg1_rev3_phos	GGTGTCCCACTCG	RTH
37	RTH_cbg1_fw_D559A_phos	<b>GC</b> AGGTCTGGATCTG	RTH
38	RTH_cbg1_fw_D559S_phos	<b>TC</b> AGGTCTGGATCTGC	RTH
39	RTH_cbg1_fw_D559C_phos	<b>TG</b> CGGTCTGGATCTG	RTH
40	RTH_cbg1_rev4_phos	CTTGATCGTGGCGGC	RTH
41	RTH_cbg1_fw_H144A_phos	<b>GCCT</b> TCGTCCCAAC	RTH
42	RTH_rhaB_D567A_fw_phos	<b>GCCT</b> GCCCGTCCTATGAACA	RTH
43	RTH_rhaB_D567C_fw_phos	<b>TGCT</b> GCCCGTCCTATGAACA	RTH
44	RTH_rhaB_D567N_fw_phos	<b>AACT</b> GCCCGTCCTATGAACA	RTH
45	RTH_rhaB_D567Q_fw_phos	<b>CAGT</b> GCCCGTCCTATGAACA	RTH

## 8 Experimental Section

46	RTH_rhaB_D567_rev_phos	GACGAACGTGTCCTCCA	RTH
47	RTH_rhaB_D579A_fw_phos	<b>GGCAGCCGCAACGAGGC</b>	RTH
48	RTH_rhaB_D579C_fw_phos	<b>TGCAGCCGCAACGAGGC</b>	RTH
49	RTH_rhaB_D579N_fw_phos	<b>AACAGCCGCAACGAGGC</b>	RTH
50	RTH_rhaB_D579Q_fw_phos	<b>CAGAGCCGCAACGAGGC</b>	RTH
51	RTH_rhaB_D579G_fw_phos	<b>GGCAGCCGCAACGAGGC</b>	RTH
52	RTH_rhaB_D579S_fw_phos	<b>TCCAGCCGCAACGAGGC</b>	RTH
53	RTH_rhaB_D579_rev_phos	GCCCACCCAGAACACCTGTT	RTH
54	RTH_rhaB_E841A_fw_phos	<b>GCGATGTATCCGAACTTTGC</b>	RTH
55	RTH_rhaB_E841C_fw_phos	<b>TGCATGTATCCGAACTTTGC</b>	RTH
56	RTH_rhaB_E841N_fw_phos	<b>AACATGTATCCGAACTTTGC</b>	RTH
57	RTH_rhaB_E841Q_fw_phos	<b>CAGATGTATCCGAACTTTGC</b>	RTH
58	RTH_rhaB_E841_rev_phos	CCAACAGGTCGTGGCAT	RTH
60	Seq_pET28_rhaB_6066	CAGAGGCAATAGCGC	A
61	Seq_Fw_EndoCCN180H_1029	GGCTGGAAGTGGGCA	A
62	Seq_Rev_EndoCCN180H_643	GCAATGACCAGGC	A
63	T7_fw	TAATACGACTCACTATAGGG	A
64	pRSET-RP	ATGCTAGTTATTGCTCAGC	A

**Table 16** Utilised and produced expression vectors.

Name	Genotype description	Origin
Base vectors		
pET-21a(+)	<i>lacI</i> , T7 Prom, T7 Term, f1 Ori, Amp <sup>R</sup> , pBR322 Ori	Novagen
pET-28a(+)	<i>lacI</i> , T7 Prom, T7 Term, f1 Ori, Kan <sup>R</sup> , pBR322 Ori	Novagen
Wild type genes		
pET-21a(+)::abg1	pET-21a(+) containing the <i>R. radiobacter</i> gene <i>abg1</i> encoding Abg with a C-terminal His-tag	This thesis
pET-21a(+)::bglU	pET-21a(+) containing the <i>M. antarcticus</i> gene <i>bglU</i> encoding BglU with a C-terminal His-tag	This thesis
pET-21a(+)::cbg1	pET-21a(+) containing the <i>R. radiobacter</i> gene <i>cbg1</i> encoding Cbg-1 with a C-terminal His-tag	This thesis
pET-28b(+)::rhaB	pET-28a(+) containing the <i>B. subtilis</i> GL1 gene <i>rhaB</i> encoding RhaB with a C-terminal His-tag	Kamila Morka
pET-DUET::bglC	pET-DUET containing the <i>P. furiosus</i> gene <i>bglC</i> encoding BglC with a N-terminal His-tag	Prof. Elling

BglC mutants		
pET-DUET::bglC_E113A	<i>bglC</i> containing the mutation E113A	This thesis
pET-DUET::bglC_E113G	<i>bglC</i> containing the mutation E113G	This thesis
pET-DUET::bglC_E113S	<i>bglC</i> containing the mutation E113S	This thesis
pET-DUET::bglC_E189C	<i>bglC</i> containing the mutation E189C	This thesis
pET-DUET::bglC_E189G	<i>bglC</i> containing the mutation E189G	This thesis
pET-DUET::bglC_E189S	<i>bglC</i> containing the mutation E189S	This thesis
pET-DUET::bglC_E316A	<i>bglC</i> containing the mutation E316A	This thesis
pET-DUET::bglC_E316G	<i>bglC</i> containing the mutation E316G	This thesis
pET-DUET::bglC_E316S	<i>bglC</i> containing the mutation E316S	This thesis
Abg1 mutants		
pET-21a(+):abg1_E358S	<i>abg1</i> containing the mutation E358S	This thesis
pET-21a(+):abg1_E358A	<i>abg1</i> containing the mutation E358A	This thesis
BglU Mutants		
pET-21a(+):bglU_E170A	<i>bglU</i> containing the mutation E170A	This thesis <sup>a</sup>
pET-21a(+):bglU_E170C	<i>bglU</i> containing the mutation E170C	This thesis <sup>a</sup>
pET-21a(+):bglU_E170S	<i>bglU</i> containing the mutation E170S	This thesis <sup>a</sup>
pET-21a(+):bglU_E377A	<i>bglU</i> containing the mutation E377A	This thesis <sup>a</sup>
pET-21a(+):bglU_E377G	<i>bglU</i> containing the mutation E377G	This thesis <sup>a</sup>
Cbg1 Mutants		
pET-21a(+):cbg1_D222A	<i>cbg1</i> containing the mutation D222A	This thesis
pET-21a(+):cbg1_D222C	<i>cbg1</i> containing the mutation D222C	This thesis
pET-21a(+):cbg1_D222S	<i>cbg1</i> containing the mutation D222S	This thesis
pET-21a(+):cbg1_Y190F	<i>cbg1</i> containing the mutation Y190F	This thesis
pET-21a(+):cbg1_Y190F_D222A	<i>cbg1</i> containing the mutations Y190F and D222A	This thesis
pET-21a(+):cbg1_H144A	<i>cbg1</i> containing the mutation H144A	This thesis
pET-21a(+):cbg1_D559A	<i>cbg1</i> containing the mutation D559A	This thesis
pET-21a(+):cbg1_D559S	<i>cbg1</i> containing the mutation D559S	This thesis
pET-21a(+):cbg1_D559C	<i>cbg1</i> containing the mutation D559C	This thesis

## 8 Experimental Section

---

RhaB mutants		
pET-28b(+):rhaB_E841G	<i>rhaB</i> containing the mutation E841G	Kamila Morka
pET-28b(+):rhaB_E841S	<i>rhaB</i> containing the mutation E841S	Kamila Morka
pET-28b(+):rhaB_E567G	<i>rhaB</i> containing the mutation E567G	Kamila Morka
pET-28b(+):rhaB_E567S	<i>rhaB</i> containing the mutation E567S	Kamila Morka
pET-28b(+):rhaB_D567C	<i>rhaB</i> containing the mutation D567C	This thesis <sup>b</sup>
pET-28b(+):rhaB_D567N	<i>rhaB</i> containing the mutation D567N	This thesis <sup>b</sup>
pET-28b(+):rhaB_D579Q	<i>rhaB</i> containing the mutation D579Q	This thesis <sup>b</sup>
pET-28b(+):rhaB_D579A	<i>rhaB</i> containing the mutation D579A	This thesis <sup>b</sup>

---

EndoCC mutant		
pET-21a(+):endoCC_N180H	pET-21a(+) containing the <i>C. cinerea</i> gene <i>endoCC</i> encoding Endo-CC with a C-terminal His-tag and the mutation N180H	<i>Genscript</i>

---

### 8.1.5 Bacterial strains

Listed in Table 17 are the bacterial strains used throughout the work of this thesis. All strains of *Escherichia coli* are derived from the K12 laboratory strain.

**Table 17** Overview of the bacterial strains and description of their genotype and application in this thesis. (DNA – Replication of plasmid DNA; Protein – Heterologous expression of the target protein; Gene – Isolation of genomic DNA as template for gene amplification)

Strain	Genotype	Reference	Application
<i>E. coli</i> DH5 $\alpha$	fhuA2 $\Delta$ (argF-lacZ)U169 phoA glnV44 $\phi$ 80 $\Delta$ (lacZ)M15 gyrA96 recA1 relA1 endA1 thi-1 hsdR17	<i>New England BioLabs Inc.</i>	DNA
<i>E. coli</i> BL21(DE3)	fhuA2 [lon] ompT gal ( $\lambda$ DE3) [dcm] $\Delta$ hsdS $\lambda$ DE3 = $\lambda$ sBamHlo $\Delta$ EcoRI-B int::(lacI::PlacUV5::T7 gene1) i21 $\Delta$ nin5	<i>New England BioLabs Inc.</i> <sup>[192]</sup>	Protein
<i>E. coli</i> Rosetta <sup>TM</sup> 2	F <sup>-</sup> ompT gal dcm lon hsdSB( <sub>r<sub>B</sub>-m<sub>b</sub></sub> ) pRARE2 (Cam <sup>R</sup> argU argW ilex glyT leuW proL metT thrT tyrU thrU)	<i>EMD Biosciences Inc. (former Novagen®)</i> <sup>[193]</sup>	Protein
<i>A. radiobacter</i> (DSMZ: DSM 7215)	Wild type	<i>Zhang et al. (2014)</i> <sup>[194]</sup>	Gene

### 8.1.6 Software

**Table 18** Commonly utilised software for analysis of biological and chemical experiments.

Name	Application	Producer
ChemBioDraw Ultra 12.0 & 16.0	Drawing chemical structures/reactions	<i>PerkinElmer Informatics</i>
Clone Manager 9.4 Professional	Planning of cloning strategies and analysis of sequencing results	<i>Scientific &amp; Educational Software</i>
enschemLab 7.0.5	Electronic lab journal	<i>Enso Software GmbH</i>
MestReNova 8.0.1-10878	Processing and analysis of NMR data	<i>Mestrelab Research S.L.</i>
OriginPro 9.0G	Statistical evaluation/ linear and non-linear regression	<i>OriginLab Corp.</i>
UCSF Chimera 1.7	Depiction of protein structures	<i>UCSF Resource for Biocomputing, Visualization and Informatics</i>
BioEdit	Evaluation of sequencing quality	<i>Ibis Therapeutics</i>
Microsoft Excel 2010	Processing of simple data	<i>Microsoft Corp.</i>
Microsoft PowerPoint 2010	Production of presentations	<i>Microsoft Corp.</i>
Microsoft Word 2016	Creation of text files	<i>Microsoft Corp.</i>

## 8.2 Molecular biological methods

### 8.2.1 Isolation of genomic DNA from *R. radiobacter*

For the extraction of the genomic DNA of *R. radiobacter* a 20 mL culture was incubated overnight and the cells harvested by centrifugation (2 min, 10,000 rpm). The resulting pellet was re-suspended in 2 mL of solution A, and after the addition of sterile glass beads (0.5 mm) vigorously mixed. The extraction proceeded in three steps. Firstly, 1 mL of the lysate was mixed thoroughly with 300  $\mu$ L Roti-Phenol and the phases separated by centrifugation for 2 min at 14,000 rpm. The upper phase was then further extracted with 3 mL Roti-phenol by mixing, followed by centrifugation for 2 min at 14,000 rpm. The third and final extraction of the upper phase was carried out with 2.5 mL chloroform/isoamylalcohol (24 : 1) solution. The genomic DNA was then precipitated by the addition of 0.2 mL P3-buffer and 0.5 mL cold abs. ethanol. The precipitated DNA was pelleted by centrifugation (15 min, 15,300 rpm, 4 °C) and the supernatant discarded. Washing of the DNA occurred by resuspension of the genomic DNA in cold ethanol (70%, v/v) and repeated centrifugation (15 min, 15,300 rpm, 4 °C). Excess ethanol was removed and the DNA dissolved by incubating in 40  $\mu$ L TE-Buffer (with 2 mg/mL RNase A added) at room temperature (~25 °C) for 30 min. The purity of the genomic DNA was checked by determination of the  $A_{260}/A_{280}$  value.

The isolated genomic DNA sample of *R. radiobacter* had a concentration of 1109 ng/ $\mu$ L. The purity of the sample was confirmed by determination of the  $A_{260}/A_{280}$  value being 1.93 ( $A_{260}/A_{230} = 1.17$ ).

**Table 19** Solutions required for the isolation of genomic DNA.

Solution	Components
TE-Buffer	10 mM TRIS-HCl 1 mM EDTA pH 8
Solution A	10 mM TRIS-HCl 1 mM EDTA 100 mM NaCl 0.1% SDS pH 8
P3-Buffer	3 M Sodium acetate, pH 5

### 8.2.2 Plasmid isolation

Isolation of desired plasmid DNA from *E. coli* cells was proceeded from a 5 mL culture, cultivated at 37 °C over night in LB-medium. The cells were pelleted by centrifugation and the supernatant discarded. The *innuPREP* DNA Mini Kit (*AnalytikJena AG*, Jena, Germany) was

applied for the isolation of the plasmid DNA from the cell pellet. The provided protocol was followed with exception of the last step. The plasmid DNA was eluted from the spin column using 20–50  $\mu\text{L}$   $\text{dH}_2\text{O}$  instead of the provided elution buffer.

### 8.2.3 DNA concentration determination

The DNA concentration of a specific sample was determined photometrical with the *NanoDrop 2000* (*Thermo Fisher Scientific*, Waltham, MA, USA) by measuring the absorption at  $\lambda = 260$  nm. The concentration was determined with 2  $\mu\text{L}$  of the DNA sample solution and with  $\text{dH}_2\text{O}$  as a reference sample. Additionally, the absorption at  $\lambda = 280$  nm was measured for determination of the purity of the DNA. This was described as the quotient of the absorption  $A_{260}/A_{280}$ .

### 8.2.4 Agarose gel electrophoresis

The size determination of DNA fragments and analysis of PCR reactions, DNA-restrictions, and plasmid isolation occurred *via* agarose gel electrophoresis.

**Table 20** Components for agarose gel electrophoresis.

Solution	Components
50x TEA buffer	2 M TRIS 50 mM EDTA (Stocksolution: 0.5 M, pH 8) 0.9 M Acetic acid
Agarose gel solution	1x TEA buffer 0.8% (w/v) agarose 0.1 ‰ Gel Red™
5x DNA loading buffer	100 mM EDTA 43% (v/v) Glycerol 0.05% (w/v) Bromophenol blue

The agarose gel solution was prepared by boiling 0.8% (w/v) agarose in TEA-buffer until complete dissolution of the agarose. After addition of the fluorescence dye Gel Red™ (*Bioticum Inc.*, Hayward, CA, USA) the solution was stored at 60 °C to avoid polymerisation during storage. The Gel Red™ dye allows the selective detection of DNA strands *via* fluorescence by intercalation with the DNA. Polymerisation after casting occurred at room temperature ( $\sim 25$  °C) for around 30 min. Samples were mixed with DNA loading buffer before loading into the agarose gel sample chambers. For size determination, 1–1.5  $\mu\text{L}$  of the

reference standard 1 kb DNA Ladder (*Thermo Scientific*, Waltham, MA, USA) was used as a size comparison. The electrophoresis was run for 26 min at 180 V submerged in TEA-buffer. Documentation of the electrophoresis results was conducted with a gel documentation system (*INTAS Science Imaging Instruments GmbH*, Göttingen, Germany).

### 8.2.5 DNA gel elution

For ligation and transformation procedures, the target DNA was required to be free of side products, which can occur in PCR reactions. The separation and isolation of the target DNA occurred after agarose gel electrophoresis by gel extraction using the *innuPREP DOUBLEpure Kit* (*AnalytikJena AG*, Jena, Germany). The desired fragment was cut out of the agarose gel using a scalpel and placed into a 2.0 mL reaction vessel. The DNA extraction was then carried out following the protocol of the kit. Differing from the protocol, the elution of the DNA from the spin column was performed using dH<sub>2</sub>O instead of the provided buffer.

### 8.2.6 DNA ligation and restriction

Self-circularisation of phosphorylated linear DNA produced by *round the horn*-PCR was carried out by ligation using the T4-DNA ligase. Depending on the presence of PCR side products, the target DNA was isolated after separation by agarose gel electrophoresis (sections 8.2.4/8.2.5). The ligation reaction mixture was incubated over night (18 h) at 18 °C and subsequently applied for transformation of competent *E. coli* cells (section 8.3.2).

**Table 21** General composition of ligation reactions for the self-circularisation of linear DNA.

Component	Volume [μL]
T4-DNA Ligase buffer (10×)	2
T4-DNA Ligase	1
PCR mix/ isolated target DNA	17

Restriction of vector DNA as preparation for cloning reactions and control of correct insertion was generally carried out using *FastDigest* restriction enzymes. The 10× *FastDigest* Buffer was applied as recommended and the reaction incubated for 1–2 h at 37 °C. Completion of the

restriction was checked by agarose gel electrophoresis (section 8.2.4). Restriction enzymes were deactivated by heating of the mixture at 80 °C for 15 min.

### 8.2.7 DNA amplification by PCR

The amplification of genes for isolation, mutagenesis or cloning purposes from genomic DNA or vectors was achieved by the polymerase chain reaction (PCR). All PCR reactions followed a general protocol and composition (Table 22). The *Phire Hot-Start II* DNA-polymerase was most commonly applied, as this polymerase yielded the best results. In certain cases the *Phusion High-Fidelity*, *KAPA-HiFi*, *Herculase II Fusion*, and *Taq* DNA-polymerase were also tested for optimal amplification of the target gene sequence. The addition of DMSO (3%, v/v) facilitated increased DNA amplification by reducing the DNA melting temperature and improving primer annealing. Verification of the DNA amplification occurred *via* agarose gel electrophoresis (section 8.2.4).

**Table 22** General composition (left) and PCR-protocol (right) used for amplification from vector or genomic DNA.

Component	Amount [ $\mu$ L]	Step	Temp. [°C]	Duration	Cycle
<i>fw</i> Primer (5 mM)	1	Initial Denaturation	98	1 min	35
<i>rw</i> Primer (5 mM)	1	Denaturation	98	30 sec	
Template DNA (20–50 ng/ $\mu$ L)	0.5	Annealing	X <sup>a</sup>	20 sec	
dNTP (10 mM)	1	Elongation	72	15 sec/kbp	
10 $\times$ Reaction-buffer	4	Final Elongation	72	10 min	
<i>Phire II Hotstart</i> DNA-Polymerase	0.4	Storage	10	$\infty$	
DMSO	0.6				
<i>ad aqua dest.</i>	20				

<sup>a</sup> Temperature of the annealing step was adjusted according to the melting temperature of the respective primers.

### Touchdown-PCR

If the standard PCR procedure did not lead to an amplification product, a variation known as a *touchdown*-PCR was applied. The procedure follows the same set-up with the addition of ten cycles before the standard 35 cycles. For each of the ten additional cycles, a stepwise decrease of the annealing temperature is applied, starting  $\sim 10^\circ$  above the annealing temperature of the employed primers. The higher temperature reduces unspecific primer

binding and enriches the target gene to achieve an improved amplification in the subsequent 35 standard PCR cycles.

### ***Nested-PCR***

Similar to the *touchdown-PCR* method, *nested-PCR* attempts to enrich the target DNA to facilitate the amplification of the target gene. The method employs two pairs of primers. The first pair binds specific to the target region, which is to be amplified. The second pair, binds upstream and downstream of the target sequence. Amplification by these primers thereby enriches the amount of DNA containing the target sequence, facilitating the amplification by the standard primers. In the *nested-PCR* applied for the isolation of *abg* from the genomic DNA of *R. radiobacter*, all four primers were employed in a single PCR reaction. It is also possible to apply this method in two consecutive PCR reactions.

### **8.2.8 Mutagenesis by inverse-PCR**

Introduction of point mutations in the glycosidase genes was performed by inverse-PCR mutagenesis methods. The inverse-PCR, in contrast to standard PCR, applies primer pairs, which 5'-ends point away from each other, therefore additionally amplifying the complete vector back bone and not just the target gene. The mutation is introduced by employing primers containing a mutation, which is built into the newly synthesized DNA strand. Vectors containing the *wt* genes were applied as the template of the inverse-PCR, except in the case of the double mutant gene *cbg1-H144A D222A* for which the pET-21a(+):*cbg1\_H144A* vector acted as the template. Subsequent to the amplification, the original template DNA was removed by restriction with DpnI, which recognises specifically the methylated DNA sequence GATC. After transformation of the competent *E. coli* cells with the potentially mutated plasmid DNA, resulting colonies are picked and the plasmids isolated for sequencing in order to confirm presence of the desired mutation (section 8.2.2 & 8.2.10).

### ***QuikChange*<sup>TM</sup>-PCR**

The *QuikChange*<sup>TM</sup>-PCR method employs complementary primers containing the point mutation in the centre of the primer pair. Binding of the primers is ensured by complementary sequences of the 3'- and 5'-end flanking the mutation. The complementary nature of the primers lead to a linear amplification of the target DNA, as primers binding to the new synthesised DNA cannot lead to further amplicates. The *QuikChange*<sup>TM</sup>-PCR followed two different procedures, depending on the success of the PCR reaction. First mutagenesis reactions were set up identically to a standard PCR (section 8.2.7). If unsuccessful, a two step PCR procedure was applied. Two separate PCR mixtures containing only the fw- or rev-primer

were run for 5 cycles and subsequently combined and the reaction run for further 18 cycles. The separate PCR reactions help to avoid primer dimerization during the PCR reaction, which can have an inhibitory effect. The template DNA was removed by DpnI restriction and the resulting mixture directly applied in a transformation of the target host (section 8.2.6 & 8.3.2).

### ***Round the horn* mutagenesis**

Contrary to the *QuikChange*<sup>™</sup>-PCR method, *round the horn*-PCR does not employ complementary primers. The mutation, deletion or insertion is incorporated in one of the primers at the 5'-end. As the primers are not complementary to each other, the amplification occurs exponential, identically to a standard PCR. The resulting DNA contains blunt-ends hindering a self-circularisation by overlaps. Therefore, primers phosphorylated at the 5'-end are applied and the circularisation caused by enzymatic ligation (section 8.2.6). The template DNA is removed by DpnI restriction and the left over mutated DNA is then directly applied in a transformation of the target host (section 8.2.6 & 8.3.2).

### **8.2.9 Gibson Assembly cloning**

The *Gibson assembly* cloning method was applied for the insertion of target genes into expression vectors. The method was developed by *Gibson et al.* in collaboration with the J. Craig Venter Institute (JCVI). The method allows the specific incorporation of large DNA fragments into a vector in an isothermal reaction. The target insertion gene is initially extended by the addition of sequences complementary to the desired vector insertion position by overlap extension PCR. The PCR product is then combined with the *Gibson assembly* master mix, which components catalyse the insertion of the target DNA into the vector (Table 23). The T5-exonuclease creates sticky-ends, which allows the annealing of complementary DNA sequences of the vector and target DNA. The gaps are subsequently filled by the present polymerase and ligated by the Taq DNA-ligase resulting in the desired construct. The assembly reaction mixture consisted of 3–6 µL linearised vector DNA, 2–4 µL insert DNA, 10 µL *Gibson assembly* master mix (Table 23), and dH<sub>2</sub>O added for a final volume of 20 µL. The reaction was incubated at 50 °C for 1 h. The assembly mixture was directly applied in the transformation of competent *E. coli* cells (section 8.3.2).

**Table 23** Composition of the master mix and ISO-buffer applied for the *Gibson assembly* carried out during the work of this thesis.

<b>Gibson assembly master mix</b>		<b>5× ISO-buffer</b>	
<b>Component</b>	<b>Amount [μL]</b>	<b>Component</b>	<b>Amount [μL]</b>
ISO-buffer (5×)	60	TRIS-HCl (1 M; pH 7.5)	500
T5-Exonuclease (100 U/mL)	24	MgCl <sub>2</sub> (2 M)	25
<i>Phusion Hot Start II</i> DNA-Polymerase (0.4 U/μL)	18	dGTP (100 mM)	10
Taq DNA-Ligase (8,000 U/mL)	39	dATP (100 mM)	10
ad <i>aqua dest.</i>	450	dTTP (100 mM)	10
		dCTP (100 mM)	10
		DTT (1 M)	50
		PEG-8000	250 mg
		NAD <sup>+</sup> (100 mM)	50

### 8.2.10 DNA sequencing

*GATC Biotech AG* (Constance, Germany) carried out sequencing of plasmid DNA samples to verify the correct target sequence insertion or mutation. The samples were sequenced using the dideoxy chain termination / cycle sequencing method developed by *Sanger*.

## 8.3 Microbiological methods

### 8.3.1 Chemically competent cells

For the transformation of *E. coli* strains with plasmid DNA it is necessary to prepare chemically competent cells of the desired bacterial host strain. Therefore, a 5 mL pre-culture (LB-medium) was prepared with the required strain and incubated over night at 37 °C. A further culture (400 mL) was inoculated with 2 mL of the pre-culture and incubated (37 °C, 120 rpm) up to an OD<sub>600</sub> of 0.4–0.6. The culture was centrifuged (sterile centrifugation cups, 10 min, 4 °C, 2,460 rpm) and the resulting pellet suspended in 10 mL of Buffer A. After incubating the cell suspension 20 min on ice, the culture was again centrifuged (10 min, 4 °C, 2,460 rpm) and subsequently suspended in 2 mL of Buffer B. The resulting cell-suspension was aliquoted into sterile tubes in 50 μL portions and immediately frozen with liquid nitrogen. The frozen cells were stored at -80 °C until needed.

**Table 24** Required buffers for preparation of chemically competent cells.

Solution	Components
Buffer A	100 mM MgCl <sub>2</sub>
Buffer B	100 mM CaCl <sub>2</sub> 15% Glycerol

Testing of the capability of plasmid uptake of newly created competent cells was tested by comparison of a transformation of the cells with a) the plasmid pET-21a(+) (1 μL, 42 ng/μL) and b) sterile dH<sub>2</sub>O. The transformation was carried out as described in section 8.3.2 and incubated on an LB-agar plate supplemented with ampicillin. Bacterial growth should only be observed for the bacteria transformed with the pET-21a(+) and not for the dH<sub>2</sub>O batch. The transformation efficiency (TE) was then determined by use of Equation 3. Additionally, the antibiotic sensitivity of the competent cells was tested in 5 mL LB-medium supplemented with ampicillin, tetracycline, chloramphenicol, streptomycine and kanamycine, incubated for 18 h at 37 °C.

**Equation 3** 
$$TE = \frac{CFU \text{ (colony forming units)}}{\text{total DNA amount } (\mu\text{g})}$$

### 8.3.2 Transformation of chemically competent *E. coli* strains

In order to express the target protein or replicate plasmid DNA, suitable host organisms were transformed with the desired plasmid DNA. Transformation of chemically competent *E. coli* cells was carried out using the heat shock method. For the transformation, 2–3 μL of the plasmid solution were added to 50 μL chemically competent cells (prepared as described in section 8.3.1) and incubated for 30 min on ice. The cells were subsequently heated in a heat block to 42 °C for 90 sec. After the heat shock, 1 mL LB-medium was added to the cell suspension and then incubated for 1 h at 37 °C. For selection, the cells were pelleted by centrifugation for 2 min at 10,000 rpm and transferred, after re-suspension in around 50 μL of sterile LB-medium, to an agar plate or pre-culture tube containing the required selection antibiotic. Colonies or growth of the pre-culture of the transformed strain was observed after incubation at 37 °C for 18 h.

### 8.3.3 Cultivation of *E. coli* strains

All media used for bacterial cultivation or protein expression was autoclaved without addition of antibiotics at 120 °C for 20 min. Media was stored if not used directly at 4 °C. Antibiotics were added to the media sterile before use. Agar plates (2% w/v; LB-medium) were inoculated with 100 µL cell suspension of transformed bacteria and spread over the plate evenly by shaking 10 sec after the addition of sterile glass beads (Ø 3 mm). Glass beads were then removed, washed with 0.1 M HCl and autoclaved for further use. Inoculated plates were incubated over night (~18 h) at 37 °C and stored up to one week at 4 °C. The cultivation of *E. coli* cultures for plasmid isolation or as pre-cultures for inoculation of expression cultures was carried out in 5 mL LB-medium in sterile test tubes (10 mL), incubated after inoculation at 37 °C for ~18 h in a test tube rotator (*Stuart*<sup>®</sup>, Staffordshire, UK). Optical densities (OD<sub>600</sub>) were measured at 600 nm using the *NanoDrop 2000c* of *Thermo Scientific Corp.* (MA, USA). Cultures for the expression of target proteins were performed on a 1 L scale with TB-medium in 3 L *Fernbach*-flasks and shaken unless otherwise stated at 120 rpm.

**Table 25** Components of cultivation media used throughout this thesis.

Lysogeny broth (LB)		Terrific broth (TB)	
Sodium chloride	1% (w/v)	Tryptone	1.2% (w/v)
Yeast extract	0.5% (w/v)	Yeast extract	2.4% (w/v)
Tryptone	1% (w/v)	Glycerol	0.4% (v/v)
		<i>Autoclaved separately:</i>	
		KH <sub>2</sub> PO <sub>4</sub>	0.2% (w/v)
		K <sub>2</sub> HPO <sub>4</sub>	1.3% (w/v)

### 8.3.4 Heterologous expression of enzymes

Protein expression of the β-glucosidases Abg, BglU, Cbg1, and the α-rhamnosidase RhaB, as well as the β-*endo*-N-acetylglucosaminidase Endo-CC N180H was carried out *via* the following procedure:

All media used during the cultivation and expression contained the respective antibiotic (100 µg/mL ampicillin, 10 µg/ml kanamycin). A pre-culture of 5 mL LB-media was inoculated with a colony of the transformed bacterial strain and incubated over night at 37 °C. TB-media was applied for the subsequent cultivation and expression. The expression culture of a volume of 1 L was incubated in 3 L *Fernbach*-flasks. The culture was inoculated to an OD<sub>600</sub> of 0.1 with the pre-culture and incubated at 37 °C until an OD<sub>600</sub> of 0.4–0.6 was reached. The induction of protein expression occurred by the addition of IPTG (final concentration 0.1 mM). After

induction, the cultures were incubated at 25 °C for 24 h. The cultures were constantly shaken at 120 rpm. Cells were harvested by centrifugation (10 min, 10,000 rpm) and the cell pellets stored at -20 °C until needed.

Protein expression of the putative  $\beta$ -galactosidase BglC of *P. furiosus* was carried out *via* the following protocol:

All media used during the cultivation and expression contained 100  $\mu$ g/mL ampicillin. When using the *E. coli* Rosetta™ 2 strain chloramphenicol (34  $\mu$ g/mL) was added in addition to ampicillin. A pre-culture of 5 mL LB-media was inoculated with a colony of the transformed bacterial strain and incubated over night at 37 °C. From this pre-culture, a second pre-culture was inoculated using 1 mL of the first pre-culture and 4 mL LB-media. This culture was incubated for 4 h at 37 °C. TB-media was applied for the subsequent cultivation and expression. Cultures of a volume of 200 mL were incubated in 1 L baffled Erlenmeyer flasks, 500 mL and 1 L cultures were incubated in 3 L *Fernbach*-flasks. The expression culture was inoculated with 1% (*v/v*) of the second pre-culture and incubated at 37 °C for 4 h ( $OD_{600}$  0.4–0.6). The induction of protein expression occurred by the addition of IPTG (0.1 mM). After induction, the cultures were incubated for 8 h at 37 °C, then at 4 °C until harvesting of the cells. The cultures were constantly shaken at 120 rpm. Cells were harvested by centrifugation (10 min, 10,000 rpm) and the cell pellets stored at -20 °C until needed. (Procedure modified from *Merker et al.*)<sup>[69]</sup>

### 8.3.5 Esculin-agar plate assay

The esculin-agar plate assay was applied for the identification of hydrolytically inactive  $\beta$ -glucosidase mutants heterologously expressed in *E. coli* BL21(DE3). Esculin (500 mg) was dissolved in 2 mL water, sterilised by filtration and added to sterile LB-agar (0.5 L). Ammonium ferric citrate (250 mg in 1 mL dH<sub>2</sub>O, sterile) and ampicillin (final concentration 100  $\mu$ g/mL) were also added to the agar solution before pouring into petri dishes to solidify. Transformed cells containing plasmids with possible mutant glucosidase variants were cultivated 18 h at 37 °C. The expression of the glucosidase was induced by addition of 2.5  $\mu$ L IPTG (50  $\mu$ M) in the centre of the agar plate. After 16–24 h incubation at ~25 °C, colonies with a functional glucosidase were distinguishable from non-functional variants by a dark brown colouration.

## 8.4 Protein biochemical methods

### 8.4.1 Cell lysis

#### Sonification

Cell disruption for protein purification/isolation was performed using sonification. The *Sonoplus* of *Bandelin electronic GmbH & Co.* (KG, Berlin) with an adequate sonotrode (depending on the volume of the sample) was applied for the procedure. A 20% (w/v) cell suspension was produced by weighing of the cell pellet and resuspension in lysis-buffer. The sonification was carried out differently depending on the target protein:

Abg, BglU, Cbg1, RhaB, Endo-CC N180H: 3× 30 s, 5× 10% cycle, max. 40% power

BglC: 2× 5 min, 5× 10% cycle, max. 40% power

All samples were cooled 1 min between sonification cycles. The cell lysates were centrifuged (10 min, 4 °C, 12,000 rpm) and the supernatant used for further purification.

**Table 26** Composition of the buffer required for cell lysis.

Buffer	Composition
Lysis-buffer	50 m KH <sub>2</sub> PO <sub>4</sub> /K <sub>2</sub> HPO <sub>4</sub> , pH 8.0, 10 mM imidazole, 1 M NaCl

#### Heat-denaturation

Cell lysates containing the wild type or mutations of BglC were further purified by a two-step heat-denaturation. The cell-free extract was heated in 2 mL reaction tubes for 30 min at 75 °C, 600 rpm (heat-denaturation I). Precipitated protein was separated from the solution *via* centrifugation and the supernatant heated once more for 30 min at 85 °C, 600 rpm (heat-denaturation II). The samples were then centrifuged once more and the enzyme solution used for biocatalytic reactions or stored at 4 °C until further use.

### 8.4.2 Protein isolation

Target proteins were isolated by immobilised metal ion affinity chromatography. The target proteins were expressed with a C-terminal His<sub>6</sub>-tag consisting of six histidine residues. For the purification, the Ni-NTA column (*Superflow Cartridge*, 5 mL; *Qiagen GmbH*, Hilden, Germany) was equilibrated with 5 column volumes (CV) of equilibration-buffer, using a peristaltic pump (*Pharmacia Fine Chemicals*, Uppsala, Sweden). The cell lysate of a 20% cell suspension in

equilibration-buffer was centrifuged for 10 min at 10,000 rpm and 4 °C. The supernatant was subsequently charged onto the Ni-NTA column pumping the solution through the column in a loop for 5 min to ensure thorough binding of the target protein to the column matrix. Excess protein and unspecific bound protein was washed out of the column with 6 CV wash-buffer I. The bound target protein was then eluted with a high concentration of imidazole by adding 2 CV of elution-buffer. The elution fraction was then further desalted, concentrated (Section 8.4.3), and used for biochemical characterisation of the enzymes or synthetic reactions. After the isolation, the Ni-NTA column was additionally washed with 3 CV of wash-buffer II in order to ensure complete removal of bound protein. Columns were stored at 4 °C flushed with 20% ethanol solution until further needed.

**Table 27** Buffers applied for protein isolation via IMAC.

<b>Buffer</b>	<b>Composition</b>
<b>Equilibration-buffer</b>	50 M KH <sub>2</sub> PO <sub>4</sub> /K <sub>2</sub> HPO <sub>4</sub> , pH 8.0, 10 mM imidazole, 1 M NaCl
<b>Wash-buffer I</b>	50 M KH <sub>2</sub> PO <sub>4</sub> /K <sub>2</sub> HPO <sub>4</sub> , pH 8.0, 20 mM imidazole, 0.3 M NaCl
<b>Elution-buffer</b>	50 M KH <sub>2</sub> PO <sub>4</sub> /K <sub>2</sub> HPO <sub>4</sub> , pH 8.0, 250 mM imidazole, 0.3 M NaCl
<b>Wash-buffer II</b>	50 M KH <sub>2</sub> PO <sub>4</sub> /K <sub>2</sub> HPO <sub>4</sub> , pH 8.0, 1 M imidazole, 0.3 M NaCl

### 8.4.3 Buffer exchange, desalting, and concentrating protein samples

After isolation of the target protein via IMAC, the sample solution (elution fraction) contains a high concentration of imidazole (~250 mM) which can damage the enzyme over time. Therefore, a desalting of the buffer is necessary. Desalting of samples containing phosphate buffers was carried out with PD-10 desalting columns containing Sephadex G-25 (*GE Healthcare Europe GmbH*, Freiburg, Germany) under gravity flow. Columns were washed and equilibrated with the desired buffer (3× 3.5 mL buffer) before adding 2.5 mL of the sample to the column. Once the sample had completely flowed through the column, the protein was eluted from the column with 3.5 mL buffer. The collected sample was then either concentrated or applied directly in further experiments. After desalting of the sample, the columns were freed of imidazole by washing thrice with 3.5 mL buffer. The columns were subsequently stored at 4 °C in 20% (v/v) ethanol.

The exchange of phosphate buffer with NH<sub>4</sub>HCO<sub>3</sub>-buffer (150 mM, pH 7.9) occurred via ultrafiltration using Vivaspin® 20 centrifugal concentrators (*Satorius AG*, Göttingen, Germany). Concentrators with a molecular weightcut-off of 10 and 50 kDa for the Abg, BglU variants and

the GalPf variants, were chosen respectively. The samples were repeatedly centrifuged for 10 min, 8,000 rpm at 4 °C and diluted with the desired  $\text{NH}_4\text{HCO}_3$ -buffer (150 mM, pH 7.9).

The Vivaspin® 20 centrifugal concentrators were also used to concentrate protein solutions with a low protein concentration. The sample was filtrated down to the desired volume by centrifugation (10 min, 4 °C, 8,000 rpm).

### 8.4.4 Protein concentration determination

Protein concentration of all samples was measured using the colorimetric Bradford-Assay.<sup>[195]</sup> The method is based on the change in absorption (at 595 nm) of *Coomassie brilliant blue* when complexed with protein structures. The samples (100  $\mu\text{L}$ ) were diluted appropriately, mixed with the Bradford-reagent (900  $\mu\text{L}$ ), and incubated for 10 min at ~25 °C. The absorption of each sample at 595 nm was measured and the protein concentration determined *via* a calibration curve (measurement of various BSA-solutions between 0–300  $\mu\text{g}/\text{mL}$ ). A calibration occurred before the measurement of each sample batch, due to possible changes of the Bradford-reagent over time.

**Table 28** Composition of the Bradford-reagent

Reagent	Composition
Bradford <sup>a</sup>	0.02% (w/v) <i>Coomassie G-250</i> 5% (v/v) ethanol 10% (v/v) phosphoric acid

<sup>a</sup> Reagent was stored in a light protected bottle at ~25 °C

### 8.4.5 Lyophilisation

The removal of residual solvent/water in synthetic products and preparation of protein samples for long-term storage was carried out by lyophilisation. The samples were therefore frozen using liquid nitrogen and then freeze-dried in the *Zirbus VaCo2 Lyophilisator* (*Zirbus technology GmbH*, Bad Grund, Germany). Lyophilised samples were stored at -20 °C or 4 °C until used in experiments.

### 8.4.6 SDS-PAGE

For the analysis of protein expression and purification, SDS-PAGE analysis of each purification fraction occurred. The SDS-PAGE gels were cast using the *BioRad Mini Protean Tetra System*. The higher concentrated separation gel was polymerised first, overlaid with *iso*-propanol to eliminate possible bubbles and ensure a straight edge of the gel. After the polymerisation, the lower concentrated stacking gel was cast over the separation gel and a sample chamber comb inserted. Two types of SDS-PAGE systems, differing in the composition of the gels and buffers, were applied during the work of this thesis, Glycine-SDS-PAGE and Tricine-SDS-PAGE. The Tricine-SDS-PAGE offers a higher resolution of proteins in the size range of 1–100 kDa.<sup>[171]</sup>

All samples were prepared with a total volume of 20  $\mu$ L by heat denaturation (98 °C, 15 min) after the addition of 4  $\mu$ L SDS-loading-buffer (5 $\times$ ). The gels were loaded in the electrophoresis chamber, with the use of SDS-chamber-buffer for the Glycine-SDS-PAGE and the Anode/Kathode-buffer for Tricine-SDS-PAGE, and run at ~25 °C, at 180 V for 1 h. Gels were then stained, after a 30 min wash step (water), with colloidal Coomassie G-250 solution over night. After removal of the staining solution, the results of the SDS-PAGE were documented by photography.

**Table 29** Composition of the solutions required for SDS-PAGE analysis of protein samples.

Solution	Composition
Glycine-SDS-PAGE	
Separation gel (12%, 4 gels)	12 mL separation gel buffer (0.6 M Tris/HCl, pH 8.8, 0.16% SDS), 7.9 mL acryl amide/bis acryl amide (30%, 37.5 : 1; <i>Carl Roth</i> ), 100 $\mu$ L APS (10% w/v), 100 $\mu$ L TEMED
Stacking gel (4.5%, 4 gels)	6.83 mL stacking gel buffer (0.13 M Tris/HCl, pH 6.8, 1.08% SDS), 1.2 mL acryl amide/bis acryl amide (30%, 37.5 : 1; <i>Carl Roth</i> ), 100 $\mu$ L APS (10% w/v), 100 $\mu$ L TEMED
SDS-Chamber-buffer (1 $\times$ )	25 mM TRIS, 192 mM glycine, 0.1% w/v SDS
Tricine-SDS-PAGE:	
Separation gel	10 mL acryl amide/bis acryl amide (30%, 37.5 : 1; <i>Carl Roth</i> ), 10 mL gel buffer (3 $\times$ ), 70 mL aqua dest., 3 g glycerol, 150 $\mu$ L APS (10% w/v), 15 $\mu$ L TEMED

Stacking gel	1.6 mL acryl amide/bis acryl amide (30%, 37.5 : 1; <i>Carl Roth</i> ), 3 mL gel buffer (3×), 7.4 mL aqua dest., 100 µL APS (10% w/v), 10 µL TEMED
Gel-buffer (3×)	3 M TRIS, 1 M HCl, 0.3% (w/v) SDS, pH 8.45
Anode-buffer (10×)	1 M TRIS, 0.225 M HCl, pH 8.9
Kathode-buffer (10×)	1 M TRIS, 1 M Tricine, 1% w/v SDS, pH 8.25
General	
SDS-loading-buffer 5x	10% (w/v) SDS, 30% (w/v) sucrose, 0.1% (w/v) bromphenolic blue, 0.5 M Tris/HCl, pH 6.8, 50 mM DTT
Colloidal Coomassie G-250 solution	2% (w/v) phosphoric acid, 10% (v/v) ethanol, 5% (w/v) aluminium sulphate, 0.02% (w/v) Coomassie brilliant blue G-250

## 8.5 Biocatalytic assays

### 8.5.1 Hydrolytic activity

Characterisation of all *wt* glycosidases was carried out using *p*-nitrophenyl glycoside substrates. For hydrolytic activity measurements of Abg, BglU, and Cbg1, 20 µL purified enzyme solution was added to 180 µL *p*-nitrophenyl glucopyranoside (**5h**, 20 mM) in NH<sub>4</sub>HCO<sub>3</sub>-buffer (150 mM, pH 7.9) or KP<sub>i</sub>-buffer (50 mM, pH 7.5) at 25 °C. For hydrolytic activity measurements of RhaB, 20 µL purified enzyme solution was added to 180 µL *p*-nitrophenyl rhamnopyranoside (**5r**, 10 mM) in KP<sub>i</sub>-buffer (50 mM, pH 7.5) at 25 °C. The absorption of released *p*-nitrophenol (**13b**) was measured at 410 nm for a 5–10 min reaction time. The *wt* BglC was characterised in citrate-phosphate-buffer (35 mM trisodium citrate, 128 mM NaH<sub>2</sub>PO<sub>4</sub>, pH 6) containing *p*-nitrophenyl glucopyranoside (**5h**, 40 mM) for 20 min at 85 °C. Before absorption measurement, 200 µL Na<sub>2</sub>CO<sub>3</sub> solution (0.2 mM) was added to the mixture. In all cases the concentration of released *p*NP **13b** was determined *via* a calibration with *p*NP (75 µM–2 mM, **13b**) in the respective buffer. Kinetic parameters were measured with substrate concentrations ranging from 100 µM–72 mM. Temperature dependency was measured identically to the hydrolytic activity in a range from 7 °C to 85 °C. All measurements were carried out in triplicate for determination of the standard deviation.

### 8.5.2 Coniferin hydrolysis

The activity of Cbg1 and mutant variants of Cbg1 towards the natural substrate coniferin (**14a**) was determined by the assay described by *Castle et al.*<sup>[85]</sup> In a microplate, 20  $\mu\text{L}$  of the to be examined enzyme solution was added to 90  $\mu\text{L}$  substrate solution (0.5 mM coniferin, 50 mM  $\text{KPi}$ -buffer, pH 7.5). The reaction was halted by addition of 20  $\mu\text{L}$   $\text{Na}_2\text{CO}_3$  solution (0.1 M) and the absorption at 490 nm recorded as a blank reading. The absorption at 490 nm was recorded once more after addition of 20  $\mu\text{L}$  *Fast Blue RR* salt solution (5 mg/mL). The *Fast Blue RR* salt (*Sigma-Aldrich*) reacts with released coniferyl alcohol (**14b**) observable as a red colouration. Calibration of the assay was carried out measuring the 490 nm absorption of various coniferyl alcohol (**14b**) concentrations.

### 8.5.3 Glycosynthase activity assay

#### Quantification of fluoride

The fluoride concentration in enzymatic reactions was measured by cleavage of TIPS $p$ NP (**23**) in aqueous acetonitrile. Therefore, after biocatalysis 20  $\mu\text{L}$  of the enzymatic reaction was added to 180  $\mu\text{L}$  acetonitrile containing 1 mM TIPS $p$ NP (**23**) in a 96-well microplate. The mixture was allowed to react for 10 min at 25  $^\circ\text{C}$  before transferring 100  $\mu\text{L}$  of the solution in to a new well for absorption measurement at 410 nm. The transfer step was necessary due to precipitate formation after addition of the enzymatic reaction mixture to the organic solution, which would disturb the absorption measurement. Calibration of the assay was carried out with varying solutions of sodium fluoride (75  $\mu\text{M}$ –2 mM). The slope of the calibration curve was used to determine the concentration of fluoride *via* absorption at 410 nm. The limit of detection (LOD) and limit of quantification (LOQ) of the developed assay was determined by linear regression (50  $\mu\text{M}$ –160  $\mu\text{M}$  NaF calibration) with  $\text{LOD} = 3 \cdot S_a/b$  and  $\text{LOQ} = 10 \cdot S_a/b$  ( $S_a$  = standard deviation of the response;  $b$  = slope of the calibration curve).<sup>[196]</sup>

#### Glycosynthase activity

For synthetic activity measurements of potential and actual glycosynthases, the fluoride, released by the conversion of the respective glycosyl fluoride donor, was determined by the fluoride quantification described above. The substrate solution containing the donor and acceptor compounds were prepared for BglU-E377A and Abg-E358S in  $\text{NH}_4\text{HCO}_3$ -buffer (150 mM, pH 7.9) and for the BglC variants E113S, E189S and E316S in citrate-phosphate-buffer (35 mM trisodium citrate, 128 mM  $\text{NaH}_2\text{PO}_4$ , pH 6). Substrates for the mutated variants of Cbg1 and RhaB were prepared in  $\text{KPi}$ -buffer (50 mM, pH 7.5). In a 96-well microplate, 20  $\mu\text{L}$  of the respective enzyme solution was added to 80  $\mu\text{L}$  of the substrate

solution to start the biocatalytic reaction. Stopping of the reaction and quantification of the released fluoride was carried out by the cleavage of TIPS $\rho$ NP (**23**) as described above.

For the acceptor screening of BglU-E377A and Abg-E358S,  $\alpha$ -GlcF **2a** was used as the donor molecule which was dissolved in  $\text{NH}_4\text{HCO}_3$ -buffer (150 mM, pH 7.89) with the acceptor molecule of interest (**15b–g**, **11a–h**, **5a/b**, **5g–l**, **5r**, **1a–c**) in a ratio of 1:2 (donor : acceptor). The screening was carried out with 24 different alcohols. Stock-solutions for each acceptor molecule **15b–g**, **11a–h**, **5a/b**, **5g–l**, **5r**, **1a–c** (80, 20, and 10 mM) and donor molecule **2a** (66,7, 16,7, and 8,3 mM) were generated. Due to the low solubility of some alcohols, 10% acetonitrile was added as a co-solvent if necessary and samples (buffer containing only the acceptor) were heated and sonicated until complete solubilisation. The screening reaction was initiated by addition of 20  $\mu\text{L}$  enzyme solution towards a mixture of 30  $\mu\text{L}$  donor- and 50  $\mu\text{L}$  acceptor stock-solutions. Reactions containing only the glycosyl donor **2a** were also carried out to exclude self-coupling of the donor. Fluoride release was subsequently quantified as described above. The reactions were carried out in triplicate and control reactions without enzyme (only the addition of buffer) were measured.

### 8.5.4 Chemical recovery experiments

#### Enzymatic assay

The recovery of activity of mutated glycosidases in the presence of external nucleophiles was determined by chemical recovery experiments. The enzymatic reaction was carried out identically to the hydrolytic activity measurements (section 8.5.1) with the addition of the external nucleophile (azide or formate) in the respective substrate solution. The cleavage of the *p*-nitrophenyl glycopyranoside was followed by absorption at 410 nm and the concentration of released *p*NP **13b** determined by calibration measurements with different *p*NP **13b** concentrations. Reactions were carried out in triplicate for determination of the standard deviation. Control reactions with no external nucleophile were measured simultaneously to exclude catalysis by the mutant glycosidase without an external nucleophile.

In the cases of Cbg1 and RhaB, the transferral of the potential glycosyl donor, produced by the chemically recovered activity, onto an acceptor was tested by adding the acceptor to the substrate solution before addition of the enzyme solution.

#### Quantification of azide

The release or incorporation of azide ions during chemical recovery experiments was determined in a microplate assay using acidic  $\text{FeCl}_3$  solution. Therefore, 20  $\mu\text{L}$  of the

enzymatic reaction was added to 80  $\mu\text{L}$  of a 40 mM  $\text{FeCl}_3$  in 10 mM HCl solution and thoroughly mixed. The absorption at 456 nm was measured immediately and the concentration of azide calculated by comparison of the absorption with a calibration (sodium azide solutions ranging from 1–10 mM). Control reactions containing no enzyme were recorded to exclude a conversion or release of azide without participation of the examined enzyme.

### 8.5.5 Glycosylation modification of RNase B

#### De-glycosylation of RNase B

To obtain the acceptor protein RNase B-GlcNAc, native RNase B was de-glycosylated by digestion with the enzyme Endo-H. The reaction mixture contained 10 mg native RNase B, 5  $\mu\text{L}$  10 $\times$  G5-buffer and 5  $\mu\text{L}$  Endo-H (1 kU) in a total volume of 50  $\mu\text{L}$  and was incubated for 12 h at 37  $^\circ\text{C}$ . The reaction was then heat-deactivated at 70  $^\circ\text{C}$  for 1 h. Centrifugation removed aggregated Endo-H enzyme and the supernatant was subjected to further reactions/analysis.

#### Glycosylation of RNase B-GlcNAc

RNase B-GlcNAc (2  $\mu\text{g}$ ) was incubated at 30  $^\circ\text{C}$  for 2 h with 150  $\mu\text{g}$  SGP **20** and 0.75 mU Endo-CC N180H in KPi-buffer (25 mM, pH 7.5) in a total volume of 10  $\mu\text{L}$ . The reaction was stopped by heating at 100  $^\circ\text{C}$  for 3 min. The product was then analysed by Tricine-SDS-PAGE.

### 8.5.6 Naringinase deactivation and activity assay

The  $\beta$ -glucosidase activity of the naringinase of *P. decumbens* was deactivated by the procedure described by Vila-Real *et al.*<sup>[103]</sup> Therefore, the lyophilised naringinase (1 mg/mL) was dissolved in the deactivation-buffer and incubated at 82  $^\circ\text{C}$  for 16 min. The enzyme solution was then kept on ice and used directly or lyophilised and stored at -20  $^\circ\text{C}$ . The activity was measured by a discontinuous activity assay for the naringinase carried out in microplate wells. Buffer A and a 2 mM *p*NPGlc **5h** or *p*NPRha **5r** substrate solution were combined with the enzyme solution (1 g/L) at room temperature ( $\sim$ 25  $^\circ\text{C}$ , Table 30). The reaction (200  $\mu\text{L}$  reaction volume) was halted after 1.5 min ( $\alpha$ -L-rhamnosidase activity) or 5 min ( $\beta$ -D-glucosidase activity) by the addition of 8.8  $\mu\text{L}$  1 M aqueous NaOH and the absorption measured at 410 nm. Calibration curves for the concentration determination of *p*-nitrophenol (**13b**) was carried out with various concentrations in Buffer A (200  $\mu\text{L}$ ) with the addition of 8.8  $\mu\text{L}$  of 1 M NaOH.

**Table 30** Composition of the buffers (left) required for deactivation and activity measurement of the naringinase of *P. decumbens* and the respective activity assay (right). The NaOH solution is added after incubation of the reaction.

Buffer	Composition	Solution	Volume [μL]
Buffer A	20 mM sodium citrate/ citric acid, pH 3.4	Buffer A	170
Deactivation-buffer	20 mM sodium citrate/ citric acid, pH 3.9	<i>p</i> NPGlc/ <i>p</i> NPRha <b>5h/r</b> (20 mM, in Buffer A)	20
		Enzyme solution (1 mg/mL)	10
		NaOH (1 M)	8.8

## 8.6 Chemical synthesis

### 8.6.1 Chromatography

#### Reaction product separation and analysis

For column chromatography, silica gel 60M (0.040–0.063 mm, 230–400 mesh) purchased from *Machery-Nagel* (Düren, Germany) was used. Respective solvent mixtures were made using low boiling petroleum ether (b.p.: 40–60 °C), ethyl acetate, dichloromethane, ethanol, methanol and water. Standard and reverse phase TLCs were carried out on POLYGRAM® SIL G/UV<sub>254</sub> with fluorescence-indicator and ALUGRAM® RP-18 W/UV<sub>254</sub> from *Machery-Nagel* (Düren, Germany). Compound visualisation was carried out *via* UV-absorption and staining with either cerium-molybdenum-staining solution [10 g Ce(SO<sub>4</sub>)<sub>2</sub>·4 H<sub>2</sub>O, 25 g phosphomolybdic acid, 60 mL conc. H<sub>2</sub>SO<sub>4</sub>, 940 mL H<sub>2</sub>O] or vanillin-staining solution (12 g vanillin, 200 mL ethanol, 5 mL H<sub>2</sub>SO<sub>4</sub>) and subsequent heating with a heat gun.

#### HPLC analysis of SGP-glycosides

HPLC analysis was carried out using the Cosmosil 5C<sub>18</sub>-MS reverse phase column (150 mm × 4.6 mm). The column was equilibrated with 0.1% (v/v) trifluoro acetic acid at a flow-rate of 0.9 mL/min. The product and substrate were eluted depending on the type of glycoside. Flavonoid substrates were eluted using a linear gradient of 0–30% (v/v) acetonitrile in 0.1% trifluoro acetic acid over 30 min and detected by absorption at 290 nm. The acceptor and product of pNPGlcNAc **5a** was eluted using a linear gradient of 0–20% (v/v) acetonitrile in 0.1% trifluoro acetic acid over 30 min and detected by absorbance at 280 nm. UDP-GlcNAc **28** reactions were analysed using 100 mM acetic acid neutralised to pH 7 with triethylamine at a flow-rate of 0.5 mL/min.

### 8.6.2 LC-MS analysis

The LC-MS analysis occurred *via* an *Agilent* 1100 Series LC-mass spectrometer (*Agilent Technologies*, Santa Clara, CA, USA) equipped with a diode array- and atmospheric pressure ionisation (API) electrospray mass detector. Compound mixtures were separated by a reversed phase Atlantis T3 column (100 mm×3.0 mm, 3 μm). Water and methanol both containing 0.1% (v/v) formic acid were applied as elution solvents. The separation occurred using the following procedure:

0.00 min H<sub>2</sub>O/MeOH (90 : 10); 4.00 min H<sub>2</sub>O/MeOH (40 : 60); 6.00 min MeOH.

The flowrate and column temperature was held constant at 0.6 mL/min and 30 °C respectively and the procedure halted after 10 min. Samples were prepared in H<sub>2</sub>O : acetonitrile (50 : 50) and the injection volume of the sample was 10 µL. Absorption was detected at the wavelengths 250 nm, 510 nm, 520 nm, 535 nm, and 540 nm. Mass detection occurred in the positive mode. Compounds were identified by the UV-absorption, mass to charge ratio ( $m/z$ ), or the measurement of reference compounds.

### 8.6.3 Mass spectrometry

For the determination of the molecular weight of the (*via* HPLC) isolated transglycosylation product (section 8.6.1) electrospray ionisation-ion trap-mass spectrometry was used. The measurement was carried out with a HCT plus ion-trap mass spectrometer operated in the negative ion mode. The nebulizer flow was 10 psi with a dry gas flow-rate of 5 L/min and a temperature of 300 °C. Samples for the ESI-MS were dissolved in 50% acetonitrile (*v/v*) in a concentration of 1 nmol/µL.

High-resolution mass spectra were measured by the Central Institute for Engineering, Electronics and Analytics (ZEA-3) of the *Forschungszentrum Jülich GmbH*. The spectra were recorded using Fourier-transform ion cyclotronresonance mass spectrometry (FT-ICR-MS) after ionisation of the sample by electrospray ionisation (ESI). Samples were provided in solution (methanol). The theoretical and recorded mass values are given for the respective compounds.

### 8.6.4 NMR-Spectroscopy

The recordings of <sup>1</sup>H- and <sup>13</sup>C-NMR-spectra were carried out using following instruments:

<sup>1</sup>H-NMR-Spectra: Bruker Avance/DRX 600 (Measurement frequency: 600 MHz)

<sup>13</sup>C-NMR-Spectra: Bruker Avance/DRX 600 (Measurement frequency: 151 MHz)

The spectra were recorded using deuterated chloroform, D<sub>2</sub>O or d<sub>6</sub>-DMSO. The <sup>1</sup>H- and <sup>13</sup>C-spectra were calibrated using the characteristic signals of CDCl<sub>3</sub> (<sup>1</sup>H: 7.26 ppm; <sup>13</sup>C: 77.00 ppm), D<sub>2</sub>O (<sup>1</sup>H: 4.79 ppm), and d<sub>6</sub>-DMSO (<sup>1</sup>H: 2.5 ppm; <sup>13</sup>C: 40.00 ppm). Chemical shifts  $\delta$  and coupling constants  $J$  are given in ppm and Hz respectively. Assignment of each signal was carried out by comparison of coupling constants  $J$  and additional DEPT-, COSY- and HSQC-spectra. Connectivity of oligosaccharides was determined by HMBC-spectra showing the coupling of a specific anomeric proton with the respective proton of the preceding

saccharide. Signal multiplicities were given the appropriate abbreviations: s (singlet), bs (broad singlet), d (doublet), t (triplet), q (quartet), m (multiplet).

### 8.6.5 IR-Spectroscopy

IR-spectra were recorded using a *PerkinElmer* SpectrumOne IR-Spectrometer. The ATR-procedure was used for each measurement and the absorption bands of each spectrum listed as wave numbers  $\tilde{\nu}(\text{cm}^{-1})$ . The analysis of the spectra was limited to only strong characteristic absorption bands, which allowed the characterisation and identification of the analysed molecule. In some cases a classification of the band is added (e.g. br = broad, w = weak). The bands were also differentiated into valence vibrations ( $\nu$ ) and deformation vibrations ( $\delta$ ).

### 8.6.6 Measurement of rotatory power ( $[\alpha]_{\text{D}}^{20}$ )

The rotatory power of each compound was measured using the polarimeter of *PerkinElmer* at 589 nm (sodium-D-line) in a tempered cylindrical cuvette (1 dm in length). The solvent, concentration ( $c = \text{g/mL}$ ) and temperature used in each measurement are given with the analytical data of the respective compound.

### 8.6.7 Melting points

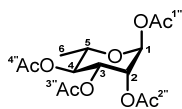
The melting points of crystalline compounds were determined using the *Point SMP-20* apparatus from *Büchi*.

### 8.6.8 Peracetylation of monosaccharides

The peracetylation of  $\beta$ -D-glucose (**11b**) was described by *Steinmann et al.* and was transferred to other monosaccharides such as  $\alpha/\beta$ -D-xylose (**11a**) and  $\alpha$ -L-rhamnose (**11e**) in this thesis.<sup>[154]</sup> The peracetylation was carried out in a 25 mL round-bottom flask with 91 mg (5.5 mmol) or 1.0 g (6.7 mmol) of the respective sugar **11a** or **11e** in 1 mL/mmol pyridine. Acetic anhydride (1.5 equiv/OH-group of the respective sugar) was slowly added to the reaction solution and the reaction stirred overnight (18 h) at room temperature ( $\sim 25^\circ\text{C}$ ). The reaction mixture was then diluted with 5 mL  $\text{Et}_2\text{O}$  and pyridine removed by extraction with saturated  $\text{CuSO}_4$ -solution. The organic phase was dried over  $\text{MgSO}_4$  and filtered through

*Celite*. The solvent was removed under reduced pressure yielding the pure product in a  $\alpha/\beta$ -anomeric mixture. The analytical data was in accordance with literature.<sup>[197]</sup>

### 1,2,3,4-Tetra-O-acetyl- $\alpha,\beta$ -L-rhamnopyranoside **22q**



#### **22b**

**C<sub>14</sub>H<sub>20</sub>O<sub>9</sub>**

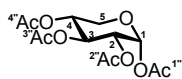
**[332.30]**

Clear syrup; Yield = 83% (1.5 g/ 4.6 mmol,  $\alpha$  :  $\beta$  mixture = 2.5 : 1);

**<sup>1</sup>H-NMR** (600 MHz, CDCl<sub>3</sub>):  $\delta$  [ppm] = 1.23 (d,  $^3J_{6,5}$  = 6.2 Hz, 3H, 6-H), 2.00 (s, 3H, Ac-H), 2.05 (s, 3H, Ac-H), 2.15 (s, 3H, Ac-H), 2.16 (s, 3H, Ac-H), 3.93 (tt,  $^3J_{5,4}$  = 12.4 Hz,  $^3J_{5,6}$  = 6.2 Hz, 1H, 5-H), 5.11 (dd,  $^3J_{4,5}$  = 10.0 Hz,  $^3J_{4,3}$  = 10.0 Hz, 1H, 4-H), 5.24 (dd,  $^3J_{2,3}$  = 3.3 Hz,  $^3J_{2,1}$  = 2.0 Hz, 1H, 2-H), 5.29 (dd,  $^3J_{3,4}$  = 10.1 Hz,  $^3J_{3,2}$  = 3.5 Hz, 1H, 3-H), 6.01 (d,  $^3J_{1,2}$  = 1.7 Hz, 1H,

1-H); **<sup>13</sup>C-NMR** (151 MHz, CDCl<sub>3</sub>):  $\delta$  [ppm] = 17.45 (CH<sub>3</sub>, C-6), 20.68, 20.76, 20.79, 20.91 (CH<sub>3</sub>, Ac), 68.64 (CH<sub>2</sub>, C-2), 68.72 (CH, C-5), 68.77 (CH, C-3), 70.48 (CH, C-4), 90.64 (CH, C-1), 168.39, 169.83, 169.85, 170.09 (CO, Ac); **IR** (ATR-film):  $\nu$  [cm<sup>-1</sup>] = 3016, 2970, 2935 (aliph. C-H-v), 1741, 1366, 1216 (ester, CO-v), 1051, 970 (C-H- $\delta$ ); **R<sub>f</sub>-Value**:  $\alpha$  0.49 (PE : EA = 1 : 1);  $\beta$  0.44 (PE : EA = 1 : 1).

### 1,2,3,4-Tetra-O-acetyl- $\alpha,\beta$ -D-xylopyranoside **22c**



#### **22c**

**C<sub>13</sub>H<sub>18</sub>FO<sub>9</sub>**

**[318.27]**

Clear syrup; Yield = 92% (1.9 g/ 6.1 mmol,  $\alpha$  :  $\beta$  mixture = 2.5 : 1);

**<sup>1</sup>H-NMR** (600 MHz, CDCl<sub>3</sub>):  $\delta$  [ppm] = 2.03 (s, 3H, Ac-H), 2.05 (s, 3H, Ac-H), 2.05 (s, 3H, Ac-H), 2.18 (s, 3H, Ac-H), 3.72 (t,  $^2J_{5,5}$  = 11.2 Hz,  $^3J_{5,4}$  = 11.2 Hz 1H, 5-H<sub>ax</sub>), 3.94 (dd,  $^2J_{5,5}$  = 11.2 Hz,  $^3J_{5,4}$  = 5.9 Hz, 1H, 5-H<sub>eq</sub>), 5.03 (m, 2H, 2/4-H), 5.47 (dd,  $^3J_{3,2}$  = 9.8 Hz,  $^3J_{3,4}$  = 9.8 Hz, 1H, 3-H), 6.62 (d,  $^3J_{1,2}$  = 3.6 Hz, 1H, 1-H); **<sup>13</sup>C-NMR** (151 MHz, CDCl<sub>3</sub>):  $\delta$  [ppm] = 20.49, 20.66,

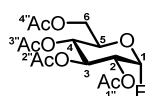
20.73, 20.86 (CH<sub>3</sub>, Ac), 60.65 (CH<sub>2</sub>, C-5), 68.67 (CH, C-4), 69.34 (CH, C-3), 69.34 (CH, C-2), 89.25 (CH, C-1), 169.00, 169.71, 169.76, 170.12 (CO, Ac); **R<sub>f</sub>-Value**: 0.49 (PE : EA = 1 : 1).

## 8.6.9 Fluorination of peracetylated glycosides

Fluorination of the peracetylated glycosides were each carried out in 100 mL plastic round-bottom flasks (Important! Plastic ware should always be used while working with hydrofluoric acid as glass wear will be degraded by the acid!). The peracetylated glycosides **22q**, **22a** or **22c** (5.68 mmol, 933 mg; 4.99 mmol, 1.95 g; 6.07 mmol, 1.93 g) were dissolved at 0 °C in HF/pyridine solution (1 mL/mmol peracetylated glycoside, 70% HF in pyridine). The reaction was stirred for 4 h at 0 °C and monitored by TLC (PE : EtOAc = 1 : 1).

After completion, the reaction was diluted with  $\text{CH}_2\text{Cl}_2$  (15 mL) and  $\text{dH}_2\text{O}$  (15 mL). Excess fluoric acid was neutralized using  $\text{K}_2\text{CO}_3$  powder and the organic phase separated from the aqueous ( $\text{K}_2\text{CO}_3$  is more effective for the neutralisation than  $\text{Na}_2\text{CO}_3$ , as  $\text{KF}$  is more soluble in  $\text{H}_2\text{O}$  than  $\text{NaF}$ ). Pyridine was removed by extraction with saturated  $\text{CuSO}_4$ -solution and the organic phase dried over  $\text{MgSO}_4$  and filtered. The solvent was removed under reduced pressure and the product purified by flash chromatography (**22d**, **22e**: PE : EA = 60 : 40, **22t**: PE : EA = 50 : 50). The analytical data was in accordance with literature.<sup>[198, 199]</sup>

### 2,3,4,6-Tetra-O-acetyl- $\alpha,\beta$ -D-glucopyranosyl fluoride **22d**

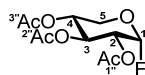


**22d**  
**C<sub>14</sub>H<sub>19</sub>FO<sub>9</sub>**  
**[350.29]**

Colourless solid, Yield = 57% (1.01 mg/ 2.88 mmol, 3 : 1  $\alpha$  :  $\beta$  mixture), 45% (797 mg/ 2.27 mmol,  $\alpha$ -anomer)

Analytical data for  $\alpha$ -anomer: **<sup>1</sup>H-NMR** (600 MHz,  $\text{CDCl}_3$ ):  $\delta$  [ppm] = 1.96 (s, 3H, Ac-H), 1.98 (s, 3H, Ac-H), 2.04 (s, 6H, Ac-H), 4.09 (dd,  $^2J_{6,6} = 12.6$  Hz, 1H, 6-H), 4.12 (m, 1H, 5-H), 4.22 (dd,  $^2J_{6,6} = 12.5$  Hz,  $^3J_{6,5} = 4.0$  Hz, 1H, 6-H), 4.89 (ddd,  $^3J_{2,F} = 24.2$  Hz,  $^3J_{2,3} = 10.2$  Hz,  $^3J_{2,1} = 2.6$  Hz, 1H, 2-H), 5.09 (dd,  $^3J_{4,3} = 9.9$  Hz,  $^3J_{4,5} = 9.9$  Hz, 1H, 4-H), 5.43 (dd,  $^3J_{3,4} = 9.9$  Hz,  $^3J_{3,2} = 9.9$  Hz, 1H, 3-H), 5.69 (dd,  $^2J_{1,F} = 52.8$  Hz,  $^3J_{1,2} = 2.4$  Hz, 1H, 1-H); **<sup>13</sup>C-NMR** (151 MHz,  $\text{CDCl}_3$ ):  $\delta$  [ppm] = 20.55, 20.61, 20.69 ( $\text{CH}_3$ , Ac), 61.2 ( $\text{CH}_2$ , C-6), 67.35 (CH, C-4), 69.40 (CH, C-3), 69.85 (CH, C-5), 70.14/70.30 (CH, C-2), 103.00/104.52 (CH, C-1), 169.43, 169.65, 169.99, 170.55 (CO, Ac); **IR** (ATR-film):  $\nu$  [ $\text{cm}^{-1}$ ] = 3012, 2958 (aliph. C-H-v), 1732, 1219 (ester, CO-v), 1035 (C-F- $\delta$ ); **R<sub>f</sub>-Value**:  $\alpha$  0.51 (PE : EA = 1 : 1),  $\beta$  0.50 (PE : EA = 1 : 1); **mp** = 109 °C (lit.: 108 °C);  **$[\alpha]_D^{20}$**  = +89 °  $\pm$  0.05 ° (c = 1.1,  $\text{CHCl}_3$ , lit.:  $[\alpha]_D^{20}$  = +90 °, c = 3.0,  $\text{CHCl}_3$ ).

### 2,3,4-Tri-O-acetyl- $\alpha$ -D-xylopyranosyl fluoride **22e**



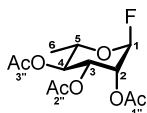
**22e**  
**C<sub>11</sub>H<sub>15</sub>FO<sub>7</sub>**  
**[278.23]**

Colourless solid; Yield = 56% (938 mg/ 3.37 mmol,  $\alpha$ -anomer);

**<sup>1</sup>H-NMR** (600 MHz,  $\text{CDCl}_3$ ):  $\delta$  [ppm] = 2.04 (s, 3H, Ac-H), 2.04 (s, 3H, Ac-H), 2.09 (s, 3H, Ac-H), 3.77 (t,  $^2J_{5,5} = 11.1$  Hz, 1H, 5- $\text{H}_{\text{ax}}$ ), 3.97 (dd,  $^2J_{5,5} = 11.2$  Hz,  $^3J_{5,4} = 5.9$  Hz, 1H, 5- $\text{H}_{\text{eq}}$ ), 4.88 (ddd,  $^3J_{2,F} = 24.1$  Hz,  $^3J_{2,3} = 10.1$  Hz,  $^3J_{2,1} = 2.7$  Hz, 1H, 2-H), 5.03 (td,  $^3J_{4,3} = 10.4$  Hz,  $^3J_{4,5} = 5.9$  Hz, 1H, 4-H), 5.49 (dd,  $^3J_{3,2} = 9.9$  Hz,  $^3J_{3,4} = 9.9$  Hz, 1H, 3-H), 5.68 (dd,  $^2J_{1,F} = 53.0$  Hz,  $^3J_{1,2} = 2.7$  Hz, 1H, 1-H); **<sup>13</sup>C-NMR** (151 MHz,  $\text{CDCl}_3$ ):  $\delta$  [ppm] = 20.56, 20.63, 20.67 ( $\text{CH}_3$ , Ac), 60.30 ( $\text{CH}_2$ , C-5), 68.21 (CH, C-4), 68.94 (CH, C-3), 70.42/70.58 (CH, C-2), 103.21/104.73 (CH, C-1), 169.82, 169.89, 170.06 (CO, Ac); **IR** (ATR-film):  $\nu$  [ $\text{cm}^{-1}$ ] = 3017, 2970 (aliph. C-H-v), 1741 (ester, CO-v), 1366 (anom. C-H-v), 1212 (ester, CO-v),

1047 (C-F- $\delta$ ); **R<sub>f</sub>-Value**: 0.54 (PE : EA = 1 : 1); **mp** = 63 °C (lit.: 87 °C); **[ $\alpha$ ]<sub>D</sub><sup>20</sup>** = +64 ° ± 0.07 ° (c = 1.0, CHCl<sub>3</sub>, lit.: [ $\alpha$ ]<sub>D</sub><sup>20</sup> = +67 °, CHCl<sub>3</sub>, c not given).

### 2,3,4-Tri-O-acetyl- $\alpha$ -L-rhamnopyranosyl fluoride **22t**



Clear syrup; Yield = 79% (1.31 g/ 4.49 mmol,  $\alpha$ -anomer, Yield of two steps: peracetylation, fluorination);

**<sup>1</sup>H-NMR** (600 MHz, CDCl<sub>3</sub>):  $\delta$  [ppm] = 1.25 (d, <sup>3</sup>J<sub>6,5</sub> = 6.2 Hz, 3H, 6-H), 1.98 (s, 3H, H-Ac), 2.04 (s, 3H, H-Ac), 2.14 (s, 3H, H-Ac), 4.02 (dq,

**22t**

<sup>3</sup>J<sub>5,4</sub> = 12.4 Hz, <sup>3</sup>J<sub>5,6</sub> = 6.2 Hz, 1H, 5-H), 5.10 (dd, <sup>3</sup>J<sub>4,5</sub> = 10.1 Hz,

**C<sub>12</sub>H<sub>17</sub>FO<sub>7</sub>**

<sup>3</sup>J<sub>4,3</sub> = 10.1 Hz, 1H, 4-H), 5.24 (ddd, <sup>3</sup>J<sub>2,F</sub> = 10.3 Hz, <sup>3</sup>J<sub>2,3</sub> = 3.5 Hz,

**[292.25]**

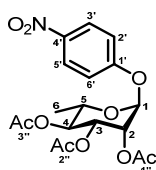
<sup>3</sup>J<sub>2,1</sub> = 1.6 Hz, 1H, 2-H), 5.36 (brs, 1H, 3-H), 5.47 (dd, <sup>2</sup>J<sub>1,F</sub> = 48.86 Hz, <sup>3</sup>J<sub>1,2</sub> = 1.5 Hz, 1H, 1-H);

**<sup>13</sup>C-NMR** (151 MHz, CDCl<sub>3</sub>):  $\delta$  [ppm] = 17.27 (CH<sub>3</sub>, C-6), 20.59, 20.69, 20.71 (CH<sub>3</sub>, Ac), 68.10 (CH, C-3), 68.21 (CH, C-2), 68.89 (CH, C-5), 69.94 (CH, C-4), 104.03/105.50 (CH, C-1);

**R<sub>f</sub>-Value**: 0.68 (PE : EA = 1 : 1).

### 8.6.10 O-Glycosylation

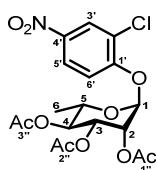
The O-glycosylation of aglycons **13b** and **13c** was generally carried out in a solution of the peracetylated glycoside in 3 mL/mmol CH<sub>2</sub>Cl<sub>2</sub>. The glycosides **22q** (4.6 mmol, 1.5 g) and **22a** (4.8 mmol, 1.9 g) were therefore dissolved in CH<sub>2</sub>Cl<sub>2</sub> and the aglycon **13b** or **13c** (1.5 equiv) and triethyl amine (0.5 equiv) were added to the solution. The lewis acid BF<sub>3</sub>·(OEt<sub>2</sub>) was added dropwise over 30 min at 0 °C to the reaction and then stirred over 72 h at room temperature (~25 °C). The reaction course was followed *via* TLC (PE : EtOAc = 1:1) and <sup>1</sup>H-NMR. Portions of saturated aqueous sodium bicarbonate (around 1 L in total) were added to the solution to extract left over starting material (extraction repeated until barely any colouration of the fresh aqueous phase occurred). The combined aqueous phases were extracted twice with a small amount of CH<sub>2</sub>Cl<sub>2</sub>. The combined organic phases were dried over MgSO<sub>4</sub>, filtered and the solvent removed under reduced pressure. The residual syrup was dissolved in a small amount of hot ethanol and the product obtained by crystallisation/precipitation and subsequent filtration (modification of the O-glycosylation method from Lee *et al.*).<sup>[153]</sup> The analytical data was in accordance with literature.<sup>[200, 201]</sup>

(4-Nitrophenyl)-2,3,4-tri-O-acetyl  $\alpha$ -L-rhamnopyranoside **22r****22r****C<sub>18</sub>H<sub>21</sub>NO<sub>10</sub>****[411.36]**

Colourless solid; Yield = 53% (1.0 g/ 2.4 mmol);

**<sup>1</sup>H-NMR** (600 MHz, CDCl<sub>3</sub>):  $\delta$  [ppm] = 1.21 (d,  $^3J_{6,5}$  = 6.3 Hz, 3H, 6-H), 2.05 (s, 3H, Ac-H), 2.07 (s, 3H, Ac-H), 2.22 (s, 3H, Ac-H), 3.90 (dq,  $^3J_{5,4}$  = 10.0 Hz,  $^3J_{5,6}$  = 6.3 Hz, 1H, 5-H), 5.18 (dd,  $^3J_{4,3}$  = 10.0 Hz,  $^3J_{4,5}$  = 10.0 Hz, 1H, 4-H), 5.45 (dd,  $^3J_{2,3}$  = 3.5 Hz,  $^3J_{2,1}$  = 1.8 Hz, 1H, 2-H), 5.49 (dd,  $^3J_{3,4}$  = 10.1 Hz,  $^3J_{3,2}$  = 3.5 Hz, 1H, 3-H), 5.57 (d,  $^3J_{1,2}$  = 1.6 Hz, 1H, 1-H), 7.19 (m, 2H, Ph-H), 8.23 (m, 2H, Ph-H); **<sup>13</sup>C-NMR** (125 MHz, CDCl<sub>3</sub>):

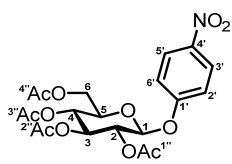
$\delta$  [ppm] = 17.42 (CH<sub>3</sub>, C-6), 20.74, 20.77, 20.87 (CH<sub>3</sub>, Ac), 67.84 (CH, C-5), 69.55 (CH, C-3), 69.71 (CH, C-2), 70.48 (CH, C-4), 95.56 (CH, C-1), 116.30, 125.91, 142.93, 160.14 (CH, Ph), 169.90, 170.05, 170.06 (CO, Ac); **IR** (ATR-film):  $\nu$  [cm<sup>-1</sup>] = 3118, 3083 (arom. C-H-v), 2980, 2936, 2916 (aliph. C-H-v), 1746 (ester, CO-v), 1594 (arom. CC-v), 1515, 1369 (NO-v), 1210 (ester, CO-v); **R<sub>f</sub>-Value**: 0.58 (PE : EA = 1 : 1).

(2-Chloro-4-nitrophenyl)-2,3,4-tri-O-acetyl  $\alpha$ -L-rhamnopyranoside **22s****22s****C<sub>18</sub>H<sub>20</sub>ClNO<sub>10</sub>****[445.81]**

Colourless solid; Yield = 32% (0.72 g/ 1.2 mmol);

**<sup>1</sup>H-NMR** (600 MHz, CDCl<sub>3</sub>):  $\delta$  [ppm] = 1.20 (d,  $^3J_{6,5}$  = 6.2 Hz, 3H, 6-H), 2.03 (s, 3H, Ac-H), 2.06 (s, 3H, Ac-H), 2.20 (s, 3H, Ac-H), 3.91 (dq,  $^3J_{5,4}$  = 12.4 Hz,  $^3J_{5,6}$  = 6.2 Hz, 1H, 5-H), 5.19 (dd,  $^3J_{4,3}$  = 9.9 Hz,  $^3J_{4,5}$  = 9.9 Hz, 1H, 4-H), 5.51 (m, 1H, 2-H), 5.53 (dd,  $^3J_{3,4}$  = 10.0 Hz,  $^3J_{3,2}$  = 3.5 Hz, 1H, 3-H), 5.63 (d,  $^3J_{1,2}$  = 1.5 Hz, 1H, 1-H), 7.28 (d,  $^3J_{Ph,Ph}$  = 9.2 Hz, 1H, Ph-H), 8.13 (dd,  $^3J_{Ph,Ph}$  = 9.1 Hz,  $^3J_{Ph,Ph}$  = 2.7 Hz, 1H, Ph-H), 8.31 (d,  $^3J_{Ph,Ph}$  = 2.7 Hz, 1H, Ph-H); **<sup>13</sup>C-NMR** (151 MHz, CDCl<sub>3</sub>):  $\delta$  [ppm] = 17.39 (CH<sub>3</sub>, C-6), 20.68, 20.76, 20.83 (CH<sub>3</sub>, Ac), 68.34 (CH, C-5), 68.49 (CH, C-3), 69.17 (CH, C-2), 70.32 (CH, C-4), 96.17 (CH, C-1), 115.01, 123.71, 124.58, 126.29, 142.73, 156.14 (CH, Ph), 169.85, 169.91, 170.01 (CO, Ac); **IR** (ATR-film):  $\nu$  [cm<sup>-1</sup>] = 3001, 2970, 2945 (aliph. C-H-v), 1741 (ester, CO-v), 1586 (arom. CC-v), 1520 (NO-v), 1366 (ester, CO-v), 1345 (NO-v), 1216 (ester, CO-v), 976 (C-Cl-v); **R<sub>f</sub>-Value**:

0.58 (PE : EA = 1 : 1); **mp** = 177 °C; **[ $\alpha$ ]<sub>D</sub><sup>20</sup>** = -93 °  $\pm$  0.21 ° (c = 1.0, CHCl<sub>3</sub>).

(4-Nitrophenyl)-2,3,4,6-tetra-O-acetyl  $\beta$ -D-glucopyranoside **22b****22b****C<sub>20</sub>H<sub>23</sub>NO<sub>12</sub>****[469.39]**

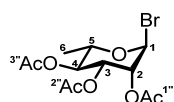
Colourless solid; Yield = 46% (1.1 g/ 2.3 mmol);

**<sup>1</sup>H-NMR** (600 MHz, CDCl<sub>3</sub>):  $\delta$  [ppm] = 2.05 (s, 3H, Ac-H), 2.07 (s, 3H, Ac-H), 2.07 (s, 3H, Ac-H), 2.08 (s, 3H, Ac-H), 3.96 (ddd, <sup>3</sup>J<sub>5,4</sub> = 10.0 Hz, <sup>3</sup>J<sub>5,6</sub> = 5.5 Hz, <sup>3</sup>J<sub>5,6</sub> = 2.4 Hz, 1H, 5-H), 4.19 (dd, <sup>2</sup>J<sub>6,6</sub> = 12.4 Hz, <sup>3</sup>J<sub>6,5</sub> = 2.4 Hz, 1H, 6-H), 4.29 (dd, <sup>2</sup>J<sub>6,6</sub> = 12.4 Hz, <sup>3</sup>J<sub>6,5</sub> = 5.5 Hz, 1H, 6-H), 5.19 (m, 1H, 4-H), 5.24 (d, <sup>3</sup>J<sub>1,2</sub> = 7.3 Hz, 1H, 1-H), 5.32 (m, 2H, 3-H/2-H), 7.09 (m, 2H, Ph-H), 8.21 (m, 2H, Ph-H); **<sup>13</sup>C-NMR** (125 MHz,

CDCl<sub>3</sub>):  $\delta$  [ppm] = 20.56, 20.56, 20.59, 20.66 (CH<sub>3</sub>, Ac), 61.82 (CH<sub>2</sub>, C-6), 68.01 (CH, C-4), 70.93 (CH, C-2/3), 72.41 (CH, C-2/3), 72.42 (CH, C-5), 98.05 (CH, C-1), 116.63, 125.79, 143.26, 161.16 (CH, Ph), 169.20, 169.37, 170.15, 170.44 (CO, Ac); **IR** (ATR-film):  $\nu$  [cm<sup>-1</sup>] = 2952 (aliph. C-H-v), 1752, 1730 (ester, CO-v), 1593 (NO-v), 1519 (arom. CC-v), 1340 (NO-v), 1210 (ester, CO-v), 1036 (ether, C-O-v), 862; **mp** = 176 °C (lit.: 175–177 °C); **[ $\alpha$ ]<sub>D</sub><sup>20</sup>** = -38 °  $\pm$  0.23 ° (c = 1.1, CHCl<sub>3</sub>, lit: [ $\alpha$ ]<sub>D</sub><sup>20</sup> = -31 °, c = 1.0, CHCl<sub>3</sub>).

**8.6.11 One-pot peracetylation and bromination of  $\alpha$ -L-rhamnose (11e)**

In a round-bottom flask 1.33 mL of HBr/AcOH (33%) was added slowly to a suspension of 1.0 g  $\alpha$ -L-rhamnose (**11e**, 6.1 mmol) in 5 mL acetic anhydride. Once all of compound **11e** had gone into solution (~5 min) further 5.65 mL HBr/AcOH (33%) was added to the solution. The reaction was followed by <sup>1</sup>H-NMR. The reaction could not be followed by TLC, as product **22u** was instable on silica gel. After completion of the reaction (24 h), the reaction was diluted with toluene (5 mL) and HBr/AcOH removed under reduced pressure (addition of solid sodium hydroxide in the solvent trap for neutralisation). The mixture was repeatedly co-evaporated with toluene. The residue was dissolved in 5 mL diethyl ether and the solvent again removed under reduced pressure resulting in the product **22u** (96%, 5.3 mmol, 1.9 g) as a brown syrup. The analytical data was in accordance with literature.<sup>[202]</sup>

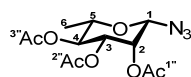
2,3,4-tri-*O*-acetyl  $\alpha$ -L-rhamnopyranosyl bromide **22u****22u****C<sub>12</sub>H<sub>17</sub>BrO<sub>7</sub>****[353.16]**

Brown syrup; Yield = 96% (1.9 g/ 5.3 mmol);

**<sup>1</sup>H-NMR** (600 MHz, CDCl<sub>3</sub>):  $\delta$  [ppm] = 1.28 (d,  $^3J_{\text{CH}_3,5}$  = 6.3 Hz, 3H, 6-H), 2.00 (s, 3H, Ac-H), 2.07 (s, 3H, Ac-H), 2.16 (s, 3H, Ac-H), 4.10 (dq,  $^3J_{5,4}$  = 10.0 Hz,  $^3J_{5,6}$  = 6.3 Hz, 1H, 5-H), 5.15 (dd,  $^3J_{4,5}$  = 10.1 Hz,  $^3J_{4,3}$  = 10.1 Hz, 1H, 4-H), 5.44 (dd,  $^3J_{2,3}$  = 3.4 Hz,  $^3J_{2,1}$  = 1.6 Hz, 1H, 2-H), 5.66 (dd,  $^3J_{3,4}$  = 10.2 Hz,  $^3J_{3,2}$  = 3.4 Hz, 1H, 3-H), 6.25 (d,  $^3J_{1,2}$  = 0.8 Hz, 1H, 1-H); **<sup>13</sup>C-NMR** (125 MHz, CDCl<sub>3</sub>):  $\delta$  [ppm] = 16.98 (CH<sub>3</sub>, C-6), 20.62, 20.75, 20.79 (CH<sub>3</sub>, Ac), 67.93 (CH, C-3), 70.32 (CH, C-4), 71.12 (CH, C-5), 72.46 (CH, C-2), 83.71 (CH, C-1), 169.64, 169.78, 169.87 (CO, Ac); **IR** (ATR-film):  $\nu$  [cm<sup>-1</sup>] = 2992, 2970, 2936 (aliph. C-H-v), 1746, 1368, 1205 (ester, C=O-v), 676 (C-Br-v);  **$[\alpha]_D^{20}$**  = -144 °  $\pm$  0.36 ° (c = 1.0, CHCl<sub>3</sub>, lit:  **$[\alpha]_D^{20}$**  = -172 °, c = 1, CHCl<sub>3</sub>).

**8.6.12 Synthesis of 2,3,4-tri-*O*-acetyl  $\beta$ -L-rhamnopyranosyl azide (22v)**

Compound **22u** (0.29 g, 0.82 mmol) was dissolved in HMPA (1.8 mL/mmol) and sodium azide (4.1 mmol, 5 equiv) added slowly to the reaction solution. The suspension was heated to 75 °C and the reaction course followed by <sup>1</sup>H-NMR. The solution was poured into ice water and the mixture extracted three times with CH<sub>2</sub>Cl<sub>2</sub>. The combined organic phases were dried over MgSO<sub>4</sub> and filtered. The solvent was removed under reduced pressure and the residue washed with ice water. The product **22v** (0.92 mmol, 0.29 mg) was dried by freezing in liquid nitrogen and lyophilisation of the sample. The analytical data was in accordance with literature.<sup>[166]</sup>

2,3,4-tri-*O*-acetyl  $\beta$ -L-rhamnopyranosyl azide **22v****22v****C<sub>12</sub>H<sub>14</sub>N<sub>3</sub>O<sub>7</sub>****[315.28]**

Colourless/yellow solid; Yield = 112% (0.29 g/ 0.92 mmol), residual HMPA present;

**<sup>1</sup>H-NMR** (600 MHz, CDCl<sub>3</sub>):  $\delta$  [ppm] = 1.31 (d,  $^3J_{6,5}$  = 6.2 Hz, 3H, 6-H), 1.98 (s, 3H, Ac-H), 2.05 (s, 3H, Ac-H), 2.19 (s, 3H, Ac-H), 3.62 (dq,  $^3J_{5,4}$  = 9.6 Hz,  $^3J_{5,6}$  = 6.2 Hz, 1H, 5-H), 4.68 (d,  $^3J_{1,2}$  = 1.0 Hz, 1H, 1-H), 4.98 (dd,  $^3J_{3,4}$  = 10.2 Hz,  $^3J_{3,2}$  = 3.3 Hz, 1H, 3-H), 5.07 (dd,  $^3J_{4,5}$  = 9.9 Hz,  $^3J_{4,3}$  = 9.9 Hz, 1H, 4-H), 5.42 (dd,  $^3J_{2,3}$  = 3.3 Hz,  $^3J_{2,1}$  = 1.2 Hz, 1H, 2-H); **<sup>13</sup>C-NMR** (125 MHz, CDCl<sub>3</sub>):  $\delta$  [ppm] = 17.37 (CH<sub>3</sub>, C-6), 20.57, 20.75, 20.76 (CH<sub>3</sub>, Ac), 69.59 (CH, C-2), 69.96 (CH, C-4), 70.99 (CH, C-3), 72.95 (CH, C-5), 84.95 (CH, C-1), 169.79, 170.07, 170.07 (CO, Ac); **IR** (ATR-film):  $\nu$  [cm<sup>-1</sup>] = 2987, 2970, 2942 (aliph. C-H-v), 2121 (azide,

N≡N-v), 1742, 1366, 1206 (ester, C=O-v), 1050;  $[\alpha]_D^{20} = +23^\circ \pm 0.11^\circ$  (c = 1.0, CHCl<sub>3</sub>, lit:  $[\alpha]_D^{20} = +114^\circ$ , c = 1, CHCl<sub>3</sub>).

### 8.6.13 Deprotection of acetylated compounds

The deprotection of acetylated compounds was either carried out using sodium methanolate in methanol (Zemplén conditions described by *Steinmann et al.*<sup>[154]</sup>) or ammonia in methanol (described by *Yamamoto et al.*<sup>[203]</sup>).

Deprotection with NaOMe/MeOH<sup>[154]</sup>:

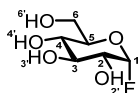
The acetylated compound (1.0 mmol) was dissolved in dry 10 mL CH<sub>2</sub>Cl<sub>2</sub> : MeOH (1 : 2) and 0.67 mL NaOMe/MeOH (0.5 M) added to the solution. The deprotection was stirred at room temperature (~25 °C) until complete deacetylation (followed by TLC). Quenching of the reaction was carried out using Dowex Monoshpere 650C (activated with aqueous HCl) and stirring for 0.5 h. The Dowex Monoshpere 650C was removed by filtration and the solvent removed under reduced pressure yielding the deacetylated product.

Deprotection using ammonia in MeOH<sup>[203]</sup>:

The acetylated compound was dissolved in NH<sub>3</sub>/MeOH (7 M) with final concentrations of 0.1 M acetylated compound and 2 M ammonia. The reaction was followed by TLC and stirred at room temperature (~25 °C) until complete deacetylation. The solvent was removed under reduced pressure and lyophilisation.

The analytical data of the deacetylated compounds was in accordance with literature.<sup>[28, 166, 198, 204, 205]</sup>

#### α-D-Glucopyranosyl fluoride **2a**



**2a**

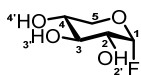
**C<sub>6</sub>H<sub>11</sub>FO<sub>5</sub>**

**[182.15]**

Colourless solid, Yield = 100% (0.35 g/ 1.9 mmol), deprotection: NH<sub>3</sub>/MeOH;

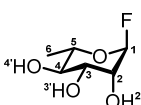
**<sup>1</sup>H-NMR** (600 MHz, d<sub>6</sub>-DMSO):  $\delta$  [ppm] = 3.12 (m, 1H, 4-H), 3.24 (m, 1H, 2-H), 3.40 (dt,  $^3J_{3,4} = 9.3$  Hz,  $^3J_{3,2} = 4.1$  Hz, 1H, 3-H), 3.49 (m, 2H, 6-H/5-H), 3.64 (dt,  $^2J_{6,6} = 9.2$  Hz,  $^3J_{6,5} = 4.6$  Hz, 1H, 6-H), 4.62 (t,  $^3J_{6',6} = 5.7$  Hz, 1H, 6'-H), 5.05 (d,  $^3J_{3',3} = 5.1$  Hz, 1H, 3'-H), 5.09 (d,  $^3J_{4',4} = 5.9$  Hz, 1H, 4'-H), 5.28 (d,  $^3J_{2',2} = 6.1$  Hz, 1H, 2'-H), 5.49 (dd,  $^2J_{1,F} = 54.1$  Hz,  $^3J_{1,2} = 2.7$  Hz, 1H,

1-H); **<sup>13</sup>C-NMR** (151 MHz, d<sub>6</sub>-DMSO):  $\delta$  [ppm] = 60.89 (CH<sub>2</sub>, C-6), 69.50 (CH, C-4), 71.67/71.83 (CH, C-2), 73.09 (CH, C-3), 76.25 (CH, C-5), 107.62/109.10 (CH, C-1); **R<sub>f</sub>-Value**: 0.26 (CH<sub>2</sub>Cl<sub>2</sub> : EtOH = 15%);  $[\alpha]_D^{20} = +92^\circ \pm 0.06^\circ$  (c = 1.1, methanol, lit.:  $[\alpha]_D^{20} = +77^\circ$ , c = 1, H<sub>2</sub>O).

$\alpha$ -D-Xylopyranosyl fluoride **2d**

**2d**  
**C<sub>5</sub>H<sub>9</sub>FO<sub>4</sub>**  
**[152.12]**

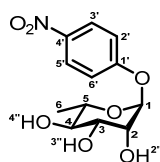
Colourless solid; Yield = 94% (0.26 g/ 1.7 mmol), deprotection: NH<sub>3</sub>/MeOH;  
**<sup>1</sup>H-NMR** (600 MHz, D<sub>2</sub>O):  $\delta$  [ppm] = 3.60 (ddd,  $^3J_{2,1} = 2.7$  Hz,  $^3J_{2,F} = 26.1$  Hz,  $^3J_{2,3} = 9.24$  Hz, 1H, 2-H), 3.63–3.73 (m, 3H, 3-H/4-H/5-H), 3.86 (dd,  $^2J_{5,5} = 10.4$  Hz,  $^3J_{5,4} = 4.7$  Hz, 1H, 5-H), 5.68 (dd,  $^2J_{1,F} = 53.4$  Hz,  $^3J_{1,2} = 2.7$  Hz, 1H, 1-H); **<sup>13</sup>C-NMR** (151 MHz, D<sub>2</sub>O):  $\delta$  [ppm] = 63.20 (CH<sub>2</sub>, C-5), 68.35 (CH, C-4), 71.09 (CH, C-2), 72.65 (CH, C-3), 107.54 (CH, C-1).

 $\alpha$ -L-Rhamnopyranosyl fluoride **2o**

**2o**  
**C<sub>6</sub>H<sub>11</sub>FO<sub>4</sub>**  
**[166.15]**

Clear syrup; Yield = 100% (0.31 g/ 0.19 mmol), deprotection: NH<sub>3</sub>/MeOH;  
**<sup>1</sup>H-NMR** (600 MHz, d<sub>6</sub>-DMSO):  $\delta$  [ppm] = 1.19 (d,  $^3J_{6,5} = 6.2$  Hz, 3H, 6-H), 3.27 (dd,  $^3J_{4,5} = 9.4$  Hz,  $^3J_{4,3} = 9.4$  Hz, 1H, 4-H), 3.43 (ddd,  $^3J_{3,4} = 9.4$  Hz,  $^3J_{3,2} = 3.2$  Hz,  $^3J_{3,3'} = 2.5$  Hz, 1H, 3-H), 3.54 (dq,  $^3J_{5,4} = 9.6$  Hz,  $^3J_{5,6} = 6.2$  Hz, 1H, 5-H), 3.76 (dd,  $^3J_{2,3} = 3.3$  Hz,  $^3J_{2,1} = 1.6$  Hz, 1H, 2-H), 5.41 (dd,  $^2J_{1,F} = 51.0$  Hz,  $^3J_{1,2} = 1.5$  Hz, 1H, 1-H); **<sup>13</sup>C-NMR** (151 MHz, CDCl<sub>3</sub>):

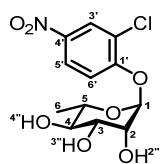
$\delta$  [ppm] = 18.18 (CH<sub>3</sub>, C-6), 69.30 (CH, C-2), 70.37 (CH, C-3), 71.52 (CH, C-4), 71.62 (CH, C-5), 108.350/109.75 (CH, C-1); **R<sub>f</sub>-Value**: 0.07 (PE : EA = 1 : 1).

4-Nitrophenyl  $\alpha$ -L-rhamnopyranoside **5r**

**5r**  
**C<sub>12</sub>H<sub>15</sub>NO<sub>7</sub>**  
**[285.25]**

Colourless solid; Yield = 97% (0.67 g/ 2.3 mmol), deprotection: NH<sub>3</sub>/MeOH;  
**<sup>1</sup>H-NMR** (600 MHz, d<sub>6</sub>-DMSO):  $\delta$  [ppm] = 1.10 (d,  $^3J_{6,5} = 6.2$  Hz, 3H, 6-H), 3.31 (ddd,  $^3J_{4,3} = 9.3$  Hz,  $^3J_{4,5} = 9.3$  Hz,  $^3J_{4,4'} = 5.8$  Hz, 1H, 4-H), 3.39 (tt,  $^3J_{5,4} = 12.3$  Hz,  $^3J_{5,6} = 6.1$  Hz, 1H, 5-H), 3.65 (ddd,  $^3J_{3,4} = 9.3$  Hz,  $^3J_{3,3'} = 5.9$  Hz,  $^3J_{3,2} = 3.4$  Hz, 1H, 3-H), 3.86 (m, 1H, 2-H), 4.82 (d,  $^3J_{3',3} = 5.9$  Hz, 1H, 3'-H), 4.93 (d,  $^3J_{4',4} = 5.7$  Hz, 1H, 4'-H), 5.17 (d,  $^3J_{2',2} = 4.5$  Hz, 1H, 2'-H), 5.57 (d,  $^3J_{1,2} = 1.8$  Hz, 1H, 1-H), 7.24 (d,

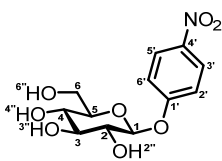
$^3J_{Ph,Ph} = 9.2$  Hz, 2H, Ph-H), 8.21 (d,  $^3J_{Ph,Ph} = 9.1$  Hz, 2H, Ph-H); **<sup>13</sup>C-NMR** (125 MHz, CDCl<sub>3</sub>):  $\delta$  [ppm] = 18.32 (CH<sub>3</sub>, C-6), 70.30 (CH, C-2), 70.54 (CH, C-5), 70.72 (CH, C-3), 72.02 (CH, C-4), 98.87 (CH, C-1), 117.11, 126.26, 142.06, 161.68 (CH, Ph); **IR** (ATR-film):  $\nu$  [cm<sup>-1</sup>] = 3498, 3427, 3324 (O-H-v), 3159 (arom. C-H-v), 2939, 2921 (aliph. C-H-v), 1592 (arom. C=C-v), 1505, 1350 (N-O-v), 1066, 1008, 976; **R<sub>f</sub>-Value**: 0.68 (CH<sub>2</sub>Cl<sub>2</sub> : EtOH 15%); **mp** = 180 °C (lit: 179 °C); **[ $\alpha$ ]<sub>D</sub><sup>20</sup>** = -151 ° ± 0.11 ° (c = 1.0, methanol; lit: [ $\alpha$ ]<sub>D</sub><sup>20</sup> = -144 °, c = 1, methanol).

2-Chloro-4-nitrophenyl  $\alpha$ -L-rhamnopyranoside **5ae**

Colourless/yellow solid; Yield = 89% (0.38 mg/ 1.2 mmol), deprotection: NaOMe/MeOH;

**<sup>1</sup>H-NMR** (600 MHz, d<sub>6</sub>-DMSO):  $\delta$  [ppm] = 1.09 (d,  $^3J_{6,5}$  = 5.8 Hz, 3H, 6-H), 3.32 (dd,  $^3J_{4,5}$  = 9.3 Hz,  $^3J_{4,3}$  = 5.8 Hz, 1H, 4-H), 3.36 (m, 1H, 5-H), 3.70 (m, 1H, 3-H), 3.91 (m, 1H, 2-H), 4.89 (d,  $^3J_{3',3}$  = 5.8 Hz, 1H, 3'-H), 5.01 (d,  $^3J_{4',4}$  = 5.2 Hz, 1H, 4'-H), 5.25 (d,  $^3J_{2',2}$  = 4.6 Hz, 1H, 2'-H), 5.72 (d,  $^3J_{1,2}$  = 1.7 Hz, 1H, 1-H), 7.51 (d,  $^3J_{\text{Ph,Ph}}$  = 9.3 Hz, 1H, Ph-H), 8.21 (dd,

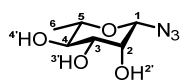
$^3J_{\text{Ph,Ph}}$  = 9.3 Hz,  $^3J_{\text{Ph,Ph}}$  = 2.2 Hz, 1H, Ph-H), 8.33 (t,  $^3J_{\text{Ph,Ph}}$  = 2.2 Hz, 1H, Ph-H); **<sup>13</sup>C-NMR** (151 MHz, d<sub>6</sub>-DMSO):  $\delta$  [ppm] = 18.27 (CH<sub>3</sub>, C-6), 70.22 (CH<sub>2</sub>, C-2), 70.68 (CH, C-5), 70.97 (CH, C-3), 71.81 (CH, C-4), 99.43 (CH, C-1), 116.36, 123.10, 124.76, 126.01, 141.95, 156.93 (CH, Ph); **IR** (ATR-film):  $\nu$  [cm<sup>-1</sup>] = 3437, 3280 (br, O-H-v), 3103, 3073 (arom. C-H-v), 3012, 2970, 2941 (aliph. C-H-v), 1730, 1585 (arom. C=C-v), 1514, 1365 (N-O-v), 1049, 734 (C-Cl-v); **R<sub>f</sub>-Value**: 0.72 (CH<sub>2</sub>Cl<sub>2</sub> : EtOH 15%); **mp** = 143 °C.

4-Nitrophenyl  $\beta$ -D-glucopyranoside **5h**

Colourless solid; Yield = 100% (1.3 g/ 4.3 mmol), deprotection: NH<sub>3</sub>/MeOH;

**<sup>1</sup>H-NMR** (600 MHz, d<sub>6</sub>-DMSO):  $\delta$  [ppm] = 3.20 (dd,  $^3J_{4,4'}$  = 13.7 Hz,  $^3J_{4,5}$  = 8.5 Hz, 1H, 4-H), 3.30 (m, 2H, 2-H/3-H), 3.43 (dd,  $^3J_{5,4}$  = 8.5 Hz,  $^3J_{5,6}$  = 5.4 Hz, 1H, 5-H), 3.49 (dd,  $^2J_{6,6}$  = 11.6 Hz,  $^3J_{6,5}$  = 5.7 Hz, 1H, 6-H), 3.70 (dd,  $^2J_{6,6}$  = 11.2 Hz,  $^3J_{6,6'}$  = 4.4 Hz, 1H, 6-H), 4.60 (t,  $^3J_{6',6}$  = 5.5 Hz, 1H, 6'-H) 5.09 (m, 2H, 4'-H/1-H), 5.16 (d,  $^3J_{2'/3',2/3}$  = 3.8 Hz, 1H, 2'/3'-H),

5.45 (d,  $^3J_{2'/3',2/3}$  = 4.2 Hz, 1H, 2'/3'-H), 7.23 (d,  $^3J_{\text{Ph,Ph}}$  = 9.0 Hz, 2H, Ph-H), 8.21 (d,  $^3J_{\text{Ph,Ph}}$  = 9.0 Hz, 2H, Ph-H); **<sup>13</sup>C-NMR** (125 MHz, d<sub>6</sub>-DMSO):  $\delta$  [ppm] = 60.99 (CH<sub>2</sub>, C-6), 69.94 (CH, C-4), 73.55 (CH, C-2/3), 76.88 (CH, C-2/3), 77.67 (CH, C-5), 100.31 (CH, C-1), 117.02, 126.17, 142.12, 162.86 (CH, Ph); **IR** (ATR-film):  $\nu$  [cm<sup>-1</sup>] = 3475, 3324 (br, O-H-v), 3016 (arom. C-H-v), 2970, 2944 (aliph. C-H-v), 1738, 1595 (N-O-v), 1435 (arom. C=C-v), 1365 (N-O-v), 1229; **R<sub>f</sub>-Value**: 0.46 (CH<sub>2</sub>Cl<sub>2</sub> : EtOH 15%); **mp** = 151 °C (lit.: 165–166 °C); **[ $\alpha$ ]<sub>D</sub><sup>20</sup>** = -86 °  $\pm$  0.12 ° (c = 1.1, methanol, lit: [ $\alpha$ ]<sub>D</sub><sup>20</sup> = +76 °, c = 0.8, methanol); **LC-MS** (API-ES, 70 eV):  $m/z$  = 324.3 [M + Na];  $t_R$  = 4.7 min.

**$\beta$ -L-Rhamnopyranosyl azide **16d****

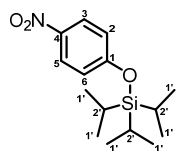
**16d**  
**C<sub>6</sub>H<sub>11</sub>N<sub>3</sub>O<sub>4</sub>**  
**[189.17]**

Brown/yellow syrup; Yield = 84% (43 mg/ 0.23 mmol), deprotection: NH<sub>3</sub>/MeOH;

**<sup>1</sup>H-NMR** (600 MHz, D<sub>2</sub>O):  $\delta$  [ppm] = 1.32 (d, <sup>3</sup>J<sub>6,5</sub> = 6.2 Hz, 3H, 6-H), 3.38 (dd, <sup>3</sup>J<sub>4,5</sub> = 9.6 Hz, <sup>3</sup>J<sub>4,3</sub> = 9.6 Hz, 1H, 4-H), 3.47 (dq, <sup>3</sup>J<sub>5,4</sub> = 9.5 Hz, <sup>3</sup>J<sub>5,6</sub> = 6.2 Hz, 1H, 5-H), 3.58 (dd, <sup>3</sup>J<sub>3,4</sub> = 9.7 Hz, <sup>3</sup>J<sub>3,2</sub> = 3.3 Hz, 1H, 3-H), 4.00 (dd, <sup>3</sup>J<sub>2,3</sub> = 3.3 Hz, <sup>3</sup>J<sub>2,1</sub> = 0.7 Hz, 1H, 2-H), 4.81 (d, <sup>3</sup>J<sub>1,2</sub> = 0.7 Hz, 1H, 1-H); **<sup>13</sup>C-NMR** (125 MHz, D<sub>2</sub>O):  $\delta$  [ppm] = 16.59 (CH<sub>3</sub>, C-6), 71.17 (CH, C-4), 71.55 (CH, C-2), 72.47 (CH, C-5), 74.38 (CH, C-3), 87.27 (CH, C-1); **IR** (ATR-film):  $\nu$  [cm<sup>-1</sup>] = 3341 (br, O-H- $\nu$ ), 2904 (aliph. C-H- $\nu$ ), 2113 (Azide, N $\equiv$ N- $\nu$ ), 1661, 1383, 1251, 1061, 983, 869, 793, 559; **R<sub>f</sub>-Value**: 0.58 (RP, CH<sub>2</sub>Cl<sub>2</sub> : EtOH 15%).

**8.6.14 Synthesis of triisopropyl-(4-nitrophenoxy)-silane (TIPSpNP, **23**)**

The synthesis of TIPSpNP (**23**) was carried out under inert atmosphere in *Schlenk*-flasks. For synthesis, 4-nitrophenol (*p*NP, **13b**, 0.70 mg, 5.0 mmol, 1.0 equiv) and imidazole (1.0 g, 15 mmol, 3.0 equiv) were dissolved with dry CH<sub>2</sub>Cl<sub>2</sub> (10 mL/mmol) and cooled to 0 °C on ice. Triisopropylsilyl chloride (2.14 mL, 10 mmol, 2.2 equiv) was added dropwise and the reaction stirred for 18 h. Excess of triisopropylsilyl chloride was hydrolysed by addition of dH<sub>2</sub>O (5 mL). The reaction mixture was extracted twice using CH<sub>2</sub>Cl<sub>2</sub>, and the combined organic phases washed with brine. The organic phase was dried over MgSO<sub>4</sub> and filtered over *Celite*<sup>TM</sup>. The solvent was removed under reduced pressure and the crude product purified by flash chromatography (PE 100%). After removal of the solvent, the product **23** was obtained as a pale yellow oil (97%, 1.4 g, 4.8 mmol). Analytical data was in accordance with literature.<sup>[206, 207]</sup>

**Triisopropyl-(4-nitrophenoxy)-silane **23****

**23**  
**C<sub>15</sub>H<sub>25</sub>NO<sub>3</sub>Si**  
**[295.45]**

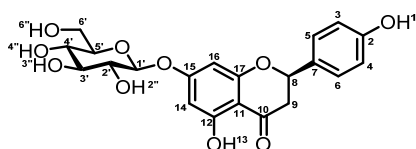
Pale yellow oil; Yield = 97% (1.43 g/ 4.84 mmol);

**<sup>1</sup>H-NMR** (600 MHz, CDCl<sub>3</sub>):  $\delta$  [ppm] = 1.11 (d, <sup>3</sup>J<sub>1',2'</sub> = 7.4 Hz, 18H, 1'-H), 1.26–1.36 (m, 3H, 2'-H), 6.91–6.94 (m, 2H, Ph-H), 8.13–8.17 (m, 2H, Ph-H); **<sup>13</sup>C-NMR** (125 MHz, CDCl<sub>3</sub>):  $\delta$  [ppm] = 12.67 (CH, C-2'), 17.81 (CH<sub>3</sub>, C-1'), 119.92 (CH, C-Ph), 125.88 (CH, C-Ph), 141.72 (C<sub>q</sub>, C-Ph), 162.09 (C<sub>q</sub>, C-Ph).

### 8.6.15 Enzymatic synthesis of prunin (1b) from naringin (1c)

A solution of naringin (**1c**, 10 mM, 58 mg, 0.1  $\mu\text{mol}$ ) in 9.5 mL citrate-buffer (20 mM, pH 3.4) was incubated at 60 °C after the addition 0.5 mL deactivated naringinase-solution (1 g/L, section 8.5.6) and shaken at 500 rpm over night (18 h). The reaction was followed on normal phase TLC plates using  $\text{CH}_2\text{Cl}_2$  and EtOH (15%) as a solvent mixture. After complete conversion, the reaction mixture was cooled to 0 °C. The precipitated product was separated *via* filtration and dissolved in acetone. The solvent was subsequently removed under reduced pressure yielding the product **1b** in a yield of 84% (37 mg, 0.84  $\mu\text{mol}$ ). The obtained analytical data was in accordance with literature.<sup>[208]</sup>

#### Naringenin-7-O- $\beta$ -D-glucoside **1b**



**1b**

$\text{C}_{21}\text{H}_{22}\text{O}_{10}$

[434.39]

Yellow solid; Yield = 84% (37 mg/ 0.84  $\mu\text{mol}$ );

**$^1\text{H-NMR}$**  (600 MHz,  $d_6$ -DMSO):  $\delta$  [ppm] = 2.75 (dt,  $^2J_{9a,9b} = 17.1$  Hz,  $^3J_{9a,8} = 3.2$  Hz, 1H, 9-H<sub>a</sub>), 3.15 (td,  $^3J_{4',5'/3'} = 9.1$  Hz,  $^3J_{4',4''} = 5.3$  Hz, 1H, 4'-H), 3.24 (m, 1H, 2'/3'-H), 3.27 (td,  $^3J_{3'/2',2'/3'} = 8.8$  Hz,  $^3J_{3'/2',3''/2''} = 4.9$  Hz, 1H, 2'/3'-H), 3.32 (9-H<sub>b</sub> overlapped by DHO-solvent signal 3.33 ppm), 3.45 (dt,  $^3J_{6'b,5'} = 5.9$  Hz,  $^2J_{6'b,6'a} = 11.7$  Hz, 1H,

6'-H<sub>b</sub>), 3.65 (m, 1H, 6'-H<sub>a</sub>), 4.56 (dd,  $^3J_{5',4'} = 10.5$  Hz,  $^3J_{5',6'b} = 5.3$  Hz, 1H, 5'-H), 4.98 (dd,  $^3J = 14.3$  Hz,  $^3J = 7.6$  Hz, 1H, 1'-H), 5.04 (d,  $^3J_{4'',4'} = 5.1$  Hz, 1H, 4''-H), 5.11 (d,  $^3J_{2''/3'',2'/3'} = 4.9$  Hz, 1H, 2''/3''-H), 5.36 (d,  $^3J_{2''/3'',2'/3'} = 5.1$  Hz, 1H, 2''/3''-H), 5.49 (m, 1H, 8-H), 6.25 (m, 2H, 14/16-H), 6.81 (d,  $^3J_{5,6} = 8.4$  Hz, 2H, 5-H/6-H), 7.34 (d,  $^3J_{3,4} = 8.5$  Hz, 2H, 3-H/4-H), 9.61 (s, 1H, 1-H), 12.06 (d,  $^4J_{13,14} = 3.8$  Hz, 1H, 13-H);  **$^{13}\text{C-NMR}$**  (125 MHz,  $d_6$ -DMSO):  $\delta$  [ppm] = 31.17 (C<sub>q</sub>), 42.50 (CH<sub>2</sub>, C-9), 61.03 (CH<sub>2</sub>, C-6'), 69.96 (CH, C-4'), 73.49 (CH, C-2'/3'), 76.90 (CH, C-2'/3'), 77.52 (CH, C-5'), 79.17 (CH, C-8), 96.70 (CH, C-14/16), 100.06 (CH, C-1'), 115.66 (CH, C-6/5), 128.94 (CH, C-3/4), 129.08 (CH, C-3/4), 158.29 (C<sub>q</sub>), 163.26 (C<sub>q</sub>), 163.46 (C<sub>q</sub>), 165.79 (C<sub>q</sub>), 197.73 (C=O, C-10); **IR** (ATR-film):  $\nu$  [ $\text{cm}^{-1}$ ] = 3324 (br, O-H-v), 3027 (arom. C-H-v), 2967, 2916 (aliph. C-H-v), 1737 (C=O-v), 1634, 1576 (arom. C=C-v), 1168 (ether, C-O-v) 1059, 1016; **R<sub>f</sub>-Value**: 0.32 ( $\text{CH}_2\text{Cl}_2$ :EtOH 15%);  **$[\alpha]_D^{20}$**  = -63 °  $\pm$  0.06 ° (c = 1.1, methanol, lit:  $[\alpha]_D^{20}$  = -72 °, c = 0.6, methanol); **LC-MS** (API-ES, 70 eV):  $m/z$  = 891.3 [2M + Na], 435.3 [M + H];  $t_R$  = 6.3 min.

### 8.6.16 Biocatalytic synthesis of $\beta$ -D-glucosides

The syntheses of various  $\beta$ -D-glucoside derivatives were catalysed by the glycosynthase variants Abg-E358S and BglU-E377A. As a general procedure, the acceptor and donor compounds were dissolved in the respective buffer and the purified enzyme solution added to the mixture, which was then incubated at 25 °C and shaken at 500 rpm. The reaction was followed by reversed phase TLC, which was stained using the vanillin staining solution (section 8.6.1).

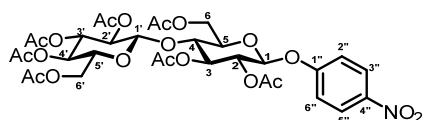
After incubation the buffer solvent was evaporated under reduced pressure and the remaining residue peracetylated by adding acetic anhydride (2.0 equiv/OH-group, calculated from the starting material) and 1 mL/mmol (starting material) pyridine. The acetylation was followed by normal phase TLC until completion. The reaction mixture was then diluted with 2 mL ethyl acetate and pyridine removed by extraction with saturated  $\text{CuSO}_4$ -solution. The organic phase was dried over  $\text{MgSO}_4$  and filtered through *Celite*<sup>TM</sup>. The solvent was removed under reduced pressure and the residual product mixture separated by column chromatography (PE : EA 1 : 1).

#### Glucosylation of *p*-nitrophenyl $\beta$ -D-glucopyranoside (**5h**)

The donor **2a** (80 mM) and acceptor **5h** (40 mM) were dissolved in 1 mL  $\text{KP}_i$ -buffer (50 mM, pH 7.0) and the reaction started by addition of 0.5 mL purified BglU-E377A solution (3.1 nM). The reaction was incubated at 25 °C for 24 h. The work-up followed the general procedure.

The analytical data of compound **5c** was in accordance with literature.<sup>[209]</sup>

*p*-Nitrophenyl 2,3,6-tri-*O*-acetyl-4-*O*-(2,3,4,6-tetra-*O*-acetyl- $\beta$ -D-glucopyranosyl)  $\beta$ -D-glucopyranoside **5c**



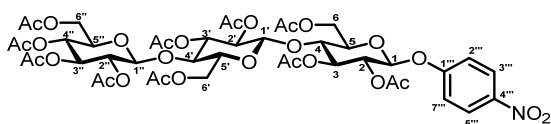
**5c**  
 $\text{C}_{32}\text{H}_{39}\text{O}_{20}$   
 [757.65]

White solid; Yield = traces;

**<sup>1</sup>H-NMR** (600 MHz,  $\text{CDCl}_3$ ):  $\delta$  [ppm] = 1,99 (s, 3H, Ac-H), 2,02 (s, 3H, Ac-H), 2,05 (s, 3H, Ac-H), 2,06 (s, 6H, Ac-H), 2,09 (s, 3H, Ac-H), 2,10 (s, 3H, Ac-H), 3,68 (ddd,  $^3J_{5,6'} = 2.4$  Hz,  $^3J_{5,6} = 4.4$  Hz,  $^3J_{5,4'} = 9.8$  Hz, 1H, 5'-H), 3,83 (ddd,  $^3J_{5,6} = 2.1$  Hz,  $^3J_{5,6} = 5.7$  Hz,  $^3J_{5,4} = 9.9$  Hz, 1H, 5-H), 3,88 (dd,  $^3J_{4,3} = 8.9$  Hz,  $^3J_{4,5} = 9.9$  Hz, 1H, 4-H), 4,06 (dd,  $^3J_{6',5'} = 2.4$  Hz,  $^3J_{6',6'} = 12.5$  Hz, 1H, 6'-H), 4,14 (dd,  $^3J_{6,5} = 5.9$  Hz,  $^3J_{6,6} = 12.0$  Hz, 1H, 6-H), 4,37 (dd,  $^3J_{6',5'} = 4.4$  Hz,  $^3J_{6',6'} = 12.5$  Hz, 1H, 6'-H), 4,53 (d,  $^3J_{6,5} = 2.1$  Hz, 1H, 6-H),

4,55 (d,  $^3J_{1',2'} = 7.9$  Hz, 1H, 1'-H), 4,95 (dd,  $^3J_{2',1'} = 7.9$  Hz,  $^3J_{2',3'} = 9.4$  Hz, 1H, 2'-H), 5,08 (t,  $^3J_{4',3'} = 9.7$  Hz, 1H, 4'-H), 5,17 (m, 2H, 3'-H, 1-H), 5,22 (dd,  $^3J_{2,1} = 7.6$  Hz,  $^3J_{2,3} = 8.9$  Hz, 1H, 2-H), 5,29 (t,  $^3J_{3,2} = 8.9$  Hz, 1H, 3-H), 7,06 (m, 2H, Ph-H), 8,20 (m, 2H, Ph-H); **R<sub>f</sub>-Value**: 0.21 (PE : EA 1 : 1).

*p*-Nitrophenyl 2,3,6-tri-*O*-acetyl-4-*O*-(hepta-*O*-acetyl- $\beta$ -D-cellobiosyl)- $\beta$ -D-glucopyranoside **5x**



**5x**

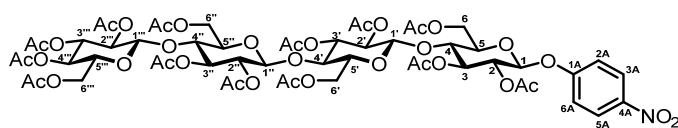
**C<sub>44</sub>H<sub>55</sub>NO<sub>28</sub>**

**[1045.90]**

White solid; Yield = 20% (8 mg/ 8  $\mu$ mol);

**<sup>1</sup>H-NMR** (600 MHz, CDCl<sub>3</sub>):  $\delta$  [ppm] = 1,92 (s, 3H, Ac-H), 1,94 (s, 3H, Ac-H), 1,94 (s, 3H, Ac-H), 1,95 (s, 3H, Ac-H), 1,97 (s, 3H, Ac-H), 1,97 (s, 3H, Ac-H), 1,99 (s, 3H, Ac-H), 2,02 (s, 6H, Ac-H), 2,09 (s, 3H, Ac-H), 3,54 (ddd,  $^3J_{5',6'} = 1.8$  Hz,  $^3J_{5',6''} = 4.9$  Hz,  $^3J_{5',4''} = 9.9$  Hz, 1H,

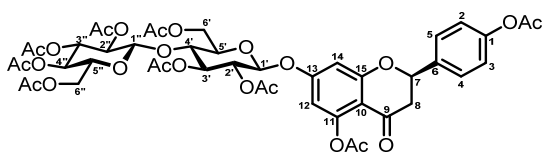
5'-H), 3,57 (ddd,  $^3J_{5',6''} = 2.5$  Hz,  $^3J_{5',6'} = 4.3$  Hz,  $^3J_{5',4''} = 9.9$  Hz, 1H, 5''-H), 3,72 (t,  $^3J_{4',3'} = 9.3$  Hz, 1H, 4'-H), 3,77 (ddd,  $^3J_{5,6} = 2.0$  Hz,  $^3J_{5,6} = 5.5$  Hz,  $^3J_{5,4} = 9.9$  Hz, 1H, 5-H), 3,79 (t,  $^3J_{4,5} = 9.8$  Hz, 1H, 4-H), 3,96 (dd,  $^3J_{6'',5''} = 2.2$  Hz,  $^3J_{6'',6''} = 12.4$  Hz, 1H, 6''-H), 4,05 (m, 2H, 6-H/6'-H), 4,29 (dd,  $^3J_{6'',5''} = 4.2$  Hz,  $^3J_{6'',6''} = 12.6$  Hz, 1H, 6''-H), 4,38 (dd,  $^3J_{6',5'} = 1.5$  Hz,  $^3J_{6',6''} = 12.3$  Hz, 1H, 6'-H), 4,43 (d,  $^3J_{1'',2''} = 7.8$  Hz, 1H, 1''-H), 4,45 (d,  $^3J_{1',2'} = 7.8$  Hz, 1H, 1'-H), 4,48 (dd,  $^3J_{6,5} = 1.7$  Hz,  $^3J_{6,6} = 11.8$  Hz, 1H, 6-H), 4,80 (dd,  $^3J_{2',1'} = 7.9$  Hz,  $^3J_{2',3'} = 9.3$  Hz, 1H, 2'-H), 4,84 (dd,  $^3J_{2'',1''} = 8.0$  Hz,  $^3J_{2'',3''} = 9.2$  Hz, 1H, 2''-H), 4,99 (t,  $^3J_{4'',3''} = 9.5$  Hz, 1H, 4''-H), 5,06 (t,  $^3J_{3'',4''} = 9.4$  Hz, 1H, 3''-H), 5,07 (t,  $^3J_{3',4'} = 9.3$  Hz, 1H, 3'-H), 5,10 (d,  $^3J_{1,2} = 7.6$  Hz, 1H, 1-H), 5,14 (dd,  $^3J_{2,1} = 7.8$  Hz,  $^3J_{2,3} = 8.9$  Hz, 1H, 2-H), 5,21 (t,  $^3J_{3,2} = 8.8$  Hz, 1H, 3-H), 6,99 (m, 2H, Ph-H), 8,12 (m, 2H, Ph-H); **<sup>13</sup>C-NMR** (125 MHz, CDCl<sub>3</sub>):  $\delta$  [ppm] = 20.49, 20,54, 20.55, 20.56, 20.57, 20.59, 20.63, 20.68, 20.77, 20.81 (CH<sub>3</sub>, Ac), 61.51 (CH<sub>2</sub>, C-6''), 61.70 (CH<sub>2</sub>, C-6), 62.02 (CH<sub>2</sub>, C-6'), 67.73 (CH, C-4''), 71.19 (CH, C-2), 71.59 (CH, C-2''), 71.77 (CH, C-2'), 72.05 (CH, C-3), 72.12 (CH, C-5''), 72.56 (CH, C-3'), 72.87 (CH, C-3''), 72.89 (CH, C-5'), 73.24 (CH, C-5), 76.01 (CH, C-4'), 76.10 (CH, C-4), 97.84 (CH, C-1), 100.50 (CH, C-1'), 100.77 (CH, C-1''), 116.58 (CH, C-Ph), 125.77 (CH, C-Ph), 143.23 (C<sub>q</sub>, C-Ph), 161.15 (C<sub>q</sub>, C-Ph), 169.06, 169.30, 169.31, 169.40, 169.67, 169.76, 170.08, 170.19, 170.21, 170.50 (C<sub>q</sub>, C-Ac); **R<sub>f</sub>-Value**: 0.15 (PE : EA 1 : 1).

***p*-Nitrophenyl trideca-*O*-acetyl cellotetraside **5y******5y****C<sub>56</sub>H<sub>71</sub>NO<sub>36</sub>****[1334.16]**

Colourless solid; Yield = 5% (2 mg, 2 μmol);

**<sup>1</sup>H-NMR** (600 MHz, CDCl<sub>3</sub>):  
δ [ppm] = 1.97 (s, 3H, Ac-H), 1.98 (s, 3H, Ac-H), 2.00 (s, 3H, Ac-H), 2.01 (s, 3H, Ac-H), 2.02 (s, 3H, Ac-H), 2.03 (s, 3H, Ac-H), 2.04 (m,6H, Ac-H), 2.05 (s, 3H, Ac-H), 2.09 (s, 6H, Ac-H), 2.15 (s, 3H, Ac-H), 2.15 (s, 3H, Ac-H), 3.57 (ddd, <sup>3</sup>J<sub>5',6'</sub> = 1.9 Hz, <sup>3</sup>J<sub>5',6''</sub> = 5.1 Hz, <sup>3</sup>J<sub>5',4'</sub> = 9.9 Hz, 1H, 5'-H), 3.59 (ddd, <sup>3</sup>J<sub>5'',6''</sub> = 2.6 Hz, <sup>3</sup>J<sub>5'',6'''</sub> = 5.9 Hz, <sup>3</sup>J<sub>5'',4''</sub> = 11.3 Hz, 1H, 5''-H), 3.63 (ddd, <sup>3</sup>J<sub>5''',6'''</sub> = 2.3 Hz, <sup>3</sup>J<sub>5''',6''''</sub> = 4.4 Hz, <sup>3</sup>J<sub>5''',4'''</sub> = 10.0 Hz, 1H, 5'''-H), 3.76 (m, 2H, 4'-H, 4''-H), 3.84 (m, 2H, 4-H, 5-H), 4.04 (dd, <sup>3</sup>J<sub>6'',5''</sub> = 2.0 Hz, <sup>3</sup>J<sub>6'',6'''</sub> = 12.5 Hz, 1H, 6''-H), 4.09–4.13 (m, 3H, 6-H/6'-H/6''-H), 4.36 (dd, <sup>3</sup>J<sub>6''',5'''</sub> = 4.4 Hz, <sup>3</sup>J<sub>6''',6''''</sub> = 12.5 Hz, 1H, 6'''-H), 4.42 (m, 2H, 6'-H, 6''-H), 4.46 (d, <sup>3</sup>J<sub>1'',2''</sub> = 7.8 Hz, 1''-H), 4.47 (d, <sup>3</sup>J<sub>1',2'</sub> = 7.8 Hz, 1'-H), 4.49 (d, <sup>3</sup>J<sub>1',2'</sub> = 7.9 Hz, 1'-H), 4.52 (dd, <sup>3</sup>J<sub>6,5</sub> = 1.9 Hz, <sup>3</sup>J<sub>6,6</sub> = 11.9 Hz, 1H, 6-H), 4.83 (dd, <sup>3</sup>J<sub>2'',1''</sub> = 8.0 Hz, <sup>3</sup>J<sub>2'',3''</sub> = 9.0 Hz, 1H, 2''-H), 4.85 (dd, <sup>3</sup>J<sub>2',1'</sub> = 8.0 Hz, <sup>3</sup>J<sub>2',3'</sub> = 9.1 Hz, 1H, 2'-H), 4.90 (dd, <sup>3</sup>J<sub>2'',1''</sub> = 7.9 Hz, <sup>3</sup>J<sub>2'',3''</sub> = 9.3 Hz, 1H, 2''-H), 5.05 (t, <sup>3</sup>J<sub>4'',3''</sub> = 9.7 Hz, 1H, 3-H), 5.11 (m, 3H, 3'''-H/3''-H/3'-H), 5.17 (d, <sup>3</sup>J<sub>1,2</sub> = 7.6 Hz, 1H, 1-H), 5.20 (dd, <sup>3</sup>J<sub>2,1</sub> = 7.6 Hz, <sup>3</sup>J<sub>2,3</sub> = 8.8 Hz, 1H, 2-H), 5.28 (t, <sup>3</sup>J<sub>3,2</sub> = 8.8 Hz, 1H, 3-H), 7:05 (m, 2H, Ph-H), 8.19 (m, 2H, Ph-H); **R<sub>f</sub>-Value**: 0.08 (PE : EA 1 : 1).**Glucosylation of naringenin-7-*O*-β-D-glucoside (**1b**)**

The donor **2a** (80 mM) and acceptor **1b** (40 mM) were dissolved in 2 mL NH<sub>4</sub>HCO<sub>3</sub>-buffer (150 mM, pH 7.9) with 10% DMSO (*v/v*) and the reaction started by addition of 3 mg purified Abg-E358S (lyophilised powder; purified with NH<sub>4</sub>HCO<sub>3</sub>-buffer, which was removed by lyophilisation). The reaction was incubated at 25 °C for 24 h. The work up followed the general procedure. The analytical data was in accordance with literature.<sup>[210]</sup>

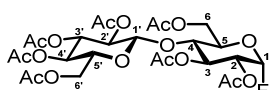
7-O-(Hepta-O-acetyl  $\beta$ -D-cellobiosyl)-5,4'-diacetyl naringenin **22i****22i****C<sub>45</sub>H<sub>50</sub>O<sub>24</sub>****[974.87]**Yellow solid; Yield = 15% (12 mg/ 12  $\mu$ mol);**<sup>1</sup>H-NMR** (600 MHz, d<sub>6</sub>-DMSO):

$\delta$  [ppm] = 1.98 (s, 6H, Ac-H), 2.01 (s, 3H, Ac-H), 2.03 (s, 3H, Ac-H), 2.04 (s, 3H, Ac-H), 2.04 (s, 3H, Ac-H), 2.09 (s, 3H, Ac-H), 2.31 (s, 3H, Ac-H), 2.37 (s, 3H, Ac-H), 2.75 (dd,  $^3J_{8a,8b}$  = 16.7 Hz,  $^3J_{8a,7}$  = 2.6 Hz, 1H, 8-H<sub>a</sub>),

3.01 (dd,  $^3J_{8b,8a}$  = 16.8 Hz,  $^3J_{8b,7}$  = 13.5 Hz, 1H, 8-H<sub>b</sub>), 3.66 (ddd,  $^3J_{5',6''}$  = 2.2 Hz,  $^3J_{5',6''}$  = 3.9 Hz,  $^3J_{5',4''}$  = 9.6 Hz, 1H, 5''-H), 3.77–3.85 (m, 2H, 7-H/4'-H), 4.04 (dd,  $^3J_{6'',5''}$  = 1.9 Hz,  $^2J_{6'',6''}$  = 12.4 Hz, 1H, 6''-H), 4.07–4.12 (m, 1H, 6'-H), 4.36 (dd,  $^3J_{6'',5''}$  = 4.4 Hz,  $^2J_{6'',6''}$  = 12.4 Hz, 1H, 6''-H), 4.48–4.57 (m, 2H, 1''-H/6'-H), 4.93 (t,  $^3J$  = 8.4 Hz, 1H, 2''/3''/4''-H), 5.07 (t,  $^3J$  = 9.5 Hz, 1H, 2''/3''/4''-H), 5.07 (d,  $^3J_{1',2'}$  = 7.5 Hz, 1H, 1'-H), 5.14 (t,  $^3J$  = 9.5 Hz, 1H, 2''/3''/4''-H), 5.18 (t,  $^3J_{2',3''}$  = 9.1 Hz, 1H, 2'-H), 5.25 (t,  $^3J_{3',2'}$  = 9.0 Hz, 1H, 3'-H), 5.44 (ddd,  $^3J_{5',6'}$  = 2.5 Hz,  $^3J_{5',6'}$  = 5.4 Hz,  $^3J_{5',4'}$  = 13.7 Hz, 1H, 5'-H), 6.33 (d,  $^3J_{14,12}$  = 2.3 Hz, 1H, 14-H), 6.51 (dd,  $^3J_{12,14}$  = 2.3 Hz,  $^3J$  = 4.3 Hz, 1H, 12-H), 7.15 (d,  $^3J_{2/3,4/5}$  = 8.5 Hz, 2H, 2-H/3-H), 7.43 (d,  $^3J_{4/5,2/3}$  = 8.5 Hz, 2H, 4-H/5-H); **HRMS** (ESI-FTMS, positive-ion): Calculated for C<sub>45</sub>H<sub>50</sub>O<sub>24</sub>Na (M + Na) = 997.2590, measured = 997.25894.

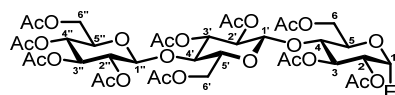
**Self-coupling of the donor  $\alpha$ -D-glucopyranosyl fluoride (2a)**

The donor **2a** (80 mM) were dissolved in 2 mL NH<sub>4</sub>HCO<sub>3</sub>-buffer (150 mM, pH 7.9) and the reaction started by addition of 3 mg purified Abg-E358S (lyophilised powder; purified with NH<sub>4</sub>HCO<sub>3</sub>-buffer, which was removed by lyophilisation). The reaction was incubated at 25 °C for 24 h. The work up followed the general procedure. The analytical data was in accordance with literature.<sup>[211]</sup>

Hepta-O-acetyl  $\alpha$ -D-cellobiosyl fluoride **22f****22f****C<sub>26</sub>H<sub>35</sub>FO<sub>17</sub>****[638.55]**Yellow solid; Yield = 7% (7 mg/ 11  $\mu$ mol);**<sup>1</sup>H-NMR** (600 MHz, CDCl<sub>3</sub>):  $\delta$  [ppm] = 1.98 (s, 3H, Ac-H), 2.01 (s, 3H, Ac-H), 2.03 (s, 3H, Ac-H), 2.04 (s, 3H, Ac-H), 2.09 (s, 3H, Ac-H), 2.09 (s, 3H, Ac-H), 2.14 (s, 3H, Ac-H), 3.67 (ddd,  $^3J_{5',6'}$  = 2.3 Hz,  $^3J_{5',6'}$  = 4.6 Hz,  $^3J_{5',4'}$  = 10.0 Hz, 1H, 5'-H), 3.83 (dd,  $^3J_{4,3}$  = 9.8 Hz,  $^3J_{4,5}$  = 9.8 Hz, 1H, 4-H), 4.04 (dd,  $^3J_{6',5'}$  = 2.3 Hz,  $^3J_{6',6'}$  = 12.5 Hz, 1H, 6'-H), 4.10 (ddd,  $^3J_{5,6}$  = 1.9 Hz,  $^3J_{5,6}$  = 4.3 Hz,  $^3J_{5,4}$  = 10.0 Hz, 1H, 5-H), 4.14 (dd,  $^3J_{6,5}$  = 4.3 Hz,  $^3J_{6,6}$  = 12.3 Hz, 1H, 6-H), 4.36 (dd,  $^3J_{6',5'}$  = 4.5 Hz,  $^3J_{6',6'}$  = 12.5 Hz, 1H, 6'-H), 4.54 (d,

$^3J_{1,2'} = 7.9$  Hz, 1H, 1'-H), 4.56 (dd,  $^3J_{6,5} = 2.0$  Hz,  $^3J_{6,6} = 12.3$  Hz, 1H, 6-H), 4.88 (ddd,  $^3J_{2,1} = 2.3$  Hz,  $^3J_{2,3} = 10.3$  Hz,  $^3J_{2,F} = 24.1$  Hz, 1H, 2-H), 4.93 (dd,  $^3J_{2',1'} = 8.0$  Hz,  $^3J_{2',3'} = 9.3$  Hz, 1H, 2'-H), 5.07 (t,  $^3J_{4',3'} = 9.6$  Hz, 1H, 4'-H), 5.15 (t,  $^3J_{3',4'} = 9.4$  Hz, 1H, 3'-H), 5.47 (dd,  $^3J_{3,2} = 10.2$  Hz,  $^3J_{3,4} = 9.4$  Hz, 1H, 3-H), 5.66 (dd,  $^2J_{1,F} = 53.0$  Hz,  $^3J_{1,2} = 2.8$  Hz, 1H, 1-H).

### 2,3,6-Tri-O-acetyl-4-O-(hepta-O-acetyl $\beta$ -cellobiosyl) $\alpha$ -D-glucopyranosyl fluoride **22g**



**22g**  
**C<sub>38</sub>H<sub>51</sub>FO<sub>25</sub>**  
**[926.80]**

Yellow solid; Yield = 1.6% (2.4 mg/ 2.6  $\mu$ mol);

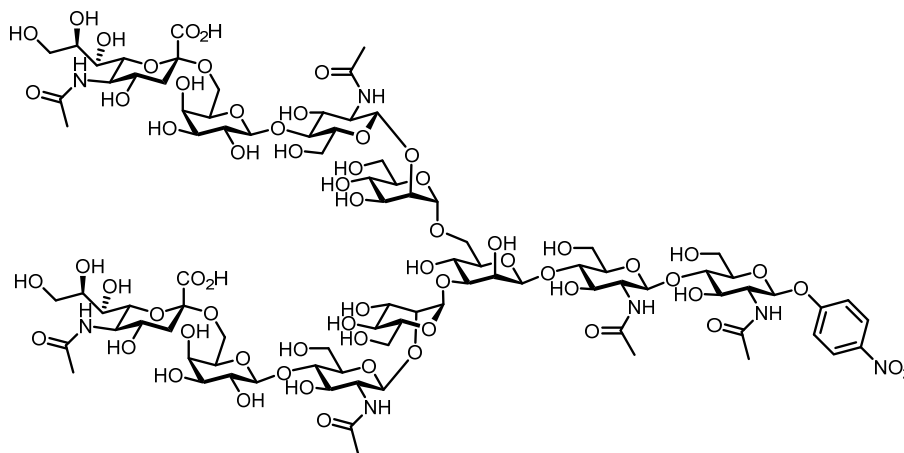
**$^1$ H-NMR** (600 MHz, d<sub>6</sub>-DMSO):  $\delta$  [ppm] = 1.98 (s, 3H, Ac-H), 2.00 (s, 3H, Ac-H), 2.00 (s, 3H, Ac-H), 2.01 (s, 3H, Ac-H), 2.02 (s, 3H, Ac-H), 2.04 (s, 3H, Ac-H), 2.09 (s, 6H, Ac-H), 2.14 (s, 3H, Ac-H), 2.15 (s, 3H, Ac-H), 3.60 (ddd,  $^3J_{5'',6''} = 1.9$  Hz,  $^3J_{5',6'} = 5.2$  Hz,  $^3J_{5',4'} = 10.0$  Hz, 1H, 5''-H), 3.64 (ddd,  $^3J_{5',6'} = 2.2$  Hz,  $^3J_{5',6'} = 4.3$  Hz,  $^3J_{5',4'} = 10.0$  Hz, 1H, 5'-H), 3.78 (t,  $^3J_{4,3} = 9.3$  Hz, 1H, 4-H), 3.81 (t,  $^3J_{4',5'} = 9.7$  Hz, 1H, 4'-H), 4.03 (dd,  $^3J_{6',5'} = 2.0$  Hz,  $^3J_{6',6'} = 12.5$  Hz, 1H, 6'-H), 4.09–4.15 (m, 3H, 6-H/5-H/6''-H), 4.34 (dd,  $^3J_{6',5'} = 4.5$  Hz,  $^3J_{6',6'} = 12.4$  Hz, 1H, 6'-H), 4.40 (dd,  $^3J_{6'',5''} = 1.8$  Hz,  $^3J_{6'',6''} = 12.0$  Hz, 1H, 6''-H), 4.48 (d,  $^3J_{1'',2''} = 7.8$  Hz, 1H, 1''-H), 4.52 (d,  $^3J_{1',2'} = 7.8$  Hz, 1H, 1'-H), 4.56 (dd,  $^3J_{6,5} = 1.6$  Hz,  $^3J_{6,6} = 11.9$  Hz, 1H, 6-H), 4.86 (dd,  $^3J_{2',1'} = 8.0$  Hz,  $^3J_{2',3'} = 9.2$  Hz, 1H, 2'-H), 4.88 (m, 1H, 2-H), 4.91 (dd,  $^3J_{2'',1''} = 7.9$  Hz,  $^3J_{2'',3''} = 9.3$  Hz, 1H, 2''-H), 5.05 (t,  $^3J_{4'',3''} = 9.6$  Hz, 1H, 4''-H), 5.11 (t,  $^3J_{3',4'} = 9.2$  Hz, 1H, 3'-H), 5.14 (t,  $^3J_{3,4} = 9.3$  Hz, 1H, 3-H), 5.46 (t,  $^3J_{3'',4''} = 9.9$  Hz, 1H, 3''-H), 5.66 (dd,  $^2J_{1,F} = 53.0$  Hz,  $^3J_{1,2} = 2.5$  Hz, 1H, 1-H).

### 8.6.17 Glycosylation of glycoside molecules by Endo-CC N180H

For the glycosylation of small glycosidic molecules 0.75 mU Endo-CC N180H was incubated with 7.5 mM SGP **20** and 10 mM of the specific acceptor molecule in KPi-buffer (25 mM, pH 7.5), in a total volume of 10  $\mu$ L. The glycosylation reaction was stopped by heat-deactivation for 3 min at 100  $^{\circ}$ C. After centrifugation, the supernatant was analysed by HPLC/LC-MS.

Following compounds were detected:

Glycosylation of *p*-nitrophenyl *N*-acetyl  $\beta$ -D-glucosaminide (**5a**)



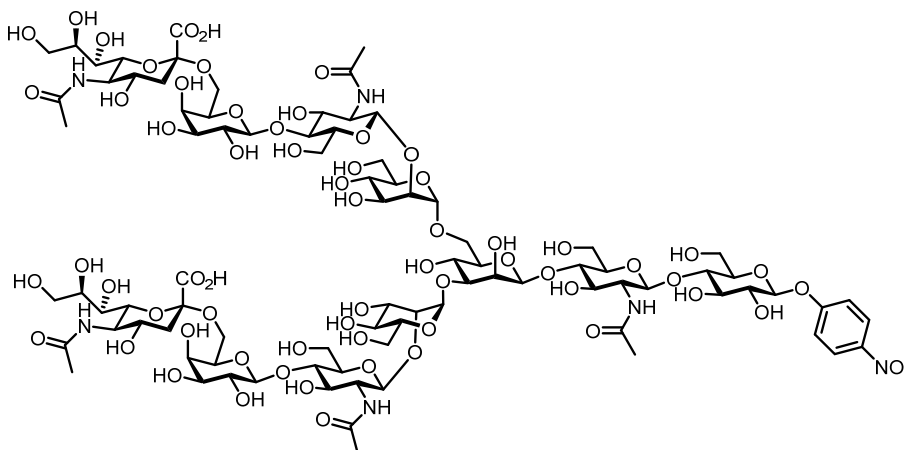
**5af**

**C<sub>90</sub>H<sub>141</sub>N<sub>7</sub>O<sub>64</sub>**

**[2343.80]**

**LC-MS** (API-ES, 70 eV):  $m/z = 1172 [M + 2H]^{2+}$ ,  $782 [M + 3H]^{3+}$ ;  $t_R = 6.0$  min.

Glycosylation of *p*-nitrophenyl  $\beta$ -D-glucopyranoside (**5h**)

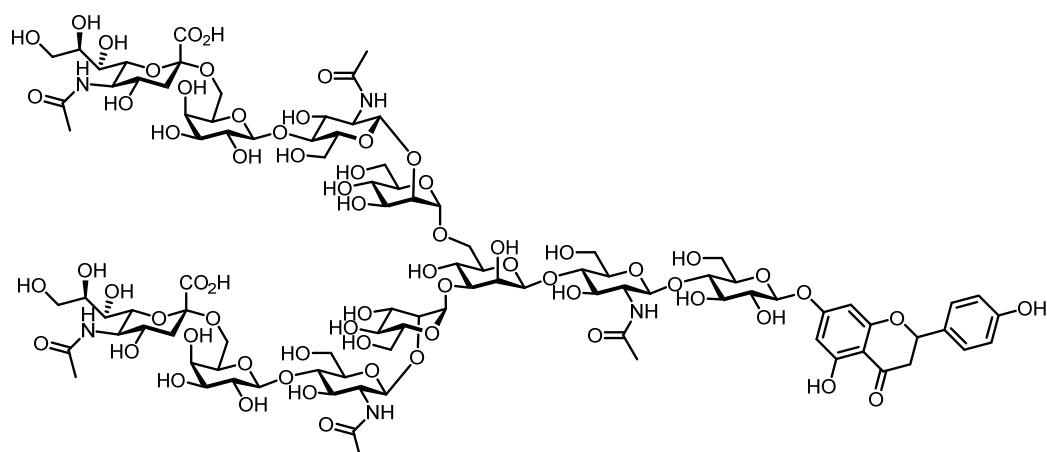


**5ag**

**C<sub>88</sub>H<sub>138</sub>N<sub>6</sub>O<sub>64</sub>**

**[2302.77]**

**LC-MS** (API-ES, 70 eV):  $m/z = 1152 [M + 2H]^{2+}$ ,  $768 [M + 3H]^{3+}$ ;  $t_R = 5.4$  min.

Glycosylation of *p*-nitrophenyl  $\beta$ -D-glucopyranoside (**5h**)**11****C<sub>97</sub>H<sub>145</sub>N<sub>5</sub>O<sub>66</sub>****[2437.20]****ESI-MS** (ESI-IT-MS, negative ion mode):  $m/z = 2436.2$  [M - H]<sup>-</sup>

## 9 APPENDIX

### 9.1 Gene and protein sequences

#### 9.1.1 Standard expression vectors

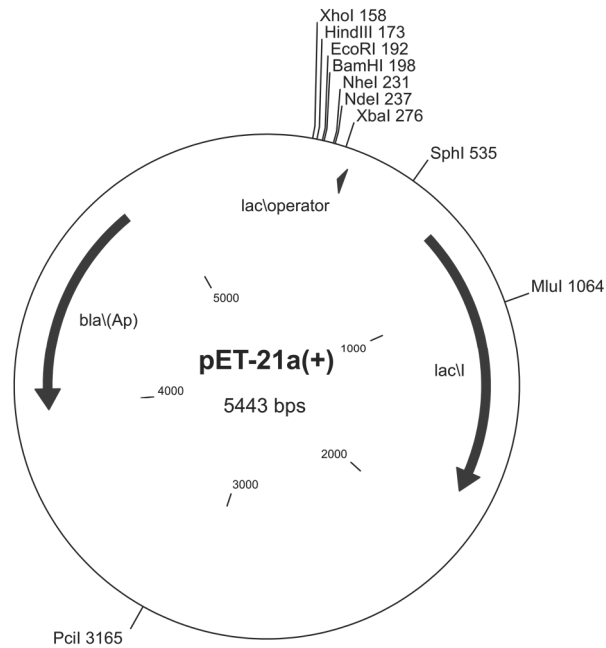


**Figure 109** Vector map of pET-21a(+) showing the positions of common restriction enzymes.

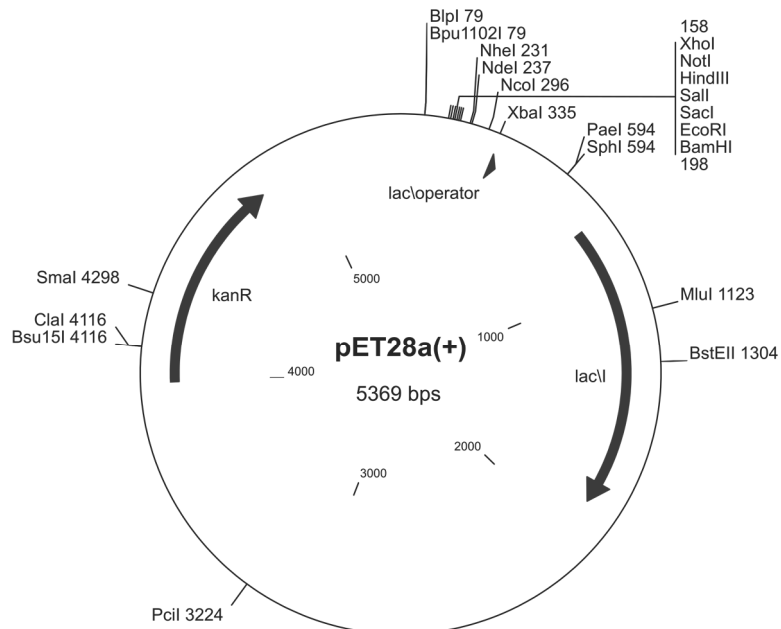


**Figure 110** Vector map of pET-28a(+) showing the positions of common restriction enzymes.

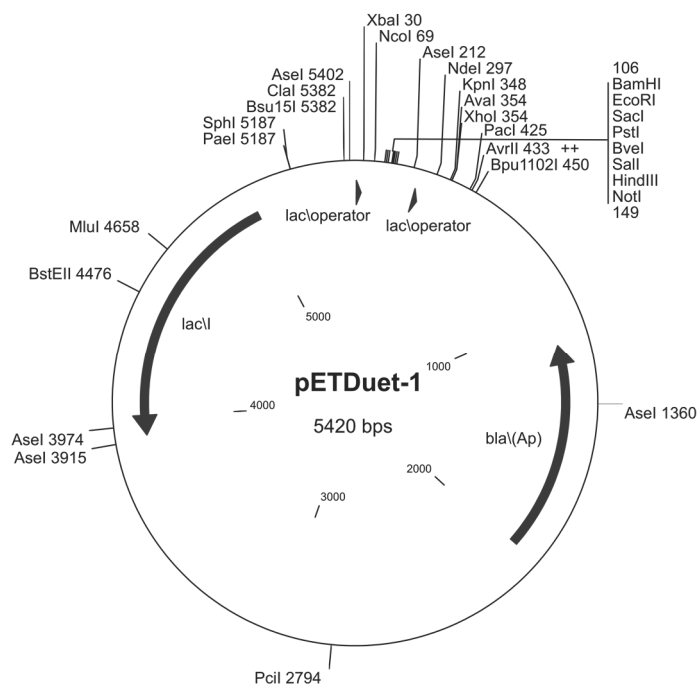


**Figure 111** Vector map of pET-Duet-1 showing the positions of common restriction enzymes.

### 9.1.2 *abg* — $\beta$ -Glucosidase of *R. radiobacter*

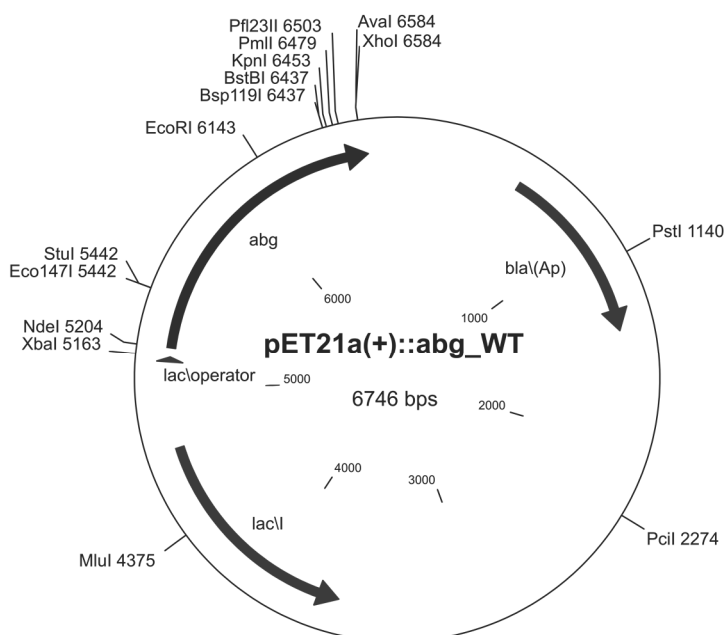


**Figure 112** Vector map of pET-21a(+)::abg\_WT containing *abg* of *R. radiobacter* in the wild type form inserted between Nde I and Xho I. The map shows the positions of common restriction enzymes.

GenBank Accession: JZLL01000080.1 (genome, Locus 39,485–40,885), KJX85806.1 (protein)

Gene Sequence (5'→3', 1404 bp, underlined nucleotides originate from the vector's His<sub>6</sub>-tag):

ATGACCGATCCCCAAACGCTTGCAGCCCGTTTCCCCGGCGATTTCTGTTTCGGCGTGG  
 CGACCGCCTCCTTCCAGATCGAGGGTGCCACCAAGGTTGACGGCCGCAAGCCATCCAT  
 CTGGGATGCCTTCTGCAACATGCCGGGCCATGTCTTCGGGCGCCACAATGGCGACGTT  
 GCCTGCGATCACTATAATCGCTGGGAGGATGATCTCGATCTCATCAAGGAAATGGGTGT  
 CGAGGCCTATCGTTTCTCATTGCCTGGCCGCGCATCATTCCCGATGGATTTCGGCCCG  
 ATCAACGAGAAGGGGCTGGATTTCTACGACCGCCTCGTCGATGGCTGCAAGGCGCGCG  
 GCATCAAGACCTATGCGACGCTTTACCATTGGGACCTGCCGCTGACACTGATGGGCGA  
 CGGCGGCTGGGCCTCGCGTTCCACCGCCCATGCCTTCAGCGTTACGCCAAGACCGT  
 CATGGCACGGCTGGGCGACCGGCTGGATGCGGTGGCGACCTTCAATGAACCCTGGTG  
 TCGGGTTTGGCTCAGCCATCTCTATGGCATCCATGCGCCGGGCGAGCGCAACATGGAA  
 GCAGCCCTTTCGGCCATGCACCACATCAACCTTGCCCATGGTTTCGGCGTTCGAGGCGT  
 CCCGCCATGTTGCGCCCAAGGTGCCGGTTCGGACTGGTGTGAACGCCCATTCGTCAT  
 CCCGGCCTCCAATAGCGACGCCGACATGAAGGCAGCTGAACGGGCATTCCAGTTCCAC  
 AACGGCGCGTTTTTTCGATCCGGTCTTCAAGGGCGAATATCCGGCCGAAATGATGGAGG  
 CCCTGGGCAGCCGCATGCCGGTGGTGGAGGCGGAAGACCTGTCCATCATCAGCCAGA  
 AGCTCGACTGGTGGGGCCTGAATTATTATACACCGATGCGCGTTGCCGACGACGCCAC  
 CGAAGGTGCGGAATTCCCTGCCACCAAACCAGCCCCGGCCGTCAGCGATGTCAAACC  
 GATATCGGCTGGGAAGTCTATGCGCCGGCGCTGCATTCCCTGGTGGAGACGCTCTACG  
 AGCGCTACGAGCTGCCCGATTGCTACATCACCGAAAATGGCGCCTGCTACAATATGGG  
 CGTCGAAAACGGCGAGGTGGATGATCAACCCCGTCTTGACTIONTACGCCGAACATCTTG  
 GTATCGTTGCTGATCTGGTGAAGGACGGTTACCCCATGCGGGGTTACTTCGCCTGGAG  
 CCTGATGGACAATTTTCAATGGGCGGAAGGGTACCGCATGCGCTTTGGCCTCGTTCAC  
 GTGGATTACGAAACGCAGGTTTCGTACGCTGAAGAACAGCGGCAAATGGTACAGCGCGC  
 TGGCATCGGGTTTTCCGAAGGGGAACCATGGTGTGGTGAAGGGGCTCGAGCACCACCA  
CCACCACCACTGA

Amino acid sequence (467 aa, underlined amino acids derive from the fused His<sub>6</sub>-tag):

MTDPQTLAARFPDGLFLGVATASFQIEGATKVDGRKPSIWDAFCNMPGHVFGRHNGDVAC  
 DHYNRWEDDLDIKEMGVEAYRFSIAWPRIIPDGFPIKGLDFYDRLVDGCKARGIKTYA  
 TLYHWDLPLTLMGDGGWASRSTAHAFQRYAKTVMARLGDRLDVATFNPEWCAVWLSHL  
 YGIHAPGERNMEAALAAMHHINLAHGFGVEASRHVAPKVPVGLVLNAHSVIPASNSDADMK  
 AAERAFQFHNGAFFDPVFKGEYPAEMMEALGSRMPVVEAEDLSISQKLDWWGLNYYTPM  
 RVADDATEGAFFPATKPAPAVSDVKTDIGWEVYAPALHSLVETLYERYELPDCYITENGACY  
 NMGVENGEVDDQPRLDYYAEHLGIVADLVKDGYPMRGYFAWSLMDNFEWAEGYRMRFGL  
 VHVDYETQVRTLNKSGKWYSALASGFPGKNGHGVVKGLEHHHHHHH

### 9.1.3 *bglU* — $\beta$ -Glucosidase of *M. antarcticus*

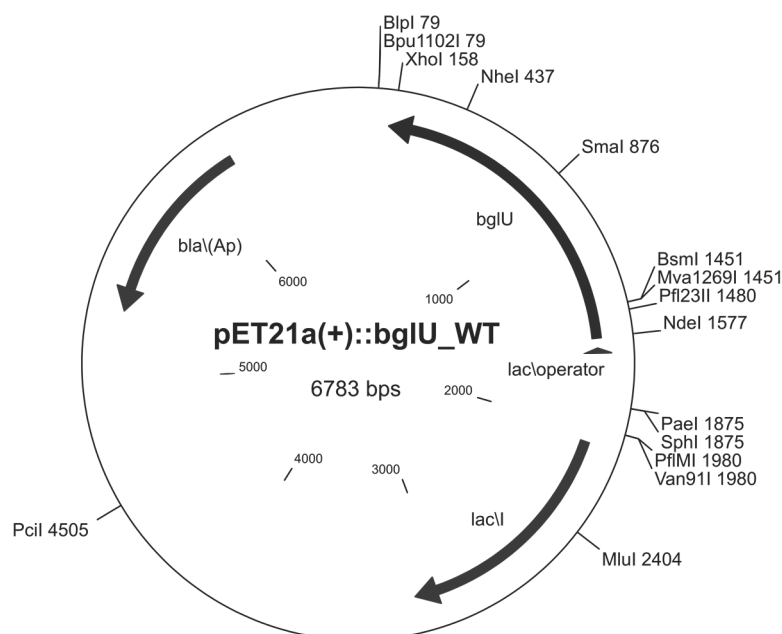


**Figure 113** Vector map of pET-21a(+):*bglU*\_WT containing *bglU* of *M. antarcticus* in the wild type form inserted between Nde I and Xho I. The map shows the positions of common restriction enzymes.

GenBank Accession: FJ483828 (gene), ACM66669 (protein)

Gene sequence (5'→3', 1443 bp, underlined nucleotides originate from the vector's His<sub>6</sub>-tag):

```

ATGATGAACCATCTAAGCCAAAAGTTTCGCATGGCCTAAGGAGTTCCTCTGGGGTAGCGC
TACCGCTGCTGCACAGATTGAGGGTGCTGGTCACTCGTACGGTAAGGAGGACAGCGTT
TGGGATGCATTCGCACGTAAGGAGGGTGCAATTGCTGGGGGAGAAAACCTTAGAGGTTG
CTGTTGATCATTACCATCGTTACCGTGAGGACGTTCAAGTAAATGCGTGAGCTGGGTCTG
GATAGCTACCGTTTCAGCACCTCTTGGGCTCGTGTTGTTCCGGGTGGTCGTACCGTTAA
CCCGGAGGGTCTGGACTTCTACAGCCGTCTGGTTGATGAACTGCTGGAAAACGGTATT
CTGCCGTGGCTGACCTTATAACCATTGGGACCTGCCGCAGGCTCTAGAGGAACGTGGAG
GTTGGACCAACCGTGAAACCAGCTACAAGTTCTTAGAGTACGCAGAAACTGTTACAGAG
AAGTTAGGTGATCGTGTTAAGCATTGGACCACCTTCAACGAGCCGCTGTGTTTCGAGCCT
GATAGGTTACGCAGCAGGTGAACACGCACCGGGGCGTCAAGAGCCTCAAGCAGCACT
GGCTGCAGTTCATCATCAGCACCTGGCACATGGTCTCGCAACCGCACGCCTGCGTGAG
CTGGGTGCAGAACACATTGGTATTACCCTGAACCTGACCAACGCAGTTCGGAACAACCC
GGGTGACCCGTTGACCTGGAGGCTGCACGTCGTGTTGATGCTCTCTGGAACCGTATG
TACCTGGACCCTGTTCTGCGTGGAAGCTACCCGGAGGATCTGCTAGAGGATGTTTCAGG
GACTCGGTCTGGCTGAGGTTATAGAGGCTGGGGATCTGGAAATTATTAGCCAGCCTATT
GATTCCTCGGTGTTAACCATTACCATGACGATAACGTATCGGGTCACCCGCTGCCGGC
AGGTCAGCCGCAGCCGTTGTTTCTACCGACAGCCGAAGTCGAGCCCTTTCGTTGGT
TCTGAATACGTTACCTTCCCGGCTCGTGATCTGCCGCGTACCGCAATGGGTTGGGAGG
TTAACCCGGAGGGTCTGCGTGTTCTGCTCAACCGTCTCAACCAGGATTACGCTAACCTA
CCGAGCCTGTACATTACCGAAAACGGTGCTAGCTACACCGACACCGTTACCGAAGCAG
GGACCGTAGAGGACCCGGAGCGTGAAGAGTACATTTTAAACCATCTAGACGCTGTTGTT
CGTGCAATAGCTGATGGTGTGACGTTTCGTGGTACTTCGTTTGGTTCGCTCCTGGATAA

```

CTTCGAGTGGGCTTGGGGTTACGCAAAGCGTTTCGGTATAATTCATGTTGACTACCAGA  
 CCCAGGTTTCGCACCATAAAGAAGCTCGGGTAAGGCATACGCTGGTCTCATAGCAGCTAAC  
 CGCACTATGGCTCTCGAGCACCACCACCACCACACTGA

Amino acid sequence (480 aa, underlined amino acids derive from the fused His<sub>6</sub>-tag):

MMNHLSQKFAWPKEFLWGSATAAAQIEGAGHSYGKEDSVWDAFARKEGAIAGGENLEVAV  
 DHYHRYREDVQLMRELGLDSYRFSTSWARVVPGGRTVNPEGLDFYSRLVDELLENGILPW  
 LTLYHWDLPQALEERGGWNTNRETSYKFLEYAETVHEKLGDRVKHWTTTFNEPLCSSLIGYAA  
 GEHAPGRQEPQAALAAVHHQHHLAHLATARLRELGAEHIGITLNLNAVPNNPGDPVDLEA  
 ARRVDALWNRMYLDPVLRGSPEDLLEDVQGLGLAEVIEAGDLEIISQPIDFLGVNHYHDDN  
 VSGHPLPAGQPQPVVPTDSPKSSPFVGVSEYVTFPARDLPRTAMGWENVPEGLRVLLNRLN  
 QDYANLPSLYITENGASYTDTVTEAGTVEDPEREYILNHLDAVVRAIADGVDVVRGYFVWSL  
 LDNFEWAWGYAKRFGIIHVDYQTQVRTIKNSGKAYAGLIAANRTMALEHHHHHHH

### 9.1.4 *bglC* — $\beta$ -Glycosidase of *P. furiosus*

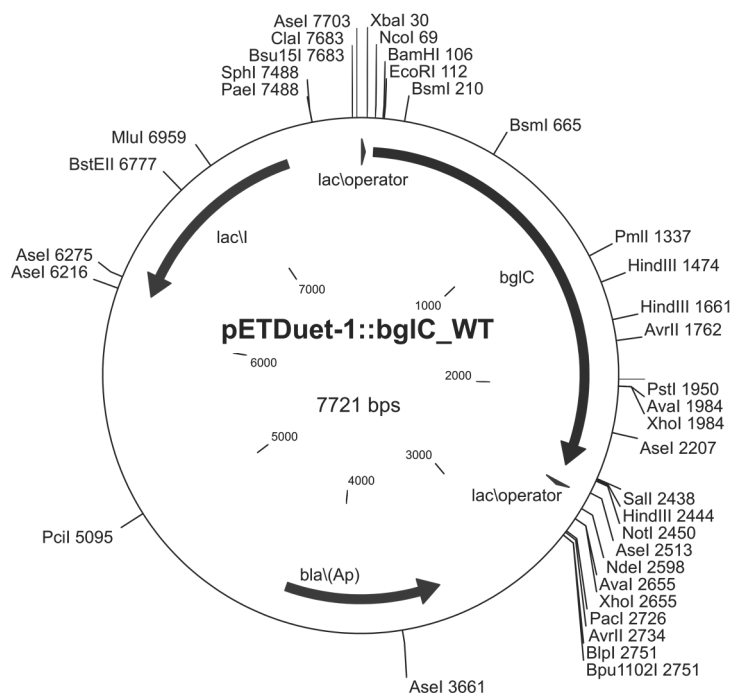


**Figure 114** Vector map of pET-Duet-1::bglC\_WT containing *bglC* of *P. furiosus* in the wild type form inserted between Nco I and Sal I. The map shows the positions of common restriction enzymes.

GenBank Accession: WP\_011011477.1 / PF\_RS01865 (gene), AAL80487 (protein)

Gene sequence (5'→3', 2367 bp, underlined nucleotides originate from the vector's His<sub>6</sub>-tag):

ATGGGCAGCAGCCATCACCATCATCACACAGCCAGGATCCGAATTCAATGGTAAAACC  
TATCTTCCTTGATGGTAAAAGGATTGTTGTTTATGGAGGTACCCTTCAGTATTTTAGAGTT  
 CCCAGGAACTCCTGGGAAAGAATGCTAAAGAAAATGAAGTCTCACGGGCTAAACACCAT  
 TGATACGTACATTGCTTGGAAATTGGCACGAGCCCCAAGAAGGACTCTTCGACTTTACTG  
 GCGAAACTCACCCCAAAGAGATCTCGTCGGTTTTCTTGATCTAGCACAAAACTCGGC  
 TTTTACGTTATCATAAGACCTGGCCCATACATTTGTGGAGAGTGGAAAAATGGAGGCAT  
 196

CCCTGAGTGGTTGATTA ACTCTCATCCAGAAACTTTGCAAAGGCCCGAATGGTACTC  
 TTCCAAGGGATATATACTATCCTCCAATCACATACCTCCATCCCCTTACTTGGAAATATG  
 TAATGAAGTGGTATGAGAATGTTTTCTATAATAAAGGAATATCTGTACTCCAATGGGG  
 GGCCTATAATAAACGTGACGATTGATGACGAACCTTCTACTGGGAACCATCTTCCAG  
 GCATTCTTGACCGATTACAACGAAATAGTAGTTAAGGAGAATGGGATCTGGCACTCTTG  
 GCTAAAGGAAA ACTACCAGTTGGATGAATTGGAGGAGAGATACGGTCAGAAGTTTTTCAG  
 ATTATGCTGAGATTGTCCCACCAACGTCATTCTCAGAGCCCCTTCCAAAGATACTCGACT  
 GGCATCACTTCAAGATATGGATGATCAACGAGTACGTAAGGATACTCTACGAAAAGATA  
 AAGAAGTACGTTGATGTTCCAATTAGCATTTTAGATCCCTATTTACTCTTAGCCGCATGG  
 AAGGAGTTTTACCTCTACGTAACCAAGCACAAAGCTCGACATCCACCTATGGACGGAGTT  
 CTGGTACTCATTCTACAGAACATTTGACTTCAAAGAAGACAGACTCGGCCACCTCTACTA  
 TAAGACGGGGGTTTATAGATATTACATAAACAAGCTGAAGACTCCCCACTAAGCATAG  
 AGACCCAAACATCCCTCGCCAATGTTATAGAGAAGGATGAGGCCGAGCTCCTCTATGCC  
 CTCTTCCAGCTTTGGGAATCCACAACATAAACTACTATCTCTACGTGGGTGGCGAAAAT  
 CCGAAAGGTTATGAATCACACAACGGAGCTACCTGGGACGTGTATTCGCCCATAGGATT  
 GGATGGAAGAGAAAGACAGCACGTGGAACCAATAAAGTGGATTGGCGAGTTCTTAAAGT  
 CTAACATGGACTTCATCGAGTCCCAACTAAAGCCAAAAGTTGCCTTTGGGATGTACGAG  
 CCTTATGAAGCCTTAAGCATGTGGGGACATCGGCCAGAAAGCTTCGAAGAGAGCGTAA  
 ATCTCCAAGAATATCTCTTTGGGGAGAGAGGATTGCTCACACTCTTGGCCATGAGCAAT  
 GTTCCCTTTGACGTCATAGACCTTGAACCTTCCACTGTAGAGGAGATGCTCCAATATGAG  
 CAGATTTGGATTTACAGCCTGGATTTTATGAGCAGAGAAGTTCAAGAAAAGCTTGCTAG  
 ATACGTGGAAGAGGGAGGAAACCTCGTGATCCTACCAACCCTTCCATCCCTTGATGAGA  
 ACATGAAGCCCTACACAAAGCTGAGGGACTTCTAGGAATTGAAGTTGAGAAGGCCAAG  
 GCAAGGGATAACATGAGGTTAATTCCTACATCAGCGTTGATGCAGAGGAGATAGACAG  
 GATGGTCGTCAGAAACGTCGTTAGGGAGGTTAAAGGAGGGAAAGCTATAGCTTGGGTT  
 GGAGATAAAGTAGTAGGGGTTATGGTAAGGAAAGGAAAGGTTCTGCAGTTGTCTTAGG  
 GTTCAGGCTTCAGTACTACTCGAGCTACCACGATCTACACAGGAAGTTTGTGATAAGAT  
 ACTCCAGCTCCAAGGGATTGAAAGGGATTTTGAAGTCTCAAACAGAGACATAATAGTAAT  
 TCCAAGAGGGAATTATCTGGTGGTGGTAAATCCAGGGACGACAAGGTTACTGGAAAA  
 GTTAGATACAGGGGTGTCGAGTTTAAATGTTGAGCTTAATAAGAGGGGAGTTCTCTACAT  
 CCCAATTAATGTGGAATAAACGGCATTAAAGTGCTCTATGCCACAGCAACTCCAGTGG  
 GAAGGGGAGAGGGAACAATTAGATTTAGAAACCATTTGGCAAATGTAAGTAAATTGCA  
 ATTAACGGCAAGATCAAGGAAGTCTCAGGGGGGTATATCCTCCAAGAGAAGAGCTCAG  
 GAGAGAAAACATCTATGTGATAAAACACGAGAGCGAAACATTGAAATAAGAGTTTAG

Amino acid sequence (788 aa, underlined amino acids derive from the fused His<sub>6</sub>-tag):

MGSSHHHHHSQDPNSMVKPIFLDGKRIVVYGGTLQYFRVPRNSWERMLKMKSHGLNTI  
 DTYIAWNWHEPQEGLDFDTGETHPQRDLVGFLDLAQKLGFYVIIRPGPYICGEWKNGGIPE  
 WLINSHPEILAKGPNGLPRDIYPPITYLHPTYLEYVMKWYENVFPIIKEYLSNGGPIINVTI  
 DDEPSYWETIFQAFLTDYNEIVVKENGIWHSWLKENYQLDELEERYGQKFSDYAEIVPPTSF  
 SEPLPKILDWHHFKIWMINEYVRILYEKIKKYVDVPISILDPYLLLAWKEFYLYVTKHKLDIHL  
 WTEFWYSFYRTFDKEDRLGHLYYKTGVYRYIYINKLKTPLSIETQTS LANVIEKDEAELLYA  
 LLPALGIHNINYYLYVGGENPKGYESHNGATWDVYSPIGLDGRERQHV EPIKWIGEF LKSNM  
 DFIESQLKPKVAFGMYPYEALSMWGH RPESFEESVNLQEYLFGERGLLTLLAMS NVPFDVI  
 DLLELSTVEEMLQYEQIWIYSLDFMSREVQEKLARYVEEGNLVILPTLPSLDENMKPYTKLR  
 DFLGIEVEKAKARDNMRLIPYISVDAEEIDRMVVRNVREVKGKAI AWVGDKVVGVMVRK  
 GKGS AVVLGFRLQYYSSYHDLHRKFVDKILQLQGIERDFEVSNRDIIVIPRGN YLVVVNPRDD

KVTGKVRVYRGVEFNVELNKRGVLYIPINVEINGIKVLYATATPVGRGEGTIRFRNHLANVTEIA  
INGKIKEVSGGYILQEKSSGEKNIYVIKHESETFEIRV

### 9.1.5 *cbg1* — $\beta$ -Glucosidase of *R. radiobacter*

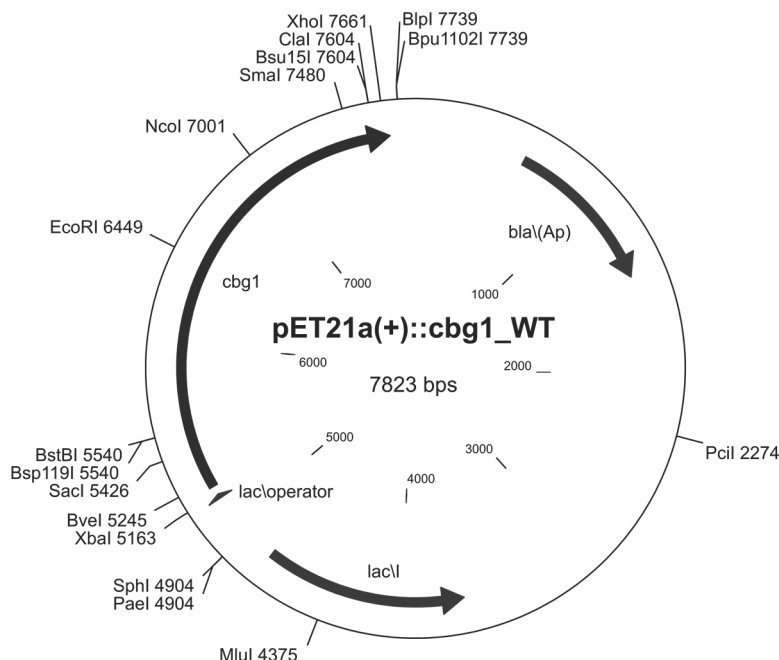


**Figure 115** Vector map of pET-21a(+):*cbg1*\_WT containing *cbg1* of *R. radiobacter* in the wild type form inserted between Nde I and Xho I. The map shows the positions of common restriction enzymes.

GenBank Accession: M59852 (gene), AAA22082 (protein)

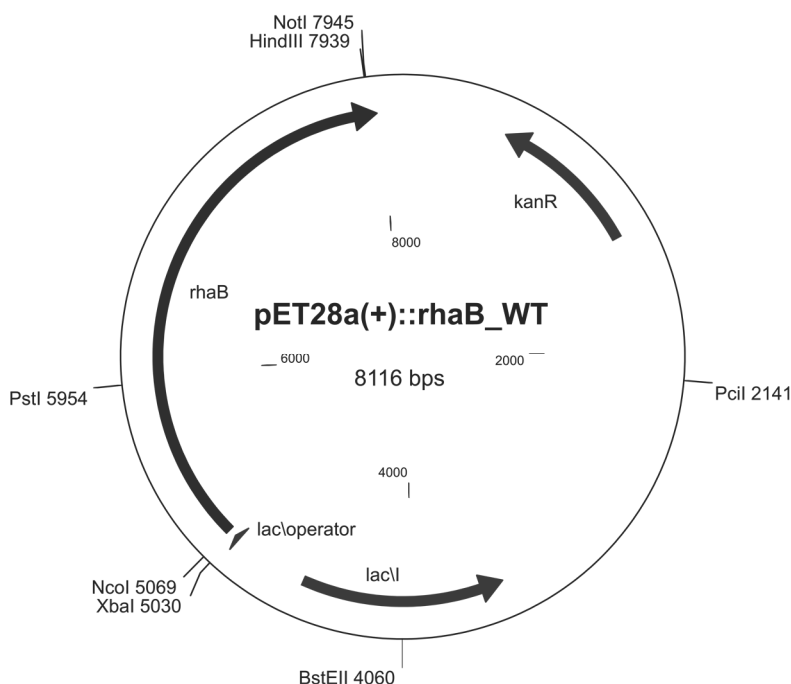
Gene sequence (5'→3', 2481 bp, underlined nucleotides originate from the vector's His<sub>6</sub>-tag):

ATGATCGACGATATTCTCGATAAGATGACACTGGAGGAGCAGGTGTCGCTGCTCTCGG  
GCGCGGATTTCTGGACGACCGTCGCGATCGAGCGGCTCGGCGTGCCGAAGATCAAGG  
TTACCGACGGCCCAATGGCGCACGCGGCGGGTTCGCTGGTTCGGCGGGCGTCAAGT  
CCGCTGCTTCCCGGTGGCAATCGCGCTTGGAGCGACGTGGGACCCGGAGCTCATCG  
AGCGCGCCGGCGTGGCGCTGGGAGGACAAGCCAAGAGCAAGGGCGCGTCCGTGCTT  
CTGGCGCCGACCGTCAACATTCACCGCTCCGGCCTCAATGGCCGCAACTTCGAATGCT  
ATTCGGAAGACCCGGCGCTGACCGCCGCCTGCGCCGTGCGCCTATATCAATGGCGTGCA  
GAGCCAGGGTGTGGCCGCCACGATCAAGCACTTCGTGCGCAACGAGTCCGAGATCGA  
GCGGCAGACCATGTCCTCCGATGTCGATGAGCGGACGCTGCGCGAAATCTATCTGCCG  
CCTTTCGAGGAGGCGGTGAAGAAGGCCGGCGTGAAGGCCGTGTCCTCTACAACA  
AGCTCAACGGCACCTATACGAGCGAAAATCCCTGGCTGCTGACGAAAGTCTGCGCGA  
GGAATGGGGCTTCGACGGCGTGGTCATGTCCGACTGGTTCGGCTCGCACTCGACGGC  
TGAAACCATCAATGCCGGGCTCGATCTGGAGATGCCGGGGCCTTGGCGGGATCGCGG  
CGAAAAGCTGGTGC CGCAGTCCGGGAAGGCAAGGTAAAGGCCGAGACCGTGC CGC  
TTCGGCACGGCGTATTCTCCTTCTGCTCGAACGCGTCCGGCGCCTTTGAAAAGGCGCCT  
GATCTCGCCGAACACGCGCTTGATCTGCCGGAAGATCGTGC GCTCATCCGCCAACTCG  
GTGCGGAGGGTGCTGTACTCCTGAAGAATGACGGAGTGCTGCCGCTTGCCAAGTCGTC

CTTCGACCAGATCGCCGTCATCGGCCCAATGCGGCTTCCGCACGCGTCATGGGCGGA  
 GGAAGCGCGCGGATTGCCGCGCATTATACGGTGAGCCCACTTGAGGGCATTTCGCGCG  
 GCGCTGTCCAACGCCAACAGCCTCCGCCATGCGGTTCGGCTGTAACAACAACCGGCTCA  
 TCGACGTCTTCAGCGGCGAGATGACGGTGAATACTTCAAGGGACGCGGCTTCGAGAG  
 CCGTCCGGTCCATGTCGAGACCGTCGAAAAGGGCGAATTCTTCTGGTTCGATCTCCGT  
 CCGGCGACCTTGATCTCGCCGATTTTTTCGGCGCGCATGACGGCGACCTTCGTGCCGCA  
 GAAACCGGTGAACACATCTTCGGCATGACCAATGCTGGGCTTGCTCGGCTGTTCGTG  
 GACGGCGAACTGGTGGTTCGATGGCTATGACGGTTGGACGAAGGGTGAGAACTTTTTTG  
 GAACCGCGAACAGCGAGCAGCGTCGGGCGGTAACGCTTGGGGCCGCACGCCGCTACC  
 GGGTTGTGGTTCGAATATGAGGCGCCGAAGGCCAGCCTGGACGGCATCAACATATGTGC  
 GCTCCGCTTCGGTGTGAAAAGCCGCTCGGCGATGCCGGGATTGCGGAGGCGGTGCA  
 AACCGCCCAGTCCGATATCGTACTGCTCCTCGTTCGGCCGTGAGGGCGAGTGGGA  
 CACCGAAGGTCTGGATCTGCCGACATGCGCCTGCCGGTTCGCCAGGAGGAGCTGAT  
 CGAGGCGGTTCGCCGAAACCAATCCCAACGTGGTTCGTGGTACTGCAAACGGGTGGTCC  
 CATCGAGATGCCATGGCTCGGCAAGGTGCGTTCGGTTCGAGATGTGGTATCCCGG  
 CCAGGAACTTGGCAATGCGCTTTCGGACGTTCTTTGGTGTGTCGAGCCTGCCGGC  
 CGCTTGCCACAGACCTTCCCGAAGGCGCTCACGGATAATTCCGCCATTACCGACGATC  
 CGTCGATCTATCCTGGCCAGGACGGCCATGTGCGCTACGCGGAAGGGATCTTCGTCCG  
 CTATCGCCATCACGATACAAGAGAGATCGAACCACTCTTCCCCTTCGGCTTCGGTCTTG  
 GCTACACCCGCTTTACCTGGGGTGCCCCGCAACTATCGGGAACGGAAATGGGGGCGG  
 ATGGTCTTACGGTGACGGTTCGATGTCACCAATATAGGCGACAGGGCGGGATCGGACGT  
 GGTGCAGCTCTATGTTCACTCTCCCAATGCCAGGGTTCGAGCGGCCGTTCAAGGAGCTG  
 CGTGCCTTTGCGAAGCTCAAGCTGGCCCCGGGCGCGACCGGTACGGCGGTGCTGAAG  
 ATCGCTCCTCGCGACTTGGCTTACTTCGATGTCGAGGCCGGTTCGTTCCGGGCTGATG  
 CGGGCAAGTACGAGCTGATCGTGGCGGCCAGCGCCATCGATATCCGGGCAAGCGTAA  
 GTATCACTTGCCGGTTCGATCATGTGATGGAGCCGCTCGAGCACCACCACCACCACCA  
CTGA

Amino acid sequence (826 aa, underlined amino acids derive from the fused His<sub>6</sub>-tag):

MIDDILDKMTLEEQVSLLSGADFWTTVAIERLGVPKIKVTDGPNRGARGGSLVGGVKSACFP  
 VAIALGATWDPELIERAGVALGGQAKSKGASVLLAPTUNIHRSGLNGRNFECYSEDPALTAA  
 CAVAYINGVQSQGVAATIKHFVANESIERQTMSSDVERTLREIYLPPFEEAVKKAGVKAV  
 MSSYNKLNQTYTSENPWLLTKVLRREEWGFVMSDWFVSHSTAETINAGLDLEMPGPW  
 RDRGEKLVAAVREGKVKAETVRASARRILLERLVGAFEKAPDLAEHALDLPEDRALIRQLG  
 AEGAVLLKNDGVLPLAKSSFDQIAVIGPNAASARVMGGGSARIAAHYTVSPLEGIRAALSNA  
 NSLRHAVGCNNRLIDVFSGEMTVEYFKGRGFESRPVHVETVEKGEFFWFDLPSGDLDLA  
 DFSARMTATFVPQETGEHIFGMTNAGLARLFVDGELVVDGYDGWTKGENFFGTANSEQRR  
 AVTLGAARRYRVVVEYEAPKASLDGINICALRFGVEKPLGDAGIAEAVETARKSDIVLLLVR  
 EGEWDEGLDLPDMRLPGRQEELIEVAETNPNVVLQTGGPIEMPWLKVRVAVLQMWY  
 PGQELGNALADVLFGDVEPAGRLPQTFPKALTDNSAITDDPSIYPGQDGHVRYAEGIFVGYR  
 HHDREIEPLFPFGFLGYTRFTWGAPQLSGTEMGADGLTVTDVTNIGDRAGSDVVQLYV  
 HSPNARVERPFKELRAFAKLKLAGATGTAVLKIAPRDLAYFDVEAGRFRADAGKYELIVAA  
 SAIDIRASVSIHLPVDHVMPELEHHHHH

9.1.6 *rhaB* —  $\alpha$ -L-Rhamnosidase of *Bacillus* sp. GL1

**Figure 116** Vector map of pET-28a(+):*rhaB*\_WT containing *rhaB* of *Bacillus* sp. GL1 in the wild type form inserted between Nco I and Hind III. The map shows the positions of common restriction enzymes.

GenBank Accession: AB046706 (Gene), BAB62315 (Protein)

Gene sequence (5'→3', 2910 bp, underlined nucleotides originate from the vector's His<sub>6</sub>-tag):

```

ATGGCAGGCAGGAATTGGAACGCTTCATGGATTTGGGGAGGACAAGAGGAGAGTCCGC
GCAACGAGTGGCGGTGCTTCCGGGGCAGCTTCGACGCGCCTGCGTCCGGTCGAGGGAC
CGGCCATGCTTCATATAACGGCGGATTCGCGATACGTACTIONTTCGTGAACGGCGAGCA
AGTGGGGAGAGGCCCGTGCCTCCTGGCCGAAGGAGCAGTTTTACGATTCGTACGAC
ATCGGCGGGCAGCTGCGCCCGGGCGTCCGCAATACGATCGCGGTGCTGGTGCTTCAT
TTCGGCGTGTGCAACTTTTATTACTTGCCTGGACGCGGGCGGGCTGATCGCCGAGATCG
AAGCCGATGGCCGCACGCTTGCCTGGACGGATGCCGCATGGCGGACGGAGCGGCTG
GGCGGACAGCGTTCCAATTCCCCTCGGATGGCCTGCCAGCAGGGATTCCGGGAAGTC
ATCGACGCGCGGAGCTGGCGGAAGACTGGGCCCTTCCGGCGTTCGACGACGGCGGC
TGGGCGCAAGCCCGATCGATCGGACCCGACAGGCACGGCGCCCTGGACCTCGCTCGTT
CCGCGCGATATTCCTTTTTTGACGGAAGAAAAGCTGTATCCCGCCTCGATCCAGTCGCT
TAGCCGGGTGAAGGCGCCCAAGTACGCAGCCGCGCTGGATCTGCGCAATCAAATGGT
GCCCGAGAGCGTTAACCATGCGAACCCCGTCTCCTACTGCGGTTATGTGGCGACGATC
CTCACGCTCGAGACAAGCGGCGTCGTACGCTCGGATCCCGACCGGCGTACGGGGG
AGCGGCGTATGGGTGACGGCGTCTTCAAACCGAGTGGACGGGCGTGCAGCCGGAG
CGATATTACAGCTTGAACCTCGCTGCAGGCGAGCATCTGGTTCTTGTGATATTACGAG
CTCCGATCATGGCGGCAGCAGCCATTTTGCATCGACAGCGAAGCGGCGTTCACGCTG
CGCTCGCCGGCCGGCGACAATGGCGTGCCGCTGGCGACGATCGGTACGTTCCGACCAG
TCCGAATACATCGATCACCGCCCGGGCAGACGGATGCAGACGGACCATCCGGATTATC
GGGCGCTGCCGGAAGCCGCGCCTACCGCCCGCGCTTGAAGCGTTCGTTCCCTGGG
TCAAGCCGTTCCGAGCCTTCGCTCTATACGGAGGAAAACGTGTTCCGGATCTAACGTATGG
CGAACGCTCGCCGAACGCAGGGCGGTGCCGAGATCCGTTCTGAACGCGATATTGCCG

```

GTTCCCGAGCCGGGCGTCCTGCCCGTATTCGAGGACGGAGACTGCGAGCTCGTCATC  
 GATCTGGGCGCGGAGCGCTCCGGGTTTATCGGCTTCGAGCTCGAAGCGCCCGCCGGT  
 ACGATCATCGATGCCTATGGCGTCGAATATATGAGAGAAGGCTACACGCAGCACACGTA  
 CGGGCTCGACAACACGTTCCGCTATATTTGCCGCGAAGGCAGACAATCGTACGTGTCC  
 CCCGTGCGCCGCGGTTTCCGGTACTTGTTCTGACCGTCAGAGGCAATAGCGCGCCGG  
 TGAAGCTGCACGAGATTTATATCCGCCAGAGCACGTACCCGGTCGCGGAACAAGGCAG  
 CTTCCGCTGCTCCGACGCGCTGCTGAACGCAACGTGGGAGATCAGCAGGCACACCACC  
 AGATTGTGCATGGAGGACACGTTCTGTCGACTGCCCGTCCTATGAACAGGTGTTCTGGG  
 TGGGCGACAGCCGCAACGAGGCGCTGGTCAACTATTACGTTTTTCGGCGAGACCGGAT  
 CGTGGAGCGCTGCCTGAATCTCGTGCCGGGCTCGGCGGACGAGACGCCGCTTTATCT  
 CGACCAGGTGCCGAGCGCATGGAGCAGCGTCATCCCGAACTGGACGTTCTTCTGGATA  
 CTCGCTTGCCGGGAATATGCCGCGCATAACGGGCAACGAAGCCTTCGCCGCCCGCATCT  
 GGCCTGCGGTGAAGCACACGCTGACGCATTATTTAGAACACATCGACGACAGCGGCCT  
 GCTGAACATGGCGGGTTGGAATCTGCTGGACTGGGCGCCGATCGACCAGCCGAACGA  
 AGGCATCGTCACCCACCAGAACCTGTTCTCGTCAAGGCGCTTCGGGATTTCGCGGGCG  
 CTTGCCGCCGCGGCCGCGCAACCGAAGAGGCAGACGCGTTTCGCGGCGCGCGCCGA  
 CTTCTGGCCGAGACGATCAACGCGGTATTGTGGGACGAGGAAAAGCGCGCTTATATC  
 GATTGCATCCACGCGGACGGGCGCCGTTTCGGACGTATACAGCATGCAGACGCAGGTC  
 GTCGCTTATCTGTGCGGGGTTGCGCAGGGCGAACCGCAAGCCGTCATCGAAGGCTAC  
 CTGTCGTCGCCCGCCGCGGCTTTTCGTACAGATCGGCAGCCCGTTTATGTCGTTTTTCTA  
 CTACGAGGCGCTCGAGAAGGCCGGCCGTCAAACGCTGATGCTCGACGACATCCGCCG  
 CAATTACGGCCAGATGCTGCGCTACGATGCCACGACCTGTTGGGAGATGTATCCGAAC  
 TTTGCGGAAAATCGCAGCAACCCGGACATGCTGACCCGCAGCCATTGCCATGCATGGT  
 CGGCGGCGCCGGGCTATTTCTGGGCTCGAGCATTCTCGGCGTCAAGCGGGGAGCTG  
 ACGGGTGGCGAACCGTCGATATCGCGCCGACGCTTGCATCTAACCTGGGCCGAAG  
 GCGTCGTGCCGCTGCCGACGGGCGGTACATCGCGGTGAGCTGGGAGTTCGTATCCG  
 CCGGCAAGCTGAAGCTGAGAATCGAGGCGCCGGAGGATATCGAGGTGAACGTGACGC  
 TGCCCGAAGGAATAGAAGGCGAAGTGACGCAGGTTAAGTATATGAGCAAGCTTGCGGC  
 CGCACTCGAGCACCACCACCACCACCTGA

Amino acid sequence (969 aa, underlined amino acids derive from the fused His<sub>6</sub>-tag):

MAGRNWNASWIWGGQEESPRNEWRCFRGSFDAPASVEGPAMLHITADSRVLFVNQEYV  
 GRGPVRSWPKEQFYDSYDIGGQLRPGVRNTIAVLVLHFGVSNFYLRGRGGLIAEIEADGR  
 TLAATDAAWRTERLGGQRSNSPRMACQQGFGEVIDARELAEDWALPAFDDGGWAQARSI  
 GPAGTAPWTSVPRDIPFLTEEKLYPASIQSLSRVKAPKYAAALDLRNQMVPESVNHANPVS  
 YCGYVATILTLETSGVVTLGFP TGVRGSGVWVDGVLQTEWTGVQPERYYSLNLAAGEHLVL  
 VDITSSDHGGSSHFAIDSEAAFTLRSPAGDNGVPLATIGTFDQSEYIDHRPGRRMQTDHPDY  
 RALPEAAPTAAALEAFASWVKPFEP SLYTEENVFGSNVWRTLAEERRAVPRSVLNAILPVPEP  
 GVLPVFEDGDCELVIDLGAERSGFIFELEAPAGTIIDAYGVEYMREGYTQHTYGLDNTRYI  
 CREGRQSYVSPVRRGFRYLFLTVRGN SAPVKLHEIYIRQSTYPVAEQGSFRCS DALLNATW  
 EISRHTTRLCMEDTFVDCPSYEQVFWVGD SRNEALVNYYVFGETEIVERCLNLVPGSADET  
 PLYLDQVPSAWSSVIPNWTFFWILACREYAAHTGNEAFAARIWPAVKHTLTHYLEHIDDSGL  
 LNMAGWNLLDWAPIDQPNEGIVTHQNLFLVKALRDSRALAAAAGATEEADAF AARADLLAE  
 TINAVLWDEEKRAYIDCIHADGRRSDVYSMQTQVVAYLCGVAQGEREAVIEGYLSSPPPAFV  
 QIGSPFMSFFYYEALEKAGRQTLMLDDIRRN YQMLRYDATT CWEMYPNFAENRSNPDM L

TRSHCHAWSAAPGYFLGSSILGVKRGADGWRTVDIAPQPCDLTWAEGVVPLPQGGHIAVS  
WEFVSAGKLRLEAPEDIEVNVTLPEGIEGEVTVQVKYMSKLAAALEHHHHHH

### 9.1.7 *endo-CC N180H* — *Endo-N-acetylglucosaminidase* variant of *C. cinerea*

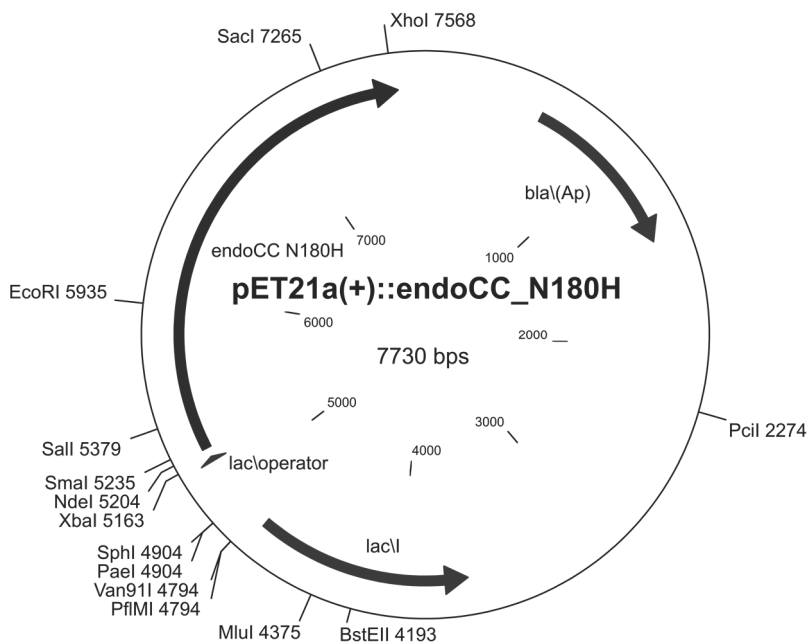


**Figure 117** Vector map of pET-21a(+)::endoCC\_N180H containing *endoCC N180H* of *C. cinerea* in the mutated form inserted between Nde I and Xho I. The map shows the positions of common restriction enzymes.

GenBank Accession: XM\_001839350 (mRNA, gene), XP\_001839402 (protein)

Gene Sequence (5'→3', 1404 bp, underlined nucleotides originate from the vector):

ATGCCTATCGCTGGGAAGAAGTTCCACCCCGGGCTCTGCCTGAGTTCTGGAGGACGT  
TCCGGGAGATGGACGAATGGCGGGCCACTCAGACTGGACCTCAGGCTCGTCCGGCTG  
AAGGCATTCTCAAGTACGTTCCACGGAAGATTCGGCCTGCTGATATCGCAGGGAAAGGT  
CGACTGTTGGTTTCTCATGACTACAAGGGAGGCTACGTCGAAGATCCCTTTTCCAAGTC  
GTATAGCTTCAATTGGTGGTTCTCGACGGATAGCTTCAACTACTTCGCTCACCACCGGA  
TAACCATTCCCCTCCGGAATGGATAAACGCTGCTCATCGCCAGGGTGTACCTATTCTC  
GGCACCATCATCTTGAAGGTGGAAGCGACGAAGACATCCTCCGGATGGTGTATCGGGA  
AAACACCAGGAAGCACCAGCAACTTCCACGCCGAACGAAACGCGGAGTACACCGTACC  
AGTTTCGTCGTACTIONACGCAACTCTTCGACAGACCTGGCTGTCGAGCGTGGATTGATG  
GTTGGCTGCTCAACGTTGAGATTGGTCTGCAGGGAGGATCAGAGCAAGCACGAGGTCT  
GGCTGCTTGGGTTGCGCTACTGCAGCAGGAGGTTTTGAAGAAGTTGGCCACATGGC  
TTGGTCATTTGGTACGACAGTGTCACTGTCCGTGGGGACCTGTGGTGGCAAGACAGGC  
TGAACGCTTTCAACTTGCCGTTCTTCTTGAATTCTTCGGGAATTTTCAAACTATTGGT  
GGTACAACGATGCACCTCAGAAACAAATCGACTTCCTTTGAGGGTTGACCCGAATCTC  
ACCGGGCAAACCGCTGAGCCGCATCAATACAACCTGCAGAAGACGATTCAAGATATCTA  
TATCGGTGTGGATGTCTGGGGACGCGGTTTCGCATGGTGGAGGAGGATTTGGTGCCTAC

AAAGCTATTGAGCACGCAGACCCGAAAGGACTCGGGTTTAGCGTTGCCCTCTTCGCTCA  
 AGGATGGACCTGGGAAACCGAGGAGGAGAAACCAGGCTGGAAGTGGGCACAGTTCTG  
 GACTACGACTCTAAACTCTGGGTTGGACCTCCCGGAGTTGTTCGAGGCACCTGACCAT  
 ACCGTCAAACCTGGCGAATACCCCTGCGTTCACGGACCCTTCCAACCCATCTCCAGCTT  
 CTTCCTGACATATCCACCTCCCGACCCGCTAGACCTGCCATTCTACACCAACTTCTGCC  
 CCGGTATCGGAGATGCGTGGTTCGTTGAGGGCAAGGAGGTCTTCCGCTCCGAGACGG  
 GTTGGACAGACATGGACAAGCAGACCACGGTTGGCGACTTGGTCTGGCCCCGACCCAA  
 GATTTATGATCTTCCATCTCAAATGCCAGTCAGGCTACGTTAAATGCGGCATTCAACTT  
 TAACGATGCGTGGAAATGGAGGAACTCGCTTCAGATCAACCTCACCGTCCCTGGAGGA  
 GCGACCACGTATGGAGCCTACTGGGTTCCCATCCAGACATTACATTCTCCAGTCGGC  
 GCCAGTACGAAGCTTCGATCGTCTACAAGCCGGGGTTGAGTGGGAAGACCCGCTTCGA  
 TGCCAAGTACGAGGTGGGTATCCGAACCATCACAGGGGAAGACCAAGGCAAGATCATC  
 TCCAACACGACGACGGAAGTTGGAAACGGTTGGCGCAAGGTGCACATTTTGTTCGAGA  
 TCGAGACGCCAGTTGAAGGAGGGTCCATCATCGTACCTTCATCCATCGGCCTGGTCATT  
 GCAGTTTCGAACGTATCAACTACCGAGCAATTTCGAGTTCCCCTTCTGGTCCGGCCAGAT  
 TACCATCCACCCCCACCTCCCGATCGTTACAAGGAGTTCAAGCCGGCCCTCCTGTGG  
 CTTTTGTTACACCTTCCGCTGGAACATAAGCCTCGATGGCACCTCACTTGGGACGT  
 CGTCGCAGCCATTGAACGCCCTCCACCAGTCGAAATTAACAACCCCGATGACGCACAAA  
 TCCCCTGGAACCTGCAGCCGACCAAACAAGAATGGTTCCCCGACTTCTCTACTTCAAT  
 GTGTACGTGCTGGAGCTCTTGATGGTGGTGGACAAGGTCCTCCACAGTGGATTGGCA  
 CGACTGGATACGATGGGGAGAAAAAGAGGTTCTTCATCTATGACGAAAGCTTGCCACCG  
 ACGTCCGGTTTAAGGAGGTTACGTTCCAGATCGAGGGCGTCCTGGAGACGGGAGAGT  
 CAACGCACTGGTACGATGCACCGGCTGCGCCGTCGGCAACGGCGGGAGGAGAGCAGA  
 AGCGGACACGACGCACCTCTCTCAAGTCCGTGCTCAGTCCGTTGCGGAGGAAGAAGTC  
 GAAGGGCGATATCTCCGTGCGCCAAGTGACTCGAGCACCAACCACCACCACCACTGA

Amino acid sequence (795 aa, underlined amino acids derive from the fused His<sub>6</sub>-tag):

MPIAGKKFHPRALPEFWRTFREMDEWRATQTGPQARPAEGILKYVPRKIRPADIAGKGRLL  
 VSHDYKGGYVEDPFSKSYSFNWWFSTDSFNFAHHRITIPPEWINAAHRQGVPI LGTIIFEG  
 GSDEDILRMVIGKTPGSTSNFHAERNAEYTPVSSYYAELFADLAVERGFDGWLLNVEIGLQ  
 GGSEQARGLAAWVALLQQEVLKKVPHGLVIWYDSVTVRGDLWWQDRLNAFNLPFFLNSS  
 GIFTNYWWYNDAPQKQIDFLSRVDPNLTGQTAEPHQYNLQKTIQDIYIGVDVWGRGSHGGG  
 GFGAYKAIEHADPKGLGFSVALFAQGWTWETEEKPGWNWAQFWDYDSKLWVGPPGVV  
 EAPDHTVKPGEYPCVHGPFQPISSFFLTYPDPDLDPFYTNFCPGIGDAWFVEGKEVFRSE  
 TGWTDMDKQTTVGDVWPRPKIYDLPSQNASQATLNAAFNFNDAWNGNSLQINLTVPGG  
 ATTYGAYWVPIQTFTFSSRRQYEASIVYKPGLSGKTRFDKYEVGIRTITGEDQGKIISNTTTE  
 VGNGWRKVHILFEIETPVEGGSIIVPSSIGLVIASVNSTTEQFEFPFLVGQITIHPLPDRYKE  
 FKPALLWLLFTPSAGTNSLDGTLTWDVVAAIERPPPVEINNPDDAQIPWNLQPTKQEWFPDF  
 LYFNVYVLELLDGGGQGPQWIGTTGYDGEKKRFFIYDESLPPTSGLRRFTFQIEGVLETGE  
 STHWYDAPAAPSATAGGEQKRTRRTSLKSVLSPLRRKSKGDISVAKLEHHHHHH

## 9.2 Codon harmonisation of *bglU*

### *Micrococcus sp. 28* [gbtct]: 51 CDS's (16439 codons)

fields: [triplet] [amino acid] [fraction] [frequency: per thousand] ([number])

UUU F 0.10 2.1 ( 34)	UCU S 0.06 3.6 ( 59)	UAU Y 0.15 2.2 ( 36)	UGU C 0.18 1.8 ( 30)
UUC F 0.90 18.8 ( 309)	UCC S 0.31 18.8 ( 309)	UAC Y 0.85 12.2 ( 201)	UGC C 0.82 8.2 ( 134)
UUA L 0.00 0.3 ( 5)	UCA S 0.09 5.6 ( 92)	UAA * 0.10 0.3 ( 5)	UGA * 0.75 2.3 ( 38)
UUG L 0.10 7.8 ( 129)	UCG S 0.25 15.1 ( 248)	UAG * 0.16 0.5 ( 8)	UGG W 1.00 14.7 ( 241)
CUU L 0.07 5.6 ( 92)	CCU P 0.12 9.8 ( 161)	CAU H 0.25 8.5 ( 139)	CGU R 0.11 11.4 ( 187)
CUC L 0.33 26.1 ( 429)	CCC P 0.31 25.1 ( 413)	CAC H 0.75 25.1 ( 412)	CGC R 0.38 39.7 ( 652)
CUA L 0.03 2.3 ( 38)	CCA P 0.13 10.8 ( 177)	CAA Q 0.15 5.2 ( 85)	CGA R 0.13 13.7 ( 226)
CUG L 0.46 36.6 ( 602)	CCG P 0.43 34.6 ( 568)	CAG Q 0.85 28.7 ( 471)	CGG R 0.28 29.6 ( 486)
AUU I 0.09 2.6 ( 42)	ACU T 0.08 4.5 ( 74)	AAU N 0.15 2.8 ( 46)	AGU S 0.07 4.3 ( 71)
AUC I 0.86 25.1 ( 412)	ACC T 0.54 31.8 ( 523)	AAC N 0.85 15.6 ( 256)	AGC S 0.22 13.0 ( 214)
AUA I 0.05 1.4 ( 23)	ACA T 0.06 3.6 ( 60)	AAA K 0.18 3.6 ( 60)	AGA R 0.03 2.9 ( 48)
AUG M 1.00 18.7 ( 308)	ACG T 0.32 18.9 ( 311)	AAG K 0.82 17.0 ( 279)	AGG R 0.08 8.3 ( 137)
GUU V 0.09 6.6 ( 108)	GCU A 0.11 14.4 ( 237)	GAU D 0.29 13.4 ( 221)	GGU G 0.15 14.5 ( 239)
GUC V 0.38 28.5 ( 468)	GCC A 0.48 63.3 ( 1040)	GAC D 0.71 33.5 ( 550)	GGC G 0.46 43.7 ( 718)
GUA V 0.04 3.3 ( 54)	GCA A 0.11 14.1 ( 232)	GAA E 0.25 12.8 ( 211)	GGA G 0.13 11.9 ( 195)
GUG V 0.48 35.7 ( 587)	GCG A 0.31 40.8 ( 670)	GAG E 0.75 38.1 ( 627)	GGG G 0.26 24.5 ( 402)

Coding GC 68.95% 1st letter GC 71.15% 2nd letter GC 55.92% 3rd letter GC 79.77%

**Figure 118** Codon usage table of *Micrococcus sp. 28*, which was used as a reference for the codon usage of *M. antarcticus* for the codon harmonisation of *bglU*.<sup>10</sup>

### *Escherichia coli* [gbtct]: 8087 CDS's (2330943 codons)

fields: [triplet] [amino acid] [fraction] [frequency: per thousand] ([number])

UUU F 0.64 24.4 ( 56791)	UCU S 0.18 13.1 ( 30494)	UAU Y 0.65 21.6 ( 50400)	UGU C 0.52 5.9 ( 13662)
UUC F 0.36 13.9 ( 32513)	UCC S 0.14 9.7 ( 22637)	UAC Y 0.35 11.7 ( 27239)	UGC C 0.48 5.5 ( 12777)
UUA L 0.18 17.4 ( 40627)	UCA S 0.18 13.1 ( 30502)	UAA * 0.58 2.0 ( 4664)	UGA * 0.33 1.1 ( 2674)
UUG L 0.13 12.9 ( 30084)	UCG S 0.11 8.2 ( 19071)	UAG * 0.09 0.3 ( 751)	UGG W 1.00 13.4 ( 31207)
CUU L 0.15 14.5 ( 33816)	CCU P 0.24 9.5 ( 22121)	CAU H 0.63 12.4 ( 28919)	CGU R 0.30 15.9 ( 37134)
CUC L 0.10 9.5 ( 22074)	CCC P 0.16 6.2 ( 14379)	CAC H 0.37 7.3 ( 17117)	CGC R 0.26 14.0 ( 32720)
CUA L 0.06 5.6 ( 12951)	CCA P 0.23 9.1 ( 21237)	CAA Q 0.35 14.4 ( 33607)	CGA R 0.09 4.8 ( 11216)
CUG L 0.38 37.4 ( 87261)	CCG P 0.37 14.5 ( 33795)	CAG Q 0.65 26.7 ( 62329)	CGG R 0.15 7.9 ( 18434)
AUU I 0.47 29.6 ( 68942)	ACU T 0.22 13.1 ( 30518)	AAU N 0.59 29.3 ( 68348)	AGU S 0.18 13.2 ( 30749)
AUC I 0.31 19.4 ( 45213)	ACC T 0.31 18.9 ( 44139)	AAC N 0.41 20.3 ( 47233)	AGC S 0.20 14.3 ( 33255)
AUA I 0.21 13.3 ( 31065)	ACA T 0.25 15.1 ( 35293)	AAA K 0.71 37.2 ( 86726)	AGA R 0.13 7.1 ( 16583)
AUG M 1.00 23.7 ( 55356)	ACG T 0.22 13.6 ( 31794)	AAG K 0.29 15.3 ( 35652)	AGG R 0.07 4.0 ( 9238)
GUU V 0.32 21.6 ( 50261)	GCU A 0.22 18.9 ( 44034)	GAU D 0.65 33.7 ( 78663)	GGU G 0.34 23.7 ( 55283)
GUC V 0.19 13.1 ( 30515)	GCC A 0.26 21.6 ( 50411)	GAC D 0.35 17.9 ( 41619)	GGC G 0.29 20.6 ( 47962)
GUA V 0.19 13.1 ( 30461)	GCA A 0.27 23.0 ( 53619)	GAA E 0.64 35.1 ( 81727)	GGA G 0.19 13.6 ( 31729)
GUG V 0.29 19.9 ( 46309)	GCG A 0.25 21.1 ( 49169)	GAG E 0.36 19.4 ( 45154)	GGG G 0.18 12.3 ( 28720)

Coding GC 47.30% 1st letter GC 53.83% 2nd letter GC 40.61% 3rd letter GC 47.45%

**Figure 119** Codon usage table of *E. coli*, which was used as a reference for the codon harmonisation of *bglU*.<sup>11</sup>

<sup>10</sup> March 2015: <http://www.kazusa.or.jp/codon/>

<sup>11</sup> March 2015: <http://www.kazusa.or.jp/codon/>

## Summary of Percent Matches:

Ref:	bglU (M. antar.)	1 to 1419	( 1419 bps)	--
2:	bglU (Cod. harm.)	1 to 1419	( 1419 bps)	74%
bglU (M. antar.)	1	atgatgaaccacttatcccaaaaattcgctggcctaaggaattcttctgtgggctcggt		
bglU (Cod. harm.)	1	.....tc..ag.....g.....a.....g.....c.c.....tagc...		
bglU (M. antar.)	61	acggcagcagcccagatcgaaggcgtggccattcttacggcaaggaagattcggctctgg		
bglU (Cod. harm.)	61	..c..t..t..a.....t..g..t.....t..c..g.....t.....g..cagc..t...		
bglU (M. antar.)	121	gacgccttcgcccgaaggaagggccatcgcaggaggtgagaacctcgaagtcgcagtg		
bglU (Cod. harm.)	121	..t..a.....a..t.....g..t..a..t..t..g..a..a..t..a..g..t..t..t		
bglU (M. antar.)	181	gaccactaccaccgctaccggaagatgtgcagctcatgcgcgaactgggcttgactcc		
bglU (Cod. harm.)	181	..t..t.....t..t.....t..g..c..t..t..a.....t..g.....t.....tag.		
bglU (M. antar.)	241	taccggttctccaccagctgggctcgcgtggtccccggggccgcaccgtgaaccccgaa		
bglU (Cod. harm.)	241	....t...ag....tct.....t..t..t..g..t..t..t.....t.....g..g		
bglU (M. antar.)	301	ggcctggatttctactcccggctggctgcagcagctgctggagaatggcatcctgcctgg		
bglU (Cod. harm.)	301	..t.....c.....ag...t.....t..t..a.....a..c..t..t.....		
bglU (M. antar.)	361	ctgacgctctaccactgggatctgccgcaggcattggaagagcggctggctggaccaac		
bglU (Cod. harm.)	361	....ct.a.....t.....c.....t.c.c.g..a..t..a..t.....		
bglU (M. antar.)	421	cgcgagacctcctacaaattcctcgaatacgggagactgtgcatgaaaagctcggcgac		
bglU (Cod. harm.)	421	..t..a...ag.....g..t..a..g.....a..a.....t..c..g.....t..a..t..t		
bglU (M. antar.)	481	cgctgaagcactggacgacgttcaacgaaccgctgtgctcttcgctgattggctacgcc		
bglU (Cod. harm.)	481	..t..t.....t.....c..c.....g.....t.....t..gagc.....a..t.....a		
bglU (M. antar.)	541	gccggcagcagcagcccccggcgcgaagaacctcaagcggcgtggcagcggctgaccac		
bglU (Cod. harm.)	541	..a..t..a..c..a.....g..t.....g.....a..a.....t..a..t..t		
bglU (M. antar.)	601	cagcatctggcccacgggtggccaccgcccactgcgcgaactggcgcggagcatatc		
bglU (Cod. harm.)	601	....c.....a..t..tc.c..a.....a..c.....t..g.....t..a..a..c..t		
bglU (M. antar.)	661	ggcatcacgctgaacctgaccaacgcggctcccgaataatcccggcgatcccggctgctg		
bglU (Cod. harm.)	661	..t..t..c.....t.....a..t.....c..c..g..t..c.....t..c.....		
bglU (M. antar.)	721	gaagcagcgcgcgcgctgcagcattgtggaaccgatgtacctggaccctgtctcgcgc		
bglU (Cod. harm.)	721	..g..t..a..t..t..t..t..tc.c.....t.....t.....t.....t.....t		
bglU (M. antar.)	781	ggttctacccccgaagacctgcttgaagcgtccagggttggggctggctgaagtcatt		
bglU (Cod. harm.)	781	..aag.....g..g..t.....a..g..t..t.....ac.c..t.....g..t..a		
bglU (M. antar.)	841	gaagcaggagacctggagatcatctcgcagccaatcgacttcttggcggtgaaccactac		
bglU (Cod. harm.)	841	..g..t..g..t.....a..t..tagc.....t..t..t..c..c..t..t.....t...		
bglU (M. antar.)	901	cacgatgacaacgtttcaggccatccgctgcccgcggccagccgcagcccggtgctgct		
bglU (Cod. harm.)	901	..t..c..t.....a..g..t..c.....g..a..t.....g..t..t...		
bglU (M. antar.)	961	accgattcgcggaagtcttcgcttttgcggcagcgagtatgtgaccttcccggcagc		
bglU (Cod. harm.)	961	....cagc.....gagc.....c..t..ttct..a..c..t.....t..t..t		
bglU (M. antar.)	1021	gacctgcccgcagccatgggctgggaagtgaatcccgaagggctgcgcgtgctgtg		
bglU (Cod. harm.)	1021	..t.....t..c..a.....t.....g..t..c..g..g..t.....t..t..c..c		
bglU (M. antar.)	1081	aaccggttgaaccaggactacgctaaccttccgctcgtgtacatcacggagaacggcgt		
bglU (Cod. harm.)	1081	....tc.c.....t.....t.....a..agc.....t..c..a.....t...		
bglU (M. antar.)	1141	tcctacaccgatacggtagcggaggccggaaccgttgaagatcccgaacgcgaggaatac		
bglU (Cod. harm.)	1141	ag.....c..c..t..c..a..a..g.....a..g..c..g..g..t..a..g...		
bglU (M. antar.)	1201	atcctcaaccacctgtatgctgtggtccgcgcatagcagcggcgtggatgtccgccc		
bglU (Cod. harm.)	1201	..tt.a.....t..a..c.....t..t..t..a.....t..t..t..t..c..t..t..t		
bglU (M. antar.)	1261	tactttgtctggtctttgctggacaatttcgaatgggcttgggctacgcaagcgttt		
bglU (Cod. harm.)	1261	....c..t.....gc.c.....t..c.....g.....t.....a.....t..c		
bglU (M. antar.)	1321	ggcattatccacgtcagattaccagaccaggtgcgaacgattaagaatagtggaagcc		
bglU (Cod. harm.)	1321	..t..a..t..t..t..c.....t.....t..c..c..a.....ctcg..t.....a		
bglU (M. antar.)	1381	tacgcagggttgattgccgcaaacctgacaatggcataa		
bglU (Cod. harm.)	1381	....t..tc.c..a..a..t.....c..t.....t..g		

**Figure 120** Alignment of the original *bglU* DNA sequence of *M. antarcticus* and the codon harmonised sequence for the homologous expression in *E. coli* BL21(DE3).

### **9.3 Content of own contribution to the published publications during the work of this thesis**

M. R. Hayes, K. A. Bochinsky, L. S. Seibt, L. Elling, J. Pietruszka, *J. Biotechnol.* **2017**, *257*, 162–170; ‘Development of a colourimetric assay for glycosynthases’.<sup>[2]</sup>

The above-mentioned publication contains the following own contribution: Conception of the project in close cooperation with Prof. Dr. Pietruszka. Synthesis and analysis of the fluoride chemosensor triisopropylsilyl chloride (**23**) and the glycosyl donor substrate  $\alpha$ -D-glucopyranosyl fluoride (**2a**). Development of the colourimetric, fluoride quantification assay in a microplate format. Structural analysis and generation of mutant variants of the  $\beta$ -glycosidase genes *abg1* and *bglC*, by application of the *QuikChange*<sup>™</sup> PCR method. The heterologous expression, isolation *via* ion metal affinity chromatography and characterisation of the *wild-type* and mutant variants of the  $\beta$ -glycosidases Abg and BglC was carried out. Examination of the acceptor substrate scope of the identified glycosynthase variants and determination of kinetic parameters. The results were summarised and evaluated within the publication. Writing of the first draft of the whole manuscript.

M. R. Hayes, J. Pietruszka, *Molecules* **2017**, *22(9)*, 1434; ‘Synthesis of glycosides by glycosynthases’.<sup>[212]</sup>

The above-mentioned publication contains the following own contribution: Literature research on the use of glycosynthases in synthesis of various glycosides was carried out and summarised in the publication. Writing of the first draft of the whole manuscript.

A. Fulton, M. R. Hayes, U. Schwaneberg, J. Pietruszka, K.-E. Jaeger, *Methods Mol. Biol.* **2018**, *1685*, 209–231; ‘High-Throughput Screening Assays for Lypolytic Enzymes’.<sup>[213]</sup>

The above-mentioned publication contains the following own contribution: Literature research towards high-throughput screenings for lipases and esterases, with a focus on enantioselectivity, was carried out and summarised in the chapter ‘High-throughput screening for lipases and esterases’. The materials and protocol for the synthesis of *p*-nitrophenyl esters and the colourimetric fingerprinting assay were described and an exemplary assay conducted for the picture example. Writing of the first drafts of the chapters ‘High-throughput screening for lipases and esterases’, ‘Materials 2.1 & 2.2’, and ‘Methods 3.1 & 3.2’.

---

## 10 REFERENCES

- [1] E. Andrés, H. Aragunde, A. Planas, *Biochem. J.* **2014**, *458*, 355; 'Screening glycosynthase libraries with a fluoride chemosensor assay independently of enzyme specificity: Identification of a transitional hydrolase to synthase mutant'.
- [2] M. R. Hayes, K. A. Bochinsky, L. S. Seibt, L. Elling, J. Pietruszka, *J. Biotechnol.* **2017**, *257*, 162-170; 'Development of a colourimetric assay for glycosynthases'.
- [3] N. R. Council, *Transforming glycoscience: A roadmap for the future*, The National Academies Press, Washington, DC, **2012**.
- [4] S. L. Flitsch, *EGSF/IBCarb joint publication* **2015**; 'A roadmap for glycoscience in europe'.
- [5] W. C. Lamanna, J. Holzmann, H. P. Cohen, X. Guo, M. Schweigler, T. Stangler, A. Seidl, M. Schiestl, *Expert Opin. Biol. Ther.* **2018**, *18*, 369-379; 'Maintaining consistent quality and clinical performance of biopharmaceuticals'.
- [6] L. Urquhart, *Nat. Rev. Drug Discovery* **2018**, *17*, 232; 'Top drugs and companies by sales in 2017'.
- [7] C. K. Schneider, *Ann. Rheum. Dis.* **2013**, *72*, 315-318; 'Biosimilars in rheumatology: The wind of change'.
- [8] J. Xiao, *Crit. Rev. Food Sci. Nutr.* **2017**, *57*, 1874-1905; 'Dietary flavonoid aglycones and their glycosides: Which show better biological significance?'.
- [9] J. Stevens, O. Blixt, L. Glaser, J. K. Taubenberger, P. Palese, J. C. Paulson, I. A. Wilson, *J. Mol. Biol.* **2006**, *355*, 1143-1155; 'Glycan microarray analysis of the hemagglutinins from modern and pandemic influenza viruses reveals different receptor specificities'.
- [10] L. Bode, *Glycobiology* **2012**, *22*, 1147-1162; 'Human milk oligosaccharides: Every baby needs a sugar mama'.
- [11] K. Nicolaou, H. J. Mitchell, *Angew. Chem., Int. Ed.* **2001**, *40*, 1576-1624; 'Adventures in carbohydrate chemistry: New synthetic technologies, chemical synthesis, molecular design, and chemical biology'.
- [12] P. Grice, S. V. Ley, J. Pietruszka, H. W. M. Priepe, E. P. E. Walther, *Synlett* **1995**, *1995*, 781-784; 'Tuning the reactivity of glycosides: Efficient one-pot oligosaccharide synthesis'.
- [13] M.-K. Cheung, N. L. Douglas, B. Hinzen, S. V. Ley, X. Pannecoucke, *Synlett* **1997**, *1997*, 257-260; 'One-pot synthesis of tetra- and pentasaccharides from monomeric building blocks using the principles of orthogonality and reactivity tuning'.
- [14] P. Grice, S. V. Ley, J. Pietruszka, H. M. I. Osborn, H. W. M. Priepe, S. L. Warriner, *Chem. - Eur. J.* **1997**, *3*, 431-440; 'A new strategy for oligosaccharide assembly exploiting cyclohexane-1,2-diacetal methodology: An efficient synthesis of a high mannose type nonasaccharide'.
- [15] John B. McArthur, X. Chen, *Biochem. Soc. Trans.* **2016**, *44*, 129-142; 'Glycosyltransferase engineering for carbohydrate synthesis'.
- [16] D. Talens-Perales, J. Polaina, J. Marín-Navarro, in *Frontier discoveries and innovations in interdisciplinary microbiology* (Ed.: P. Shukla), Springer India, New Delhi, **2016**, pp. 9-31.
- [17] D. E. Koshland, *Biol. Rev.* **1953**, *28*, 416-436; 'Stereochemistry and the mechanism of enzymatic reactions'.
- [18] G. J. Davies, K. S. Wilson, B. Henrissat, *Biochem. J.* **1997**, *321*; 'Nomenclature for sugar-binding subsites in glycosyl hydrolases'.
- [19] P. M. Danby, S. G. Withers, *ACS Chem. Biol.* **2016**; 'Advances in enzymatic glycoside synthesis'.
- [20] B. Bissaro, P. Monsan, R. Faure, M. J. O'Donohue, *Biochem. J.* **2015**, *467*; 'Glycosynthesis in a waterworld: New insight into the molecular basis of transglycosylation in retaining glycoside hydrolases'.
- [21] L. F. Mackenzie, Q. Wang, R. A. J. Warren, S. G. Withers, *J. Am. Chem. Soc.* **1998**, *120*, 5583-5584; 'Glycosynthases: Mutant glycosidases for oligosaccharide synthesis'.

- [22] C. Malet, A. Planas, *FEBS Lett.* **1998**, *440*, 208-212; 'From  $\beta$ -glucanase to  $\beta$ -glucansynthase: Glycosyl transfer to  $\alpha$ -glycosyl fluorides catalyzed by a mutant endoglucanase lacking its catalytic nucleophile'.
- [23] B. Cobucci-Ponzano, F. Conte, M. Mazzone, E. Bedini, M. M. Corsaro, M. Rossi, M. Moracci, *Biocatal. Biotransform.* **2008**, *26*, 18-24; 'Design of new reaction conditions for characterization of a mutant thermophilic  $\alpha$ -L-fucosidase'.
- [24] B. Cobucci-Ponzano, C. Zorzetti, A. Strazzulli, E. Bedini, M. M. Corsaro, G. Sulzenbacher, M. Rossi, M. Moracci, *Biocatal. Biotransform.* **2012**, *30*, 288-295; 'Exploitation of  $\beta$ -glycosyl azides for the preparation of  $\alpha$ -glycosynthases'.
- [25] M. Umekawa, W. Huang, B. Li, K. Fujita, H. Ashida, L.-X. Wang, K. Yamamoto, *J. Biol. Chem.* **2008**, *283*, 4469-4479; 'Mutants of *Mucor hiemalis* endo- $\beta$ -N-acetylglucosaminidase show enhanced transglycosylation and glycosynthase-like activities'.
- [26] J.-H. Shim, H.-M. Chen, J. R. Rich, E. D. Goddard-Borger, S. G. Withers, *Prot. Eng. Des. Select.* **2012**, *25*, 465-472; 'Directed evolution of a  $\beta$ -glycosidase from *Agrobacterium* sp. to enhance its glycosynthase activity toward C3-modified donor sugars'.
- [27] Y.-W. Kim, S. S. Lee, R. A. J. Warren, S. G. Withers, *J. Biol. Chem.* **2004**, *279*, 42787-42793; 'Directed evolution of a glycosynthase from *Agrobacterium* sp. increases its catalytic activity dramatically and expands its substrate repertoire'.
- [28] J. Wei, X. Lv, Y. Lü, G. Yang, L. Fu, L. Yang, J. Wang, J. Gao, S. Cheng, Q. Duan, C. Jin, X. Li, *Eur. J. Org. Chem.* **2013**, *2013*, 2414-2419; 'Glycosynthase with broad substrate specificity – an efficient biocatalyst for the construction of oligosaccharide library'.
- [29] S. Pengthaisong, C.-F. Chen, S. G. Withers, B. Kuaprasert, J. R. Ketudat Cairns, *Carbohydr. Res.* **2012**, *352*, 51-59; 'Rice Bglu1 glycosynthase and wild type transglycosylation activities distinguished by cyclophellitol inhibition'.
- [30] J. K. Fairweather, M. J. McDonough, R. V. Stick, D. M. G. Tilbrook, *Aust. J. Chem.* **2004**, *57*, 197-205; 'Some approaches to glycosylated versions of methyl  $\beta$ -acarviosin'.
- [31] D. L. Jakeman, A. Sadeghi-Khomami, *Biochemistry* **2011**, *50*, 10359-10366; 'A  $\beta$ -(1,2)-glycosynthase and an attempted selection method for the directed evolution of glycosynthases'.
- [32] J. M. Macdonald, R. V. Stick, D. M. G. Tilbrook, S. G. Withers, *Aust. J. Chem.* **2003**, *55*, 747-752; 'Synthesis with glycosynthases: Cello-oligomers of isofagomine and a tetrahydrooxazine as cellulase inhibitors'.
- [33] T. Pozzo, M. Plaza, J. Romero-García, M. Faijes, E. N. Karlsson, A. Planas, *J. Mol. Cat. B: Enz.* **2014**, *107*, 132-139; 'Glycosynthases from *Thermotoga neapolitana*  $\beta$ -glucosidase 1A: A comparison of  $\alpha$ -glucosyl fluoride and *in situ*-generated  $\alpha$ -glycosyl formate donors'.
- [34] T. Pozzo, J. Romero-García, M. Faijes, A. Planas, E. Nordberg Karlsson, *Glycobiology* **2017**, *27*, 165-175; 'Rational design of a thermostable glycoside hydrolase from family 3 introduces  $\beta$ -glycosynthase activity'.
- [35] I. Park, H. Lee, J. Cha, *Biotechnol Lett* **2014**, *36*, 789-796; 'Glycoconjugates synthesized *via* transglycosylation by a thermostable  $\alpha$ -glucosidase from *Thermoplasma acidophilum* and its glycosynthase mutant'.
- [36] M. Yang, G. J. Davies, B. G. Davis, *Angew. Chem.* **2007**, *119*, 3959-3962; 'A glycosynthase catalyst for the synthesis of flavonoid glycosides'.
- [37] V. Codera, K. J. Edgar, M. Faijes, A. Planas, *Biomacromolecules* **2016**, *17*, 1272-1279; 'Functionalized celluloses with regular substitution pattern by glycosynthase-catalyzed polymerization'.
- [38] H. Aragunde, E. Castilla, X. Biarnés, M. Faijes, A. Planas, *Carbohydr. Res.* **2014**, *389*, 85-92; 'A transitional hydrolase to glycosynthase mutant by Glu to Asp substitution at the catalytic nucleophile in a retaining glycosidase'.
- [39] D. H. Kwan, S. Ernst, M. P. Kötzler, S. G. Withers, *Glycobiology* **2015**, *25*, 806-811; 'Chemoenzymatic synthesis of a type 2 blood group A tetrasaccharide and

- development of high-throughput assays enables a platform for screening blood group antigen-cleaving enzymes'.
- [40] A. Strazzulli, B. Cobucci-Ponzano, S. Carillo, E. Bedini, M. M. Corsaro, G. Pocsfalvi, S. G. Withers, M. Rossi, M. Moracci, *Glycobiology* **2017**, *27*, 425-437; 'Introducing transgalactosylation activity into a family 42  $\beta$ -galactosidase'.
- [41] E. D. Goddard-Borger, C. Tysoe, S. G. Withers, *Carbohydr. Res.* **2016**, *435*, 97-99; 'Glycosynthase mediated synthesis of psychosine'.
- [42] J. R. Rich, A.-M. Cunningham, M. Gilbert, S. G. Withers, *Chem. Commun.* **2011**, *47*, 10806-10808; 'Glycosphingolipid synthesis employing a combination of recombinant glycosyltransferases and an endoglycoceramidase glycosynthase'.
- [43] G.-Y. Yang, C. Li, M. Fischer, C. W. Cairo, Y. Feng, S. G. Withers, *Angew. Chem.* **2015**, *127*, 5479-5483; 'A fret probe for cell-based imaging of ganglioside-processing enzyme activity and high-throughput screening'.
- [44] M. Henze, S. Schmidtke, N. Hoffmann, H. Steffens, J. Pietruszka, L. Elling, *ChemCatChem* **2015**, *7*, 3131-3139; 'Combination of glycosyltransferases and a glycosynthase in sequential and one-pot reactions for the synthesis of type 1 and type 2 *N*-acetylactosamine oligomers'.
- [45] M. Henze, D.-J. You, C. Kamerke, N. Hoffmann, C. Angkawidjaja, S. Ernst, J. Pietruszka, S. Kanaya, L. Elling, *J. Biotechnol.* **2014**, *191*, 78-85; 'Rational design of a glycosynthase by the crystal structure of  $\beta$ -galactosidase from *Bacillus circulans* (BgaC) and its use for the synthesis of *N*-acetylactosamine type 1 glycan structures'.
- [46] M. J. Vázquez, J. L. Alonso, H. Domínguez, J. C. Parajó, *Trends Food Sci. Technol.* **2000**, *11*, 387-393; 'Xylooligosaccharides: Manufacture and applications'.
- [47] Y.-W. Kim, H. Chen, S. G. Withers, *Carbohydr. Res.* **2005**, *340*, 2735-2741; 'Enzymatic transglycosylation of xylose using a glycosynthase'.
- [48] Y. Honda, M. Kitaoka, *J. Biol. Chem.* **2006**, *281*, 1426-1431; 'The first glycosynthase derived from an inverting glycoside hydrolase'.
- [49] Y.-W. Kim, D. T. Fox, O. Hekmat, T. Kantner, L. P. McIntosh, R. A. J. Warren, S. G. Withers, *Org. Biomol. Chem.* **2006**, *4*, 2025-2032; 'Glycosynthase-based synthesis of xylo-oligosaccharides using an engineered retaining xylanase from *Cellulomonas fimi*'.
- [50] M. Sugimura, M. Nishimoto, M. Kitaoka, *Biosci. Biotechnol. Biochem.* **2006**, *70*, 1210-1217; 'Characterization of glycosynthase mutants derived from glycoside hydrolase family 10 xylanases'.
- [51] A. Ben-David, T. Bravman, Y. S. Balazs, M. Czjzek, D. Schomburg, G. Shoham, Y. Shoham, *ChemBioChem* **2007**, *8*, 2145-2151; 'Glycosynthase activity of geobacillus stearothermophilus GH52  $\beta$ -xylosidase: Efficient synthesis of xylooligosaccharides from  $\alpha$ -D-xylopyranosyl fluoride through a conjugated reaction'.
- [52] A. Khasin, I. Alchanati, Y. Shoham, *Appl. Environ. Microbiol.* **1993**, *59*, 1725-1730; 'Purification and characterization of a thermostable xylanase from *Bacillus stearothermophilus* T-6'.
- [53] A. Ben-David, G. Shoham, Y. Shoham, *Chem. Biol.* **2008**, *15*, 546-551; 'A universal screening assay for glycosynthases: Directed evolution of glycosynthase XynB2 (E335G) suggests a general path to enhance activity'.
- [54] E. D. Goddard-Borger, B. Fiege, E. M. Kwan, S. G. Withers, *ChemBioChem* **2011**, *12*, 1703-1711; 'Glycosynthase-mediated assembly of xylanase substrates and inhibitors'.
- [55] A. Trincone, B. Cobucci-Ponzano, B. Di Lauro, M. Rossi, Y. Mitsuishi, M. Moracci, *Extremophiles* **2001**, *5*, 277-282; 'Enzymatic synthesis and hydrolysis of xylogluco-oligosaccharides using the first archaeal  $\alpha$ -xylosidase from *Sulfolobus solfataricus*'.
- [56] O. Spadiut, F. M. Ibatullin, J. Peart, F. Gullfot, C. Martinez-Fleites, M. Ruda, C. Xu, G. Sundqvist, G. J. Davies, H. Brumer, *J. Am. Chem. Soc.* **2011**, *133*, 10892-10900; 'Building custom polysaccharides in vitro with an efficient, broad-specificity xyloglucan glycosynthase and a fucosyltransferase'.

- [57] O. Nashiru, D. L. Zechel, D. Stoll, T. Mohammadzadeh, R. A. J. Warren, S. G. Withers, *Angew. Chem.* **2001**, *113*, 431-434; ' $\beta$ -Mannosynthase: Synthesis of  $\beta$ -mannosides with a mutant  $\beta$ -mannosidase'.
- [58] K. Yamamoto, B. G. Davis, *Angew. Chem., Int. Ed.* **2012**, *51*, 7449-7453; 'Creation of an  $\alpha$ -mannosynthase from a broad glycosidase scaffold'.
- [59] M. Jahn, D. Stoll, R. A. J. Warren, L. Szabo, P. Singh, H. J. Gilbert, V. M. A. Ducros, G. J. Davies, S. G. Withers, *Chem. Commun.* **2003**, 1327-1329; 'Expansion of the glycosynthase repertoire to produce defined manno-oligosaccharides'.
- [60] S. G. Withers, R. A. J. Warren, I. P. Street, K. Rupitz, J. B. Kempton, R. Aebbersold, *J. Am. Chem. Soc.* **1990**, *112*, 5887-5889; 'Unequivocal demonstration of the involvement of a glutamate residue as a nucleophile in the mechanism of a retaining glycosidase'.
- [61] D. E. Trimbur, R. A. Warren, S. G. Withers, *J. Biol. Chem.* **1992**, *267*, 10248-10251; 'Region-directed mutagenesis of residues surrounding the active site nucleophile in  $\beta$ -glucosidase from *Agrobacterium faecalis*'.
- [62] S. G. Withers, K. Rupitz, D. Trimbur, R. A. J. Warren, *Biochemistry* **1992**, *31*, 9979-9985; 'Mechanistic consequences of mutation of the active site nucleophile Glu358 in *Agrobacterium*  $\beta$ -glucosidase'.
- [63] Q. Wang, D. Trimbur, R. Graham, R. A. J. Warren, S. G. Withers, *Biochemistry* **1995**, *34*, 14554-14562; 'Identification of the acid/base catalyst in *Agrobacterium faecalis*  $\beta$ -glucosidase by kinetic analysis of mutants'.
- [64] H. Prade, L. F. Mackenzie, S. G. Withers, *Carbohydr. Res.* **1997**, *305*, 371-381; 'Enzymatic synthesis of disaccharides using *Agrobacterium* sp.  $\beta$ -glucosidase'.
- [65] C. Mayer, D. L. Jakeman, M. Mah, G. Karjala, L. Gal, R. A. J. Warren, S. G. Withers, *Chem. Biol.* **2001**, *8*, 437-443; 'Directed evolution of new glycosynthases from *Agrobacterium*  $\beta$ -glucosidase: A general screen to detect enzymes for oligosaccharide synthesis'.
- [66] C. Mayer, D. L. Zechel, S. P. Reid, R. A. J. Warren, S. G. Withers, *FEBS Lett.* **2000**, *466*, 40-44; 'The E358S mutant of *Agrobacterium* sp.  $\beta$ -glucosidase is a greatly improved glycosynthase'.
- [67] K. M. Borges, S. R. Brummet, A. Bogert, M. C. Davis, K. M. Hujer, S. T. Domke, J. Szasz, J. Ravel, J. Diruggiero, C. Fuller, *Genome Sci. Technol.* **1996**, *1*, 37-46; 'A survey of the genome of the hyperthermophilic archaeon, *Pyrococcus furiosus*'.
- [68] D. L. Maeder, R. B. Weiss, D. M. Dunn, J. L. Cherry, J. M. González, J. DiRuggiero, F. T. Robb, *Genetics* **1999**, *152*, 1299-1305; 'Divergence of the hyperthermophilic archaea *Pyrococcus furiosus* and *P. horikoshii* inferred from complete genomic sequences'.
- [69] D. Merker, Bachelor thesis, RWTH Aachen (RWTH Aachen), **2013**.
- [70] B. L. Cantarel, C. Rancurel, P. M. Coutinho, T. Bernard, V. Lombard, B. Henrissat, *Nucleic Acids Res.* **2008**, *37*, D233-D238; 'The carbohydrate-active enzymes database (Cazy): An expert resource for glycogenomics'.
- [71] B. Henrissat, G. Davies, *Curr. Opin. Struct. Biol.* **1997**, *7*, 637-644; 'Structural and sequence-based classification of glycoside hydrolases'.
- [72] M. Gelo-Pujic, E. Guibe-Jampel, A. Loupy, A. Trincone, *J. Chem. Soc., Perkin Trans. 1* **1997**, 1001-1002; 'Enzymatic glycosidation in dry media under microwave irradiation'.
- [73] J. Van Lieshout, M. Faijes, J. Nieto, J. Van Der Oost, A. Planas, *Archaea* **2004**, *1*; 'Hydrolase and glycosynthase activity of *endo*-1,3- $\beta$ -glucanase from the thermophile *Pyrococcus furiosus*'.
- [74] G. Perugino, A. Trincone, A. Giordano, J. van der Oost, T. Kaper, M. Rossi, M. Moracci, *Biochemistry* **2003**, *42*, 8484-8493; 'Activity of hyperthermophilic glycosynthases is significantly enhanced at acidic pH'.
- [75] A. Trincone, A. Giordano, G. Perugino, M. Rossi, M. Moracci, *Bioorg. Med. Chem. Lett.* **2003**, *13*, 4039-4042; 'Glycosynthase-catalysed syntheses at pH below neutrality'.
- [76] R. Cavicchioli, T. Charlton, H. Ertan, S. M. Omar, K. S. Siddiqui, T. J. Williams, *Microb. Biotechnol.* **2011**, *4*, 449-460; 'Biotechnological uses of enzymes from psychrophiles'.

- [77] S. Brethauer, C. E. Wyman, *Bioresour. Technol.* **2010**, *101*, 4862-4874; 'Review: Continuous hydrolysis and fermentation for cellulosic ethanol production'.
- [78] N. Aghajari, R. Haser, G. Feller, C. Gerday, *Protein Sci.* **1998**, *7*, 564-572; 'Crystal structures of the psychrophilic  $\alpha$ -amylase from *Alteromonas haloplanctis* in its native form and complexed with an inhibitor'.
- [79] A. Andolfo, A. Amoresano, C. Gerday, G. Marino, I. Petrescu, I. Zocchi, M. M. Corsaro, *Glycobiology* **2000**, *10*, 451-458; 'Structural characterization of a xylanase from psychrophilic yeast by mass spectrometry'.
- [80] S. Yang, C. Hua, Q. Yan, Y. Li, Z. Jiang, *Carbohydr. Polym.* **2013**, *92*, 784-791; 'Biochemical properties of a novel glycoside hydrolase family 1  $\beta$ -glucosidase (PtBglu1) from *Paecilomyces thermophila* expressed in *Pichia pastoris*'.
- [81] H.-X. Fan, L.-L. Miao, Y. Liu, H.-C. Liu, Z.-P. Liu, *Enzyme Microb. Technol.* **2011**, *49*, 94-99; 'Gene cloning and characterization of a cold-adapted  $\beta$ -glucosidase belonging to glycosyl hydrolase family 1 from a psychrotolerant bacterium *Micrococcus antarcticus*'.
- [82] L. M. Zanphorlin, P. O. de Giuseppe, R. V. Honorato, C. C. C. Tonoli, J. Fattori, E. Crespim, P. S. L. de Oliveira, R. Ruller, M. T. Murakami, *Sci. Rep.* **2016**, *6*, 23776; 'Oligomerization as a strategy for cold adaptation: Structure and dynamics of the GH1  $\beta$ -glucosidase from *Exiguobacterium antarcticum* B7'.
- [83] L.-L. Miao, Y.-J. Hou, H.-X. Fan, J. Qu, C. Qi, Y. Liu, D.-F. Li, Z.-P. Liu, *Appl. Environ. Microbiol.* **2016**, *82*, 2021; 'Molecular structural basis for the cold adaptedness of the psychrophilic  $\beta$ -glucosidase BglU in *Micrococcus antarcticus*'.
- [84] J. W. Morris, R. O. Morris, *Proc. Natl. Acad. Sci.* **1990**, *87*, 3614-3618; 'Identification of an *Agrobacterium tumefaciens* virulence gene inducer from the pinaceous gymnosperm *Pseudotsuga menziesii*'.
- [85] L. A. Castle, K. D. Smith, R. O. Morris, *J. Bacteriol.* **1992**, *174*, 1478-1486; 'Cloning and sequencing of an *Agrobacterium tumefaciens*  $\beta$ -glucosidase gene involved in modifying a vir-inducing plant signal molecule'.
- [86] A. Singh, K. Hayashi, T. T. Hoa, Y. Kashiwagi, K. Tokuyasu, *Biochem. J.* **1995**, *305*, 715-719; 'Construction and characterization of a chimeric  $\beta$ -glucosidase'.
- [87] K. Hayashi, A. Singh, C. Aoyagi, A. Nakatani, K. Tokuyasu, Y. Kashiwagi, *Biotechnology for improved foods and flavors* **1996**; 'Chimeric  $\beta$ -glucosidases with increased heat stability'.
- [88] D. K. Watt, H. Ono, K. Hayashi, *Biochim. Biophys. Acta, Protein Struct. Mol. Enzymol.* **1998**, *1385*, 78-88; '*Agrobacterium tumefaciens*  $\beta$ -glucosidase is also an effective  $\beta$ -xylosidase, and has a high transglycosylation activity in the presence of alcohols'.
- [89] K. Goyal, Y. K. Kim, M. Kitaoka, K. Hayashi, *J. Mol. Cat. B: Enz.* **2001**, *16*, 43-51; 'Construction and characterization of chimeric enzymes of the *Agrobacterium tumefaciens* and *Thermotoga maritima*  $\beta$ -glucosidases'.
- [90] L. Ying, M. Kitaoka, K. Hayashi, *Biosci. Biotechnol. Biochem.* **2004**, *68*, 1113-1118; 'Effects of truncation at the non-homologous region of a family 3  $\beta$ -glucosidase from *Agrobacterium tumefaciens*'.
- [91] M. Kitaoka, T. Takahashi, L. Ying, K. Hayashi, *J. Appl. Glycosci.* **2011**, *58*, 129-132; 'Self-transferring product inhibition observed during the hydrolysis of aryl- $\beta$ -D-glucopyranosides by a  $\beta$ -glucosidase from *Agrobacterium tumefaciens*'.
- [92] E. Yoshida, M. Hidaka, S. Fushinobu, T. Koyanagi, H. Minami, H. Tamaki, M. Kitaoka, T. Katayama, H. Kumagai, *Biochem. J.* **2010**, *431*, 39-49; 'Role of a PA14 domain in determining substrate specificity of a glycoside hydrolase family 3  $\beta$ -glucosidase from *Kluyveromyces marxianus*'.
- [93] S. J. Williams, S. G. Withers, *Carbohydr. Res.* **2000**, *327*, 27-46; 'Glycosyl fluorides in enzymatic reactions'.
- [94] B. Cobucci-Ponzano, C. Zorzetti, A. Strazzulli, S. Carillo, E. Bedini, M. M. Corsaro, D. A. Comfort, R. M. Kelly, M. Rossi, M. Moracci, *Glycobiology* **2011**, *21*, 448-456; 'A novel  $\alpha$ -D-galactosynthase from *Thermotoga maritima* converts  $\beta$ -D-galactopyranosyl azide to  $\alpha$ -galacto-oligosaccharides'.

- [95] M. Okuyama, K. Matsunaga, K.-i. Watanabe, K. Yamashita, T. Tagami, A. Kikuchi, M. Ma, P. Klahan, H. Mori, M. Yao, A. Kimura, *FEBS J.* **2017**, *284*, 766-783; 'Efficient synthesis of  $\alpha$ -galactosyl oligosaccharides using a mutant *Bacteroides thetaiotaomicron* retaining  $\alpha$ -galactosidase (BtGH97b)'.
- [96] C. Bayon, M. Moracci, M. J. Hernaiz, *RSC Adv.* **2015**, *5*, 55313-55320; 'A novel, efficient and sustainable strategy for the synthesis of  $\alpha$ -glycoconjugates by combination of a  $\alpha$ -galactosynthase and a green solvent'.
- [97] J. Wada, Y. Honda, M. Nagae, R. Kato, S. Wakatsuki, T. Katayama, H. Taniguchi, H. Kumagai, M. Kitaoka, K. Yamamoto, *FEBS Lett.* **2008**, *582*, 3739-3743; '1,2- $\alpha$ -L-fucosynthase: A glycosynthase derived from an inverting  $\alpha$ -glycosidase with an unusual reaction mechanism'.
- [98] B. Cobucci-Ponzano, F. Conte, E. Bedini, M. M. Corsaro, M. Parrilli, G. Sulzenbacher, A. Lipski, F. Dal Piaz, L. Lepore, M. Rossi, M. Moracci, *Chem. Biol.* **2009**, *16*, 1097-1108; ' $\beta$ -Glycosyl azides as substrates for  $\alpha$ -glycosynthases: Preparation of efficient  $\alpha$ -L-fucosynthases'.
- [99] H. Sakurama, S. Fushinobu, M. Hidaka, E. Yoshida, Y. Honda, H. Ashida, M. Kitaoka, H. Kumagai, K. Yamamoto, T. Katayama, *J. Biol. Chem.* **2012**, *287*, 16709-16719; '1,3-1,4- $\alpha$ -L-Fucosynthase that specifically introduces lewis *a/x* antigens into type-1/2 chains'.
- [100] Y. Sugiyama, A. Gotoh, T. Katoh, Y. Honda, E. Yoshida, S. Kurihara, H. Ashida, H. Kumagai, K. Yamamoto, M. Kitaoka, T. Katayama, *Glycobiology* **2016**, *26*, 1235-1247; 'Introduction of H-antigens into oligosaccharides and sugar chains of glycoproteins using highly efficient 1,2- $\alpha$ -L-fucosynthase'.
- [101] Y. Sugiyama, T. Katoh, Y. Honda, A. Gotoh, H. Ashida, S. Kurihara, K. Yamamoto, T. Katayama, *Biosci. Biotechnol. Biochem.* **2017**, *81*, 283-291; 'Application study of 1,2- $\alpha$ -L-fucosynthase: Introduction of Fuca1-2Gal disaccharide structures on *N*-glycan, ganglioside, and xyloglucan oligosaccharide'.
- [102] V. Yadav, P. K. Yadav, S. Yadav, K. D. S. Yadav, *Process Biochem.* **2010**, *45*, 1226-1235; ' $\alpha$ -L-Rhamnosidase: A review'.
- [103] H. Vila-Real, A. J. Alfaia, M. R. Bronze, A. R. T. Calado, M. H. L. Ribeiro, *Enzyme Res.* **2011**, *2011*, 11; 'Enzymatic synthesis of the flavone glucosides, prunin and isoquercetin, and the aglycones, naringenin and quercetin, with selective L-rhamnosidase and D-glucosidase activities of naringinase'.
- [104] Y.-S. Lee, J.-Y. Huh, S.-H. Nam, D. Kim, S.-B. Lee, *J. Food Sci.* **2013**, *78*, C411-C415; 'Synthesis of quercetin-3-O-glucoside from rutin by *Penicillium decumbens* naringinase'.
- [105] N. Thuan, R. Pandey, T. Thuy, J. Park, J. Sohng, *Appl. Biochem. Biotechnol.* **2013**, *171*, 1956-1967; 'Improvement of regio-specific production of myricetin-3-O- $\alpha$ -L-rhamnoside in engineered *Escherichia coli*'.
- [106] A. Trincone, *Biomolecules* **2015**, *5*, 2160; 'Uncommon glycosidases for the enzymatic preparation of glycosides'.
- [107] K. De Winter, D. Šimčíková, B. Schalck, L. Weignerová, H. Pelantova, W. Soetaert, T. Desmet, V. Křen, *Bioresour. Technol.* **2013**, *147*, 640-644; 'Chemoenzymatic synthesis of  $\alpha$ -L-rhamnosides using recombinant  $\alpha$ -L-rhamnosidase from *Aspergillus terreus*'.
- [108] L. Lu, Q. Liu, L. Jin, Z. Yin, L. Xu, M. Xiao, *PLOS ONE* **2015**, *10*, e0140531; 'Enzymatic synthesis of rhamnose containing chemicals by reverse hydrolysis'.
- [109] L. Xu, X. Liu, Z. Yin, Q. Liu, L. Lu, M. Xiao, *Appl Microbiol Biotechnol* **2016**, *100*, 10385-10394; 'Site-directed mutagenesis of  $\alpha$ -L-rhamnosidase from *Alternaria* sp. L1 to enhance synthesis yield of reverse hydrolysis based on rational design'.
- [110] Z. Fujimoto, A. Jackson, M. Michikawa, T. Maehara, M. Momma, B. Henrissat, H. J. Gilbert, S. Kaneko, *J. Biol. Chem.* **2013**, *288*, 12376-12385; 'The structure of a *Streptomyces avermitilis*  $\alpha$ -L-rhamnosidase reveals a novel carbohydrate-binding module Cbm67 within the six-domain arrangement'.
- [111] E. C. O'Neill, C. E. M. Stevenson, M. J. Paterson, M. Rejzek, A.-L. Chauvin, D. M. Lawson, R. A. Field, *Proteins: Struct., Funct., Bioinf.* **2015**, *83*, 1742-1749; 'Crystal

- structure of a novel two domain GH78 family  $\alpha$ -rhamnosidase from *Klebsiella oxytoca* with rhamnose bound'.
- [112] Z. Cui, Y. Maruyama, B. Mikami, W. Hashimoto, K. Murata, *J. Mol. Biol.* **2007**, *374*, 384-398; 'Crystal structure of glycoside hydrolase family 78  $\alpha$ -L-rhamnosidase from *Bacillus* sp. GL1'.
- [113] W. Hashimoto, H. Nankai, N. Sato, S. Kawai, K. Murata, *Arch. Biochem. Biophys.* **1999**, *368*, 56-60; 'Characterization of  $\alpha$ -L-rhamnosidase of *Bacillus* sp. GL1 responsible for the complete depolymerization of gellan'.
- [114] W. Hashimoto, O. Miyake, H. Nankai, K. Murata, *Arch. Biochem. Biophys.* **2003**, *415*, 235-244; 'Molecular identification of an  $\alpha$ -L-rhamnosidase from *Bacillus* sp. Strain GL1 as an enzyme involved in complete metabolism of gellan'.
- [115] Z. Cui, Y. Maruyama, B. Mikami, W. Hashimoto, K. Murata, *Acta Crystallogr., Sect. F* **2006**, *62*, 646-648; 'Crystallization and preliminary crystallographic analysis of the family GH78  $\alpha$ -L-rhamnosidase RhaB from *Bacillus* sp. GL1'.
- [116] M. Umekawa, T. Higashiyama, Y. Koga, T. Tanaka, M. Noguchi, A. Kobayashi, S.-i. Shoda, W. Huang, L.-X. Wang, H. Ashida, K. Yamamoto, *Biochim. Biophys. Acta, Gen. Subj.* **2010**, *1800*, 1203-1209; 'Efficient transfer of sialo-oligosaccharide onto proteins by combined use of a glycosynthase-like mutant of *Mucor hiemalis* endoglycosidase and synthetic sialo-complex-type sugar oxazoline'.
- [117] W. Huang, H. Ochiai, X. Zhang, L.-X. Wang, *Carbohydr. Res.* **2008**, *343*, 2903-2913; 'Introducing *N*-glycans into natural products through a chemoenzymatic approach'.
- [118] M. Noguchi, T. Tanaka, H. Gyakushi, A. Kobayashi, S.-i. Shoda, *J. Org. Chem.* **2009**, *74*, 2210-2212; 'Efficient synthesis of sugar oxazolines from unprotected *N*-acetyl-2-amino sugars by using chloroformamidinium reagent in water'.
- [119] M. Noguchi, T. Fujieda, W. C. Huang, M. Ishihara, A. Kobayashi, S.-i. Shoda, *Helv. Chim. Acta* **2012**, *95*, 1928-1936; 'A practical one-step synthesis of 1,2-oxazoline derivatives from unprotected sugars and its application to chemoenzymatic  $\beta$ -*N*-acetylglucosaminidation of disialo-oligosaccharide'.
- [120] M. Umekawa, C. Li, T. Higashiyama, W. Huang, H. Ashida, K. Yamamoto, L.-X. Wang, *J. Biol. Chem.* **2010**, *285*, 511-521; 'Efficient glycosynthase mutant derived from *Mucor hiemalis* endo- $\beta$ -*N*-acetylglucosaminidase capable of transferring oligosaccharide from both sugar oxazoline and natural *N*-glycan'.
- [121] K. Sakaguchi, T. Katoh, K. Yamamoto, *Biotechnol. Appl. Biochem.* **2016**, *63*, 812-819; 'Transglycosidase-like activity of *Mucor hiemalis* endoglycosidase mutants enabling the synthesis of glycoconjugates using a natural glycan donor'.
- [122] M. N. Amin, W. Huang, R. M. Mizanur, L.-X. Wang, *J. Am. Chem. Soc.* **2011**, *133*, 14404-14417; 'Convergent synthesis of homogeneous Glc<sub>1</sub>Man<sub>9</sub>GlcNAc<sub>2</sub>-protein and derivatives as ligands of molecular chaperones in protein quality control'.
- [123] Y. Tomabechi, G. Krippner, P. M. Rendle, M. A. Squire, A. J. Fairbanks, *Chem. - Eur. J.* **2013**, *19*, 15084-15088; 'Glycosylation of pramlintide: Synthetic glycopeptides that display in vitro and in vivo activities as amylin receptor agonists'.
- [124] R. Kowalczyk, M. A. Brimble, Y. Tomabechi, A. J. Fairbanks, M. Fletcher, D. L. Hay, *Org. Biomol. Chem.* **2014**, *12*, 8142-8151; 'Convergent chemoenzymatic synthesis of a library of glycosylated analogues of pramlintide: Structure-activity relationships for amylin receptor agonism'.
- [125] S.-Q. Fan, W. Huang, L.-X. Wang, *J. Biol. Chem.* **2012**, *287*, 11272-11281; 'Remarkable transglycosylation activity of glycosynthase mutants of Endo-D, an endo- $\beta$ -*N*-acetylglucosaminidase from *Streptococcus pneumoniae*'.
- [126] J. P. Giddens, J. V. Lomino, M. N. Amin, L.-X. Wang, *J. Biol. Chem.* **2016**, *291*, 9356-9370; 'Endo-F3 glycosynthase mutants enable chemoenzymatic synthesis of core-fucosylated triantennary complex type glycopeptides and glycoproteins'.
- [127] J. D. McIntosh, M. A. Brimble, A. E. S. Brooks, P. R. Dunbar, R. Kowalczyk, Y. Tomabechi, A. J. Fairbanks, *Chem. Sci.* **2015**, *6*, 4636-4642; 'Convergent chemo-enzymatic synthesis of mannosylated glycopeptides; targeting of putative vaccine candidates to antigen presenting cells'.

- [128] C. Toonstra, M. N. Amin, L.-X. Wang, *J. Org. Chem.* **2016**, *81*, 6176-6185; 'Site-selective chemoenzymatic glycosylation of an HIV-1 polypeptide antigen with two distinct *N*-glycans via an orthogonal protecting group strategy'.
- [129] Q. Yang, Y. An, S. Zhu, R. Zhang, C. M. Loke, J. F. Cipollo, L.-X. Wang, *ACS Chem. Biol.* **2017**, *12*, 1665-1673; 'Glycan remodeling of human erythropoietin (EPO) through combined mammalian cell engineering and chemoenzymatic transglycosylation'.
- [130] T. Yamaguchi, M. N. Amin, C. Toonstra, L.-X. Wang, *J. Am. Chem. Soc.* **2016**, *138*, 12472-12485; 'Chemoenzymatic synthesis and receptor binding of mannose-6-phosphate (M6P)-containing glycoprotein ligands reveal unusual structural requirements for M6P receptor recognition'.
- [131] F. Tang, Y. Yang, Y. Tang, S. Tang, L. Yang, B. Sun, B. Jiang, J. Dong, H. Liu, M. Huang, M.-Y. Geng, W. Huang, *Org. Biomol. Chem.* **2016**, *14*, 9501-9518; 'One-pot *N*-glycosylation remodeling of IgG with non-natural sialylglycopeptides enables glycosite-specific and dual-payload antibody-drug conjugates'.
- [132] Y. Eshima, Y. Higuchi, T. Kinoshita, S.-i. Nakakita, K. Takegawa, *PLOS ONE* **2015**, *10*, e0132859; 'Transglycosylation activity of glycosynthase mutants of *endo*- $\beta$ -*N*-acetylglucosaminidase from *Coprinopsis cinerea*'.
- [133] Y. Higuchi, Y. Eshima, Y. Huang, T. Kinoshita, W. Sumiyoshi, S.-i. Nakakita, K. Takegawa, *Biotechnol Lett* **2017**, *39*, 157-162; 'Highly efficient transglycosylation of sialo-complex-type oligosaccharide using *Coprinopsis cinerea* endoglycosidase and sugar oxazoline'.
- [134] S. Manabe, Y. Yamaguchi, J. Abe, K. Matsumoto, Y. Ito, *R. Soc. Open Sci.* **2018**, *5*, 171521; 'Acceptor range of *endo*- $\beta$ -*N*-acetylglucosaminidase mutant Endo-CC N180H: From monosaccharide to antibody'.
- [135] D. G. Gibson, in *Methods in enzymology*, Vol. 498 (Ed.: V. Christopher), Academic Press, **2011**, pp. 349-361.
- [136] R. C. Kasana, A. Gulati, *J. Basic Microbiol.* **2011**, *51*, 572-579; 'Cellulases from psychrophilic microorganisms: A review'.
- [137] S. Shipkowski, J. E. Brenchley, *Appl. Environ. Microbiol.* **2005**, *71*, 4225; 'Characterization of an unusual cold-active  $\beta$ -glucosidase belonging to family 3 of the glycoside hydrolases from the psychrophilic isolate *Paenibacillus* sp. Strain C7'.
- [138] J. Zhou, R. Zhang, P. Shi, H. Huang, K. Meng, T. Yuan, P. Yang, B. Yao, *Appl Microbiol Biotechnol* **2011**, *92*, 305-315; 'A novel low-temperature-active  $\beta$ -glucosidase from symbiotic *Serratia* sp. TN49 reveals four essential positions for substrate accommodation'.
- [139] F. Madeira, Y. M. Park, J. Lee, N. Buso, T. Gur, N. Madhusoodanan, P. Basutkar, A. R. N. Tivey, S. C. Potter, R. D. Finn, R. Lopez, *Nucleic Acids Res.* **2019**; 'The EMBL-EBI search and sequence analysis tools apis in 2019'.
- [140] M. Fuhrmann, A. Hausherr, L. Ferbitz, T. Schödl, M. Heitzer, P. Hegemann, *Plant Mol. Biol.* **2004**, *55*, 869-881; 'Monitoring dynamic expression of nuclear genes in *Chlamydomonas reinhardtii* by using a synthetic luciferase reporter gene'.
- [141] F. T. Robb, D. L. Maeder, J. R. Brown, J. DiRuggiero, M. D. Stump, R. K. Yeh, R. B. Weiss, D. M. Dunn, in *Methods in enzymology*, Vol. Volume 330, Academic Press, **2001**, pp. 134-157.
- [142] D. R. P. Murray, *Biochem. J.* **1930**, *24*, 1890-1896; 'The inhibition of esterases by excess substrate'.
- [143] C. Zheng, C. J. Lanczycki, D. Zhang, D. I. Hurwitz, F. Chitsaz, F. Lu, G. H. Marchler, J. S. Song, J. He, L. Y. Geer, L. Han, M. Gwadz, M. K. Derbyshire, N. Thanki, N. R. Gonzales, R. C. Geer, R. A. Yamashita, S. Lu, S. H. Bryant, Y. Bo, Z. Wang, A. Marchler-Bauer, *Nucleic Acids Res.* **2016**, *45*, D200-D203; 'CDD/SPARCLE: Functional classification of proteins via subfamily domain architectures'.
- [144] M. Eda, M. Ishimaru, T. Tada, *Acta Crystallogr., Sect. F* **2015**, *71*, 153-156; 'Expression, purification, crystallization and preliminary X-ray crystallographic analysis of tomato  $\beta$ -galactosidase 4'.

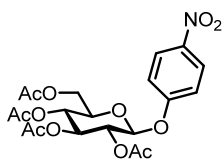
- [145] U. Ohto, K. Usui, T. Ochi, K. Yuki, Y. Satow, T. Shimizu, *J. Biol. Chem.* **2012**, *287*, 1801-1812; 'Crystal structure of human  $\beta$ -galactosidase: Structural basis of GM1 gangliosidosis and morquio B diseases'.
- [146] K. Palani, D. Kumaran, S. Burley, S. Swaminathan, **2011**.
- [147] W. Cheng, L. Wang, Y.-L. Jiang, X.-H. Bai, J. Chu, Q. Li, G. Yu, Q.-L. Liang, C.-Z. Zhou, Y. Chen, *J. Biol. Chem.* **2012**, *287*, 22910-22918; 'Structural insights into the substrate specificity of *Streptococcus pneumoniae*  $\beta$ -(1,3)-galactosidase BgaC'.
- [148] S. Mine, M. Watanabe, S. Kamachi, Y. Abe, T. Ueda, *J. Biol. Chem.* **2017**, *292*, 4996-5006; 'The structure of an archaeal  $\beta$ -glucosaminidase provides insight into glycoside hydrolase evolution'.
- [149] T. Tanaka, T. Fukui, H. Atomi, T. Imanaka, *J. Bacteriol.* **2003**, *185*, 5175; 'Characterization of an *exo*- $\beta$ -D-glucosaminidase involved in a novel chitinolytic pathway from the hyperthermophilic archaeon *Thermococcus kodakaraensis* KOD1'.
- [150] D. J. Vocadlo, G. J. Davies, *Curr. Opin. Chem. Biol.* **2008**, *12*, 539-555; 'Mechanistic insights into glycosidase chemistry'.
- [151] F. C. Harrison, J. Van Der Leek, *Am. J. Public Hygiene* **1909**, *19*, 557-563; 'Aesculin bile salt media for water analysis'.
- [152] D. H. Juers, B. W. Matthews, R. E. Huber, *Protein Sci.* **2012**, *21*, 1792-1807; 'LacZ  $\beta$ -galactosidase: Structure and function of an enzyme of historical and molecular biological importance'.
- [153] Y. S. Lee, E. S. Rho, Y. K. Min, B. T. Kim, K. H. Kim, *J. Carbohydr. Chem.* **2001**, *20*, 503-506; 'Practical  $\beta$ -stereoselective O-glycosylation of phenols with penta-O-acetyl- $\beta$ -D-glucopyranose'.
- [154] A. Steinmann, J. Thimm, M. Matwiejuk, J. Thiem, *Macromolecules* **2010**, *43*, 3606-3612; 'Formation of homooligosaccharides using base-promoted glycosylation of unprotected glycosyl fluorides'.
- [155] P. Sokkalingam, C.-H. Lee, *J. Org. Chem.* **2011**, *76*, 3820-3828; 'Highly sensitive fluorescence "turn-on" indicator for fluoride anion with remarkable selectivity in organic and aqueous media'.
- [156] D. A. Armbruster, T. Pry, *Clin. Biochem. Rev.* **2008**, *29*, S49-52; 'Limit of blank, limit of detection and limit of quantitation'.
- [157] H. Bisswanger, *Enzyme kinetics: Principles and methods*, John Wiley & Sons, **2008**.
- [158] M. Kanehisa, *Post-genome informatics*, Oxford University Press (OUP), **2000**.
- [159] S. Marcinowsdki, H. Grisebach, *Eur. J. Biochem.* **1978**, *87*, 37-44; 'Enzymology of lignification'.
- [160] W. Hösel, E. Surholt, E. Borgmann, *Eur. J. Biochem.* **1978**, *84*, 487-492; 'Characterization of  $\beta$ -glucosidase isoenzymes possibly involved in lignification from chick pea (*Cicer arietinum* L.) cell suspension cultures'.
- [161] R. V. Stick, K. A. Stubbs, *Tetrahedron: Asymmetry* **2005**, *16*, 321-335; 'From glycoside hydrolases to thioglycoligases: The synthesis of thioglycosides'.
- [162] Z. Györgydeák, L. Szilágyi, H. Paulsen, *J. Carbohydr. Chem.* **1993**, *12*, 139-163; 'Synthesis, structure and reactions of glycosyl azides'.
- [163] W. J. Hennen, H. M. Sweers, Y. F. Wang, C. H. Wong, *J. Org. Chem.* **1988**, *53*, 4939-4945; 'Enzymes in carbohydrate synthesis. Lipase-catalyzed selective acylation and deacylation of furanose and pyranose derivatives'.
- [164] D. Drueckhammer, W. Drueckhammer, R. Hennen, C. Pederson, I. Barbas, T. Gautheron, C.-H. Krach, Wong, *Synthesis* **1991**, *1991*, 499-525; 'Enzyme catalysis in synthetic carbohydrate chemistry'.
- [165] D. Kadereit, H. Kadereit, Waldmann, *Chem. Rev.* **2001**, *101*, 3367-3396; 'Enzymatic protecting group techniques'.
- [166] Z. Györgydeák, L. Szilágyi, *Liebigs Ann. Chem.* **1985**, *1985*, 103-112; 'Darstellung und  $^1\text{H}$ -NMR-spektroskopische untersuchung anomerer 6-desoxyhexopyranosylazide'.
- [167] K. P. R. Kartha, H. J. Jennings, *J. Carbohydr. Chem.* **1990**, *9*, 777-781; 'A simplified, one-pot preparation of acetobromosugars from reducing sugars'.

- [168] K. Tsuge, M. Kataoka, Y. Seto, *J. Anal. Toxicol.* **2001**, *25*, 228-236; 'Rapid determination of cyanide and azide in beverages by microdiffusion spectrophotometric method'.
- [169] A. Seko, M. Koketsu, M. Nishizono, Y. Enoki, H. R. Ibrahim, L. R. Juneja, M. Kim, T. Yamamoto, *Biochim. Biophys. Acta, Gen. Subj.* **1997**, *1335*, 23-32; 'Occurrence of a sialylglycopeptide and free sialylglycans in hen's egg yolk'.
- [170] B. Sun, W. Bao, X. Tian, M. Li, H. Liu, J. Dong, W. Huang, *Carbohydr. Res.* **2014**, *396*, 62-69; 'A simplified procedure for gram-scale production of sialylglycopeptide (SGP) from egg yolks and subsequent semi-synthesis of Man<sub>3</sub>GlcNAc oxazoline'.
- [171] H. Schägger, *Nat Protoc.* **2006**, *1*, 16-22; 'Tricine-SDS-PAGE'.
- [172] A. Trincone, G. Perugino, M. Rossi, M. Moracci, *Bioorg. Med. Chem. Lett.* **2000**, *10*, 365-368; 'A novel thermophilic glycosynthase that effects branching glycosylation'.
- [173] L.-L. Miao, H.-X. Fan, J. Qu, Y. Liu, Z.-P. Liu, *Appl Microbiol Biotechnol* **2017**, *101*, 2033-2041; 'Specific amino acids responsible for the cold adaptedness of *Micrococcus antarcticus*  $\beta$ -glucosidase BglU'.
- [174] K. Haneda, T. Oishi, H. Kimura, T. Inazu, *Bioorg. Med. Chem.* **2018**, *26*, 2092-2098; 'Development of a microbioreactor for glycoconjugate synthesis'.
- [175] J. Mayer, B. Kranz, L. Fischer, *J. Biotechnol.* **2010**, *145*, 387-393; 'Continuous production of lactulose by immobilized thermostable  $\beta$ -glycosidase from *Pyrococcus furiosus*'.
- [176] A. Schwarz, M. S. Thomsen, B. Nidetzky, *Biotechnol. Bioeng.* **2009**, *103*, 865-872; 'Enzymatic synthesis of  $\beta$ -glucosylglycerol using a continuous-flow microreactor containing thermostable  $\beta$ -glycoside hydrolase CelB immobilized on coated microchannel walls'.
- [177] J. M. Whitelock, R. V. Iozzo, *Chem. Rev.* **2005**, *105*, 2745-2764; 'Heparan sulfate: A complex polymer charged with biological activity'.
- [178] M. M. Fuster, J. D. Esko, *Nat. Rev. Cancer* **2005**, *5*, 526-542; 'The sweet and sour of cancer: Glycans as novel therapeutic targets'.
- [179] P. Fialová, L. Weignerová, J. Rauvolfová, V. Přikrylová, A. Pišvejcová, R. Ettrich, M. Kuzma, P. Sedmera, V. r. Křen, *Tetrahedron* **2004**, *60*, 693-701; 'Hydrolytic and transglycosylation reactions of *N*-acyl modified substrates catalysed by  $\beta$ -*N*-acetylhexosaminidases'.
- [180] H. Ochiai, M. Ohmae, T. Mori, S. Kobayashi, *Biomacromolecules* **2005**, *6*, 1068-1084; 'Bottom-up synthesis of hyaluronan and its derivatives via enzymatic polymerization: Direct incorporation of an amido functional group'.
- [181] S. Kobayashi, M. Ohmae, H. Ochiai, S.-i. Fujikawa, *Chem. - Eur. J.* **2006**, *12*, 5962-5971; 'A hyaluronidase supercatalyst for the enzymatic polymerization to synthesize glycosaminoglycans'.
- [182] S. Kobayashi, H. Morii, R. Itoh, S. Kimura, M. Ohmae, *J. Am. Chem. Soc.* **2001**, *123*, 11825-11826; 'Enzymatic polymerization to artificial hyaluronan: A novel method to synthesize a glycosaminoglycan using a transition state analogue monomer'.
- [183] S.-i. Fujikawa, M. Ohmae, S. Kobayashi, *Biomacromolecules* **2005**, *6*, 2935-2942; 'Enzymatic synthesis of chondroitin 4-sulfate with well-defined structure'.
- [184] J. Müllegger, H.-M. Chen, W. Y. Chan, S. P. Reid, M. Jahn, R. A. J. Warren, H. M. Salleh, S. G. Withers, *ChemBioChem* **2006**, *7*, 1028-1030; 'Thermostable glycosynthases and thioglycoligases derived from *Thermotoga maritima*  $\beta$ -glucuronidase'.
- [185] E. D. Soli, A. S. Manoso, M. C. Patterson, P. DeShong, D. A. Favor, R. Hirschmann, A. B. Smith, *J. Org. Chem.* **1999**, *64*, 3171-3177; 'Azide and cyanide displacements via hypervalent silicate intermediates'.
- [186] D. P. Temelkoff, M. Zeller, P. Norris, *Carbohydr. Res.* **2006**, *341*, 1081-1090; '*N*-glycoside neoglycotrimers from 2,3,4,6-tetra-*O*-acetyl- $\beta$ -D-glucopyranosyl azide'.
- [187] S. Dedola, D. L. Hughes, S. A. Nepogodiev, M. Rejzek, R. A. Field, *Carbohydr. Res.* **2010**, *345*, 1123-1134; 'Synthesis of  $\alpha$ - and  $\beta$ -D-glucopyranosyl triazoles by CuAAC

- 'click chemistry': Reactant tolerance, reaction rate, product structure and glucosidase inhibitory properties'.
- [188] M. Jahn, S. G. Withers, *Biocatal. Biotransform.* **2003**, *21*, 159-166; 'New approaches to enzymatic oligosaccharide synthesis: Glycosynthases and thioglycoligases'.
- [189] L. Ge, J. Xie, T. Wu, S. Zhang, L. Zhao, G. Ding, Z. Wang, W. Xiao, *Int. J. Food Sci. Technol.* **2017**, *52*, 2596-2603; 'Purification and characterisation of a novel  $\alpha$ -L-rhamnosidase exhibiting transglycosylating activity from *Aspergillus oryzae*'.
- [190] L. Liu, A. R. Prudden, G. P. Bosman, G.-J. Boons, *Carbohydr. Res.* **2017**, *452*, 122-128; 'Improved isolation and characterization procedure of sialylglycopeptide from egg yolk powder'.
- [191] Y. Zou, Z. Wu, L. Chen, X. Liu, G. Gu, M. Xue, P. G. Wang, M. Chen, *J. Carbohydr. Chem.* **2012**, *31*, 436-446; 'An efficient approach for large-scale production of sialylglycopeptides from egg yolks'.
- [192] F. W. Studier, B. A. Moffatt, *J. Mol. Biol.* **1986**, *189*, 113-130; 'Use of bacteriophage T7 RNA polymerase to direct selective high-level expression of cloned genes'.
- [193] B. A. Moffatt, F. W. Studier, *Cell* **1987**, *49*, 221-227; 'T7 lysozyme inhibits transcription by T7 RNA polymerase'.
- [194] L. Zhang, X. Li, F. Zhang, G. Wang, *Standards in Genomic Sciences* **2014**, *9*, 574-584; 'Genomic analysis of *Agrobacterium radiobacter* DSM 30147<sup>T</sup> and emended description of *A. radiobacter* (Beijerinck and Van Delden 1902) Conn 1942 (approved lists 1980) emend. Sawada *et al.* 1993'.
- [195] M. M. Bradford, *Anal. Biochem.* **1976**, *72*, 248-254; 'A rapid and sensitive method for the quantitation of microgram quantities of protein utilizing the principle of protein-dye binding'.
- [196] A. Shrivastava, V. Gupta, *Chron. Young Sci.* **2011**, *2*, 21-25; 'Methods for the determination of limit of detection and limit of quantitation of the analytical methods'.
- [197] L. Shi, G. Zhang, F. Pan, *Tetrahedron* **2008**, *64*, 2572-2575; 'Fe<sub>2</sub>(SO<sub>4</sub>)<sub>3</sub>·XH<sub>2</sub>O-catalyzed per-O-acetylation of sugars compatible with acid-labile protecting groups adopted in carbohydrate chemistry'.
- [198] D. H. Brauns, *J. Am. Chem. Soc.* **1923**, *45*, 833-835; 'Fluoro-acetyl derivatives of sugars'.
- [199] R. Miethchen, G. Kolp, *J. Fluorine Chem.* **1993**, *60*, 49-55; 'Reactions with and in anhydrous hydrogen fluoride systems. Part 8. Triethylamine trishydrofluoride — a convenient reagent for the stereoselective synthesis of glycosyl fluorides'.
- [200] H. M. Burke, T. Gunnlaugsson, E. M. Scanlan, *Org. Biomol. Chem.* **2016**, *14*, 9133-9145; 'Glycosylated lanthanide cyclen complexes as luminescent probes for monitoring glycosidase enzyme activity'.
- [201] S. Inaba, M. Yamada, T. Yoshino, Y. Ishido, *J. Am. Chem. Soc.* **1973**, *95*, 2062-2063; 'Synthetic studies by the use of carbonates. IV. New method for the synthesis of glycosyl compounds by the use of 1-O-aryloxycarbonyl sugar derivatives'.
- [202] B. Capon, P. M. Collins, A. A. Levy, W. G. Overend, *J. Chem. Soc.* **1964**, 3242-3254; 'Reactions at position 1 of carbohydrates. Part V. Nucleophilic displacement reactions of acetylglycosyl halides'.
- [203] K. Yamamoto, *Biosci. Biotechnol. Biochem.* **2012**, *76*, 1815-1827; 'Biological analysis of the microbial metabolism of hetero-oligosaccharides in application to glycototechnology'.
- [204] O. Westphal, H. Feier, *Chem. Ber.* **1956**, *89*, 582-588; 'Darstellung künstlicher Antigene mit determinanten Zuckerguppen, II. Mittel.: Synthese der *p*-aminophenyl-O- $\alpha$ -glykoside von L-fucose, L-rhamnose, D-galaktose und D-mannose'.
- [205] S. Tejima, S. Ishiguro, *Chem. Pharm. Bull.* **1967**, *15*, 255-263; 'Thiiosugars, X. Studies on glycosyl *N,N*-dialkyldithiocarbamates'.
- [206] J. C. Ellington, E. M. Arnett, *J. Am. Chem. Soc.* **1988**, *110*, 7778-7785; 'Kinetics and thermodynamics of phenolate silylation and alkylation'.

- 
- [207] A. Khalafi-Nezhad, R. Fareghi Alamdari, N. Zekri, *Tetrahedron* **2000**, *56*, 7503-7506; 'Efficient and selective protection of alcohols and phenols with triisopropylsilyl chloride/imidazole using microwave irradiation'.
- [208] G. G. Zapesochnaya, V. A. Kurkin, V. B. Braslavskii, N. V. Filatova, *Chem. Nat. Compd.* **2002**, *38*, 314-318; 'Phenolic compounds of *Salix acutifolia* bark'.
- [209] B. Capon, D. S. Rycroft, J. W. Thomson, *Carbohydr. Res.* **1979**, *70*, 145-149; 'The <sup>13</sup>C NMR spectra of peracetylated cello-oligosaccharides'.
- [210] F. Sonmez, M. Nebioglu, S. Besoluk, M. Arslan, M. Zengin, M. Kucukislamoglu, *Nat. Prod. Res.* **2013**, *27*, 631-638; 'The first total synthesis of apigenin 7-O-β-D-cellobiosyl-4'-O-β-D-glucopyranoside isolated from *Salvia uliginosa*'.
- [211] S. Tsegay, R. J. Williams, S. J. Williams, *Carbohydr. Res.* **2012**, *357*, 16-22; 'Synthesis of glycosyl fluorides from thio-, seleno-, and telluroglycosides and glycosyl sulfoxides using aminodifluorosulfonium tetrafluoroborates'.
- [212] M. R. Hayes, J. Pietruszka, *Molecules* **2017**, *22*, 1434; 'Synthesis of glycosides by glycosynthases'.
- [213] A. Fulton, M. R. Hayes, U. Schwaneberg, J. Pietruszka, K.-E. Jaeger, in *Protein engineering: Methods and protocols* (Eds.: U. T. Bornscheuer, M. Höhne), Springer New York, New York, NY, **2018**, pp. 209-231.

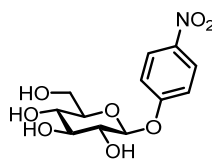
## 11 LIST OF SYNTHESISED MOLECULES



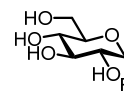
**22b**  
 $C_{20}H_{23}NO_{12}$   
 [469.40]  
 MH029ac



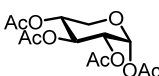
**22d**  
 $C_{14}H_{19}FO_9$   
 [350.29]  
 MH022



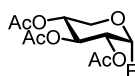
**5h**  
 $C_{12}H_{15}NO_8$   
 [301.25]  
 MH029dep



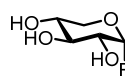
**2a**  
 $C_6H_{11}FO_5$   
 [182.15]  
 MH025



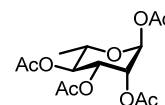
**22c**  
 $C_{13}H_{18}O_9$   
 [318.28]  
 MH020



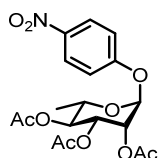
**22e**  
 $C_{11}H_{15}FO_7$   
 [278.23]  
 MH024



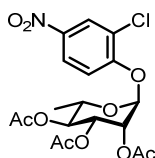
**2d**  
 $C_5H_9FO_4$   
 [152.12]  
 MH\_D\_018



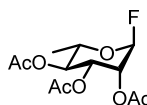
**22q**  
 $C_{14}H_{20}O_9$   
 [332.30]  
 MH021



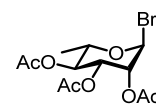
**22r**  
 $C_{18}H_{21}NO_{10}$   
 [411.36]  
 MH023a



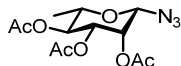
**22s**  
 $C_{18}H_{20}ClNO_{10}$   
 [445.81]  
 MH030acyl



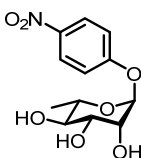
**22t**  
 $C_{12}H_{17}FO_7$   
 [315.28]  
 MH026



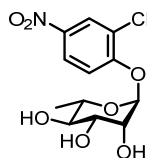
**22u**  
 $C_{12}H_{17}BrO_7$   
 [353.16]  
 MH036



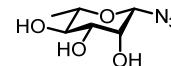
**22v**  
 $C_{12}H_{17}N_3O_7$   
 [315.28]  
 MH037



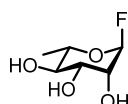
**5r**  
 $C_{12}H_{15}NO_7$   
 [285.25]  
 MH023b



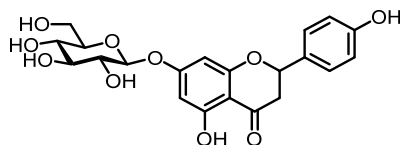
**5ae**  
 $C_{12}H_{14}ClNO_8$   
 [319.67]  
 MH030



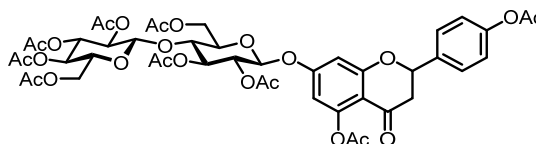
**16d**  
 $C_6H_{11}N_3O_4$   
 [189.17]  
 MH038



**2o**  
 $C_6H_{11}FO_4$   
 [166.15]  
 MH027a

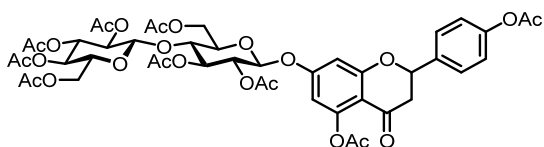


**1b**  
 $C_{21}H_{22}O_{10}$   
 [434.39]  
 MH016

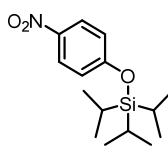


**22i**  
 $C_{45}H_{50}O_{24}$   
 [974.87]  
 MH\_D\_Syn03

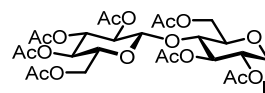
11 List of Synthesised Molecules



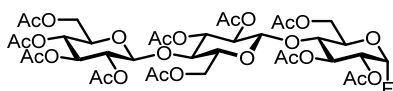
**22i**  
**C<sub>45</sub>H<sub>50</sub>O<sub>24</sub>**  
**[974.87]**  
 MH\_D\_Syn03



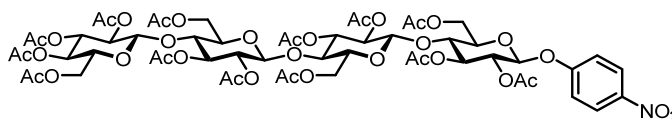
**23**  
**C<sub>15</sub>H<sub>25</sub>NO<sub>3</sub>Si**  
**[295.45]**  
 MH\_D\_023



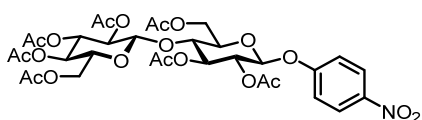
**22f**  
**C<sub>26</sub>H<sub>35</sub>FO<sub>17</sub>**  
**[638.55]**  
 MH\_D\_Syn01



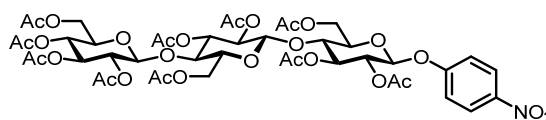
**22g**  
**C<sub>38</sub>H<sub>51</sub>FO<sub>25</sub>**  
**[926.80]**  
 MH\_D\_Syn01



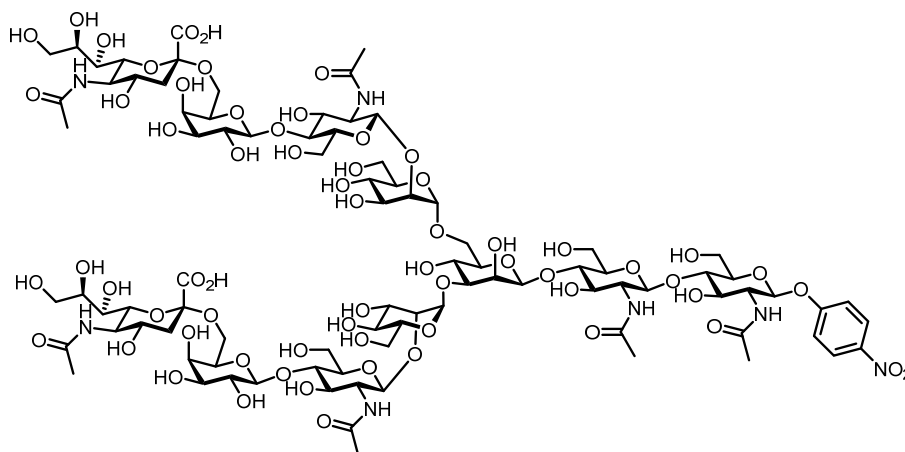
**5y**  
**C<sub>56</sub>H<sub>71</sub>NO<sub>36</sub>**  
**[1334.16]**  
 LS\_Synth\_01



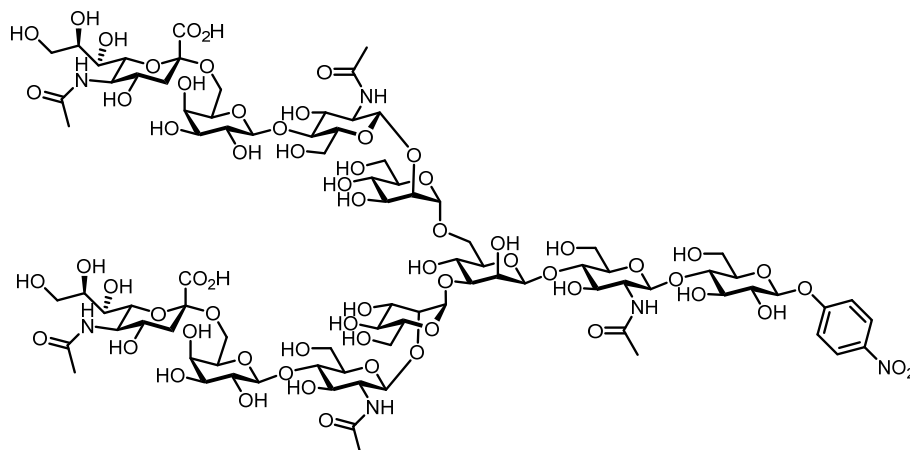
**5c**  
**C<sub>32</sub>H<sub>39</sub>O<sub>20</sub>**  
**[757.65]**  
 LS\_Synth\_01



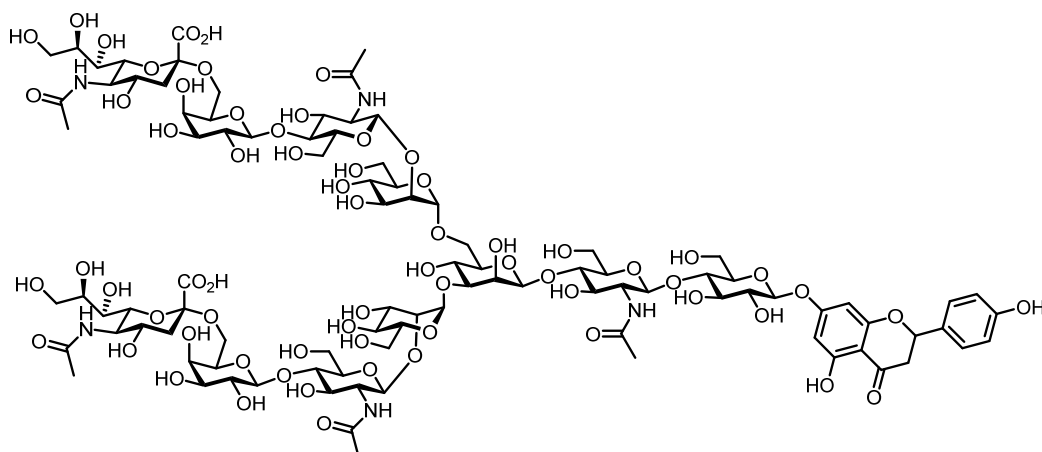
**5x**  
**C<sub>44</sub>H<sub>55</sub>NO<sub>28</sub>**  
**[1045.90]**  
 LS\_Synth\_01



**5af**  
**C<sub>90</sub>H<sub>141</sub>N<sub>7</sub>O<sub>64</sub>**  
**[2343.80]**  
 MH05V09



**5ag**  
**C<sub>88</sub>H<sub>138</sub>N<sub>6</sub>O<sub>64</sub>**  
**[2302.77]**  
MH05V02



**1l**  
**C<sub>97</sub>H<sub>145</sub>N<sub>5</sub>O<sub>66</sub>**  
**[2437.20]**  
MH05V01

## 12 ACKNOWLEDGEMENTS

It has been a long journey, from taking my first steps in the lab during my apprenticeship, expanding my knowledge during my studies of biochemistry, and now finally reaching the end of my doctoral thesis! On this journey, countless people have come and gone. People, who not only inspired and motivated me, but also shaped my path and helped me reach the goals I have achieved. Each and every one was equally special but at this point I would like to give special thanks to the persons, which made this doctoral thesis possible.

First of all, of course, a special thank you to Prof. Dr. Jörg Pietruszka! Thank you for introducing me to the world of sugars. For the trust you gave, allowing me to follow my ideas and interests and to create and shape the project in all its entirety. The project has come a long way since our first discussion about simply 'taking a sugar away and adding another in its place'! For all the inspirational discussions in your office, which often led to me leaving with more questions than before, but taught me to focus and to look at problems from a different angle. Also, for all the non-scientific discussions about board games and theme parks, which were always fun. But most of all, for constantly throwing me in the deep end, even though you know I don't like it! I have learnt so much, not only scientifically, but also in general for life during my time at the IBOC.

I would also like to thank Prof. Dr. Urlacher for her willingness to take over the evaluation of this thesis as a second evaluator.

A big thank you to the Jürgen Manchot Stiftung and the International Research Training Group 'SeleCa' for the financial support during my doctoral thesis. Also, for the opportunity and organisation of my research internship in Japan. A special thanks to all the doctoral students of SeleCa, the time in Aachen or Osaka wouldn't have been the same without you crazy people! Furthermore, thank you to Prof. Fujiyama and Guest Associate Prof. Ohashi and all the students of the Fujiyama lab. Thank you for welcoming me so heartily into the institute and teaching me about Japanese culture. Here also a special thanks to Anne-Katrin Bachon, I will never forget the travels and great evenings with food and beer and (of course!) our two nights partying in Osaka! It was an unforgettable experience.

Even though the time during the doctoral thesis was not always easy, all my great colleagues at the IBOC made the time easier and enjoyable. Many thanks go out to all the people who have worked together with me in any way at the IBOC. To Tom, thank you for all your help and biochemical input. Your advice was always received gratefully! To Yvonne, who taught me many practical tricks in the chemistry lab during my first internship in the IBOC and in turn became a great friend on whom I can always rely on. To Caro, who taught me all I know on

the biology side and was always a source of inspiration. To Roza, whose laugh always brightened the day in the lab and in the train on the way home. To all the former members of the IBOC, you were always ready to help and always reminded me why I chose to stay! Also, to all the ladies, who took part in the 'Mädels und Marc - Just Dance' evenings. To Moni, Rainer, Bea, and Vera, you keep the IBOC running, even if we don't always notice it. And of course a special thank you to Birgit! You were always there to help, even if you were actually too busy and didn't have any time. Thank you for all your help, filling in the countless forms, organising financial stuff and always being ready to call anyone to get the information we need. Our time at the IBOC wouldn't be as easy without you.

Of course, I thank not only the former doctoral students but also all of my bachelor students and the apprentices of the IBOC. Thank you, Lisa and Bianca for contributing to the Team Sugar and always coming to the lab motivated! I enjoyed the time supervising you and am glad I could show you that sugars can also be fun. A big thank you to Kevin! The time with you was so much fun. I couldn't have managed much of the work, if you hadn't been there to help. I am very proud to have contributed to your education and am excited to see where your path leads you. And I of course cannot forget Dennis (D---is)! Thank you for all the fun talks in the bio lab and showing everybody that leading a 'normal' student life doesn't mean you can't achieve great scientific goals.

As most of our time is spent in the lab, I of course have to thank all of my co-workers in Lab 308. Thank you to Claudia, Andreas, Kevin, David, Julia, Hannah K., and Pascal. The time in the lab with you was never boring and I always looked forward to coming to the lab in the morning. A special thanks to Andreas, for all the countless questions about picture quality, formatting, and Origin, which you always answered patiently. This thesis would not look the same without you. Also thank you for always listening, even when you don't really have the time.

A big thanks also to all the current colleagues of the IBOC. I have enjoyed my time at the IBOC thanks to all of you. Even if the day did not start well, I knew I could look forward to lunch and have a great time with all of you in the kitchen. I will never forget the interesting and funny discussions about food and the world in the kitchen, but also during all the barbeques, Christmas parties, in the Venn, and during game evenings.

Furthermore, I would like to send a huge thanks to Jan, Hannah and Roxy. First of all for the correction of my thesis. You helped me loads and I am very grateful. Thank you Jan for helping with this 'complicated' thesis and for all the gossip on our train trips to and from work. It's never boring with you around! Thank you Hannah for the special time in the 'Bio'. Seeing the basket in the kitchen when I arrive at work always brightens my day. Thank you for all the help, time,

and friendship you have given. My time at the IBOC would not be the same without you. And what would life at the IBOC have been without my 'lab wife' Roxy? Thank you for everything! All the hours spent in the RurTalBahn, in Aachen, on the motor way, at the university, in Japan, and in the IBOC. I enjoyed all the time with you and am so proud to see how you developed over the time we spent together. I learnt so much from you.

Last but not least, thank you to my family and especially to Alex. It has probably not been easy with me during the time of my thesis (especially while I was writing), but you have always been there for me. Thank you for always motivating me, distracting me, and just being there. Knowing I always have your support helps me get through so many challenges. But mostly, thank you for putting up with me the way I am.

## 13 DECLARATION

I hereby certify, that the present doctoral thesis, supervised by Prof. Dr. Jörg Pietruszka at the Institute of Bioorganic Chemistry at the Heinrich Heine University Düsseldorf and Forschungszentrum Jülich, was written by me independently and without the use of unauthorised aids. The work and writing of this doctoral thesis was conducted in accordance with the 'Principles of ensuring good scientific practice at the Heinrich Heine University Düsseldorf'.

The present doctoral thesis has only been presented to the Faculty of Mathematics and Natural Sciences of the Heinrich Heine University Düsseldorf. There has been no other attempt of reaching a doctoral degree before.

Marc Richard Hayes